THE BUMP AT THE END OF THE RAILWAY BRIDGE

A Dissertation

by

JENNIFER ELIZABETH NICKS

Submitted to the Office of Graduate Studies of
Texas A&M University
in partial fulfillment of the requirements for the degree of

DOCTOR OF PHILOSOPHY

December 2009

Major Subject: Civil Engineering

THE BUMP AT THE END OF THE RAILWAY BRIDGE

A Dissertation

by

JENNIFER ELIZABETH NICKS

Submitted to the Office of Graduate Studies of
Texas A&M University
in partial fulfillment of the requirements for the degree of

DOCTOR OF PHILOSOPHY

Approved by:

Chair of Committee,	Jean-Louis Briaud
Committee Members,	Charles Aubeny
	Gary Fry
	Alan Palazzolo
Head of Department,	John Niedzwecki

December 2009

Major Subject: Civil Engineering

ABSTRACT

The Bump at the End of the Railway Bridge. (December 2009)

Jennifer Elizabeth Nicks, B.S.; M.Eng., Texas A&M University

Chair of Advisory Committee: Dr. Jean-Louis Briaud

The bump at the end of the railway bridge is a result of differential movement between the bridge deck and the approach embankment. The movement can have the form of a bump or a dip. Either defect in the track geometry can cause significant problems in track performance.

The current state of practice was evaluated by conducting a literature review and an industry survey. According to the survey, approximately half of all railway bridges are affected by the bump/dip. The total annual cost for repairing these bridge transition problems is estimated at $26 million. This does not take into account the considerable cost resulting from speed reductions that railroads must place on trains at these locations. In addition to the increased maintenance costs, the bump/dip leads to higher impact loads, uncomfortable rides and possible safety hazards.

The track response due to the bump at the end of the bridge was evaluated by creating a 4-D finite element model of the train, track structure and track substructure. The motion of the train model across a bridge/approach transition, with and without a bump/dip, was then simulated using LS-DYNA. It was found that a track modulus differential alone (no bump/dip) at a bridge/approach location leads to impact forces as

well as increased ballast and subgrade pressures on the approach. This instigates the formation of a bump or dip in the track. The track response is increased when a bump/dip is present in the track profile. A parametric study looking at the influence of train direction, train speed, bump/dip size, approach embankment soil modulus, approach tie material, bridge tie material, bridge deck type, ballast thickness and approach tie length on the magnitude of impact forces, track deflection, ballast and subgrade pressures was also performed with the model.

Finally, a design solution to minimize the bump at the end of the bridge is proposed. The solution involves installing varying length steel bars into a soft subgrade approach embankment. The solution addresses both the settlement and track modulus differential between the bridge and the embankment. A full-scale field test of this prototype solution is underway.

ACKNOWLEDGEMENTS

I would first like to thank my committee chair, Dr. Jean-Louis Briaud for his direction and support throughout the course of this research. Dr. Briaud has been a great advisor and mentor, providing me with valuable opportunities to broaden my knowledge and further myself in my chosen field. His enthusiasm and leadership inspired me to pursue geotechnical engineering and become involved in the professional community. My other committee members, Dr. Gary Fry, Dr. Charles Aubeny and Dr. Alan Palazzolo also deserve thanks for their guidance and support. Without Dr. Fry, I would not have come to appreciate rail research as much as I do. Thanks also go to my friends, colleagues and the geotechnical engineering faculty for making my time at Texas A&M University a great experience.

Appreciation and thanks are also reserved for Dr. Akram Abu-Odeh who took the time to help me while I was learning LS-DYNA. Without his help, this dissertation would have taken much longer. I am also thankful to Matt Dick for providing information on the dimensions and material properties for vehicle and rail components which helped me in building the finite element model used in my research.

I also want to extend my gratitude to the Association of American Railroads which provided the support for my continued research studies. Those who have been especially helpful in this sponsored research are Dave Davis, Rafael Jimenez and Duane Otter from the Transportation Technology Center (TTC) in Pueblo, CO. Spending a

summer with them at their facility was a great experience that helped me gain further insight into my own research.

Finally, thanks to my mother, father and the rest of my family for their encouragement and love. My mother deserves special credit as she gave me a strong work ethic and a drive to succeed. My father, who unfortunately passed away before I completed this dissertation, brought me up to respect math, science and engineering. I also want to recognize my boyfriend, Jason Lee, who has been a great sounding board for my thoughts and ideas regarding this topic. This achievement is because of him and my family.

TABLE OF CONTENTS

Page

ABSTRACT iii

ACKNOWLEDGEMENTS v

TABLE OF CONTENTS vii

LIST OF FIGURES xiii

LIST OF TABLES xxiv

1. INTRODUCTION 1

    1.1 Problem Statement 1
    1.2 Objectives 2
    1.3 Research Approach 3
    1.4 Procedure 4
    1.5 Significance of Research 10
    1.6 Organization of Dissertation 11

2. BACKGROUND 13

    2.1 Overview of North American Railways 13
        2.1.1 Track Structure 14
            2.1.1.1 Superstructure 14
            2.1.1.2 Substructure 16
        2.1.2 Freight Railroads 17
        2.1.3 Organizations 17
    2.2 Track Modulus 19
        2.2.1 Definition 19
        2.2.2 Estimating Track Modulus 19
            2.2.2.1 Beam on Elastic Foundation Method 19
            2.2.2.2 Deflection Basin Method 23
            2.2.2.3 Pyramid Load Distribution Method 24
            2.2.2.4 Limitations 25
        2.2.3 Measuring Track Modulus 27
            2.2.3.1 Deflection Basin Test 27
            2.2.3.2 Single Point Load Test 27
            2.2.3.3 Track Loading Vehicle (TLV) 28

Page

2.2.3.4 Real-Time Measurement System 32
2.2.4 Typical Track Modulus Values 33
2.2.5 Factors Influencing the Track Modulus 34
2.3 Wheel/Rail Forces 35
2.3.1 Wheel-Rail Contact Models 36
2.3.2 Loading Frequencies 36
2.3.3 Stress Distributions 38
2.3.4 Design Guidelines 41
2.4 Ballast Material 43
2.4.1 Ballast Specifications 44
2.4.2 Ballast Settlement 44
2.4.3 Ballast Problems 46
2.4.4 Ballast Maintenance 47
2.5 Track Settlement 49
2.6 Computer Models 50
2.6.1 Vehicle Dynamics Models 50
2.6.2 Track Substructure Models 52
2.6.3 LS-DYNA 53

3. LITERATURE REVIEW 54

3.1 General Findings 54
3.2 Causes 55
3.2.1 Differential Track Modulus 56
3.2.2 Quality of Approach Fill 57
3.2.3 Impact Loads 58
3.2.4 Ballast Material 59
3.2.5 Drainage 59
3.2.6 Damping 60
3.2.7 Abutment Type 61
3.2.8 Bridge Joint 63
3.2.9 Traffic Considerations 64
3.2.10 Quality of Construction 64
3.3 Previous Studies 65
3.3.1 Track Modulus Issues 65
3.3.1.1 Wheel/Rail Forces 66
3.3.1.2 Track Deflection 68
3.3.2 Bump Profile 70
3.3.3 Dip Profile 74
3.3.4 Track Response Criteria 76
3.3.4.1 Wheel/Rail Forces 76
3.3.4.2 Deflection 77

Page

3.3.4.3 Ballast and Subgrade Pressures 77
3.4 Mitigation Methods 78
3.4.1 Highways 79
3.4.2 Railway 81
3.4.2.1 Reduce Approach Settlement 81
3.4.2.2 Minimize Differential Track Modulus 83
3.4.2.2.1 Decrease Modulus on Bridge 84
3.4.2.2.2 Increase Modulus on Approach 85
3.4.2.3 Reduce Ballast Wear and Movement 86
3.4.2.4 Increase Damping 87

4. SURVEY OF CURRENT PRACTICE 88

4.1 Survey Description 88
4.2 Current State of Problem 88
4.3 Causes 90
4.4 Detection and Repair Methods 90
4.5 Design and Construction Procedures 93

5. 4-D FINITE ELEMENT MODEL 96

5.1 Description of Vehicle and Track Model 96
5.1.1 Vehicle 96
5.1.2 Track 100
5.1.3 Wheel/Rail Contact 102
5.2 Approach Embankment 105
5.2.1 Material Properties 106
5.2.2 Soil Damping 107
5.3 Bridge 107
5.4 Boundary Conditions 110
5.5 Model Validation 111

6. TRACK RESPONSE AT BRIDGE/APPROACH LOCATION 115

6.1 Track Modulus Transition 115
6.1.1 Static Response 115
6.1.2 Dynamic Response 117
6.1.3 Cyclic Response 124
6.2 Bump Profile 133
6.3 Dip Profile 138

7. PARAMETRIC STUDY 144

Page

7.1 Train Direction 147
7.1.1 Bump Results 148
7.1.2 Dip Results 152
7.1.3 Summary 156
7.2 Train Velocity 156
7.2.1 Bump Results 157
7.2.2 Dip Results 161
7.2.3 Summary 164
7.3 Bump/Dip Size 166
7.3.1 Bump Results 167
7.3.2 Dip Results 173
7.3.3 Bump/Dip Slope and Velocity Results 178
7.3.4 Summary 184
7.4 Subgrade/Fill Modulus 191
7.4.1 Bump Results 192
7.4.2 Dip Results 196
7.4.3 Summary 196
7.5 Approach Tie Material 200
7.5.1 Bump Results 201
7.5.2 Dip Results 201
7.5.3 Summary 202
7.6 Bridge Tie Material 205
7.6.1 Bump Results 206
7.6.2 Dip Results 206
7.6.3 Summary 207
7.7 Bridge Deck Type 210
7.7.1 Bump Results 210
7.7.2 Dip Results 211
7.7.3 Summary 212
7.8 Ballast Thickness 215
7.8.1 Bump Results 216
7.8.2 Dip Results 217
7.8.3 Summary 217
7.9 Approach Tie Length 220
7.9.1 Bump Results 221
7.9.2 Dip Results 222
7.9.3 Summary 222
7.10 Summary 225

8. FIELD TEST OF PROTOTYPE DESIGN SOLUTION 234

8.1 Proposed Solution 234

Page

8.1.1 Description 234
8.1.2 Design Concept 237
8.2 Base Case Field Test 238
8.2.1 Site Location 238
8.2.1.1 Description 239
8.2.1.2 Soil Conditions 240
8.2.1.3 Track Modulus 241
8.2.1.4 Previous Site Behavior 243
8.2.2 Instrumentation and Measurements 243
8.2.3 Base Case Test Results 246
8.2.3.1 Track Modulus 247
8.2.3.2 TOR Elevations 248
8.2.3.3 Wheel/Rail Forces 252
8.2.3.4 Cross Section Elevations 256
8.2.3.5 Subgrade Settlement 258
8.2.3.6 Subgrade Pressures 259
8.3 Solution Design 260
8.3.1 Numerical Simulations 261
8.3.1.1 Model Description 262
8.3.1.2 Base Case Results 263
8.3.1.3 Design Alternatives 269
8.3.1.4 Optimization Results 273
8.3.1.5 Summary 277
8.3.2 Recommended Solution 279
8.4 Design Solution Field Test 285
8.4.1 Installation 285
8.4.2 Cost 293

9. CONCLUSIONS 294

9.1 Survey 294
9.2 Parametric Study 296
9.3 Design Solution for Track Transitions 311
9.4 Future Related Research 313

REFERENCES 314

APPENDIX A 325

APPENDIX B 331

APPENDIX C 359

Page

APPENDIX D 360

APPENDIX E 377

APPENDIX F 476

VITA 575

LIST OF FIGURES

FIGURE Page

1.1 Schematic of (a) a bump (b) a dip at the bridge transition zone 1

2.1 Track layout side view (Selig and Waters 1994) 15

2.2 Track layout cross-section (Selig and Waters 1994)..... 15

2.3 Track deflection profile under a single point load 21

2.4 Track deflection profile under two point loads 22

2.5 Deflection basin method (Selig and Li 1994) 23

2.6 Pyramid load distribution 24

2.7 Moving mass on a simply supported beam 26

2.8 Track loading vehicle (Li et al. 2004a) 29

2.9 Independent reference frame for camera/laser system (Li et al. 2004a) 30

2.10 Offset based track deflection measurement (Li et al. 2004a)..... 31

2.11 Effects of track components on track modulus (Selig and Waters 1994) .. 35

2.12 Stress distribution in railway track structure (Selig and Waters 1994)..... 39

2.13 Impact percentage for concrete bridges 42

2.14 Ballast, subballast and subgrade contributions to total settlements (Selig and Waters 1994) 45

2.15 Tamping action (Selig and Waters 1994)..... 48

2.16 Effect of progressive fouling on length of tamping cycle (Selig and Waters 1994) 48

3.1 Contributing factors to bump/dip development (After Briaud et al. 1997) 56

FIGURE Page

3.2 Types of abutment foundations (Briaud et al. 1997)..... 61

3.3 Typical closed (high) abutment (Briaud et al. 1997) 62

3.4 Typical pedestal (spill-through) abutment (Briaud et al. 1997) 63

3.5 Typical perched abutment (Briaud et al. 1997)..... 63

3.6 Static beam deflection with variable track modulus (Hunt 1997)..... 69

3.7 Track settlement response to cyclic loading (Hunt 1997)..... 70

3.8 Simulated rail displacement in a stiffness transition under moving load (Banimahd and Woodward 2007) 71

3.9 Effect of transition length on wheel/rail forces (Banimahd and Woodward 2007) 72

3.10 Track transition with bump angle (Reprinted from Lei and Mao 2004 with permission from Elsevier)..... 73

3.11 Maximum vertical wheel/rail force for different bump angles (Reprinted from Lei and Mao 2004 with permission from Elsevier)..... 74

3.12 Effect of void height and speed on wheel/rail forces (Banimahd and Woodward 2007) 75

3.13 Approach slab schematic (Seo et al. 2002) 79

3.14 Configuration of pile-supported approach slab (Bakeer et al. 2005, With permission from ASCE)..... 80

3.15 BASP schematic (Reid and Buchanan 1984)..... 82

5.1 Model vehicle dimensions..... 97

5.2 Cross-section of wheel with elastic and rigid elements 98

5.3 Model truck suspension system..... 100

5.4 Rigid beams connecting side frame model to axle..... 101

FIGURE Page

5.5 Rail model 101

5.6 Wheel/Rail contact surfaces 102

5.7 Free body diagram of forces on truck model 104

5.8 Approach model cross-section 105

5.9 Open deck bridge model 108

5.10 Ballast deck bridge model 108

5.11 Bridge beam model 109

5.12 Soil springs for bridge model 109

5.13 Boundary constraints on model (cross-section) 110

5.14 Boundary constraints on model (side view) 111

5.15 Comparison of model and analytical solution for track deflection 112

5.16 LS-DYNA wheel/rail reaction forces for open track 113

5.17 FFT of unfiltered wheel/rail reaction force signal from simulation on open track 114

6.1 Track deflection profile under subsequent static point loads 116

6.2 Track modulus profile under subsequent static point loads 117

6.3 (a) Wheel/Rail forces (b) Axle accelerations and (c) Track deflection due to a stiffness change alone at a bridge/approach location (v = 22.2 m/s) 118

6.4 Ballast pressure for a track modulus change alone at a bridge/approach location (v = 22.2 m/s) 121

6.5 Subgrade pressure for a track modulus change alone at a bridge/approach location (v = 22.2 m/s) 123

FIGURE Page

6.6 Track deflection under cyclic load for a track modulus change alone at a bridge/approach location (v = 22.2 m/s)..... 125

6.7 DDF vs. N or MGT under cyclic load for a track modulus change alone at a bridge/approach location (v = 22.2 m/s)..... 126

6.8 Reaction force under cyclic load for a track modulus change alone at a bridge/approach location (v = 22.2 m/s)..... 127

6.9 DLF vs. N or MGT under cyclic load for a track modulus change alone at a bridge/approach location (v = 22.2 m/s)..... 127

6.10 Ballast pressure under cyclic load for a track modulus change alone at a bridge/approach location (v = 22.2 m/s)..... 128

6.11 Average ballast pressure vs. N or MGT under cyclic load for a track modulus change alone at a bridge/approach location (v = 22.2 m/s) 129

6.12 DBF vs. N or MGT under cyclic load for a track modulus change alone at a bridge/approach location (v = 22.2 m/s)..... 130

6.13 Subgrade pressure under cyclic load for a track modulus change alone at a bridge/approach location (v = 22.2 m/s)..... 131

6.14 Average subgrade pressure vs. N or MGT under cyclic load for a track modulus change alone at a bridge/approach location (v = 22.2 m/s) 132

6.15 DSF vs. N or MGT under cyclic load for a track modulus change alone at a bridge/approach location (v = 22.2 m/s)..... 132

6.16 (a) Wheel/Rail forces (b) Axle accelerations and (c) Track deflection due to a 1:150 bump at a bridge/approach location (v = 22.2 m/s) 134

6.17 Track deflection comparison: no slope vs. 1:150 bump (v = 22.2 m/s)..... 136

6.18 Ballast pressure resulting from a 1:150 bump (v = 22.2 m/s) 136

6.19 Subgrade pressure resulting from a 1:150 Bump (v = 22.2 m/s) 137

FIGURE Page

6.20 (a) Wheel/Rail forces (b) Axle accelerations and (c) Track deflection due to a 1:150 Dip at a bridge/approach location (v = 22.2 m/s) 139

6.21 Track deflection comparison: no Slope vs. 1:150 dip (v = 22.2 m/s) 140

6.22 Ballast pressure resulting from a 1:150 dip (v = 22.2 m/s) 142

6.23 Subgrade pressure resulting from a 1:150 dip (v = 22.2 m/s) 142

7.1 (a) Wheel/Rail forces (b) Axle accelerations and (c) Track deflection due to moving off of the bridge on to an approach embankment with a 1:150 bump (v = 22.2 m/s) 149

7.2 Ballast pressure due to moving off of the bridge on to an approach embankment with a 1:150 bump (v = 22.2 m/s) 150

7.3 Subgrade pressure due to moving off of the bridge on to an approach embankment with a 1:150 bump (v = 22.2 m/s) 151

7.4 Wheel/Rail forces (b) Axle accelerations and (c) Track deflection due to a truck moving off of the bridge on to an approach embankment with a 1:150 dip (v = 22.2 m)..... 153

7.5 Ballast pressure due to a truck moving off of the bridge on to an approach embankment with a 1:150 dip (v = 22.2 m/s) 155

7.6 Subgrade pressure due to a truck moving off of the bridge on to an approach embankment with a 1:150 dip (v = 22.2 m/s) 155

7.7 10 Hz filtered reaction force comparison for various velocities (Bump)... 158

7.8 Track displacement comparison for various velocities (Bump)..... 159

7.9 Ballast pressure comparison for various velocities (Bump)..... 160

7.10 Subgrade pressure comparison for various velocities (Bump)..... 160

7.11 10 Hz filtered reaction force comparison for various velocities (Dip) 162

7.12 Track displacement comparison for various velocities (Dip) 162

FIGURE Page

7.13 Ballast pressure comparison for various velocities (Dip) 163

7.14 Subgrade pressure comparison for various velocities (Dip) 163

7.15 (a) DLF, (b) DDF, (c) DBF and (d) DSF vs. velocity for the bump and the dip 165

7.16 (a) Bump (b) Dip dimensions for parametric study (equal lengths) 167

7.17 (a) Bump (b) Dip dimensions for parametric study (equal heights) 167

7.18 10 Hz filtered reaction force comparison for various bump slopes of equal length (Bump) 168

7.19 Track deflection comparison for various bump slopes of equal length (Bump) 169

7.20 Ballast pressure comparison for various bump slopes of equal length (Bump) 169

7.21 Subgrade pressure comparison for various bump slopes of equal length (Bump) 170

7.22 (a) DLF, (b) DDF, (c) DBF and (d) DSF vs. bump slope 172

7.23 10 Hz filtered reaction force comparison for 1:50 bump slopes (Bump)... 173

7.24 10 Hz filtered reaction force comparison for various dip slopes of equal length (Dip) 174

7.25 Track deflection comparison for various dip slopes of equal length (Dip) 174

7.26 Ballast pressure comparison for various dip slopes of equal length (Dip) 175

7.27 Subgrade pressure comparison for various dip slopes of equal length (Dip) 175

7.28 (a) DLF, (b) DDF, (c) DBF and (d) DSF vs. dip slope 177

FIGURE Page

7.29 DLF vs. (a) Bump slope and (b) dip slope for different velocities 179

7.30 DDF vs. (a) Bump slope and (b) dip slope for different velocities 181

7.31 DBF vs. (a) Bump slope and (b) dip slope for different velocities 182

7.32 DSF vs. (a) Bump slope and (b) dip slope for different velocities..... 183

7.33 DLF vs. Bump angle 185

7.34 DDF vs. Bump angle 185

7.35 DBF vs. Bump angle 186

7.36 DSF vs. Bump angle..... 186

7.37 DLF vs. Dip angle 187

7.38 DDF vs. Dip angle..... 187

7.39 DBF vs. Dip angle 188

7.40 DSF vs. Dip angle 188

7.41 Tolerable bump/dip slope vs. velocity based on DLF results 189

7.42 Tolerable bump slope vs. velocity based on DSF results..... 190

7.43 Effect of soil modulus on track modulus 192

7.44 10 Hz filtered reaction force comparison for various fill/subgrade moduli (Bump) 193

7.45 Track deflection comparison for various fill/subgrade moduli (Bump) 194

7.46 Ballast pressure comparison for various fill/subgrade moduli (Bump) 195

7.47 Subgrade pressure comparison for various fill/subgrade moduli (Bump) . 195

7.48 (a) DLF, (b) DDF, (c) DBF and (d) DSF vs. soil modulus 198

7.49 Track deflection comparison for various fill/subgrade moduli (Dip) 199

FIGURE Page

7.50 DLF vs. approach tie material 202
7.51 DDF vs. approach tie material 203
7.52 DBF vs. approach tie material 203
7.53 DSF vs. approach tie material 204
7.54 DLF vs. bridge tie material 208
7.55 DDF vs. bridge tie material 208
7.56 DBF vs. bridge tie material 209
7.57 DSF vs. bridge tie material 209
7.58 Ballast pressure comparison for bridge deck type (Bump) 211
7.59 DLF vs. bridge deck type 213
7.60 DDF vs. bridge deck type 213
7.61 DBF vs. bridge deck type 214
7.62 DSF vs. bridge deck type 214
7.63 Ballast thicknesses considered 216
7.64 DLF vs. ballast thickness 218
7.65 DDF vs. ballast thickness 219
7.66 DBF vs. ballast thickness 219
7.67 DSF vs. ballast thickness 220
7.68 Tie lengths considered 221
7.69 DLF vs. tie length 223
7.70 DDF vs. tie length 224

FIGURE Page

7.71 DBF vs. tie length 224

7.72 DSF vs. tie length 225

8.1 Proposed solution sketch 235

8.2 FAST HTL test sections 238

8.3 LTM cross-section 239

8.4 LTM longitudinal cross-section 240

8.5 Measured track modulus at LTM section 242

8.6 Subgrade measurements for proposed test case 246

8.7 Vertical track modulus of LTM section (base case) 248

8.8 TOR Elevations for LTM section (base case) 249

8.9 Change in TOR elevation vs. MGT for LTM dip (log-log scale) 251

8.10 Change in TOR elevation vs. MGT for LTM dip (arithmetic scale) 251

8.11 Vertical wheel load measurements (a) front wheels (b) back wheels at a velocity of 8.9 m/s (base case) 253

8.12 Vertical wheel load measurements (a) front wheels (b) back wheels at a velocity of 13.4 m/s (base case) 254

8.13 Vertical wheel load measurements (a) front wheels (b) back wheels at a velocity of 17.9 m/s (base case) 254

8.14 DLF vs. velocity for field test (base case) 255

8.15 Cross-section elevations for LTM at Tie 130 256

8.16 Difference in cross-section elevations for 0 MGT and 50 MGT at Tie 130 257

8.17 Subgrade settlement for LTM taken between Ties 126 and 127 259

FIGURE Page

8.18 Subgrade pressure in LTM under Tie 125 260

8.19 Finite element model of the LTM section 262

8.20 Simulation track modulus compared to measured track modulus..... 264

8.21 Wheel/Rail forces at LTM section from numerical model (base case)..... 265

8.22 Track deflection at LTM section from numerical model (base case 266

8.23 Ballast pressure at LTM section from numerical model (base case) 267

8.24 Subgrade pressure at LTM section from numerical model (base case) 268

8.25 Design Alternative 1: Uniform bar lengths with 1.83 m longest bar and 44 total bars..... 270

8.26 Design Alternative 2: Equal bar length decrease with 1.83 m longest bar and 44 bars total..... 270

8.27 Design Alternative 3: Unequal bar length decrease with 1.83 m longest bar and 44 total bars..... 271

8.28 Design Alternative 4: Unequal bar length decrease with 2.13 m longest bar and 44 total bars..... 271

8.29 Design Alternative 5: Equal bar length decrease with 1.83 m longest bar and 88 total bars..... 272

8.30 Design Alternative 6: Unequal bar length decrease with 1.83 m longest bar and 88 total bars..... 272

8.31 10 Hz wheel/rail force comparison for solution design alternatives at LTM section 273

8.32 Track deflection under the back axle comparison for solution design alternatives at LTM section..... 274

8.33 Ballast pressure comparison for solution design alternatives at LTM section..... 275

FIGURE Page

8.34 Subgrade pressure comparison for solution design alternatives at LTM section 276

8.35 DLF for track transition design alternatives 278

8.36 DBF for track transition design alternatives 278

8.37 DSF for track transition design alternatives 279

8.38 Track deflection comparison for recommended solution design and base case simulation 281

8.39 Ballast pressure comparison for recommended solution design and base case simulation 281

8.40 Subgrade pressure comparison for recommended solution design and base case simulation 282

8.41 Track modulus comparison for recommended solution design and base case simulation 282

8.42 Pile skin friction and end bearing 283

8.43 Interface between control and LTM section at FAST 285

8.44 Dywidag bars 287

8.45 Ballast removal between Ties 127 and 128 at location of settlement rod 288

8.46 Schematic of actual installation (settlement rods are in red) 288

8.47 Initial driving of the rods using an impact hammer 289

8.48 Forklift used as impact hammer 290

8.49 Drive rod to install the steel bars 291

8.50 Vibratory driver 291

8.51 Vibratory driver used to install steel bars 292

LIST OF TABLES

TABLE		Page
3.1	Allowable subgrade bearing pressures (Selig and Waters 1994)	78
4.1	Companies responding to the survey	88
4.2	Factors contributing to the formation of the bump	91
4.3	Current bump detection methods	92
4.4	Current bump repair methods	93
4.5	Current bump design procedures	94
4.6	Current bridge/approach construction procedures	95
5.1	Model vehicle properties	96
5.2	Model component weights	98
5.3	Approach model material properties	106
6.1	Cyclic response summary	133
6.2	Track response summary for reference cases	143
7.1	Bump parametric study cases	145
7.2	Dip parametric study cases	146
7.3	Train direction results summary	156
7.4	Velocity results summary (Bump)	161
7.5	Velocity results summary (Dip)	164
7.6	Bump slope (equal lengths) results summary (Bump)	170
7.7	Bump slope (equal heights) results summary (Bump)	171

TABLE Page

7.8 Dip slope (equal lengths) results summary (Dip) 176

7.9 Dip slope (equal heights) results summary (Dip) 178

7.10 Bump/Dip slope (equal heights) and velocity results summary 184

7.11 Soil modulus results summary (Bump) 196

7.12 Soil modulus results summary (Dip) 196

7.13 Material properties of model ties 200

7.14 Approach tie material summary (Bump) 201

7.15 Approach tie material summary (Dip) 202

7.16 Bridge tie material summary (Bump) 206

7.17 Bridge tie material summary (Dip) 207

7.18 Bridge deck type summary (Bump) 211

7.19 Bridge deck summary (Dip) 212

7.20 Ballast thickness summary (Bump) 217

7.21 Ballast thickness summary (Dip) 217

7.22 Tie length summary (Bump) 222

7.23 Tie length summary (Dip) 222

7.24 Parametric study summary 226

7.25 Evaluation of tolerable limits for parametric study 228

7.26 Overall ranking for parametric study (Bump) 229

7.27 Overall ranking for parametric study (Dip) 231

8.1 Base case measurement schedule 244

TABLE Page

8.2 Solution field test measurement schedule 244

8.3 Change in TOR elevation for LTM dip (base case) 250

8.4 Material properties for LTM numerical model 263

8.5 Design alternative summary 277

9.1 Parametric study conclusion: reference cases 297

9.2 Parametric study conclusion: train direction (Bump) 298

9.3 Parametric study conclusion: train direction (Dip) 298

9.4 Parametric study conclusions: train velocity (Bump) 299

9.5 Parametric study conclusions: train velocity (Dip) 299

9.6 Parametric study conclusions: bump slope 300

9.7 Parametric study conclusions: dip slop 301

9.8 Parametric study conclusions: soil modulus (Bump) 303

9.9 Parametric study conclusions: soil modulus (Dip) 304

9.10 Parametric study conclusion: approach tie material (Bump) 304

9.11 Parametric study conclusion: approach tie material (Dip) 305

9.12 Parametric study conclusion: bridge tie material (Bump) 306

9.13 Parametric study conclusion: bridge tie material (Dip) 306

9.14 Parametric study conclusion: bridge deck type (Bump) 307

9.15 Parametric study conclusion: bridge deck type (Dip) 307

9.16 Parametric study conclusion: ballast thickness (Bump) 308

9.17 Parametric study conclusion: ballast thickness (Dip) 309

TABLE Page

9.18 Parametric study conclusion: approach tie length (Bump) 309

9.19 Parametric study conclusion: approach tie length (Dip) 310

1. INTRODUCTION

1.1 PROBLEM STATEMENT

The bump at the end of the bridge is classified as a track geometry degradation problem. It occurs in the track transition zone located at the interface between the approach embankment and the bridge structure (Fig. 1.1). It can take two forms: a bump (Fig. 1.1a) or a dip (Fig. 1.1b). For brevity, the phrase "the bump at the end of the bridge" will be used to refer to either condition of the bump or the dip throughout this dissertation.

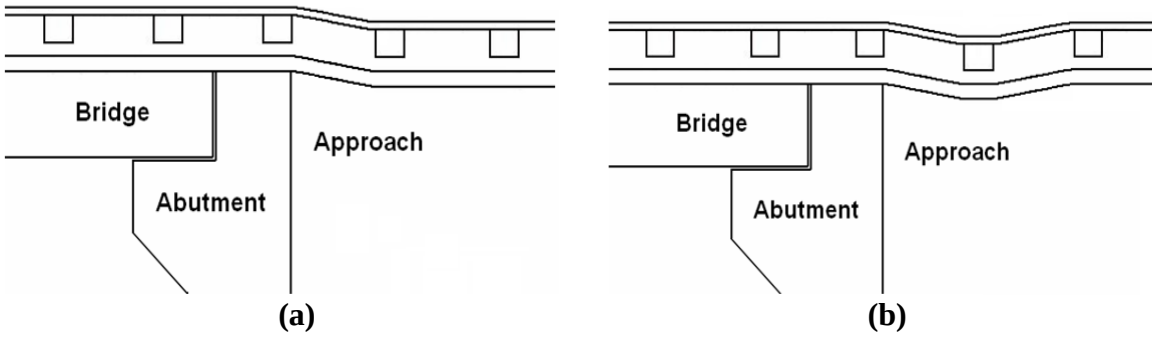

Figure 1.1 - Schematic of (a) a bump (b) a dip at the bridge transition zone

The bump develops as a result of an overall differential settlement between the two structures. The approach embankment is typically made of compressible fill material whereas the bridge deck is founded on deep piles. Under the same loading, the approach

---

This dissertation follows the style of the *Journal of Geotechnical and Geoenvironmental Engineering*.

structure will settle more than the bridge structure. This causes a bump to form in the track. The dip, however, develops as a result of localized settlement on the approach whereas the bridge deck is founded on deep piles. Under the same loading, the approach structure will settle more than the bridge structure. This causes a bump to form in the track. The dip, however, develops as a result of localized settlement on the approach embankment. As the bump/dip forms, greater impact forces will occur as the train passes over the defect in the track. This will lead to further degradation, thus a bigger bump/dip. The bump at the end of the railway bridge is a result of this repeated process.

The bump/dip can cause significant problems in track performance. According to an industry survey conducted during the course of this research (Section 4), approximately half of all railway bridges are affected by the bump/dip. The total annual cost for repairing these bridge transition problems is estimated at $26 million, which does not take into account the considerable cost resulting from speed reductions that railroads must place on trains at these problem locations. In addition to the increased maintenance costs, the bump/dip leads to higher impact loads, increased ballast and subgrade pressures, uncomfortable rides and possible safety hazards.

1.2 OBJECTIVES

The proposed plan of research is organized around the following research objectives:

1) Evaluate the current state of the bump problem in the railroad industry.
2) Investigate the complete track response resulting from a bump/dip.
3) Quantify an acceptable slope for track geometry under freight traffic.

4) Examine the influence of various design components on track response for the bump/dip.
5) Develop a prototype track transition solution and assist in analyzing the performance of a full-scale field test.

1.3 RESEARCH APPROACH

The bump at the end of the railway bridge may never be completely eliminated. There are too many factors involved in its formation, and oftentimes, these factors are site-dependent. This makes a global solution to the problem difficult to identify. What can be done about the problem is to find ways to minimize the bump/dip to a tolerable slope. This will reduce impact loading and track degradation.

An acceptable slope has yet to be adequately defined for the bump/dip. To do this, an industry survey was conducted to determine the opinions on what is acceptable (Section 4), and a 4-D dynamic numerical model was developed to simulate a train passing over a bridge approach system using the program LS-DYNA (Section 5). Using this model, different size bumps and dips were imposed into the track structure (Section 7). The resulting impact forces, track deflection, ballast and subgrade pressures that were generated by the bump/dip were then evaluated. Based on the survey and simulation results, an acceptable slope can be defined.

In addition to the size of the bump/dip, there are several track design components that may influence the severity of a bump/dip. These can include ballast thickness, tie length and tie material to name a few. The relationship between these components and

the bump/dip problem had not been fully investigated. With the same 4-D model developed during this research, however, a parametric study was conducted to evaluate the influence of these various components on the bump/dip problem (Section 7).

Finally, to complement the numerical simulations, a design has been proposed to minimize the bump/dip in revenue service to an acceptable ramp rather than a steep step (Section 8). A full scale field test of this solution, built with the help of the Association of American Railroads (AAR) and the Technology Transportation Center, Inc. (TTCI), is currently being tested.

1.4 PROCEDURE

A thoughtful procedure is planned in order to achieve the stated research objectives. The steps for each objective are outlined below:

A) Evaluate the current state of the bump problem in the railroad industry:

1) Prepare and send out a questionnaire addressing the following:
    a. Current state of the problem (number of affected bridges, maintenance cost, track structure characteristics, typical bump/dip sizes, loading)
    b. Current detection methods for the bump/dip
    c. Causes for the bump problem
    d. Current maintenance/repair methods
    e. Design solutions to prevent the bump/dip
    f. Research areas

2) Review the responses from the survey and summarize

Since it is unclear how many railway bridges are affected by the bump problem, a survey of railroad professionals is necessary to determine the extent of the problem. The questionnaire consists of 26 questions. It was sent out to railway bridge engineers, maintenance-of-way workers, researchers, managers and government regulators. This broad spectrum of opinions will give insight into the nature and extent of the problem. A survey of this kind, focusing on the bump/dip problem, had not previously been performed in the railroad industry.

B) Investigate the complete track response resulting from a bump/dip

1) Prepare the mesh for a track model, an embankment model, a bridge model and a truck model (two axles, half the weight of a standard freight railcar). Impose a bump/dip in the embankment model leading up to the bridge model. Modeling will be accomplished using a finite element pre-processor program: HyperMesh.
2) Use the powerful finite element program LS-DYNA to simulate the motion of a truck across the bridge/approach transition.
3) Evaluate the complete response:
    a. Track deflection
    b. Wheel/rail forces
    c. Axle accelerations
    d. Ballast pressures

e. Subgrade pressures

4) Verify the finite element model by running simulations with no slope in track and comparing the general trends of the results with those found in the literature. This includes track deflection, axle acceleration and wheel/rail forces.

The effects of track geometry defects such as bumps/dips at the bridge/approach location have not yet been fully investigated. More research is available on the bump than the dip, yet the findings from the bump research are limited mainly to wheel/rail forces. It is important to evaluate the complete response because focusing on one type of result can be misleading. LS-DYNA allows for the response under a moving load (with realistic suspension characteristics) to be evaluated. Validating the model by comparing the general trends from the LS-DYNA output to results found in the literature will lend credibility the simulations.

C) Quantify an acceptable slope for track geometry under freight traffic

1) Prepare several bridge/approach models with different bump slopes and dip slopes imposed in the embankment. Bump/dip slopes will range from 1:50 to 1:250. This is included in a large parametric study.
2) Use LS-DYNA to simulate the truck motion across various bump/dip sizes.
5) Evaluate the complete response:
    a. Track deflection
    b. Wheel/rail forces

c. Axle accelerations

d. Ballast pressures

e. Subgrade pressure

3) Quantify an acceptable slope based on survey results and established criteria:

a. Track deflection should be less than 6.4 mm for durability (Talbot 1918, Lundgren & Martin 1970)

b. Wheel/rail forces should be less than 1.5 times the static load to avoid increased track settlement rate (Plotkin and Davis 2008)

c. Ballast pressures should be less than or equal to 450 kPa for wood ties and 590 kPa for concrete ties (AREMA 2008)

d. Subgrade pressures are limited to 140 kPa for all soil conditions (AREMA 2008)

There is no standard or criteria for track slopes due to running surface defects. Criteria are available for runoff slopes (FRA 2002), but that is for drainage concerns and has nothing to do with wheel/rail forces and increased track deflection. According to Zhai et al. (2001) and Lei and Mao (2004), the bump slope should not be steeper than 1:150. This is based on dynamic load alone and does not consider the complete response. No investigations into the dip geometry have been found.

D) Examine the influence of various design components on track response for the bump/dip

1) Conduct a parametric study using LS-DYNA:
    a. Train Direction (on to bridge, off of bridge)
    b. Train Velocity (ranging from 8.9 m/s to 44.7 m/s)
    c. Bump/Dip Slope (ranging from 1:50 to 1:250)
    d. Subgrade/Fill modulus (ranging from 20 MPa to 100 MPa)
    e. Approach tie material (concrete, wood, plastic) including additional materials (rubber tie pads, rubber rail seat pads, ballast mats)
    f. Bridge tie material (concrete, wood, plastic) including additional materials (rubber tie pads, rubber rail seat pads)
    g. Bridge deck type (open or ballasted) including additional materials (ballast mats)
    h. Ballast thickness (ranging from 152.4 mm to 304.8 mm)
    i. Tie length (ranging from 2.1 m to 3.6 m)
2) Evaluate the complete response:
    a. Track deflection
    b. Wheel/rail forces
    c. Axle accelerations
    d. Ballast pressures
    e. Subgrade pressures
3) Provide conclusions based on the parametric study

The reference case for the parametric study is based on the results from the industry survey conducted at the beginning of this research. After analyzing this case, a single design component was changed for each simulation and run through LS-DYNA until every case had been examined. The impact of many of these components has been theorized and measured as it relates to track stiffness, but their effect due to a bump/dip has not yet been investigated.

E) Develop a prototype track transition solution and assist in analyzing the performance of a full-scale field test

1) Propose a solution for existing bridges that will address both stiffness and settlement issues at the bridge/approach location.
2) Prepare a model of the solution using HyperMesh.
3) Optimize the design of the solution using LS-DYNA based on the track response:
    a. Track deflection
    b. Wheel/rail forces
    c. Ballast pressures
    d. Subgrade pressures
4) Prepare an instrumentation and monitoring plan for the full-scale field test
5) Assist in analyzing the performance of a full-scale field test of this solution:
    a. Track stiffness
    b. Subgrade pressures
    c. Track settlement

d. Subgrade settlement

e. Wheel loads

6) Verify the model using results from the field test:

a. Wheel/rail forces across the transition

b. Subgrade pressures

The proposed solution was designed to strengthen the subgrade while limiting cost and track downtime. Similar soil inclusion solutions, such as stone columns and pile-supported embankments, have performed well in the past but require the track structure to be completely removed in order to install. This is often avoided unless it is new construction or track maintenance costs become too frequent and expensive.

1.5 SIGNIFICANCE OF RESEARCH

The bump at the end of the bridge is not a new problem. In fact, the bump/dip problem has already been thoroughly investigated for highway bridges. There are several major differences, however, between highways and railways. For example, the loading environment between highways and railways is very different. The maximum weight of an 18-wheeler, the largest vehicle on highways, is 356 kN (80 kips). By comparison, freight cars for heavy axle load trains can weigh as much as 1400 kN (315 kips). This equates to approximately 4 times more load on railways than on highways. The impact of the bump/dip is therefore different and must be investigated to the same degree as for highway bridges.

While it has long been a concern for railroads, studies on the bridge approach location have thus far focused more on vehicle dynamics rather than on track substructure issues. With the use of the 4-D finite element model, more insight can be gained into track deflections, ballast and subgrade pressures that have not been examined until now. Combining this new knowledge with the existing knowledge will provide a well rounded look into this complex issue for railway bridges.

Another major difference between highways and railways is the maintenance and construction considerations. A common solution to prevent bump/dip problems on highway bridges is to install an approach slab. This is not a feasible solution for existing railway bridges, however, as railways are under strict time constraints for track work.

Currently, for existing railway bridges, railroads do not have a solution; they continually maintain the problem by ballast tamping. For new bridges, several possible solutions have been tried with varying success. Railroads want a solution for existing bridges, however, that will avoid significant track down-time. The solution proposed in this research takes this into account. It can be installed relatively rapidly without removing any of the track structure. This research will have practical applications for the railroad industry.

1.6 ORGANIZATION OF DISSERTATION

The previous work on this topic is presented in Section 2 while important background information is given in Section 3. The current state of practice in the railroad industry is then investigated in Section 4. Section 5 discusses the development of the 4-D model

used to simulate the bridge approach transition. The track response at a bridge/approach location is then discussed in Section 6. The results of a large parametric study are then presented in Section 7. Section 8 discusses a proposed solution to remedy the bump problem for existing bridges. A full-scale field using this solution is also described in Section 8. Finally, recommendations and conclusions from the research are given in Section 9.

2. BACKGROUND

2.1 OVERVIEW OF AMERICAN RAILWAYS

The railway system is a vital component of the transportation infrastructure in America. Without contributions from the railroad industry, countries would not have been able to progress and prosper as quickly as they did. The railway system consists of freight traffic and public transit.

Freight traffic involves the movement of goods from one area to another. It comprises the bulk of the railroad business (Hay 1982). Over 40% of America's freight is moved by the freight railroad system (AAR 2008). This is more than any other form of transportation. The fuel efficiency of railroads is also better than other forms of transportation. For a ton of freight, railroads can move 436 miles per gallon of fuel (AAR 2008). For these reasons, the U.S. Department of Transportation (DOT) predicted that freight railroad demand would increase 88% by 2035. This increased strain on the track system, which already experiences very high loading, will require advanced technology and methods to reduce maintenance and operating costs.

Public transit involves the movement of people from one area to another. Track loading may not be as high, but riding quality is very important. The railway lines used by freight traffic are also largely used by passenger traffic (AAR 2008). The problems associated with freight tracks can have an impact on passenger rail services. The bump at the end of the railway bridge is therefore a concern for both freight and public transportation. For freight trains, the main issue is the maintenance cost associated with

repairing bump/dip problems due to impact loads at the bridge/approach location. For public transit, the main issue is reducing car body accelerations that can affect the people inside.

This dissertation is mainly focused on the issue as it pertains to freight traffic. Although the problem is universal, the loading environment and primary interests are different. Improvements made for freight traffic, however, will also benefit passenger rail.

2.1.1 Track Structure

The track structure consists of elements comprising the superstructure and substructure (Figs. 2.1 – 2.2). The superstructure consists of the rails, ties, and fastening system while the substructure consists of the ballast, subballast, and subgrade. The response of the superstructure has been thoroughly investigated. The substructure response, is more unknown, however. This is because the substructure is made of natural materials whose behavior is not easy to predict.

2.1.1.1 Superstructure

The rails serve to guide the train while transferring the load to the ties. The main problems occurring with the rails are defects and discontinuities that can cause high impact loads affecting the entire track structure (Lim 2004). Rail is made of steel and typically comes in lengths of 12 m or shorter. The standard gage between two rails, which is the inside spacing between the rail head faces, is 1435 mm in North America

(Selig and Waters 1994). Rail sections are often given in terms of sizes, based on weight per length of rail. A common rail section in North America is the 662 N/m (136 lb/yd) rail.

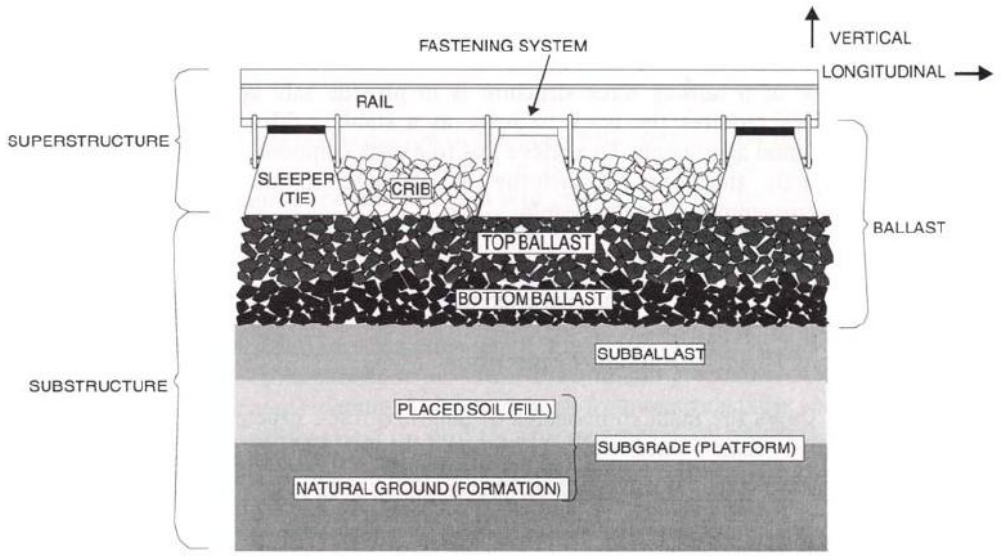

Figure 2.1 - Track layout side view (Selig and Waters 1994)

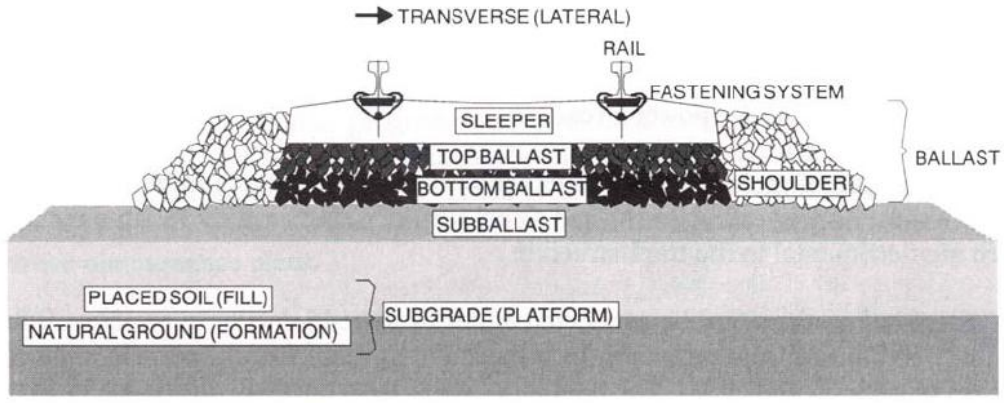

Figure 2.2 – Track layout cross-section (Selig and Waters 1994)

The ties, or sleepers, play an important role the track structure. They serve as a platform to anchor the rails, restraining any lateral, longitudinal or vertical movement. They also help distribute loading to the track substructure. The majority of sleepers in America are made of wood, although concrete ties are gaining favor due to longevity (Schneider 2006). Ties have also been made out of a composite plastic material and steel. Typical sleeper dimensions in America are 229 mm (9 in) width by 2.59 m (8.5 ft) length. They are commonly spaced at 495 mm (19.5 in) centers, although in practice, this can vary along the track structure.

The fastening system acts to bind the rails to the sleepers. These can be in the form of driven cut spikes (most common), screw spikes, anchor spikes and elastic clips. The type of fastening system can have a big impact on the track response under load and should be considered.

2.1.1.2 Substructure

The ballast is made of a granular material. It acts as a shock absorber for the loads on the track superstructure. It also helps to restrain the ties from movement. The subballast is the layer of granular material separating the ballast and subgrade. The granular particles are smaller in size than the ballast, however. The main function of the subballast is to prevent penetration between the ballast and subgrade.

The subgrade is the ultimate foundation for the track structure. It can be homogenous or layered. It is often advantageous to remove a portion of the subgrade and

backfill with a quality material. This is sometimes not economical or necessary to do, however.

2.1.2 Freight Railroads

Freight railroads are broken down into categories based on revenue: Class I, regional and local linehaul. Class I railroads are those with revenue of at $346.8 million; regional railroads are those with revenue between $40 and $346.8 million and/or operate at least 350 miles of track; local linehaul railroads are those with revenue less than $40 million and/or operate less than 350 miles of track (AAR 2008). As of 2006, there are 7 Class I railroads, 33 regional railroads and 323 local linehaul railroads in America.

Although Class I railroads comprise only 1% of freight railroads, they account for 67% of the mileage and 93% of the revenue. The American Class I railroads are comprised of 7 companies: Burlington Northern Santa Fe Railway (BNSF), CSX Transportation (CSX), Grand Trunk Corporation, Kansas City Southern Railway (KCS), Norfolk Southern (NS) Combined Railroad Subsidiaries, Soo Line Railroad and Union Pacific Railroad (UP). Other major North American railroads are: Canadian National Railway (CN), Canadian Pacific Railway (CP), Ferrocarril Mexicano (FXE) and Kansas City Southern de Mexico (KCSM).

2.1.3 Organizations

The top government agency responsible for enforcing safety regulations, promoting rail research, and recommending policy is the Federal Railroad Administration (FRA) within

the U.S. Department of Transportation (DOT). The FRA sponsors and conducts research, both applied and theoretical. One organization that receives funding from the FRA is the Association of American Railways (AAR).

The AAR is a professional organization comprised of members that include the major freight railroads in North America along with Amtrak. AAR advocates for rail issues with elected officials and leaders. A subsidiary of AAR is the Transportation Technology Center, Inc. (TTCI). TTCI is a research and development facility. They test a number of issues related to rail research that enhances safety, reliability and productivity. TTCI is located in Pueblo, CO in a facility owned by the FRA. AAR also sponsors research at the University level through the Affiliated Laboratory program. Currently, only 4 universities participate in this program: Texas A&M University, the University of Illinois at Urbana-Champaign and Virginia Tech.

The American Railway Engineering and Maintenance-of-Way Association (AREMA) is a professional organization comprised of members that include railroad employees and researchers. AREMA produces the "Manual for Railway Engineering" each year that provides guidelines on the design, construction and maintenance of railway infrastructure. The technical committees within AREMA are responsible for the development of these guidelines.

2.2 TRACK MODULUS

An important parameter used to characterize track quality is the vertical track modulus. Every component of the track structure, including the rails, ties, fasteners, ballast, subballast and subgrade, has an impact on the modulus (Farritor 2006).

2.2.1 Definition

The track modulus is defined as the supporting force per unit length of track per unit track deflection (Selig and Li 1994). It has been referred to as the "modulus of elasticity of rail support" (Zarembski 1989c). The track modulus is considered an indicator of track quality and performance (Arnold et al. 2006). It is directly related to the track deflection under the moving load of a railcar (Hay 1982).

2.2.2 Estimating Track Modulus

There are a variety of theoretical methods available to estimate the track modulus. The most common are the beam on elastic foundation, deflection basin, and pyramid load distribution methods.

2.2.2.1 Beam on Elastic Foundation Method

The method traditionally used by railway engineers is the beam on elastic foundation model (BOEF). A common elastic foundation model was introduced by Winkler (1867). The application of this model to railway tracks has been investigated (Zarembski and Choros 1980, Hay 1982, Cai et al. 1994, Kerr 2002, Norman et al. 2004). The model

simplifies the track structure into an infinitely long beam (the rail) supported by evenly distributed linear springs representing a continuous elastic foundation (Iwnicki 2006). The stiffness of the springs used in the model (u) is the track modulus. It represents a combination of the tie, ballast and subgrade stiffnesses (Hay 1982).

Note that other elastic foundation models are available, including the Pasternak (1954) foundation model, the Filonenko-Borodich (1940) model and the Vlasov and Leont'ev (1960) model. These models are extensions of the Winkler (1987) model and help overcome some of the shortcomings associated with the simple Winkler model (Tanahashi 2007). These improved models are more complex and require more computational effort; therefore, the Winkler model is recommended for practical design (Hay 1982).

The BOEF method is based on the differential equation shown in Eq. 2.1.

$$EI\frac{d^4y(x)}{dx^4}+uy(x)=q(x) \tag{2.1}$$

where EI is the flexural rigidity of the beam, y(x) is the vertical deflection of the beam at a location x away from the load, u is the track modulus, and q(x) is the distributed load equivalent to the wheel loads (Cai et al. 1994). The equation is based on vertical equilibrium for an element of the beam under consideration. It is solved by finding the solution for the general equation where q(x) equals zero (Hetényi 1946). Loading on the beam is accounted for when solving for the constants of integration. For a single point load (or wheel load), P, the solution to the differential equation (Eq. 2.1) is given by Eq. 2.2 (Hetényi 1946).

$$y(x) = \frac{P\beta}{2u} e^{-\beta x} (\cos \beta x + \sin \beta x) \tag{2.2}$$

where β is the damping factor (Eq. 2.3).

$$\beta = \left(\frac{u}{4EI} \right)^{\frac{1}{4}} \tag{2.3}$$

A representative deflection profile of the track, based on the BOEF method, is shown in Fig. 2.3. Since the foundation is considered elastic, the law of superposition can be used if more than one wheel, or point load, is present to estimate the track deflection under multiple loads (Hetényi 1946). Hetényi (1946) also presents solutions for various loading and boundary conditions.

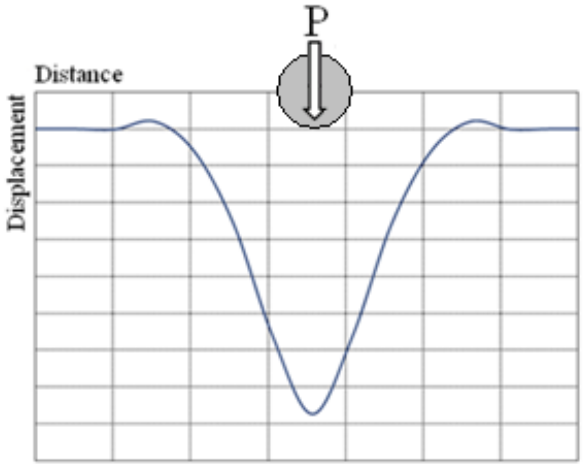

Figure 2.3 – Track deflection profile under a single point load

For two wheels (one axle), a representative deflection profile of the track is shown in Fig. 2.4. The dotted lines represent the track deflection if only the single load

was present. Note that the deflection under two wheels is larger than under a single wheel.

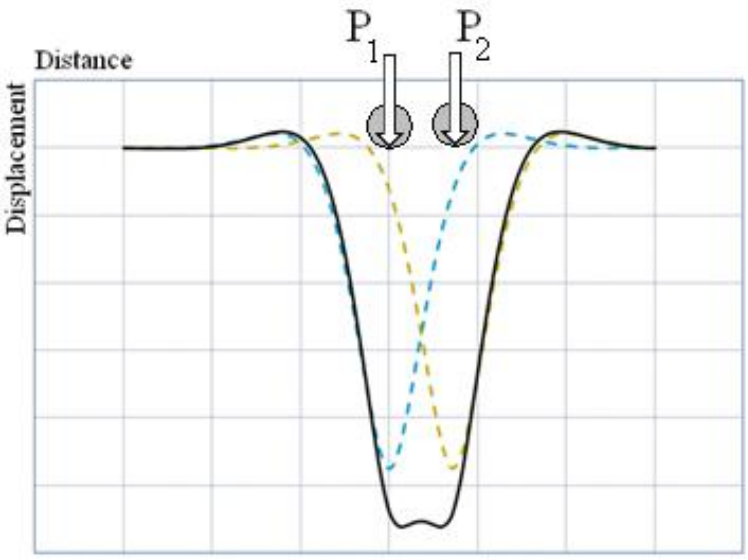

Figure 2.4 –Track deflection profile under two point loads

Knowing the measured track deflection, Eq. 2.2 can be rearranged to calculate the track modulus, u (Eq. 2.4) where y_0 is the maximum deflection at the point load location (x=0). Note that the ratio of load to maximum deflection (P/y_0) is referred to as the track stiffness.

$$u = \frac{1}{4}\left(\frac{1}{EI}\right)^{\frac{1}{3}}\left(\frac{P}{y_0}\right)^{\frac{4}{3}} \tag{2.4}$$

2.2.2.2 Deflection Basin Method

Another method to estimate the track modulus is the deflection basin method (Talbot 1918, Selig and Li 1994, Cai et al. 1984, Norman et al. 2004). This method is based on vertical equilibrium of an infinitely long beam, including the applied rail forces and the supporting rail forces (Fig. 2.5). The track modulus is the ratio of these applied forces to the total area of track deflection, which is measured as the area between the original rail position and the deflected rail position (Selig and Li 1994). The track modulus is then calculated according to Eq. 2.5.

$$u = \frac{\sum_{j=1}^{n} P_j}{A_\delta} = \frac{\sum_{j=1}^{n} P_j}{S\sum_{i=1}^{m} \delta_i} \tag{2.5}$$

where P is the load, n is the number of point loads, u is the track modulus, A_δ is the deflection basin area, S is the center-to-center tie spacing, m is the number of ties which deflect under the vertical loads, and δ_i is the track deflection at a particular location (Selig and Li 1994).

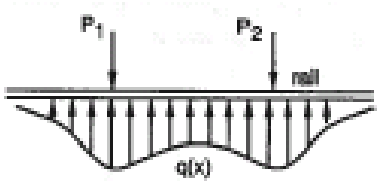

Figure 2.5 – Deflection basin method (Selig and Li 1994)

To measure the track modulus in the field, several deflections are required with this method whereas with the BOEF method, only one deflection measurement is needed. It also does not explicitly account for the rail-bending rigidity whereas the BOEF method does take this into account. It is therefore not a recommended method to measure track modulus (Kerr and Shenton 1985).

2.2.2.3 Pyramid Load Distribution Method

The pyramid load distribution method (PLD) is another method to calculate the vertical track modulus (Cai et al. 1994, Norman et al. 2004). This method assumes a pyramidal stress distribution with uniform stresses at a given depth (Fig. 2.6). An equivalent spring stiffness (K_e) for the entire rail support system is used which accounts for the stiffness of the rail pad, tie, ballast and subgrade separately, much like springs in series. The ballast stiffness is based on the elastic modulus of the ballast along with its internal friction angle (Cai et al. 1994). The subgrade stiffness is based on the internal friction angle of the soil along with the subgrade modulus (k_s). Typical values for k_s are given by Das (1998).

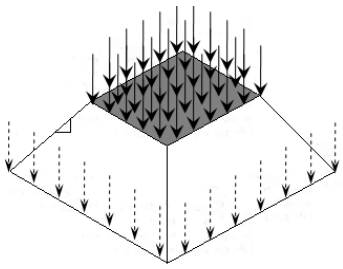

Figure 2.6 –Pyramid load distribution

The track modulus is then calculated as the ratio of K_e to the tie spacing, S (Eq. 2.6). Similar to the deflection basin method, the PLD method does not account for the rail-bending rigidity. It is useful, however, for a quick estimate that does not require direct measurement of deflection under load (Cai et al. 1994).

$$u = \frac{K_e}{S} \tag{2.6}$$

2.2.2.4 Limitations

The main limitation with the BOEF model is that the track substructure is estimated in terms of spring stiffnesses. The substructure is more complex than a single stiffness value, however. The soil parameters can vary with the displacement characteristics of the track, the geometry of the soil-structure system and the loading history (Chang et al. 1980).

Estimating the track stiffness, and thus the track modulus, often assumes a linear load-deflection behavior. This means that, regardless of the load placed on the track, the track modulus would be the same. According to laboratory tests (Zarembski 1989b), however, this is not the case. The modulus varies depending on the load placed on the track; higher loads result in higher track moduli. This is due to the non-linearity of the ballast and subgrade materials. Using a cubic model (Lu 2008) to describe the supporting medium, as opposed to the linear Winkler model, will produce more accurate results for track response. It is rarely used in industry, however, which prefers the Winkler model (Lu 2008). When measuring the track modulus, it is therefore important

to test the track at a load level representative of the actual loads that will be placed on the track.

Another limitation of the foundation models is that the calculated or measured deflection is for static loading only (Iwnicki 2006). Track deflection and loading stresses, however, due to moving loads are slightly larger than those calculated assuming a static load (Timoshenko 1926). Several studies have been conducted for track response under a concentrated moving load (Timoshenko 1926, Steele 1967, Choros and Adams 1979, Frýba 1999). Studies have also been conducted assuming a line load moving force (Lu & Xuejun 1998, Sun 2001). The easiest method, however, is to model the track as a simply supported beam with a moving concentrated force (Fig. 2.7). The differential equation for this method (Frýba 1999) is given by Eq. 2.7.

$$EJ\frac{\partial y^4(x,t)}{\partial x^4}+\mu\frac{\partial y^2(x,t)}{\partial t^2}+2\mu\omega_b\frac{\partial y(x,t)}{\partial t}=\delta(x-vt)P \qquad (2.7)$$

where E is the elastic modulus of the beam, J is the constant moment of inertia of the beam cross section, y is the deflection, x is the length coordinate, t is time, μ is the constant mass per unit length of the beam, ω_b is the circular frequency of damping for the beam, δ is the Dirac delta function, v is the constant velocity, and P is the force. The solution to the equation can be found in Frýba (1999).

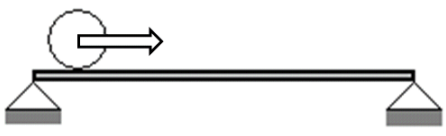

Figure 2.7 - Moving mass on a simply supported beam

2.2.3 Measuring Track Modulus

Traditionally, vertical track modulus was measured statically. A static force was placed on the rail and the corresponding deflection was measured with survey equipment. The methods of measurement typically involved either a deflection basin test or a single load point test.

The advantage of the traditional measurement method with survey equipment is that a stationary reference frame can be used to measure rail deflection. The disadvantage is that it only provides data for a single section of track. To look at an entire length of track would be too time-consuming and costly.

2.2.3.1 Deflection Basin Test

The deflection basin test, or vertical equilibrium method, involves placing one or two point loads on the rail and measuring the total area of track deflection. This is accomplished by measuring the deflection at multiple locations along the track. The track modulus is then calculated according to Eq. 2.5.

2.2.3.2 Single Point Load Test

To simplify measurements and save time, a single point load test can be employed. This test involves placing one point load on the rail and measuring the resulting maximum track deflection (y_0). The track modulus can then be calculated according to the BOEF method (Eq. 2.4).

2.2.3.3 Track Loading Vehicle (TLV)

To solve the problem of time, another method has been developed at the Transportation Technology Center, Inc. (TTCI) to measure vertical track modulus using their track loading vehicle (TLV), shown in Fig. 2.8. This system, consisting of an instrumentation coach, the TLV, and an empty tank car, is capable of measuring the modulus at speeds up to 4.5 m/s (10 mph). A locomotive is used to move the TLV system along the track. The TLV's other applications have included measuring track gage strength, bridge strength, longitudinal rail force, flange climb derailments, and track panel shift strength (Li et al. 2004a).

The TLV is a loaded train car with five wheel-sets: 4 standard wheel sets and a center load bogie. The static wheel loads of the standard wheel sets are 138 kN (31 kips). The center load bogie can be raised and lowered from the car by hydraulic actuators to apply the vertical test loading to the track. This load bogie can apply loads in the range of 4 to 267 kN (1 to 60 kips), but a standard vertical track modulus test uses a vertical load of 178 kN (40kips) (Thompson and Li 2002). The resulting deflections from the applied constant load are measured using a non-contact laser/camera system mounted in front of and behind the center load bogie.

Figure 2.8 - Track loading vehicle (Li et al. 2004a)
Reproduced with permission of TRB

The empty tank car is set up similar to the TLV with a center load bogie and a laser/camera system. The static wheel loads of the empty tank car are 62 kN (14 kips). The center load bogie only applies loads up to around 9 kN (2 kips). This small force is used to ensure that the wheel stays in contact with the rail during the measurement. The laser/camera system on the empty tank car then measures the unloaded rail deflection. An empty tank car is used because the static wheel loads on the TLV produce a deflection basin that could impact the deflection measurements at the center of the car. The lower wheel loads of the empty tank car produce a negligible deflection basin at the center of the car (Li et al. 2004b).

The non-contact laser/camera system used to measure deflections on both the TLV and empty tank car is set up on two independent reference frames located on the

car bodies (Fig. 2.9). The lasers project a light beam onto the rail (Li et al. 2004a). The distance between the laser/camera system and the rail is calculated using the high-speed camera and triangulation. Software is employed to take a continuous reading as the TLV moves along the track.

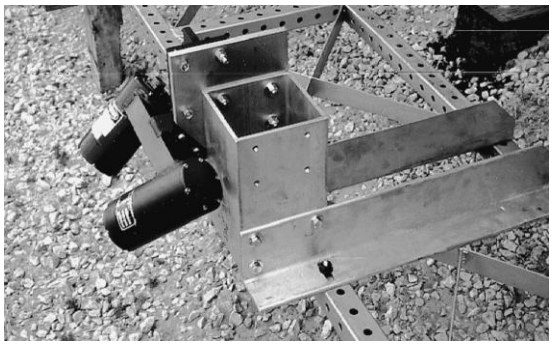

Figure 2.9 - Independent reference frame for camera/laser system (Li et al. 2004a) Reproduced with permission of TRB

A total of three distance measurements are taken to form the rail profile. Two are from the camera/laser system installed on either side of the center load bogie. The middle, or center, measurement comes from the center load bogie itself. Chordal offset measurements are then calculated for both the loaded and unloaded rail profiles (Fig. 2.10). The difference between the loaded and unloaded chordal offset measurements is the vertical deflection of the track due to the load. The track modulus is then calculated according to Eq. 2.4. The accuracy of the deflection measurements is 0.25 mm (0.1 in) (Li et al. 2004a).

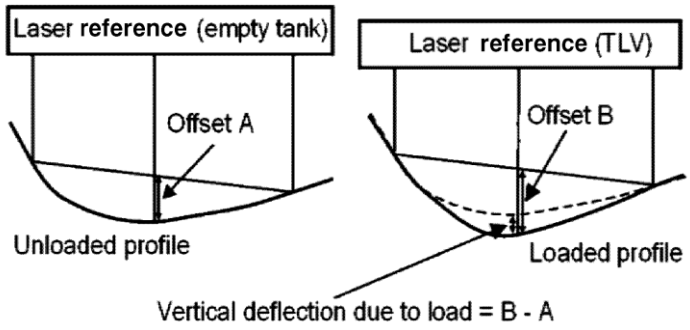

Figure 2.10 – Offset based track deflection measurement (Li et al. 2004a)
Reproduced with permission of TRB

To obtain a dynamic track modulus, two runs of the TLV system are required. The first run is at the standard 178 kN (40 kips) and the second run is at 44 kN (10kips). The loaded and unloaded track profiles are found for both runs. The 44 kN used in the second run serves as a seating load run to remove any slack in the track. Deflections are measured as previously described with the camera/laser system. The dynamic track modulus resulting from these two runs is found using Eq. 2.8, based on the Winkler model.

$$u = \frac{1}{4}\left(\frac{1}{EI}\right)^{\frac{1}{3}}\left[\left(\frac{P_1 - P_2}{y_1 - y_2}\right)\right]^{\frac{4}{3}} \tag{2.8}$$

where u is the track modulus, E is the modulus of elasticity of the rail, I is the moment of inertia of the rail, P_1 is the heavy load (178 kN), P_2 is the seating load (44 kN), y_1 is the rail deflection due to the heavy load, and y_2 is the rail deflection due to the seating load.

This two run test also allows for the support of the subgrade to be investigated. It is assumed that the seating load run provides information about the support of the rail,

ties and ballast. The heavy load of 178 kN provides information about the entire track structure including the subgrade. The difference in deflection between the two runs will then give you information about the support characteristics of the subgrade alone.

The TLV has been validated using the traditional survey measurements. There are some slight discrepancies in the TLV readings compared to the optical survey readings, but the magnitude and wave-form of the deflection measurements are reasonably similar. The difference is likely a result of the relative nature of the offset-based measurements (Li et al. 2004a).

While the TLV system is capable of accurately measuring the vertical modulus, there are some limitations. First, the maximum speed of measurement is 4.5 m/s (10 mph). This restricts the length of track that can be measured in a reasonable amount of time. The cost of the equipment, as well as qualified personnel, is another disadvantage. The TLV has had limited use in the railroad industry because of these reasons (Lu et al. 2007).

2.2.3.4 Real-Time Measurement System

Another similar method has been developed at the University of Nebraska-Lincoln (Norman et al. 2003). The system is capable of measuring the track modulus at revenue service speeds. A separate test consist is not necessary as with the TLV as the camera/laser system is directed attached to the railcar body. The two lasers produce an outline of the rail head seen by the camera. As the rail displaces, the distance, d, between the two lasers' outlines will change. If the rail "sinks" into weak subgrade, d will

increase. The change in distance, as measured with the camera, represents the rail deflection. The corresponding track modulus, using the Winkler model, is then calculated.

As this system is more fully developed and the results adequately validated, track modulus measurement may become more mainstream among the railroad industry. Considering the track modulus is widely used as a measure of track quality, a useful measurement device for track modulus is necessary. If trains were equipped with a simple, inexpensive system to measure track modulus, problem areas in the track could be identified more quickly resulting in increased safety.

2.2.4 Typical Track Modulus Values

The track modulus is highly sensitive to materials of the track structure and substructure. It will vary depending on the rails, ties, fasteners, ballast, subballast and subgrade (Farritor 2006). A track modulus value less than 10 N/mm/mm will cause significant track degradation and should be avoided (Jenks 2006). Stable track structures are considered to have a track modulus between 17 N/mm/mm and 69 N/mm/mm. Higher track modulus values will lead to increased dynamic loads. Typical values for common tie configurations on main-line track are given by AREMA (2008) and Hay (1982).

For a new wood tie track, immediately after tamping, the track modulus is around 7 N/mm/mm (AREMA 2008). After traffic passes over the wood tie track and compacts the track substructure, the modulus increases to about 21 N/mm/mm. This is the about the same track modulus as for a plastic composite tie track that has also been compacted

by traffic. Concrete ties stiffen the track. A common track modulus for this case is around 41 N/mm/mm. These values are representative of track modulus for open track. For a bridge/approach location, typical track modulus values for the approach can range from 14 N/mm/mm to 41 N/mm/mm while typical track modulus values for the bridge can range from 55 N/mm/mm to 83 N/mm/mm (Plotkin et al. 2006).

2.2.5 Factors Influencing the Track Modulus

There are a variety of factors that play a role in the track modulus. Mentioned earlier, the rail, subgrade, ballast, subballast, ties, tie pads, and fasteners all impact the track modulus (Farritor 2006). To investigate the influence of various components on the track modulus, several studies have been conducted (Stewart and Selig 1982, Stewart 1985, Selig and Li 1994). These studies involved the use of the computer model developed by Chang et al. (1980): GEOTRACK.

The findings from the parametric studies (Fig. 2.11) indicate that the subgrade resilient modulus has the strongest influence on track modulus (Selig and Li 1994). As the modulus increases, the track modulus increases. The thickness of the subgrade also plays a major role; as soil thickness increases, the track modulus decreases. The tie material (concrete or wood), tie spacing, ballast resilient modulus and subballast resilient modulus do not significantly control the track modulus.

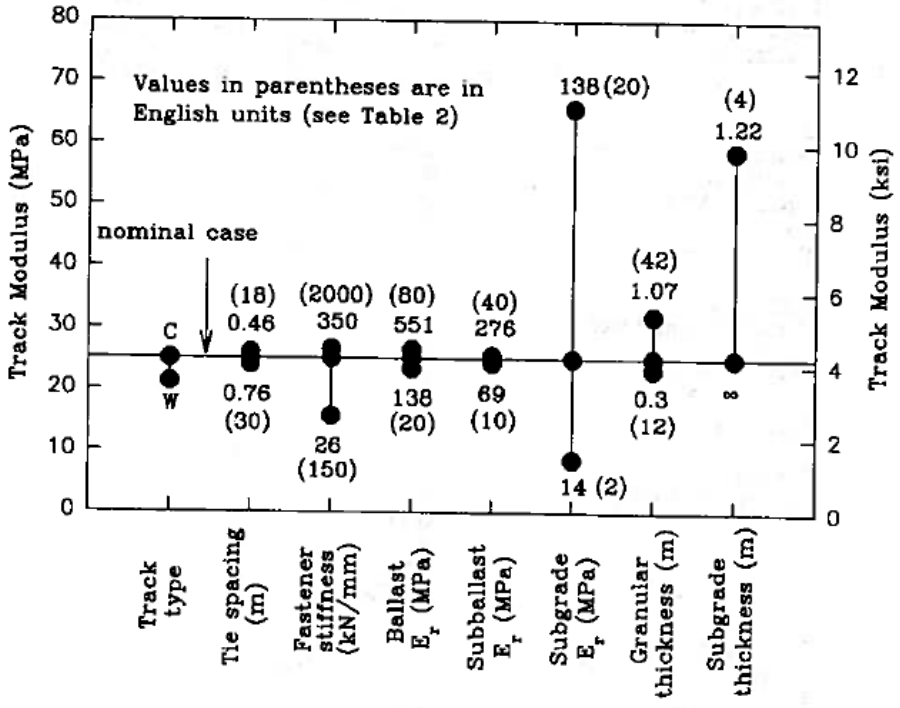

Figure 2.11 – Effects of track components on track modulus (Selig and Waters 1994) Reproduced with permission of TRB

2.3 WHEEL/RAIL FORCES

The nature of wheel/rail forces has been investigated through wheel-rail contact models and actual measurement. The results provide insight into the load frequencies and load transfer through the track structure. Note that only vertical loading is of concern in this present study. Railways do experience other forms of loading, including lateral and longitudinal loads, but this is outside the scope of this research.

2.3.1 Wheel-Rail Contact Models

Since the rail and the wheel materials are not perfectly rigid, some elastic deformation takes at their contact. This occurs, not at a single point, but over a contact patch of about 10 – 15 mm long (Iwnicki 2006). A common method to solve this problem is to represent the patch with contact spring. The Hertzian contact formulation can then be used to calculate wheel-rail forces. There are a number of theoretical models available to quantify the wheel-rail contact forces using this approach (Jenkins et al. 1974, Kalker 1979, Ahlbeck 1980, Knothe & Grassie 1993, Wu & Thompson 2001). Non-Hertzian models are also available to quantify impact forces (Kalker 1990).

2.3.2 Loading Frequencies

Loading frequencies can range from 0.5 Hz to over 1000 Hz (Frederick and Round 1985). For track irregularities, the high-frequency loads (>100 Hz) corresponding to wheel impact are termed P1 forces; they are high amplitude but short duration. The low-frequency loads (around 50 Hz) corresponding to wheel bounce are termed P2 forces; they are lower amplitude but long duration.

P1 forces, which can be as high as 3.5 times the static load, are known to contribute to tie cracking (Zarembski and Bell 2002). The rails and the ties both absorb these high frequency forces so that they are not transmitted through to the ballast or the subgrade (Frederick and Round, 1985). The effects of the P1 forces therefore greatly influence wheel/rail contact behavior but do not affect ballast or subgrade settlement. P2 forces, on the other hand, which can be as high as 2.5 times the static load, are known to

contribute to ballast and subgrade degradation (Zarembski and Bell 2002). Both forces are known to increase with train speed and ramp angles (Frederick and Round 1985). Not much can be done about the high frequency forces, but the lower frequency loads can be manipulated through design changes in track stiffness (Singh et al. 2004).

P1 and P2 forces are often calculated according to Ahlbeck (1980) and Jenkins et al. (1974). Both P1 and P2 forces should not exceed certain limits. For new wheels, P1 forces should not exceed 400 kN; P2 forces should not exceed 250 kN; P1 and P2 combined forces should not exceed 600 kN (Jenkins et al. 1974). Similarly for old, worn wheels, P1 forces should not exceed 425 kN; P2 forces should not exceed 250 kN; P1 and P2 combined forces should not exceed 625 kN.

In addition to the frequencies related to impact loads, normal vibrations on railways result in three main vertical resonances: deflection mode (pinned-pinned) of the rail beam, rail vibrating on pad mode, and rail/sleepers shifting on the ballast stiffness mode (Lee and Chiu 2005). These tend to occur in the range of 725 Hz – 1 kHz, 473 Hz – 670 Hz and around 100 Hz, respectively. Singh et al. (2004) also provide similar typical frequencies for the various modes: about 200 Hz for the movement of rail and ties on the ballast, about 500 Hz for the movement of rail relative to ties on the railpads, 800 to 1500 Hz for movement of the rails on ties and 25 to 40 Hz for the movement of the ballast and the track above it on the subgrade. Frequency response can be obtained by performing a Fast Fourier Transform of wheel load data which is often expressed in the time domain. This will give the dominant frequencies of interest in the signal.

To analyze the signal using a FFT analysis, a window should to be applied to correct for leakage. The window ensures that at the beginning and end of the signal, the value is exactly zero. There are a number of windows to choose from depending on the quality of the signal and the application. For this study, a Hanning window was employed in the FFT analysis. This common window was chosen because it is best for random signals, good for frequency resolution and spectral leakage and fair for amplitude accuracy (LDS 2003). FFT analysis was performed using MATLAB. The code used in MATLAB to perform the FFTs is available in Appendix C.

2.3.3 Stress Distributions

The impact loads on the track structure are transmitted through the ties, ballast and subgrade (Fig. 2.12). Ensuring uniformity in the pressure distribution is important in preventing differential track settlement. To avoid increased subgrade settlement, the track loads must be sufficiently reduced through a good load-distributing structure. This is a key function of the track structure (Zarembski 1989a). The main components of this structure are the ties and the ballast (Hay 1982).

When a wheel load is placed on the track, it is distributed amongst several ties (Fig. 2.12). The outer ties actually experience an uplift force due to the track deflection. This must be restrained by the rails and the ties. If not, the tie will move up down due to a passage of the wheel. This can cause a pumping action on the track leading to track deterioration (Selig and Waters 1984).

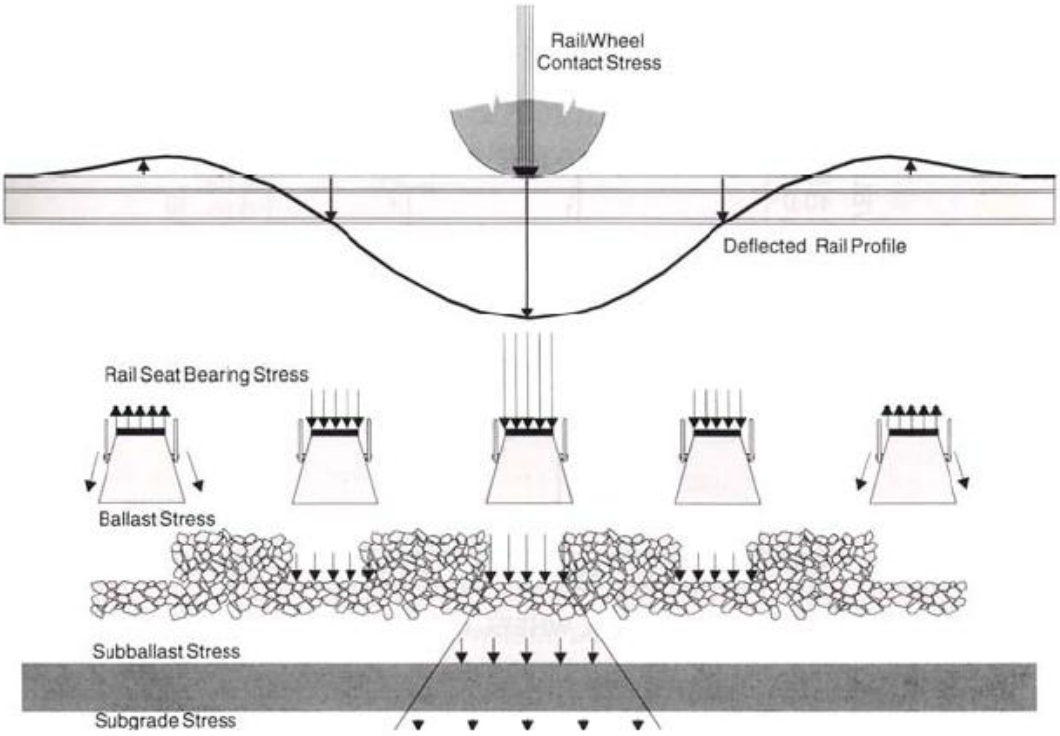

Figure 2.12 - Stress distribution in railway track structure (Selig and Waters 1994)

The entire length of the tie does not carry the load; only the outer thirds of the tie does Hay (1982). Usual practice for a tie spacing of 0.5 m is to assume only 40% of the axle load is present on one tie (Hay 1982). For larger tie spacing, the axle load percentage considered is increased to as much as 60%. The load from the ties is then distributed through the ballast.

According to Hay (1982), the unit pressure spread by the tie to the ballast (p_a) can easily be calculated using Eq. 2.9. Note that Eq. 2.9 is valid for wood ties. For concrete ties, the bearing area is assumed to be the whole tie area, not just the outer

thirds of the tie (Selig & Waters 1994). For concrete ties, the results of Eq. 2.9 should be multiplied by 2/3 to obtain the pressure.

$$p_a = \frac{2P}{\frac{2}{3}bL} = \frac{3P}{bL} \tag{2.9}$$

where P is the wheel load (reduced by 40% for a tie spacing of 0.5 m), b is the tie width, L is the tie length and 2/3bL is the total tie bearing area. A more accurate bearing area, however, takes into account the effect of tie thickness (t). The pressure spread by the tie to the ballast for this case can then be calculated by Eq. 2.10 (AREMA 2008).

$$p_a = \frac{2P}{2\left[b(L-60)\left(1-\frac{0.018(L-60)}{t^{0.75}}\right)\right]} \tag{2.10}$$

where p_a is in psi, P is in lb_f, b is in inches, L is in inches and t is in inches. To convert p_a to kPa, multiply the results of Eq. 2.10 by 6.9. Based on the AREMA Manual for Railway Engineering (2009), p_a should be less than or equal to 450 kPa (65 psi) for wood ties and 590 kPa (85 psi) for concrete ties.

Eq. 2.11 represents the pressure at the top of the subgrade under the ballast (Talbot 1918).

$$p_c = \frac{16.8p_a}{h^{1.25}} \tag{2.11}$$

where p_c is the pressure at the top of the subgrade (in psi), p_a is the pressure at the top of the ballast (in psi) and h is ballast depth (in inches). Another common method to calculate the surface subgrade pressure is by using the Japanese National Railways (JNR) equation (Eq. 2.12).

$$p_c = \frac{50 p_a}{10 + h^{1.35}} \tag{2.12}$$

where p_c is the pressure at the top of the subgrade (in psi), p_a is the pressure at the top of the ballast (in psi) and h is ballast depth (in centimeters). It is important to be consistent with units in these equations. To convert p_c to kPa, multiply the results of Eqs. 2.11-2.12 by 6.9. Based on the AREMA Manual for Railway Engineering (2008), the subgrade pressure should be less than or equal to 140 kPa (20 psi) for all soil conditions.

2.3.4 Design Guidelines

The AREMA Manual for Railway Engineering (2008) provides guidelines to determine dynamic impact loads on open track and on bridge structures. For continuous track with no rail joints, AREMA (2008) describes the total dynamic load on the track (P_{tot}) as a product of the static load (P_{static}) and a dynamic load factor (DLF) (Eq. 2.13). The DLF is calculated according to Eq. 2.14.

$$P_{tot} = DLF \;\; P_{static} \tag{2.13}$$

$$DLF = 1 + \frac{33V}{100D} \tag{2.14}$$

where V is the train velocity (in mph) and D is the wheel diameter (in inches). To convert V and D to SI units of m/s and m, multiply by 0.45 and 0.025, respectively. Eq. 2.14 indicates that as the train speed increases, the DLF will also increase. Conversely, as the wheel diameter increases, the DLF will decrease. The maximum threshold limit for allowable dynamic force is 445 kN (100 kips) according to AREMA (2008).

AREMA (2008) also provides guidelines to determine the impact loads on bridges. The impact load (IL) is calculated as an impact percentage (I) of live load (LL) on the track (IL = I*LL). IL depends on the bridge type: concrete or steel or concrete.

For concrete bridge structures, the impact percentage is estimated as a function of span length (L) (Eq. 2.15, Fig. 2.13). Note that Eq. 2.15 is valid for ballasted deck spans and substructure elements. It cannot be used for direct fixation tracks.

$$\begin{aligned} I &= 60\% \quad && for\ L \le 4m \\ I &= \frac{125}{\sqrt{L}}\% \quad && for\ 4\text{m} \le L \le 39m \\ I &= 20\% \quad && for\ L > 39m \end{aligned} \tag{2.15}$$

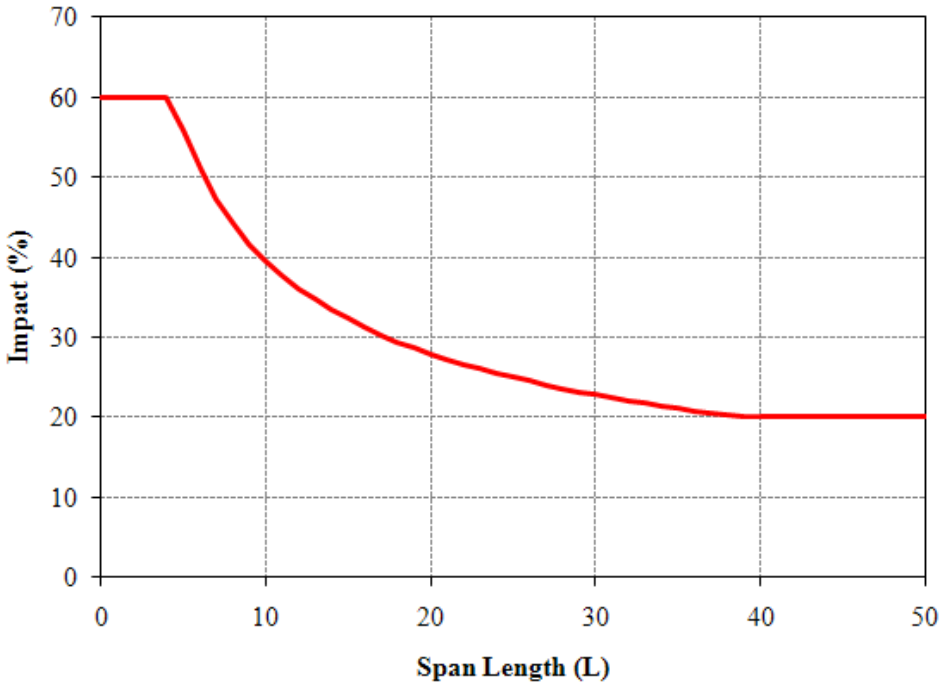

Figure 2.13 – Impact percentage for concrete bridges

For steel bridge structures, the impact load resulting from both vertical and rocking effects must be calculated. The impact percentage for vertical effects on freight cars is described by Eq. 2.16. In Eq. 2.16, L is not necessarily the span length. It is the length (in ft) of the center-to-center supports for stringers or other main members. To convert L from meters to ft, multiply by 3.281.

$$\begin{aligned} I &= 40 - \frac{3L^2}{1600} \qquad for\ L < 80\ ft \\ I &= 16 + \frac{600}{L - 30} \quad for\ \mathrm{L} \geq 80\ \mathrm{ft} \\ I &= 20\% \qquad for\ L > 39m \end{aligned} \tag{2.16}$$

Rocking effects are due to the lateral rocking of a train which transfers load from one rail to the other during motion. This is accounted for by placing a force couple: on one rail, the load is acting downwards while on the other rail, the load is acting upwards. It is calculated as 20% of the wheel load without impact (AREMA 2008). Eq. 2.16 is valid for open deck bridges only. The impact percentage should be reduced by 10% for a ballasted deck bridge (AREMA 2008).

2.4 BALLAST MATERIAL

The ballast acts as a shock absorber for the dynamic load. The quality and depth of the ballast material is therefore important to adequately absorb load and limit track settlement. If the ballast material is poor, a number of problems both related and unrelated to the bump problem can occur.

2.4.1 Ballast Specifications

The quality and depth of the ballast material is important. AREMA (2008) provides guidelines for the selection of ballast including the grading specifications. Typically, uniformly graded ballast (aka poorly graded) will perform better than broadly graded ballast (aka well graded) (Selig and Waters 1984). This has been confirmed with lab tests (Raymond 1977).

The minimum ballast and subballast depths for mainline track in North America range from 150-350 mm and 100-305 mm, respectively (Raymond 1978). AREMA (2008), however, recommends 305 mm for a minimum ballast thickness and 150 mm for a minimum subballast thickness. Alternatively, the required thickness for stability can be calculated by rearranging Eq. 2.11 and solving for the minimum required ballast depth (Eq. 2.17).

$$h = \left(\frac{16.8 p_a}{p_c} \right)^{\frac{4}{5}} \tag{2.17}$$

If the ballast thickness is too small, excessive subgrade pressures could result. This includes increasing the pore water pressure throughout the subgrade. This could lead to increased settlement and possible subgrade failure. It can also cause subgrade attrition whereby the fines in the subgrade move up and infiltrate the ballast.

2.4.2 Ballast Settlement

Ballast settlement accounts for most of the total settlement in railways (Fig. 2.14). It typically consists of rapid immediate settlement after placement followed by gradual

consolidation. There is not a simple linear relationship between number of loads and ballast settlement.

The settlement of the ballast, as a function of load cycles, can be estimated according to Eq. 2.18 (Indraratna et al. 2006).

$$s_{b,N} = aN^b \tag{2.18}$$

where $s_{b,N}$ is the ballast settlement as a function of number of cycles, a is the settlement after one cycle, N is the number of cycles and b is an empirical coefficient found from nonlinear regression analysis.

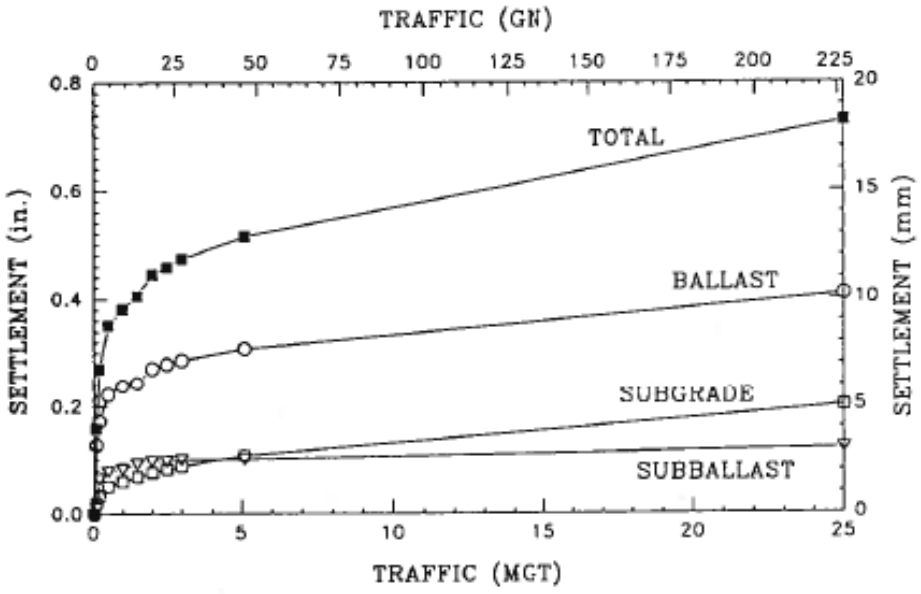

Figure 2.14 – Ballast, subballast and subgrade contributions to total settlements (Selig and Waters 1994)

In the railroad business, number of cycles is usually expressed in terms of million gross tons (MGT) of traffic. In this case, Eq. 2.19 can be used to calculate ballast settlement (Selig & Waters 1994).

$$s_{b,MGT} = a_1(MGT)^c \tag{2.19}$$

where $s_{b,MGT}$ is the ballast settlement as a function of MGT, a_1 is the settlement after one MGT and c is an empirical coefficient found from nonlinear regression analysis equal to b in Eq. 2.18. The relationship between number of cycles and MGT is expressed in Eq. 2.20 (Selig & Waters 1994).

$$\frac{N}{MGT} = \frac{10^6}{A_t N_a} \tag{2.20}$$

where A_t is the total axle load in tons and N_a is the number of axles/load cycles.

2.4.3 Ballast Problems

Oftentimes, after repeated load, the ballast gets pulverized and ballast fouling becomes an issue. Fouling of the ballast occurs when the ballast contains a significant amount of particles less than 6 mm in diameter (Selig and Waters 1984). When placed in service, new ballast will have less than 2% by weight of fouling components (Selig and Waters 1994). In addition to ballast breakage from traffic, fouling can also occur by infiltration from outside sources including coal or other material droppings and wind-blown soil. Fines generated through subgrade attrition, can also clog the ballast resulting in mud pumping.

Reducing the amount of ballast fouling is important because the fouling material can limit the drainage properties of the ballast. Trapped water will increase pore pressures, erosion and ballast deterioration. In addition, the fines produced during fouling may act as a cementitious material binding ballast particles together. This could lead to a hard spot in the ballast that is less capable of absorbing the impact forces (Raymond 1977).

If the ballast absorbs too much energy, it has a tendency to migrate. To prevent migration beneath the track, the ballast material must have sufficient angularity to bind together (Li et al. 2003). If the ballast moves a significant amount, ballast memory becomes a problem. This means that maintenance efforts such as tamping and surfacing will not correct the problem as the ballast will return to its displaced location. Ballast memory causes increased impact loads and thus, increased differential settlement. The way to avoid this is to optimize the energy absorption of the ballast. This can be accomplished through inclusions under the ballast such as hot mix asphalt (HMA), ballast mats, and other geosynthetic materials which provide damping to the track structure.

2.4.4 Ballast Maintenance

The most common way to correct track geometry is through ballast tamping (Fig. 2.15). This helps to lift the track and fill in any voids that may have resulted from ballast fouling. The process loosens the ballast by rearranging the particles from a compacted position. This means that as soon as traffic loads the area, immediate settlement will

occur. Densification of the ballast will then continue to occur under repeated traffic loadings as shown in Fig. 2.16 (Selig & Waters 1994).

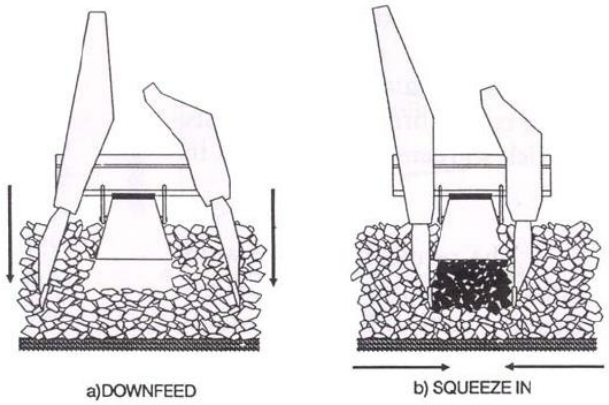

Figure 2.15 – Tamping action (Selig and Waters 1994)

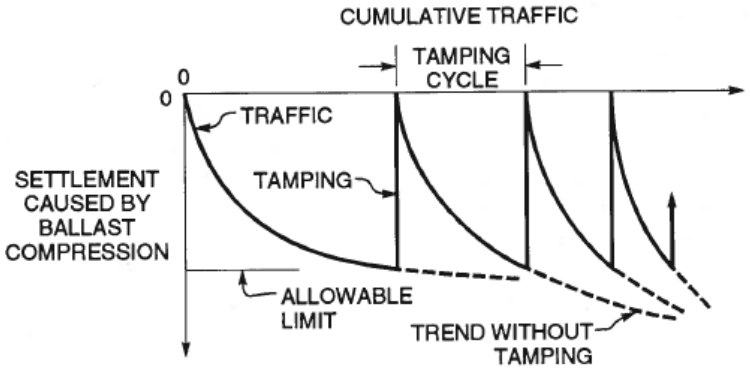

Figure 2.16 –Effect of progressive fouling on length of tamping cycle (Selig and Waters 1994)

If the ballast is fouled, termed dirty ballast, then it must be cleaned to allow for adequate drainage and support. Traditionally, shoulder cleaning has been used to clean

the ballast (Hay 1982). Other methods, such as sledding, plowing and undercutting are also used to clean ballast.

2.5 TRACK SETTLEMENT

The settlement of track has been estimated thus far using mathematical models. The models typically do not take into account the soil properties of the subgrade or the ballast. Rather, they are empirical in nature, relating to the magnitude of the load as well as the number of load cycles applied to the track.

The settlement of track occurs in 2 phases (Dahlberg 2001): immediate settlement and long-term settlement. The first phase generally results from the initial ballast compaction directly after tamping. The second phase, however, results from consolidation of the subgrade and ballast breakdown. A critical review of the available models to predict track settlement is given by Dahlberg (2001).

The track settlement model used in the U.S. is described by Alva-Hurtado and Selig (1981). Their model relates the total permanent strain to the number of cycles (Eq. 2.21).

$$\varepsilon = \varepsilon_1 \; 1 + C\log(N) \tag{2.21}$$

where ε is the total permanent strain, ε_1 is the permanent strain after the first load cycle, N is the number of cycles and C is a dimensionless material constant typically ranging from 0.2 to 0.4 (Selig and Waters 1994). The relationship between settlement and number of cycles (in log scale) is linear.

2.6 COMPUTER MODELS

There are a number of models available to investigate the dynamics of rail traffic on the track structure. The models tend to focus on either the vehicle or the track. Vehicle dynamics models will center in on the vehicle model leaving the track substructure models very simple. Other models, however, have a well developed track substructure model but a simple vehicle model. The choice is dependent on the area of interest.

2.6.1 Vehicle Dynamics Models

The AAR relies heavily on their in-house program NUCARS (New and Untried Car Analytic Regime Simulation) since it was created in the late 1980's. It is also available commercially by railroad companies and suppliers. NUCARS is a general multi-body rail vehicle dynamics computer simulation model (NUCARS 2009). It is a great tool to study the interaction between vehicle and track. It has the capability to model both rail vehicle transient and steady state response (Blader et al. 1989). NUCARS is very useful in studying vehicle behavior including hunting, rock-and-roll, curve entry and steady state curving (Elkins et al. 1990). NUCARS employs a discrete support track model with springs and dampers representing the track substructure.

Bumps/dips and other track geometries can be modeled with NUCARS, however, the typical applications include vehicle design optimization, derailment investigation, track component design, vehicle certification, wheel and rail profile design optimization, vehicle ride quality, wheel/rail lubrication studies, rolling contact fatigue studies and dynamic clearance envelope calculations (NUCARS 2009). The outputs of

the program include body motions, eigenvalues, wheel/rail forces, contact stresses, suspension forces, wheel and rail wear and simulated transducers. It cannot provide track deflection, ballast or subgrade pressures. No study has been found using NUCARS to measure wheel/rail forces at a bridge/approach location with an imposed bump/dip. NUCARS has been used, however, to measure the impact of an abrupt stiffness change. This will be discussed further in the literature review presented in the next section (Section 3).

NUCARS has been benchmarked with a number of other commercially available railway vehicle simulation programs including VAMPIRE, GENSYS, SIMPACK and ADAMS/Rail-MEDYNA in the Manchester Benchmark Study (Iwnicki 1999). The benchmarking study involved the comparison of the results from each simulation program using two simple vehicles and four matching track cases. In general, all programs produced similar results giving confidence to the use of any of them by railroad professionals.

The main problem with most of these available codes used for rail specific applications is that, while they are great for vehicle dynamics, they do not provide much information below the track. The ballast and subgrade are modeled as elastic springs and dampers. The bump at the end of the railway bridge, however, primarily involves mechanisms in the track substructure. The use of these programs would therefore not be beneficial for this purpose.

2.6.2 Track Substructure Models

There are models available that pay special attention to the influence of the substructure: ILLITRACK, GEOTRACK and KENTRACK (Selig and Waters 1994). ILLITRACK is a 2-D finite element model developed at the University of Illinois. It actually consists of two 2-D models with output from one model (longitudinal) serving as input to the other model (transverse). This simulates a 3-D domain. The properties of the substructure are inputs from the user and van vary in the longitudinal and transverse directions. There is no vehicle model associated with ILLITRACK, only the substructure model. A single vertical force is used to simulate vehicle loading. Robnett et al. (1975) provide further details.

GEOTRACK is a 3-D multi-layer model used to determine the track structure's elastic response. It allows for the calculation of track deflection, track modulus, ballast and subgrade deformations and ballast and subgrade pressures. In total, there are 5 layers under the track and ties: ballast, subballast, subgrade layer 1, subgrade layer 2 and bedrock. Each layer is composed of a linear elastic material with material properties defined by the user. There is no vehicle model associated with GEOTRACK. Loading is represented as a single vertical load. The effects of multiple loads can be found using single loads and the method of superposition. Chang et al. (1980) provide further details.

KENTRACK is a 3-D multi-layer model similar to GEOTRACK (Selig & Waters 1994). The main differences between the two programs are that KENTRACK allows for finite element modeling of the ties and for multiple wheel forces on the track. It is mainly used as a structural design tool for railway trackbeds (Rose & Konduri

2006). It was originally developed to model track with HMA underlayment. Its use has since been expanded for applications without a HMA layer. Huang et al. (1984) and Rose and Konduri (2006) provide further details.

ILLITRACK, GEOTRACK and KENTRACK are all useful programs, but are not capable of handling the complex issue of the bump/dip at the end of the railway bridge. Vehicle interactions with the track are important in accurately describing the wheel/rail forces on the track at the bridge approach location.

2.6.3 LS-DYNA

LS-DYNA is a commercially available general purpose transient dynamic finite element program (LS-DYNA 2007). It works with an explicit solver. There are a number of uses for LS-DYNA including automotive crashworthiness and occupant safety, sheet metal forming, aerospace applications, earthquake analysis, biomedical research and civil engineering applications to name a few. Its use in railway applications has thus far mainly focused on crash impacts and dynamic analysis of bridges (not including the bump at the end of the railway bridge). Its use in bridge approach transition studies, however, is slowly starting to gain traction. The benefits of LS-DYNA are that both a vehicle and track substructure model can be developed to fully analyze the problem of the bump at the end of the railway bridge.

3. LITERATURE REVIEW

The bump at the end of the bridge is not a new problem. Both the highway and railroad industry face this difficulty. Although they share many of the same contributing factors that lead to the bump, the solutions employed to alleviate the problem are quite different. A comprehensive literature review on the topic was conducted to determine the past knowledge and practice for the bump at the end of the bridge.

3.1 GENERAL FINDINGS

The FRA (1993) estimated that there were about 101,000 railway bridges in the US (not including rapid-transit operations). This number has likely increased since that time. After reviewing the literature, however, it is unclear how many of these railway bridges are affected by the bump problem. To close this gap, a survey of railroad professionals was conducted during the course of this research to determine the extent of the problem (Section 4). Based on a similar highway survey conducted by Briaud et al. (1997), about 150,000 out of 600,000 US highway bridges (as of 1995), about 25%, experienced problems. This percentage is expected to be higher for railways due to the much higher loading environment.

Based on the AAR's 2008 Strategic Research Initiatives (SRI) Plan (R. Jimenez, personal communication, June 2008), the cost of railway bridge transition repairs is estimated as $26 million per year ($16 million for steel bridges and $10 million for concrete bridges). This figure does not take into account the significant cost resulting

from slow orders that railroads must impose in problem locations. A slow order is a speed restriction where trains must travel at slower-than-line speeds to operate safely (Solomon 2006). By comparison, the cost of repair for highway bridges has been estimated at $100 million per year (Seo 2003). The expense is much higher for highway bridges than railway bridges. This is likely due to the total number of bridges in service.

3.2 CAUSES

The bump/dip is a result of a repeated process that starts with differential settlement between the approach embankment and the bridge structure. As the settlement increases, loading on the track structure will also increase. This causes even more track degradation, thus a bigger bump/dip. There are a number of factors leading to the development of a bump/dip in the track (Fig. 3.1).

Most of these contributing factors depend on local site conditions which complicates the problem as a “one size fits all” type solution is difficult to identify. Several studies have been conducted concerning the causes of the bump at the end of the bridge for both the highway industry (Dupont and Allen 2002, Briaud et al. 1997, Long et al. 1998, Seo 2003, Seo et al. 2002, Stark et al. 1995, Wahls 1990) and for the railway industry (Davis et al. 2003, Jenks 2006, Li et al. 2003, Li and Davis 2005, Plotkin et al. 2006).

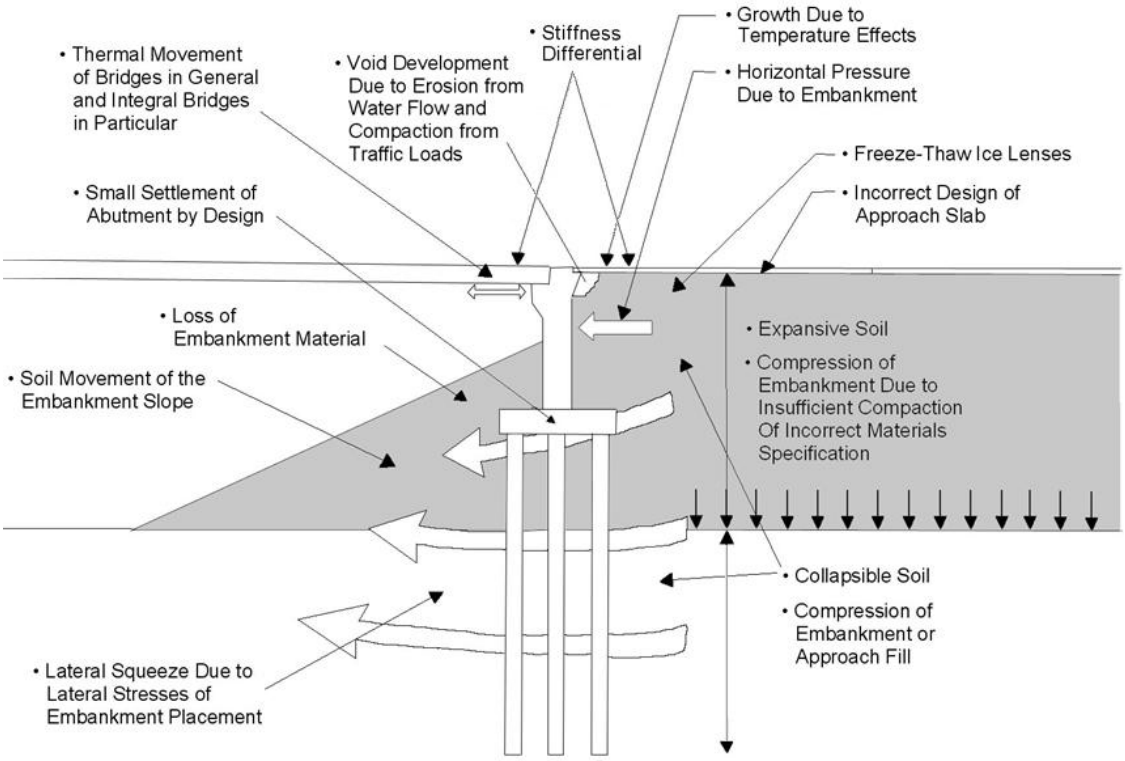

Figure 3.1 - Contributing factors to bump/dip development (After Briaud et al. 1997)

3.2.1 Differential Track Modulus

The most commonly held belief is that the bump is a result of an abrupt change in the vertical track modulus, or stiffness, between the approach and the bridge structures (Davis and Plotkin 2009). In general, the approach embankment will have a low track modulus compared to the stiff bridge. Typical track modulus values for the approach can range from 14 N/mm/mm to 41 N/mm/mm while typical track modulus values for the bridge can range from 55 N/mm/mm to 83 N/mm/mm (Plotkin et al. 2006). Differential

settlement has been shown to result from a track with a low modulus (Read et al. 1994, Ebersohn et al. 1993).

By itself, the stiffness differential does not contribute to significant dynamic impact loads (Davis and Plotkin 2009, Plotkin et al. 2006). It can contribute to running surface defects in the track, however, that will eventually lead to increased differential settlement and uneven ballast wear, amplifying the impact loads at the bridge approach location even more. The dynamic loads caused by this are approximately 1.5 to 3 times the static load (Davis et al. 2003). To avoid track degradation, uniform stiffness should be maintained along the length of the track if possible. This is often difficult as variations in track modulus can result from alternative ballast/subgrade conditions, uneven construction effects and track service life (Cai et al. 1994).

3.2.2 Quality of Approach Fill

The quality of the fill and embankment material significantly impacts the degradation of the approach geometry. In addition, the subgrade material has the largest influence on the track modulus (Selig and Waters 1994). Poor quality material can cause differential settlement and erosion. In some cases, the natural soil found at the site will be used for the approach fill. Oftentimes, however, it is advantageous to import soil with the desired characteristics.

Using rock, gravel, and sand deposits will lessen the long-term settlement effects seen at the bridge approach (Briaud et al. 1997). This is because these cohesionless soils typically fully compress immediately after load is placed. Highly compressible clays or

silts, organic clays that may decay and excessive vegetation at the surface are considered unfavorable for the fill and embankment material (Li et al. 2003). Clays should be avoided, if possible, because they exhibit long-term settlement, creep, and shrink-swell characteristics. It is often difficult and expensive to replace the soil at the site though. If clay must be used, proper drainage must then be ensured.

3.2.3 Impact Loads

Impact loads both contribute to and result from the bump at the end of the railway bridge. They result from wheel and/or track defects. For a perfectly smooth track with good, uniform ballast conditions, there would be hardly any increased dynamic loads (Fredrick and Round 1985). Unfortunately, this is rarely the case. In the case of a bump or dip at the bridge approach location, for example, impact loads mainly occur as a result of the change in the track profile geometry and stiffness. Note that only vertical loading is of concern in this present study. Railways do experience other forms of loading, including lateral and longitudinal loads, but this is outside the scope of this research.

To detect high impact loads in service, railroads use the Wheel Impact Load Detector (WILD). This system incorporates strain gages welded to the wheels (Stratman et al. 2007). Currently, the load limit for the WILD devices, set by the Association of American Railroads (AAR) is 400.3 kN (AAR 2005). Once this threshold has been met, the wheels are removed from service.

3.2.4 Ballast Material

The ballast acts as a shock absorber for the dynamic load. The quality and depth of the ballast material is therefore important to adequately absorb load and limit track settlement. If the ballast material is poor, a number of problems both related and unrelated to the bump problem can occur.

If the ballast absorbs too much energy, it has a tendency to migrate. If the ballast moves a significant amount, ballast memory becomes a problem. This means that maintenance efforts such as tamping and surfacing will not correct the problem as the ballast will return to its displaced location. Ballast memory causes increased impact loads and thus, increased differential settlement. At a bridge/approach location, this can cause a bump or a dip to form.

3.2.5 Drainage

Drainage is an important component that must be considered in the design of any structure. The drainage system employed should serve several functions including intercepting/diverting groundwater and surface water from the track structure, removing water from under the tie throughout the ballast material and containing/channeling streams (Hay 1982, Selig and Waters 1994).

A good design for the fill can be negated with poor drainage. For bridge approaches, poor drainage can lead to erosion and instability of the embankment fill. As water is allowed to enter and pool in the voids beneath the approach zone, scour and erosion takes place (Li et al. 2003). This impacts the strength and consolidation

characteristics of the fill material and can also amplify vegetation problems. In addition to impacting the subgrade, poor drainage can also play a role in tie and ballast deterioration, frost heave and ice. Proper designs must be in place to ensure adequate drainage around the track. AREMA (2008) provides recommendations for several drainage designs.

3.2.6 Damping

At track transitions, damping differs between the approach and bridge structures. This is due to the materials on which the track rests. The approach, made of fill, decays accelerations faster than the bridge structure, typically made of a stiffer material such as concrete. Track damping also serves to dissipate energy from impact loads on the track. The high frequency loads tend to disperse energy higher in the track structure than lower frequencies (Wanek 2006). This means that ballast and subgrade deterioration are due, in part, to the low frequency loads that are dispersed lower in the track structure.

According to Sasaoka and Davis (2005), 52.5 kN/m/sec/tie/rail (300 lb/in/sec/tie/rail) is considered an optimum damping value for railway track. Based on field tests, however, actual damping of open deck bridges and ballast is around 8.8 kN/m/sec/tie/rail (50 lb/in/sec/tie/rail). Damping can be added to these structures in the form of rail seat pads, under tie pads and ballast mats.

3.2.7 Abutment Type

The abutment serves to support the structural loads while helping to retain the approach embankment (Briaud et al. 1997). The design and geometry of the abutment is therefore a critical factor to the bump problem. The choice of foundation for the abutment (Fig. 3.2) depends on the location of the bridge, the soil type used, and the loading on the bridge (Seo 2003). Typically, abutments built on piles are likely to see degradation of track geometry (Li et al. 2003). Abutments supported by shallow foundations within the embankment will tend to settle with the embankment (Wahls 1990). This results in less differential settlement. Most railway bridge abutments, however, are supported by deep foundations.

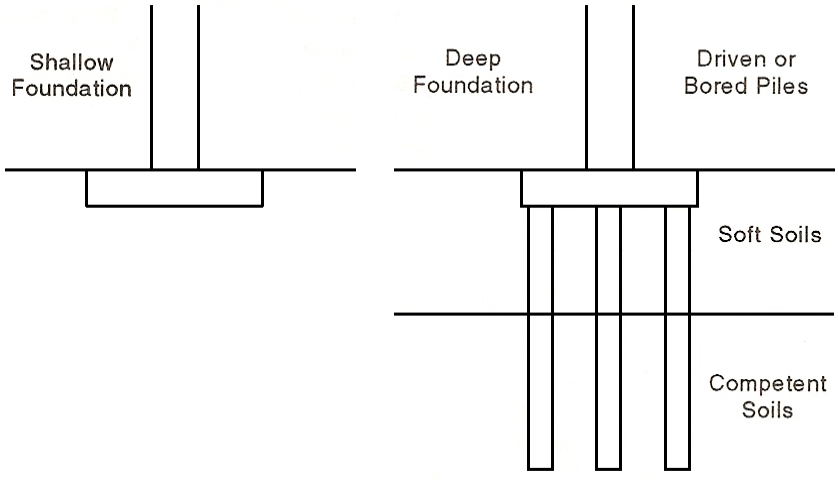

Figure 3.2 - Types of abutment foundations (Briaud et al. 1997)

Closed (high) and pedestal (spill-through) abutments lead to problems because of insufficient compaction of the fill material close to the structure (Fig. 3.3 and Fig. 3.4, respectively). This leads to increased differential settlement. A perched (stub) abutment simplifies compaction problems as it is constructed after the embankment (Fig. 3.5). Higher lateral earth pressures are found more on closed abutments than on pedestal or perched abutments (Seo 2003). Spill-through and stub abutments lack lateral confinement and can lead to rougher approaches (Mahmood 1990). Weak lateral confinement contributes to increased soil erosion and thus, increased embankment settlement.

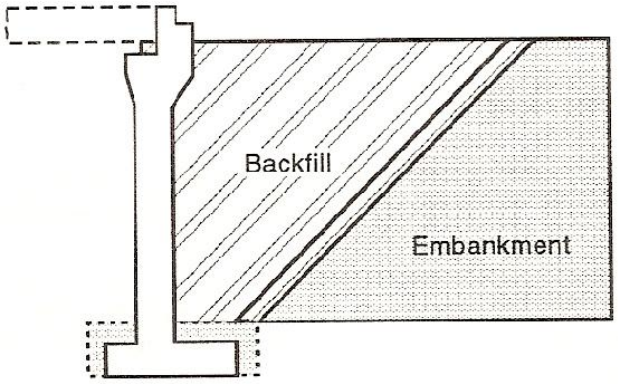

Figure 3.3 - Typical closed (high) abutment (Briaud et al. 1997)

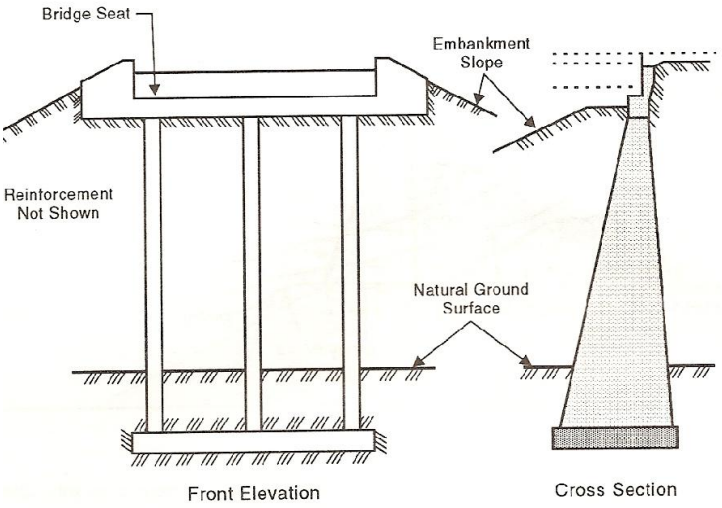

Figure 3.4 - Typical pedestal (spill-through) abutment (Briaud et al. 1997)

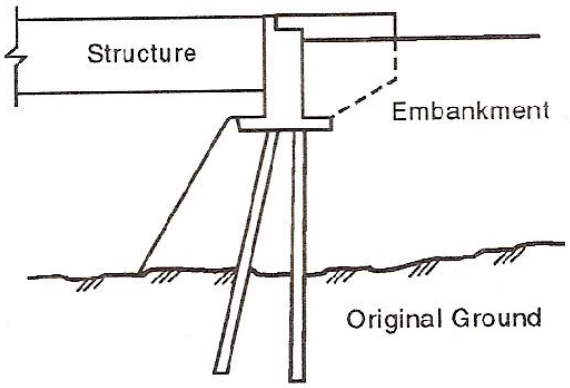

Figure 3.5 - Typical perched abutment (Briaud et al. 1997)

3.2.8 Bridge Joint

The bridge joint, or end connection, is another important factor to consider. A rough joint will lead to increased impact loads and erosion (Li et al. 2003). If the joint is not securely placed, water can enter the system causing erosion and increased pressure on

the abutment wall (Briaud et al. 1997). Typically, integral end bents are used and perform well. Thermal stresses, however, can cause longitudinal deformations in the joints causing voids to form behind the abutment (Li et al. 2003). Erosion can then occur as water enters these voids.

3.2.9 Traffic Considerations

It is expected under consolidation theory that heavier axle loads will lead to larger settlement. The suspension quality of the vehicle will also impact track loads (Li et al. 2003). Trains with better suspension properties will be more able to attenuate rail profile deviations making the transition smoother. This leads to decreased impact loads. While the effect on impact loads is relatively small, the vehicle suspension system has a big influence on the train ride and component performance (Jenkins et al. 1974).

Impact loads are also affected by the speed of the train. Increased speeds will naturally lead to increased wheel loads. Lateral and longitudinal forces due to braking or throttling of a train must also be considered. These lateral forces can lead to significant problems such as ballast migration and differential settlement.

3.2.10 Quality of Construction

Quality control must be established with any construction project. Poor craftsmanship can lead to significant problems such as improper compaction of the backfill. Improper compaction can increase the settlement of the embankment material relative to the

bridge structure (Li et al. 2003). Shortcuts in construction practices should be avoided to ensure a stable bridge approach.

3.3 PREVIOUS STUDIES

The complete track response resulting from a bump/dip in the track at the bridge/approach location has not been investigated yet. A few studies have looked at a bump or dip track geometry and the resulting wheel/rail forces, but the effects of the bump/dip go beyond wheel/rail forces. Most studies have focused on the bump at the end of the railway bridge as a track modulus transition issues since it is considered the leading contributing factor in railway bump/dips. These studies typically look at the track response due a track modulus change only though and do not including a track geometry change such as the bump or dip.

3.3.1 Track Modulus Issues

According to Davis and Plotkin (2009), the most commonly held belief in the railroad industry is that the bump is a result of increased forces due to an abrupt change in the vertical track modulus, or stiffness, between the approach and the bridge structures. Several measurements have been made quantifying the track modulus at bridge sites. For example, Li and Davis (2007) reported TLV results from a bridge site near Marysville Kansas. As expected, the bridge is significantly stiffer than the approach embankment. In fact, the track modulus on the bridge is about double the track modulus on the

approach. Wheel/rail forces resulting from the stiffness differential, however, were not measured in this study.

3.3.1.1 Wheel/Rail Forces

The magnitude of forces and the effect of a bump/dip at the bridge approach location have not been well documented thus far. One study (Davis and Plotkin 2009) presents actual force measurements, taken by the FRA's research car T-16 across both open deck and ballasted deck bridges outside of Baltimore, MD. Results from these tests indicate that crossing the stiffness change alone does not produce any appreciable dynamic forces. In fact, if the bridge locations were not marked in the results, it would be very hard to tell where the bridges were since no significant impact force above noise level was detected. The stiffness values for the bridge and the approach section in this case were not reported.

Other studies (Plotkin et al. 2006) indicate that a stiffness change alone will produce a DLF of less than 10%. Including a surface defect such as a bump or a dip will increase the dynamic load by 1.5 to 3 times the static load (Plotkin et al. 2006). The effect of a stiffness change alone (less than 10%) is therefore considered negligible compared to effect of a bump/dip in the track.

In a NUCARS study presented by Sasaoka and Davis (2005), the effect of track modulus on the maximum vertical wheel loads on a crossing diamond was found. It concluded that a stiffness change alone will not significantly affect the impact loads on the track. A modulus variation can create running surface defects, however, which can

lead to a bump/dip in the track. It is more important to ensure a level track than a continuous vertical track stiffness (Hunt & Newland 1996).

Namura and Suzuki (2007) investigated the effect of stiffness changes in the track. The stiffness changes were due to different track structures, such as from ballasted track to slab track. While the study is not focused on bridges, the results are still helpful since they help describe effects of stiffness changes alone. Using axle box acceleration data, it was found that as the train moved from the softer track (ballasted) to the stiffer track (slab), an impact was produced on the softer track (ballasted). Similarly, as the train moved from the stiffer track (slab) to the softer track (ballasted), an impact was also produced on the softer track. In both cases, the impact is on the soft side. Also clear from the figure is that moving from the soft to stiff track produced a higher axle force than moving from the stiff to soft track. These measurements are in agreement with results produced by Lundqvist et al. (2006) using LS-DYNA.

This is contrasted by results from Plotkin et al. (2006) though. Using NUCARS, various degrees of abrupt track modulus change were modeled to simulate the bridge approach condition. The simulation results show that the peak force occurs on the bridge side, or the stiffer side, right before the train crosses over to the approach. The exact details of the model were not reported.

Ribeiro et al. (2008) also looked at the dynamic analysis of transition zones for high speed railway lines. There was no imposed bump or dip, just a level track over two soils with varying stiffnesses. A 2-D track model and a 3-D track model were simulated with ANSYS and LS-DYNA, respectively. The exact track modulus values in the model

are unknown. The train model, representing a ICE2 train locomotive, moved from the soft soil to the stiffer soil. Outputs included sleeper-ballast contact forces and wheel/rail forces. The results indicate that a stiffness change produces an impact between the wheels and rail and the back wheels experience a different force response than the front wheels.

This is confirmed by Frederick and Round (1985) who found from actual force measurements that the trailing axle of the bogie exerts higher impact forces than the leading axle. The results show that the peak force on the front axles is independent from the train speed whereas the peak force on the back axles has a relatively linear relationship with train speed. Results from Zarembski (1989d) also suggest this behavior. Frederick (1978), however, suggests that dynamic forces are a function of mass times the square of the velocity (mv^2), regardless of the track profile.

3.3.1.2 Track Deflection

Hunt and Newland (1996) describe a simple bogie model moving along a track with variable stiffness. The stiffness of the track has a cosine variation along a transition length, L. The displacement profile and normalized force for a single wheel bogie moving on and off of the bridge resulting from the stiffness variation is reported.

Hunt (1997) investigated the problem of track settlement near bridge abutments due to variations in track stiffness. Using a discrete element track model, a single force was applied to the track and the corresponding deflections were estimated (Fig. 3.6). The

bending stiffness of the beam was held constant while the track modulus was linearly varied across a transition length of 2 m.

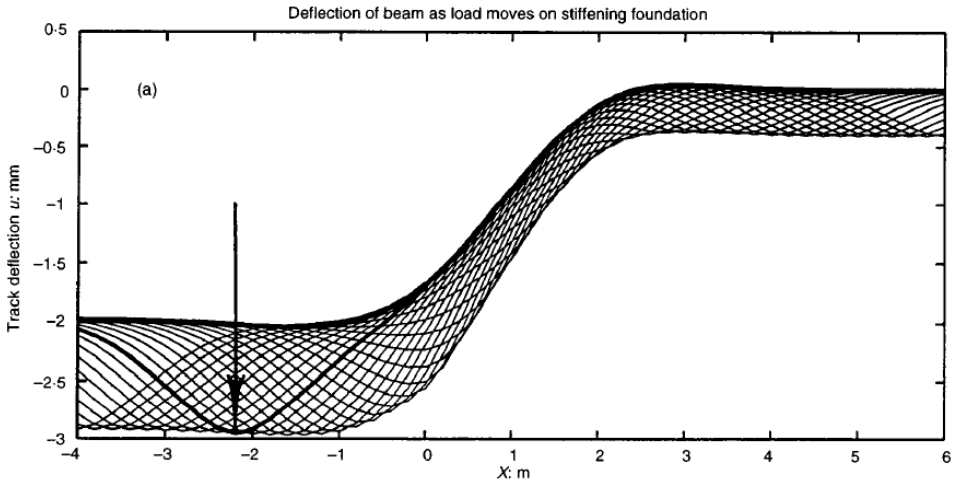

Figure 3.6 - Static beam deflection with variable track modulus (Hunt 1997)

Incorporating a bogie model, Hunt (1997) also calculated the dynamic forces applied on the track due to moving from a low stiffness to a high stiffness with a linear stiffness variation. This stiffness variation is assumed to occur at the bridge/approach location. The deflection and forces due to the bogie moving off of the bridge onto the approach (from a stiff to a soft stiffness) was previously described by Hunt and Newland (1996). Finally, with the same vehicle and track model, the progressive track settlement under cyclic loading was estimated (Fig. 3.7).

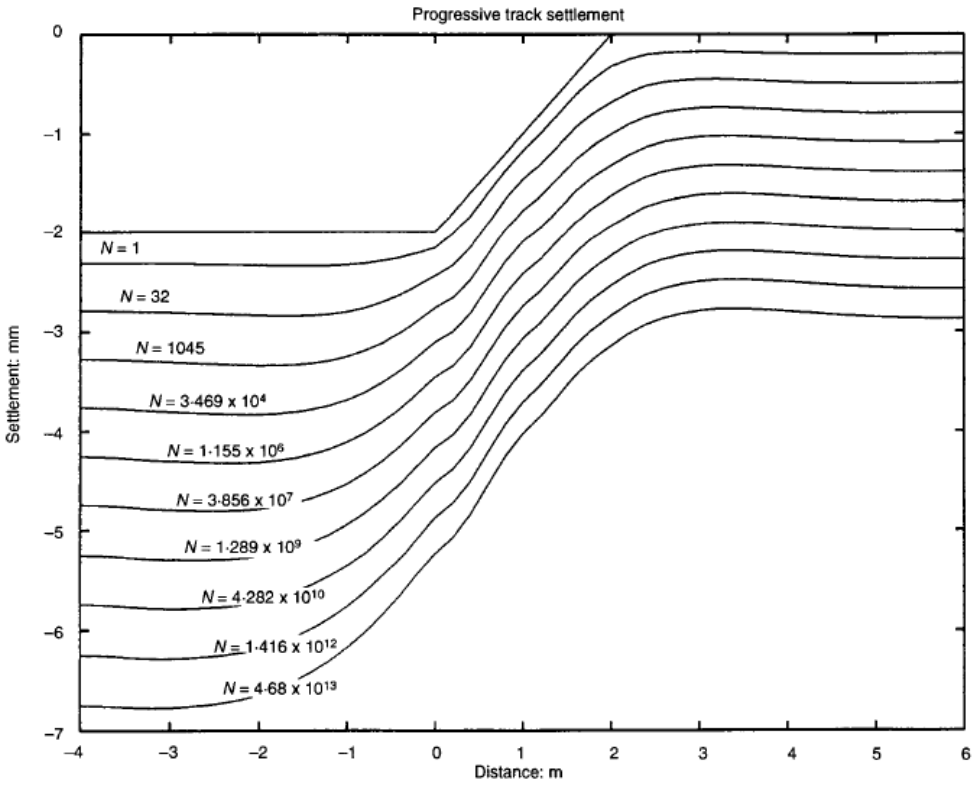

Figure 3.7 - Track settlement response to cyclic loading (Hunt 1997)

3.3.2 Bump Profile

Banimahd and Woodward (2007) looked at effect of speed, sleeper voiding and track stiffness changes on track response using 3-D finite element modeling. The track deflection at a transition zone was first estimated with their model (Fig. 3.8). This agrees with the previous results from Hunt (1997). The track deflection begins to change on the soft side of the transition leading up to the stiff side. This is attributed to the flexural stiffness of the rail. The wheel/rail forces due to the stiffness change alone were negligible though. The deflection profile at the transition zone can be broken down into transition length (L) and change in deflection (h).

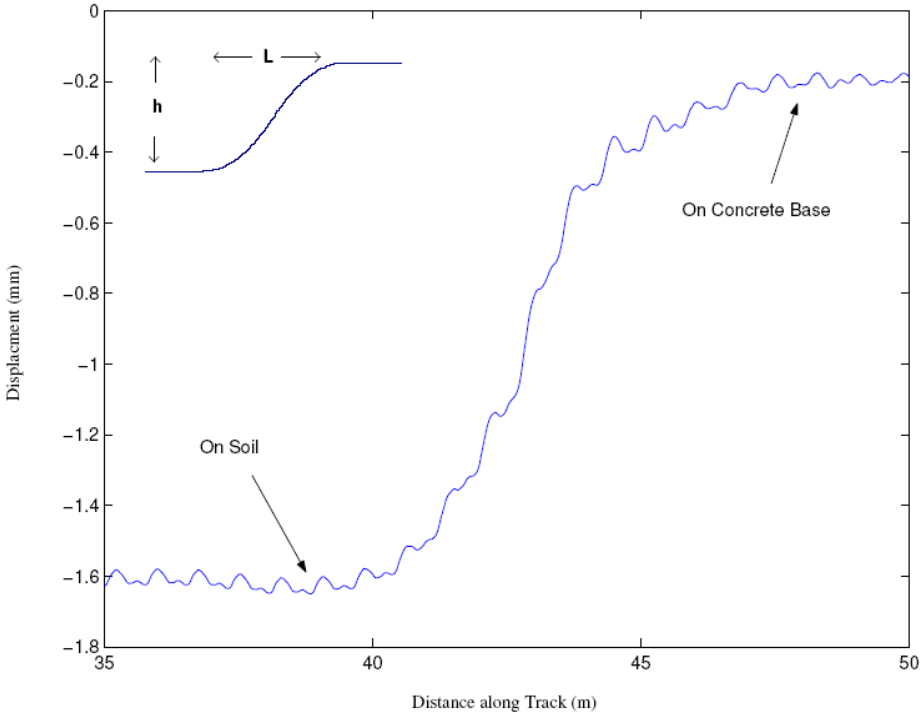

Figure 3.8 - Simulated rail displacement in a stiffness transition under moving load (Banimahd and Woodward 2007)

Using a track irregularity model, Banimahd and Woodward (2007) looked at the influence of difference transition lengths and changes in deflection on wheel/rail interaction forces at 20 m/s (45 mph) and at 70 m/s (156 mph). The results at 20 m/s (45 mph) are presented in Fig. 3.9. The exact details of the model, including vehicle and track properties, were not presented in the paper. The results indicate a linear relationship where increasing L will decrease the DLF and increasing h will increase the

DLF. Increasing the velocity was also found to increase the DLF. The effect was maximized with short transition lengths and minimized with long transition lengths.

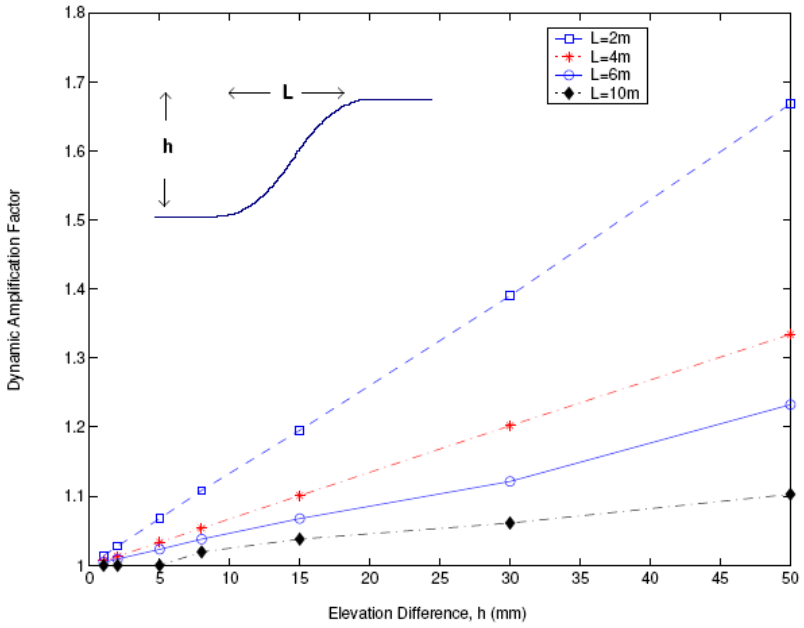

Figure 3.9 - Effect of transition length on wheel/rail forces (Banimahd and Woodward 2007)

Zhai et al. (2001) used a theoretical model, simulated with computer software named VICT, to investigate the wheel/rail forces due to a bump or track irregularity. The inputs for the bump included the length of the transition section and the bump angle (α) (Fig. 3.10). Japanese railways restrict the value of α to help maintain the bridge approach location.

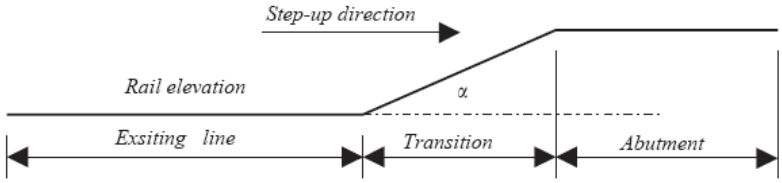

Figure 3.10 - Track transition with bump angle (Reprinted from Lei and Mao 2004 with permission from Elsevier)

With the model, the wheel/rail force for a train at 160 km/hr (100 mph) crossing over a ramp with a transition length of 10 m and an α of 0.004 (0.229^{o}) was found. Running the simulation with other deflection angles shows that there is a linear relationship between maximum load and α. Based on the Britain Rail standard for the P2 force (250 kN), the deflection angle should be less than 0.0065 (0.372^{o}) for a train speed of 160 km/hr. This corresponds to a slope of 1:154 in this case.

Lei and Mao (2004) looked at both track modulus transition zones as well as the classic bump at the end of the bridge for high speed railways using a dynamic computational model employing the finite element method. The track substructure was modeled as spring stiffnesses. The model for transition zones looked at transition changes of 10 times to 100 times the conventional track modulus. The model for the bump looked at different angles (α) for the bump (Fig. 3.10). Results include maximum wheel/rail forces and vertical accelerations of the car body and rail. All of the models had the train moving from a low stiffness to a high stiffness, or from the approach to the bridge.

The authors (Lei and Mao 2004) found that the change in stiffness at the bridge approach location has little effect on the maximum wheel/rail force. This result agrees with the findings of Sasaoka and Davis (2005), Plotkin et al. (2006) and Plotkin and Davis (2009). They also found that the bump angle and train velocity has a significant influence on the wheel/rail forces (Fig. 3.11). The relationship between the DLF and α is linear. These forces are for a TGV (French high speed train) locomotive.

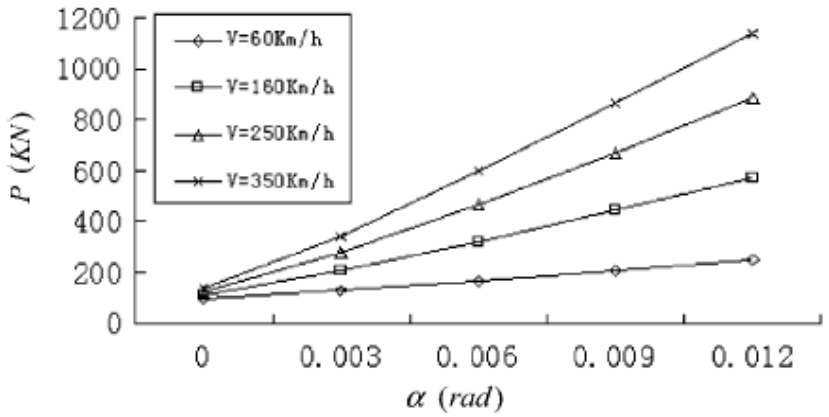

Figure 3.11 - Maximum vertical wheel/rail force for different bump angles (Reprinted from Lei and Mao 2004 with permission from Elsevier)

3.3.3 Dip Profile

With the same model used to find the effects of a bump profile, Banimahd and Woodward (2007) looked at the effect of faulted transitions due to voided sleepers. This causes a "dip" in the originally straight track deflection under moving load. Looking at

various voids of 1 m in length, the effect of velocity and void height on the DLF was found (Fig. 3.12).

As velocity is increased, the DLF increased; similarly, as void height increased, the DLF also increased. It is important to note that the geometry was not imposed in the track. The geometry was based on track deflections under moving load. The track geometry without a load present is considered straight.

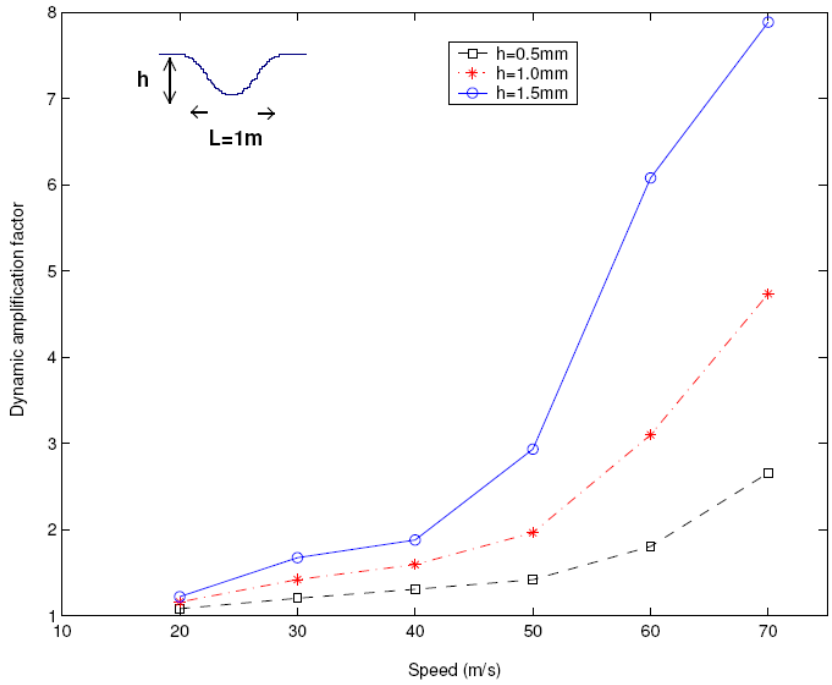

Figure 3.12 - Effect of void height and speed on wheel/rail forces (Banimahd and Woodward 2007)

Jenkins et al. (1974) also examined the effect of a dip profile in the track. Rail displacement, wheel/rail forces and rail bending moments due to a dip were found. Using theoretical equations described in the paper, different dip angles were also

investigated. The study found that both P1 and P2 forces are proportional to the product of the total joint angle and the speed ($2\alpha V$).

3.3.4 Track Response Criteria

To characterize the complete track response, wheel/rail forces, track deflection, ballast and subgrade pressures must be analyzed. Limits and criteria have been established for each of these response components.

3.3.4.1 Wheel/Rail Forces

Based on a track settlement model developed by TTCI (Davis et al. 2007), there is a linear relationship between the rate of settlement increase and an increase in load. According to Plotkin and Davis (2008), a 50% increase in the load felt under the track is necessary to produce a noticeable difference in differential track settlement rate of 25%. This means that the DLF must be 1.5 or higher to see any appreciable settlement requiring more frequent maintenance than usual. Note that dynamic load may be higher than 1.5 times the static load, but if it is too high a frequency, then the ballast and subgrade will not feel the effects. This is discussed in Section 2.

Both P1 and P2 forces should not exceed certain limits as well. For new wheels, P1 forces should not exceed 400 kN; P2 forces should not exceed 250 kN; P1 and P2 combined forces should not exceed 600 kN (Jenkins et al. 1974). Similarly for old, worn wheels, P1 forces should not exceed 425 kN; P2 forces should not exceed 250 kN; P1 and P2 combined forces should not exceed 625 kN.

3.3.4.2 Deflection

After reviewing the literature, the track deflection resulting from a bump/dip in the track has not yet been quantified. Deflection criteria are available, however, that limit the amount of deformation that track can handle. According to Lundgren and Martin (1970), the maximum desirable deflection for heavy axle loads is 6.4 mm (0.25 in). This deflection should not be exceeded whether on open track or on a bump/dip.

3.3.4.3 Ballast and Subgrade Pressures

Based on the AREMA Manual for Railway Engineering (2008), ballast pressures should be less than or equal to 450 kPa (65 psi) for wood ties and 590 kPa (85 psi) for concrete ties. Similarly, for subgrade pressures, AREMA (2008) recommends that the subgrade pressure should be less than or equal to 140 kPa (20 psi) for all soil conditions. Since soil conditions vary, Selig and Waters (1994) presented new values for allowable pressure based on soil type (Table 3.1). Methods to calculate ballast and subgrade pressures have been presented in Section 2. Frederick and Round (1985) suggest that when dynamic forces are very large, the highest pressures on the ballast and subballast will occur when the axle is not directly overhead.

Table 3.1 – Allowable subgrade bearing pressures (Selig and Waters 1994)

Subgrade Description	In-Place Consistency	Allowable Pressure below Track	
		psi	kPa
Well graded mixture of fine and coarse grained soils: glacial till, hardpan, boulder clay (GW-GC, GC, SC)	Very compact	65 - 100	450 - 690
Gravel, gravel-sand mixtures, boulder-gravel mixtures (GW, GP, SW, SP)	Very compact	55 - 85	380 - 590
	Medium to Compact	40 - 60	280 - 410
	Loose	25 - 50	170 - 350
Coarse to medium sand, sand with little gravel (SW, SP)	Very compact	30 - 50	210 - 350
	Medium to Compact	25 - 30	170 - 210
	Loose	15 - 25	100 - 170
Fine to medium sand, silty or clayey medium to coarse sand (SW, SM, SC)	Very compact	25 - 40	170 - 280
	Medium to Compact	15 - 30	100 - 210
	Loose	8 - 15	60 - 100
Fine sand, silty or clayey medium to fine sand (SP, SM, SC)	Very compact	25 - 30	170 - 210
	Medium to Compact	15 - 25	100 - 170
	Loose	8 - 15	60 - 100
Homogeneous inorganic clay, sandy or silty clay (CL, CH)	Very stiff to hard	25 - 50	170 - 350
	Medium to stiff	8 - 25	60 - 170
	Soft	4 - 8	30 - 60
Inorganic silt, sandy or clayey silt, varved silt-clay-fine sand (ML, MH)	Very stiff to hard	15 - 30	100 - 210
	Medium to stiff	8 - 25	60 - 170
	Soft	4 - 8	30 - 60

3.4 MITIGATION METHODS

A thorough literature review was then conducted to determine mitigation practices used to prevent the bump at the end of the bridge. The solutions have widely varied for both highways and railways. While some solutions may be advantageous for highway applications, they may not be as useful for railway applications and vice-versa.

3.4.1 Highways

Several solutions have been proposed and used to remedy the bump problem for highways. The most common solution is the approach slab (Fig. 3.13). According to Briaud et al. (1997), the main function of approach slabs is to provide a ramp for the differential settlement between the approach embankment and the bridge. They also prevent water infiltration and erosion of the embankment. Approach slabs are typically 6-12 m long and 225.-30.5 m thick and are supported on one end by the bridge abutment and on the other end by either a sleeper slab or the subgrade itself (Seo 2003). The design, methodology, materials, and construction techniques used by states tend to vary greatly (Hoppe 1999).

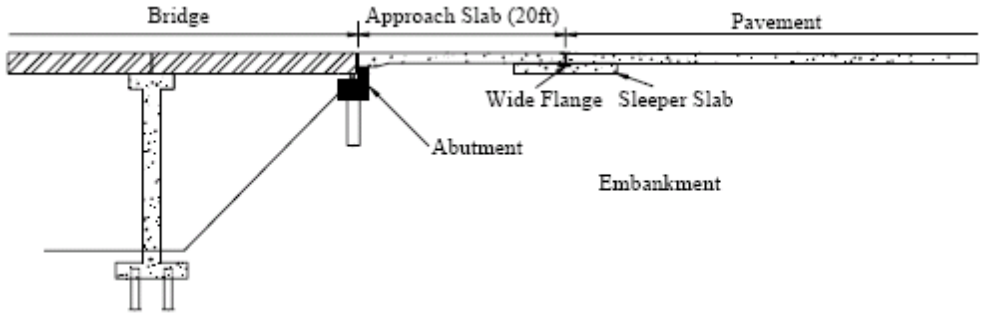

Figure 3.13 –Approach slab schematic (Seo et al. 2002)

Helwany et al. (2003) reported on using segmental block-faced geosynthetic-reinforced soil (GRS) bridge abutments to alleviate bridge approach settlement. Compared to conventional gravity walls, GRS abutments are also more economical and easier to construct. According to the authors, GRS abutments can potentially be used

without piling. A shallow foundation for the abutment would ensure that the abutment moved with the soil, minimizing the bump problem.

Bakeer et al. (2005) report on the performance of pile-supported bridge approach slabs used in Louisiana highways (Fig. 3.14). The piles were empirically designed and installed with the approach slabs after excessive settlement occurred with the slab alone. After review, it was found that, in general, pile-supported bridge approach slabs performed relatively well but some still performed poorly. This inconsistency is attributed to site conditions and differences in drag load. A "trial and error" process of determining the pile lengths is recommended.

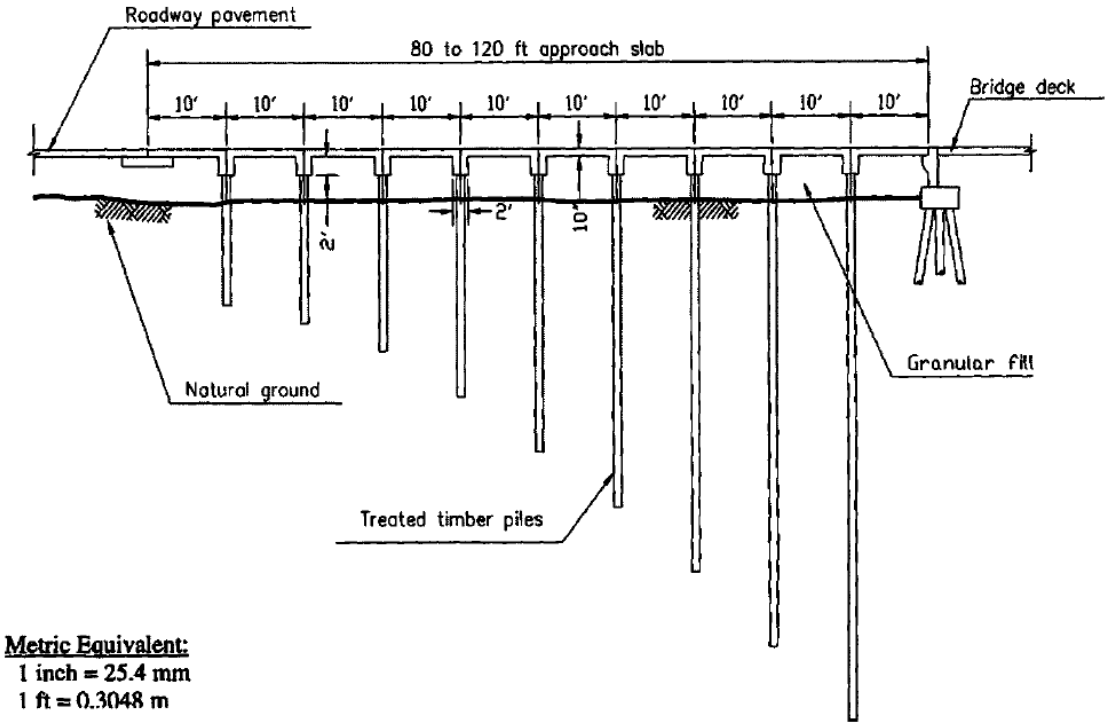

Figure 3.14 - Configuration of pile-supported approach slab (Bakeer et al. 2005) with permission from ASCE

Reid and Buchanan (1984) describe a similar solution to the highway bump problem due to soft soils: the Bridge Approach Support Piling (BASP) system (Fig. 3.15). BASP consists of a geo-membrane atop varying length piles with individual reinforced concrete caps. The idea is for the piles to reduce the load on the surrounding soil in a smooth transition from the bridge abutment to the natural soil of the approach. The membrane serves to encourage soil arching between the pile caps. This solution was proposed over the previous solution of constructing the embankment first, preloading it to speed up settlement and then building the bridge structure because of both time and cost. After monitoring several bridge sites, the BASP proved successful as no apparent differential settlement at the bridge sites were measured.

3.4.2 Railways

For railways, solutions are often defined in terms of categories depending on the main cause behind the problem. These include solutions to reduce settlement of the approach structure, minimize the change in stiffness, reduce ballast wear and movement and increase damping. The choice of solution will typically depend on site dependent factors.

3.4.2.1 Reduce Approach Settlement

The approach structure will likely settle more than the bridge structure. There are several options available to reduce the settlement of the approach structure. For one, adequate drainage must be ensured. Fluctuations in the water content of the soil could pose problems and lead to erosion within the embankment fill. The fill and embankment

materials should also be specified and confirmed. The specification of the approach material is perhaps the most critical action made during construction (Li et al. 2003).

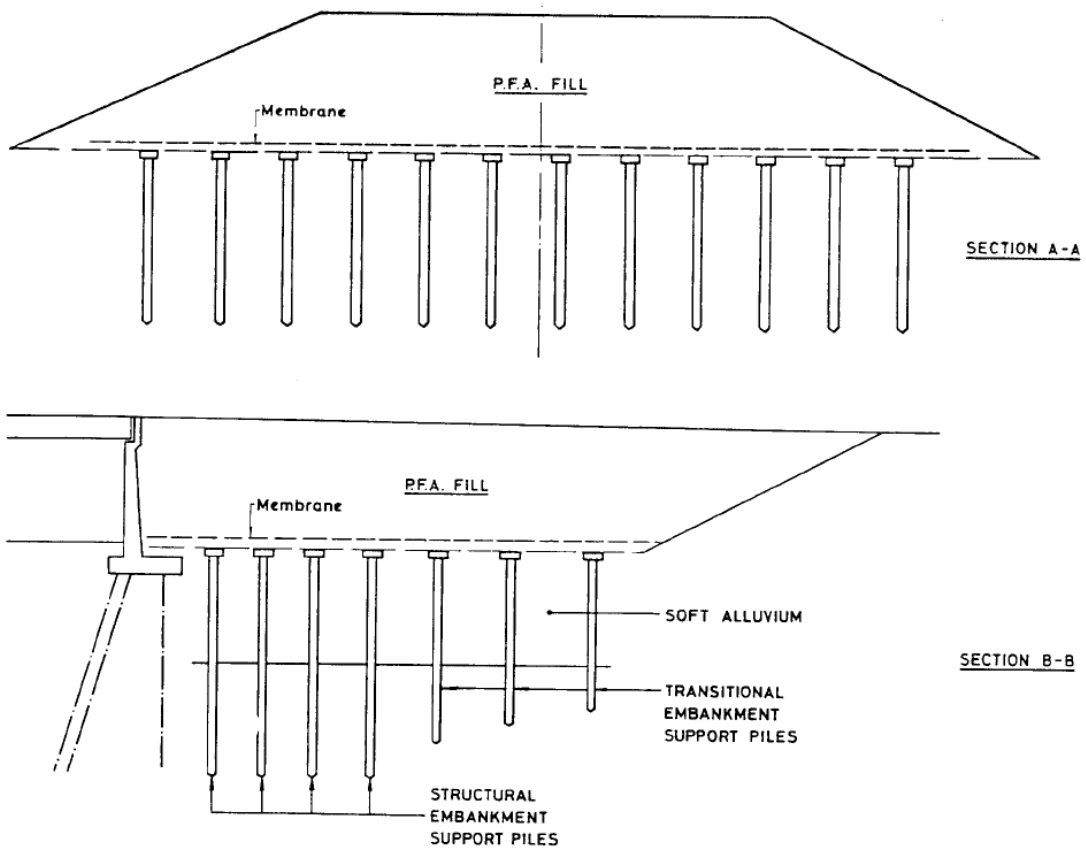

Figure 3.15 - BASP schematic (Reid and Buchanan 1984)

If poor materials are naturally at the site, they should be removed or stabilized by using piles (or other columns), deep soil mixing columns, stone columns, or grout. Piles are used to transfer the load, mainly through skin friction, from the track above to the subgrade reducing the amount of settlement. Deep soil mixing, stone columns and

grouting are used to strengthen the embankment soil by incorporating a hard material into the soil. This provides a strong and relatively incompressible material. Placing inclusions into the soil will therefore strengthen the fill and reduce movements. The cost and down-time of the track for this construction are issues though. These types of solutions are more applicable to new bridge construction.

Li and Davis (2005) reported on field tests of three different solutions installed on the approach on top of the subgrade below the ballast to alleviate the bump problem. The solutions involved 1) a 30 m (100 ft) long, 0.2 m (8 in) thick hot mix asphalt (HMA) underlayment, 2) a 30 m, 0.2 m thick geocell confined subballast layer, and 3) a 3 m (10 ft) long, 2 m (6.75 ft) thick cement stabilized backfill. A control test was also performed with standard track construction at another bridge site. The solutions were designed to reduce the stress on the subgrade, thereby reducing subgrade settlement. They also served to stiffen up the approach section. After running train operations across each ballasted deck concrete bridge site, however, it was found that none of the solutions improved the bump problem compared to the control test. While the track modulus of the approaches increased with each solution, there was still a large differential modulus between the bridge and the approach structures. It was concluded that the change in track modulus must be reduced more gradually to avoid large bump problems.

3.4.2.2 Minimize Differential Track Modulus

Across the bridge transition zone, the modulus increases from the approach structure to the bridge structure. The change in stiffness does create conditions likely to cause track

degradation. To reduce running surface defects, measures must be taken to accommodate the change in stiffness at the bridge transition zone. This can be achieved by either reducing the stiffness on the bridge structure or gradually increasing the stiffness on the approach structure.

3.4.2.2.1 Decrease Modulus on Bridge

One of the most common methods used to reduce the stiffness of the bridge structure is through the placement of pads or mats. Typically made of rubber or polyurethane, they are designed for a desired stiffness on the bridge to approximately match that of the surrounding track (Li et al. 2003). Along with decreasing the stiffness on the bridge, pads or mats can be used to help with damping. They are also cost-effective and relatively easy to install within a short amount of time.

There are four main options: rail seat pads, tie plate pads, under tie pads and ballast mats. Rail seat pads are placed directly under the rail seat between the rail and the tie plate; tie plate pads are placed directly under the tie plate; under tie pads are located directly underneath the tie above the ballast; ballast mats are placed under the ballast section. Each type helps to dissipate track loadings and vibrations. The placement of the pads is determined by where in the track structure damping is needed.

The material of the ties can also be varied to reduce impact loads due to changing stiffness. There are several different materials ties can be made from including timber, concrete, plastic, and steel. To determine the effect of different tie materials on track stiffness, revenue service testing was conducted at test sites in Marysville, Kansas and

Salem, Illinois (Sasaoka 2006). The bridges tested had a concrete span ballasted deck. The stiffness differential between the bridge and the approach structures was minimized the most by using plastic ties (Reiff and Sasaoka 2003).

Installing rubber pads to the bottom of concrete ties is another promising method to reduce the track stiffness differential. The rubber pads tested at the sites actually decreased the bridge modulus to a value lower than the approach modulus. Two different types of rubber pads were tested. Made by two different companies, both pads seemed to work similarly.

3.4.2.2.2 Increase Modulus on Approach

The stiffness on the approach structure can be gradually increased through approach slabs, gradually increasing the length of the ties, placing a layer of HMA, geocell, or other similar material above the subgrade, or using extra rails between or outside of the running rails.

Approach slabs are commonly built as a cantilever with the fixed end supported by the rigid bridge structure. The free end is then supported by the subgrade. The main purpose of approach slabs is to provide a ramp for the differential settlement (Hoppe 1999). Rather than a bump, a slope develops which can lessen the impact effects on the track. The allowable criterion for this slope is less than 1:200 for highways (Briaud et al. 1997). For railways, the limits for this slope have yet to be defined exactly. Another purpose of approach slabs is to prevent water from leaking in between the embankment and the bridge structure. This prevents erosion and soil movement.

Typically, the approach slab thickness decreases further from the bridge in order to modify the stiffness of the track over the approach (Li et al. 2003). The use of an approach slab depends on the amount of anticipated differential settlement, the degree of compaction, and the quality of drainage. For highways, the use of an approach slab has a significant impact on reducing the bump problem (Briaud et al. 1997). The disadvantage of an approach slab lies in maintenance costs and slab repairs. This occurs when settlements exceed their designed tolerable limits (Hoppe 1999).

Another method used to increase the track stiffness in the approach section is to gradually increase the length of the ties in the approach zone (Li et al. 2003). This reduces the amount of differential settlement between the bridge and approach structures. Standard gauge track ties are typically 8’ to 8.5’ in length. The length impacts the surface area over which the load is spread onto the ballast. Also, reducing tie spacing and increasing the tie width can help increase the stiffness of the approach (AREMA 2008).

3.4.2.3 Reduce Ballast Wear and Movement

Ballast memory causes increased impact loads and thus, increased differential settlement. The way to avoid this is to optimize the energy absorption of the ballast. This can be done using retaining walls or bonding agents. The movement of the ballast can be restricted through the placement of side retaining walls which help to control the lateral and vertical displacement of the ballast. Another method is to use a bonding agent to glue the ballast particles together (Li et al. 2003).

3.4.2.4 Increase Damping

At track transitions, damping differs between the approach and bridge structures. The approach tends to help decay accelerations faster than the bridge, indicating more damping (Sasaoka 2006). Damaging vibrations on the track are a result of inadequate damping in the system. As impact loads are placed on the bridge structure, the track must be able to sufficiently dissipate the resulting energy. The use of rubber pads under ties is not just for reducing the modulus on the bridge structure. Laboratory tests point to an increase of 50% in damping levels on bridges by using rubber pads under concrete ties (Sasaoka 2006).

4. SURVEY OF CURRENT PRACTICE

4.1 SURVEY DESCRIPTION

The current views on the causes, problems and mitigation measures associated with the bump at the end of the bridge are reviewed in this section. These views were found through a survey which was distributed across the world to various railroad companies and personnel. Fourteen responses, representing nine different companies (Table 4.1), were returned for evaluation. The survey questionnaire can be found in Appendix A. A complete list and summary of the responses is located in Appendix B.

Table 4.1 - Companies responding to the survey

No. of Responders	Company
1	Austrian Railways
1	Canadian National
1	Canadian Pacific Railway
1	FRA
1	Norfolk Southern
1	Queensland Rail
1	Savage Industries/CANAC
2	Transportation Technology Center, Inc.
5	Union Pacific

4.2 CURRENT STATE OF PROBLEM

Based on the survey responses, the bump problem affects, on average, 51% of railroad bridges. This is double the number of highway bridges that are affected. The typical

bridge consists of an open bridge deck (with height less than or equal to 3.05 m) resting on a deep foundation (e.g. piles) with no skew. As a majority, the respondents did not know what type of soil is typically used as compacted fill or as foundation soil.

A tolerable bump has yet to be strictly defined in the railroad industry. Most companies rely on visual inspections rather than measurements in deciding when to fix the bump problem. The annual cost of maintenance for the affected bridges of each company, including both internal and contracted, is estimated at $23 million total. This represents an average cost for each railroad company of $2.55 million per year. In other terms, the average cost for each railroad company is approximately $6,000 per million gross tons (MGT). The estimated annual cost from the survey is close to the figure of $26 million per year predicted in AAR's 2008 Strategic Research Initiatives (SRI) plan. Although the respondents do not see the bump as a major problem, it is a nuisance that leads to track degradation and increased maintenance costs.

Among those surveyed, the typical bump size ranges from ¼" to 4" with an average difference in elevation of 1.3" along the rail profile. The horizontal length over which the bump occurs also varies, ranging from 4' to 50' with an average of approximately 17'. This leads to an average slope for current bumps equal to approximately 1:150. This slope is worse than the tolerable slope of 1:200 allowed for highway bridges (Briaud et al., 1997). It is also not acceptable according to those surveyed, who defined a tolerable slope for railroad bridges as about 1:250.

4.3 CAUSES

The common causes of the bump problem were evaluated by the survey respondents. Each respondent ranked a given contributing factor on a scale of 1 to 4, with 1 representing the “most common” and 4 representing “never a factor.” The results are summarized in Table 4.2. Based on these results, the most common factors leading to the bump are settlement of the fill, differential track modulus, poor surfacing, improper tamping and poor maintenance practices. The least common were lateral movement of the bridge abutment, settlement of the natural soil under the bridge abutment and poor construction specifications.

The cases where the problem appears to be worse are when: the bridge is an open deck bridge, the bridge is made of concrete and has concrete ties, concrete approach ties are used and wet conditions are present. Conversely, the cases where the problem appears to be minimized are when: the bridge is a ballasted deck bridge, the bridge/approach location is well maintained and there is good drainage.

4.4 DETECTION AND REPAIR METHODS

Finding the exact location and nature of the bump requires inspection of the track on and near a bridge site. There are many current detection methods used by companies to find the problem (Table 4.3). The most common is through visual inspection. Many bumps/dips are fairly shallow, however, so it may not be visually noticed until the problem is more severe. The track geometry evaluation car is another widely used

method to measure and depict the rail profile. Since the car simulates the loading of an actual railcar on the track, the results are more accurate.

Table 4.2 - Factors contributing to the formation of the bump

Ranking	Topic
1	Settlement of fill
1	Others: difference in track modulus at transition, poor surfacing, not tamping approach properly, poor maintenance practices by bridge and track forces
3	Poor drainage
3	Dynamic impact of cars
5	Poor compaction of ballast on fill
5	Differential settlement between bridge and fill
7	Poor joints
7	Bridge type
7	Poor fill material
10	Loss of fill by erosion
10	Abutment type
10	Settlement of natural soil under the fill
13	Too rigid a bridge foundation
14	Poor construction practices
14	Temperature cycle
16	Poor construction specifications
17	Settlement of natural soil under the bridge abutment
18	Lateral movement of the bridge abutment

Table 4.3 – Current bump detection methods

Ranking	Topic
1	Visual inspection
2	Track geometry evaluation car
3	Complaints from user
4	Ridability (subjective)
5	Ridability (quantitative)
6	Ride quality accelerometers
7	Non-destructive tests (NDT)
Others	Measure track stiffness or use survey equipment

Complaints from the user and subjective ridability are similar to visual inspections. These types of methods provide companies the information that a bump exists and if it is relatively dangerous. The size and slope of the bump/dip, however, are not quantified.

To help quantify the effects of the bump, ride quality accelerometers are typically placed on a locomotive to measure the response of the car on the track. Locations with degradation, such as at the bridge transition zone, will be detected with these instruments. Non-destructive tests (NDT) are rarely used to detect the problem.

Once a problem has been detected, the proper repair method can be chosen (Table 4.4). The most popular among those surveyed is leveling by ballast tamping. Tamping of the ballast tries to pack the ballast back underneath the track to make it more durable. Assuming ballast memory has not become a problem, this method works well. The more expensive methods, such as improving the properties of the fill or natural soil under the fill, retrofitting with an approach slab, and mud jacking are less desirable for repair.

4.5 DESIGN AND CONSTRUCTION PROCEDURES

It is easier to deal with the bump problem for new bridge construction rather than for an old bridge because the design and construction can be controlled. Current practice concerning the bump varies among railroad companies. A standard design procedure across the industry has not been made. The most common methods used during the design stage are listed in Table 4.5.

Table 4.4 – Current bump repair methods

Ranking	Topic
1	Leveling by ballast tamping
2	Eliminate rail joints from the transition area
3	Others: track surfacing, retrofit track on bridge to match approach stiffness, dig out mud and replace track ties and ballast, install transition ties (longer bridge approach ties)
4	Drainage improvements
5	Retrofit with an approach slab
6	Improve the properties of the natural soil under the fill
7	Improve the properties of the fill
8	Mud jacking
9	Remove and replace approach slab

Table 4.5 – Current bump design procedures

Ranking	Topic
1	Better cooperation between the track maintenance supervisor and bridge maintenance supervisor
2	Improve drainage provisions
3	Avoid open deck bridges
4	Specify better backfill
4	Use more rigorous compaction specifications
6	Other: avoid skew, particularly for open deck bridges
7	Confine the approach fill parallel to track retaining walls
8	Design better joint at bridge-embankment connection
9	Use a properly designed approach slab
10	Design the bridge abutment and approach fill so they settle by approximately the same amount
11	Allow for more settlement under the bridge abutment
12	Place the bridge abutment on spread footings

Based on the survey, the most popular design measure is to simply have better cooperation between the track maintenance supervisor and the bridge maintenance supervisor. Another common design procedure for new bridges is to improve drainage and avoid open deck bridges. Open deck bridges, as opposed to ballasted deck bridges, are more rigid creating higher impact forces and thus, bigger bumps/dips at the bridge/approach location.

The least used design procedure is to place the bridge abutment on spread footings. Currently, abutments are founded on deep piles to restrain vertical settlement. If the abutment was placed on a shallow foundation such as spread footings, however, the bridge would tend to move with the embankment fill. This would reduce differential movement. Bridge stability and soil bearing capacity must be taken into account before using a shallow foundation though.

Construction practices are as important as the design stage for new bridges. The methods used could impact the formation of a bump at the end of the bridge (Table 4.6). The most popular procedure recommended by those surveyed is to have better compaction control of the fill. Typically, current compaction methods do not allow for compaction very close to the bridge abutment because of the lack of adequate space for the equipment at this location. This can lead to differential settlement and possible erosion of the fill. Other mitigation methods include stiffening up the approach embankment with various solution methods as discussed in Section 3.

The survey provided valuable information about the state of practice for the railroad industry concerning the bump at the end of the bridge. The main conclusion from the survey is that differential settlement must be accommodated so that a tolerable ramp can develop as opposed to a steep bump. It seems as if the bump is unavoidable in the long-term. Solutions and factors to minimize the bump/dip that does form are necessary, however, to mitigate the problem.

Table 4.6 – Current bridge/approach construction procedures

Ranking	Topic
1	Better compaction control of the fill
2	Others: geo-piers, longer bridge approach transition ties, prevent ballast runoff at approaches by installing L-walls
3	Install rubber pads under ties on bridge
4	Improved abutment design
5	Waiting period after the fill construction prior to placing the abutment
6	Install rubber pads under ties on fill

5. 4-DIMENSIONAL FINITE ELEMENT MODEL

To better understand the system, HyperMesh was used to model the components involved while LS-DYNA was used to simulate the dynamic motion. HyperMesh is a powerful pre-processor and LS-DYNA, according to FEA Information (2006), is "the most advanced general purpose nonlinear finite element program capable of simulating complex real world [dynamic] problems."

5.1 VEHICLE AND TRACK MODELS

5.1.1 Vehicle

Typical dimensions for an 890 kN (100 ton) capacity freight car were used in the model (Fig. 5.1). All material and section properties, except for the wheel and the suspension springs and dampers, were assumed to be rigid and solid, respectively.

Table 5.1 – Model vehicle properties

Component	Material	ρ (kg/m^3)	E (MPa)	v	K_s (N/m)	C_d (N s/m)	Section
Wheel	Rigid (Elastic Contact)	7850	200000	0.28	-	-	Solid
Axle	Rigid	7850	200000	0.28	-	-	Solid
Side Frame	Rigid	3816	200000	0.28	-	-	Solid
Bolster	Rigid	2897	200000	0.28	-	-	Solid
Car Mass	Rigid	2.2E+07	200000	0.28	-	-	Solid
Spring	Elastic	-	-	-	2257535	-	Discrete
Damper	Viscous	-	-	-	-	25000	Discrete

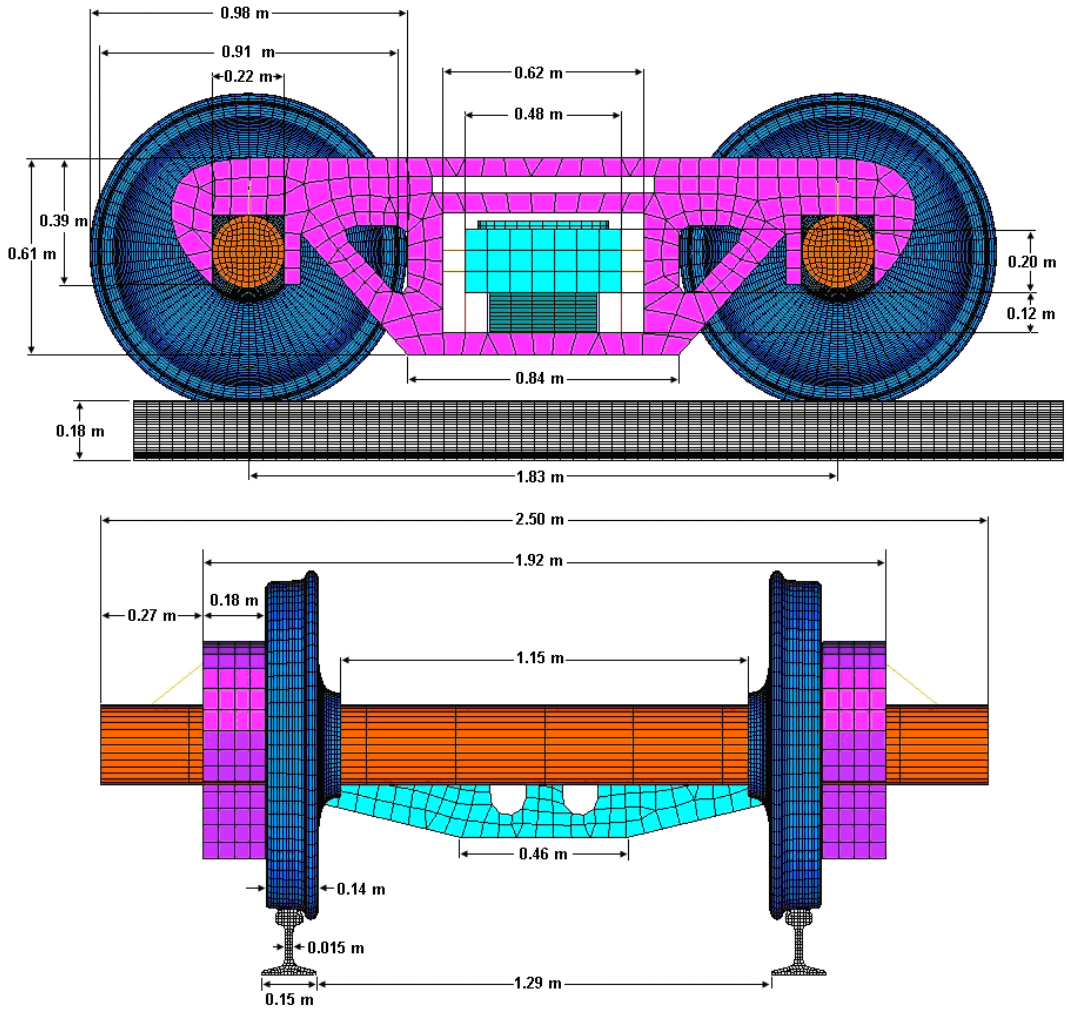

Figure 5.1 – Model vehicle dimensions

Material properties for the wheel and axle components were assumed to be representative of steel, with a density of 7850 kg/m^3 (0.49 kcf), a modulus of 200,000 MPa (4.18x10^6 ksf), and a Poisson's ratio of 0.28. The wheel is assumed to be rigid except for the contact surface of the wheel (Fig. 5.2). This technique is useful to mimic the contact behavior, yet save on computation time. The densities for the side frame, bolster, and car mass components, however, were chosen based on an assumed weight

(Table 5.2). The values do not reflect actual values for steel. This is because the side frame and bolster are not complete solid sections in reality.

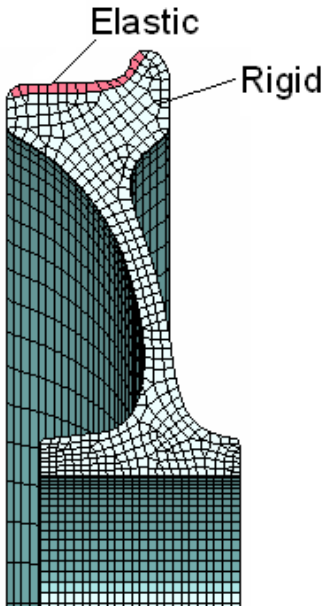

Figure 5.2 - Cross-section of wheel with elastic and rigid elements

Table 5.2 – Model component weights

Component	Weight (N)	No. of Components	Total Component Weight (N)
Wheel	3557.5	4	14230
Axle	7632.8	2	15265.6
Side Frame	4389.2	2	8778.4
Bolster	4561.9	1	4561.9
Car Mass	541949.4	1	541949.4
Spring	-	4	-
Damper	-	4	-
		Total Weight (N)	584785.3
		Weight/Wheel (N)	**146196.325**

To account for this in the vehicle model, which consists entirely of solid sections, the density of the side frame and bolster were changed to 3816 kg/m^3 (0.24 kcf) and 2897 kg/m^3 (0.18 kcf), respectively. The car mass, located in the centerplate of the bolster, served to simulate the loading of half a fully loaded, 890 kN (100 ton) railcar. The density of the car mass was therefore chosen as 2.2x10^7 kg/m^3 (1370.33 kcf) rather than the typical value of 7850 kg/m^3 for steel. The total weight of the model is therefore 584785 N (131500 lb), or 146.2 kN/wheel (32.9 kips/wheel).

Four discrete element springs and dampers were used to simulate the suspension of the truck (Fig. 5.3). Each spring has a stiffness coefficient, K_s, of 2,257,535 N/m (12889.7 lb/in), and each damper had a damping coefficient, C_d, of 25,000 N s/m (142.74 lb s/in). The spring stiffness, K_s, was chosen based on a load rate, K, of 25,783 lb/in (4,515,300 N/m) for a spring grouping of 9 outer and 5 inner D5 springs (ASF User's Guide). This K value represents the stiffness of one side of the truck. Since the model contains two springs per side, the number is divided by 2 to obtain K_s. The damping coefficient, C_d, was chosen based on an average value from a previous survey (Sun et al., 2003).

To limit the bolster's horizontal, back-and-forth motion, two very stiff horizontal side springs, with negligible weight, were added to each side of the bolster connecting it to the side frames. A high stiffness, K_{ss}= 5 x 10^9 N/m (2.8 x 10^7 lb/in), was assigned to these components. In reality, friction wedges are used to constrain the bolster within the side frame. For this simple truck model, however, side springs are considered adequate

to model the constraint. If vehicle dynamics are of concern, then the friction wedges should be included.

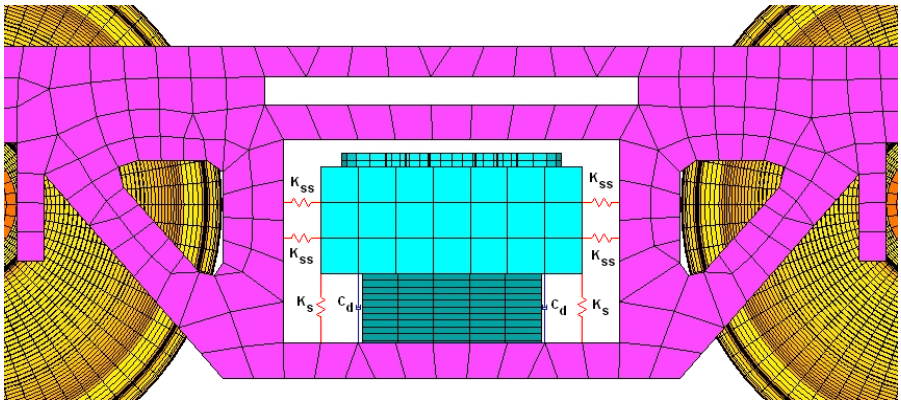

Figure 5.3 – Model truck suspension system

Rigid beams of insignificant mass and finite length are attached to the side frames directly above the axis of rotation to the center of the axle (Fig. 5.4). This serves to connect the two components and ensure their relative positions during movement. Spherical joints are used to define the rotation of the axles (LSTC 2007). They are placed at the interface between the rigid beams and the axles.

5.1.2 Track

The track was modeled after a 661.6 N/m (136 lb/yd) rail. As such, the beam area and moment of inertia were assigned as 8.58 x 10^{-3} m^2 (13.3 in^2) and 3.9 x 10^{-5} mm^4 (94 in^4), respectively (AREMA, 2008). The track is modeled as beam elements that are rigidly

connected to shell elements around it (Fig. 5.5). The beam elements actually define the behavior of the rail. The shell elements serve only to define the contact shape of the rail. The track is attached with revolute joints to the tie. The ties are made of wood and have dimensions of 0.22 m x 0.17 m x 2.59 m. The ties are spaced at 0.5 m center-to-center.

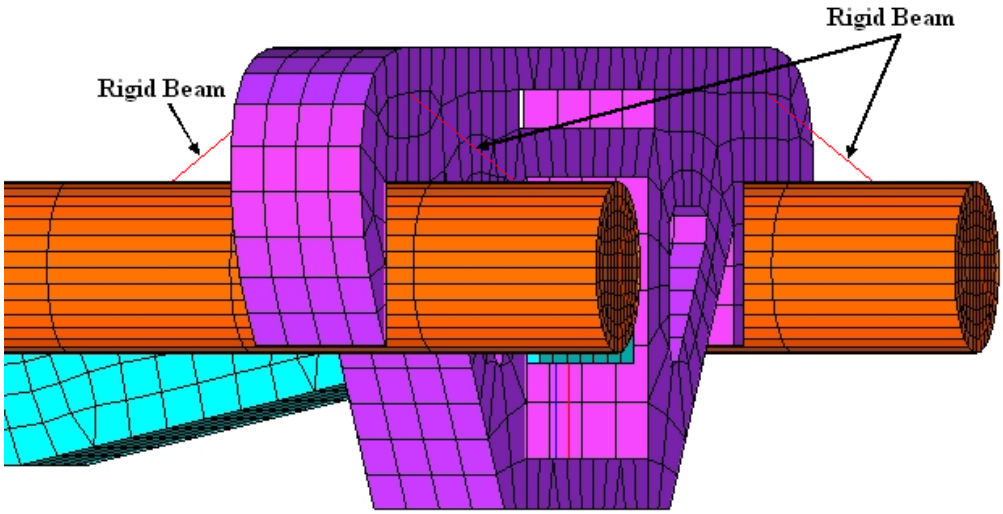

Figure 5.4 - Rigid beams connecting side frame model to axle

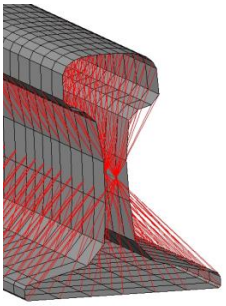

Figure 5.5 - Rail model

5.1.3 Wheel/Rail Contact

A “Surface_To_Surface” contact was defined in LS-DYNA between the outer surfaces of the wheel and the tracks (Fig. 5.6). The penalty method is used to define the contact between the two surfaces. The outer, elastic elements of the wheel comprise the slave surface while the top, outer elements of the track comprise the master surface. If the slave nodes penetrate the master nodes, a penalty algorithm will place normal interface springs between the contact surface and the penetrating nodes (Hallquist 2006).

In LS-DYNA, friction is based on a Coulomb formulation (Hallquist 2006). A value of 0.4 was given for the static friction coefficient. A value of 0.35 was given for the dynamic coefficient of friction.

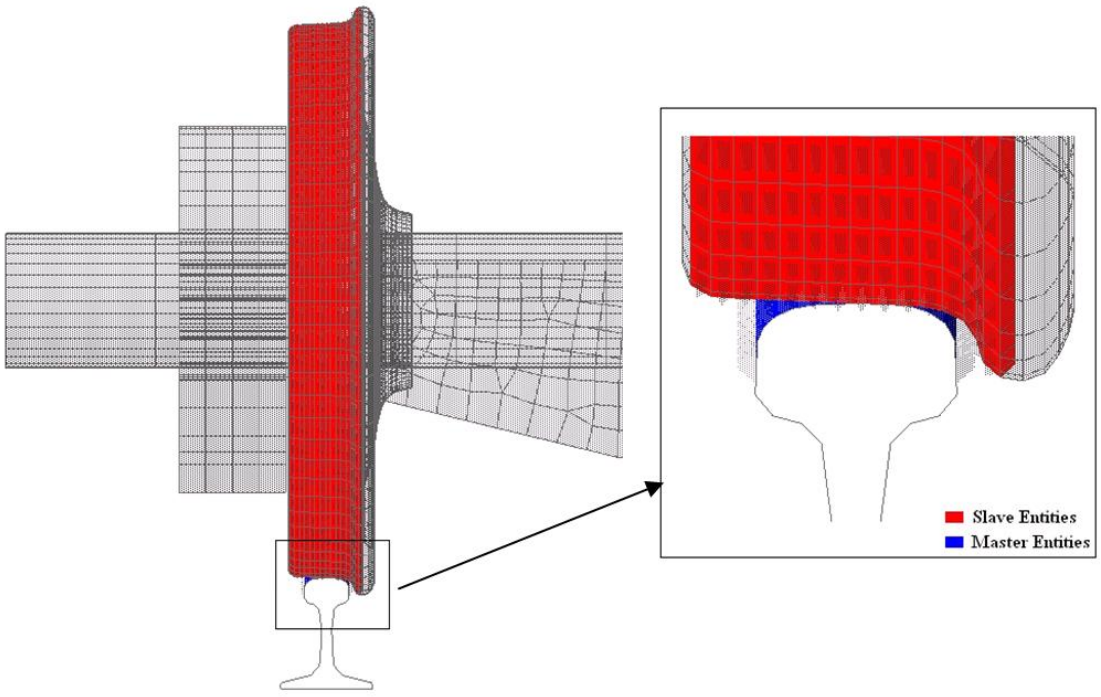

Figure 5.6 - Wheel/Rail contact surfaces

The vertical wheel/rail forces between the contact surfaces were calculated according to Newton's second law of motion ($F = \Sigma ma$). The acceleration time histories of each truck component were used to calculate the wheel/rail forces. These included the front and back wheel sets (A_F and A_B), the right and left side frames (S_R and S_L) and the car body (C). The accelerations of the car body include the response of the suspension system. A free-body diagram of the truck is shown in Fig. 5.7. Note that LS-DYNA does provide a result called "rcforc" which is supposed to give the reaction force between the wheel and rail contact surfaces. On level track, the rcforc results are equal to those calculated, but not on the bump/dip where the values are elevated above expectations. The reason behind this has not been found.

The normal force (N) between the wheel and the rail is therefore solved through equilibrium (Eq. 5.1).

$$F = \sum_{i=1:N}^{N} m_i a_i \tag{5.1}$$

where m is the mass of the component, a is the acceleration of the component and N is the total number of components. The normal force (and friction force) between the wheel and rail is assumed to be equal for all wheels. This means that rocking or rolling is not captured by the reaction forces. While this does not represent actual conditions, it simplifies the analysis and provides average forces.

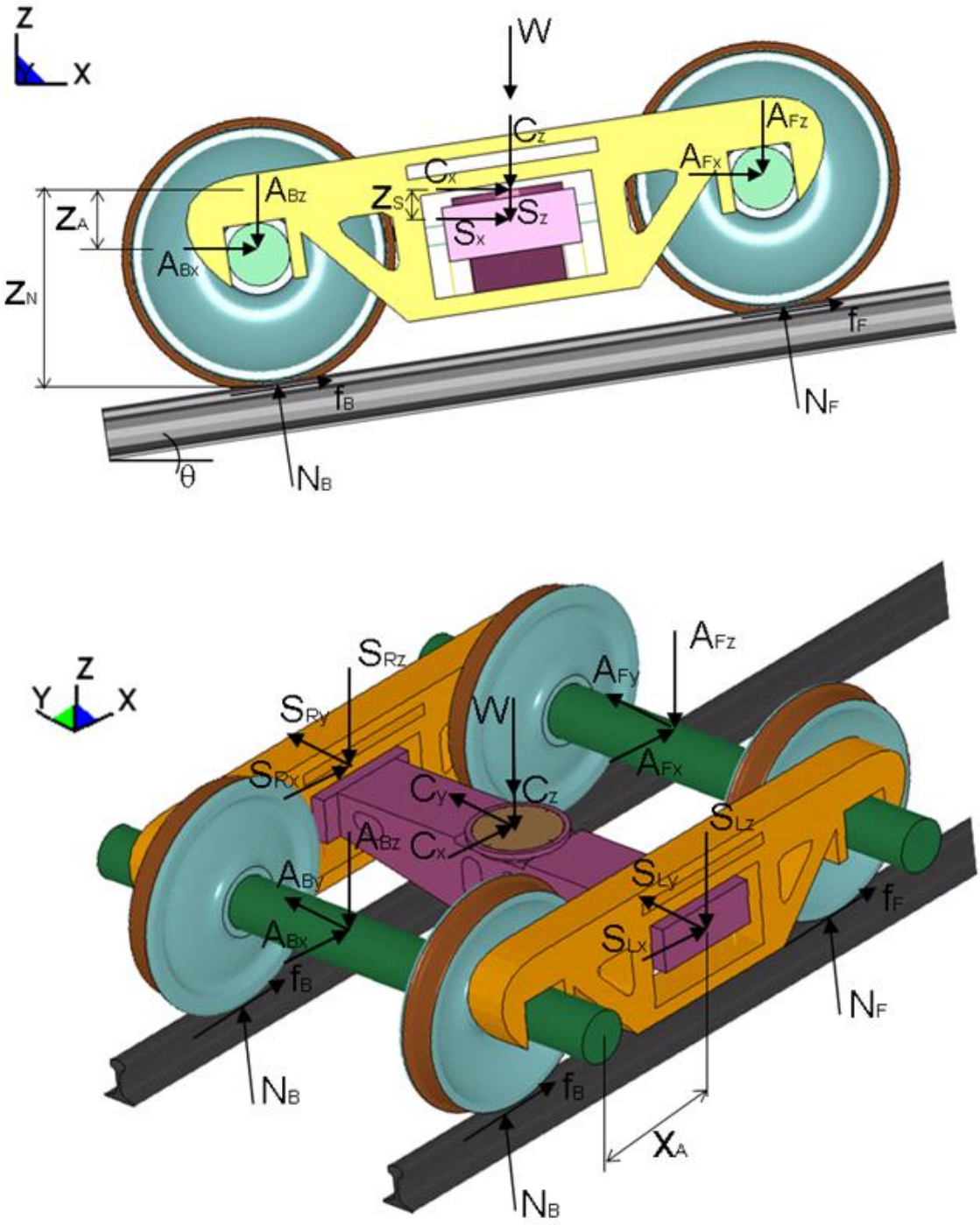

Figure 5.7 - Free body diagram of forces on truck model

The difference between the front and back wheel forces is also small. Data recorded with instrumented wheel sets (Section 8) indicates that at 17.9 m/s, the difference between the front and back wheel/rail forces was only about 1.5%. The equilibrium equation used to calculate the wheel/rail forces is presented in Eq. 5.2.

$$N = \frac{1}{4}\begin{pmatrix} W\cos\theta + m_{A_F} A_{F,z}\cos\theta + m_{A_B} A_{B,z}\cos\theta + m_{A_F} A_{F,x}\sin\theta + m_{A_B} A_{B,x}\sin\theta + \ldots \\ \ldots + m_{S_L} S_{L,z}\cos\theta + m_{S_R} S_{R,z}\cos\theta + m_{S_L} S_{L,x}\sin\theta + m_{S_R} S_{R,x}\sin\theta + \ldots \\ \ldots + m_C C_z \cos\theta + m_C C_x \sin\theta \end{pmatrix} \quad (5.2)$$

5.2 APPROACH EMBANKMENT

The approach embankment is comprised of the ballast, subballast, fill material, and natural subgrade material (Fig. 5.8). The thickness of the ballast and subballast is approximately 0.26 m (10 in) and 0.15 m (6 in) thick, respectively. The total granular thickness under the rail is therefore 0.41 m (16 in). The fill and the natural subgrade are 1.85 m (6 ft) and 2.86 m (9.4 ft) thick, respectively.

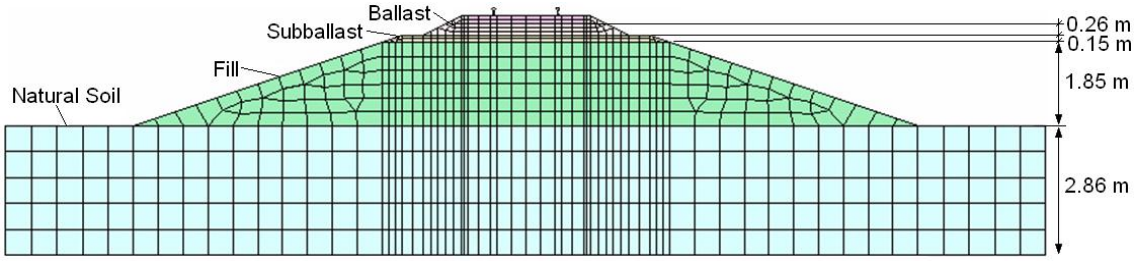

Figure 5.8 - Approach model cross-section

5.2.1 Material Properties

The properties of each layer are given Table 5.3, where E is the modulus of elasticity, ρ is the mass density, v is Poisson's ratio, G is the shear modulus, and v_s is the shear wave velocity. G and v_s were calculated according to Eqs. 5.3 and 5.4. The properties were chosen such that the approach track modulus equals 32 N/mm/mm (4700 lb/in/in).

Table 5.3 – Approach model material properties

Material	ρ (kg/m^3)	E (MPa)	G (MPa)	v_s (m/s)	μ
Ballast	1836	150	57.7	177.3	0.3
Subballast	2173	80	29.6	116.8	0.35
Fill	1836	35	13	84	0.35
Soil	1836	20	7.4	63.5	0.35

$$G = \frac{E}{2(1+\upsilon)} \tag{5.3}$$

$$v_s = \sqrt{\frac{G}{\rho}} \tag{5.4}$$

Each layer is assumed to be an elastic material. Soil is not perfectly elastic, but under small strain conditions, it is a good assumption. Permanent deformations therefore cannot be found with this initial model. Since this is a new model, however, it is important to look at the problem in the simplest fashion as with an elastic soil model. Adding soil constitutive models, such as Drucker-Prager, should follow to examine the effect on permanent deformations of the track substructure. It is outside the scope of this research though.

5.2.2 Soil Damping

Soil damping was incorporated into the model using the Rayleigh damping. In this type of damping, the damping matrix ([C]) is assumed to be proportional to both the mass ([M]) and stiffness ([K]) matrices (Eq. 5.5).

$$[C] = \alpha[M] + \beta[K] \tag{5.5}$$

Rearranging Eq. 5.5, the proportionality constants, α and β, are found knowing the natural frequencies of the soil (ω_i) and the damping ratio (ξ) (Eq. 5.6). In Eq. 5.6, δ_{ij} is the Dirac delta function. An equivalent natural frequency for the entire track substructure was calculated using a weighted average of the shear wave velocity ($v_{s,avg}$) in Eq. 5.7.

$$2\omega_i \xi_i \delta_{ij} = \alpha + \beta\omega_i^2 \tag{5.6}$$

$$\omega_i = \frac{\pi v_{s,avg}}{2H}\ 2i - 1 \tag{5.7}$$

The first (i = 1) and third modes (i = 3) of the natural frequency were used, along with a damping ratio of 5% to calculate α and β as 2.15 and 0.00065, respectively. The transition section, where the bump or the dip is located, has the same material and damping properties as the approach section.

5.3 BRIDGE

Two bridge models were developed for this study: an open deck bridge and a ballast deck bridge (Figs. 5.9-5.10). An open deck bridge does not have ballast underneath the ties whereas a ballast deck bridge does. The ballast serves to make the bridge less stiff

than an open deck bridge and also aids in track damping. As such, a ballast deck bridge is less severe than a open deck bridge. This is confirmed by the results of the survey discussed in Section 4.

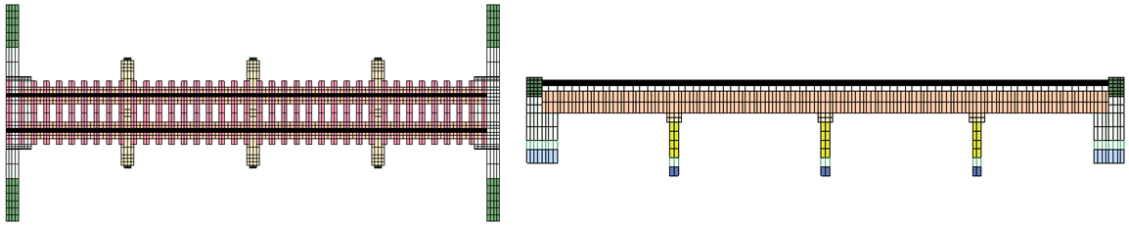

Figure 5.9 - Open deck bridge model

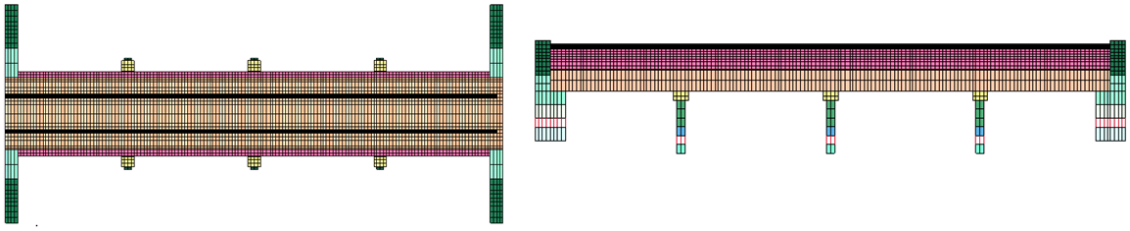

Figure 5.10 - Ballast deck bridge model

For both bridges, the bridge beams were modeled as steel W30x108 sections. Similar to the track, the bridge beams have shell elements rigidly tied around them to give the shape of the beam in the model (Fig. 5.11). The ballast thickness for the ballast deck bridge is approximately 257 mm (10 in). The bridge deck holding the ballast is made of concrete.

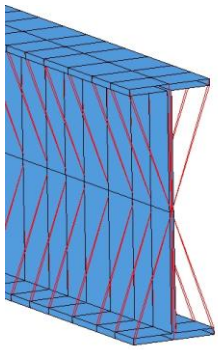

Figure 5.11 - Bridge beam model

Springs are attached to the bottom of the abutment and to the piles to simulate the soil (Fig. 5.12). In reality, the piles would extend deep to a competent soil layer. To simulate this condition without increasing the number of elements in the model, the soil supporting the piles is modeled as springs. A spring stiffness of 1250 N/mm (7138 lb/in) for each spring was chosen based on a bridge track modulus of 83 N/mm/mm (12000 lb/in/in).

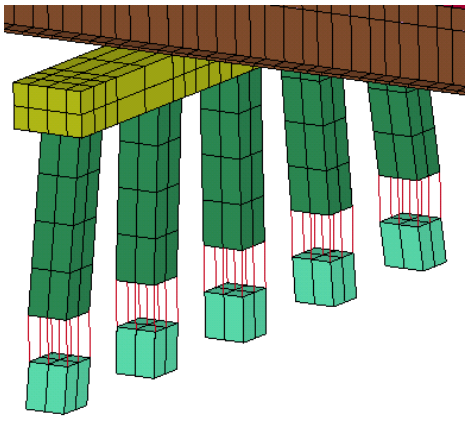

Figure 5.12 - Soil springs for bridge model

In total, the entire model has approximately 270,000 – 300,000 elements. Using finite element analysis, there are many different types of results that can be produced. For this study, the reaction force between the wheel and the rail, the track deflection, the ballast pressures and the subgrade pressures are the results of interest. These will provide a complete picture of the track response due to a bump/dip in the track profile.

5.4 BOUNDARY CONDITIONS

The boundary conditions imposed on the model include roller supports which allow for the vertical motion on the sides of the approach embankment model. Pin supports, restricting movement at the bottom of the model, were also imposed to simulate a bedrock location (Fig. 5.13 and Fig. 5.14).

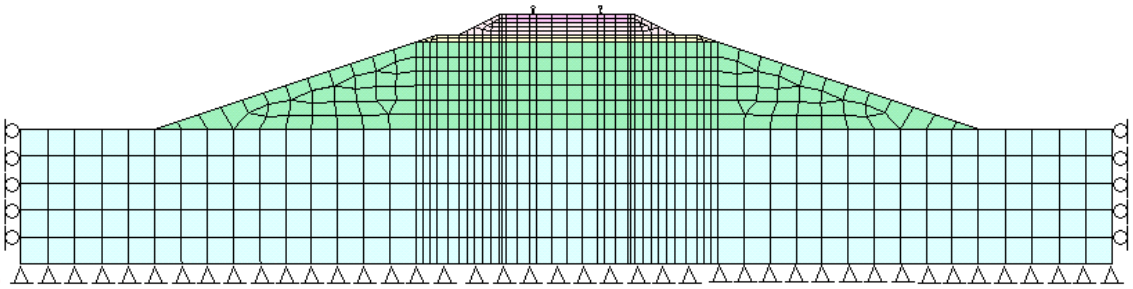

Figure 5.13 –Boundary constraints on model (cross-section)

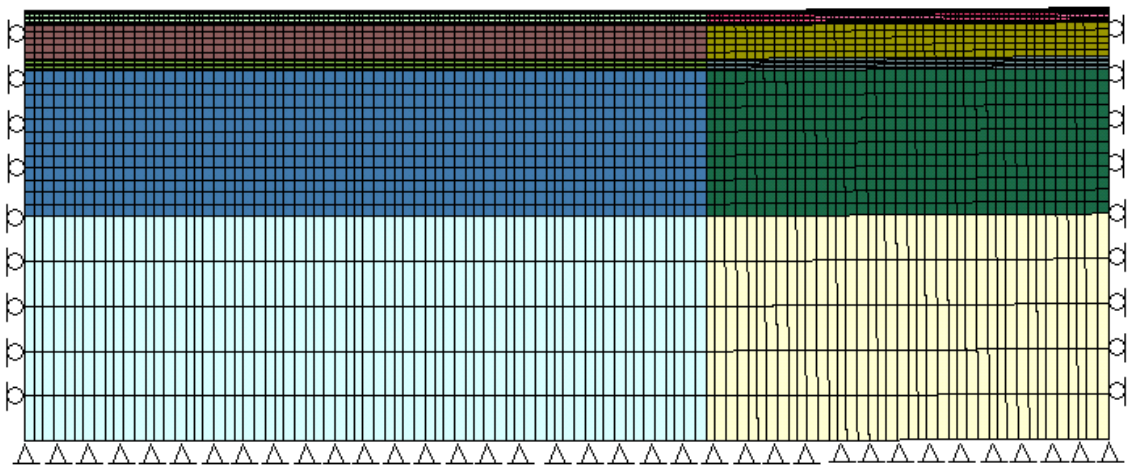

Figure 5.14 - Boundary constraints on model (side view)

5.5 MODEL VALIDATION

Before relying on the model to simulate the bump at the end of the railway bridge, it must first be validated. This is accomplished statically by comparing the track deflection to the analytical solution (Eq. 2.2). In the model, a point load of 100 kN was placed on the center of the rail head at a location on the track right above the tie. The subsequent track deflection was found (Fig. 5.15). Good agreement is seen between the model and the analytical solution. The track deflection over 1 m away from the point load, however, differs slightly between the model and the analytical solution. This is likely due to the nature of the finite element model. The track components, such as the ties, are connected to the ballast and do not allow for separation at the nodes. This restricts the upward movement of the track in the model.

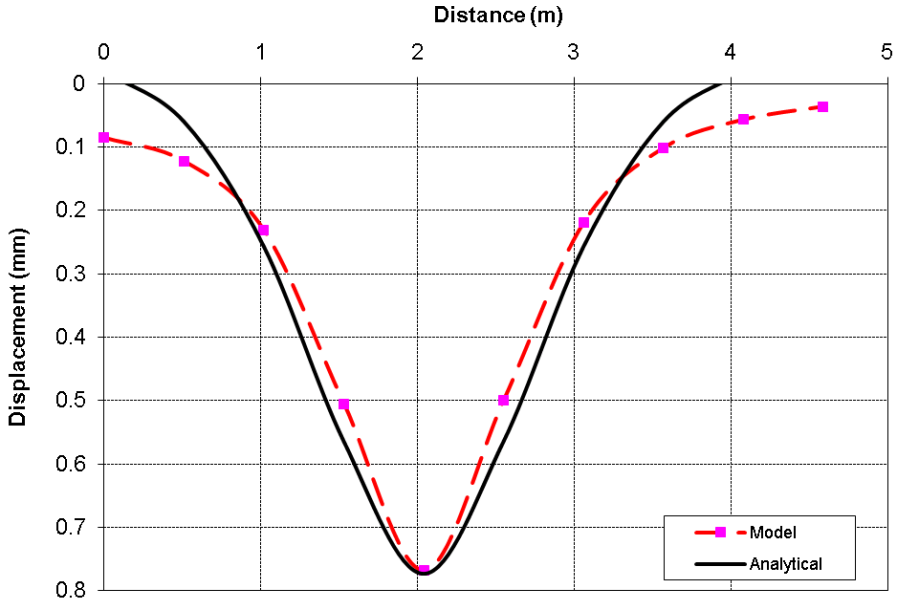

Figure 5.15 – Comparison of model and analytical solution for track deflection

The model was validated dynamically by simulating the vehicle moving across the approach embankment with no bump or dip. As expected, the reaction force between the wheel and the rail is centered on the static wheel load of 146 kN (Fig. 5.16). The sampling rate for the data is 2000 Hz. The unfiltered force signal is mainly produced by high frequency loadings. Forces representing P2 forces are also present at around 50 Hz.

An FFT of this signal shows dominant frequencies, however, between a range of 400 to 600 Hz with the peak around 450 Hz (Fig. 5.17). These frequencies are reasonable according to reported values in the literature (Section 2) and correspond to the movement of the rail relative to the ties (Singh et al. 2004). This mode shape was validated at 450 Hz by running an implicit analysis using LS-DYNA. Further dynamic validation of the model will occur in later sections. This includes comparing the model

results for track deflection and subgrade pressure to that found in the literature and through field testing.

A 10 Hz SAE low pass filter was applied to the unfiltered force signal. This filtering technique removes the high frequency components of the signal. A value of 10 Hz was chosen based on a review of the literature. FRA filtering requirements are 10 Hz for vehicle/car body accelerations and 25 Hz for wheel/rail force measurements (FRA 2003). Similarly, Australian railway standards suggest filtering all acceleration signals below 10 Hz (Bleakley 2006). This value of 10 Hz is likely chosen because, at typical freight speeds, the meaningful characteristic frequencies are less than 10 Hz (Oldknow and Reiff 2006). Low frequencies are also more of a factor for ballast and subgrade deterioration which largely impacts the bump at the end of the bridge.

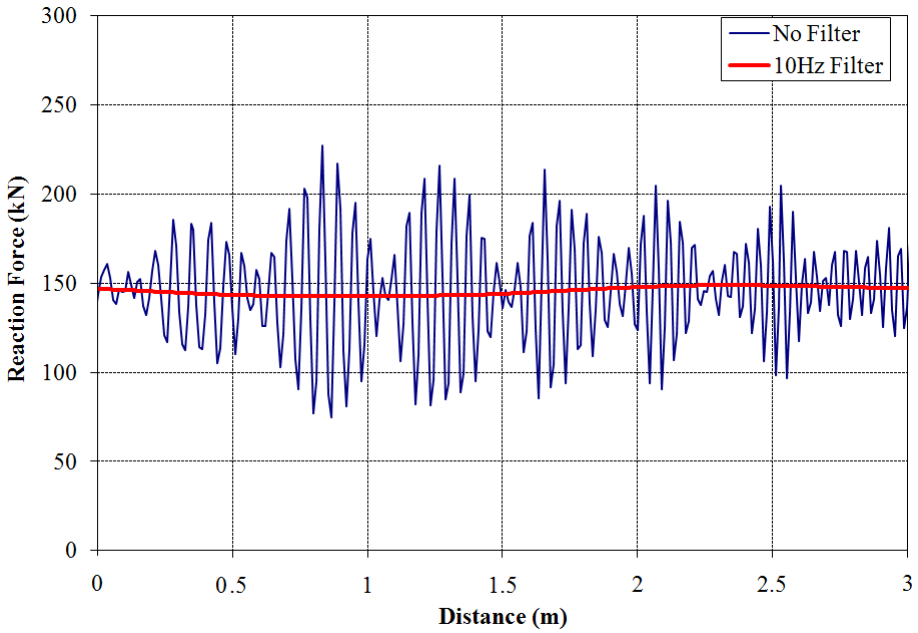

Figure 5.16 – LS-DYNA wheel/rail reaction forces for open track

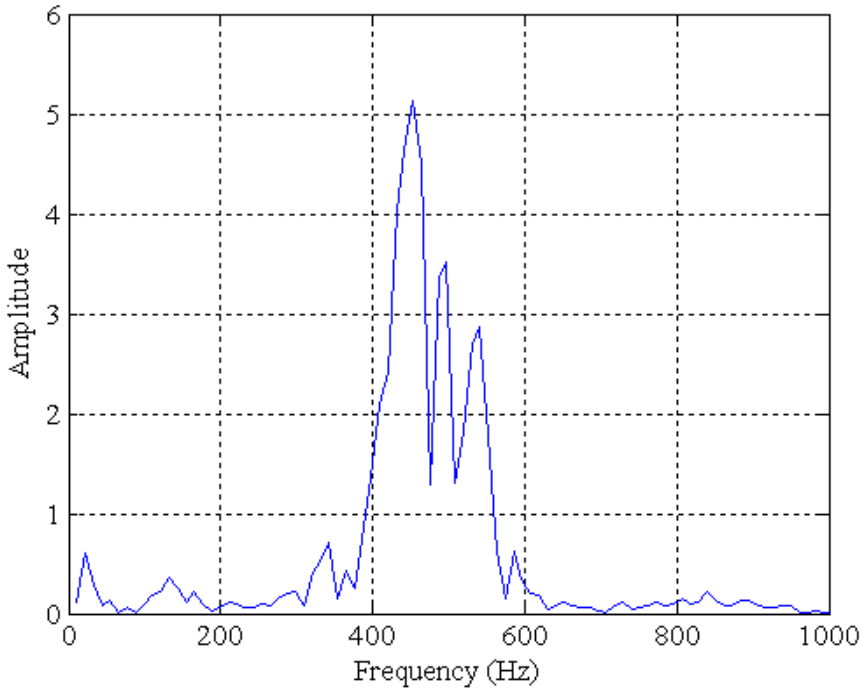

Figure 5.17 – FFT of unfiltered wheel/rail reaction force signal from simulation on open track

6. TRACK RESPONSE AT BRIDGE/APPROACH LOCATION

The complete track response includes the track deflection, wheel/rail forces, ballast pressures and subgrade pressures. This set of results has not been fully analyzed as it relates to the bump at the end of the railway bridge as of yet. Before looking at the track response due to a bump or dip, it is important to evaluate the response due to a track modulus change alone at the bridge/approach location.

6.1 TRACK MODULUS TRANSITION

The effect of a track modulus change alone at the bridge/approach location has been evaluated by simulating the model described previously in Section 5 using LS-DYNA. The approach, which has a track modulus of 32 N/mm/mm, is softer than the bridge, which has a track modulus of 83 N/mm/mm.

6.1.1 Static Response

The effect of a static point load on the track was first evaluated using LS-DYNA. Using the track and track substructure models discussed in Section 5, a single force of 100 kN was placed on the top, center node of the track over a tie on the approach embankment (Tie 24). The resulting track deflection for this tie (Tie 24) was then evaluated (Fig. 6.1). This process was repeated for the subsequent ties on the approach leading up the bridge abutment (Ties 25-28). The track deflection envelope was then found (Fig. 6.1).

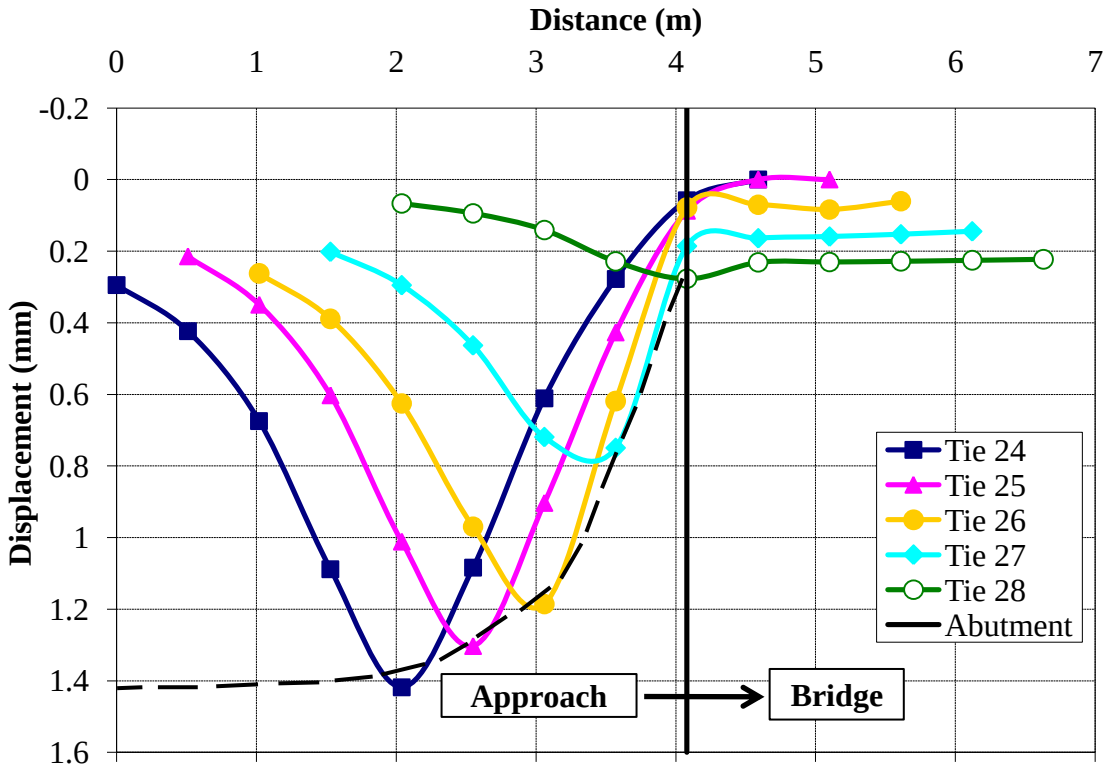

Figure 6.1 - Track deflection profile under subsequent static point loads

Since the bridge cannot deform as much as the soft approach, the track close to the bridge structure must deform less and less to accommodate the change in track modulus. The shape closely matches that found by Hunt (1997) in Fig. 3.6, helping to validate the model. Using Eq. 2.4, the track modulus profile can then be evaluated (Fig. 6.2). The track deflection and the track modulus both have similar profiles leading up to the bridge.

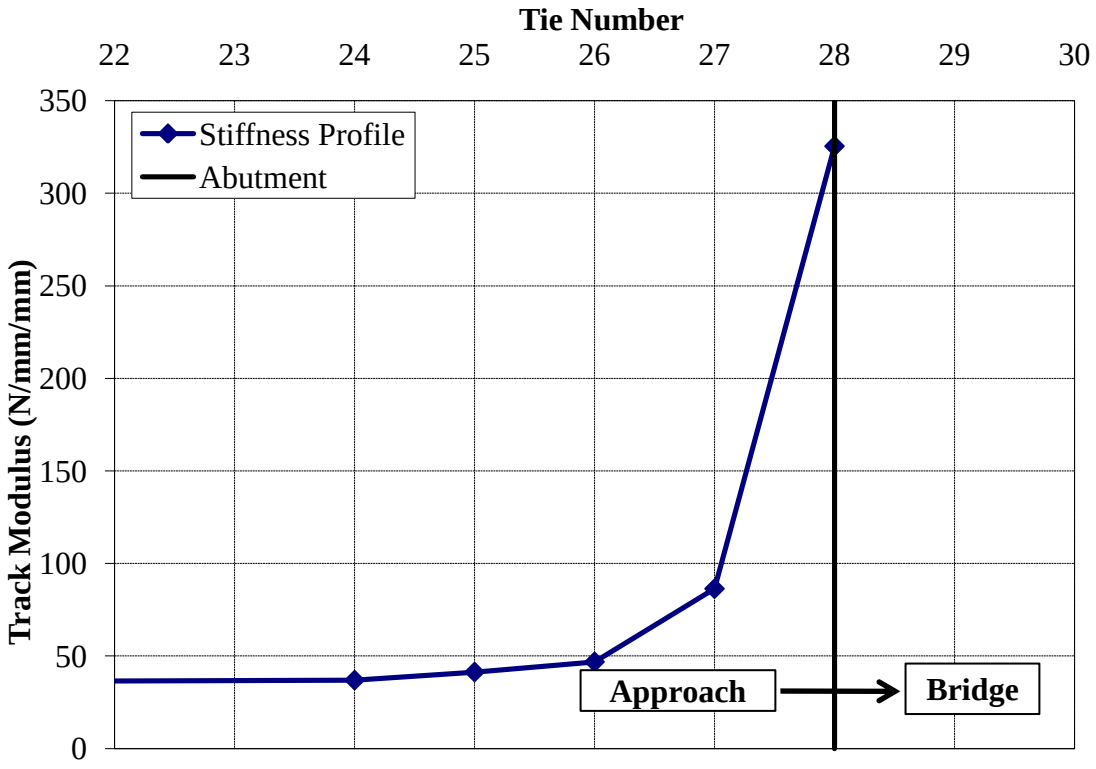

Figure 6.2 –Track modulus profile under subsequent static point loads

6.1.2 Dynamic Response

After evaluating the static response, the response of the track to a moving vehicle is then modeled. In this simulation, the truck (with a static wheel load of 146 kN) is moving from the approach embankment onto the bridge at a velocity of 22.2 m/s (50 mph). The resulting wheel/rail reaction forces, axle accelerations and track deflection are shown in Fig. 6.3. Note that in the figure, the direction of motion is from left (the approach) to right (the bridge).

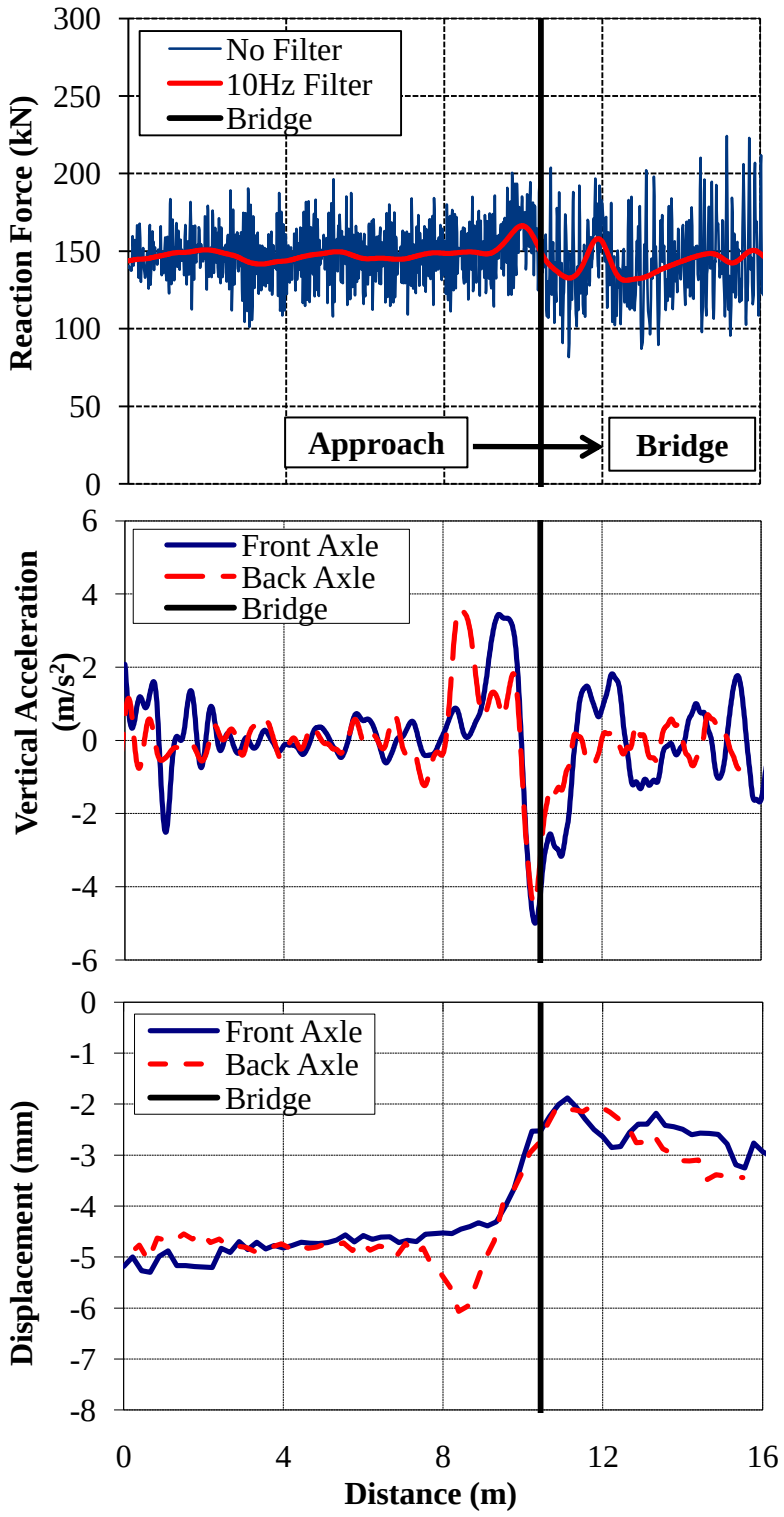

Figure 6.3 - (a) Wheel/Rail forces (b) Axle accelerations and (c) Track deflection due to a stiffness change alone at a bridge/approach location (v = 22.2 m/s)

The wheel/rail reaction forces (calculated from component accelerations) and the individual axle accelerations have been filtered with a cut-off frequency of 10 Hz according to FRA standards (FRA 2003). It is clear that an impact occurs on the approach before the truck crosses over the bridge (Fig. 6.3a). This can only be due to the track modulus change at that location since no defects are present in the track in this case.

Since the reaction force incorporates effects of the suspension system, it is often easier to examine the front and back axle accelerations independently to see the individual responses (Fig. 6.3b). Both the front and the back axles experience an impact on the approach embankment before the bridge, but the impacts are at different locations on the approach. This trend agrees with the axle acceleration results from Namura and Suzuki (2007). It is explained by looking at the track deflection (Fig. 6.3c).

The deflection profile under the front axle, due to the track modulus change, closely matches that found under static loading (Fig. 6.1), but the deflection under the back axle is different. Track deflection increases under the back axle approximately 2 m from the bridge abutment. This is due to the weight transfer between the front and back axles; as the front axle unloads, weight is transferred to the back wheels compressing the track further. This causes an impact on the back axle (Fig. 6.3b).

Based on BOEF theory (Eq. 2.4), the deflection under a 146 kN wheel load (292 kN axle force) for an approach track modulus of 32 N/mm/mm is 4.6 mm. This static deflection is reasonably matched by the model, which has an average track deflection of approximately 4.8 mm under the moving back wheel (Fig. 6.3b). The increased

deflection under the back axle is, at a maximum, 6.06 mm. The ratio of the maximum track deflection (d_{max}) to the static deflection (d_{static}) in this case is 1.27 and is termed the dynamic deflection factor (DDF) (Eq. 6.1). Based on the deflection limit of 6.4 mm (Lundgren and Martin 1970), this is less than the tolerable DDF of 1.40.

$$DDF = \frac{d_{max}}{d_{static}} \tag{6.1}$$

Similarly, to evaluate the increase in load due to a track modulus change at the bridge/approach location, the dynamic load factor (DLF) will be used. The DLF is the ratio of the maximum total wheel load (P_{max}) to the static wheel load (P_{static}) (Eq. 6.2). In this case, the static wheel load is 146 kN.

$$DLF = \frac{P_{max}}{P_{static}} \tag{6.2}$$

The DLF, based on the 10 Hz filter, is 1.14 in this case. This means that a stiffness change of about 50 N/mm/mm produced a 14% increase in the load. While this is not a significant increase, it is enough to instigate the process of track degradation leading to even higher impact loads and thus, a bigger bump.

The ballast pressure profile as the truck moves across the bridge is shown in Fig. 6.4. Note that compression is considered negative in all the pressure graphs presented in this study. While referring to pressures in the text, however, compression is considered positive. The data was collected on the surface of the ballast directly underneath the centerline of the rail and ties. The oscillations in the ballast pressure profile are likely due to some rocking effects of the suspension system during movement.

The average ballast pressure is approximately 400 kPa. This agrees well with the ballast pressure calculated in Eq. 2.9 of 380 kPa when the tie load is 50% of the axle load. Using the recommended tie load as 40% of axle load (Hay 1982), the ballast pressure is calculated as 305 kPa. The ballast pressure is reduced right near the bridge abutment where the bump ends. This pressure differential near the bridge abutment can lead to uneven ballast degradation close to the abutment.

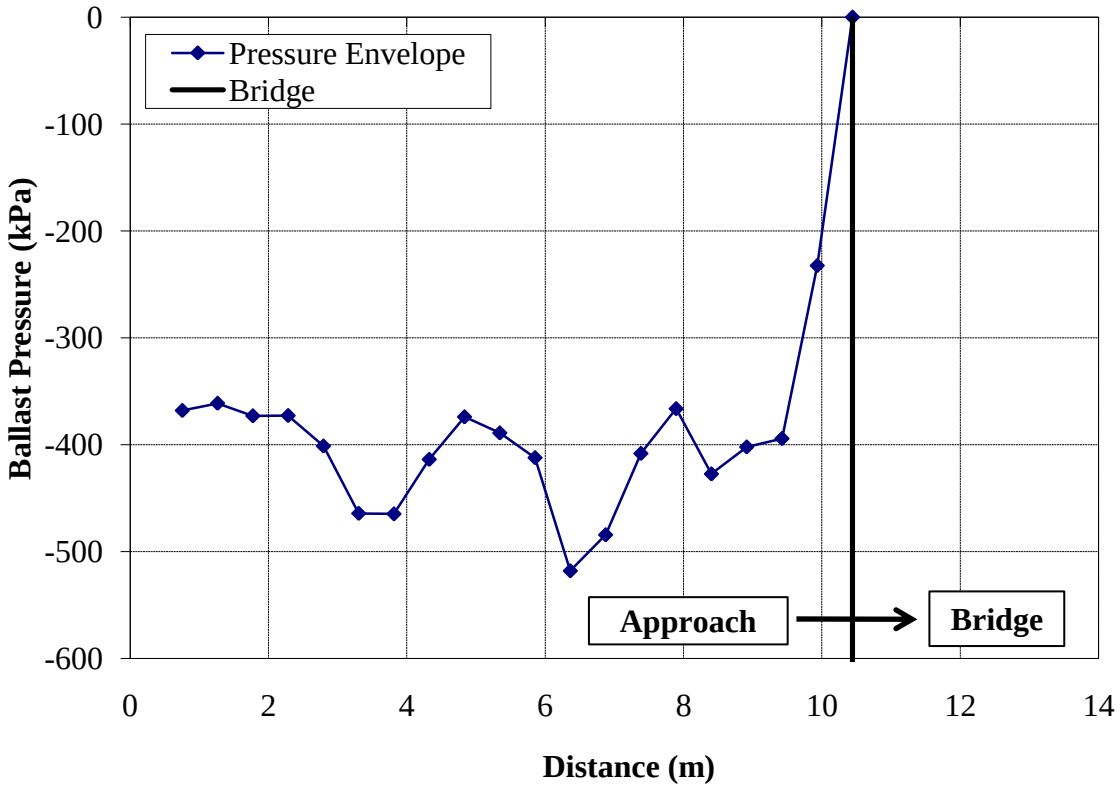

Figure 6.4 - Ballast pressure for a track modulus change alone at a bridge/approach location (v = 22.2 m/s)

To evaluate the increase in ballast pressure due to a track modulus change at the bridge/approach location, the dynamic ballast pressure factor (DBF) will be used. The DBF is the ratio of the maximum ballast pressure (B_{max}) to the average, static ballast pressure (B_{static}) (Eq. 6.3).

$$DBF = \frac{B_{max}}{B_{static}} \tag{6.3}$$

The DBF is 1.30 in this case. The ballast pressure limit of 450 kPa for wood ties (AREMA 2008) has been exceeded in this case, but the ballast pressure limit of 590 kPa for concrete ties (AREMA 2008) has not been exceeded. None of the pressure data was filtered in this study. This means that a stiffness change of about 50 N/mm/mm produced a 30% increase in the ballast pressure.

The subgrade pressure profile as the truck moves across the bridge is shown in Fig. 6.5. The data was collected on the surface of the subgrade directly underneath the centerline of the rail, ties, ballast and subballast. Again, the oscillations in the subgrade pressure profile are likely due to some rocking effects of the suspension system during movement. The average subgrade pressure is approximately 72 kPa. This differs from the subgrade pressure calculated with the JNR equation (Eq. 2.12) of about 125 kPa.

The maximum subgrade pressure is approximately 2 m from the bridge abutment. Note that this is at the same location as the impact due to the back axle (Fig. 6.3b). Closer to the bridge abutment, however, the subgrade pressure is reduced much like for the ballast pressure. In this case, however, a tensile pressure of 11 kPa occurs right before the bridge abutment. This is likely due to the truck unloading that occurs at

this location (Fig. 6.3b). This pressure differential near the bridge abutment can lead to uneven subgrade degradation.

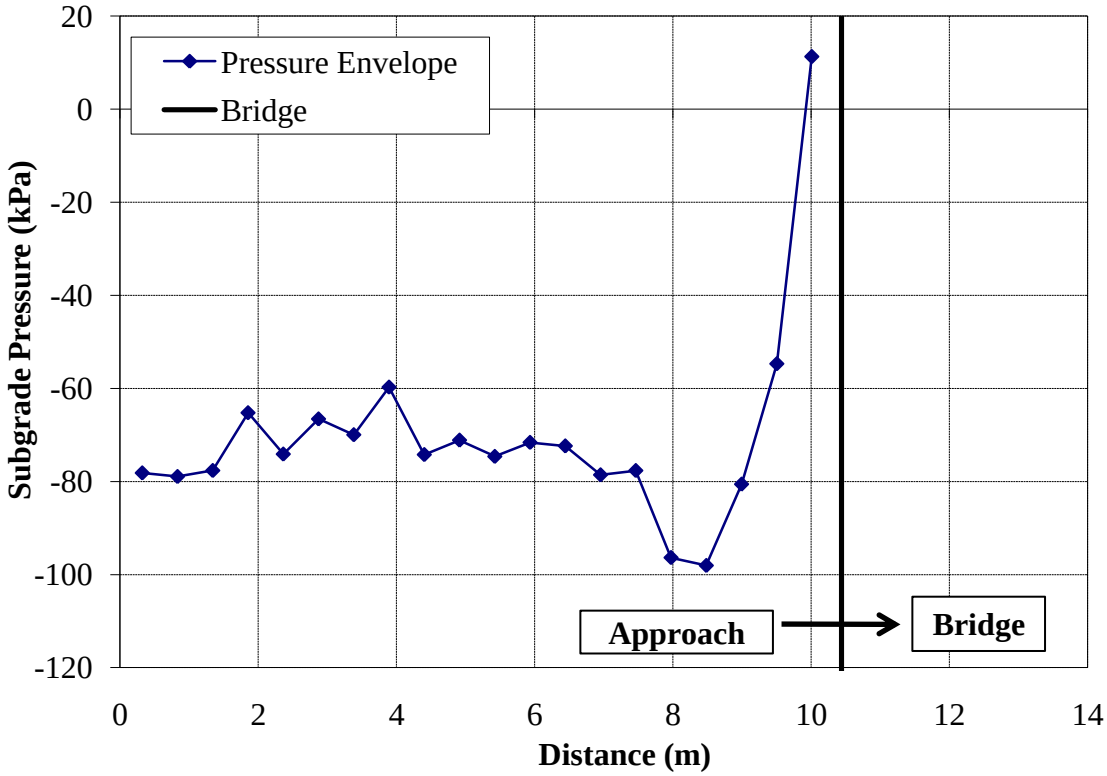

Figure 6.5 - Subgrade pressure for a track modulus change alone at a bridge/approach location (v = 22.2 m/s)

To evaluate the increase in subgrade pressure due to a track modulus change at the bridge/approach location, the dynamic subgrade pressure factor (DSF) will be used. The DSF is the ratio of the maximum subgrade pressure (S_{max}) to the average, static subgrade pressure (S_{static}) (Eq. 6.4). Again, in this case the static subgrade pressure is 72 kPa.

$$DSF = \frac{S_{max}}{S_{static}} \tag{6.4}$$

The DSF is approximately 1.36 in this case. The subgrade pressure limit of 140 kPa (AREMA 2008) has not been exceeded. None of the pressure data was filtered in this study. This means that a stiffness change of about 50 N/mm/mm produced an almost 40% increase in the subgrade pressure.

6.1.3 Cyclic Response

Since the track substructure materials are elastic, permanent deformations and track response cannot be directly found. The cyclic response of the track structure can be modeled, however, by altering the material properties of the ballast, subballast, fill and subgrade. This is accomplished by changing the modulus of elasticity for each layer depending on the cycle of interest (Eq. 6.5).

$$E_N = E_0 N^{-a} \tag{6.5}$$

where E_N is the modulus of elasticity at cycle N, E_0 is the initial modulus of elasticity and a is an exponent depending on the material. This process was completed for one cycle, one thousand cycles, one million cycles and one billion cycles. To put in terms of MGT, use Eq. 2.20.

The track deflection profile under both the front axle and back axle will change depending on the number of cycles (Fig. 6.6). As expected, the track displaces more as the system is cycled. After only 1000 cycles (0.07 MGT), the track deflection exceeds the deflection criteria for durability (Lundgren and Martin 1970). The slope of the

deflection envelope also changes; it gets steeper as the number of cycles increases. These trends for track deflection under cyclic load are very similar to that found by Hunt (1997) (Fig. 3.7).

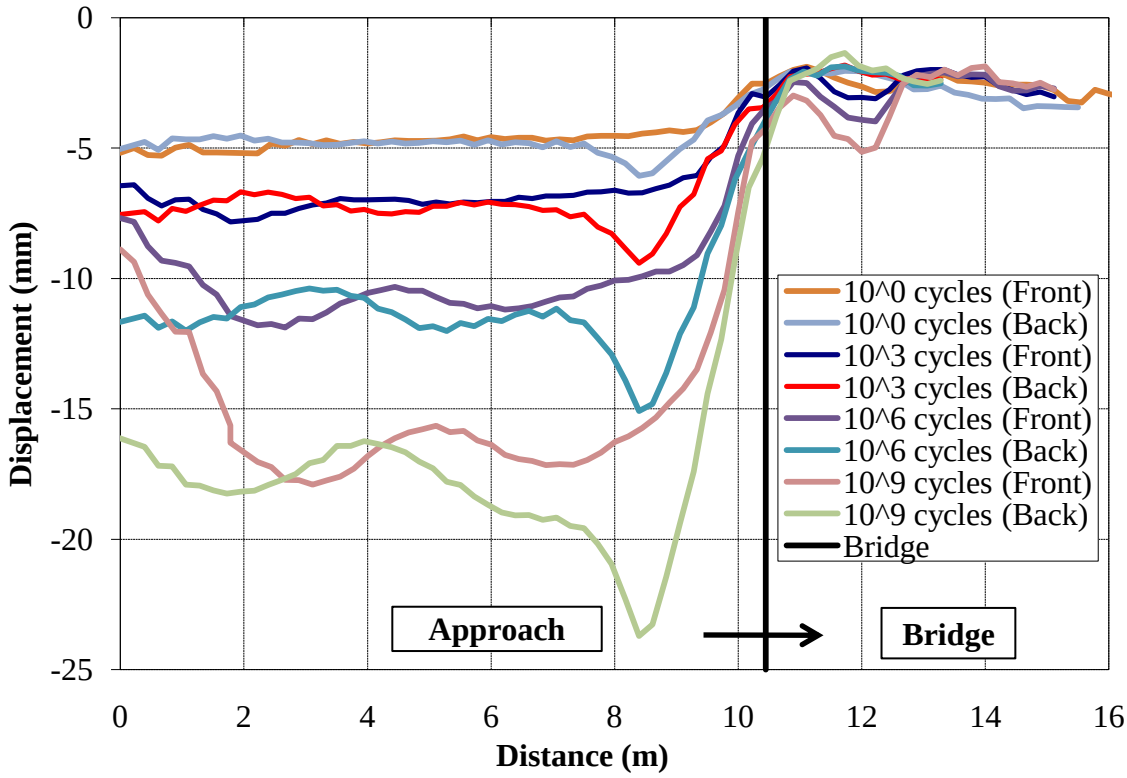

Figure 6.6 - Track deflection under cyclic load for a track modulus change alone at a bridge/approach location (v = 22.2 m/s)

While the maximum deflection increases, the average deflection also increases. In terms of DDF, therefore, there is not a big difference with the number of cycles (in log scale) (Fig. 6.7). While there is a linear relationship on the semi-log scale, where an

increase in the number of cycles increases the DDF, the difference between the DDF at 10^9 cycles and at 10^0 cycles is only 0.10 (or 10%).

Increased track deflections due to cyclic effects will then lead to higher impact loads (Fig. 6.8). Plotting this in terms of the DLF on a log scale for N (or MGT), a linear relationship is found between the maximum impact load and the number of cycles (Fig. 6.9). This allows for prediction of the DLF after even more cycles.

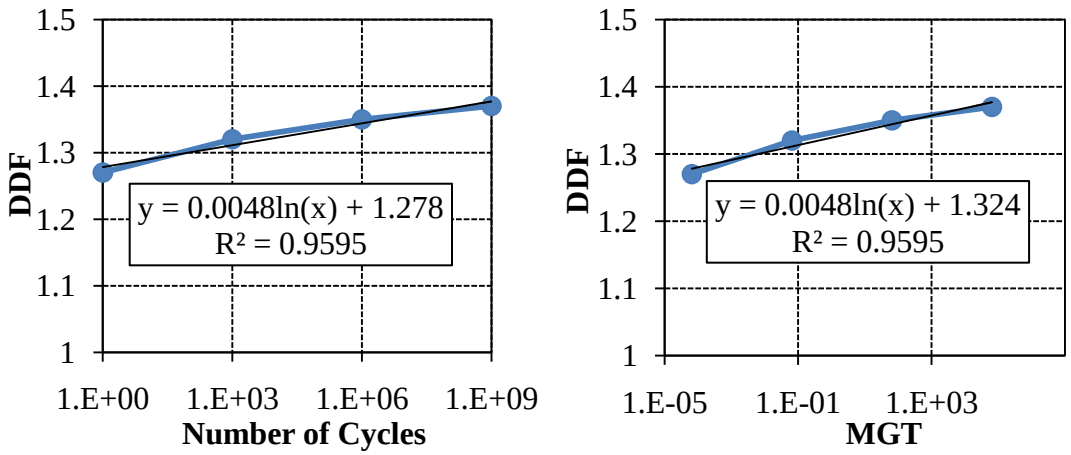

Figure 6.7 - DDF vs. N or MGT under cyclic load for a track modulus change alone at a bridge/approach location (v = 22.2 m/s)

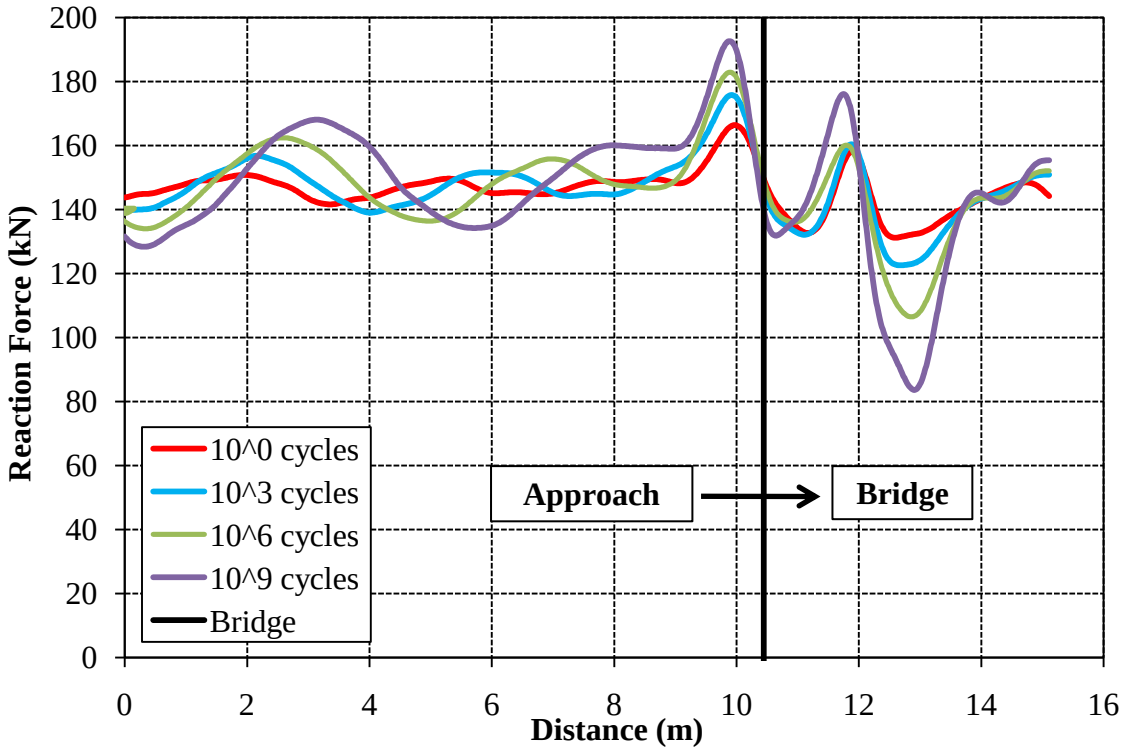

Figure 6.8 - Reaction force under cyclic load for a track modulus change alone at a bridge/approach location (v = 22.2 m/s)

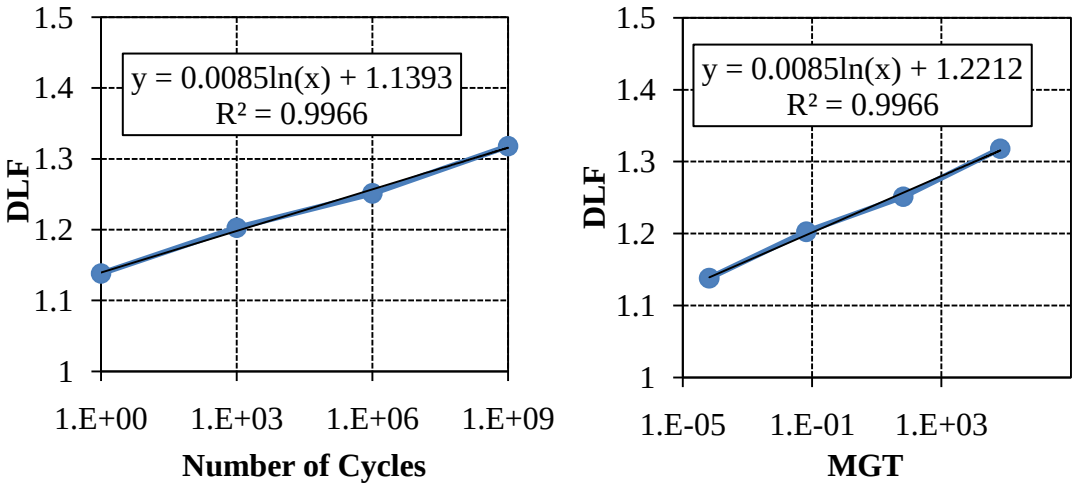

Figure 6.9 - DLF vs. N or MGT under cyclic load for a track modulus change alone at a bridge/approach location (v = 22.2 m/s)

The ballast pressure profiles as the truck moves across the bridge are shown in Fig. 6.10. From the figure, it is shown that the average ballast pressure on the approach embankment decreases with the number of cycles. This is because, as the ballast degrades, the confining pressure and stiffness is reduced. For 1 cycle, 1000 cycles, 1000000 cycles and 1000000000 cycles, the average ballast pressure (in compression) is approximately 400 kPa, 350 kPa, 300 kPa and 230 kPa, respectively. There is a linear relationship between the average ballast pressure and the number of cycles in this case (Fig. 6.11).

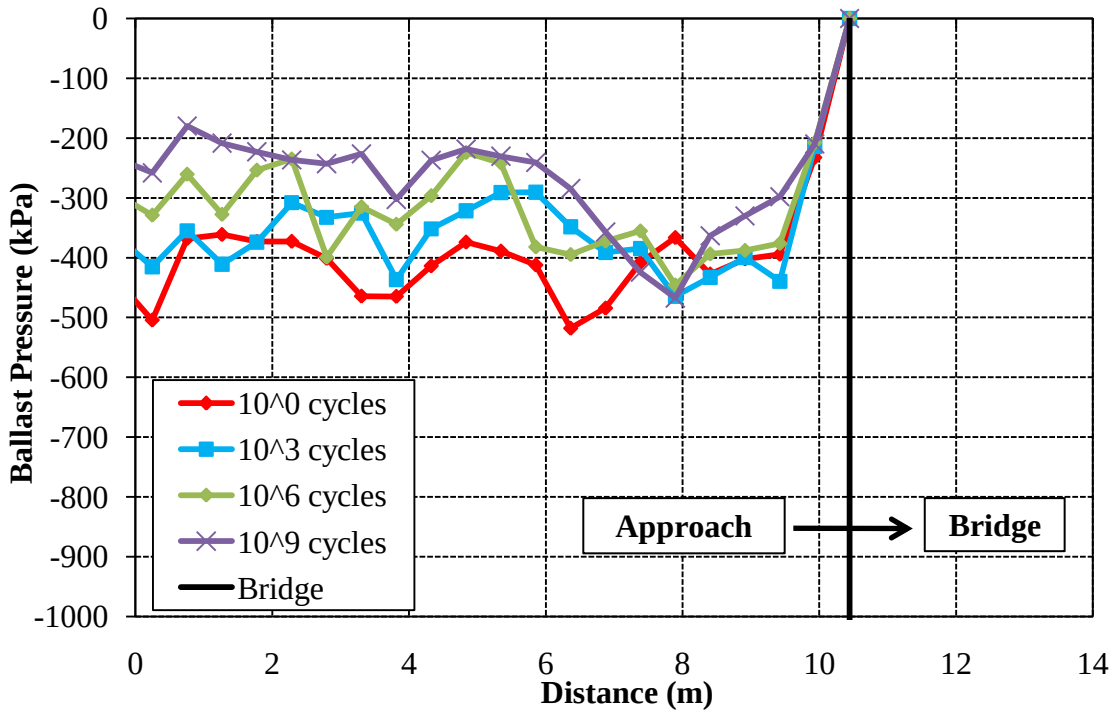

Figure 6.10 - Ballast pressure under cyclic load for a track modulus change alone at a bridge/approach location (v = 22.2 m/s)

While the average ballast pressure on the approach embankment decreases with the number of cycles (or MGTs), the DBF (and thus the maximum ballast pressure) tends to increase (Fig. 6.12). Unlike for the DDF and DLF, however, the linear relationship is weak. The maximum ballast pressure for each cycle (except for 10^6 cycles) slightly exceeds the ballast pressure threshold of 450 kPa for wood ties (AREMA 2008). The maximum ballast pressure for 10^6 cycles (446 kPa) was just below the threshold. This means that the ballast will likely experience fouling and abrasion which could lead to bump/dip formation and other problems.

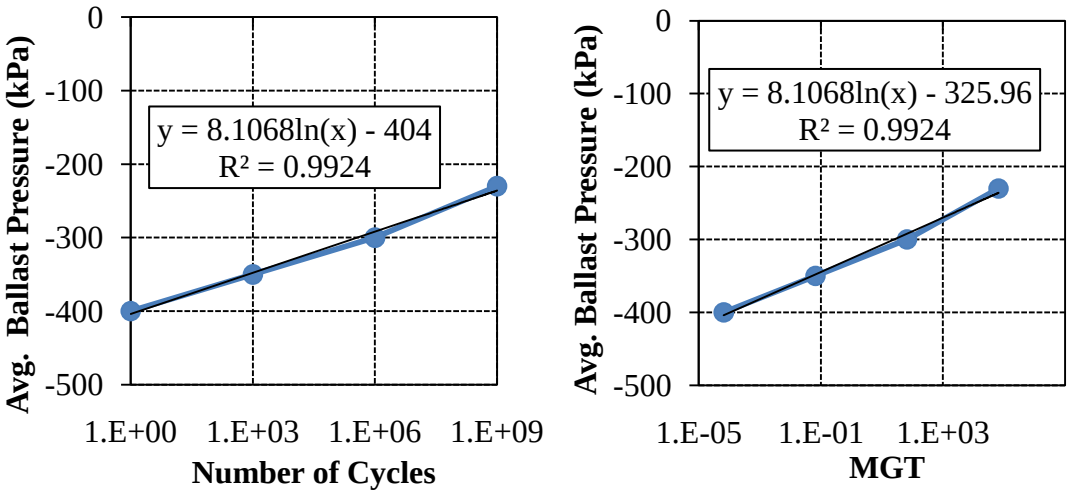

Figure 6.11 - Average ballast pressure vs. N or MGT under cyclic load for a track modulus change alone at a bridge/approach location (v = 22.2 m/s)

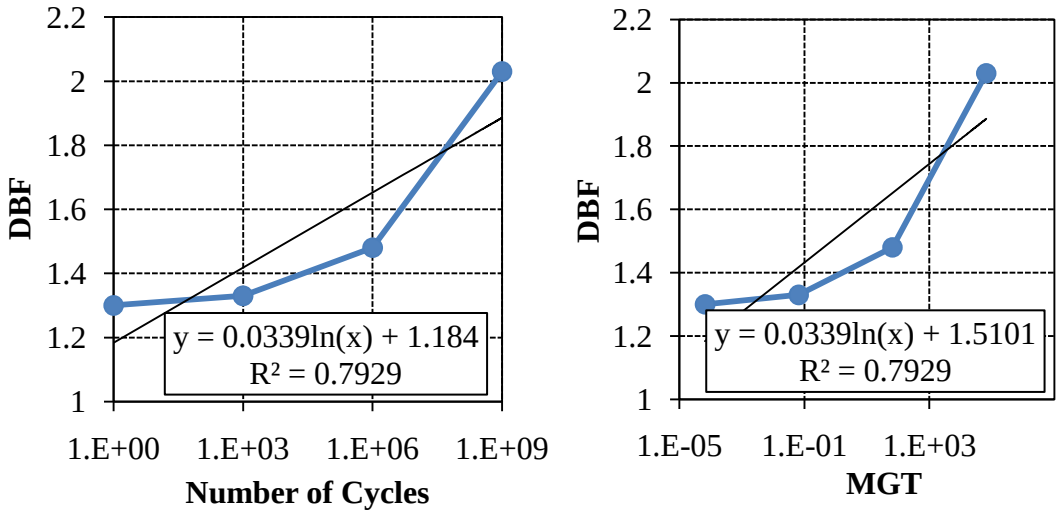

Figure 6.12 - DBF vs. N or MGT under cyclic load for a track modulus change alone at a bridge/approach location (v = 22.2 m/s)

The subballast pressure profiles as the truck moves across the bridge are shown in Fig. 6.13. While the average subgrade pressure on the approach embankment decreases with the number of cycles, it is not significantly affected by the number of cycles (Fig. 6.14). For 1 cycle, 1000 cycles, 1000000 cycles and 1000000000 cycles, the average subgrade pressure is approximately 72 kPa, 66 kPa, 61 kPa and 58 kPa, respectively. So after 1 billion cycles (or MGT), the subgrade pressure decreased only by 14 kPa.

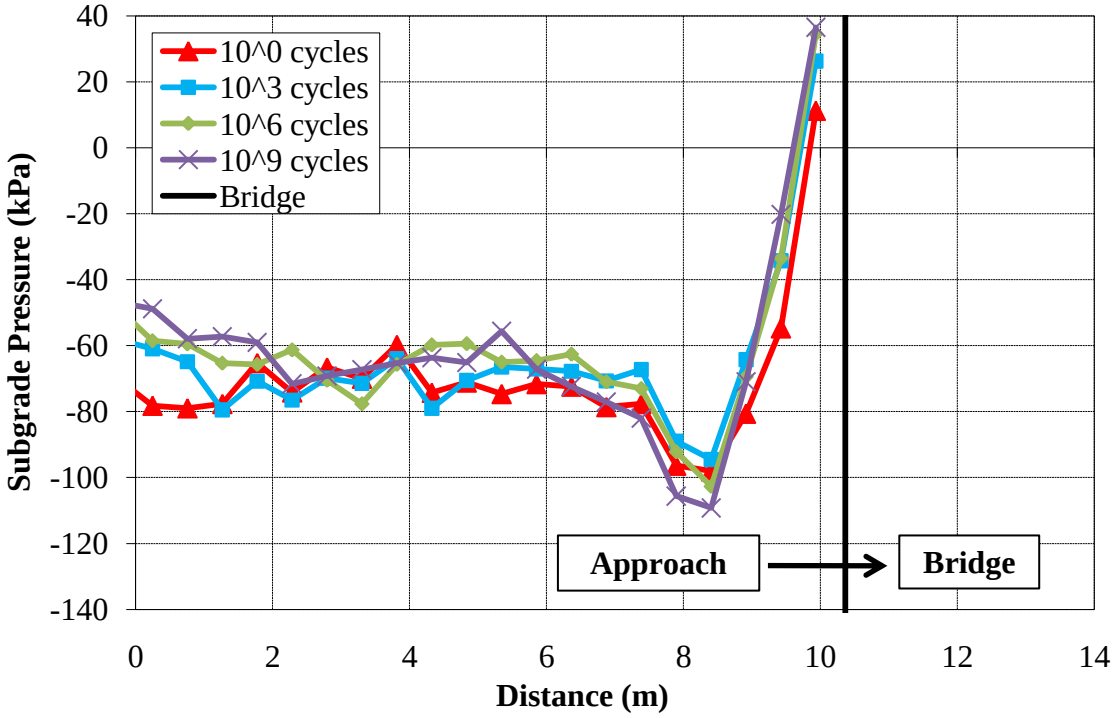

Figure 6.13 - Subgrade pressure under cyclic load for a track modulus change alone at a bridge/approach location (v = 22.2 m/s)

As with ballast pressures, there is a linear relationship between the average subgrade pressure and the number of cycles in this case (Fig. 6.14). This is also true in terms of the DSF (Fig. 6.15). While the average subgrade pressure on the approach embankment decreases with the number of cycles (or MGTs), however, the DSF increases. None of the subgrade pressures in this cyclic study exceeded the subgrade pressure threshold of 140 kPa (AREMA 2008). A complete summary of the DDF, DLF, DBF and DSF results are presented in Table 6.1.

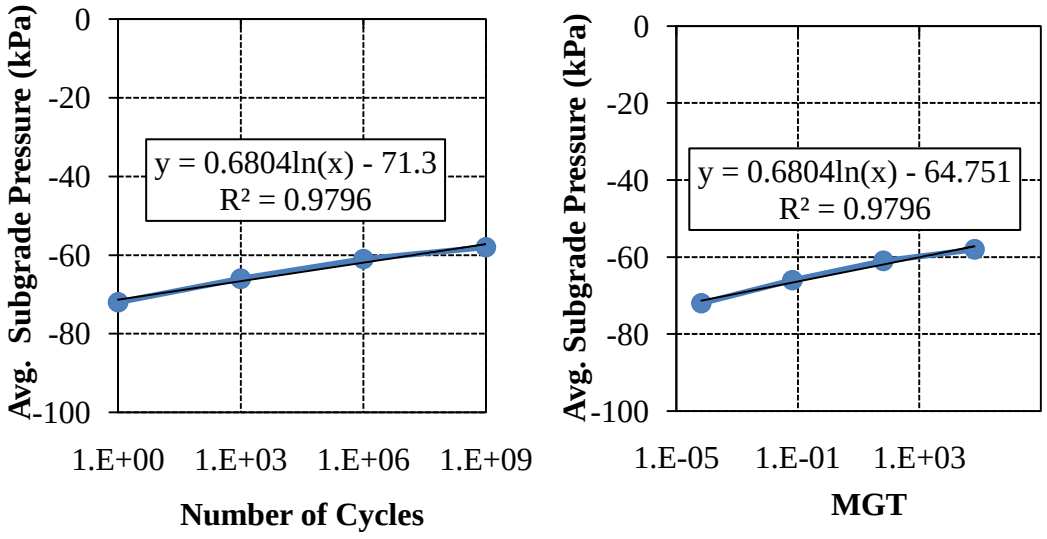

Figure 6.14 - Average subgrade pressure vs. N or MGT under cyclic load for a track modulus change alone at a bridge/approach location (v = 22.2 m/s)

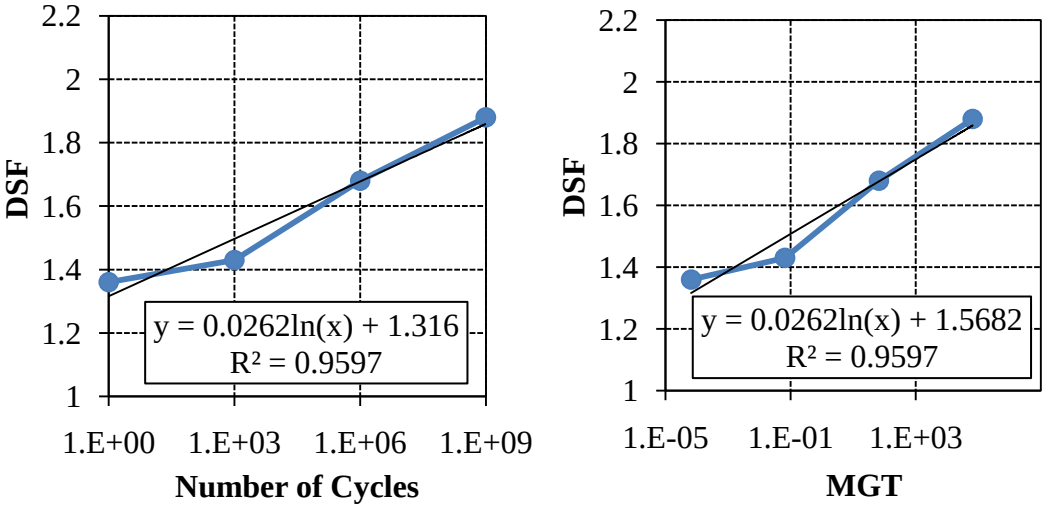

Figure 6.15 - DSF vs. N or MGT under cyclic load for a track modulus change alone at a bridge/approach location (v = 22.2 m/s)

Table 6.1 – Cyclic response summary

MGT	N	DDF	DLF	DBF	DSF
6.60E-05	1.00E+00	1.27	1.14	1.3	1.36
6.60E-02	1.00E+03	1.32	1.20	1.33	1.43
6.60E+01	1.00E+06	1.35	1.25	1.48	1.68
6.60E+04	1.00E+09	1.37	1.32	2.03	1.88

6.2 BUMP PROFILE

In addition to a stiffness change, including a track geometry change in the form of a bump increases the impact forces, track deflection, ballast pressures and subgrade pressures. To examine the effect, a bump with a slope of 1:150 was imposed in the model. The length of the bump is 5.1 m and the height of the bump is 33 mm. The truck model moves at a speed of 22.2 m/s over the bump. These values were chosen based on the averages from the survey (Section 4). The reaction forces, axle accelerations and track deflection for this case are presented in Fig. 6.16.

The first two impacts seen in Fig. 6.16a represent the front and back wheels hitting the bump, respectively. The third impact force is due to the track modulus change and resulting change in the displacement profile. Looking at the front and back axles independently (Fig. 6.16b), both respond similarly to the bump in the track but differently to the track modulus change near the bridge. This mimics the response due to a track modulus change alone (Fig. 6.3b). The reason is explained by the different track deflection profiles under the front and back wheels (Fig. 6.16c). Weight transfer to the back wheel is apparent as the truck's front axle entered the bump and then crossed over the bridge.

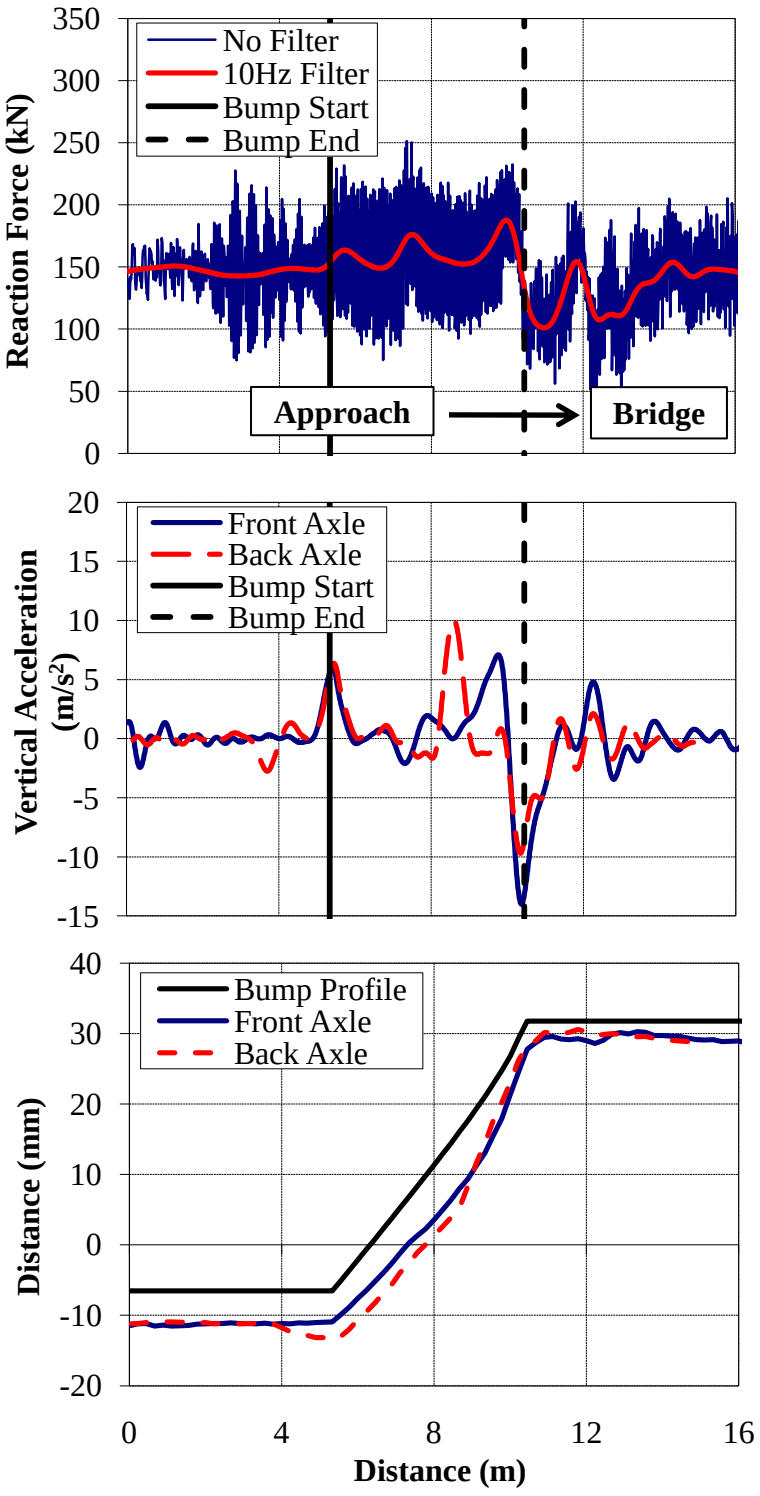

Figure 6.16 - (a) Wheel/Rail forces (b) Axle accelerations and (c) Track deflection due to a 1:150 bump at a bridge/approach location (v = 22.2 m/s)

The DLF for this case is 1.28. This means that a stiffness change of about 50 N/mm/mm, along with a 1:150 bump in the track, produced a 28% increase in the load. This is double the increase found for a stiffness change alone. A DLF of 1.28 is still not considered significant because it is under 1.5 (Plotkin and Davis 2008), but the bump will only get more severe with the number of cycles.

To compare the deflection response between no slope and a 1:150 bump, the track displacement for the 1:150 bump was corrected for grade (Fig. 6.17). The track deflection is significantly increased under a bump profile. The slope of the deflection envelope becomes steeper for the bump as well. These factors suggest that the impact due to a bump is more severe than an impact due to a track stiffness change alone. In fact, the track deflection exceeds the tolerable limits of less than 6.4 mm (Lundgren and Martin 1970). The DDF for this case is 2.40; the DDF for no slope was 1.40.

The ballast pressures resulting from a 1:150 bump are shown in Fig. 6.18. The ballast pressures more than double when there is a bump in the track as opposed to no slope in the track. The ballast pressures exceed the AREMA (2008) guidelines. These increased ballast pressures in the transition zone will lead to further degradation in this location. The DBF for this case is 2.33.

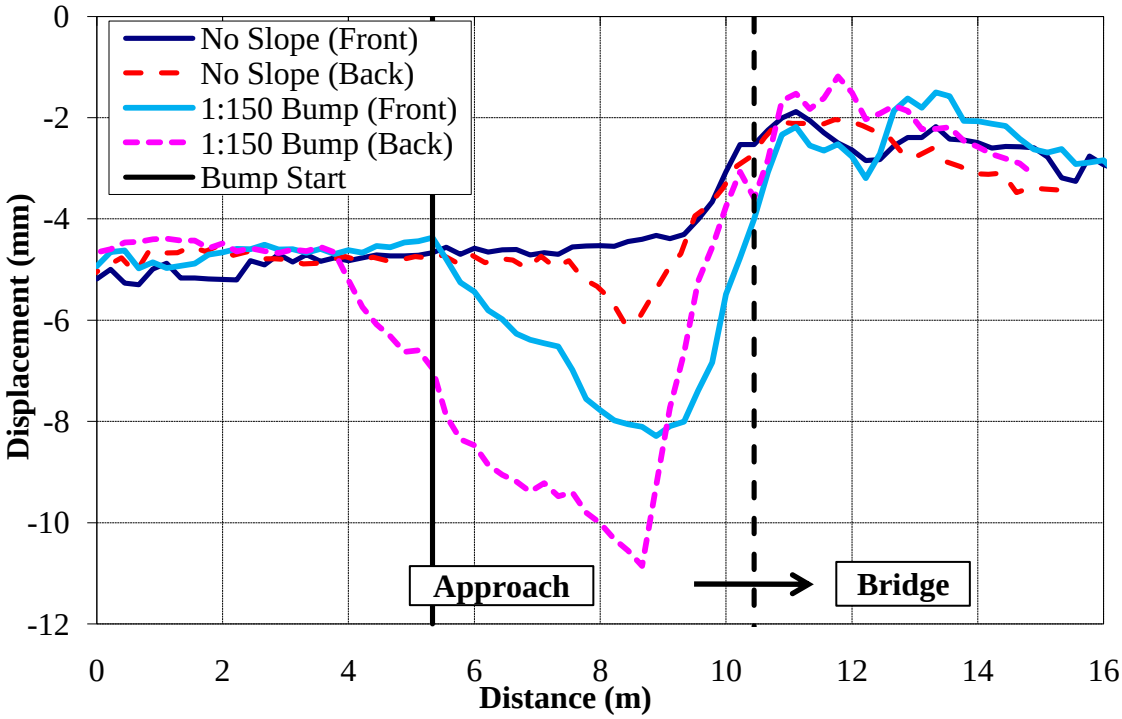

Figure 6.17 - Track deflection comparison: no slope vs. 1:150 bump (v = 22.2 m/s)

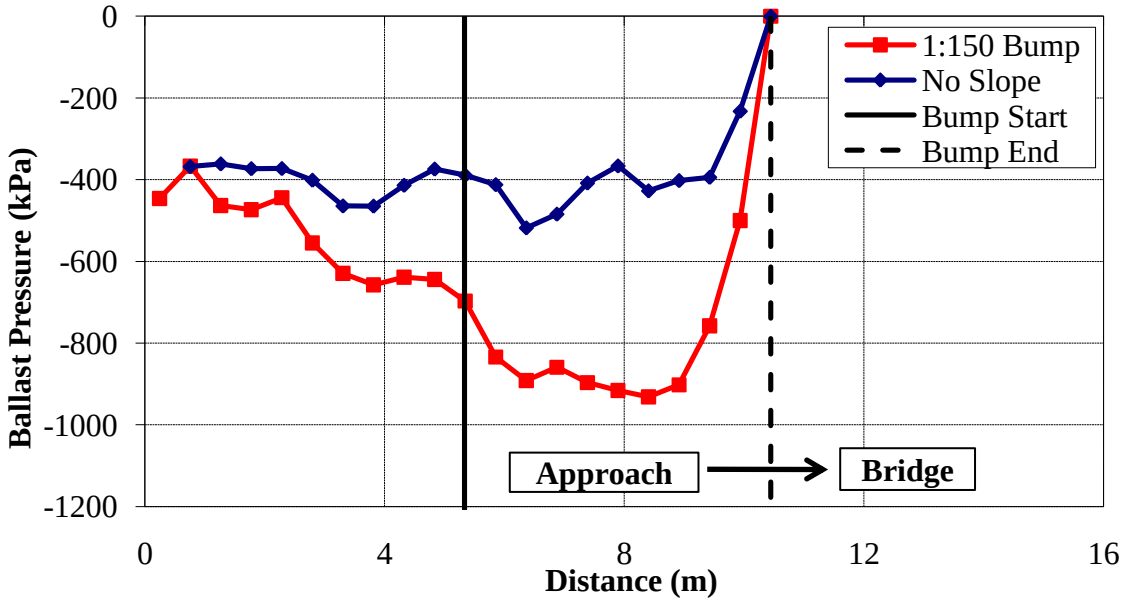

Figure 6.18 - Ballast pressure resulting from a 1:150 bump (v = 22.2 m/s)

The subgrade pressures resulting from a 1:150 bump are shown in Fig. 6.19. The difference in subgrade pressures between no slope and a 1:150 bump is not as high as for the ballast pressures; there is approximately a 60% increase in subgrade pressures due to a bump. The DSF for this case is 2.18. As with ballast pressures, the subgrade pressures exceed the AREMA (2008) guidelines.

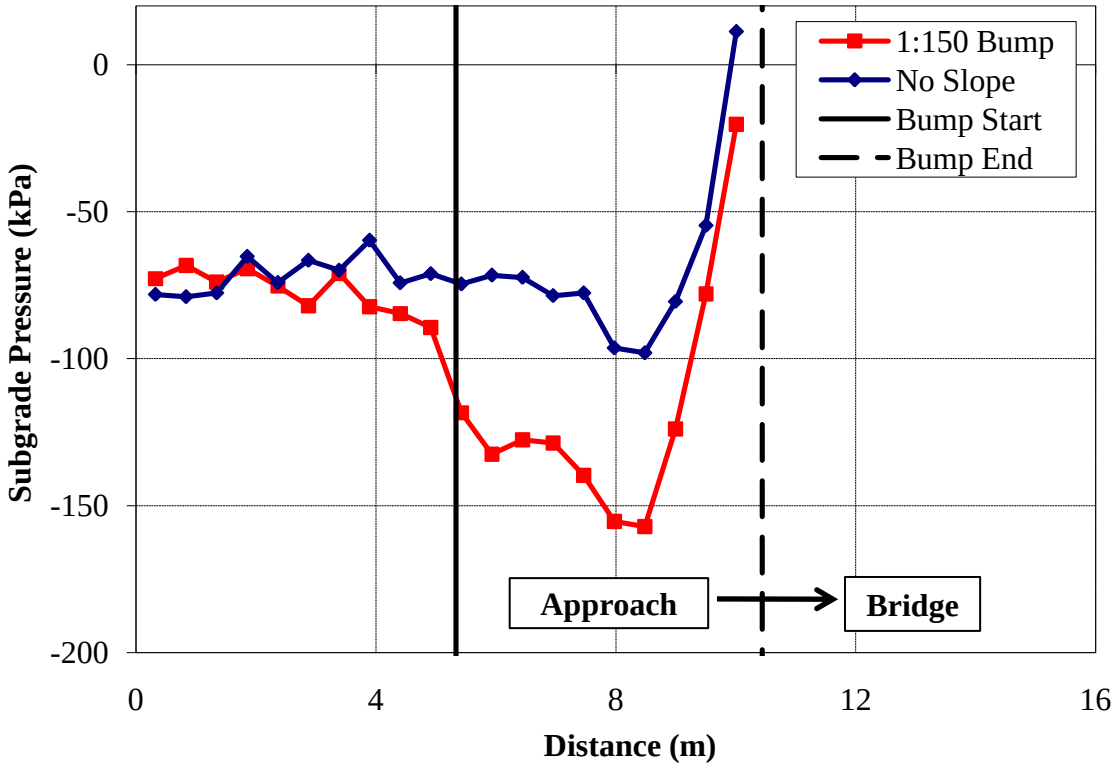

Figure 6.19 - Subgrade pressure resulting from a 1:150 Bump (v = 22.2 m/s)

6.3 DIP PROFILE

The effect of imposing a dip profile in the track, along with a stiffness change, is seen in Fig. 6.20. As the truck enters the down slope of the dip, an unloading occurs for both the front wheel and the back wheel (Fig. 6.20a). An impact is then seen as the truck reaches the bottom of the dip and begins travelling on the up slope of the dip. The impact due to the track modulus change is also present, but is not as severe as the impact due to the truck reaching the bottom of the dip.

The DLF for this case is 1.45. This means that a stiffness change of about 50 N/mm/mm, along with a 1:150 dip in the track, produced a 45% increase in the load. This is more than three times the increase found for a stiffness change alone and about one and a half times the increase found for a bump and stiffness change. This is approaching the DLF limit of 1.5.

Looking at the front and back axles independently (Fig. 6.20b), both respond similarly to the beginning of the dip in the track but differently to the bottom of the dip and the track modulus change near the bridge. This occurs as a result of the track deflection under the front and back wheels (Fig. 6.20c). As with the bump and no slope, the track beneath the back wheel on a dip experiences more deflection than the front wheel.

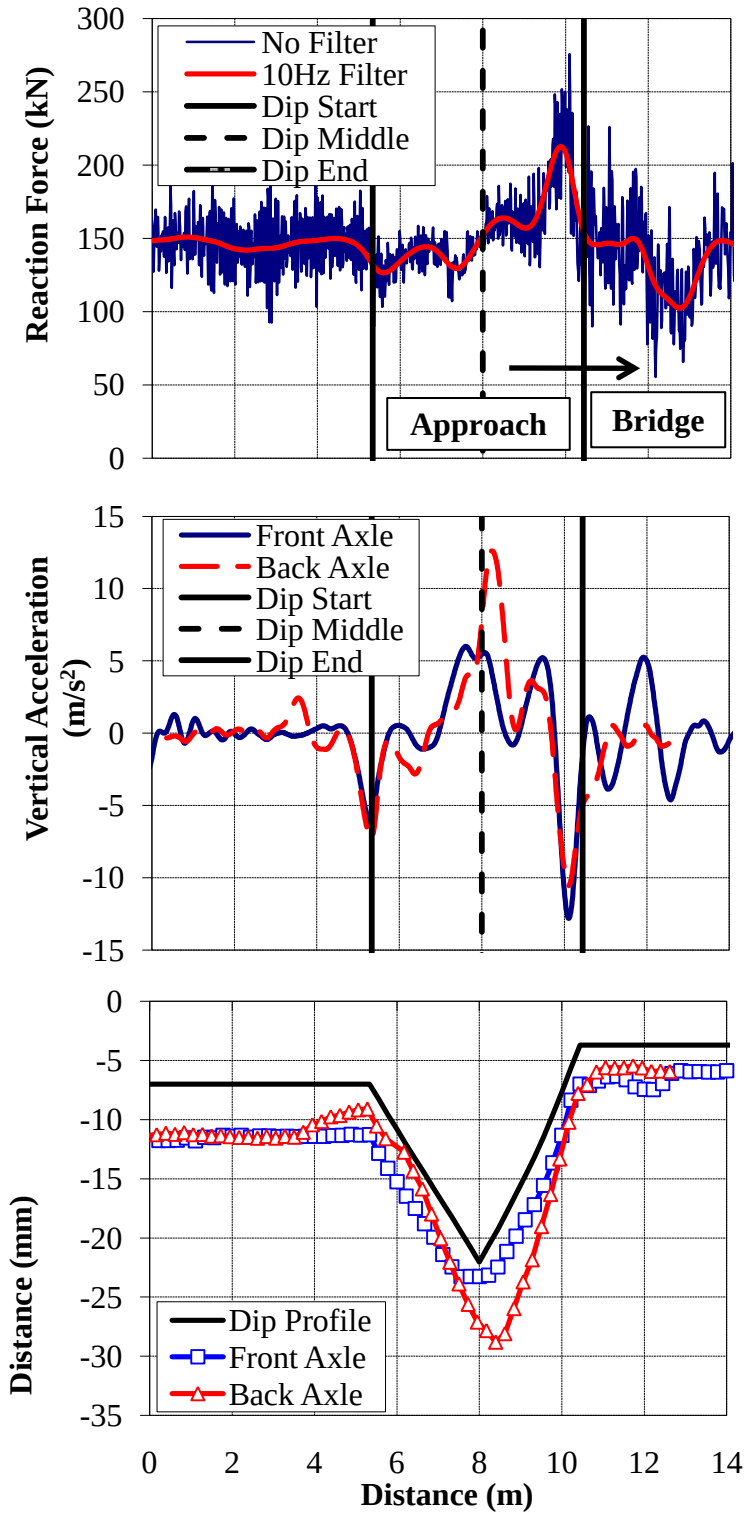

Figure 6.20 - (a) Wheel/Rail forces (b) Axle accelerations and (c) Track deflection due to a 1:150 Dip at a bridge/approach location (v = 22.2 m/s)

To compare the deflection response between no slope and a 1:150 dip, the track displacement for the 1:150 dip was corrected for grade (Fig. 6.21). The track deflection decreases for the front axle as it travels on the down slope of the dip. The track then compresses more as the front wheel travels on the upslope of the dip. The track deflection under the back axle begins to decrease at the point when the front axle enters the down slope of the dip. The distance between the front and back axle is 1.8 m.

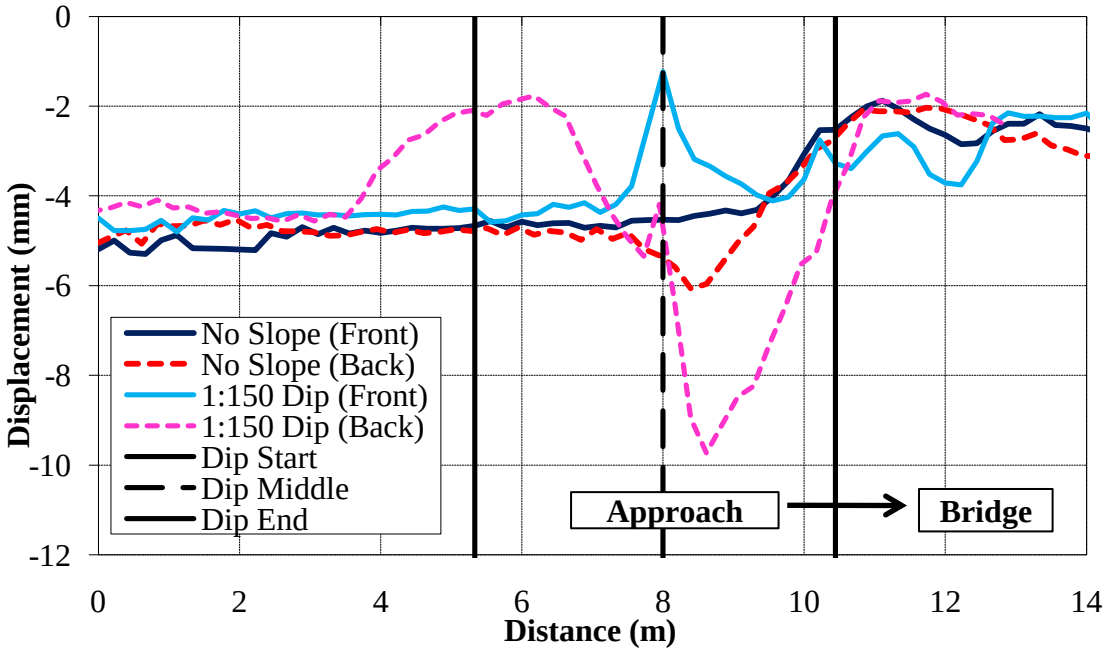

Figure 6.21 - Track deflection comparison: no Slope vs. 1:150 dip (v = 22.2 m/s)

As the back axle reaches the bottom and travels the upslope of the dip, the track deflection greatly increases over that for no slope. This suggests that the impact due to a dip is more severe than an impact due to a track stiffness change alone. The deflection

under the back wheel exceeds tolerable track deflection limits (Lundgren and Martin 1970) while the deflection under the front wheel does not. The DDF for this case, 2.24, is slightly lower than for the bump. This is because the track deflection was decreased on the down slope of the dip, causing the maximum magnitude of track deflection to be less than for the bump of the same size. The total change in track deflection, accounting for the relief on the down slope, however, is greater for the dip than for the bump.

The ballast pressures resulting from a 1:150 dip are shown in Fig. 6.22. The ballast pressures more than double when there is a dip in the track as opposed to no slope in the track. Similar to the track deflection under the back axle, the ballast pressure decreases on the down slope of the dip and increases on the up slope of the dip. This would likely increase the formation of the dip in the track. The DBF for this case is 2.14. As with the 1:150 bump, the ballast pressures for a 1:150 dip exceed AREMA (2008) guidelines for maximum ballast pressure.

The subgrade pressures resulting from a 1:150 dip are shown in Fig. 6.23. Again, a reduction in the subgrade pressure is found on the down slope of the dip. The subgrade pressure is increased, however, on the up-slope of the dip as compared to no slope. The DSF for this case is 1.78. Unlike for a 1:150 bump, the subgrade pressures for a 1:150 dip do not exceed the AREMA (2008) guidelines.

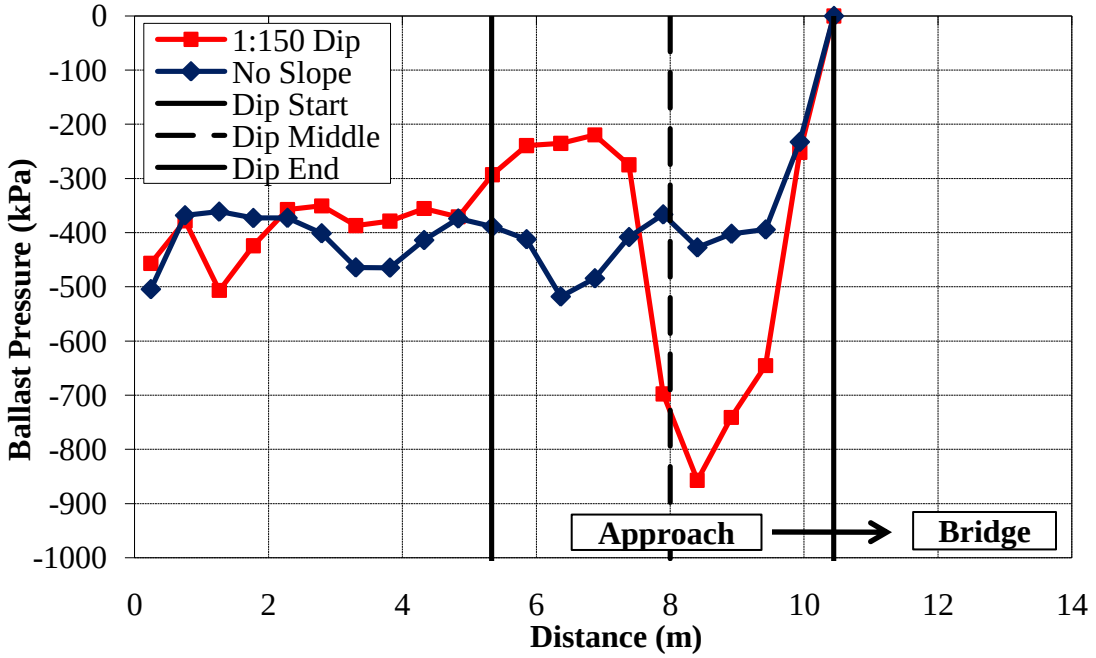

Figure 6.22 - Ballast pressure resulting from a 1:150 dip (v = 22.2 m/s)

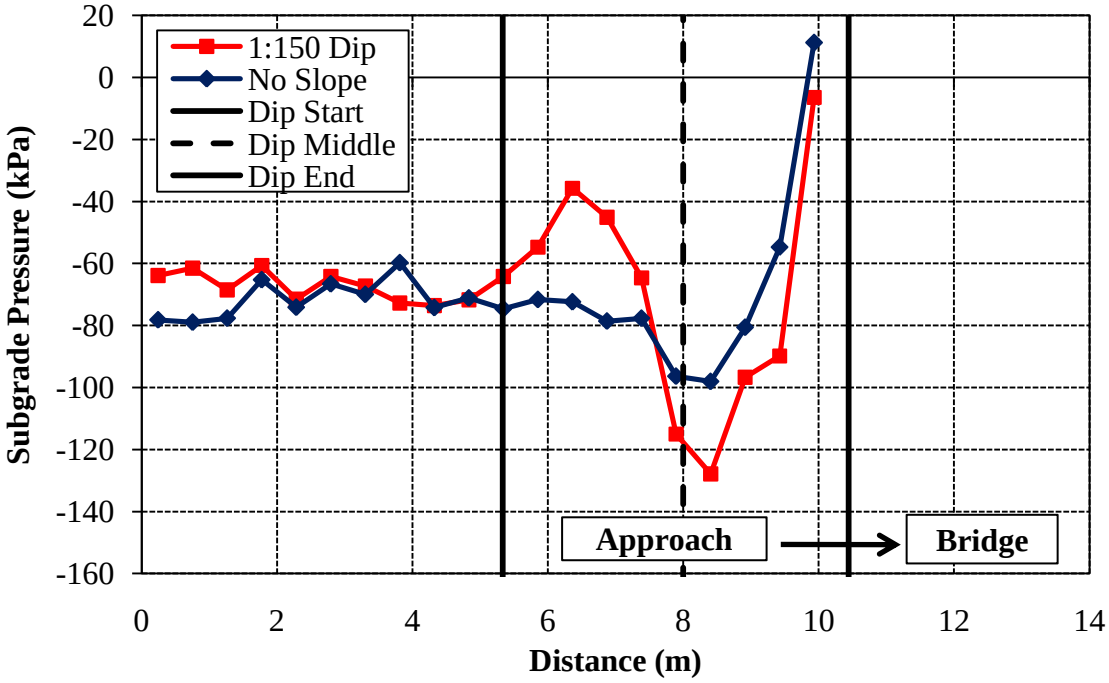

Figure 6.23 – Subgrade pressure resulting from a 1:150 dip (v = 22.2 m/s)

To briefly summarize, the DDF for no slope, a 1:150 bump and a 1:150 dip is 1.4, 2.4 and 2.24, respectively. The track deflection for the cases with a 1:150 bump and dip both exceeded the desirable limit for durability of 6.4 mm (Lundgren and Martin 1970). The DLF for no slope, a 1:150 bump and a 1:150 dip is 1.14, 1.28 and 1.45, respectively. None of these cases exceed the DLF limit of 1.5. The DBF for no slope, a 1:150 bump and a 1:150 dip is 1.30, 2.33 and 2.14, respectively. Both the bump and the dip exceed the AREMA maximum ballast pressure limitation where, for these cases, the DBF equals 1.12 (1.5 for concrete ties). The DSF for no slope, a 1:150 bump and a 1:150 dip is 1.36, 2.18 and 1.78. Only the bump profile exceeds the AREMA maximum subgrade pressure limitation where, for these cases, the DSF equals 1.94. The results are summarized in Table 6.2.

Table 6.2 – Track response summary for reference cases

Case	DDF	DLF	DBF	DSF
No Slope	1.4	1.14	1.3	1.36
1:150 Bump	2.4	1.28	2.33	2.18
1:150 Dip	2.24	1.45	2.14	1.78

Based on the results, it is concluded that a 1:150 bump with a track modulus change of 50 N/mm/mm and a vehicle speed of 22.2 m/s is more severe than a 1:150 dip under the same conditions. This does not mean that bumps, in general, cause more problems than dips. The result is applicable to these cases only. The effect of other factors on the severity of the bump and dip will be examined in a full parametric study.

7. PARAMETRIC STUDY

To determine the influence of various components on the bump/dip problem, a parametric study was conducted. The previous case with an approach and bridge track modulus of 31 MN/m/m (4500 lb/in/in) and 83 MN/m/m (12000 lb/in/in), respectively, serves as a reference off of which the parameters are varied. The reference case for the bump includes wood ties on both the bridge and approach, 2.6 m (8.5 ft) tie lengths, an open deck steel bridge, 254 mm (10 in) ballast thickness, 22.2 m/s (50 mph) truck velocity, a bump length of 5.1 m (16.7 ft), a bump height of 33 mm (1.3 in), and a bump/dip slope of 1:150. The reference case for the dip is exactly the same as for the bump except for the dip height, which is 16 mm (0.6 in). Using the reference case, each parameter is varied one at a time, for both the bump and the dip, to study its impact on the system. For this parametric study, the parameters varied include:

1) Train direction
2) Truck velocity
3) Bump/Dip size
4) Subgrade/Fill modulus
5) Approach tie material
6) Bridge tie material
7) Bridge deck type
8) Ballast thickness
9) Approach tie length

The parametric study for the bump is defined in Table 7.1. The parametric study for the dip is defined in Table 7.2. In both tables, the reference case is shown in blue, while the parameter varied in each case is shown in red. In total, there are 100 unique cases, including the reference cases.

Table 7.1 - Bump parametric study cases

Case	Truck		Approach					Bump			Bridge	
	Velocity (m/s)	Direction	Tie Material	Ballast Depth (mm)	Tie Length (m)	Fill Mod. (MPa)	Soil Mod. (MPa)	Vertical Elev. (mm)	Horiz. Dist. (m)	Slope	Bridge Type	Tie Material
Ref.	22.2	On To	Wood	254	2.6	35	20	33	5.1	1:150	Open Deck	Wood
1	50	Off Of	Wood	254	2.6	35	20	33	5.1	1:150	Open Deck	Wood
2	8.9	On To	Wood	254	2.6	35	20	33	5.1	1:150	Open Deck	Wood
3	15.6	On To	Wood	254	2.6	35	20	33	5.1	1:150	Open Deck	Wood
4	33.5	On To	Wood	254	2.6	35	20	33	5.1	1:150	Open Deck	Wood
5	44.7	On To	Wood	254	2.6	35	20	33	5.1	1:150	Open Deck	Wood
6	22.2	On To	Wood	254	2.6	35	20	100	5.1	1:50	Open Deck	Wood
7	22.2	On To	Wood	254	2.6	35	20	50	5.1	1:100	Open Deck	Wood
8	22.2	On To	Wood	254	2.6	35	20	25	5.1	1:200	Open Deck	Wood
9	22.2	On To	Wood	254	2.6	35	20	20	5.1	1:250	Open Deck	Wood
10	15.6	On To	Wood	254	2.6	35	20	33	1.6	1:50	Open Deck	Wood
11	22.2	On To	Wood	254	2.6	35	20	33	1.6	1:50	Open Deck	Wood
12	33.5	On To	Wood	254	2.6	35	20	33	1.6	1:50	Open Deck	Wood
13	44.7	On To	Wood	254	2.6	35	20	33	1.6	1:50	Open Deck	Wood
14	15.6	On To	Wood	254	2.6	35	20	33	3.3	1:100	Open Deck	Wood
15	22.2	On To	Wood	254	2.6	35	20	33	3.3	1:100	Open Deck	Wood
16	33.5	On To	Wood	254	2.6	35	20	33	3.3	1:100	Open Deck	Wood
17	44.7	On To	Wood	254	2.6	35	20	33	3.3	1:100	Open Deck	Wood
18	15.6	On To	Wood	254	2.6	35	20	33	6.6	1:200	Open Deck	Wood
19	22.2	On To	Wood	254	2.6	35	20	33	6.6	1:200	Open Deck	Wood
20	33.5	On To	Wood	254	2.6	35	20	33	6.6	1:200	Open Deck	Wood
21	44.7	On To	Wood	254	2.6	35	20	33	6.6	1:200	Open Deck	Wood
22	15.6	On To	Wood	254	2.6	35	20	33	8.4	1:250	Open Deck	Wood
23	22.2	On To	Wood	254	2.6	35	20	33	8.4	1:250	Open Deck	Wood
24	33.5	On To	Wood	254	2.6	35	20	33	8.4	1:250	Open Deck	Wood
25	44.7	On To	Wood	254	2.6	35	20	33	8.4	1:250	Open Deck	Wood
26	15.6	On To	Wood	254	2.6	35	20	0	0	0	Open Deck	Wood
27	22.2	On To	Wood	254	2.6	35	20	0	0	0	Open Deck	Wood
28	33.5	On To	Wood	254	2.6	35	20	0	0	0	Open Deck	Wood
29	44.7	On To	Wood	254	2.6	35	20	0	0	0	Open Deck	Wood
30	22.2	On To	Wood	254	2.6	20	20	33	5.1	1:150	Open Deck	Wood
31	22.2	On To	Wood	254	2.6	50	50	33	5.1	1:150	Open Deck	Wood
32	22.2	On To	Wood	254	2.6	100	100	33	5.1	1:150	Open Deck	Wood
33	22.2	On To	Concrete	254	2.6	35	20	33	5.1	1:150	Open Deck	Wood
34	22.2	On To	Plastic	254	2.6	35	20	33	5.1	1:150	Open Deck	Wood
35	22.2	On To	Conc. w/Rubber Pads	254	2.6	35	20	33	5.1	1:150	Open Deck	Wood
36	22.2	On To	Wood w/Rubber Pads	254	2.6	35	20	33	5.1	1:150	Open Deck	Wood
37	22.2	On To	Wood w/Rubber Tie Pads	254	2.6	35	20	33	5.1	1:150	Open Deck	Wood
38	22.2	On To	Conc. w/Rubber Tie Pads	254	2.6	35	20	33	5.1	1:150	Open Deck	Wood
39	22.2	On To	Wood	254	2.6	35	20	33	5.1	1:150	Open Deck	Concrete
40	22.2	On To	Wood	254	2.6	35	20	33	5.1	1:150	Open Deck	Plastic
41	22.2	On To	Wood	254	2.6	35	20	33	5.1	1:150	Open Deck	Wood w/Rubber Pads
42	22.2	On To	Wood	254	2.6	35	20	33	5.1	1:150	Open Deck	Conc. w/Rubber Pads
43	22.2	On To	Wood	254	2.6	35	20	33	5.1	1:150	Ballast Deck	Wood
44	22.2	On To	Wood	254	2.6	35	20	33	5.1	1:150	Open Deck	Wood w/Ballast Mat
45	22.2	On To	Wood	152.4	2.6	35	20	33	5.1	1:150	Open Deck	Wood
46	22.2	On To	Wood	203.2	2.6	35	20	33	5.1	1:150	Open Deck	Wood
47	22.2	On To	Wood	304.8	2.6	35	20	33	5.1	1:150	Open Deck	Wood
48	22.2	On To	Wood	406.4	2.6	35	20	33	5.1	1:150	Open Deck	Wood
49	22.2	On To	Wood	254	2.1	35	20	33	5.1	1:150	Open Deck	Wood
50	22.2	On To	Wood	254	3	35	20	33	5.1	1:150	Open Deck	Wood
51	22.2	On To	Wood	254	3.6	35	20	33	5.1	1:150	Open Deck	Wood

Table 7.2 – Dip parametric study cases

Case	Truck		Approach					Dip			Bridge	
	Velocity (m/s)	Direction	Tie Material	Ballast Depth (mm)	Tie Length (m)	Fill Mod. (MPa)	Soil Mod. (MPa)	Vertical Elev. (mm)	Horiz. Dist. (m)	Slope	Bridge Type	Tie Material
Ref.	22.2	On To	Wood	254	2.6	35	20	16	5.1	1:150	Open Deck	Wood
1	50	Off Of	Wood	254	2.6	35	20	16	5.1	1:150	Open Deck	Wood
2	8.9	On To	Wood	254	2.6	35	20	16	5.1	1:150	Open Deck	Wood
3	15.6	On To	Wood	254	2.6	35	20	16	5.1	1:150	Open Deck	Wood
4	33.5	On To	Wood	254	2.6	35	20	16	5.1	1:150	Open Deck	Wood
5	44.7	On To	Wood	254	2.6	35	20	16	5.1	1:150	Open Deck	Wood
6	22.2	On To	Wood	254	2.6	35	20	46	5.1	1:50	Open Deck	Wood
7	22.2	On To	Wood	254	2.6	35	20	23	5.1	1:100	Open Deck	Wood
8	22.2	On To	Wood	254	2.6	35	20	11	5.1	1:200	Open Deck	Wood
9	22.2	On To	Wood	254	2.6	35	20	9	5.1	1:250	Open Deck	Wood
10	15.6	On To	Wood	254	2.6	35	20	16	1.6	1:50	Open Deck	Wood
11	22.2	On To	Wood	254	2.6	35	20	16	1.6	1:50	Open Deck	Wood
12	33.5	On To	Wood	254	2.6	35	20	16	1.6	1:50	Open Deck	Wood
13	44.7	On To	Wood	254	2.6	35	20	16	1.6	1:50	Open Deck	Wood
14	15.6	On To	Wood	254	2.6	35	20	16	3.3	1:100	Open Deck	Wood
15	22.2	On To	Wood	254	2.6	35	20	16	3.3	1:100	Open Deck	Wood
16	33.5	On To	Wood	254	2.6	35	20	16	3.3	1:100	Open Deck	Wood
17	44.7	On To	Wood	254	2.6	35	20	16	3.3	1:100	Open Deck	Wood
18	15.6	On To	Wood	254	2.6	35	20	16	6.6	1:200	Open Deck	Wood
19	22.2	On To	Wood	254	2.6	35	20	16	6.6	1:200	Open Deck	Wood
20	33.5	On To	Wood	254	2.6	35	20	16	6.6	1:200	Open Deck	Wood
21	44.7	On To	Wood	254	2.6	35	20	16	6.6	1:200	Open Deck	Wood
22	15.6	On To	Wood	254	2.6	35	20	16	8.4	1:250	Open Deck	Wood
23	22.2	On To	Wood	254	2.6	35	20	16	8.4	1:250	Open Deck	Wood
24	33.5	On To	Wood	254	2.6	35	20	16	8.4	1:250	Open Deck	Wood
25	44.7	On To	Wood	254	2.6	35	20	16	8.4	1:250	Open Deck	Wood
26	15.6	On To	Wood	254	2.6	35	20	0	0	0	Open Deck	Wood
27	22.2	On To	Wood	254	2.6	35	20	0	0	0	Open Deck	Wood
28	33.5	On To	Wood	254	2.6	35	20	0	0	0	Open Deck	Wood
29	44.7	On To	Wood	254	2.6	35	20	0	0	0	Open Deck	Wood
30	22.2	On To	Wood	254	2.6	20	20	16	5.1	1:150	Open Deck	Wood
31	22.2	On To	Wood	254	2.6	50	50	16	5.1	1:150	Open Deck	Wood
32	22.2	On To	Wood	254	2.6	100	100	16	5.1	1:150	Open Deck	Wood
33	22.2	On To	Concrete	254	2.6	35	20	16	5.1	1:150	Open Deck	Wood
34	22.2	On To	Plastic	254	2.6	35	20	16	5.1	1:150	Open Deck	Wood
35	22.2	On To	Conc. w/Rubber Pads	254	2.6	35	20	16	5.1	1:150	Open Deck	Wood
36	22.2	On To	Wood w/Rubber Pads	254	2.6	35	20	16	5.1	1:150	Open Deck	Wood
37	22.2	On To	Wood w/Rubber Tie Pads	254	2.6	35	20	16	5.1	1:150	Open Deck	Wood
38	22.2	On To	Conc. w/Rubber Tie Pads	254	2.6	35	20	16	5.1	1:150	Open Deck	Wood
39	22.2	On To	Wood	254	2.6	35	20	16	5.1	1:150	Open Deck	Concrete
40	22.2	On To	Wood	254	2.6	35	20	16	5.1	1:150	Open Deck	Plastic
41	22.2	On To	Wood	254	2.6	35	20	16	5.1	1:150	Open Deck	Wood w/Rubber Pads
42	22.2	On To	Wood	254	2.6	35	20	16	5.1	1:150	Open Deck	Conc. w/Rubber Pads
43	22.2	On To	Wood	254	2.6	35	20	16	5.1	1:150	Ballast Deck	Wood
44	22.2	On To	Wood	254	2.6	35	20	16	5.1	1:150	Open Deck	Wood w/Ballast Mat
45	22.2	On To	Wood	152.4	2.6	35	20	16	5.1	1:150	Open Deck	Wood
46	22.2	On To	Wood	203.2	2.6	35	20	16	5.1	1:150	Open Deck	Wood
47	22.2	On To	Wood	304.8	2.6	35	20	16	5.1	1:150	Open Deck	Wood
48	22.2	On To	Wood	406.4	2.6	35	20	16	5.1	1:150	Open Deck	Wood
49	22.2	On To	Wood	254	2.1	35	20	16	5.1	1:150	Open Deck	Wood
50	22.2	On To	Wood	254	3	35	20	16	5.1	1:150	Open Deck	Wood
51	22.2	On To	Wood	254	3.6	35	20	16	5.1	1:150	Open Deck	Wood

The reference case was largely chosen based on average results from the survey of railroad professionals (Section 4). Most of the parameters chosen were based on their possible effect on the track modulus. This could, in turn, affect the track response due to a bump or dip in the track geometry. Train direction, train velocity and bump/dip size are

the exceptions. These parameters are important because the severity of the problem is influenced by these factors. The results of the parametric study include the wheel/rail reaction forces, vertical axle accelerations, track deflection, dynamic load factor (DLF), dynamic ballast pressure factor (DBF) and dynamic subgrade pressure factor (DSF) for each case. Note that in each figure presented, the direction of traffic is from left to right.

7.1 TRAIN DIRECTION

The direction of the truck, whether it goes on to the bridge or comes off of the bridge, will have an influence on the track response. For the case of a train going on to the bridge, the train is traveling from a softer material (the approach) to a harder material (the bridge). Since the bridge is not as deformable as the approach, an impact will occur. This has been shown in the previous section (Section 6) for the case of truck moving on to a bridge with no bumps or dips in the approach track geometry. For the case of a train moving off of the bridge, the train is traveling from a harder material (the bridge) to a softer material (the approach). The approach will tend to deform with the load causing any impact on the track to be less severe.

To determine the effect of train direction, a case was simulated with the truck moving off of the bridge on to the approach embankment for both the bump and the dip. The results are then compared to the reference case where the truck moves in the opposite direction, off of the approach embankment on to the bridge.

7.1.1 Bump Results

The track response resulting from the bump reference case, where the truck travels on to the bridge was previously presented in Section 6 (Figs. 6.15 to 6.18). The results for a train moving off of the bridge onto an approach embankment with a 1:150 bump, however, are presented in Fig. 7.1. The truck is moving from left to right in the figure.

From the reaction forces between the wheel and the rail (Fig. 7.1a), it is shown that no impact occurs when the truck exits the bridge and moves on to the approach embankment bump. An unloading actually occurs at this location for both the front and the back axles (Fig. 7.1b). Therefore, as the truck moves from the bridge, an area of high track modulus, to the approach embankment, an area of low track modulus, an initial decrease of track loading will occur. The maximum low frequency impacts on the track will occur at the end of the bump on the approach embankment. So, for either direction, the highest impact force occurs on the soft side of the track transition.

The DLF for this case is 1.13. This is small compared to the case with the truck is moving on to the bridge where the DLF is 1.28. This is a 15% difference in impact load for the two cases.

The track deflection for a truck moving off of the bridge is shown in Fig. 7.1c. There is very little deflection along the bump slope. This suggests that full contact is not established between the wheel and rail. Once the truck enters the level portion of the approach after the bump, full track deflection is again seen. The DDF is thus very small, at 1.02. The small track deflection on the bump is reflected in the ballast and subgrade pressures.

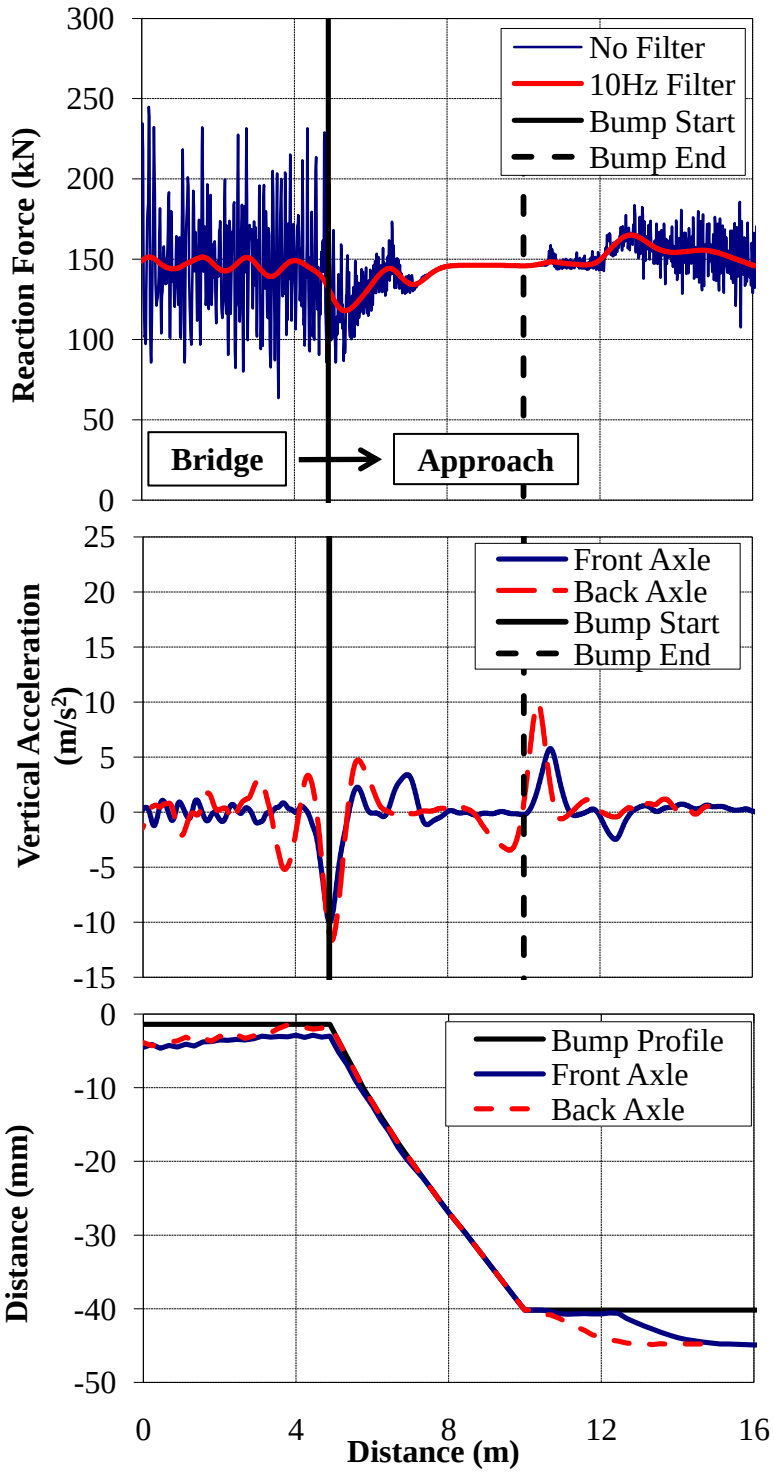

Figure 7.1 - (a) Wheel/Rail forces (b) Axle accelerations and (c) Track deflection due to moving off of the bridge on to an approach embankment with a 1:150 Bump (v = 22.2 m/s)

The ballast pressures resulting from a truck moving off of the bridge are shown in Fig. 7.2. On the bump, ballast pressures are considerably reduced to as little as 13 kPa (compression). A slight increase in ballast pressure is seen on the level portion of the approach, about 2.8 m from the end of the bump. The DBF for this case, using the average ballast pressure of 400 kPa found previously, is 1.1. This is a significant reduction from the DBF of 2.32 for the case with the truck moving on to the bridge.

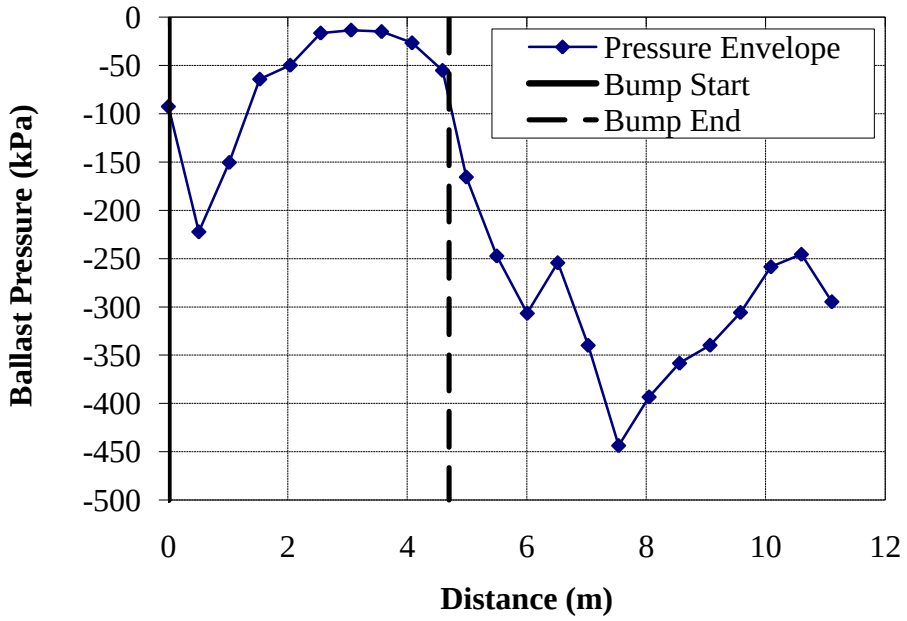

Figure 7.2 - Ballast pressure due to moving off of the bridge on to an approach embankment with a 1:150 Bump (v = 22.2 m/s)

The subgrade pressures resulting from a truck moving off of the bridge are shown in Fig. 7.3. As with the ballast pressures, the subgrade pressures are reduced on the bump from the average pressure of 72 kPa (compression) found earlier. The

subgrade pressures do not fully develop until after the truck has left the bump and moved on to the level approach embankment. The DSF in this case is 1.05, a significant reduction from the DSF of 2.18 for the case with the truck moving on to the bridge.

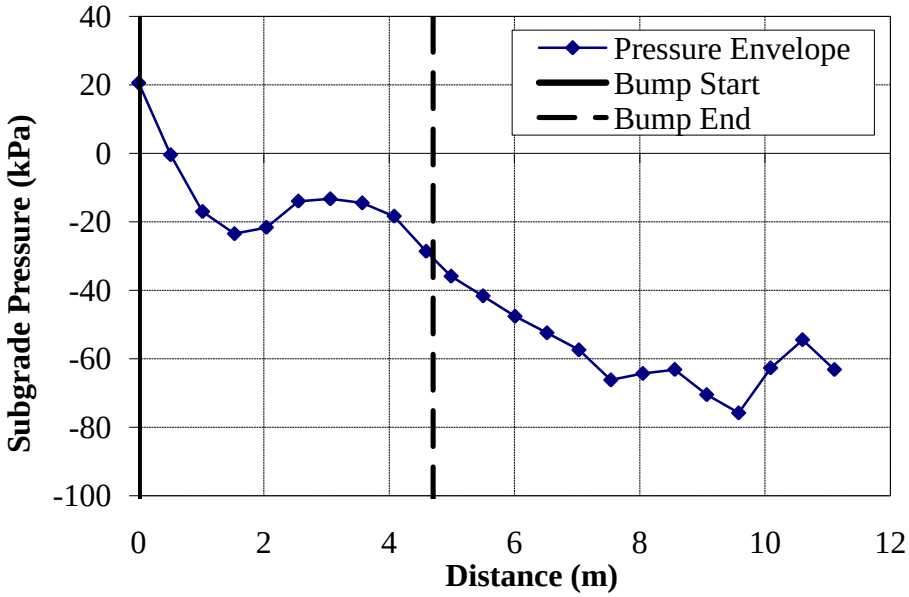

Figure 7.3 - Subgrade pressure due to moving off of the bridge on to an approach embankment with a 1:150 Bump (v = 22.2 m/s)

From these results, it is clear that coming off of the bridge is less severe than going on to the bridge when a 1:150 bump is present. The DLF, DDF, DBF and DSF are all considerably greater for the case of a truck moving on to the bridge than for the case of a truck moving off of the bridge.

7.1.2 Dip Results

The track response resulting from the dip reference case, where the truck travels on to the bridge was previously presented in Section 6 (Figs. 6.15 to 6.18). A case where the truck travels in the opposite direction, off of the bridge on to the approach, was simulated. Similarly to the case with a bump, no impact occurs when the truck first exits the bridge (Fig. 7.4a). At the bottom of the dip, however, both the front and the back axle experience an impact (Fig. 7.4b). Another unloading then occurs as the truck moves up the dip on to the level approach.

The response is comparable to the response found from the reference case as the truck moves up the dip onto the bridge (Fig. 6.19c). The main difference is that there is no impact right before the dip end for this case (off of bridge) (Fig. 7.4b). This is because the truck is moving from the dip to the approach where both have relatively the same track modulus. The impact seen before the dip end in Fig. 6.19c, is because the truck is moving from the dip to the bridge where a large track modulus change is present.

The DLF for this case is 1.27. This is small compared to the case with the truck is moving on to the bridge where the DLF is 1.45. This is an 18% difference in impact load for the two cases. This is about the same difference as for the bump.

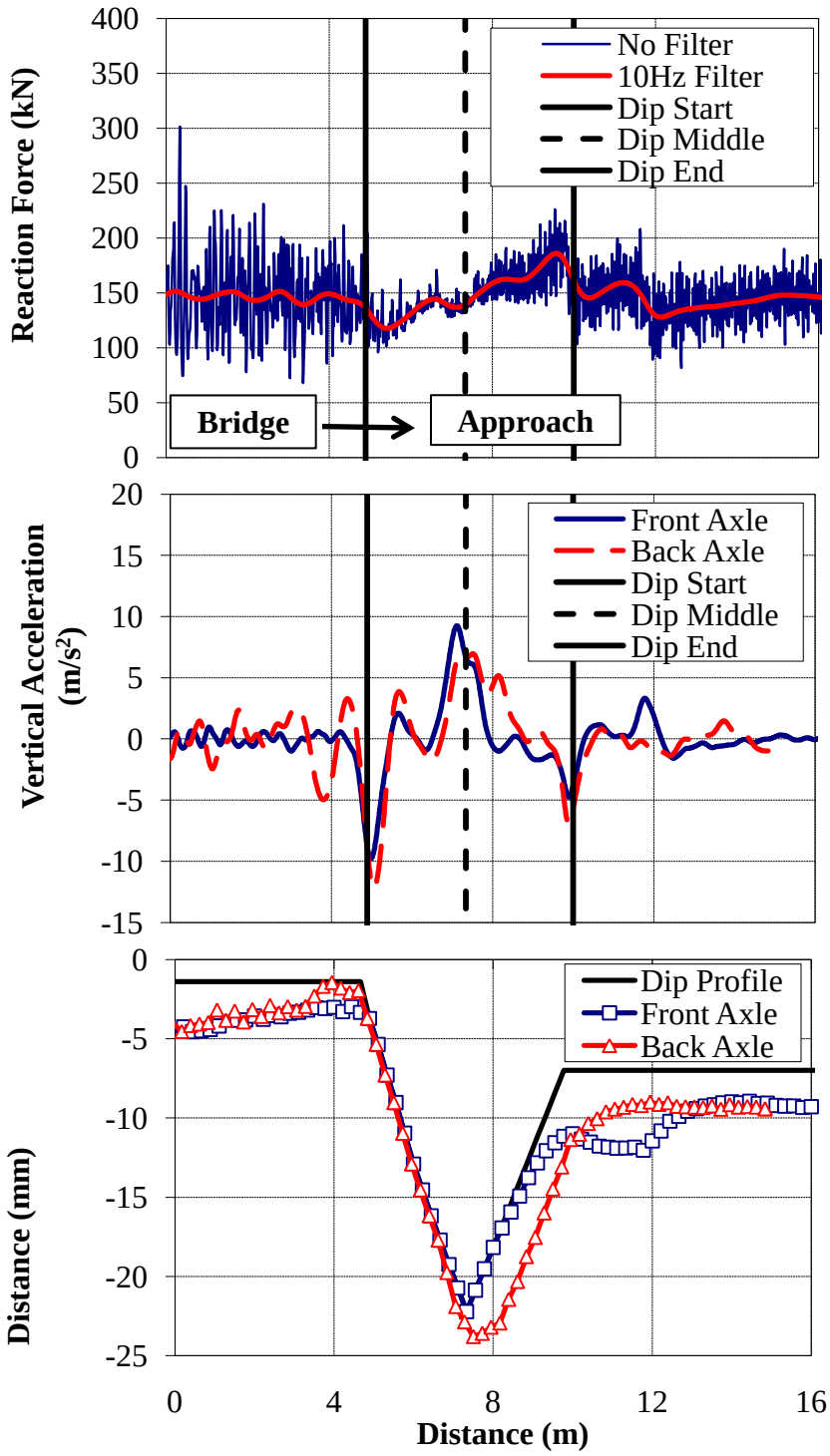

Figure 7.4 - (a) Wheel/Rail forces (b) Axle accelerations and (c) Track deflection due to a truck moving off of the bridge onto an approach embankment with a 1:150 Dip (v = 22.2 m/s)

The track deflection for a truck moving off a bridge onto a 1:150 dip is shown in Fig. 7.4c. As with the bump, there is very little track deflection on the down-slope of the dip as the truck enters the approach from the bridge. The maximum deflection is at a different location depending on which axle is passing. The maximum deflection under the front axle occurs at the end of the dip as it transitions to the approach embankment; the maximum deflection under the back axle, however, occurs near the bottom, or middle, of the dip. Both occur as the back axle enters the upslope of the dip. The DDF is 1.45, higher than for the bump of same size.

The ballast pressure for this case is shown in Fig. 7.5. The ballast pressure is increased on one side of the dip (the side that the truck is moving up and over) and on the approach near the dip. The ballast pressure then gradually reduces to the average ballast pressure of 400 kPa (compression).

The subgrade pressure responds similarly (Fig. 7.6). The DBF and DSF are 1.57 and 1.70, respectively. To compare, the DBF and DSF for the reference case are 2.14 and 1.78, respectively. As with the bump, the case with the truck moving on to the bridge is more severe than this case with the truck moving off of the bridge.

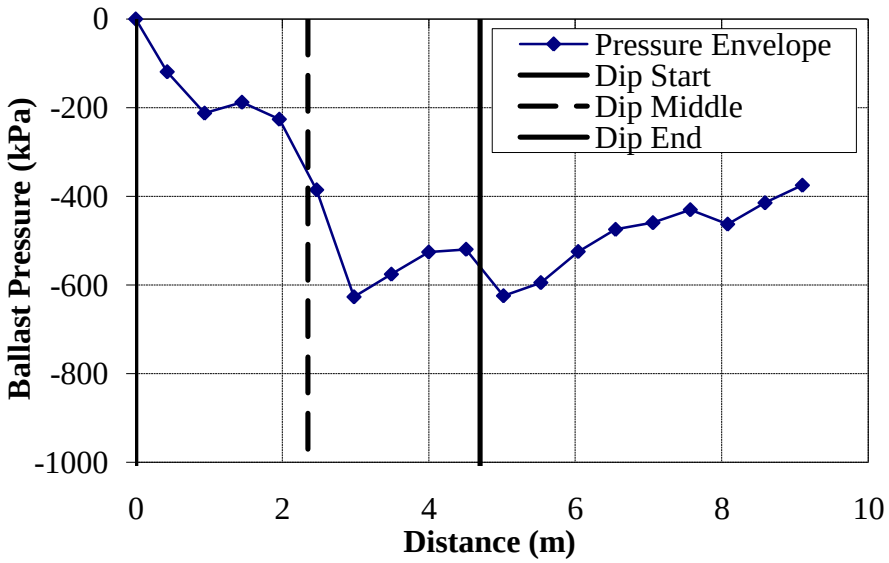

Figure 7.5 - Ballast pressure due to a truck moving off of the bridge onto an approach embankment with a 1:150 Dip (v = 22.2 m/s)

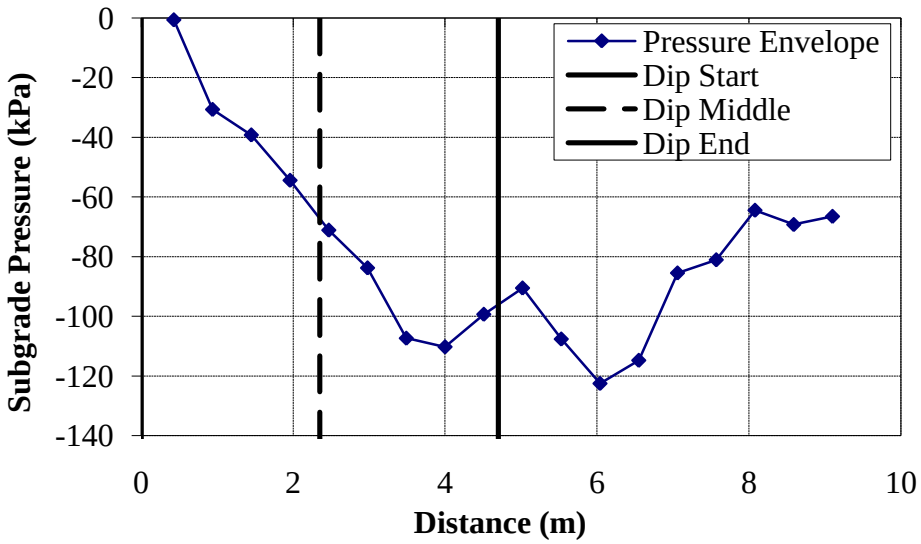

Figure 7.6 - Subgrade pressure due to a truck moving off of the bridge onto an approach embankment with a 1:150 Dip (v = 22.2 m/s)

7.1.3 Summary

The results for these bump and dip cases are summarized in Table 7.3. It is clear that the case with the truck moving on to the bridge is more severe than this case with the truck moving off of the bridge. Also, the response due to a 1:150 dip is more of a problem than due to a 1:150 bump. This is because the truck must still pass over the upslope of the dip which is, in a way, a small bump. When the truck is moving off of the bridge onto the 1:150 bump, there is no upslope to traverse, only a down-slope.

Table 7.3 – Train direction results summary

		BUMP				DIP			
Case No.	**Direction**	**DLF**	**DDF**	**DBF**	**DSF**	**DLF**	**DDF**	**DBF**	**DSF**
Ref.	On To Bridge	1.28	2.4	2.33	2.18	1.45	2.24	2.14	1.78
1	Off Of Bridge	1.13	1.02	1.10	1.05	1.27	1.45	1.57	1.70

7.2 TRAIN VELOCITY

The velocity was varied in this parametric study from 8.9 m/s (20 mph) to 44.7 m/s (100 mph). It is expected that a higher velocity will produce a higher dynamic load factor. The kinetic energy (KE) of the truck is a function of its mass (m) and velocity (v), given by Eq. 7.1. Therefore, if the velocity is increased, the kinetic energy will increase by the velocity squared. This higher energy at impact will result in larger DLFs, DDFs, DBFs and DSFs.

$$KE = \frac{1}{2}mv^2 \tag{7.1}$$

7.2.1 Bump Results

The complete set of results for wheel/rail reaction forces, vertical axle accelerations, track deflection, ballast pressures and subgrade pressures for each velocity case can be found in Appendix E. As expected, as the velocity increases, the reaction forces also increase (Fig. 7.7). For a velocity of 8.9 m/s, the impact right before the bridge at the end of the bump, which results from the track modulus differential, almost disappears. Therefore, to avoid large impacts on the track, trains should travel slowly over the bridge/approach location. This is often not feasible, however, as it could delay traffic considerably. In trouble locations, however, slow orders must be placed to limit the wheel/rail forces.

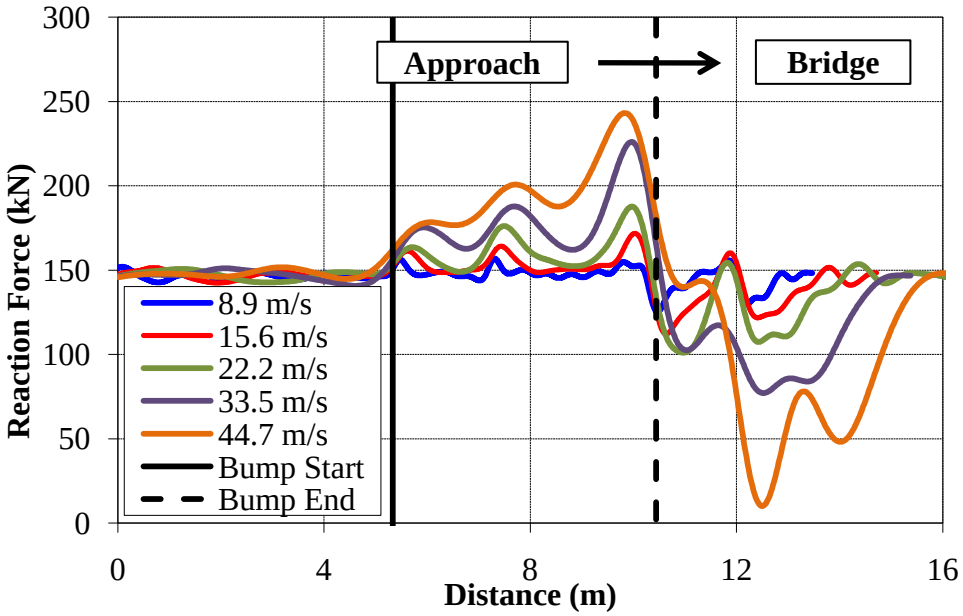

Figure 7.7 – 10 Hz filtered reaction force comparison for various velocities (Bump)

Track deflection is also affected by the train velocity (Fig. 7.8). The track deflection profile in Fig. 7.8 and all subsequent deflection figures is under the back axle only since the response is more severe than the front axle. Along with maximum displacement, the steepness of the track deflection profile also increases with increasing velocity. This leads to the larger impact forces as seen in Fig. 7.7. The only case that does not exceed the desirable limit of 6.4 mm is the case with a truck velocity of 8.9 m/s.

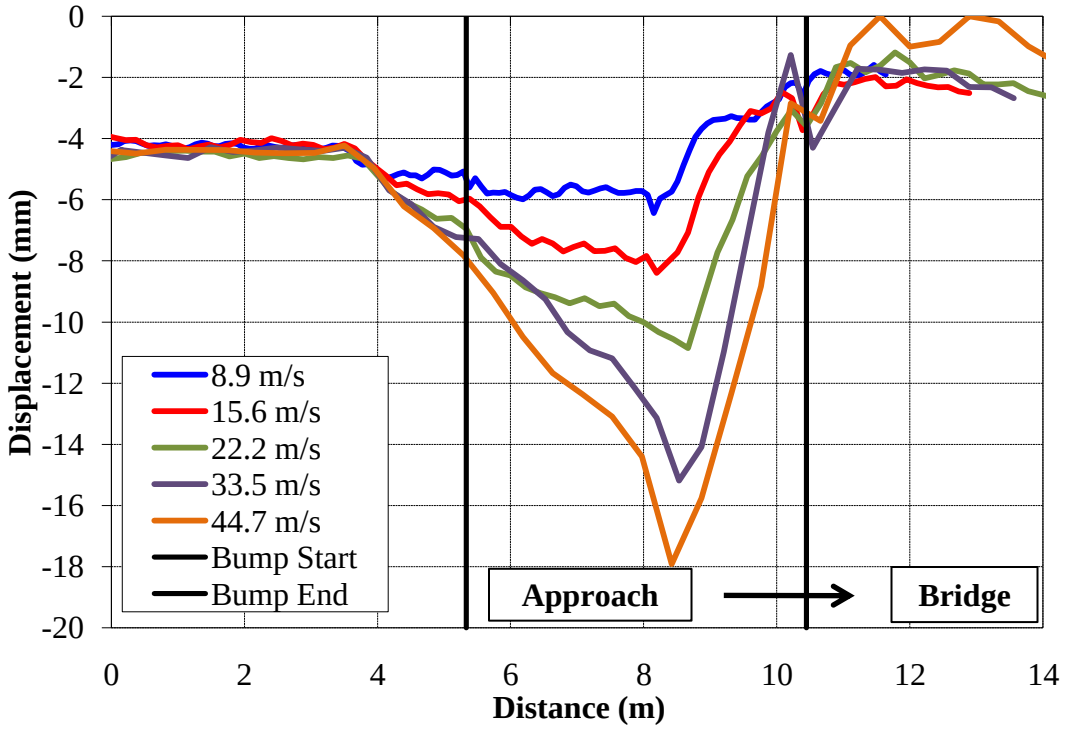

Figure 7.8 – Track displacement comparison for various velocities (Bump)

Similarly, ballast pressures (Fig. 7.9) and subgrade pressures (Fig. 7.10) are increased with increasing velocity. It is interesting to note that at higher velocities in the study (33.5 m/s and 44.7 m/s), the ballast and subgrade pressures peak at a location about 2 m away from the bridge abutment whereas for the lower velocities, the ballast and subgrade pressures are more uniformly increased across the bump. This could indicate that a dip is more likely to form at higher velocities and a bump is more likely to form at lower velocities.

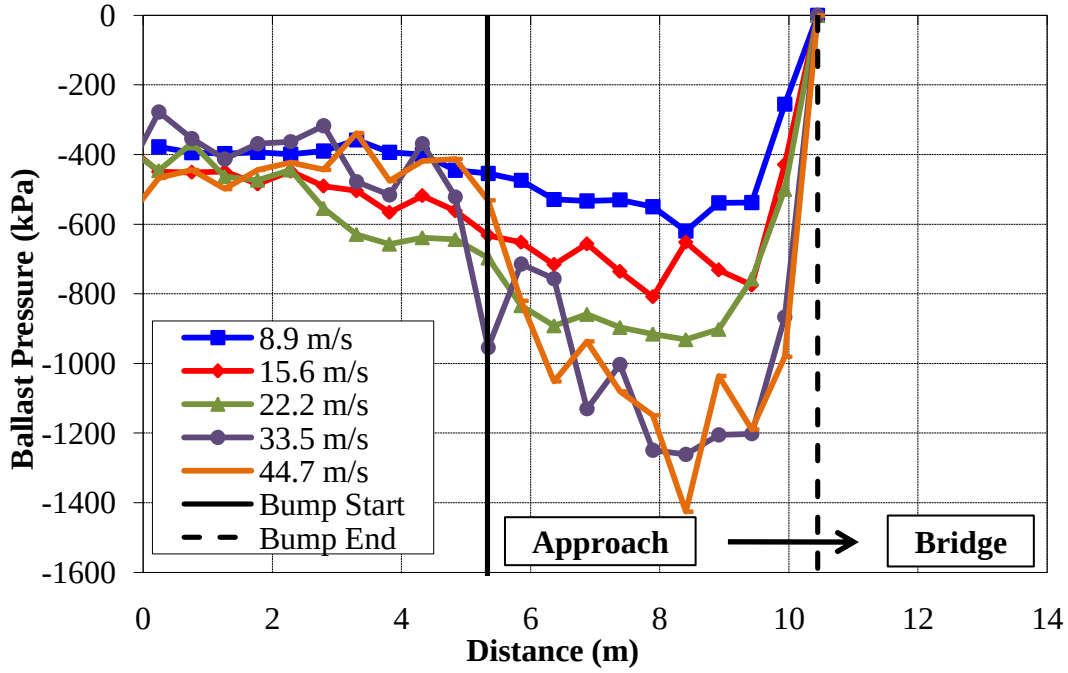

Figure 7.9 - Ballast pressure comparison for various velocities (Bump)

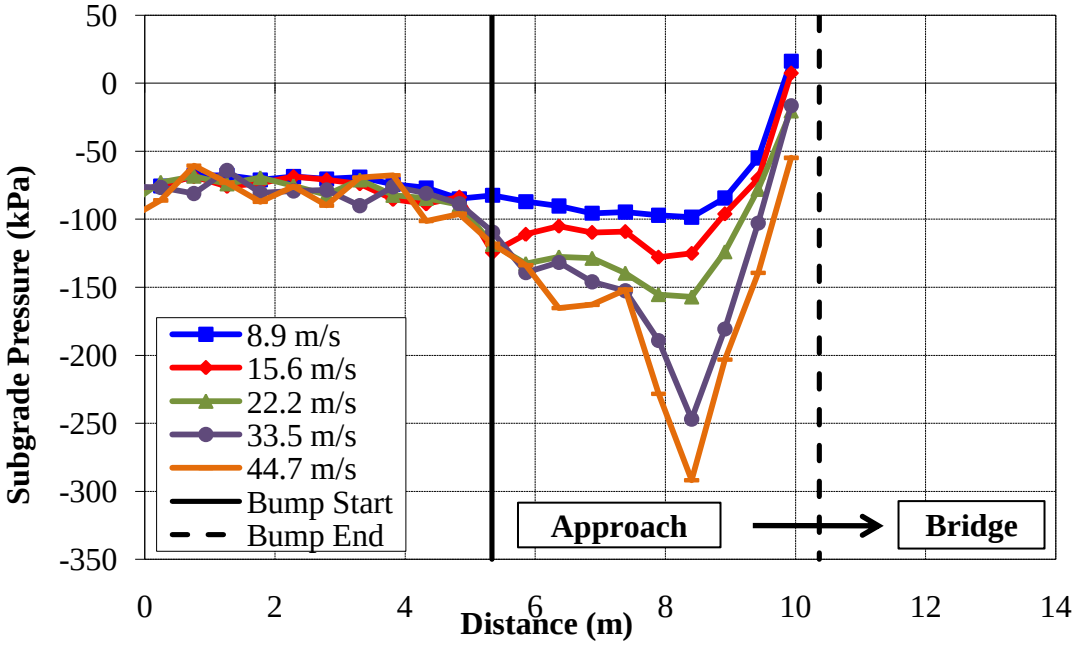

Figure 7.10 - Subgrade pressure comparison for various velocities (Bump)

The maximum ballast pressures for every case are above the limit of 450 kPa (AREMA 2008). This indicates that ballast fouling and tie abrasion could be an issue. The subgrade pressure limit of 140 kPa (AREMA 2008) is exceeded by each case except when the truck velocity is 8.9 m/s and 15.6 m/s. The results for DLF, DDF, DBF and DSF for varying velocities over the bump problem are summarized in Table 7.4.

Table 7.4 – Velocity results summary (Bump

Velocity (m/s)	DLF	DDF	DBF	DSF
8.9	1.07	1.46	1.55	1.37
15.6	1.18	1.83	2.02	1.78
22.2	1.28	2.40	2.33	2.18
33.5	1.55	3.45	3.15	3.43
44.7	1.66	4.07	3.56	4.05

7.2.2 Dip Results

The complete set of plots for wheel/rail reaction forces, vertical axle accelerations, track deflection, ballast pressures and subgrade pressures for each velocity case concerning the dip can be found in Appendix F. In general, an increase in truck velocity leads to an increase in impact forces (Fig. 7.11), track deflection (Fig. 7.12) ballast pressures (Fig. 7.13) and subgrade pressures (Fig. 7.14).

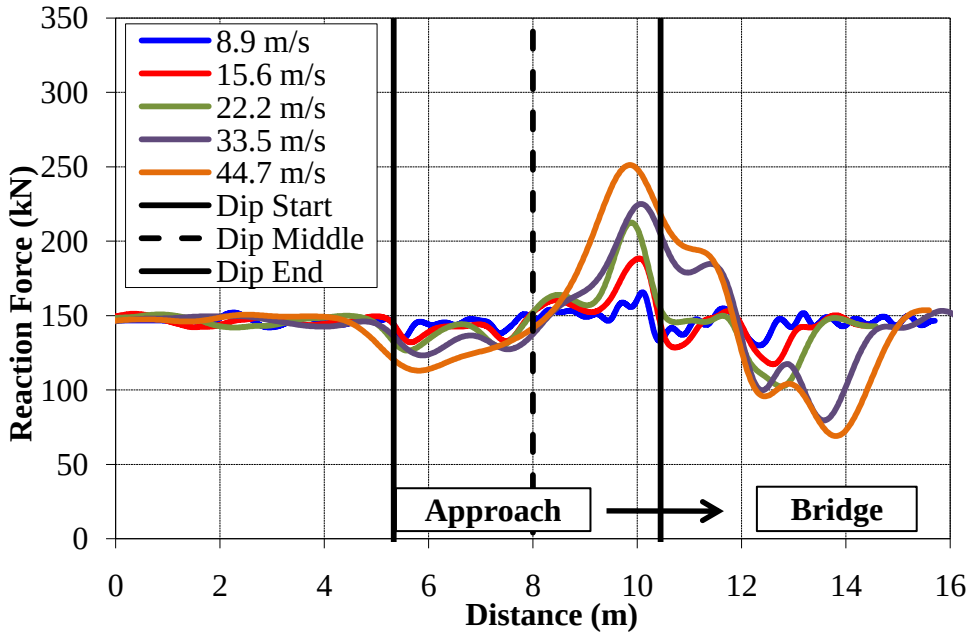

Figure 7.11 – 10 Hz filtered reaction force comparison for various velocities (Dip)

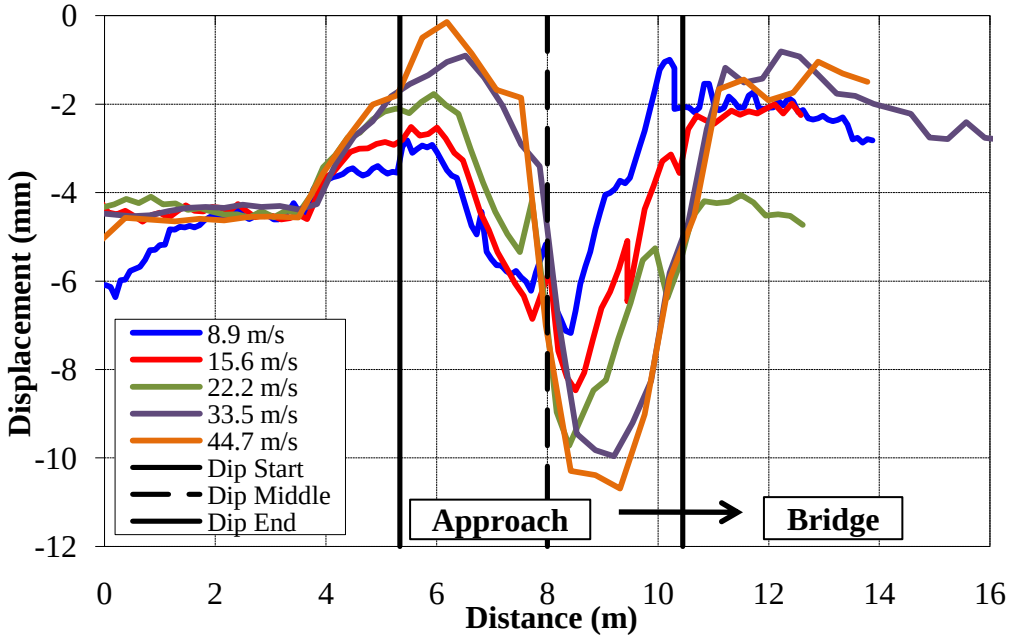

Figure 7.12 - Track displacement comparison for various velocities (Dip)

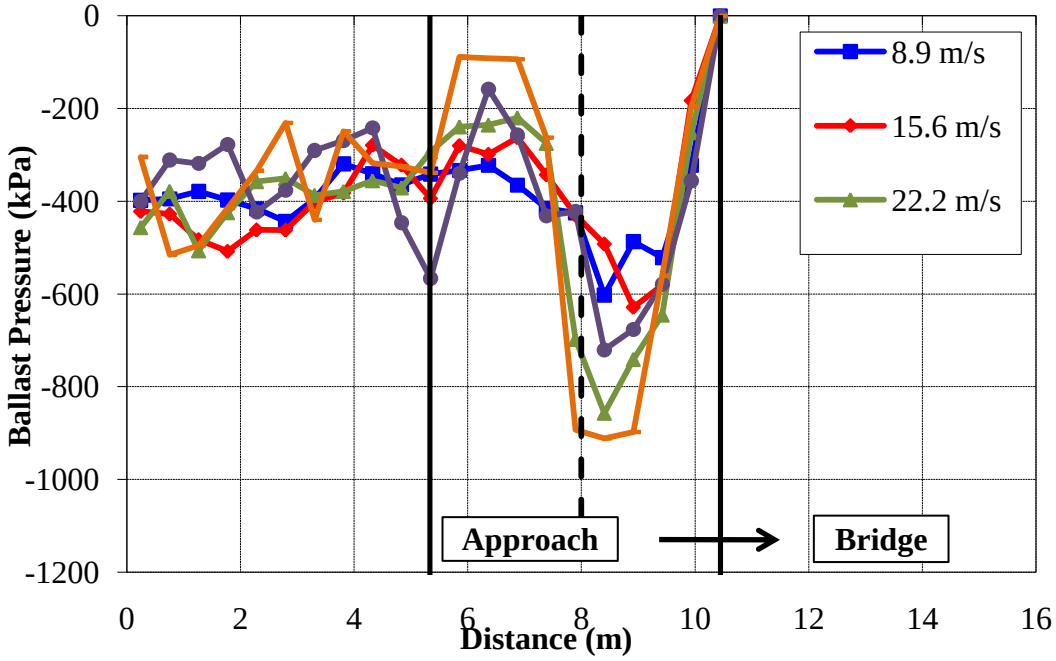

Figure 7.13 – Ballast pressure comparison for various velocities (Dip)

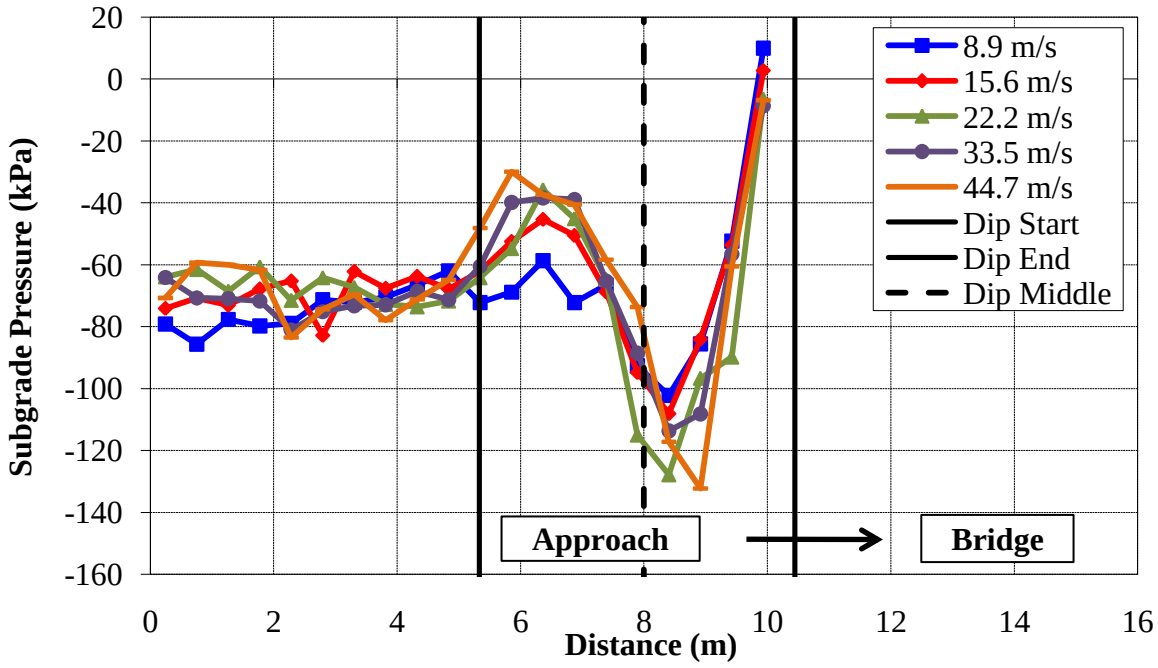

Figure 7.14 – Subgrade pressure comparison for various velocities (Dip)

The DLF limit of 1.5 is exceeded only when the velocity reaches at least 33.5 m/s, The track deflection and ballast pressure limits are exceeded for every case, even the slowest case with a truck velocity of 8.9 m/s. Unlike for the bump, however, all cases are below the subgrade pressure limit. The results for DLF, DDF, DBF and DSF are presented in Table 7.5.

Table 7.5 – Velocity results summary (Dip)

Velocity (m/s)	DLF	DDF	DBF	DSF
8.9	1.13	1.63	1.51	1.42
15.6	1.29	1.92	1.57	1.5
22.2	1.45	2.24	2.14	1.78
33.5	1.54	2.26	1.8	1.58
44.7	1.72	2.43	2.28	1.84

7.2.3 Summary

The results for both the bump and the dip have been summarized graphically in Fig. 7.15. The trends for DLF, DDF, DBF and DSF for the bump and the dip are all fairly linear. The steepness of this trend is typically higher for the bump, however, than for the dip. This suggests that velocity is a bigger factor for a bump than for a dip.

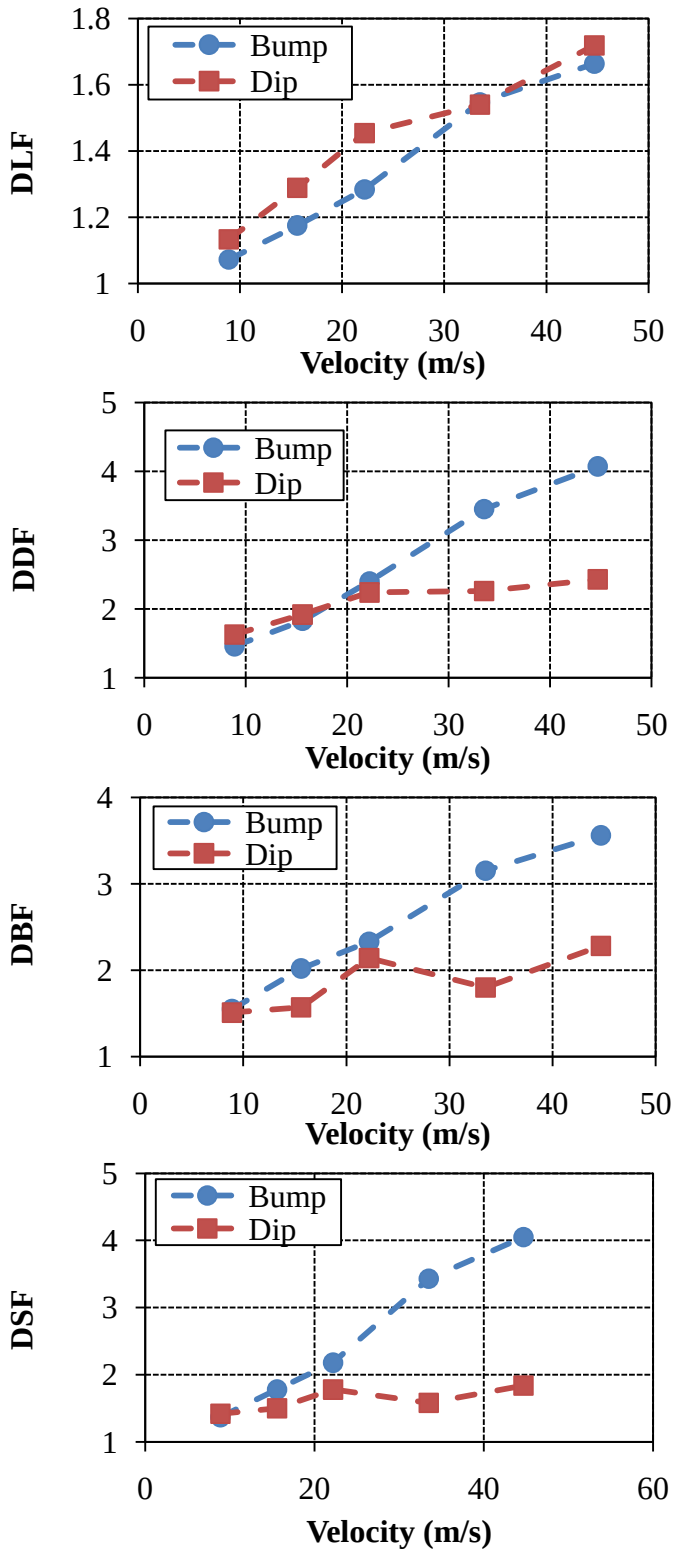

Figure 7.15 – (a) DLF, (b) DDF, (c) DBF and (d) DSF vs. velocity for the bump/dip

While the dip experiences higher DLFs than the bump, the opposite is true for both the DBF and DSF. This is because the ballast and subgrade pressures generated by a bump have longer to develop than for the dip in these cases as the upslope of the dip (which is like a bump in itself) is only half the length of the bump cases.

7.3 BUMP/DIP SIZE

In this parametric study, the bump/dip slopes examined are: 1:50, 1:100, 1:150, 1:200, 1:250 and no slope. The effect of bump/dip slope on the track response was investigated first by keeping the length (L) of the bump/dip the same and varying the height (H) depending on the desired slope (Fig. 7.16). Then, the effect of bump/dip slope on the track response was investigated by keeping the height (H) of the bump/dip the same and varying the length (L) depending on the desired slope (Fig. 7.17). It is expected that the track response will be more severe with a steeper bump/dip slope than a shallow bump slope.

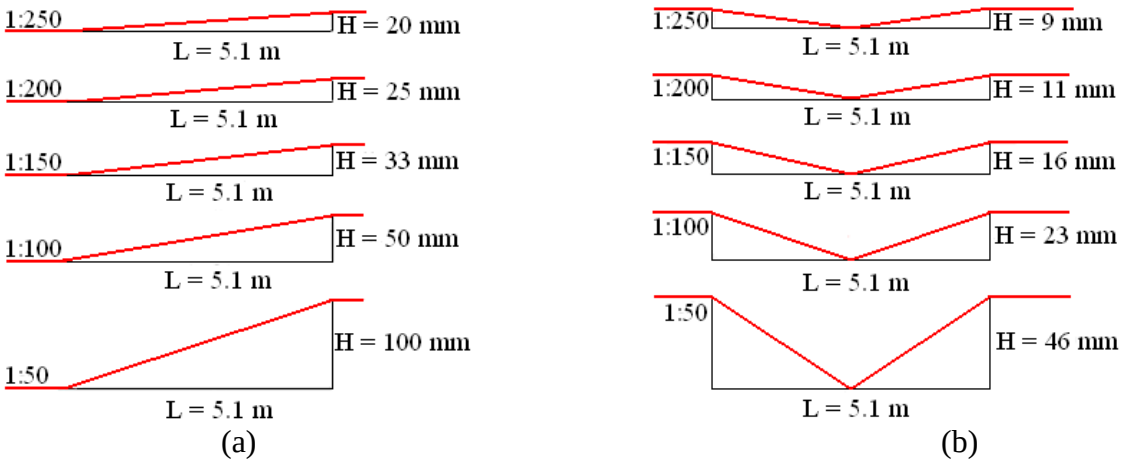

Figure 7.16 - (a) Bump (b) Dip dimensions for parametric study (equal lengths)

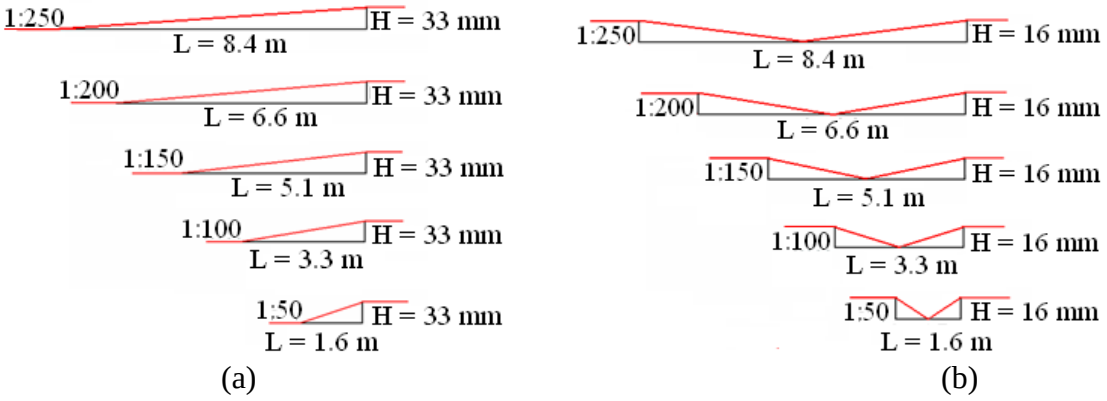

Figure 7.17 - (a) Bump (b) Dip dimensions for parametric study (equal heights)

7.3.1 Bump Results

The complete set of plots for wheel/rail reaction forces, vertical axle accelerations, track deflection, ballast pressures and subgrade pressures for each bump slope can be found in Appendix E. As expected, the wheel/rail forces do increase with bump slope steepness (Fig. 7.18) for bump slopes that have equal lengths (Fig. 7.16a). It is interesting to note

that for a steep slope of 1:50, the maximum forces that occur on the bump are due to the change in geometry, not due to the track modulus differential between the bridge and the approach as with the other shallower slopes. This suggests that if a slope is steep enough, the track geometry is more influential on impact forces than a change in track modulus.

The track deflection, ballast pressure and subgrade pressure profiles for slopes with equal lengths are presented in Figs. 7.19, Fig. 7.20 and Fig. 7.21, respectively. Every case with a bump slope exceeds the track deflection, ballast pressure and subgrade pressure limit criteria. The results for the DLF, DDF, DBF and DSF for different slopes with equal lengths are summarized in Table 7.6.

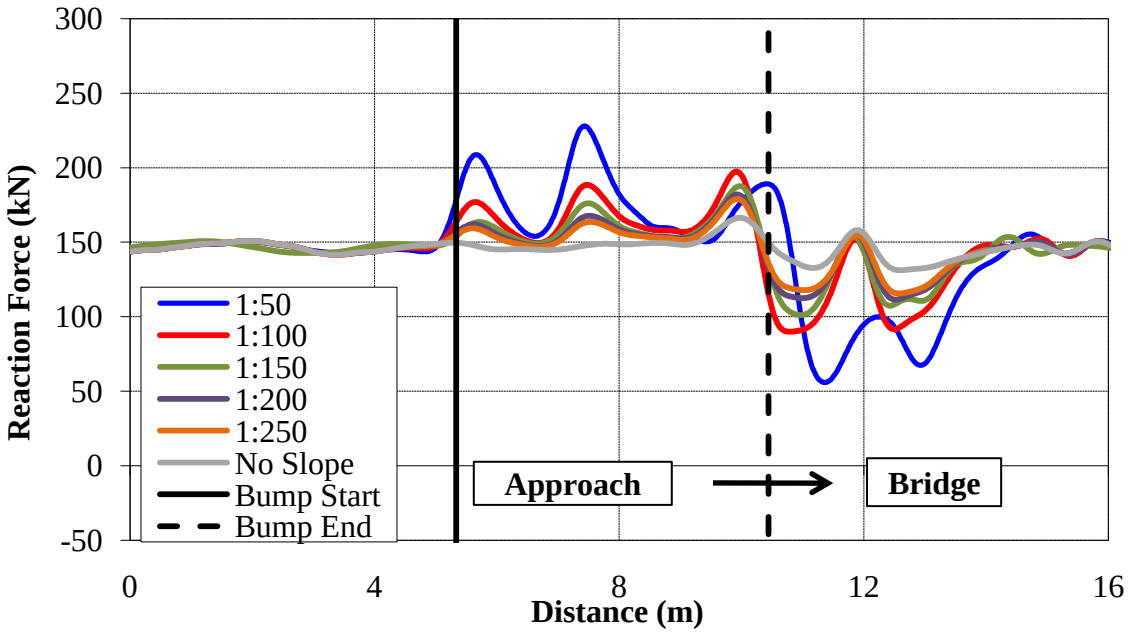

Figure 7.18 - 10 Hz filtered reaction force comparison for various bump slopes of equal length (Bump)

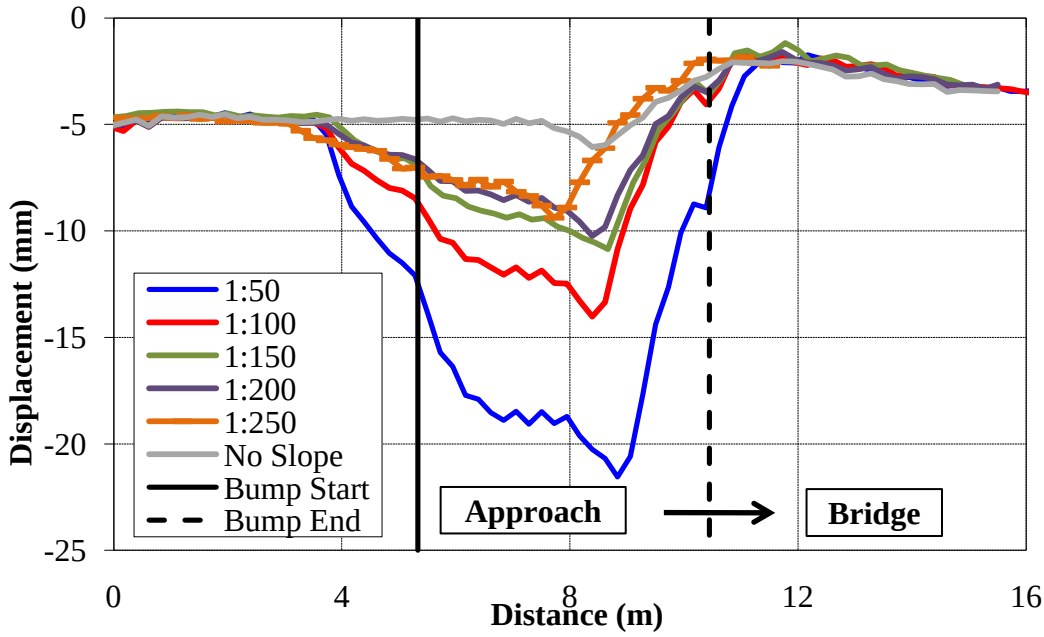

Figure 7.19 – Track deflection comparison for various bump slopes of equal length (Bump)

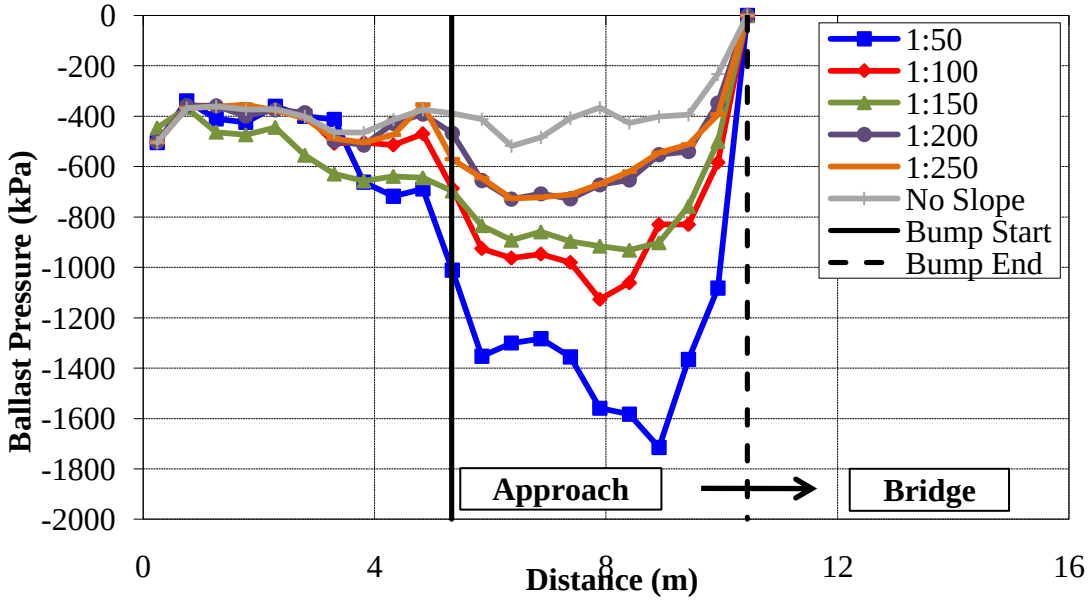

Figure 7.20 – Ballast pressure comparison for various bump slopes of equal length (Bump)

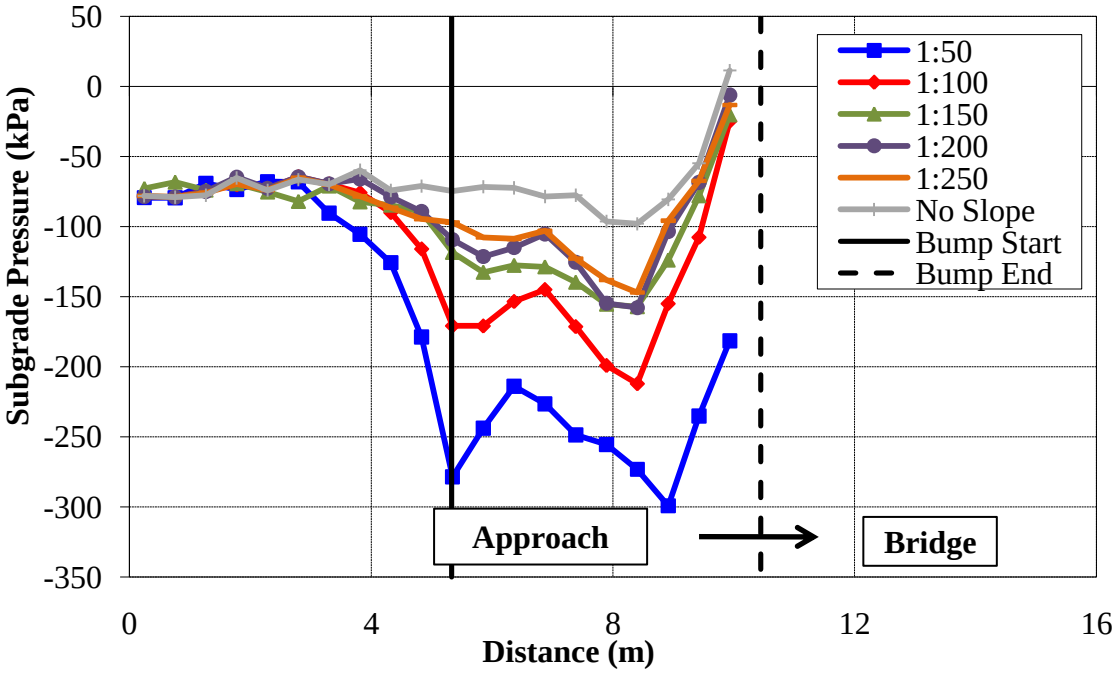

Figure 7.21 – Subgrade pressure comparison for various bump slopes of equal length (Bump)

Table 7.6 – Bump slope (equal lengths) results summary (Bump)

Bump Slope	Bump Length (m)	Bump Height (mm)	DLF	DDF	DBF	DSF
1:50	5.1	101.6	1.56	4.60	4.29	4.16
1:100	5.1	50.8	1.35	2.93	2.82	2.94
1:150	5.1	33	1.28	2.40	2.33	2.18
1:200	5.1	25.4	1.24	2.16	1.82	2.19
1:250	5.1	20.3	1.22	1.98	1.82	2.04
No Slope	0	0	1.14	1.40	1.30	1.36

Simulations were also performed on bump slopes with equal heights and varying lengths (Fig. 7.17a). A summary of the DLF, DDF, DBF and DSF results for these cases

are presented in Table 7.7. The results were then graphically compared to the previous results for bump slopes with equal lengths (Fig. 7.22).

Table 7.7 - Bump slope (equal heights) results summary (Bump)

Bump Slope	Bump Length (m)	Bump Height (mm)	DLF	DDF	DBF	DSF
1:50	1.7	33	1.45	3.24	3.54	3.05
1:100	3.3	33	1.40	2.88	2.67	2.75
1:150	5.1	33	1.28	2.93	2.33	2.18
1:200	6.6	33	1.23	2.20	2.19	2.07
1:250	8.3	33	1.20	2.10	1.80	1.95
No Slope	0	0	1.14	1.98	1.30	1.36

Fig. 7.22 suggests that the height and length of the bump does not matter as much as the overall slope. The only exception is for the steep slope of 1:50 where the slope with the greater bump height is more severe. This is likely because the length of the 1:50 bump, with equal height to the reference case, is shorter than the length between the two axles of the truck. While this does not change the impact due to the initial geometry change, it does reduce the subsequent impact on the track (Fig. 7.23).

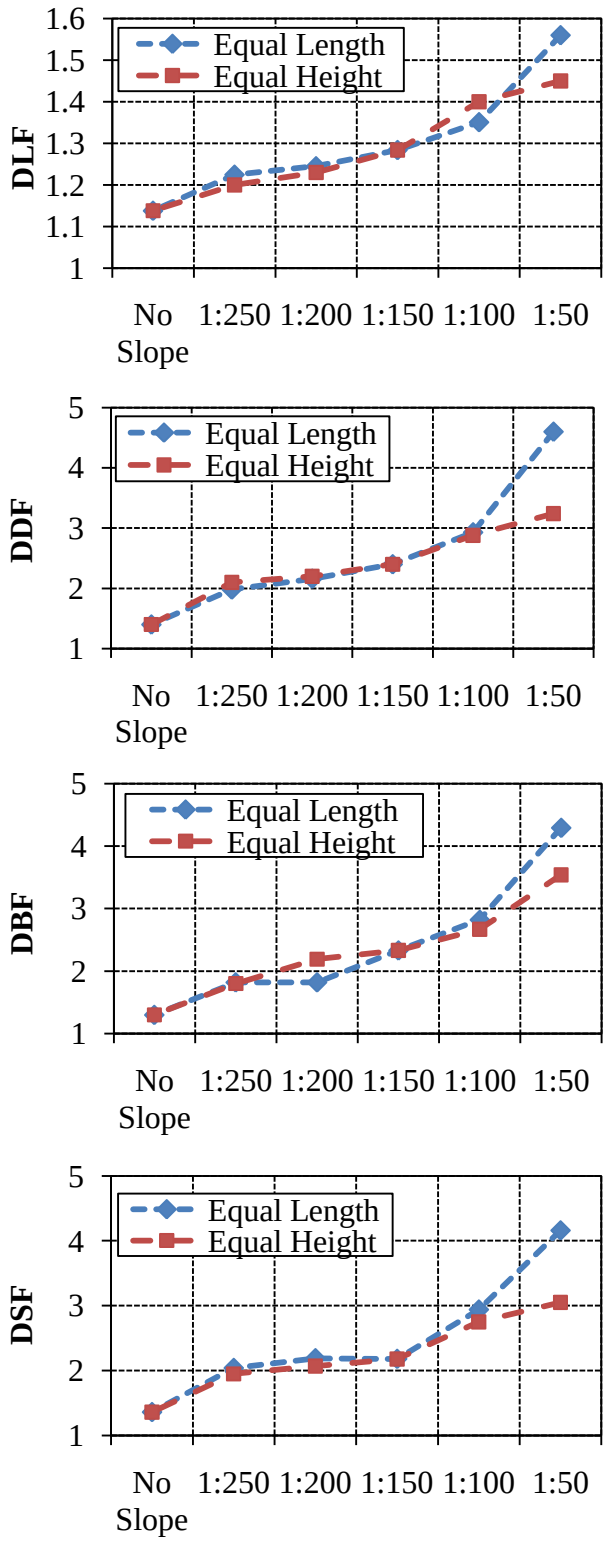

Figure 7.22 – (a) DLF, (b) DDF, (c) DBF and (d) DSF vs. bump slope

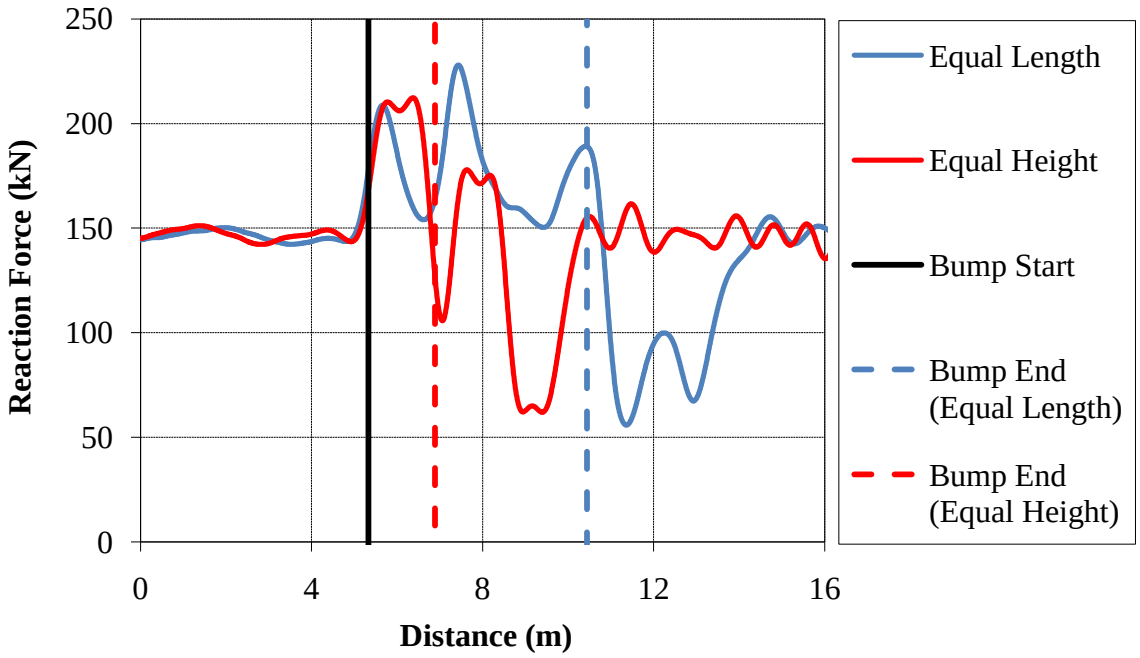

Figure 7.23 - 10 Hz filtered reaction force comparison for 1:50 bump slopes (Bump)

7.3.2 Dip Results

The complete set of plots for wheel/rail reaction forces, vertical axle accelerations, track deflection, ballast pressures and subgrade pressures for each dip slope can be found in Appendix F. As with the bump, simulations were first performed on dip slopes with equal lengths and varying heights (Fig. 7.16b). The reaction force, track deflection, ballast and subgrade pressure profiles for each of these cases are shown in Fig. 7.24, Fig. 7.25, Fig. 7.26 and Fig. 7.27, respectively.

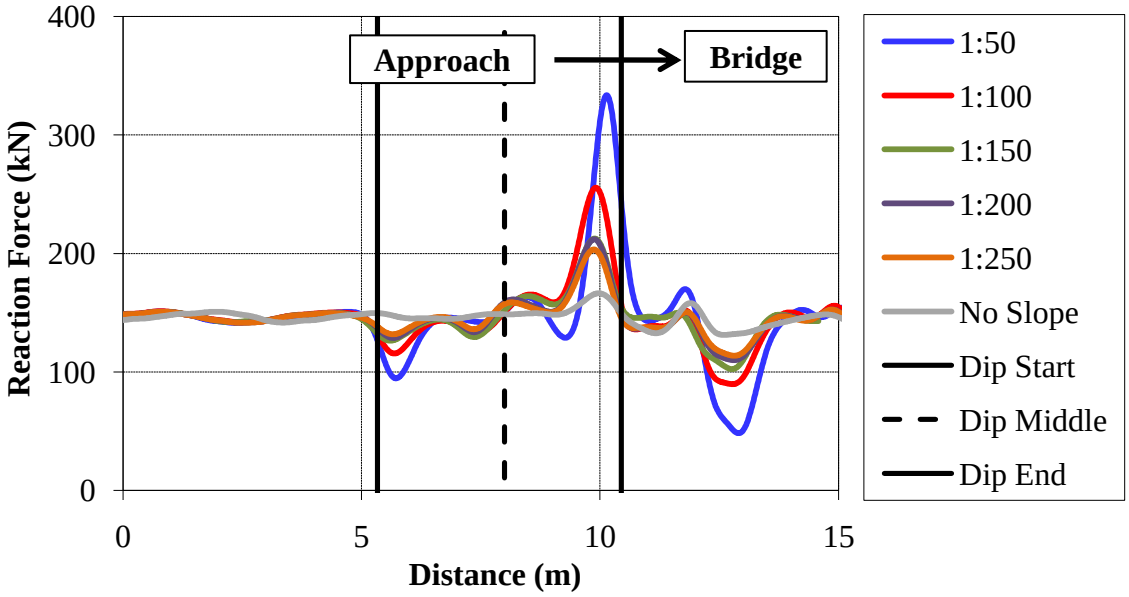

Figure 7.24 - 10 Hz filtered reaction force comparison for various dip slopes of equal length (Dip)

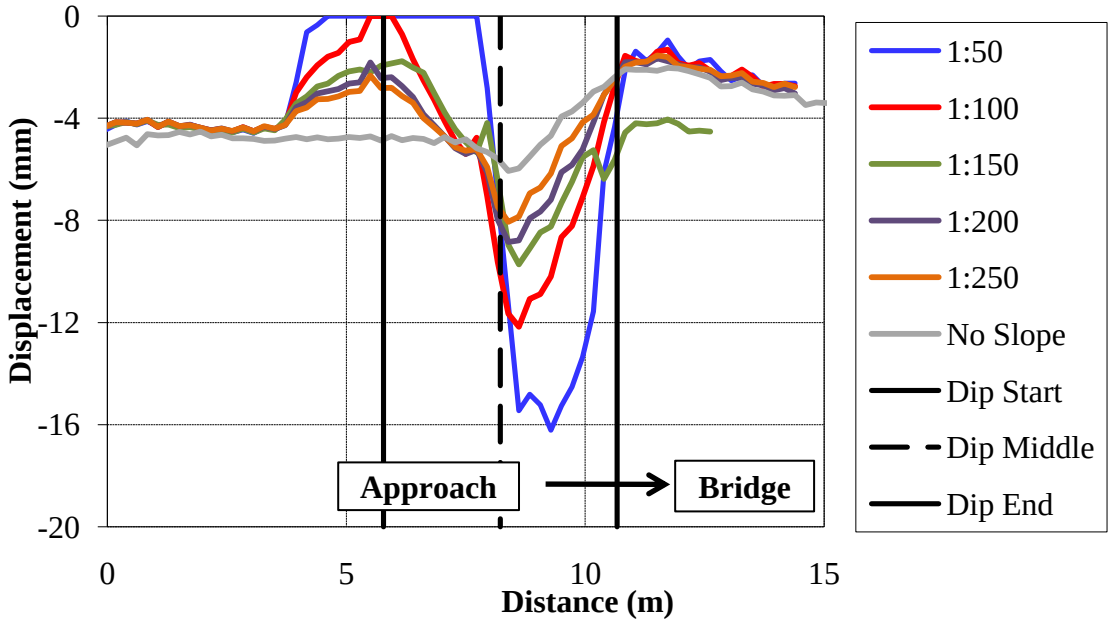

Figure 7.25 – Track deflection comparison for various dip slopes of equal length (Dip)

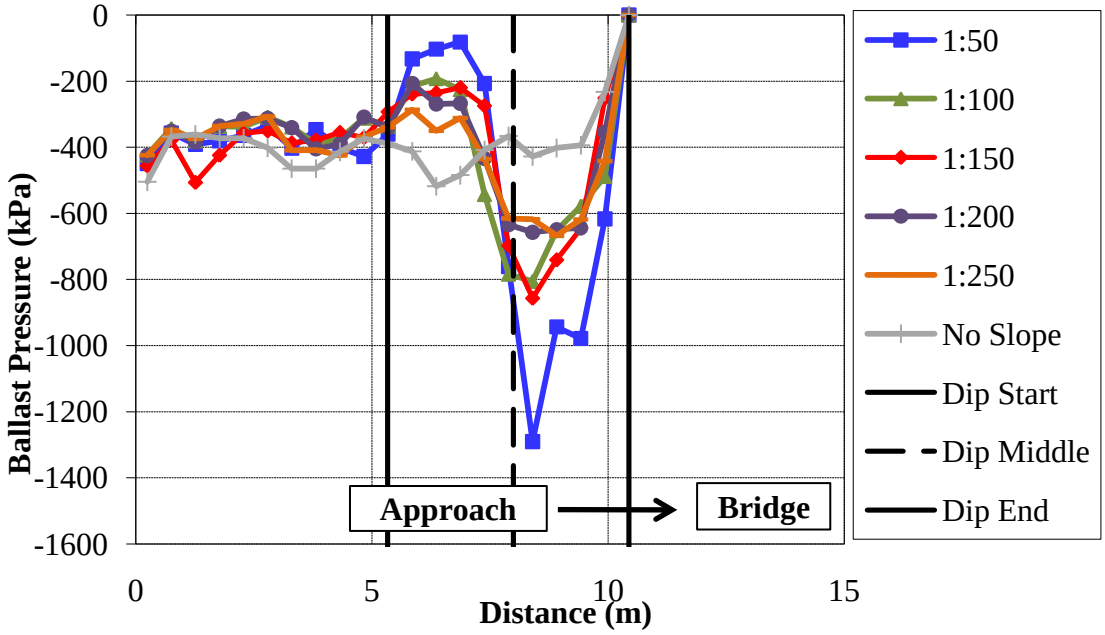

Figure 7.26 – Ballast pressure comparison for various dip slopes of equal length (Dip)

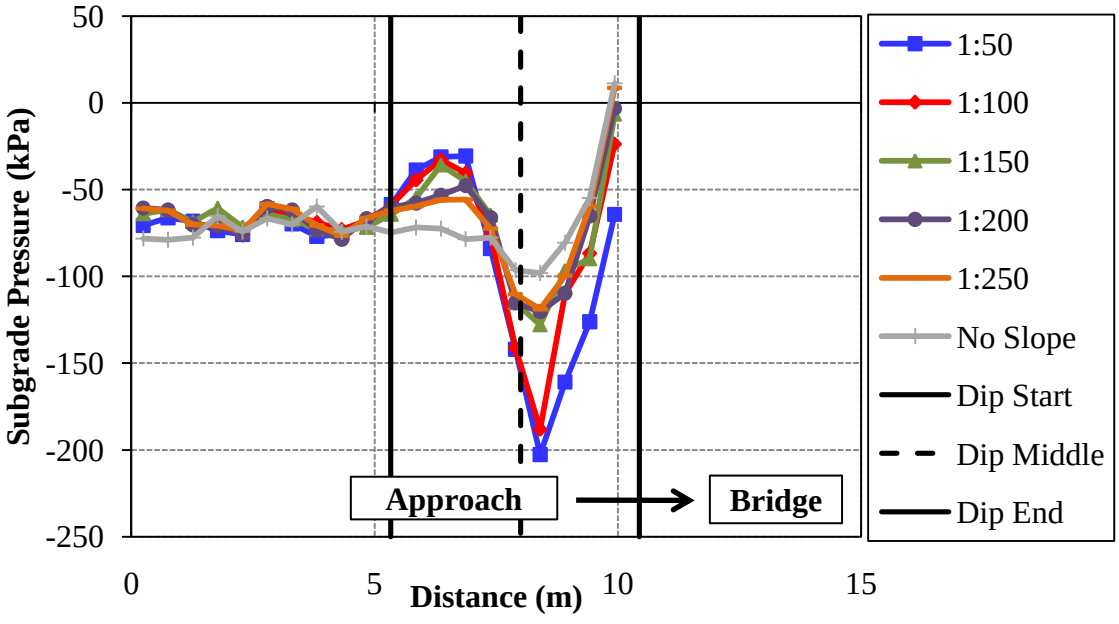

Figure 7.27 - Subgrade pressure comparison for various dip slopes of equal length (Dip)

It is interesting to note that for dip slopes of 1:100 and 1:50, the track deflection actually goes to zero before and after the truck first enters the bump (Fig. 7.25). This occurs for approximately 40 milliseconds. This could pose a serious danger as full contact between the truck and the track is not present. Reducing the bump slope, however, eliminates this problem. Unfortunately, every bump slope case still exceeds the 6.4 mm limit. The only case that does not is the case with no bump slope. The results are summarized in Table 7.8.

Table 7.8 – Dip slope (equal lengths) results summary (Dip)

Dip Slope	Dip Length (m)	Dip Height (mm)	DLF	DDF	DBF	DSF
1:50	5.1	46	2.28	3.74	3.23	2.81
1:100	5.1	23	1.75	2.83	2.01	2.61
1:150	5.1	16	1.45	2.24	2.14	1.78
1:200	5.1	11	1.45	2.06	1.64	1.67
1:250	5.1	9	1.39	1.88	1.67	1.65
No Slope	0	0	1.14	1.29	1.3	1.36

Cases concerning the dip slope with equal heights and varying lengths (Fig. 7.17b) were then examined. Unlike for the bump, the dip dimensions, along with the overall slope, play a role in the DLF, DDF, DBF and DSF (Fig. 7.28). For dips with equal length, a clear trend is seen where increasing slope steepness increases the severity of the response. The same is not true, however, for dip slopes with equal heights. This suggests that dip length is not as big a factor as dip height.

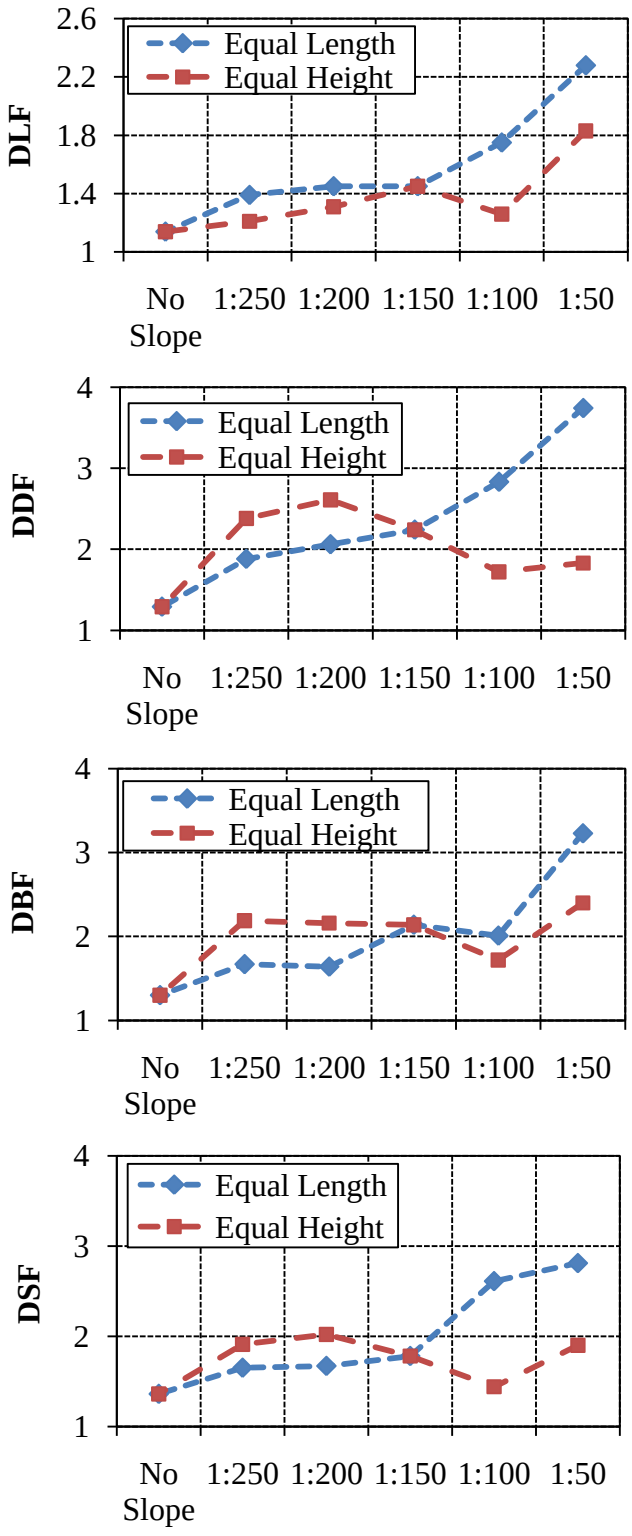

Figure 7.28 – (a) DLF, (b) DDF, (c) DBF and (d) DSF vs. dip slope

While a general trend is visible between dip slopes with equal heights and the DLF, there is not a strong correlation for DDF, DBF and DSF. In fact, the profile of these are similar themselves, having a sinusoidal shape rather than a linear shape. A summary of the results for dip slopes with equal heights is found in Table 7.9.

Table 7.9 - Dip slope (equal heights) results summary (Dip)

Dip Slope	Dip Length (m)	Dip Height (mm)	DLF	DBF	DSF
1:50	1.6	16	1.83	2.4	1.9
1:100	3.3	16	1.26	1.72	1.44
1:150	5.1	16	1.45	2.14	1.78
1:200	6.6	16	1.31	2.16	2.02
1:250	8.4	16	1.21	2.19	1.91
No Slope	0	0	1.14	1.3	1.36

7.3.3 Bump/Dip Slope and Velocity Results

Next, the impact of velocity on various bump/dip slopes was investigated. Velocities of 15.6 m/s, 22.2 m/s, 33.5 m/s and 44.7 m/s were simulated for each bump and dip slope of 1:50, 1:100, 1:150, 1:200 and 1:250. The bump and dip slopes all had equal heights of 33 mm and 16 mm and varying lengths according to Fig. 7.17a and 7.17b, respectively. These slopes were chosen because, for the dip, the response is more unusual. The results indicate that DLF increases with steeper bump/dip slopes and with velocity (Fig. 7.29).

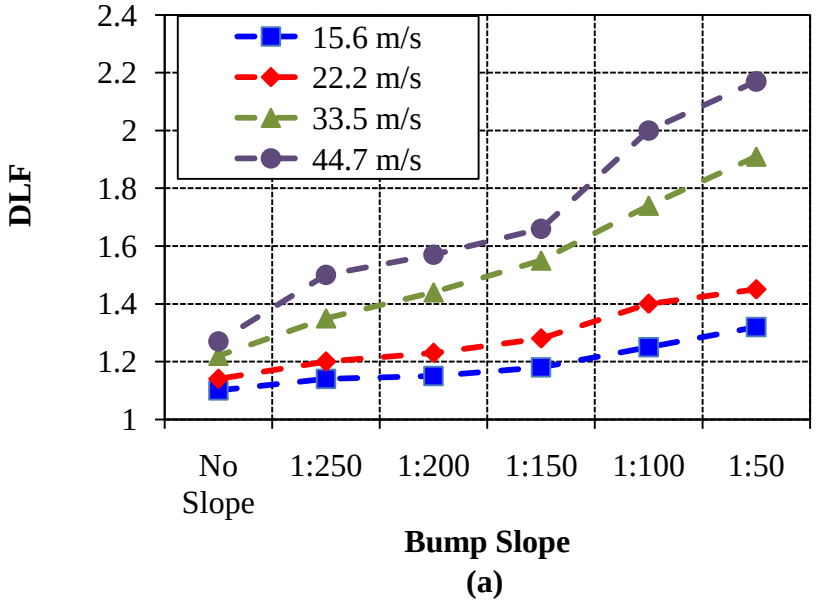

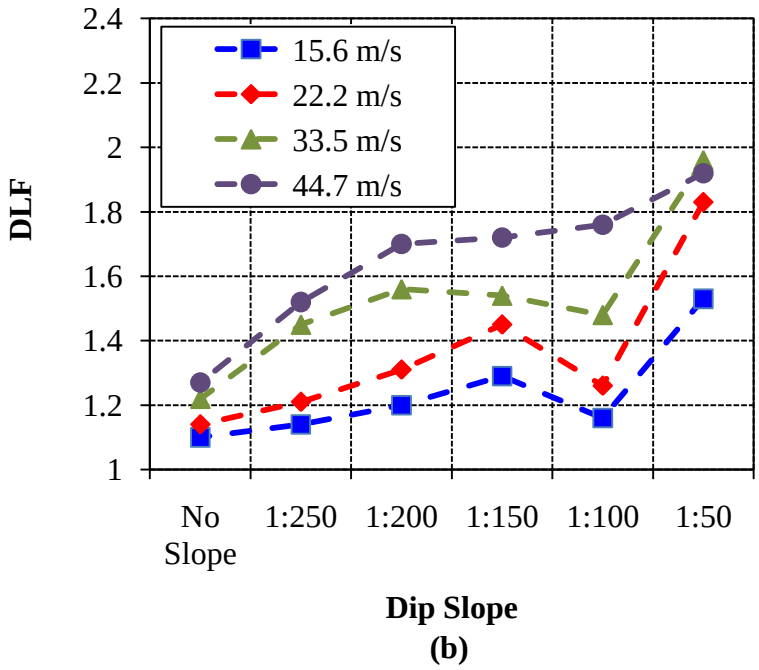

Figure 7.29 - DLF vs. (a) bump slope and (b) dip slope for different velocities

The relationship between DLF and bump slope and dip slope is fairly linear. This agrees with the results from Lei and Mao (2004). For the steeper slopes of 1:100 and 1:50, the DLF is higher for the bump than for the dip while for shallower slopes of 1:150 or less, the DLF is higher for the dip than for the bump. This is likely due to the short distance of the dip upslope as it relates to the distance between the two axles, or 1.8 m. For example, a length of 3.3 m for a 1:100 dip, means that the front axle of the truck has completely passed over the down-slope of the dip and is on the upslope of the dip before the back axle even reaches the dip. This works to reduce the severity of the steep slope. It is important to note that not all slopes of 1:100 will act this way. As previously mentioned, it depends on the length of the dip and the length between the two axles.

Results for the DDF (Fig. 7.30), DBF (Fig. 7.31) and DSF (Fig. 7.32) show that the bump is more severe than the dip. The velocity is also a bigger factor for the bump than for the dip. Also, as previously found for dips of equal heights at 22.2 m/s (Fig. 7.28), there is not a strong correlation between dip slope and DDF, DBF and DSF for any velocity studied. This is not the case for bump slopes of equal heights, where, in general, an increase in bump steepness leads to an increase in DDF, DBF and DSF. A complete summary of these results is presented in Table 7.10.

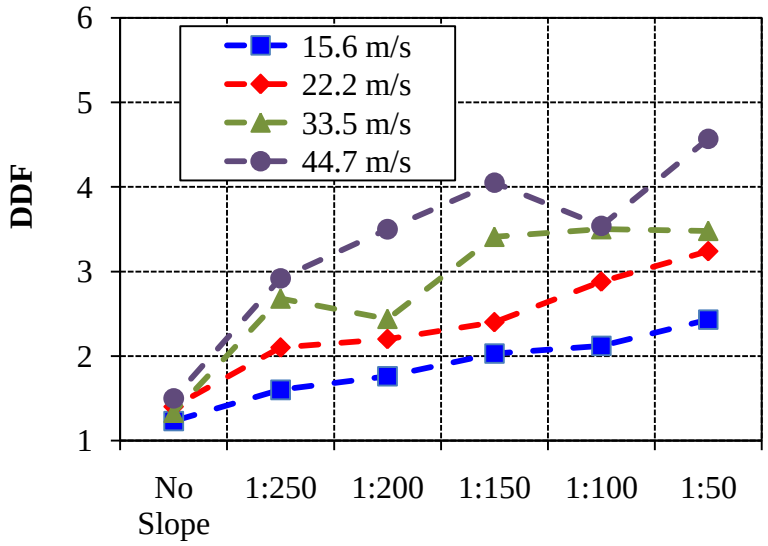

(a)

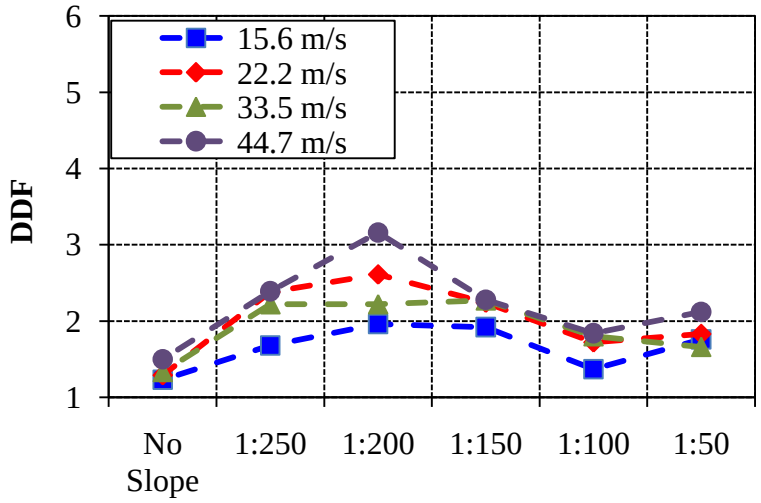

(b)

Figure 7.30 - DDF vs. (a) bump slope and (b) dip slope for different velocities

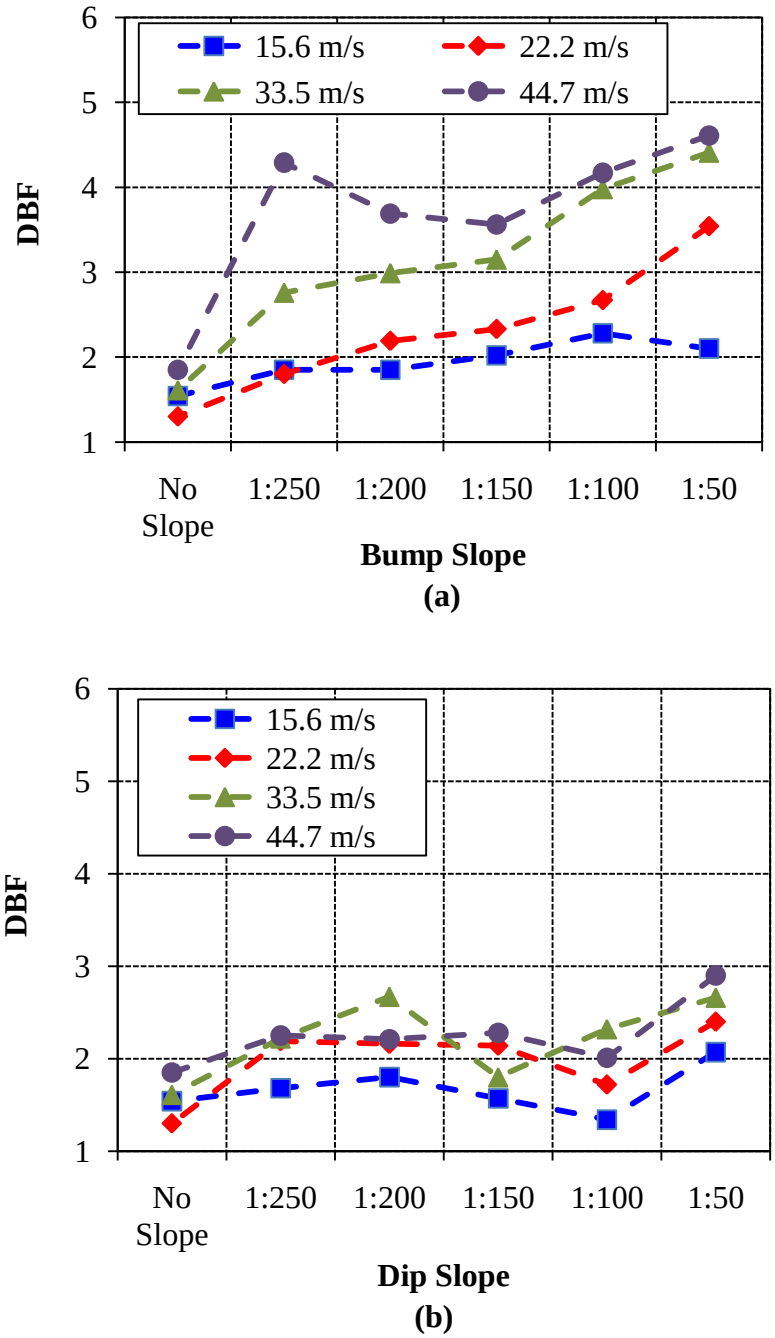

Figure 7.31 - DBF vs. (a) bump slope and (b) dip slope for different velocities

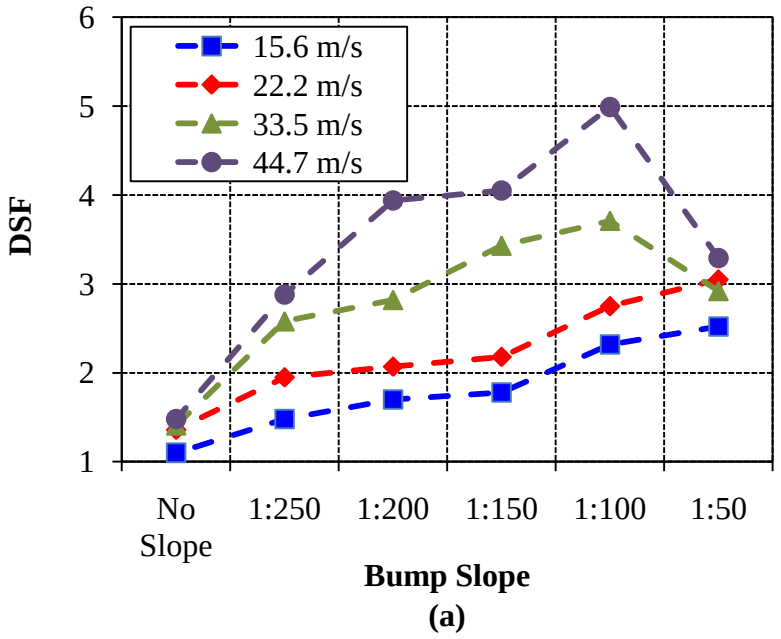

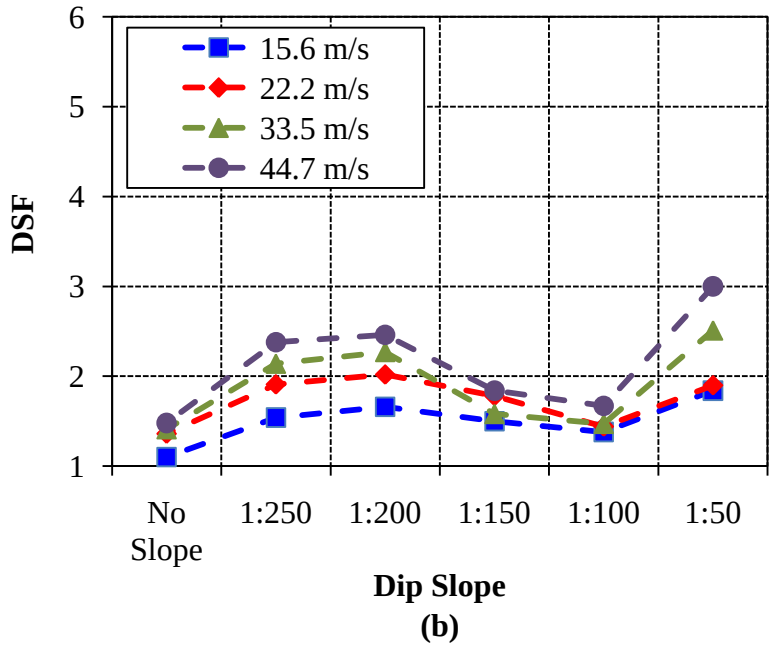

Figure 7.32 - DSF vs. (a) bump slope and (b) dip slope for different velocities

Table 7.10 – Bump/Dip slope (equal heights) and velocity results summary

		BUMP				DIP			
Bump/Dip Slope	**Velocity (m/s)**	**DDF**	**DLF**	**DBF**	**DSF**	**DDF**	**DLF**	**DBF**	**DSF**
1:50	15.6	2.43	1.32	2.10	2.52	1.76	1.53	2.07	1.84
	22.2	3.24	1.45	3.54	3.05	1.83	1.83	2.40	1.90
	33.5	3.48	1.91	4.41	2.92	1.66	1.96	2.66	2.51
	44.7	4.57	2.17	4.61	3.29	2.12	1.92	2.90	3.00
1:100	15.6	2.12	1.25	2.28	2.32	1.37	1.16	1.34	1.38
	22.2	2.88	1.40	2.67	2.75	1.72	1.26	1.72	1.44
	33.5	3.50	1.74	3.98	3.71	1.80	1.48	2.32	1.47
	44.7	3.54	2.00	4.17	4.99	1.84	1.76	2.01	1.67
1:150	15.6	2.03	1.18	2.02	1.78	1.92	1.29	1.57	1.50
	22.2	2.40	1.28	2.33	2.18	2.24	1.45	2.14	1.78
	33.5	3.41	1.55	3.15	3.43	2.27	1.54	1.80	1.58
	44.7	4.05	1.66	3.56	4.05	2.28	1.72	2.28	1.84
1:200	15.6	1.76	1.15	1.85	1.70	1.96	1.20	1.80	1.66
	22.2	2.20	1.23	2.19	2.07	2.61	1.31	2.16	2.02
	33.5	2.44	1.44	2.99	2.82	2.22	1.56	2.67	2.27
	44.7	3.50	1.57	3.69	3.94	3.16	1.70	2.21	2.46
1:250	15.6	1.60	1.14	1.85	1.48	1.68	1.14	1.68	1.54
	22.2	2.10	1.20	1.80	1.95	2.38	1.21	2.19	1.91
	33.5	2.68	1.35	2.76	2.58	2.22	1.45	2.22	2.14
	44.7	2.92	1.50	4.29	2.88	2.39	1.52	2.25	2.38
No Slope	15.6	1.23	1.10	1.54	1.10	1.23	1.10	1.54	1.10
	22.2	1.40	1.14	1.30	1.36	1.29	1.14	1.30	1.36
	33.5	1.33	1.22	1.61	1.41	1.33	1.22	1.61	1.41
	44.7	1.50	1.27	1.85	1.48	1.50	1.27	1.85	1.48

7.3.4 Summary

To establish tolerable slopes depending on the train velocity, the results were re-plotted in terms of bump (Fig. 7.33 – Fig. 7.36) and dip angles (Fig. 7.37 - Fig. 7.40). The respective limits for DLF, DDF, DBF and DSF are also shown on the figures. Only the angles corresponding to each velocity that are under this limit are tolerable.

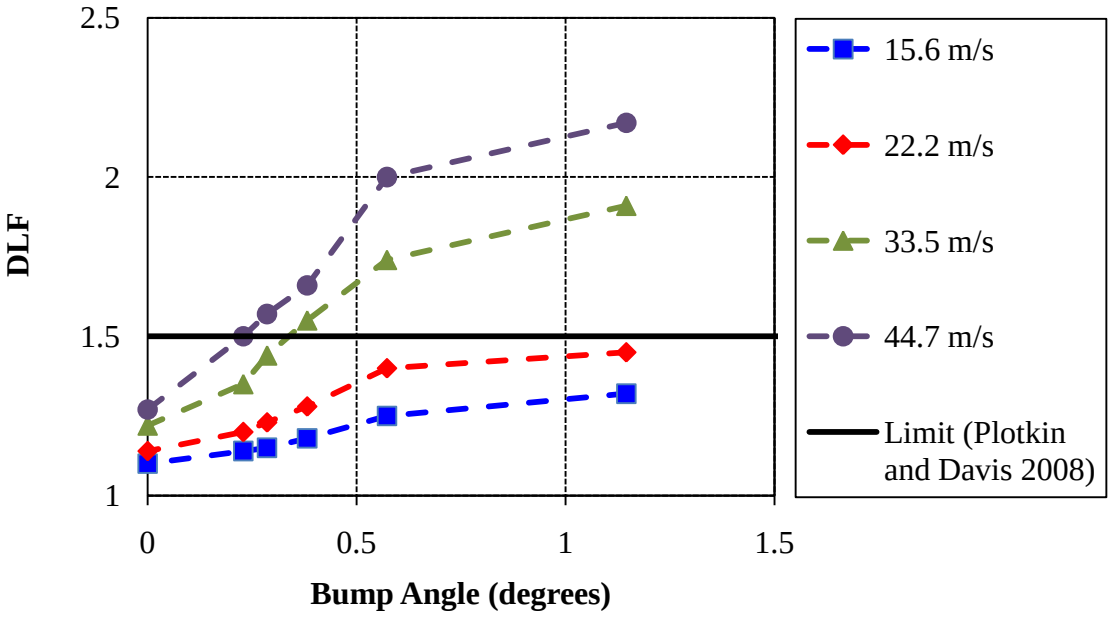

Figure 7.33 – DLF vs. bump angle

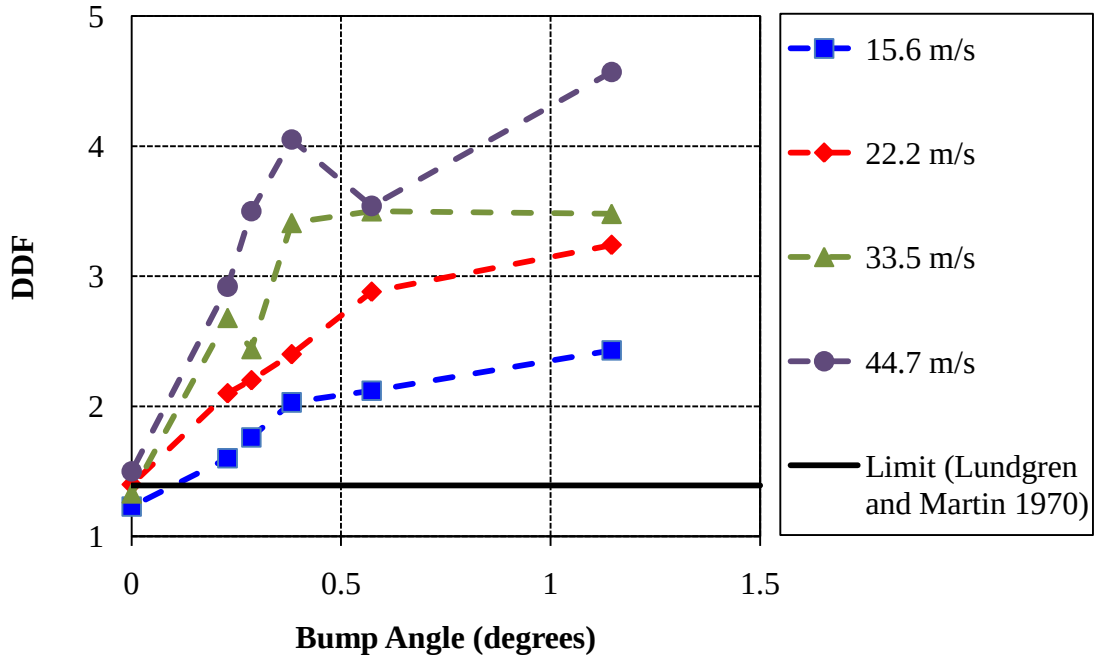

Figure 7.34 – DDF vs. bump angle

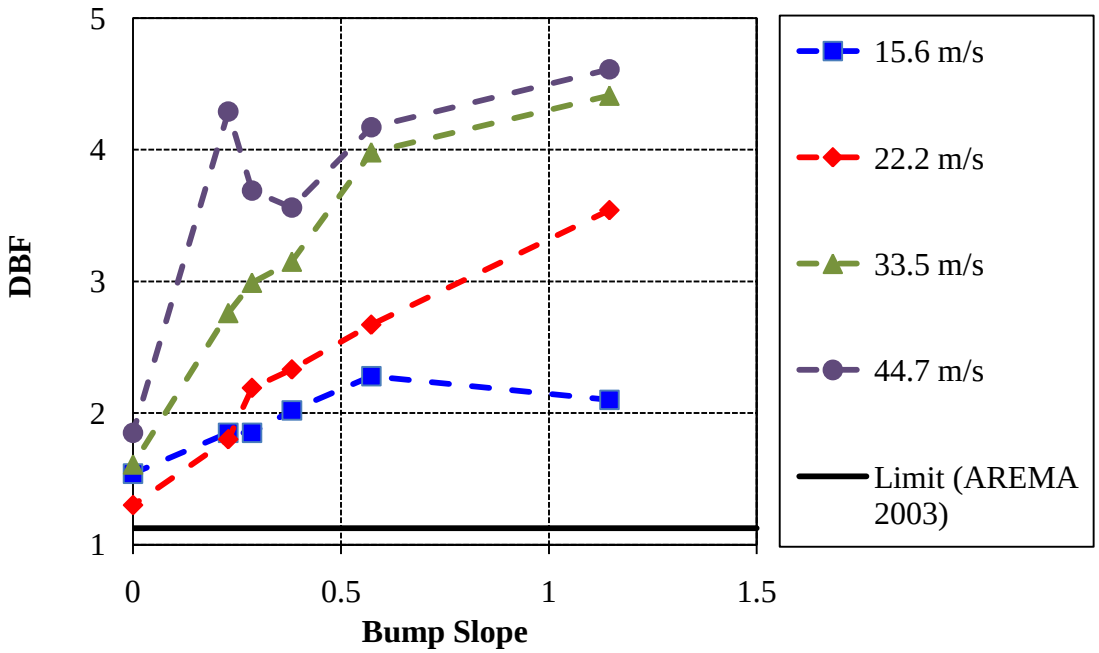

Figure 7.35 – DBF vs. bump angle

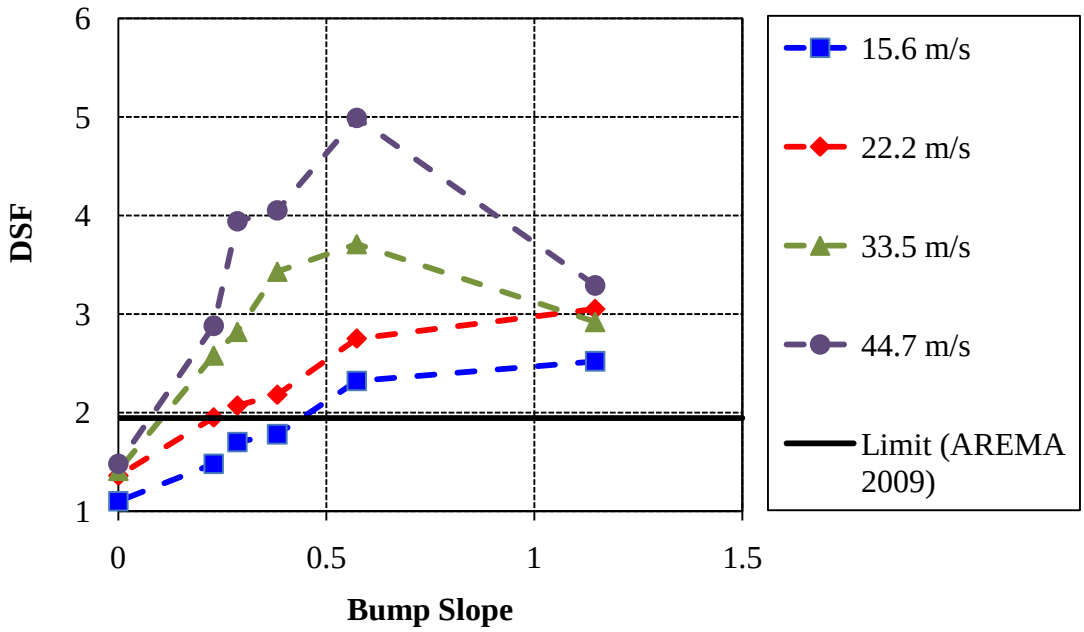

Figure 7.36 – DSF vs. bump angle

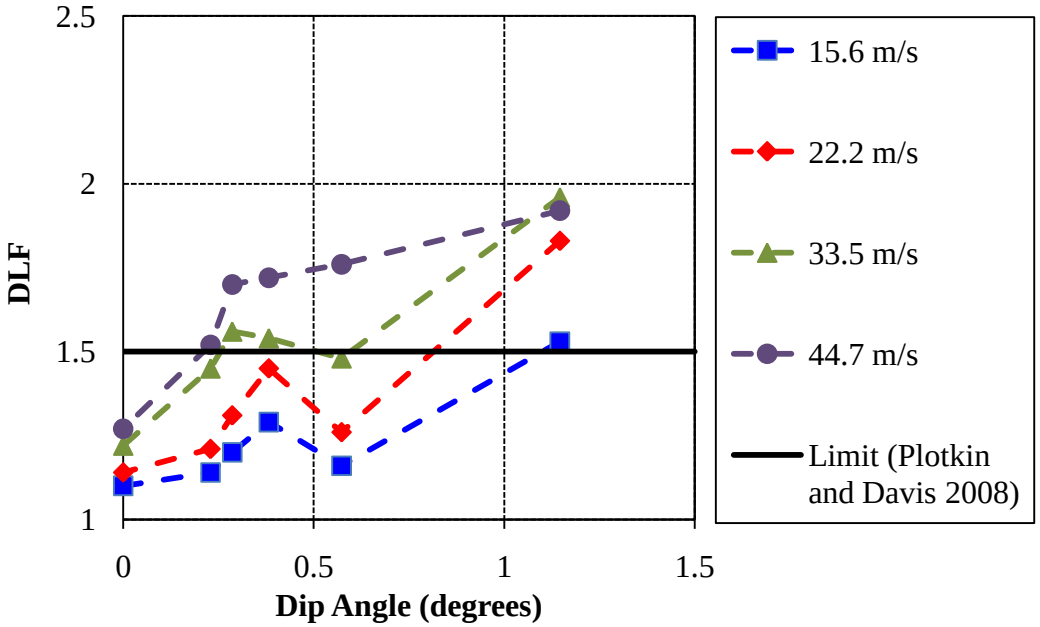

Figure 7.37 – DLF vs. dip angle

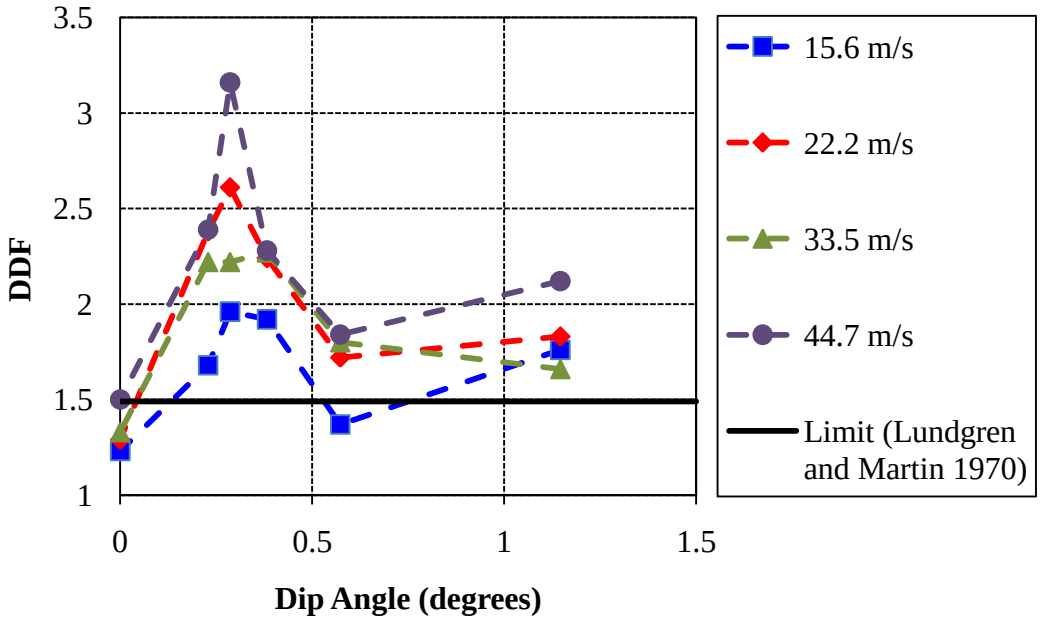

Figure 7.38 – DDF vs. dip angle

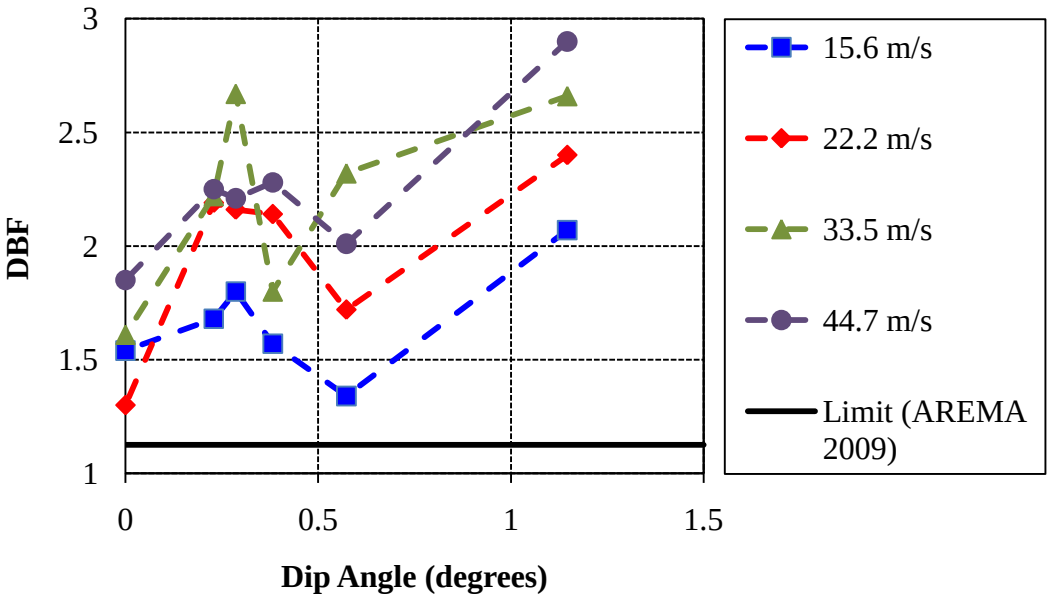

Figure 7.39 – DBF vs. dip angle

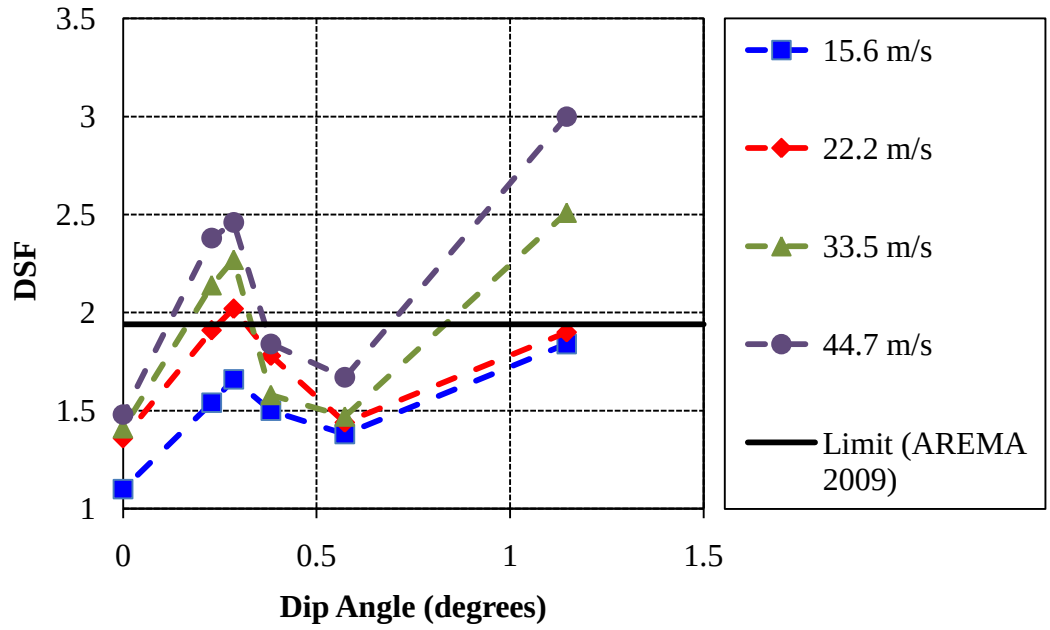

Figure 7.40 – DSF vs. dip angle

For both the bump and the dip, the tolerable slope is evaluated based on the DLF (Fig. 7.41). The relationship between bump/dip slope and velocity is relatively linear. The corresponding "best-fit" equations are shown in the figure. These equations can be used to determine the tolerable slope for a certain velocity for the model inputs. For the range of velocities tested in this parametric study, the maximum tolerable bump/dip slope, based on DLF, is approximately 1:250. This is the tolerable slope provided by the respondents of the industry survey (Section 4).

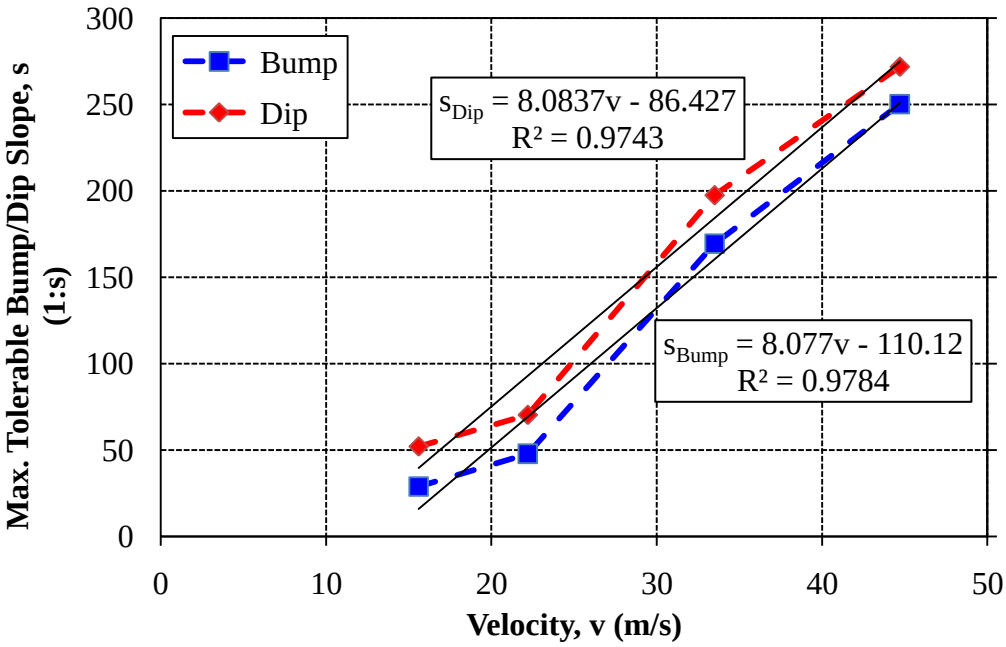

Figure 7.41 – Tolerable bump/dip slope vs. velocity based on DLF results

The tolerable slope for a bump is also evaluated based on the DSF (Fig. 7.42). As with the DLF, the relationship between the tolerable slope and velocity is linear. Since

there is no correlation between the DSF, DDF and DBF for the dip, a tolerable slope for these results cannot be evaluated. Tolerable slopes corresponding to the DDF and DBF for the bump are also not evaluated. This is because the results for these cases are above the limits for deflection and ballast pressure, respectively.

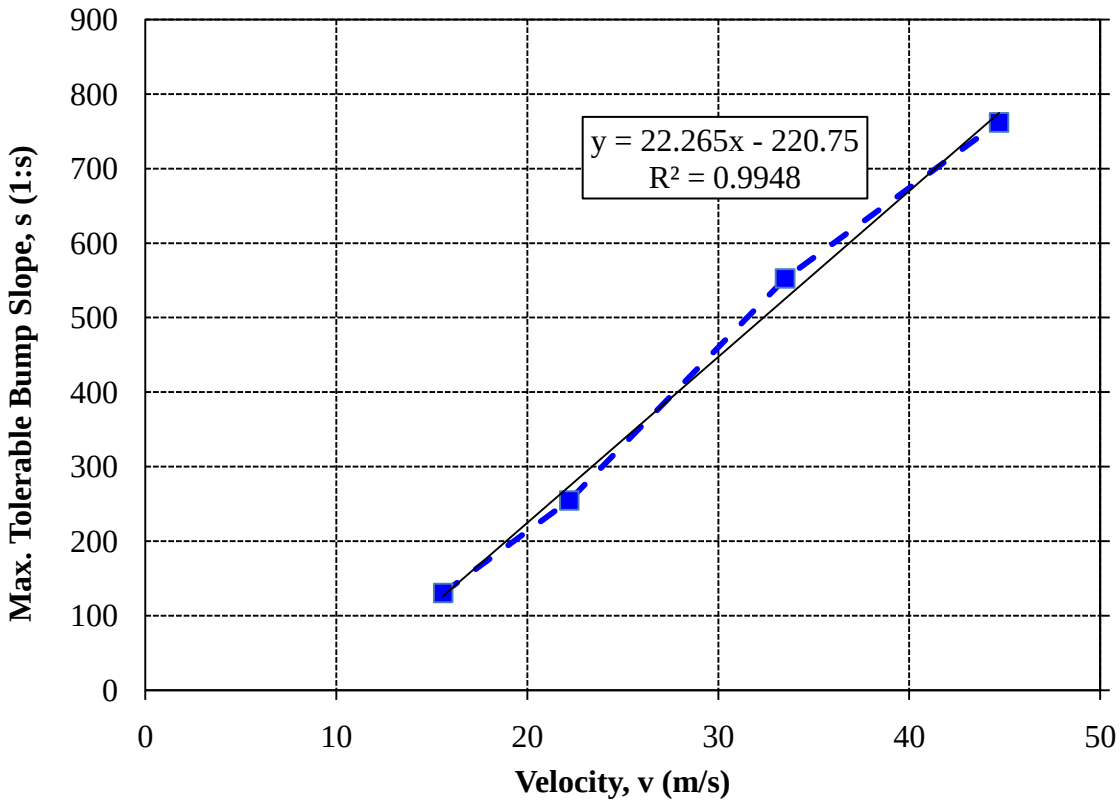

Figure 7.42 - Tolerable bump slope vs. velocity based on DSF results

For the range of velocities tested in this parametric study, the maximum tolerable bump/dip slope, based on DSF, is approximately 1:750. This is significantly higher than for the DLF, which was 1:250. To allow for a steeper tolerable slope, the velocity must

be reduced. While Fig. 7.41 and Fig. 7.42 are useful, they are only applicable to the inputted model properties. Similar figures can be developed for other cases by modeling the specific dimensions and material properties of the actual site. A dimensional analysis could also be performed after more cases are evaluated to obtain charts that are applicable to all cases.

7.4 SUBGRADE/FILL MODULUS

The modulus of the subgrade or fill has a dominant influence on the track modulus (Selig and Li 1994). Changing the soil modulus would therefore have a significant effect on the track response for the bump and the dip. The reference case included a fill with a modulus of 35 MPa and a subgrade with a modulus of 20 MPa. To simplify the analysis, the effect of the subgrade modulus on the DLF, DDF, DBF and DSF was investigated by having an equal modulus value for both the fill and the subgrade.

Soil moduli of 20 MPa, 50 MPa and 100 MPa were evaluated for both the bump and the dip. These equate to approach track moduli of 30 N/mm/mm, 50 N/mm/mm and 80 N/mm/mm, respectively. There is a clear relationship between the soil modulus and the track modulus (Fig. 7.43).

The case with a soil modulus of 100 MPa (80 N/mm/mm track modulus) is very close to matching the track modulus of the bridge (83 N/mm/mm). It is therefore expected that there will be little impact due to the track modulus change near the bridge abutment. The track modulus of 30 N/mm/mm for a soil modulus of 20 MPa is very close to matching the reference case (31 N/mm/mm). The expected response should

therefore be very similar to the reference case. The bump/dip slope and velocity for each case is 1:150 and 22.2 m/s, respectively.

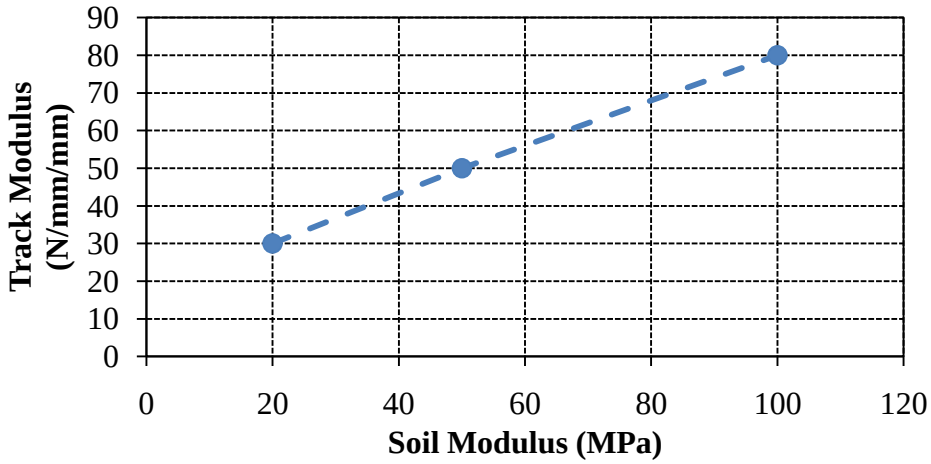

Figure 7.43 – Effect of soil modulus on track modulus

7.4.1 Bump Results

The complete set of plots for wheel/rail reaction forces, vertical axle accelerations, track deflection, ballast pressures and subgrade pressures for each soil moduli can be found in Appendix E. As expected, the wheel/rail impact due to the track modulus change is greater for a soft soil with a low modulus than for a stiffer soil (Fig. 7.44). This suggests that reducing the track modulus differential between the bridge and the approach will result in lower impact forces. It is interesting to note, however, that for a stiff soil with a high modulus, the impact due to the initial geometry change is greater than for a softer

soil. The difference is smaller than the difference resulting from a track modulus change though.

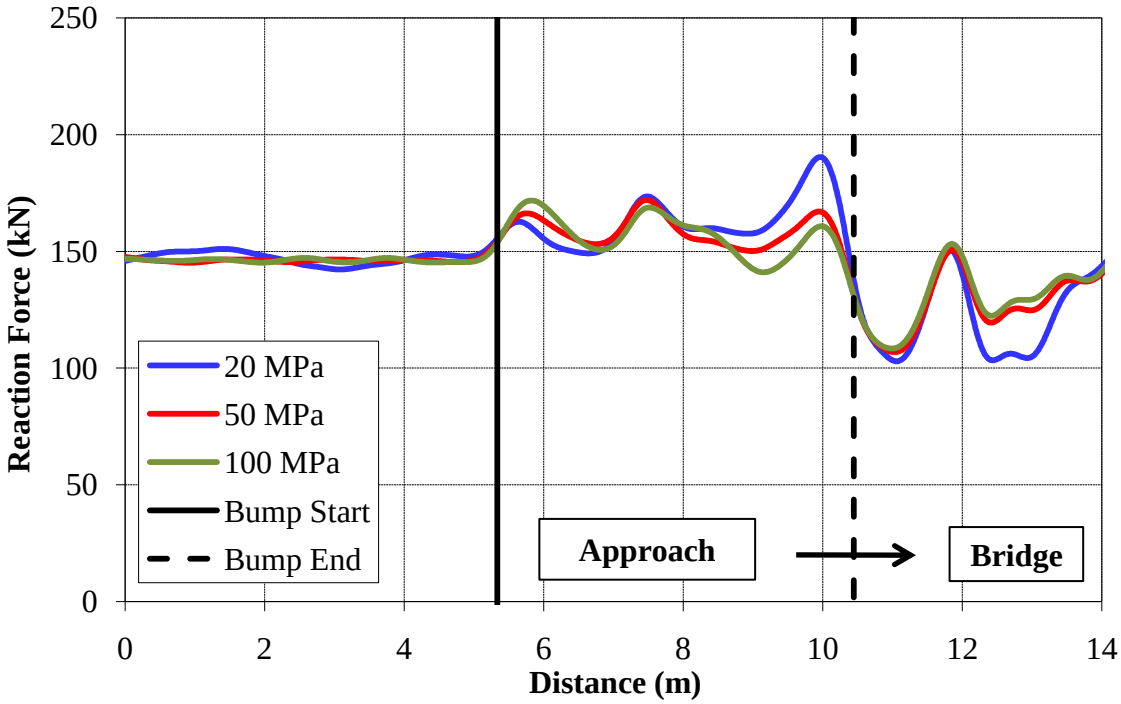

Figure 7.44 - 10 Hz filtered reaction force comparison for various fill/subgrade moduli (Bump)

Also as expected, the maximum track displacement is greatest for a soil modulus of 20 MPa and decreases with increasing soil modulus (Fig. 7.45). The steepness of the profile before the bridge abutment is also more severe for lower soil moduli causing the impact at this location to be higher. Only the case with a soil modulus of 100 MPa produced track deflections under the limit of 6.4 mm.

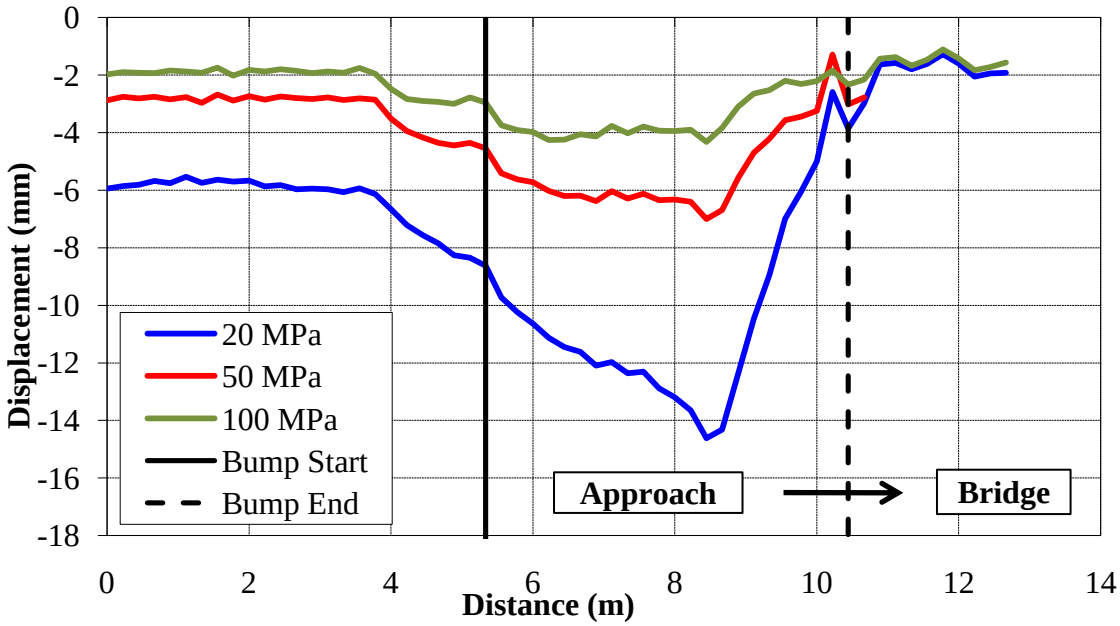

Figure 7.45 – Track deflection comparison for various fill/subgrade moduli (Bump)

The average ballast pressure on the approach embankment does not depend on the soil modulus; it is still at 400 kPa in compression (Fig. 7.46). The maximum ballast pressure, however, changes depending on the soil modulus. Surprisingly, the maximum ballast pressure for these cases is for a soil modulus of 50 MPa, not 100 MPa. More simulations are necessary in the future to determine if this is an isolated incident or if the maximum ballast pressure is independent of the soil modulus.

The average subgrade pressure does depend on the soil modulus; it decreases (in compression) with decreasing soil modulus (Fig. 7.47). The maximum subgrade pressure also decreases with decreasing soil modulus. The ratio, or DSF, however, increases with decreasing soil modulus. The results are as expected. A summary of the results for DLF, DDF, DBF and DSF for these cases are given in Table. 7.11.

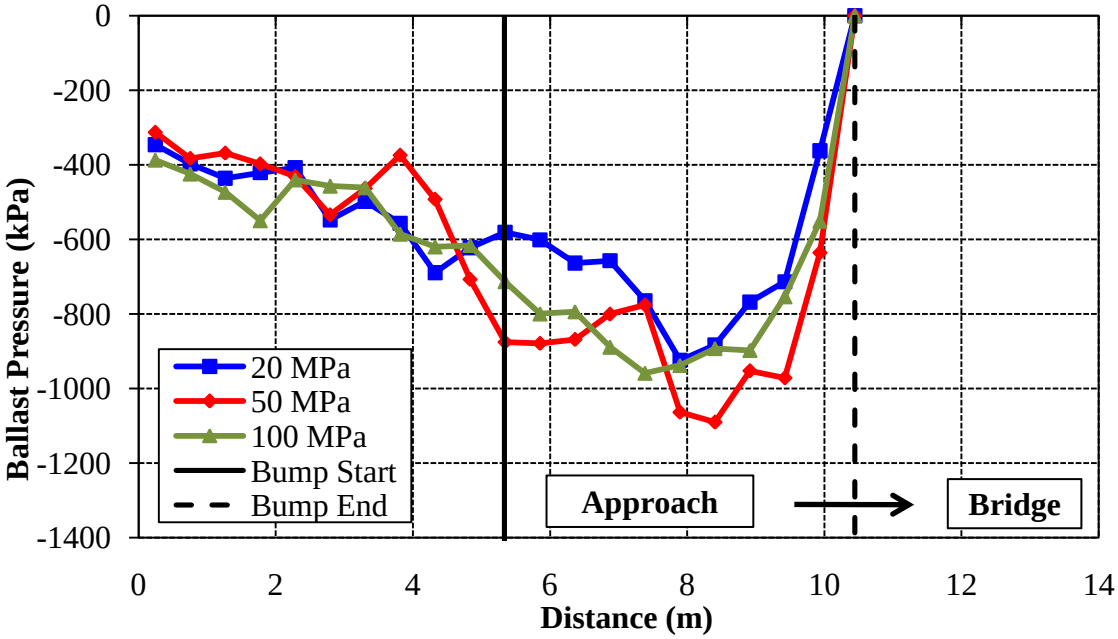

Figure 7.46 – Ballast pressure comparison for various fill/subgrade moduli (Bump)

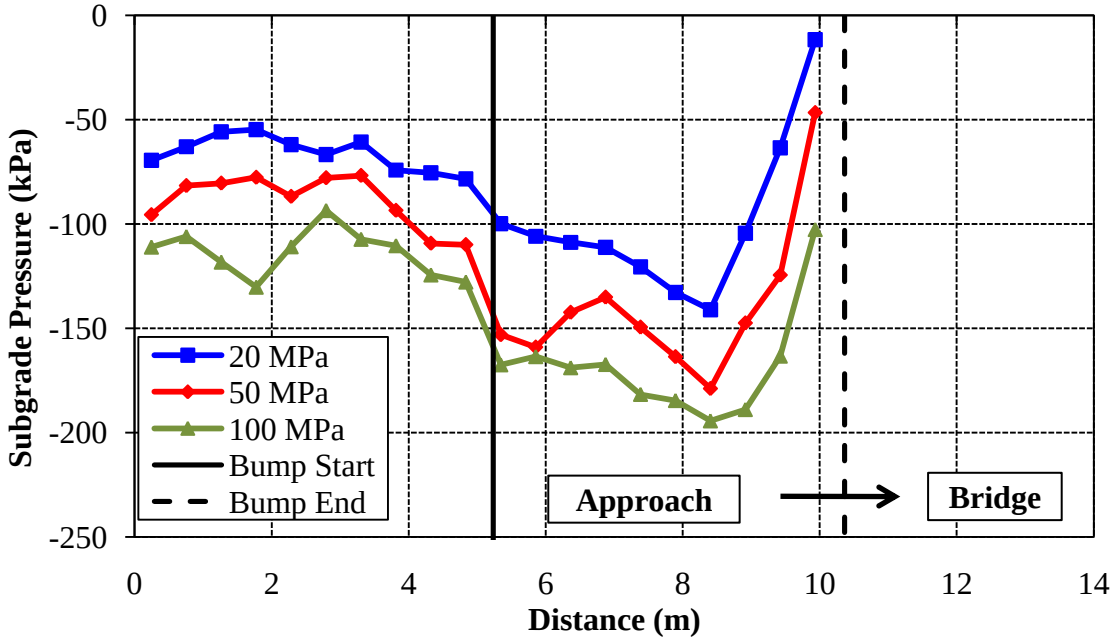

Figure 7.47 - Subgrade pressure comparison for various fill/subgrade moduli (Bump)

Table 7.11 – Soil modulus results summary (Bump)

Fill/Subgrade Modulus (MPa)	DLF	DDF	DBF	DSF
20	1.30	2.54	2.31	2.20
50	1.18	2.5	2.72	2.10
100	1.18	2.29	2.4	1.80

7.4.2 Dip Results

The complete set of plots for wheel/rail reaction forces, vertical axle accelerations, track deflection, ballast pressures and subgrade pressures for each soil moduli can be found in Appendix F. The results for impact forces, track deflection, ballast and subgrade pressures are similar in nature to those found for the bump (Figs. 7.44-7.47). A summary of the DLF, DBF and DSF results are in Table 7.12.

Table 7.12 – Soil modulus results summary (Dip)

Fill/Subgrade Modulus (MPa)	DLF	DDF	DBF	DSF
20	1.44	2.04	1.89	1.78
50	1.41	2.41	2.08	1.75
100	1.35	2.19	2.06	1.72

7.4.3 Summary

The results for both the bump and the dip have been summarized graphically in Fig. 7.48. For the DLF, the general trend is that the DLF increases with decreasing soil

moduli (Fig. 7.48a). This is because the track modulus differential is increased. So, a soft soil for an approach embankment will tend to result in higher dynamic loads.

The exception to this is for the bump, where the DLF for a soil modulus of 50 MPa is the same as for a soil modulus of 100 MPa. This is explained by looking at a comparison of the reaction forces (Fig. 7.44). The impact at the beginning of the bump under the front axle for a soil modulus of 100 MPa is equal to the impact at the same location under the back axle for a soil modulus of 50 MPa. If a track modulus change alone is present (no bump), then the DLF for the 100 MPa soil would be less than for the 50 MPa soil. For both cases, the impact due to the track modulus change is less than the impact due to the track geometry change. The DLF for the dip is, as with the previous other cases, higher than for the bump.

The DDF results suggest that the DDF increases with decreasing soil modulus (Fig. 7.48b). One large exception is for the dip with a soil modulus of 20 MPa. The DDF is lower than for the cases having larger soil moduli of 50 and 100 MPa. Note that the maximum displacement is still largest for the case having a soil modulus of 20 MPa though and will still cause more problems than the cases with higher soil moduli (Fig. 7.49).

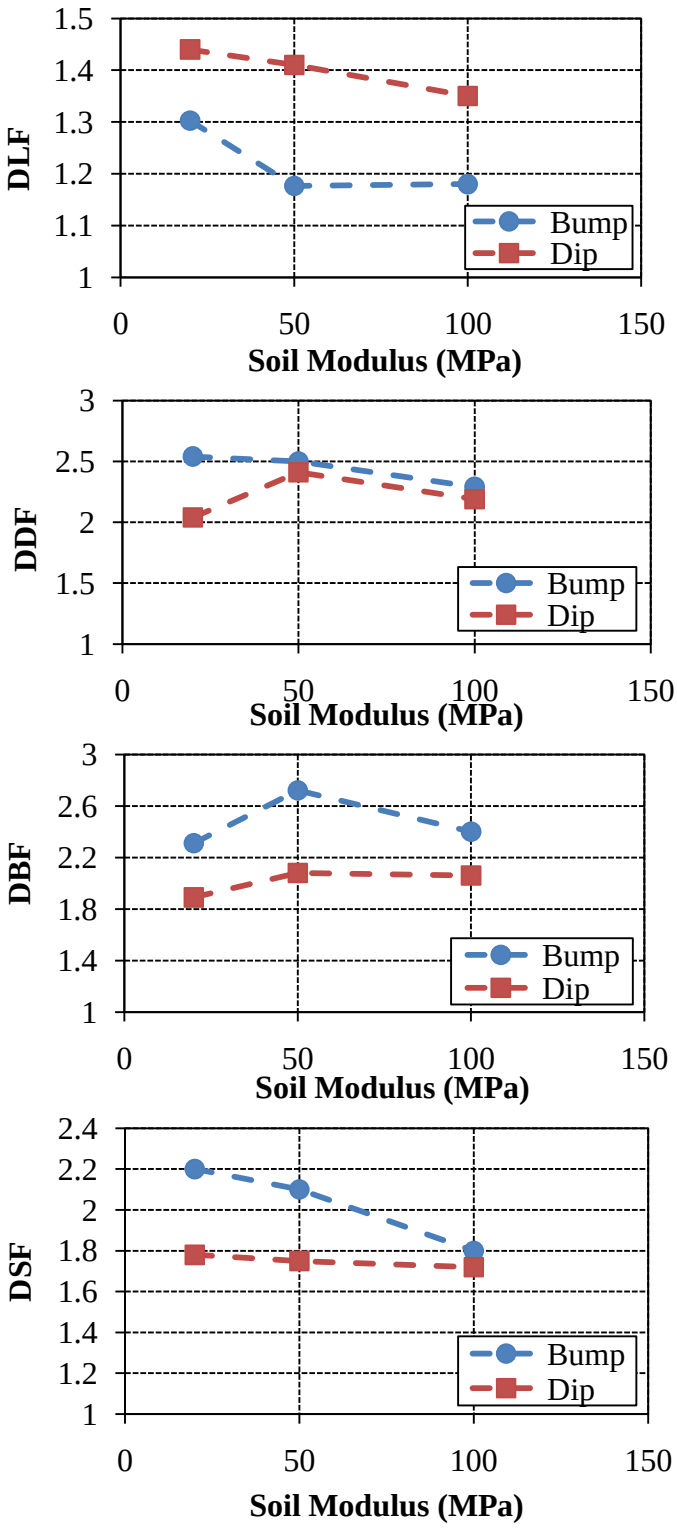

Figure 7.48 - (a) DLF, (b) DDF, (c) DBF and (d) DSF vs. soil modulus

There is not a strong correlation between the DBF and the soil modulus (Fig. 7.48c). This suggests that the maximum ballast pressure is not dependent on the modulus of the soil. More simulations are needed to verify this finding. For the DSF, the general trend is that the DSF decreases with increasing soil moduli (Fig. 7.48d). This means that a weaker soil is worse for the bridge/approach location than a stiffer soil.

For both the DBF and the DSF, the response is greater for the bump than for the dip. This is due to the stress reduction that occurs on the down-slope of the dip which, in turn, reduces the maximum pressure on the up slope of the dip. The bump, however, does not experience any significant stress reduction along the approach embankment.

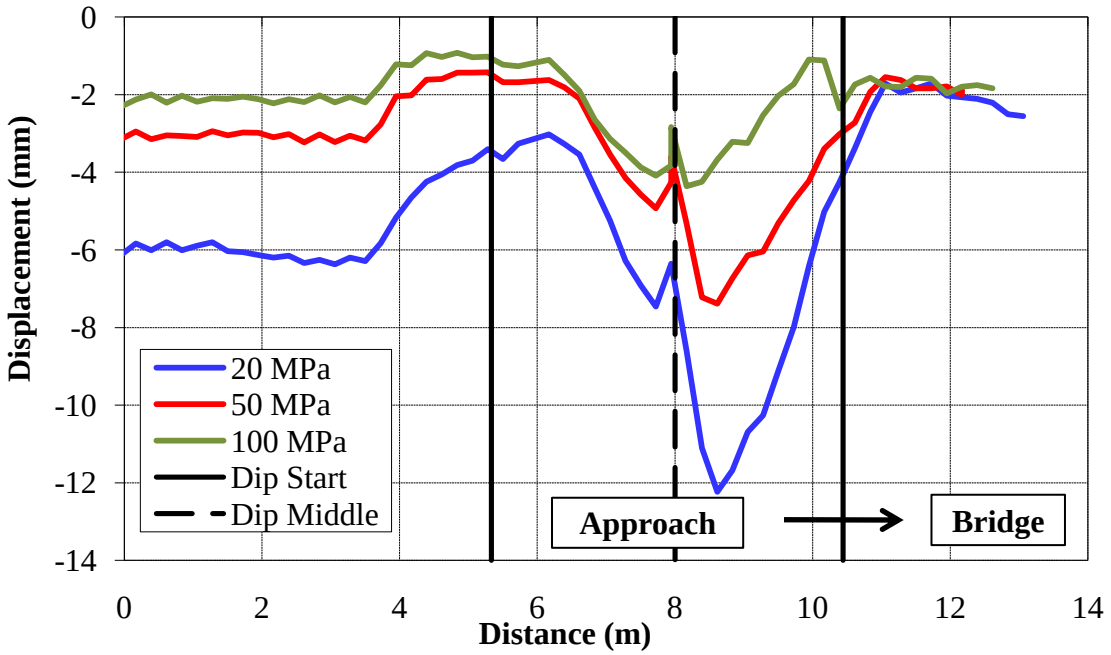

Figure 7.49 - Track deflection comparison for various fill/subgrade moduli (Dip)

7.5 APPROACH TIE MATERIAL

The approach tie material was varied to determine the effect on the track response. Wood, concrete and plastic ties were modeled. The wood and concrete tie mechanical and material properties were determined from AREMA (2008) (Table 7.13). The material properties for the plastic composite tie was chosen to match the PermaTie^{TM} specifications (Rex Crick, personal communication, May 15, 2008). Rubber pads under the rail seat and under the tie were also considered in this analysis. The material properties of these pads can be varied depending on the desired response.

Table 7.13 – Material properties of model ties

Tie Material	ρ (kg/m^3)	E (Mpa)	v
Wood	943.5	12300	0.33
Plastic	1065	1172	0.35
Concrete	2400	20000	0.2
Rubber Pads	1522	7	0.3

According to Selig and Li (1994), the material of the approach ties only has a small effect on the track modulus. The track response is therefore not expected to vary considerably for different approach tie materials. Adding the rubber pads, however, should make more of a difference than just changing the tie material.

7.5.1 Bump Results

The complete set of plots for wheel/rail reaction forces, vertical axle accelerations, track deflection, ballast pressures and subgrade pressures for each approach tie material can be found in Appendix E. A complete summary of the results for the bump cases is shown in Table 7.14.

Table 7.14 – Approach tie material summary (Bump)

Approach Tie Material	DLF	DDF	DBF	DSF
Wood w/Rubber Rail Seat Pads	1.4	2.84	3.84	2.92
Concrete w/Rubber Rail Seat Pads	1.42	2.84	3.44	2.96
Wood w/Rubber Tie Pads	1.31	2.16	2.45	2.92
Concrete w/Rubber Tie Pads	1.31	2.14	2.3	2.89
Wood	1.28	2.40	2.33	2.18
Plastic	1.3	2.55	2.85	2.47
Concrete	1.28	2.50	2.54	2.09

7.5.2 Dip Results

The complete set of plots for wheel/rail reaction forces, vertical axle accelerations, track deflection, ballast pressures and subgrade pressures for each approach tie material can be found in Appendix F. A complete summary of the results for the bump cases is shown in Table 7.15.

Table 7.15 – Approach tie material summary (Dip)

Approach Tie Material	DLF	DDF	DBF	DSF
Wood w/Rubber Rail Seat Pads	1.57	2.38	2.83	2.23
Concrete w/Rubber Rail Seat Pads	1.57	2.34	2.51	2.28
Wood w/Rubber Tie Pads	1.58	2.54	1.89	2.41
Concrete w/Rubber Tie Pads	1.56	2.51	1.61	2.49
Wood	1.45	2.24	2.14	1.78
Plastic	1.46	2.35	2.24	1.91
Concrete	1.46	2.28	1.88	1.81

7.5.3 Summary

The DLF, DDF, DBF and DSF results for both the bump and the dip have been summarized graphically in Fig. 7.50, Fig. 7.51, Fig. 7.52 and Fig. 7.53, respectively. All of the results show a similar trend for the bump as for the dip.

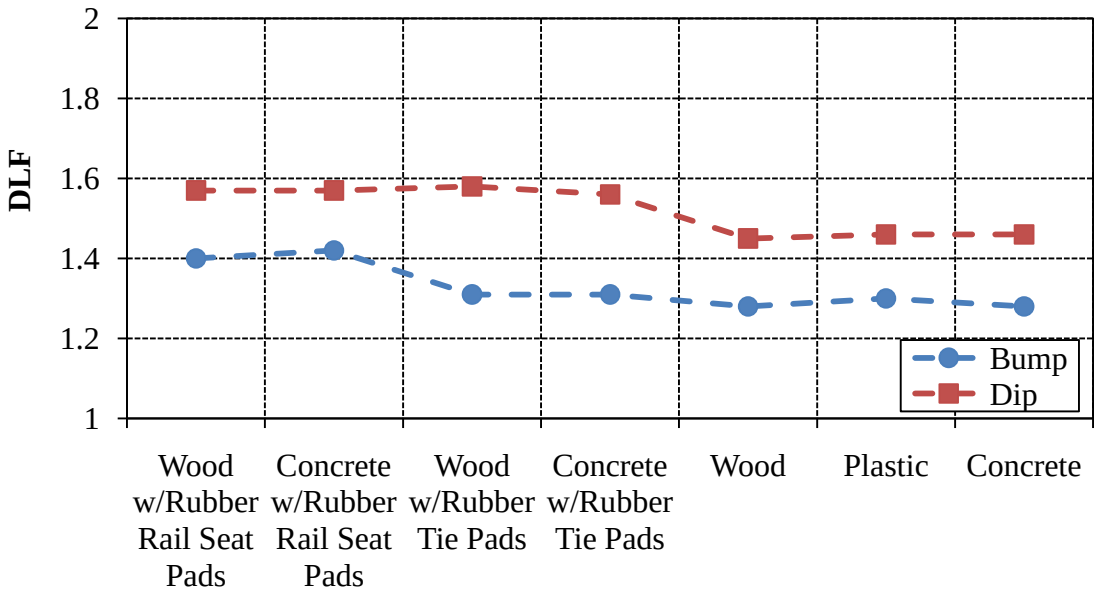

Figure 7.50 – DLF vs. approach tie material

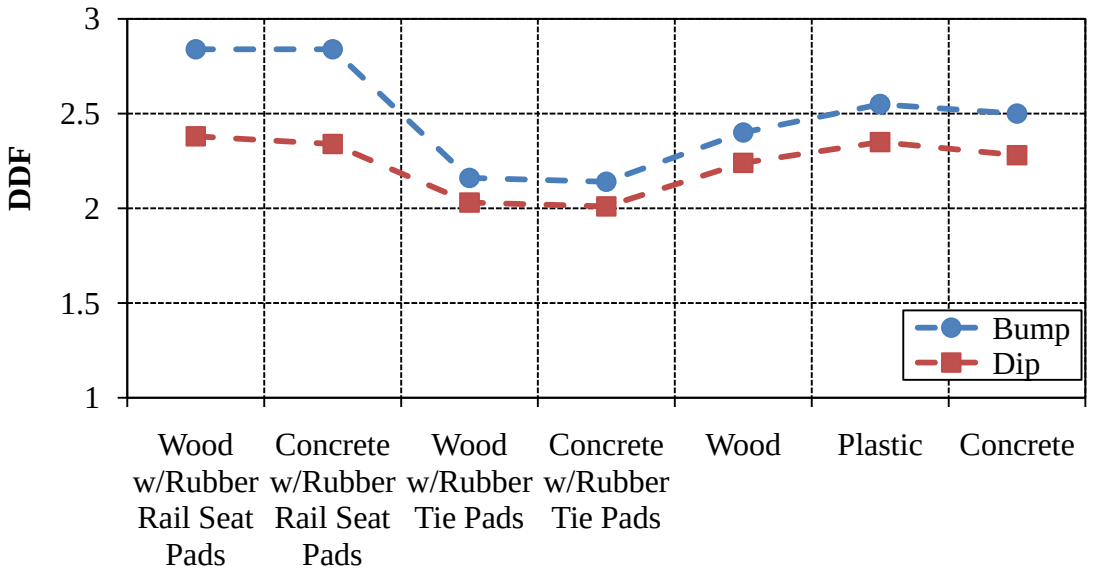

Figure 7.51 – DDF vs. approach tie material

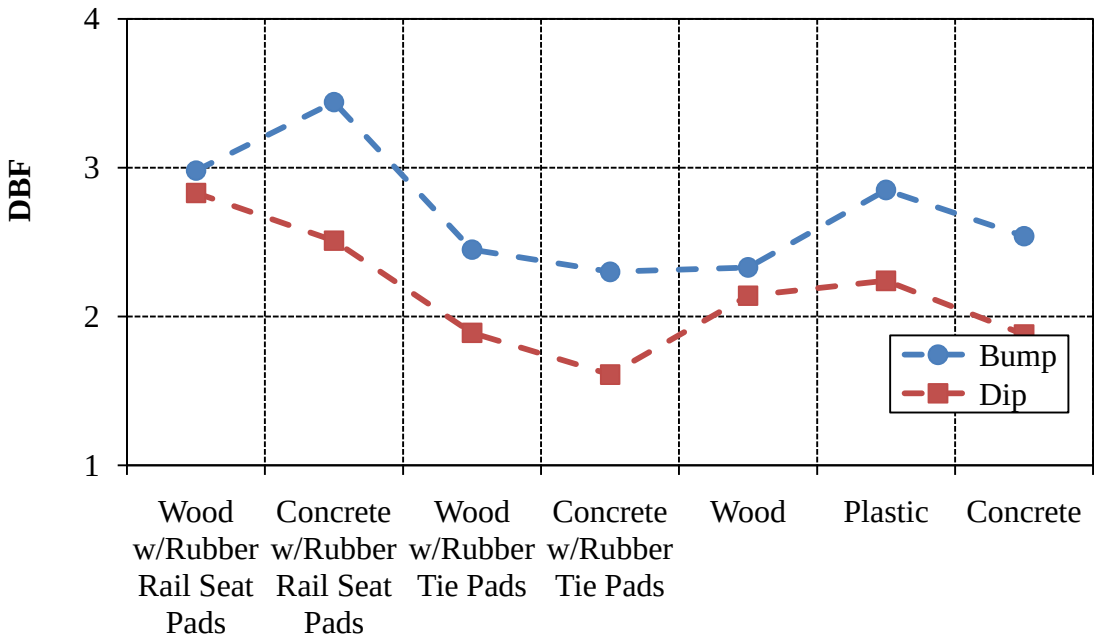

Figure 7.52 – DBF vs. approach tie material

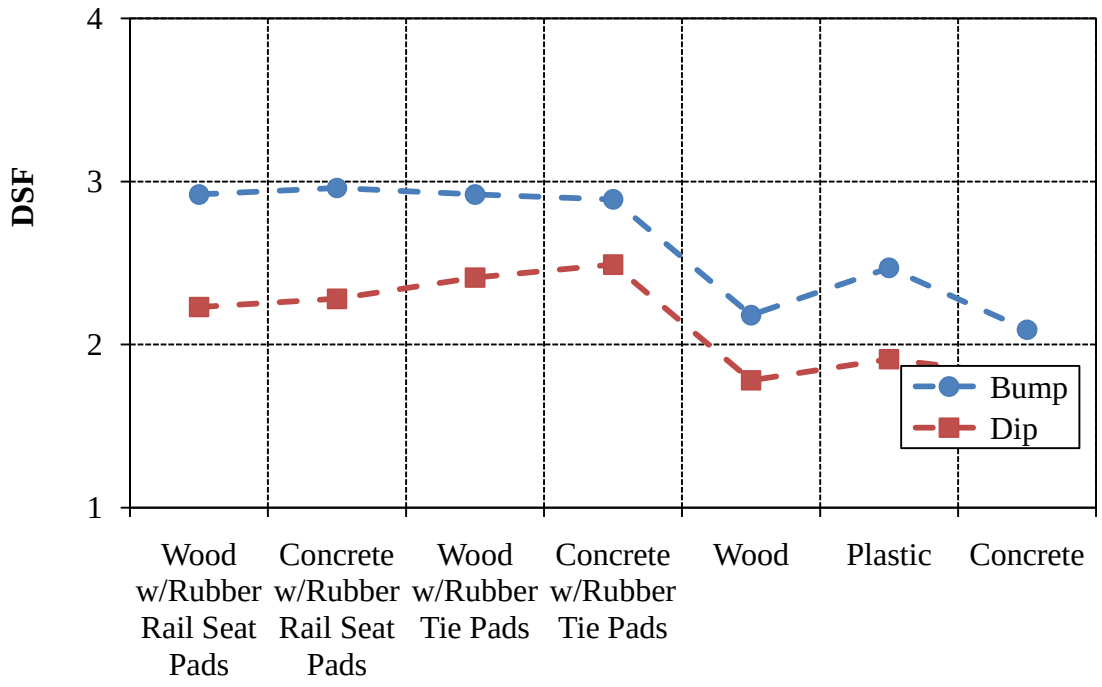

Figure 7.53 - DSF vs. approach tie material

The results indicate that approach tie material does not have a big impact on DLF (Fig. 7.50). Adding rubber pads on the approach, however, will increase the DLF. The increase is due to the track modulus change; adding rubber rail seat pads makes the track softer especially compared to the bridge. Just changing the tie material, however, does not make much difference in the track modulus.

The lowest value for DDF on the bump and dip was obtained by including rubber pads underneath the tie (Fig. 7.51). The tie material, whether wood or concrete, did not affect this. The highest value for DDF on the bump and dip was obtained by including rubber rail seat pads. Looking at the maximum deflections (Appendix E and F), the cases with rubber rail seat pads experienced the highest deflection followed by the cases with

rubber under tie pads. The average ballast pressure for the ties with both types of rubber pads was also increased.

Since adding rubber rail seat pads will soften the approach, higher ballast pressures result (Fig. 7.52). Also, since wood is not as stiff as concrete, the highest DBF occurs for wood with rubber rail seat pads. The lowest ballast pressures occur for ties with rubber tie pads. This is likely due to the fact that the interface between the tie and the ballast is padded with a soft material that helps absorb some of the dynamic loads.

Comparing the DSF for each case, ties with rubber pads tend to have larger subgrade pressures as compared to ties without rubber pads (Fig. 7.53). For both the bump and the dip, there is not a big difference between rubber rail seat pads and rubber tie pads. The same is true for tie material.

7.6 BRIDGE TIE MATERIAL

The bridge tie material was varied to determine the effect on the track response. Wood, concrete and plastic ties were modeled. Rubber pads under the rail seat and under the tie were also considered in this analysis. It was seen in the previous section that changing the approach ties did not have a large impact on the DLF, DDF, DBF and DSF, but adding rubber pads did make a slight difference. It is expected that the results will look similarly for different bridge tie materials.

7.6.1 Bump Results

The complete set of plots for wheel/rail reaction forces, vertical axle accelerations, track deflection, ballast pressures and subgrade pressures for each bridge tie material can be found in Appendix E. A complete summary of the results for the bump cases is shown in Table 7.16.

Table 7.16 – Bridge tie material summary (Bump)

Bridge Tie Material	DLF	DDF	DBF	DSF
Wood w/Rubber Rail Seat Pads	1.2	2.35	2.33	2.13
Concrete w/Rubber Rail Seat Pads	1.2	2.38	2.35	2.15
Wood	1.28	2.41	2.33	2.18
Plastic	1.28	2.5	2.32	2.28
Concrete	1.28	2.53	2.41	2.24

7.6.2 Dip Results

The complete set of plots for wheel/rail reaction forces, vertical axle accelerations, track deflection, ballast pressures and subgrade pressures for each bridge tie material can be found in Appendix F. A complete summary of the results for the bump cases is shown in Table 7.17.

Table 7.17 – Bridge tie material summary (Dip)

Bridge Tie Material	DLF	DDF	DBF	DSF
Wood w/Rubber Rail Seat Pads	1.42	2.48	2.11	1.80
Concrete w/Rubber Rail Seat Pads	1.41	2.48	2.08	1.72
Wood	1.45	2.24	2.14	1.78
Plastic	1.46	2.37	2.17	1.75
Concrete	1.46	2.39	2.21	1.82

7.6.3 Summary

The bridge tie material does not seem to have any influence on the DLF, DDF, DBF or DSF (Fig. 7.54, Fig. 7.55 Fig. 7.56 and Fig. 7.57, respectively). This is because the bridge tie material does not significantly affect the track modulus of the bridge. Since each simulation case models similar track modulus differentials, the track response for each case is also similar. Adding rubber pads on the bridge also does not affect the response on the approach.

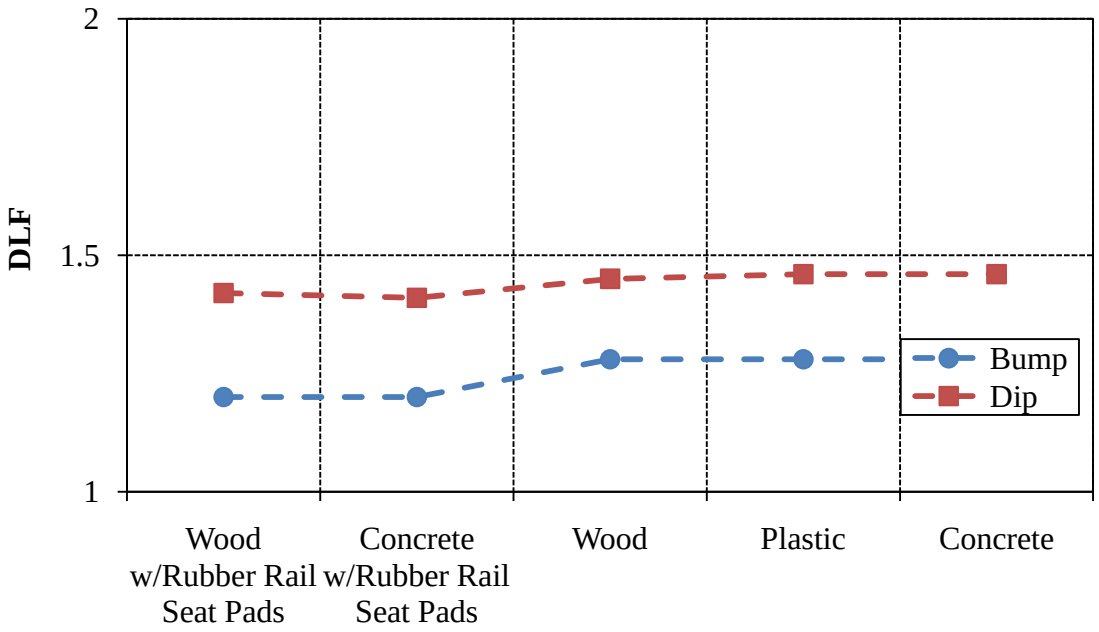

Figure 7.54 –DLF vs. bridge tie material

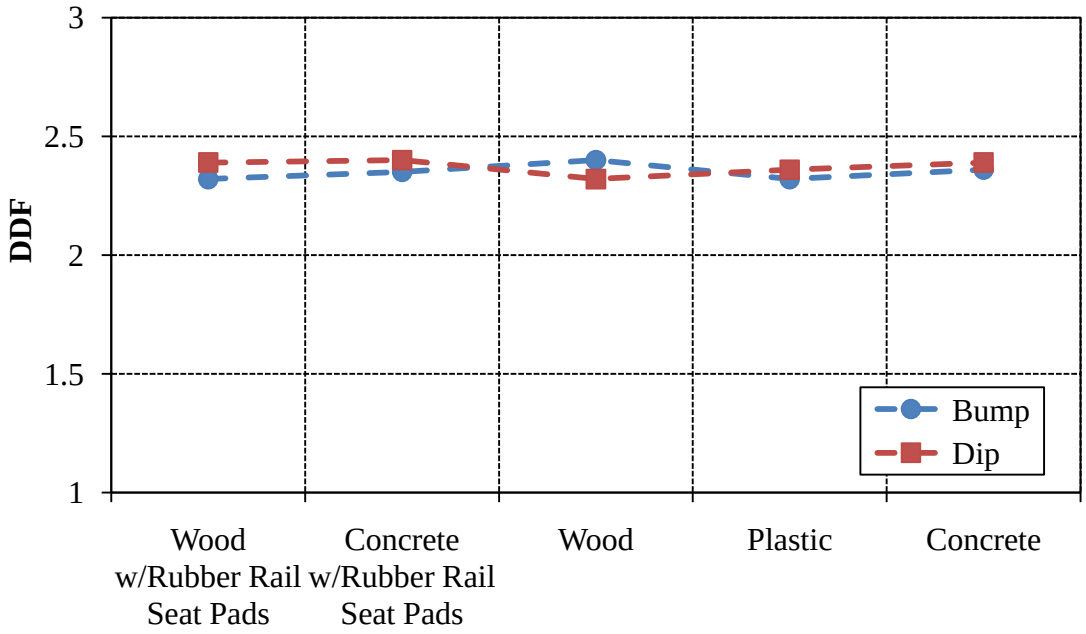

Figure 7.55 – DDF vs. bridge tie material

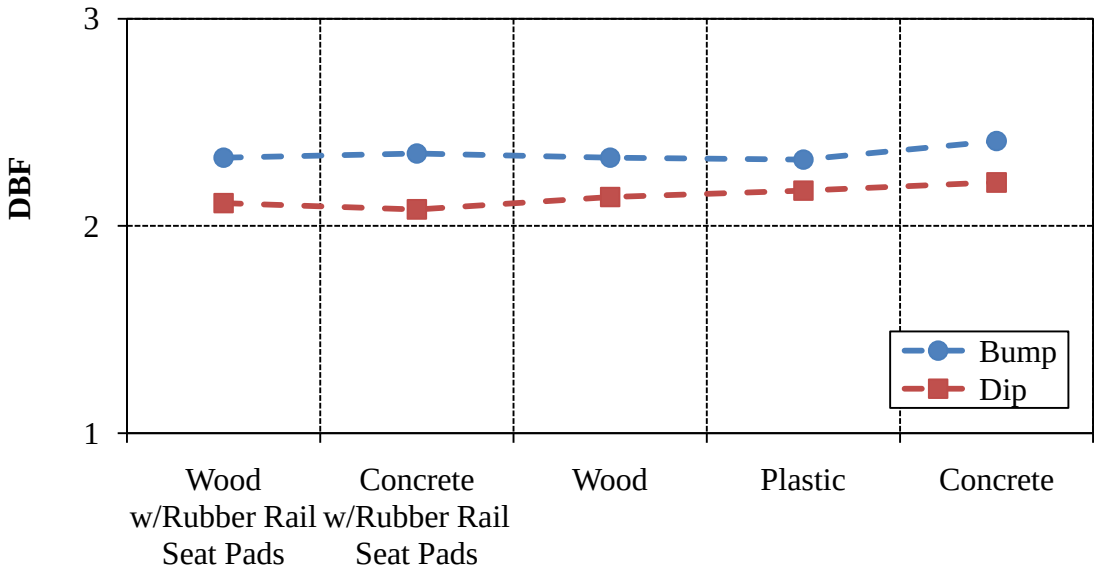

Figure 7.56 – DBF vs. bridge tie material

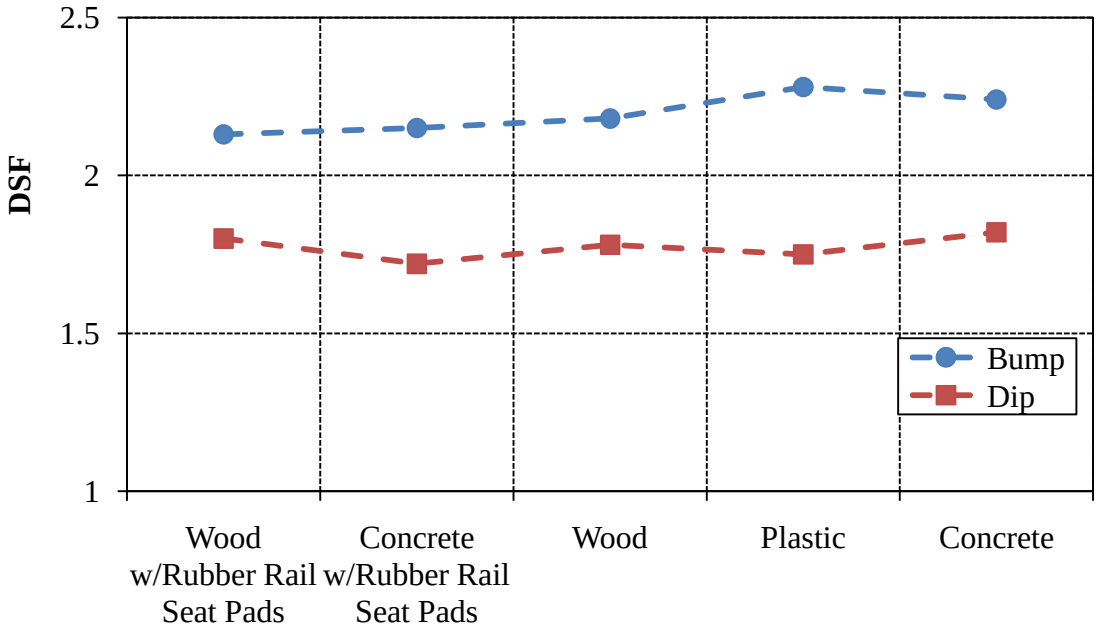

Figure 7.57 – DSF vs. bridge tie material

7.7 BRIDGE DECK TYPE

According to the survey conducted during this research (Section 4), locations with ballasted deck bridges have fewer problems than site with open deck bridges. This is because ballasted deck bridges are less stiff than open deck bridges, reducing the track modulus differential between the approach embankment and the bridge. Adding ballast mats under the ballast on a ballasted deck bridge should also serve to reduce to the track modulus on the bridge, lessening the track response.

7.7.1 Bump Results

The complete set of plots for wheel/rail reaction forces, vertical axle accelerations, track deflection, ballast pressures and subgrade pressures for each bridge deck type can be found in Appendix E. Comparing the reaction forces for each case, the impact due to the track modulus change is largest for the stiffest deck type, the open deck bridge. The impact is least for the ballast deck with a ballast mat. The impacts due to the track geometry change of the bump, however, are very similar no matter what bridge deck type is present.

Looking at the ballast pressure profile (Fig. 7.58), the maximum ballast pressure occurs at the abutment for ballasted deck bridges. The ballast mat acts to lessen the ballast pressure at this location though. Along the bump transition, the ballast pressures are all relatively similar, with those for an open deck bridge being slightly higher. The subgrade pressures are also very similar, not really affected by the bridge deck type. A complete summary of the results for the bump cases is shown in Table 7.18.

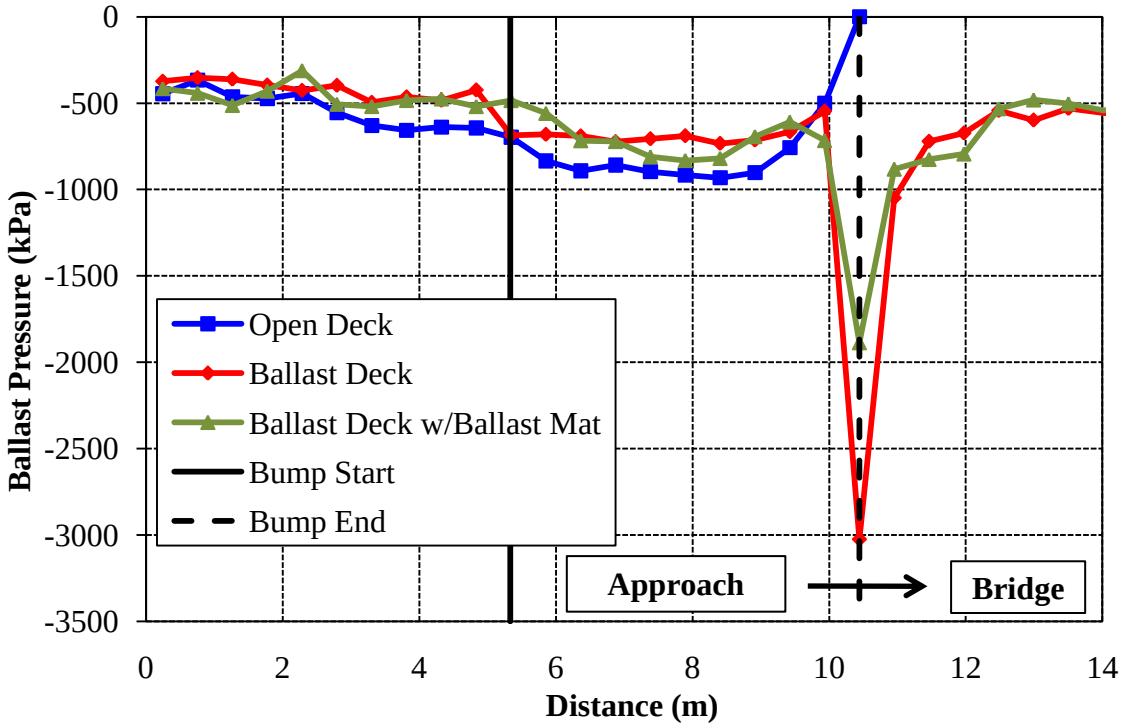

Figure 7.58 – Ballast pressure comparison for bridge deck type (Bump)

Table 7.18 – Bridge deck type summary (Bump)

Bridge Deck Type	DLF	DDF	DBF	DSF
Open Deck	1.28	2.40	2.33	2.18
Ballasted Deck	1.22	2.46	1.62 (7.56)	2.30
Ballasted Deck w/Ballast Mat	1.17	2.12	2.08 (4.72)	2.36

7.7.2 Dip Results

The complete set of plots for wheel/rail reaction forces, vertical axle accelerations, track deflection, ballast pressures and subgrade pressures for each bridge deck type can be found in Appendix F. Similar result trends for reaction forces, ballast and subgrade

pressures were found for the dip as with the bump. A complete summary of the results for the bump cases is shown in Table 7.19.

Table 7.19 – Bridge deck type summary (Dip)

Bridge Deck Type	DLF	DDF	DBF	DSF
Open Deck	1.45	2.24	2.14	1.78
Ballasted Deck	1.34	1.96	4.24	1.51
Ballasted Deck w/Ballast Mat	1.33	1.98	4.02	1.56

7.7.3 Summary

The results for DLF, DDF, DBF and DSF for bridge deck type are shown in Fig. 7.59, Fig. 7.60, Fig. 7.61 and Fig. 7.62, respectively. The bridge deck type does have an influence on the DLF (Fig. 7.59). The stiffer open deck bridges result in higher DLFs than the softer ballasted deck bridges. Adding a ballast mat reduces the track modulus for the ballasted deck bridge even further resulting in a smaller DLF for both the bump and the dip.

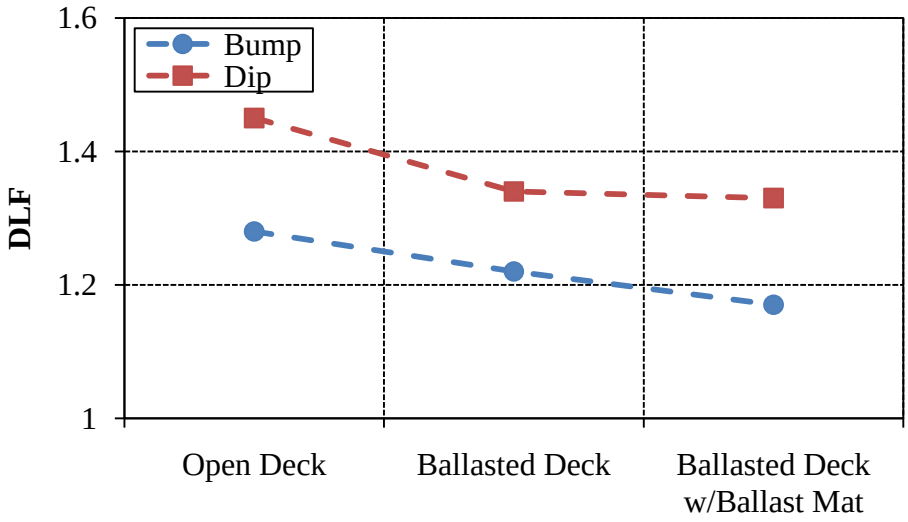

Figure 7.59 – DLF vs. bridge deck type

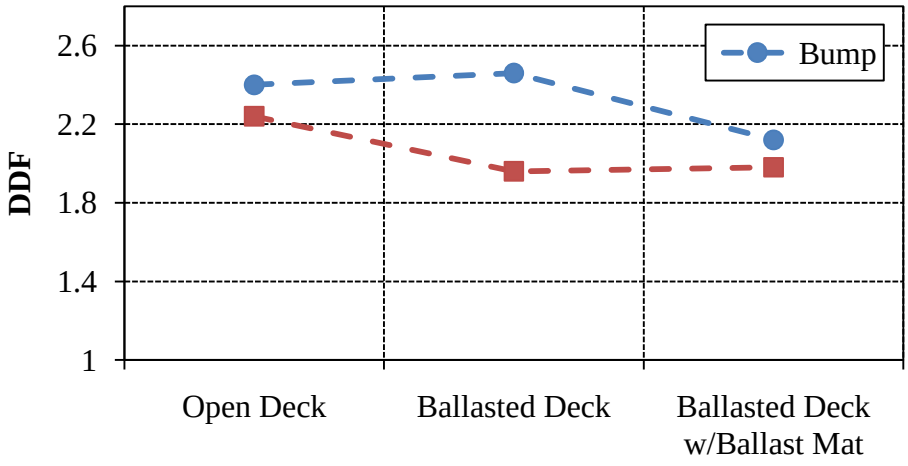

Figure 7.60 –DDF vs. bridge deck type

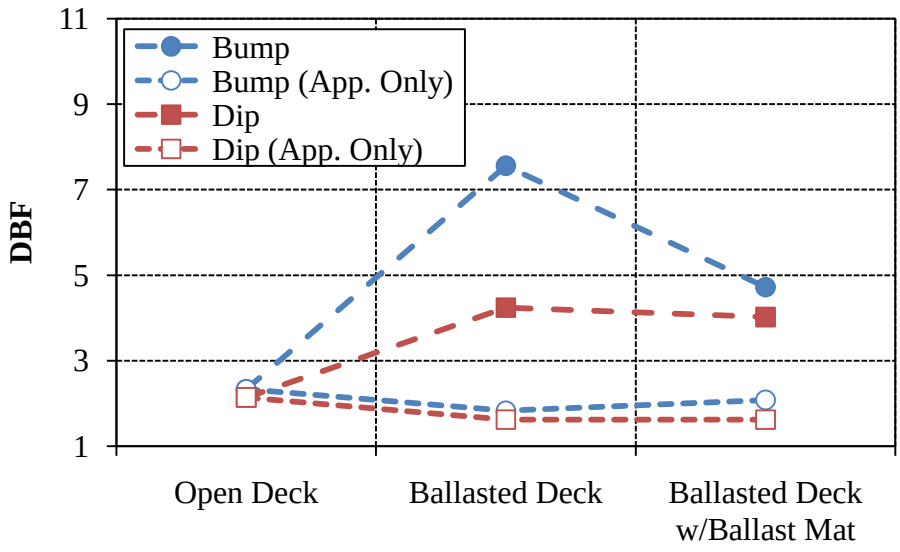

Figure 7.61 – DBF vs. bridge deck type

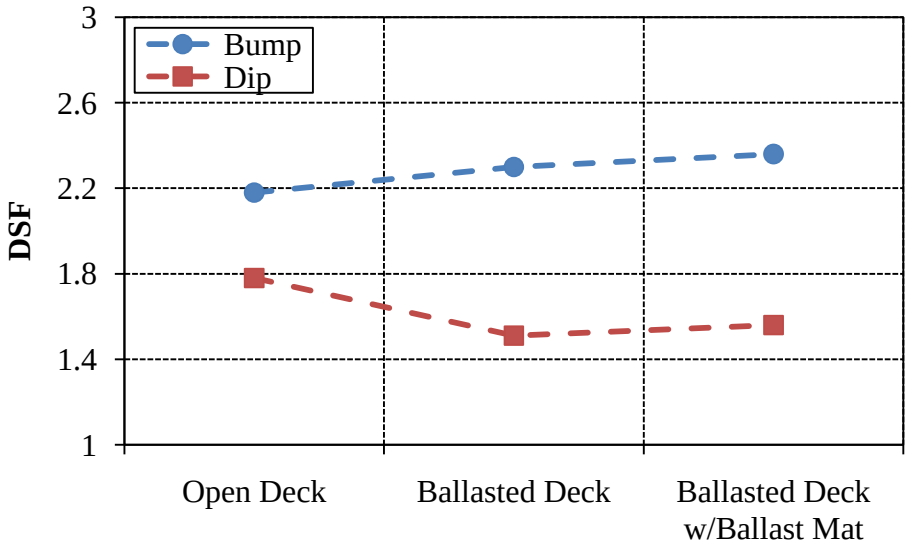

Figure 7.62 - DSF vs. bridge deck type

The approach embankment leading to an open deck bridge will generally experience more deflection than a ballast deck bridge with a ballast mat (Fig. 7.60). The ballast pressures on the approach are also higher for open deck bridges than for ballast deck bridges (Fig. 7.61). For ballasted deck bridges, the maximum ballast pressure actually occurs at the bridge abutment (Fig. 7.58). The maximum ballast pressure decreases when a ballast mat is included though. For open deck bridges, there is no ballast at this location. To accurately compare the ballast pressures and the DBF, the maximum ballast pressure is also found on the approach only (not accounting for any ballast on the bridge deck).

The DSF for the bump is at a minimum when an open deck bridge is present (Fig. 7.62). Conversely, the DSF for the dip is at a maximum when an open deck bridge is present. The difference in DSF between the bridge deck types is small though. This suggests that the bridge deck type is not a significant factor in terms of subgrade pressures.

7.8 BALLAST THICKNESS

The track modulus is not significantly affected by increasing the ballast thickness (Redden et al., 2002). Therefore, it will likely not have much influence on the impact loads. Increasing the thickness of the ballast, however, should help to reduce ballast and subgrade stresses. This, in turn, will help to reduce settlement of the approach leading to a smaller bump/dip formation.

Simulations were performed looking at varying thicknesses of ballast: 152.4 mm, 203.2 mm, 254 mm, 304.8 mm and 406.4 mm (Fig. 7.63). For each new thickness, the damping parameters for the ballast, subballast, subgrade and natural soil were recalculated, but the values were practically equal to the initial alpha and beta damping parameters calculated for the base case.

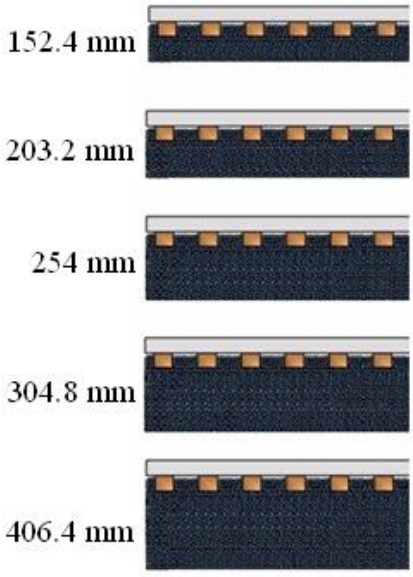

Figure 7.63 - Ballast thicknesses considered

7.8.1 Bump Results

The complete set of plots for wheel/rail reaction forces, vertical axle accelerations, track deflection, ballast pressures and subgrade pressures for each ballast thickness can be found in Appendix E. The complete summary of the results for the bump cases is shown in Table 7.20.

Table 7.20 – Ballast thickness summary (Bump)

Ballast Thickness (mm)	DLF	DDF	DBF	DSF
152.4	1.31	2.87	2.88	2.5
203.2	1.26	2.38	2.49	2.28
254	1.28	2.4	2.33	2.18
304.8	1.25	2.33	2.48	2.07
406.4	1.28	2.14	2.12	2.04

7.8.2 Dip Results

The complete set of plots for wheel/rail reaction forces, vertical axle accelerations, track deflection, ballast pressures and subgrade pressures for each ballast thickness can be found in Appendix F. The complete summary of the results for the bump cases is shown in Table 7.21.

Table 7.21 - Ballast thickness summary (Dip)

Ballast Thickness (mm)	DLF	DDF	DBF	DSF
152.4	1.51	1.88	2.16	1.73
203.2	1.49	1.93	1.77	1.94
254	1.45	2.24	2.14	1.78
304.8	1.52	2	1.87	1.6
406.4	1.52	1.81	1.74	1.44

7.8.3 Summary

The results are presented graphically in Figs. 7.64-7.67. As expected, for both the bump and the dip, the ballast thickness does not influence the DLF (Fig. 7.64). For the bump,

the DLF is approximately 1.3 for all ballast thicknesses; for the dip, the DLF is approximately 1.5 for all ballast thicknesses. For the bump, as the ballast thickness decreases, the DDF increases (Fig. 7.65). While the ballast thickness plays a role in the DDF for the bump, there is not strong correlation for the dip.

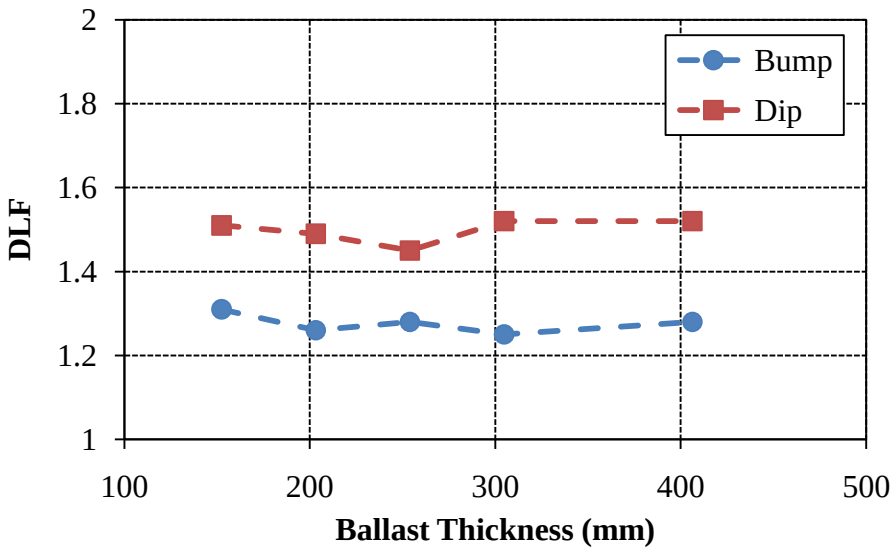

Figure 7.64 – DLF vs. ballast thickness

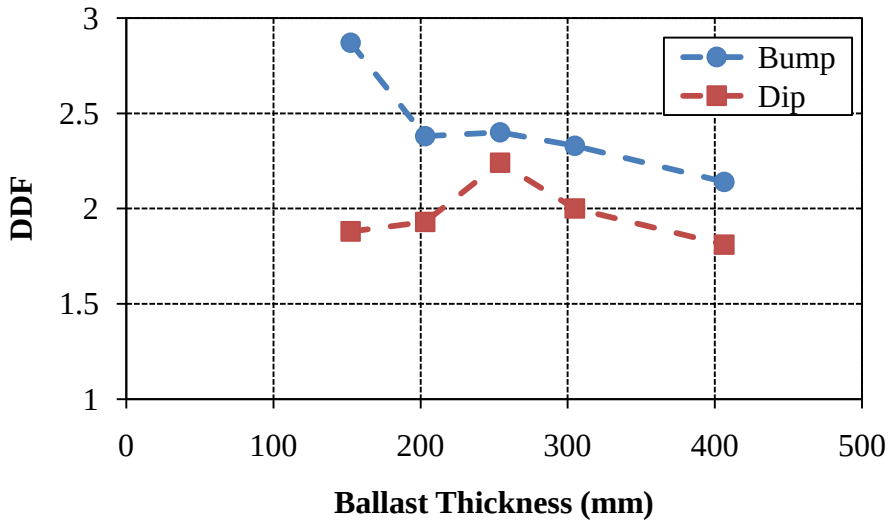

Figure 7.65 – DDF vs. ballast thickness

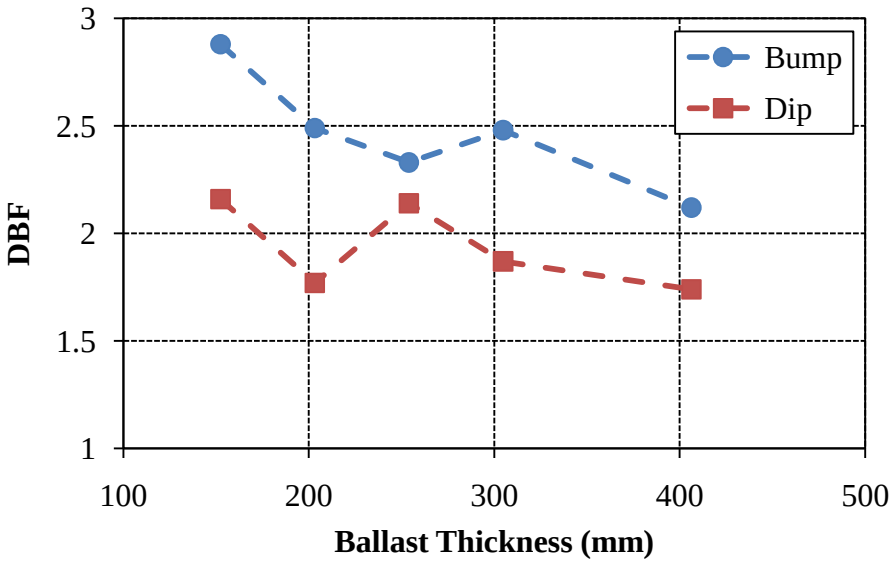

Figure 7.66 – DBF vs. ballast thickness

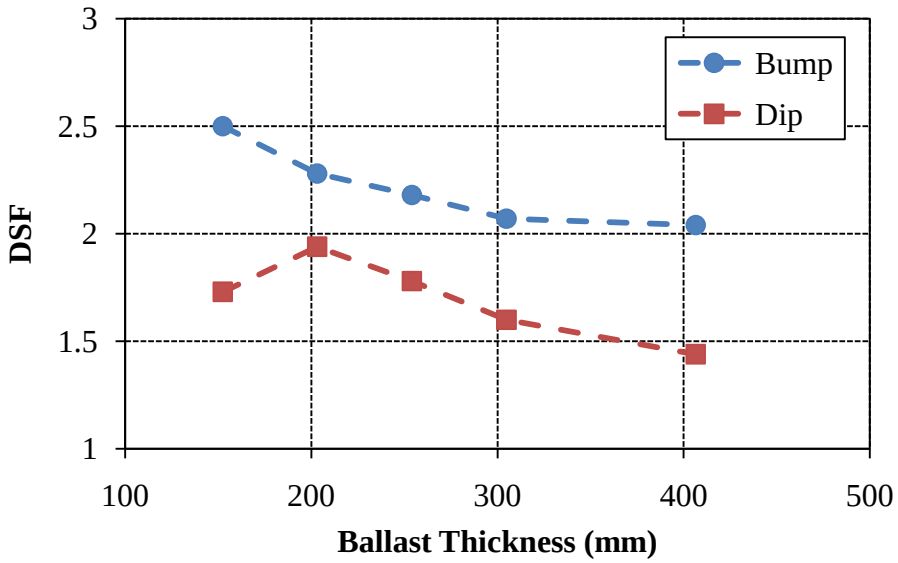

Figure 7.67 – DSF vs. ballast thickness

The ballast thickness does influence the ballast and subgrade pressures though. In general, the DBF and DSF both decrease with increasing ballast thickness (Fig. 7.66 and Fig. 7.67, respectively). While there is some slight variability in the results, it is safe to assume that pressure is reduced with increasing ballast thickness.

7.9 APPROACH TIE LENGTH

The ties considered in the parametric study were 2.1 m, 2.6 m, 3 m and 3.6 m in length (Fig. 7.68). Increasing the length of the ties will not affect the approach stiffness considerably (Sussman and Selig 1998). It is therefore expected that the length of the ties will not have a big impact on the impact loads. While it may not influence the DLF, tie length may have an impact on the subgrade stresses. The longer tie increases the area

over which the impact loads are spread which should decrease the ballast and subgrade pressures. Increasing the tie length may therefore help reduce settlement of the approach.

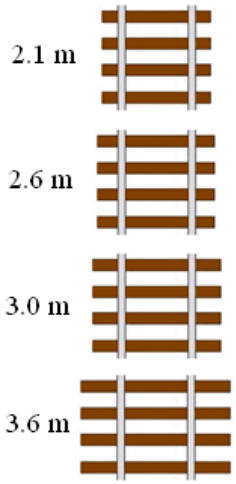

Figure 7.68 – Tie lengths considered

7.9.1 Bump Results

The complete set of plots for wheel/rail reaction forces, vertical axle accelerations, track deflection, ballast pressures and subgrade pressures for each tie length can be found in Appendix E. The complete summary of the results for the bump cases is shown in Table 7.22.

Table 7.22 – Tie length summary (Bump)

Tie Length (m)	DLF	DDF	DBF	DSF
2.1	1.31	2.7	2.5	2.41
2.6	1.28	2.4	2.33	2.18
3	1.31	2.68	2.39	2.25
3.6	1.31	2.7	2.38	2.33

7.9.2 Dip Results

The complete set of plots for wheel/rail reaction forces, vertical axle accelerations, track deflection, ballast pressures and subgrade pressures for each tie length can be found in Appendix F. The complete summary of the results for the bump cases is shown in Table 7.23.

Table 7.23 – Tie length summary (Dip)

Tie Length (m)	DLF	DDF	DBF	DSF
2.1	1.52	2.14	1.94	1.79
2.6	1.45	2.24	2.14	1.78
3	1.5	1.84	1.73	1.86
3.6	1.5	1.82	1.68	1.90

7.9.3 Summary

As expected, for both the bump and the dip, the tie length does not influence the DLF (Fig. 7.69). As with ballast thicknesses, the DLF for the bump is approximately 1.3 for all tie lengths; the DLF for the dip is approximately 1.5 for all tie lengths. There is also not a strong correlation between the tie length and the DDF, DBF and DSF (Fig. 7.70,

Fig. 7.71 and Fig. 7.72, respectively). There is a slight trend of higher ballast pressures for smaller tie lengths, but the response is not greatly affected. The results suggest that the change in pressure and track response due to increasing tie lengths is negligible compared to the other factors present.

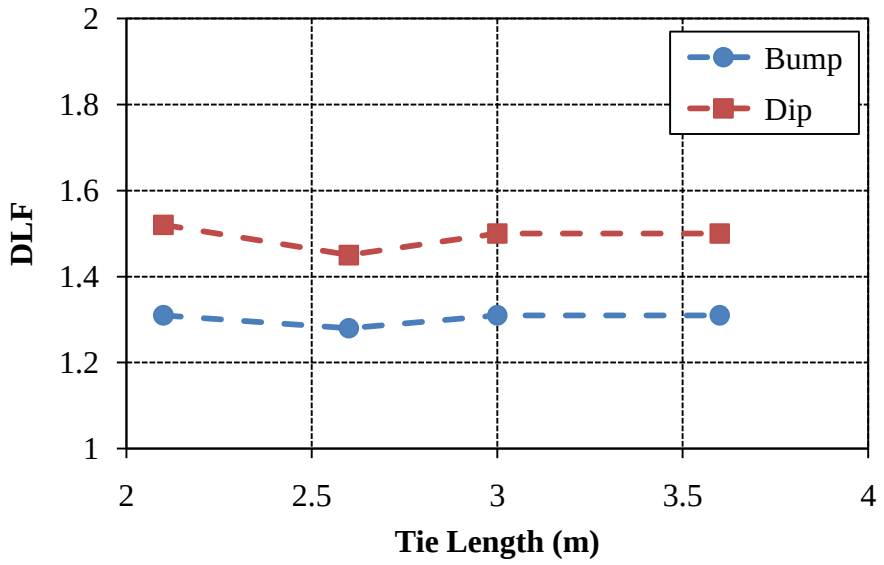

Figure 7.69 – DLF vs. tie length

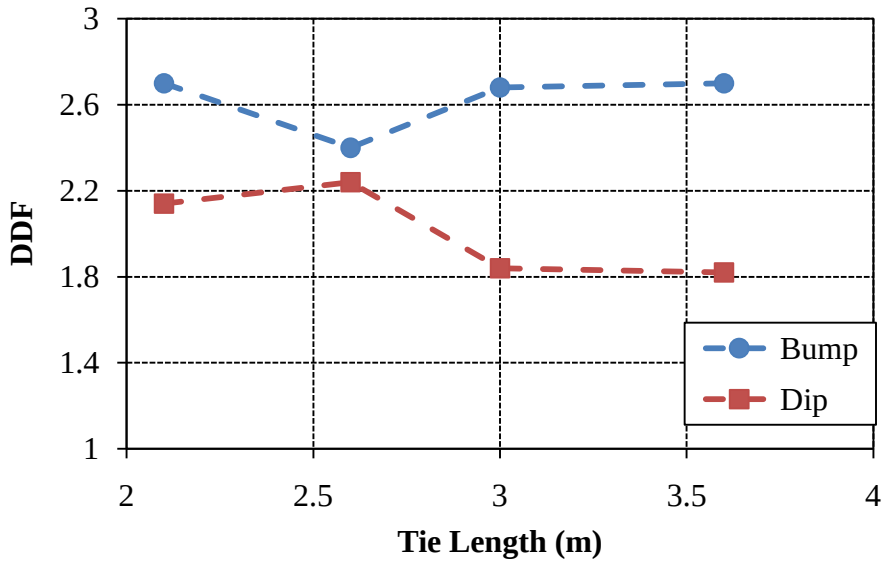

Figure 7.70 –DDF vs. tie length

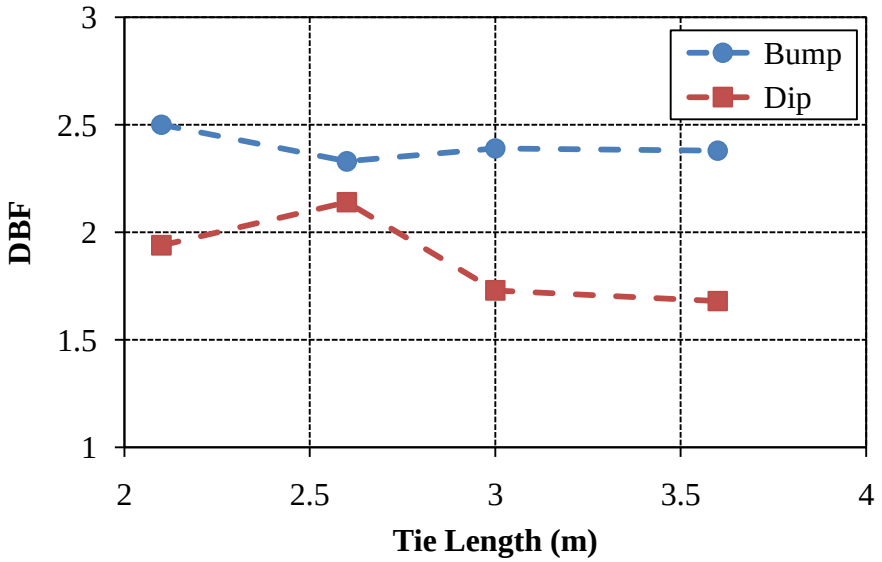

Figure 7.71 – DBF vs. tie length

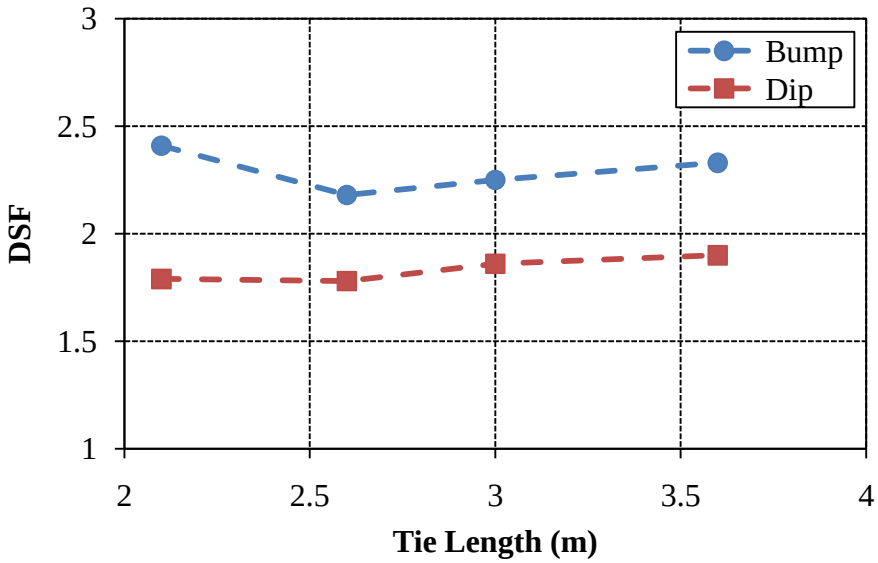

Figure 7.72 - DSF vs. tie length

7.10 SUMMARY

A complete recording of the DLF, DDF, DBF and DSF for each case in the parametric study is shown in Table 7.24. Assuming that the limitations for force, deflection, ballast pressures and subgrade pressures are all equally important, a ranking of the cases can be performed. First, the cases are evaluated based on how many tolerable limitations they exceed (Table 7.25). The cases with equal number of exceedances (for both the bump and the dip separately) are then ranked amongst themselves based on the results.

For example, case number 1 for the bump does not exceed any tolerable limits (for the dip, the ballast pressures are exceeded). This is the only case that has one exceedance for the bump, so it is ranked number 1 (Table 7.26). For the dip, there are four other cases besides case number 1 that each has only one exceedance. These five

cases are then ranked together for each limitation separately. So, for DLF, each case is ranked. Then, for track deflection, each case is ranked again and so on. Combining the total rank of each limitation provides the total ranking. The lowest sum corresponds to the best case. This was done for every case with the bump and the dip. The resulting overall rankings are shown in Table 7.27 for the bump and Table 7.28 for the dip.

Table 7.24 – Parametric study summary

Case	Bump				Dip			
	DDF	**DLF**	**DBF**	**DSF**	**DDF**	**DLF**	**DBF**	**DSF**
Ref.	2.40	1.28	2.33	2.18	2.24	1.45	2.14	1.78
1	1.02	1.13	1.10	1.05	1.45	1.27	1.57	1.70
2	1.46	1.07	1.55	1.37	1.63	1.13	1.51	1.42
3	1.83	1.18	2.02	1.78	1.92	1.29	1.57	1.50
4	3.45	1.55	3.15	3.43	2.26	1.54	1.80	1.58
5	4.07	1.66	3.56	4.05	2.43	1.72	2.28	1.84
6	4.60	1.56	4.29	4.16	3.74	2.28	3.23	2.81
7	2.93	1.35	2.82	2.94	2.83	1.75	2.01	2.61
8	2.16	1.24	1.82	2.19	2.06	1.45	1.64	1.67
9	1.98	1.22	1.82	2.04	1.88	1.39	1.67	1.65
10	2.43	1.32	2.10	2.52	1.76	1.53	2.07	1.84
11	3.24	1.45	3.54	3.05	1.83	1.83	2.40	1.90
12	3.48	1.91	4.41	2.92	1.66	1.96	2.66	2.51
13	4.57	2.17	4.61	3.29	2.12	1.92	2.90	3.00
14	2.12	1.25	2.28	2.32	1.37	1.16	1.34	1.38
15	2.88	1.40	2.67	2.75	1.72	1.26	1.72	1.44
16	3.50	1.74	3.98	3.71	1.80	1.48	2.32	1.47
17	3.54	2.00	4.17	4.99	1.84	1.76	2.01	1.67
18	1.76	1.15	1.85	1.70	1.96	1.20	1.80	1.66
19	2.20	1.23	2.19	2.07	2.61	1.31	2.16	2.02
20	2.44	1.44	2.99	2.82	2.22	1.56	2.67	2.27
21	3.50	1.57	3.69	3.94	3.16	1.70	2.21	2.46
22	1.60	1.14	1.85	1.48	1.68	1.14	1.68	1.54
23	2.10	1.20	1.80	1.95	2.38	1.21	2.19	1.91

Table 7.24 Cont'd

Case	Bump				Dip			
	DDF	DLF	DBF	DSF	DDF	DLF	DBF	DSF
24	2.68	1.35	2.76	2.58	2.22	1.45	2.22	2.14
25	2.92	1.50	4.29	2.88	2.39	1.52	2.25	2.38
26	1.23	1.10	1.54	1.10	1.23	1.10	1.54	1.10
27	1.40	1.14	1.30	1.36	1.29	1.14	1.30	1.36
28	1.33	1.22	1.61	1.41	1.33	1.22	1.61	1.41
29	1.50	1.27	1.85	1.48	1.50	1.27	1.85	1.48
30	2.54	1.30	2.31	2.20	2.04	1.44	1.89	1.78
31	2.50	1.18	2.72	2.10	2.41	1.41	2.08	1.75
32	2.29	1.18	2.40	1.80	2.19	1.35	2.06	1.72
33	2.50	1.28	2.54	2.09	2.28	1.46	1.88	1.81
34	2.55	1.30	2.85	2.47	2.35	1.46	2.24	1.91
35	2.14	1.42	3.44	2.96	2.51	1.57	2.51	2.28
36	2.16	1.42	3.44	2.96	2.54	1.57	2.83	2.23
37	2.84	1.31	2.45	2.92	2.38	1.58	1.89	2.41
38	2.84	1.31	2.30	2.89	2.34	1.56	1.61	2.49
39	2.53	1.28	2.41	2.24	2.39	1.46	2.21	1.82
40	2.50	1.28	2.32	2.28	2.37	1.46	2.17	1.75
41	2.35	1.20	2.33	2.13	2.48	1.42	2.11	1.80
42	2.38	1.20	2.35	2.15	2.48	1.41	2.08	1.72
43	2.46	1.22	7.56	2.30	1.96	1.34	4.24	1.51
44	2.12	1.17	4.72	2.36	1.98	1.33	4.02	1.56
45	2.87	1.31	2.88	2.50	1.88	1.51	2.16	1.73
46	2.38	1.26	2.49	2.28	1.93	1.49	1.60	2.03
47	2.33	1.25	2.48	2.07	2.00	1.52	1.87	1.60
48	2.14	1.28	2.12	2.04	1.81	1.52	1.74	1.44
49	2.70	1.31	2.50	2.41	2.14	1.52	1.94	1.79
50	2.68	1.31	2.39	2.25	1.84	1.50	1.73	1.86
51	2.70	1.31	2.38	2.33	1.82	1.50	1.68	1.90

Table 7.25 – Evaluation of tolerable limits for parametric study

Case	DLF ≤ 1.5?		B_{max} ≤ 450 kPa (wood ties) or B_{max} ≤ 590 kPa (concrete ties)?		S_{max} ≤ 140 kPa?		d_{max} ≤ 6.4 mm?	
	Bump	Dip	Bump	Dip	Bump	Dip	Bump	Dip
Ref.	Y	Y	N	N	N	Y	N	N
1	Y	Y	Y	N	Y	Y	Y	Y
2	Y	Y	N	N	Y	Y	Y	N
3	Y	Y	N	N	Y	Y	N	N
4	N	N	N	N	N	Y	N	N
5	N	N	N	N	N	Y	N	N
6	N	N	N	N	N	N	N	N
7	Y	N	N	N	N	N	N	N
8	Y	Y	N	N	N	Y	N	N
9	Y	Y	N	N	N	Y	N	N
10	Y	N	N	N	N	Y	N	N
11	Y	N	N	N	N	Y	N	N
12	N	N	N	N	N	N	N	N
13	N	N	N	N	N	N	N	N
14	Y	Y	N	N	N	Y	N	N
15	Y	Y	N	N	N	Y	N	N
16	N	Y	N	N	N	Y	N	N
17	N	N	N	N	N	Y	N	N
18	Y	Y	N	N	Y	Y	N	N
19	Y	Y	N	N	N	N	N	N
20	Y	N	N	N	N	N	N	N
21	N	N	N	N	N	N	N	N
22	Y	Y	N	N	Y	Y	N	N
23	Y	Y	N	N	N	Y	N	N
24	Y	Y	N	N	N	N	N	N
25	N	N	N	N	N	N	N	N
26	Y	Y	N	N	Y	Y	Y	Y
27	Y	Y	N	N	Y	Y	Y	Y
28	Y	Y	N	N	Y	Y	N	Y
29	Y	Y	N	N	Y	Y	N	Y
30	Y	Y	N	N	N	Y	N	N
31	Y	Y	N	N	N	N	N	N

Table 7.25 Cont'd.

Case	DLF ≤ 1.5?		B_{max} ≤ 450 kPa (wood ties) or B_{max} ≤ 590 kPa (concrete ties)?		S_{max} ≤ 140 kPa?		d_{max} ≤ 6.4 mm?	
	Bump	Dip	Bump	Dip	Bump	Dip	Bump	Dip
32	Y	Y	N	N	N	Y	Y	Y
33	Y	Y	N	N	N	Y	N	N
34	Y	Y	N	N	N	Y	N	N
35	Y	N	N	N	N	N	N	N
36	Y	N	N	N	N	N	N	N
37	Y	N	N	N	N	N	N	N
38	Y	N	N	N	N	N	N	N
39	Y	Y	N	N	N	Y	N	N
40	Y	Y	N	N	N	Y	N	N
41	Y	Y	N	N	N	Y	N	N
42	Y	Y	N	N	N	Y	N	N
43	Y	Y	N	N	N	Y	N	N
44	Y	Y	N	N	N	Y	N	N
45	Y	N	N	N	N	Y	N	N
46	Y	Y	N	N	N	N	N	N
47	Y	N	N	N	N	Y	N	N
48	Y	N	N	N	N	Y	N	N
49	Y	N	N	N	N	Y	N	N
50	Y	N	N	N	N	Y	N	N
51	Y	N	N	N	N	Y	N	N

Table 7.26 – Overall ranking for parametric study (Bump)

Case	Rank	Brief Description	DLF	DBF	DSF	DDF
1	1	Direction: Off of Bridge	1.13	1.10	1.05	1.02
26	2	No Slope @ 15.6 m/s	1.10	1.54	1.10	1.23
27	3	No Slope @ 22.2 m/s	1.14	1.30	1.36	1.40
2	4	1:150 @ 8.9 m/s	1.07	1.55	1.37	1.46
22	5	1:250 (Equal Height) @ 15.6 m/s	1.14	1.85	1.48	1.60
28	6	No Slope @ 33.5 m/s	1.22	1.61	1.41	1.33
18	7	1:200 (Equal Height) @ 15.6 m/s	1.15	1.85	1.70	1.76

Table 7.26 Cont'd

Case	Rank	Brief Description	DLF	DBF	DSF	DDF
29	8	No Slope @ 44.7 m/s	1.27	1.85	1.48	1.50
3	9	1:150 @ 15.6 m/s	1.18	2.02	1.78	1.83
32	10	100 MPa Soil Modulus	1.18	2.40	1.80	2.29
23	11	1:250 (Equal Height) @ 22.2 m/s	1.20	1.80	1.95	2.10
9	12	1:250 (Equal Length)	1.22	1.82	2.04	1.98
48	13	406.4 mm Ballast Thickness	1.28	2.12	2.04	2.14
44	23	Ballast Deck Bridge with a Ballast Mat	1.17	4.72	2.36	2.12
19	14	1:200 (Equal Height) @ 22.2 m/s	1.23	2.19	2.07	2.20
8	15	1:200 (Equal Length)	1.24	1.82	2.19	2.16
41	16	Wood Bridge Ties with Rubber Rail Seat Pads	1.20	2.33	2.13	2.35
42	17	Concrete Bridge Ties with Rubber Rail Seat Pads	1.20	2.35	2.15	2.38
14	18	1:100 (Equal Height) @ 15.6 m/s	1.25	2.28	2.32	2.12
43	30	Ballast Deck Bridge	1.22	7.56	2.30	2.46
47	19	304.8 mm Ballast Thickness	1.25	2.48	2.07	2.33
Ref.	20	1:150 (Equal Length, Equal Height) @ 22.2 m/s	1.28	2.33	2.18	2.40
31	21	50 MPa Soil Modulus	1.18	2.72	2.10	2.50
40	22	Plastic Bridge Ties	1.28	2.32	2.28	2.50
46	24	203.2 mm Ballast Thickness	1.26	2.49	2.28	2.38
33	25	Concrete Approach Ties	1.28	2.54	2.09	2.50
30	26	20 MPa Soil Modulus	1.30	2.31	2.20	2.54
39	27	Concrete Bridge Ties	1.28	2.41	2.24	2.53
10	28	1:50 (Equal Height) @ 15.6 m/s	1.32	2.10	2.52	2.43
50	29	3 m Approach Tie Length	1.31	2.39	2.25	2.68
51	31	3.6 m Approach Tie Length	1.31	2.38	2.33	2.70
34	33	Plastic Approach Ties	1.30	2.85	2.47	2.55
49	35	2.1 m Approach Tie Length	1.31	2.50	2.41	2.70
38	32	Concrete Approach Ties with Rubber Tie Pads	1.31	2.30	2.89	2.84
37	34	Wood Approach Ties with Rubber Tie Pads	1.31	2.45	2.92	2.84
35	36	Concrete Approach Ties with Rubber Rail Seat Pads	1.42	3.44	2.96	2.14
36	37	Wood Approach Ties with Rubber Rail Seat Pads	1.42	3.44	2.96	2.16
45	38	152.4 mm Ballast Thickness	1.31	2.88	2.50	2.87
24	39	1:250 (Equal Height) @ 33.5 m/s	1.35	2.76	2.58	2.68

Table 7.26 Cont'd

Case	Rank	Brief Description	DLF	DBF	DSF	DDF
20	40	1:200 (Equal Height) @ 33.5 m/s	1.44	2.99	2.82	2.44
15	41	1:100 (Equal Height) @ 22.2 m/s	1.40	2.67	2.75	2.88
7	42	1:100 (Equal Length)	1.35	2.82	2.94	2.93
11	43	1:50 (Equal Height) @ 22.2 m/s	1.45	3.54	3.05	3.24
25	44	1:250 (Equal Height) @ 44.7 m/s	1.50	4.29	2.88	2.92
4	45	1:150 @ 33.5 m/s	1.55	3.15	3.43	3.45
21	46	1:200 (Equal Height) @ 44.7 m/s	1.57	3.69	3.94	3.50
16	47	1:100 (Equal Height) @ 33.5 m/s	1.74	3.98	3.71	3.50
12	48	1:50 (Equal Height) @ 33.5 m/s	1.91	4.41	2.92	3.48
5	49	1:150 @ 44.7 m/s	1.66	3.56	4.05	4.07
6	50	1:50 (Equal Length)	1.56	4.29	4.16	4.60
17	51	1:100 (Equal Height) @ 44.7 m/s	2.00	4.17	4.99	3.54
13	52	1:50 (Equal Height) @ 44.7 m/s	2.17	4.61	3.29	4.57

Table 7.27 – Overall ranking for parametric study (Dip)

Case	Rank	Brief Description	DLF	DBF	DSF	DDF
26	1	No Slope @ 15.6 m/s	1.10	1.54	1.10	1.23
27	2	No Slope @ 22.2 m/s	1.14	1.30	1.36	1.29
28	3	No Slope @ 33.5 m/s	1.22	1.61	1.41	1.33
1	4	Direction: Off of Bridge	1.27	1.57	1.70	1.45
29	5	No Slope @ 44.7 m/s	1.27	1.85	1.48	1.50
14	6	1:100 (Equal Height) @ 15.6 m/s	1.16	1.34	1.38	1.37
2	7	1:150 @ 8.9 m/s	1.13	1.51	1.42	1.63
22	8	1:250 (Equal Height) @ 15.6 m/s	1.14	1.68	1.54	1.68
15	9	1:100 (Equal Height) @ 22.2 m/s	1.26	1.72	1.44	1.72
3	10	1:150 @ 15.6 m/s	1.29	1.57	1.50	1.92
43	14	Ballast Deck Bridge	1.34	1.62	1.51	1.96
44	15	Ballast Deck Bridge with a Ballast Mat	1.33	1.62	1.56	1.98
18	11	1:200 (Equal Height) @ 15.6 m/s	1.20	1.80	1.66	1.96
9	12	1:250 (Equal Length)	1.39	1.67	1.65	1.88
8	13	1:200 (Equal Length)	1.45	1.64	1.67	2.06
32	16	100 MPa Soil Modulus	1.35	2.06	1.72	2.19
16	17	1:100 (Equal Height) @ 33.5 m/s	1.48	2.32	1.47	1.80
30	18	20 MPa Soil Modulus	1.44	1.89	1.78	2.04

Table 7.27 Cont'd

Case	Rank	Brief Description	DLF	DBF	DSF	DDF
42	19	Concrete Bridge Ties with Rubber Rail Seat Pads	1.41	2.08	1.72	2.48
Ref.	20	1:150 (Equal Length, Equal Height) @ 22.2 m/s	1.45	2.14	1.78	2.24
23	22	1:250 (Equal Height) @ 22.2 m/s	1.21	2.19	1.91	2.38
33	21	Concrete Approach Ties	1.46	1.88	1.81	2.28
41	24	Wood Bridge Ties with Rubber Rail Seat Pads	1.42	2.11	1.80	2.48
40	23	Plastic Bridge Ties	1.46	2.17	1.75	2.37
34	25	Plastic Approach Ties	1.46	2.24	1.91	2.35
39	26	Concrete Bridge Ties	1.46	2.21	1.82	2.39
48	27	406.4 mm Ballast Thickness	1.52	1.74	1.44	1.81
51	28	3.6 m Approach Tie Length	1.50	1.68	1.90	1.82
50	29	3 m Approach Tie Length	1.50	1.73	1.86	1.84
47	30	304.8 mm Ballast Thickness	1.52	1.87	1.60	2.00
46	31	203.2 mm Ballast Thickness	1.49	1.60	2.03	1.93
10	32	1:50 (Equal Height) @ 15.6 m/s	1.53	2.07	1.84	1.76
45	33	152.4 mm Ballast Thickness	1.51	2.16	1.73	1.88
17	34	1:100 (Equal Height) @ 44.7 m/s	1.76	2.01	1.67	1.84
4	35	1:150 @ 33.5 m/s	1.54	1.80	1.58	2.26
31	36	50 MPa Soil Modulus	1.41	2.08	1.75	2.41
49	37	2.1 m Approach Tie Length	1.52	1.94	1.79	2.14
19	38	1:200 (Equal Height) @ 22.2 m/s	1.31	2.16	2.02	2.61
24	39	1:250 (Equal Height) @ 33.5 m/s	1.45	2.22	2.14	2.22
11	40	1:50 (Equal Height) @ 22.2 m/s	1.83	2.40	1.90	1.83
5	41	1:150 @ 44.7 m/s	1.72	2.28	1.84	2.43
38	32	Concrete Approach Ties with Rubber Tie Pads	1.31	2.30	2.89	2.84
20	43	1:200 (Equal Height) @ 33.5 m/s	1.56	2.67	2.27	2.22
25	45	1:250 (Equal Height) @ 44.7 m/s	1.52	2.25	2.38	2.39
37	44	Wood Approach Ties with Rubber Tie Pads	1.58	1.89	2.41	2.38
35	46	Concrete Approach Ties with Rubber Rail Seat Pads	1.57	2.51	2.28	2.51
36	47	Wood Approach Ties with Rubber Rail Seat Pads	1.57	2.83	2.23	2.54
12	48	1:50 (Equal Height) @ 33.5 m/s	1.96	2.66	2.51	1.66
21	49	1:200 (Equal Height) @ 44.7 m/s	1.70	2.21	2.46	3.16
7	50	1:100 (Equal Length)	1.75	2.01	2.61	2.83

Table 7.27 Cont'd

Case	Rank	Brief Description	DLF	DBF	DSF	DDF
13	51	1:50 (Equal Height) @ 44.7 m/s	1.92	2.90	3.00	2.12
6	52	1:50 (Equal Length)	2.28	3.23	2.81	3.74

8. FIELD TEST OF PROTOTYPE DESIGN SOLUTION

8.1 PROPOSED SOLUTION

After evaluating the current mitigation methods (Section 3), it is clear that there are a number of solutions for new bridge construction that are performing well: approach slabs, bridge approach support piling, stone columns and HMA underlayment. These solutions address settlement and track modulus issues at the bridge/approach location. To install these types of solutions, the track structure must be completed removed to access the subgrade. This can cause significant track downtime leading to economic loss. Depending on the cost, railroads may simply maintain the problem rather than fix it. The solutions are therefore not as feasible for existing bridges.

A new solution is proposed in this section for approach embankments with soft subgrades at existing bridges. It will reduce the settlement on the approach and minimize the track modulus differential with the bridge. Full-scale field testing and numerical simulations of the proposed solution design will analyze the performance under actual traffic conditions.

8.1.1 Description

The proposed solution for the bump/dip problem involves installing varying length steel bars between the ties into the subgrade (Fig. 8.1). These pile-like elements will strength and stiffen the subgrade. The tops of the bars will begin directly underneath the ballast so as not to interfere with any future ballast tamping activities. The steel bars can be

vibro-driven into place without removing any of the track structure. The installation can be done either from the side of the track or directly from a bogie on top of the track depending on available equipment and right-of-way issues.

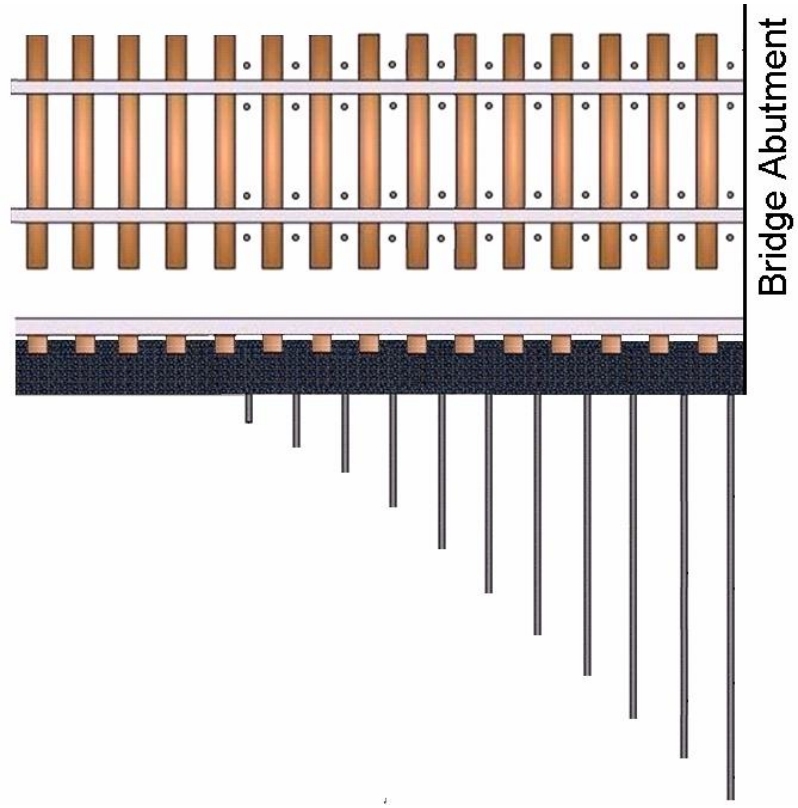

Figure 8.1 – Proposed solution sketch

The diameter of the steel bars is recommended at 35 mm (1.375 in). Although two bars could theoretically be placed within the distance between two ties, it is not practical construction-wise. The proposed solution therefore involves a total of four bars between each tie: two inside the tracks, and two outside of the tracks. The distance that

the bars should extend beyond the bridge abutment is based on the soil conditions of the subgrade. A soft soil will require a longer distance of soil strengthening than a harder soil.

The total number of steel bars, spacing, depth, and length are also determined based on the local site conditions. For example, the depth of the steel bars closest to the bridge abutment should extend the deepest to a competent soil layer. The depth of subsequent piles will decrease so as to soften the stiffness transition and is determined based on the soil strength of the approach embankment. If the soil is very soft, the change in depth between the steel bars will be smaller than if the soil is stronger.

The bar length decrease may also not be linear as depicted in Fig. 8.1. This assumes a uniform subgrade. If the subgrade is layered, as with an imported fill and natural soil embankment, then the bar length decrease will be non-linear. For a subgrade with a weaker layer over a stronger layer, the bars may need to be longer for a greater distance and then gradually decrease. Conversely, for a subgrade with a stronger layer of a weaker layer, the bars may need to longer for a shorter distance and then more rapidly decrease. If the thickness of the top layer is large enough, however, then the embankment can be assumed to be uniform and a linear bar length decrease can be used. While the details of the solution will vary depending on the site, the solution itself should be applicable at any bridge location.

8.1.2 Design Concept

The proposed solution addresses both the differential track modulus and differential settlement issues. The varying length of the steel bars serves to gradually stiffen the approach embankment. Rather than having a sharp discontinuity at the bridge abutment, a gentle track stiffness transition will be created by the solution. This will reduce the impact force, track deflection, ballast pressures and subgrade pressures resulting in less track degradation.

The stress due to the train load is transferred through the ties and ballast to the subgrade. Inclusions in the soil, such as the proposed steel bars, will take most of the load transfer in a process called soil arching (Terzaghi 1943). This is because the steel bars are much less compressible than the surrounding soil. As loading occurs, shear stresses develop between the piles and the subgrade which causes the piles to carry a higher load. This also means that the stress will be reduced on the subgrade around the piles. This will reduce the sharpness of the settlement profile of the subgrade. The varying length of the steel bars will provide for an acceptable ramp in the track up to the bridge, rather than a steep bump.

While the proposed solution is applicable to any site, the exact design is subject to local site conditions. This means that the design is not a “one size fits all” solution. Site investigations must still be performed to determine the soil properties. The proposed solution can then be designed to account for the local conditions.

8.2 BASE CASE FIELD TEST

To validate the effectiveness of the proposed solution at minimizing the bump at the end of the railway bridge, a full-scale field is being conducted with the support of the AAR and the Transportation Technology Center, Inc. (TTCI).

8.2.1 Site Location

TTCI's facility in Pueblo, CO, called the Facility for Acceleration Service Testing (FAST), consists of more than 48 miles of railroad tracks used for research testing. The High Tonnage Loop (HTL) at FAST, which has 4.8 miles of track, is divided into test sections specifically for research under heavy axle loads (Fig. 8.2). The traffic on the HTL is running at a maximum of 17.9 m/s (40 mph). While there are a couple of full-scale test bridges on the HTL, none have experienced any bump/dip problems. This makes testing the proposed solution at a test bridge site difficult without importing a soft subgrade to force a bump problem to solve.

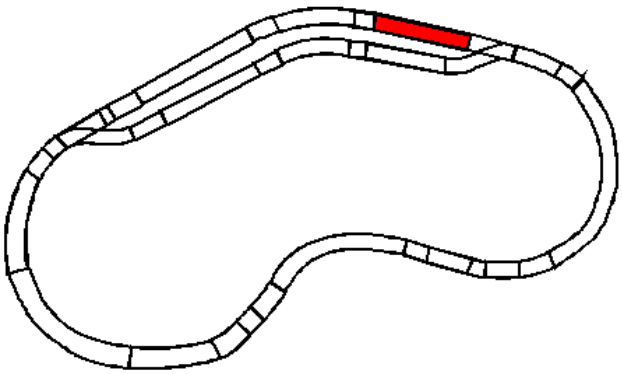

Figure 8.2 – FAST HTL test sections

8.2.1.1 Description

One test section on the HTL, Section 29, already has an imported soft clay subgrade and is called the Low Track Modulus (LTM) Section (shown in red in Fig. 8.2). The LTM section consists of a 213 m (700 ft) long, 3.6 m (12 ft) wide, 1.5 m (5 ft) deep trench filled with Mississippi Buckshot clay (Fig. 8.3). The clay section is lined with a geomembrane to prevent moisture loss to the surrounding silty sand.

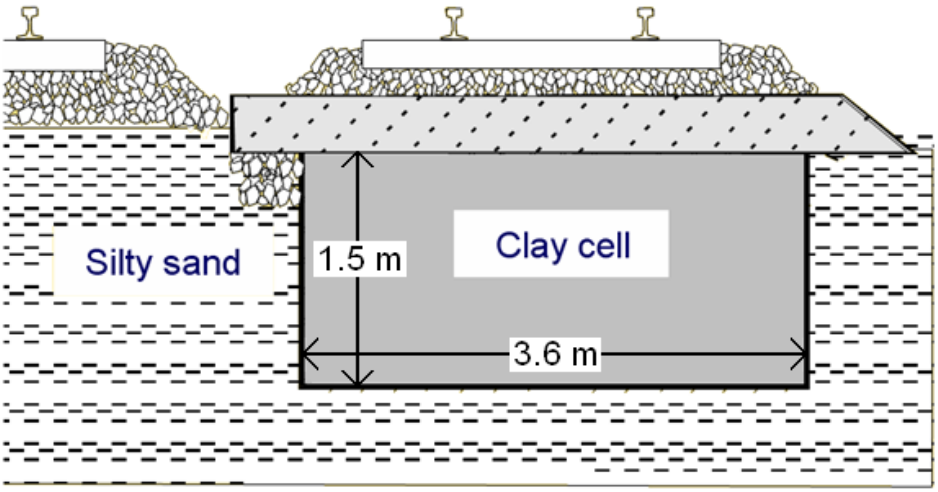

Figure 8.3 – LTM cross-section

While the LTM section is not at a bridge/approach location, the track modulus differential between the soft clay and the surrounding natural soil will serve to mimic the track response and behavior at a bridge site. Prior to its use for the prototype design test, the LTM section was being used to test both 203.2 mm and 101.6 mm thick hot mix asphalt (HMA) sections above the subgrade (Li et al. 2001). A 30.5 m (100 ft) section of

the 203.2 mm (8 in) HMA therefore had to be removed before testing of the prototype solution (Fig. 8.4). The prototype solution will be placed from the beginning of the clay section (far right in Fig. 8.4) and extend towards the 101.6 mm HMA (towards the left in Fig. 8.4).

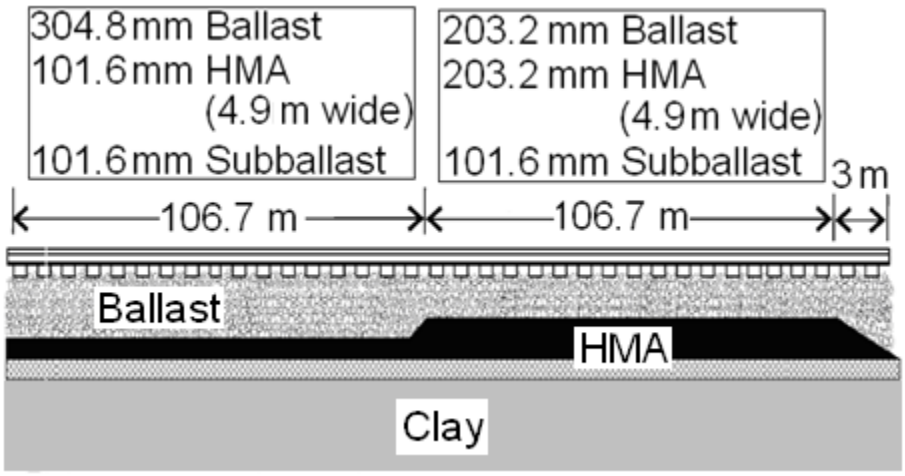

Figure 8.4 –LTM longitudinal cross-section

8.2.1.2 Soil Conditions

The soft clay used in the LTM section is a highly plastic Mississippi Buckshot Clay. Comprehensive soil testing has been conducted on this clay soil to determine its properties (Miller et al. 2000). The USCS classification is CH. The total mass density of the clay is assumed to equal approximately 2000 kg/m^3. The friction angle is 22.7^o and the cohesion intercept is 15.9 kPa (2.3 psi). The undrained shear strength is approximately 31 kPa. The average liquid limit, plastic limit, and plasticity index for the

clay soil are 64%, 26% and 38%, respectively. The clay was installed with a moisture content of 33%. Since a membrane was placed around the entire trench, the moisture is maintained within the clay. Subsequent tests over the years confirm that the water content has been stable (LoPresti and Li 2005).

The California Bearing Ratio (CBR) for the clay, which is a measure of strength, is at 1%, indicating a very low strength soil (LoPresti and Li 2005). CPT testing at the site indicated an average tip resistance between 5 MPa and 15 MPa (Li 2000). The resilient modulus varies between approximately 13.8 MPa (2000 psi) and 20.7 MPa (3000 psi), also indicating a soft clay (Read and Li 1995).

The natural soil at the site is a competent silty sand. The USCS classification is SM. The total mass density of the silty sand is calculated as 1874 kg/m^3, based on the reported dry density of 1970 kg/m^3 and the moisture content of approximately 5% (Li 2000). Li (2000) also recommends using a resilient modulus value between 55.2 MPa and 137.9 MPa for design and analysis. CPT testing at the site indicated an average tip resistance between 2 MPa and 10 MPa. At shallow depths, above about 1 m, the tip resistance of the natural soil can reach almost 25 MPa.

8.2.1.3 Track Modulus

The track modulus in the LTM section has been found to range from about 13.8 N/mm/mm (2000 lb/in/in) to 17.2 N/mm/mm (2500 lb/in/in) (Li et al. 1997). The strong silty sand that comprises the natural subgrade at FAST has a track modulus that ranges from 27.6 N/mm/mm (4000 lb/in/in) to 41.4 N/mm/mm (6000 lb/in/in). To help increase

the track modulus differential and better model the bridge/approach location, concrete ties were installed over the natural subgrade soil (wood ties remain over the LTM section).

The track modulus profile across the LTM section is shown in Fig. 8.5. The profile was taken after removal of the HMA section, prior to running any new traffic on the LTM section (at 0 MGT). Right at the interface between the control and the LTM sections, the track modulus differential is approximately 10 N/mm/mm. The track modulus profile will likely change, however, once traffic runs across the test section. This is because the ballast rearranges and consolidates from the neatly placed condition prior to any traffic.

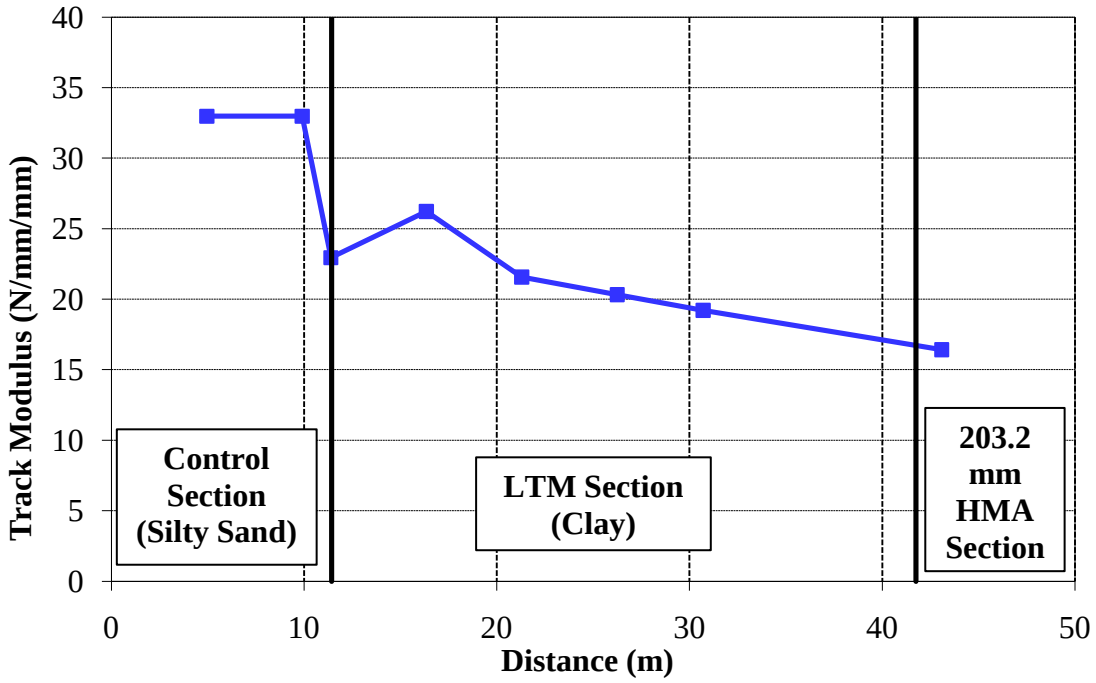

Figure 8.5 – Measured track modulus at LTM section

8.2.1.4 Previous Site Behavior

Shortly after the initial installation of the LTM section in 1991, track geometry degradation became a problem, resulting in frequent surfacing and track rebuilding (Li et al., 1997). It was concluded that the problem was progressive shear failures in the subgrade. As the train passed over the rails, the soil was pushed outward and upward to the ballast shoulder.

One reason for the progressive shear failures may have been due to the confinement of the clay layer. Since the clay cannot move laterally beyond the 3.6 m trench boundary, it tends to move up and out under heavy loading. Another reason was the appearance of free standing water around the track. This could have caused the subgrade stresses to increase resulting in the excessive deformation. A drainage ditch has since been placed to alleviate the problem.

After 17 years since installation, the clay cell may have consolidated and stabilized. A base case test was therefore conducted after removal of the HMA to determine if a bump/dip would even form in the track. The base case also serves to ensure that the progressive shear failures seen shortly after the initial installation of the clay layer are no longer a problem. More information on the base case is provided later in this section.

8.2.2 Instrumentation and Measurements

The type and amount of measurements are vital in evaluating the effectiveness of the proposed solution. A base case trial, where traffic runs over the LTM section with no

solution, will be tested first. This will allow for comparison once the proposed solution is installed. It will also help validate the numerical model created to analyze the LTM section. The following measurements are suggested: track modulus, top-of-rail (TOR) elevation, wheel/rail forces, cross-section elevation, subgrade settlement and subgrade pressure. The measurement schedule for the base case is listed in Table 8.1. The suggested measurement schedule for the field test of the solution is listed in Table 8.2.

Table 8.1 – Base case measurement schedule

MGT	Track Modulus	TOR Elevations	Wheel/Rail Forces	Cross Section	Subgrade Settlement	Subgrade Pressure
0	Y	Y	N	Y	Y	N
5	N	Y	N	N	Y	N
25	N	Y	N	Y	Y	Y
34	Y	N	N	N	N	N
50	N	Y	N	Y	Y	N
63	Y	N	Y	N	N	N

Table 8.2 – Solution field test measurement schedule

MGT	Track Modulus	TOR Elevations	Wheel/Rail Forces	Cross Section	Subgrade Settlement	Subgrade Pressure
0	Y	Y	N	Y	Y	N
5	N	Y	N	Y	Y	N
25	N	Y	N	Y	Y	Y
34	Y	N	N	N	N	N
50	N	Y	N	Y	Y	N
63	Y	Y	Y	Y	Y	N

The track modulus for both the control section and the LTM section should be measured using the TLV. This will show the track modulus differential before and after a solution is installed. If the proposed solution works as intended, the track modulus differential will be reduced from the base case measurements.

The track deflection profile needs to be measured as well. This can be done in regular intervals of traffic, not just before and after the test. This will show how the track profile changes with traffic. If a bump forms, it will be clearly indicated by the track profile. Ideally, a tolerable ramp will develop with the solution rather than a steep bump/dip.

Wheel/rail forces are also important to measure. Since the bump at the end of the railway bridge is influenced by vertical impact loads on the track structure, it is important to minimize the vertical wheel/rail forces for this problem. To determine if the solution does this, instrumented wheel sets, which use strain gages, are used to take these readings during traffic. Data is recorded a sampling rate of 1000 Hz and filtered at 250 Hz.

Elevations of the LTM cross-section are essential to ensure that the subgrade is not experiences progressive shear failure. This would be noticed by looking for movements in the cross-section elevation. As mentioned previously, this has been a problem before when the subgrade was initially installed in 1991.

The response of the subgrade will be evaluated by measuring both the settlement and the subgrade pressure (Fig. 8.6). The settlement of the clay layer in the LTM is measured using settlement rods that extend to the surface of the clay. Elevations of the

top of the rod determine the settlement at various intervals of traffic. Initial elevations will be taken prior to both the base case test and the field test. The subgrade pressure will be measured using pressure cells that are installed at the top of the subgrade. Readings will be taken under traffic conditions at 17.9 m/s and at 6.7 m/s to get the maximum pressure that occurs. The proposed solution should reduce the both the subgrade settlement and pressure from the base case.

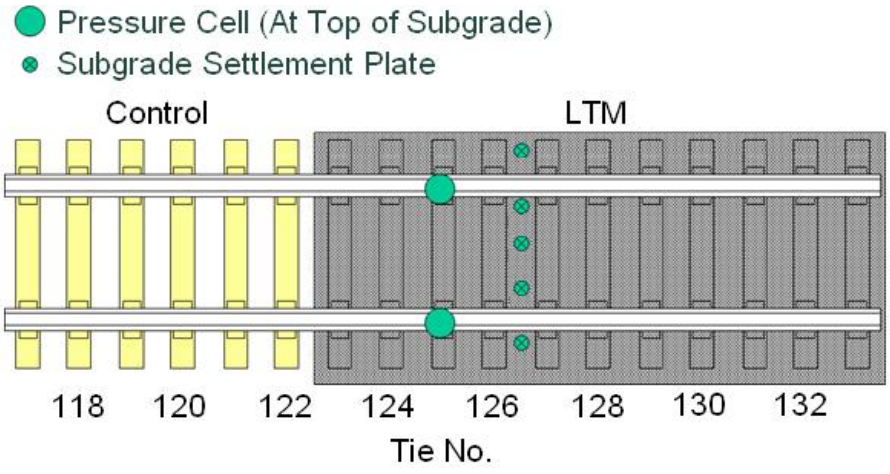

Figure 8.6 - Subgrade measurements for proposed test case

8.2.3 Base Case Test Results

The base case was established by taking measurements before the proposed solution was installed. It will serve as a comparison to evaluate the solution design. As mentioned in the previous section, the track modulus, top-of-rail (TOR) elevation, wheel/rail forces, cross section elevation, subgrade settlement and subgrade pressure were all measured at

various traffic intervals for the base case. The measurement schedule is detailed in Table 8.1.

8.2.3.1 Track Modulus

The vertical track modulus was measured with the TLV at 0 MGT, 34 MGT and 63 MGT (Fig. 8.7). The track modulus on the LTM section did not vary considerably with traffic; it is around 20 N/mm/mm. The track modulus on the control section, however, significantly increased from 33 N/mm/mm to a maximum of 90 N/mm/mm after 34 MGT. It reduced from this high value to a maximum of 65 N/mm/mm after more traffic at 63 MGT. The difference is due to the track substructure rearranging after loading. For example, the ballast compacts after loading from the just-placed state initially. As traffic continues, the ballast particles will break down making the track less stiff.

The maximum track modulus differential is 13 N/mm/mm, 65 N/mm/mm and 45 N/mm/mm for 0 MGT, 34 MGT and 63 MGT, respectively. After traffic, the track modulus differential at the test section is representative of the track modulus differential at an actual bridge/approach location. It is interesting to note that when the 203.2 mm HMA underlayment was present in the LTM section, there was very little differential between the control and LTM sections. As such, no bump/dip problems were ever reported for the HMA.

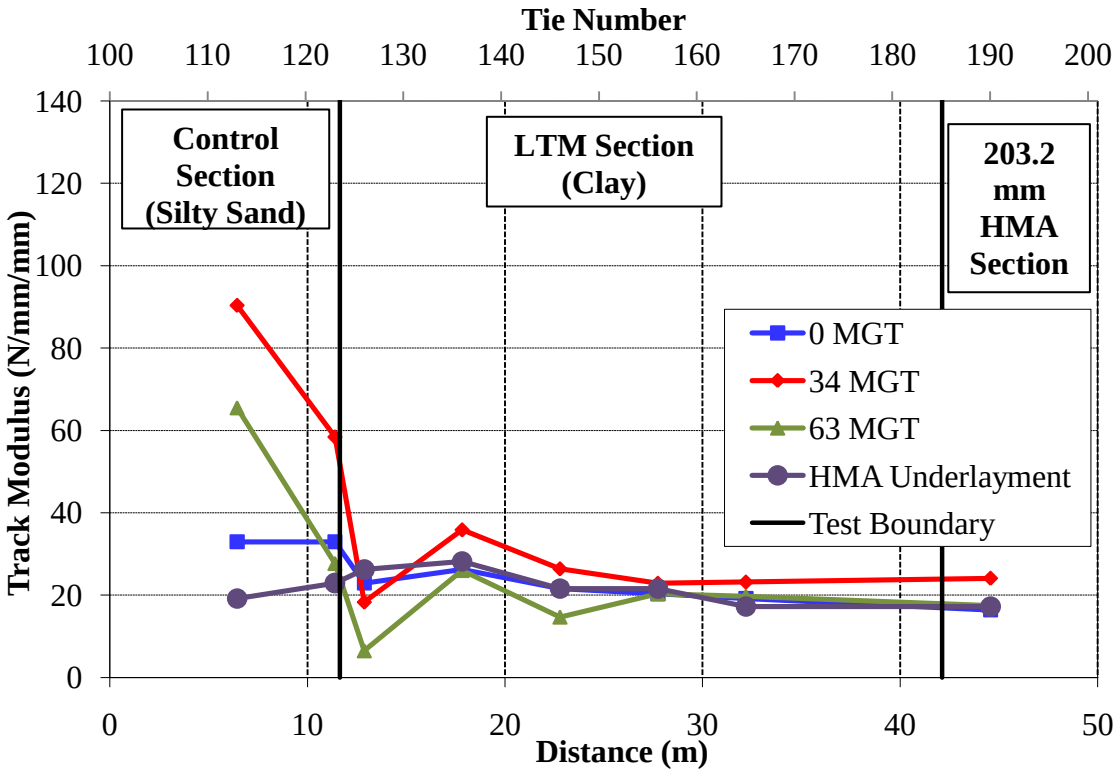

Figure 8.7 - Vertical track modulus of LTM section (base case)

8.2.3.2 TOR Elevations

The TOR elevations were taken at 0 MGT, 5 MGT, 25 MGT and 50 MGT. The difference in elevations for each traffic interval from the initial elevations at 0 MGT are shown in Fig. 8.8. The LTM section actually settled less than the center of the control section which is unexpected. The softer clay of the LTM should compress more than the stiffer silty sand of the control section. The reason is likely due to the fact that the clay is confined and can therefore not fully compress.

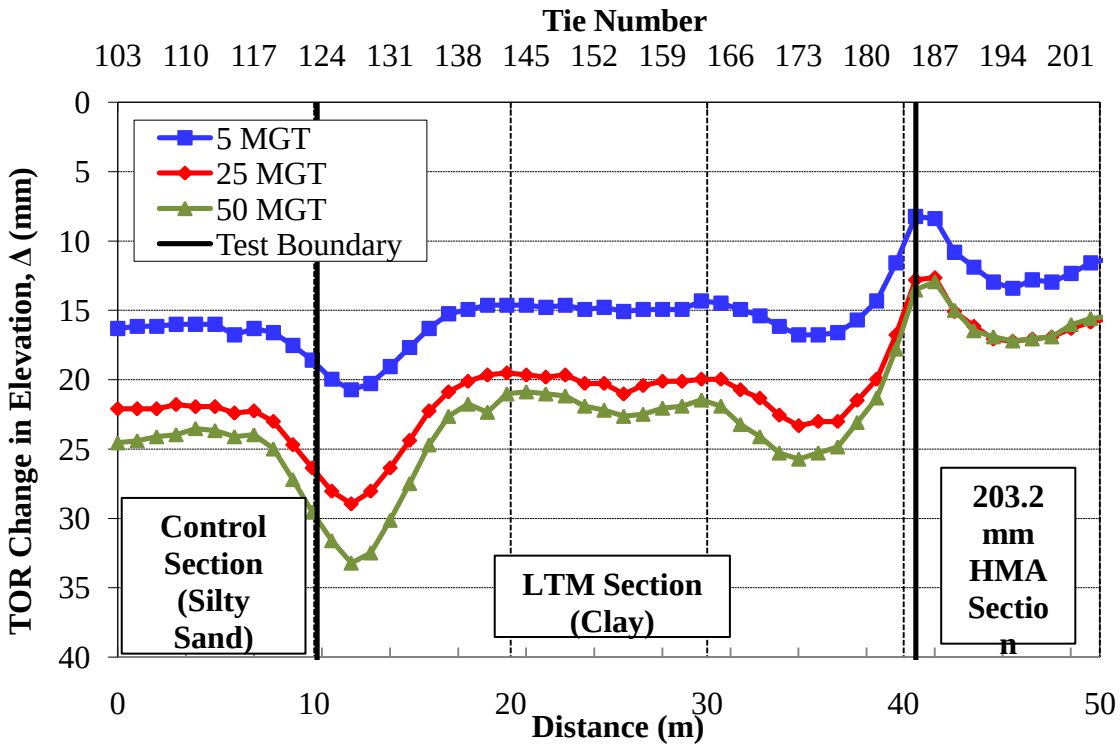

Figure 8.8 – TOR Elevations for LTM section (base case)

It is clear from the Fig. 8.8, however, that a dip has formed at the interface between the control section and the LTM section. After 50 MGT, the maximum dip height and length are approximately 11 mm and 10 m, respectively. Since only half of the dip length is involved in each dip slope, the slope of the dip after 50 MGT is about 1:450. This is a fairly shallow slope, but it will continue to progress after more traffic. The progression can be estimated without further field testing by looking at the cyclic rate of degradation.

The cyclic rate of degradation for the dip at the interface between the LTM and control sections can be observed by looking at three defining locations for the dip: at the

end of the dip on the control section, at the deepest point of the dip and at the end of the dip on the LTM section. From Fig. 8.8, these locations are at 7 m, 12 m and 17 m, respectively. At each location, the change in TOR elevation was recorded (Table 8.3). Plotting these values in log-log scale, a linear relationship between the TOR elevation change and the number of MGT is found for each of the three dip locations (Fig 8.9). This relationship is also plotted in arithmetic scale (Fig. 8.10).

Table 8.3 – Change in TOR elevation for LTM dip (base case)

	Change in TOR Elevation (mm)		
MGT	**7 m**	**12 m**	**17 m**
5	16.31	20.73	15.24
25	22.25	28.96	20.88
50	23.96	33.22	22.64

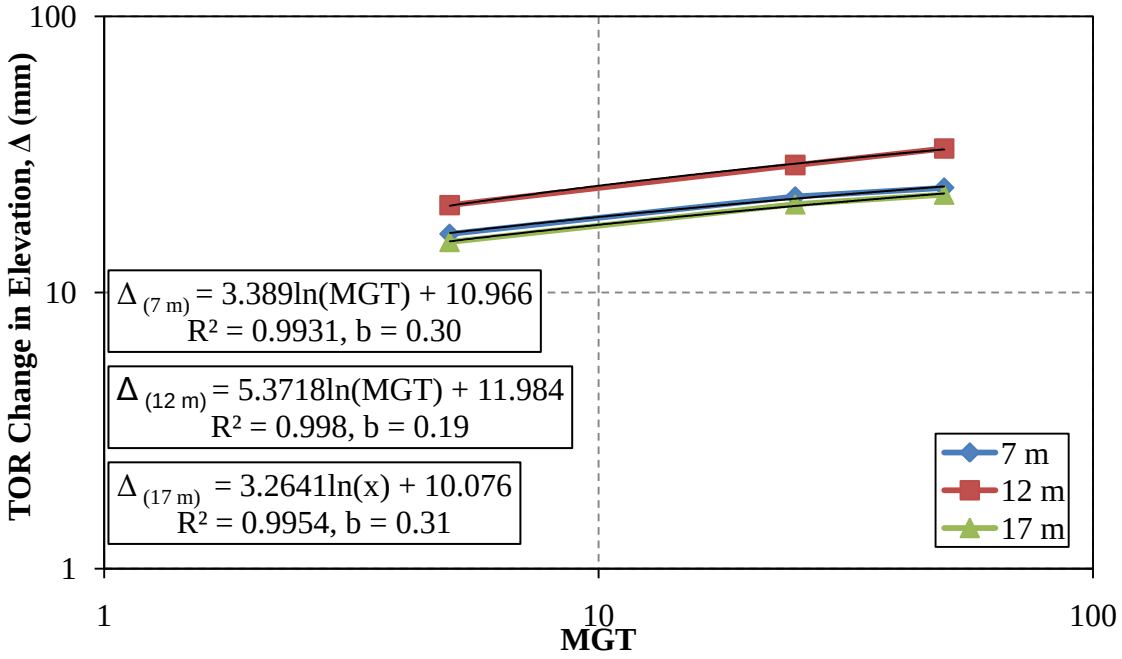

Figure 8.9 - Change in TOR elevation vs. MGT for LTM dip (log-log scale)

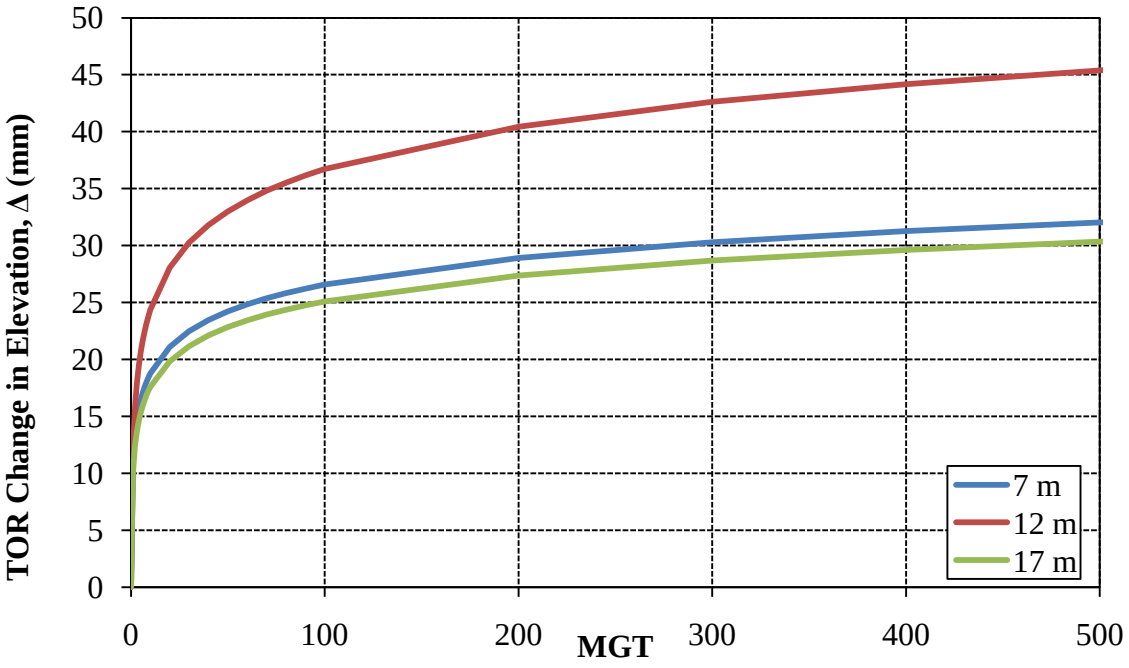

Figure 8.10 - Change in TOR elevation vs. MGT for LTM dip (arithmetic scale)

The slope of each line (b) in Fig. 8.9 is called the cyclic stress component and ranges from 0.19 to 0.31. The higher values for b correspond to the ends of the dip while the lower value for b corresponds to the deepest point of the dip. This means that the deepest point of the dip will degrade faster than the ends of the dip. Future change in TOR elevations can be estimated according to Eq. 8.1.

$$\Delta = N^b \tag{8.1}$$

After 500 MGT, the end of the dip on the control section will have deflected 32 mm from the initial elevation; the end of the dip on the LTM section will have deflected 30 mm; the deepest point of the dip will have deflected 45 mm. This means that the maximum dip height is 15 mm. Assuming the length of the dip remains unchanged (10 m total), the maximum slope of the dip is estimated to equal 1:333 after 500 MGT. It will take 6000 MGT before the slope exceeds the tolerable limit of 1:250 set by the survey. The results indicate that the biggest change in displacement occurs early in the number of cycles; as MGT increases, the change in displacement between each cycle will decrease (Fig. 8.10).

8.2.3.3 Wheel/Rail Forces

The wheel loads as the train passed over the transition section were measured using instrumented wheelsets. The vertical loads for the front and back wheels, taken at 8.9 m/s, 13.4 m/s and 17.9 m/s, are shown in Fig. 8.11, Fig. 8.12 and Fig. 8.13, respectively. The train is moving in a counterclockwise direction along the FAST HTL loop, or from the control section on to the LTM section. The carrot in the figures is the location where

the LTM begins. The low frequency waves in the measurements indicate that rocking and rolling of the train car occurred throughout the run.

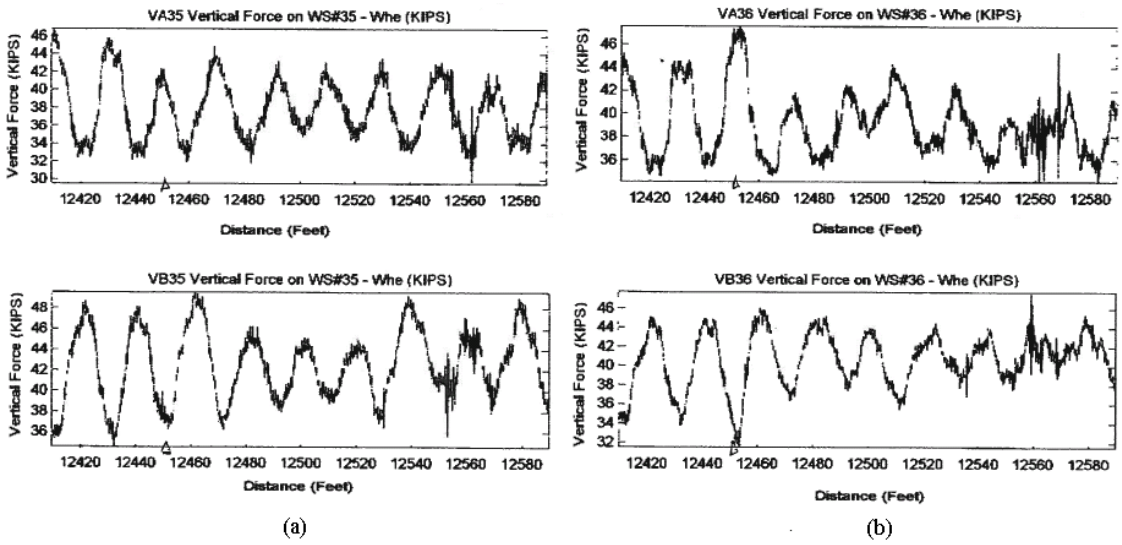

Figure 8.11 - Vertical wheel load measurements (a) front wheels (b) back wheels at a velocity of 8.9 m/s (base case) – Note: 1 kip = 4.45 kN, 1 ft = 0.3048 m

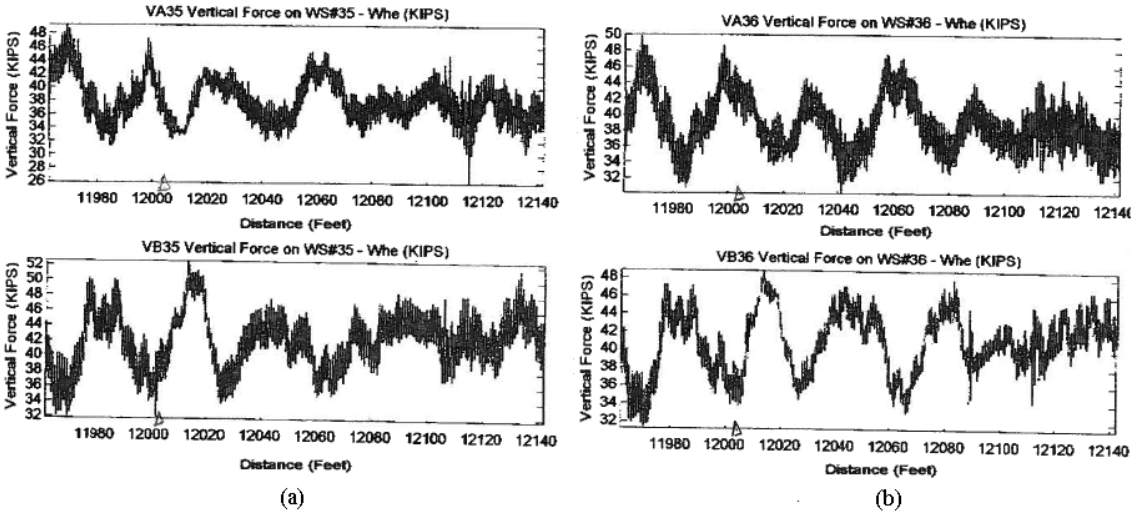

Figure 8.12 - Vertical wheel load measurements (a) front wheels (b) back wheels at a velocity of 13.4 m/s (base case) – Note: 1 kip = 4.45 kN, 1 ft = 0.3048 m

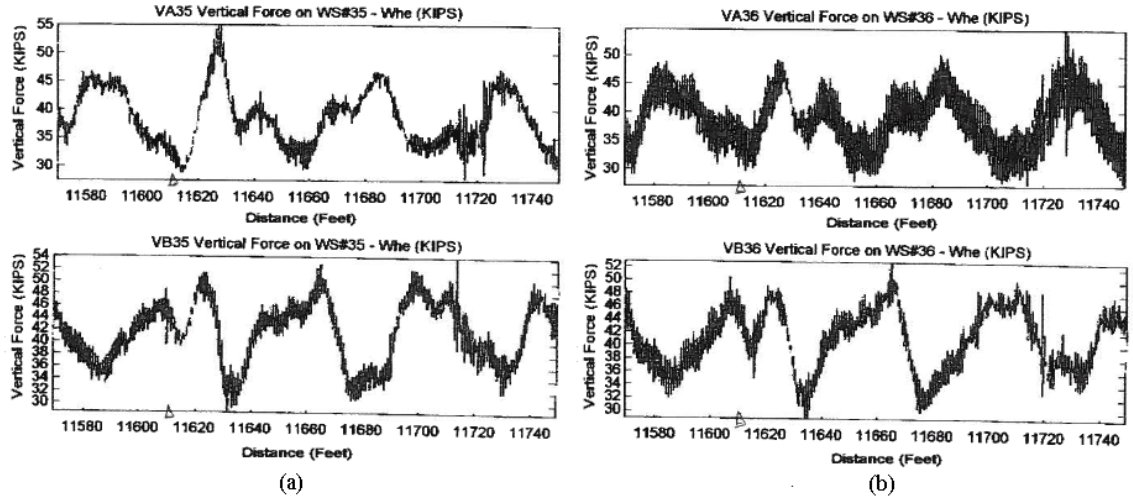

Figure 8.13 - Vertical wheel load measurements (a) front wheels (b) back wheels at a velocity of 17.9 m/s (base case) – Note: 1 kip = 4.45 kN, 1 ft = 0.3048 m

It is difficult to identify the transition section just by looking at the wheel load measurements. A slight increase in amplitude is seen at 17.9 m/s for the front axle's

inner wheel (closest to the bypass track), but not for any other wheels. The same is true for all the wheels at other velocities. Although the load does not increase significantly, a dip has still formed at the transition.

The maximum wheel force does increase with increasing velocity though. To illustrate, the DLF was calculated and compared to velocity (Fig. 8.14). The relationship is relatively linear. This agrees with the numerical simulation results found from the parametric study. Note that the maximum wheel force was not necessarily at the transition.

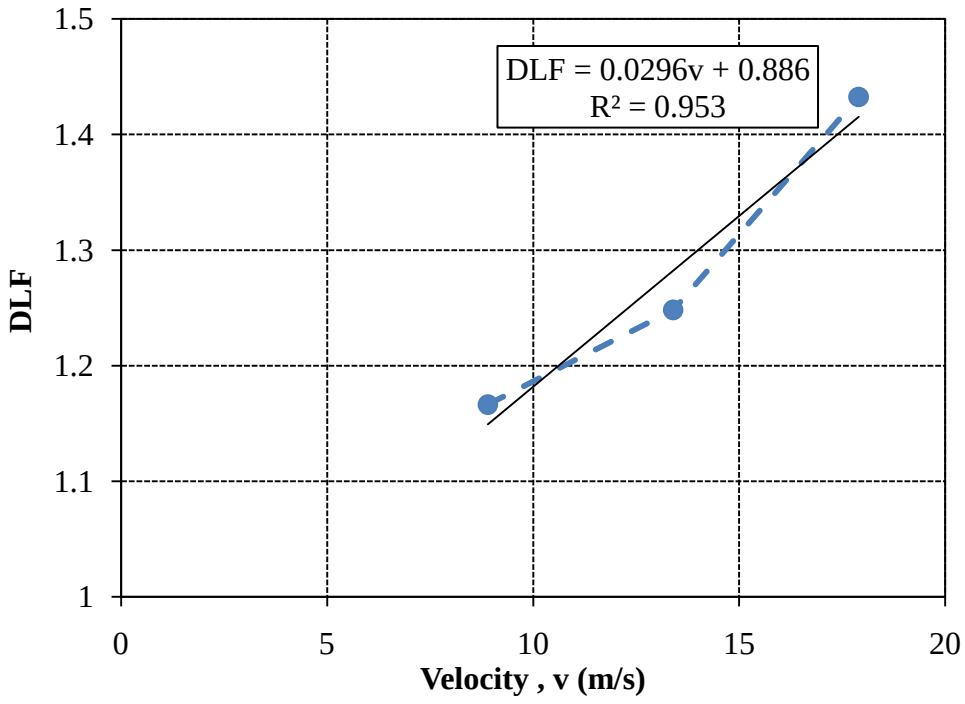

Figure 8.14 – DLF vs. velocity for field test (base case)

8.2.3.4 Cross Section Elevations

The cross section elevations of the track and the ballast shoulders at the LTM were taken at 0 MGT, 25 MGT and 50 MGT (Fig. 8.15). The elevations were taken at Tie No. 130 (Fig. 8.6), about 3.5 m away from the transition between the LTM and control sections. The zero location in Fig. 8.15 represents the centerline of the track. The inside of the track is represented by the negative location values while the outside of the track is represented by the positive location values. Taking the difference between the cross section elevations at 0 MGT and 50 MGT, the track settlement is calculated (Fig. 8.16).

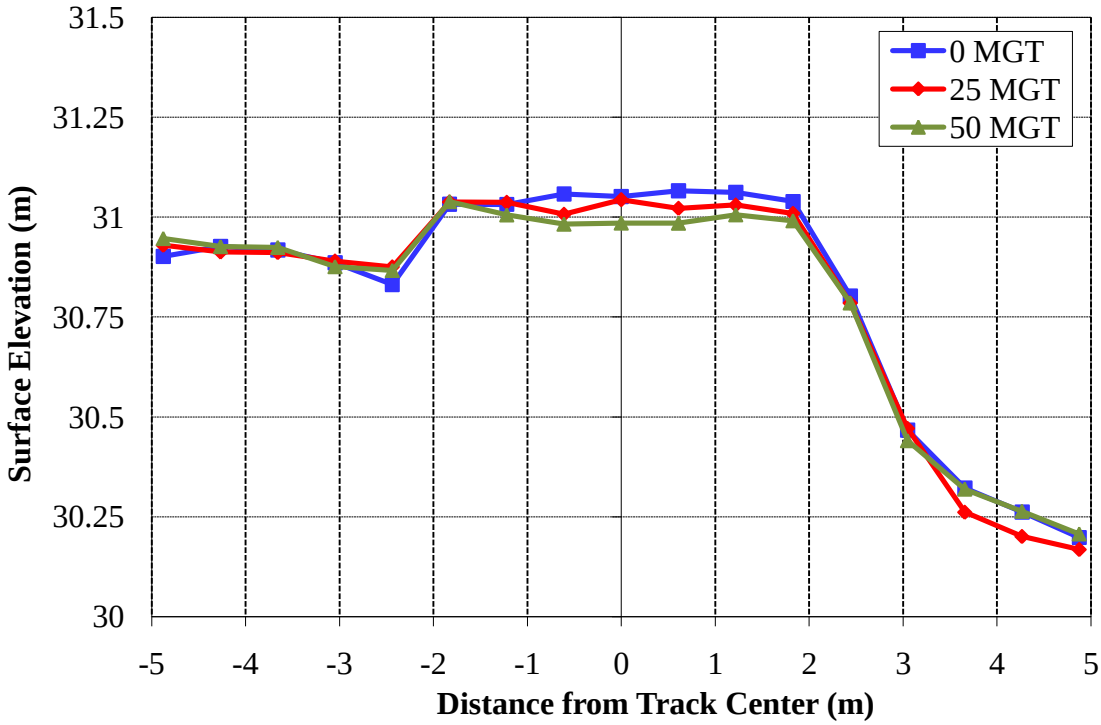

Figure 8.15 – Cross-section elevations for LTM at Tie 130

The maximum track settlement, found 0.6 m from the centerline of the track, is equal to 80 mm (3 inches). Under the rails, the track settlement is approximately 60 mm and 70 mm. Under the tie ends, the track settlement is around 15 mm and 55 mm. From Fig. 8.16, it is clear that there is some heave on portions of the ballast shoulders with the maximum calculated heave of 45 mm. This occurs outside of the clay trench boundaries.

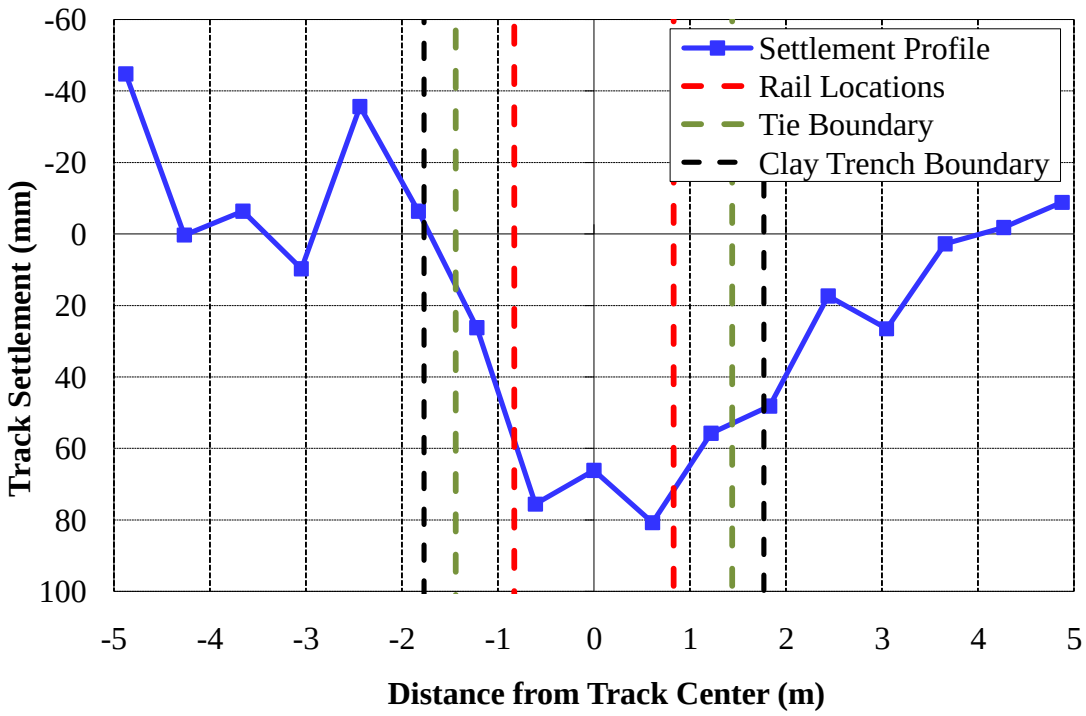

Figure 8.16 – Difference in cross-section elevations for 0 MGT and 50 MGT at Tie 130

8.2.3.5 Subgrade Settlement

The settlement of the subgrade was measured by taking survey elevations of 5 settlement rods installed in the subgrade between Tie 126 and Tie 127 (Fig. 8.6). Readings were taken at 0 MGT, 5 MGT, 25 MGT and 50 MGT (Fig. 8.17). From the figure, the term "field" represents a location outside of the rails near the ends of the ties; the term "gage" represents a location inside of the rails; the term "inside" represents the location near the bypass track (Fig. 8.2); the term "outside" represents the location away from the bypass track.

There has not been uniform settlement across the subgrade. The maximum subgrade settlement of approximately 11.5 mm occurs on the outside gage. The difference in subgrade settlement could be due to track modulus changes cross the length of the tie. The inside location is close to a bypass track so it is stiffer than the outside location which only has a ballast shoulder (Fig. 8.15).

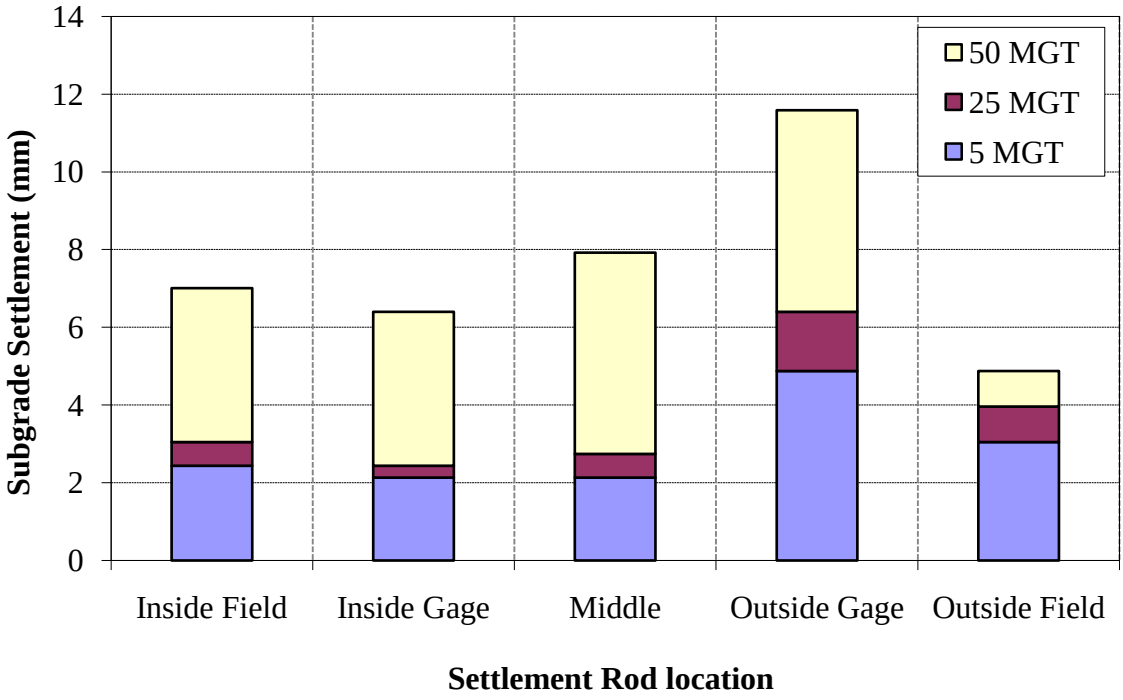

Figure 8.17 – Subgrade settlement for LTM taken between Ties 126 and 127

8.2.3.6 Subgrade Pressures

The subgrade pressure was measured using pressure cells located at the surface of the subgrade under Tie 125 (Fig. 8.6). Readings were taken only once, at 25 MGT during traffic. Pressures were recorded under traffic conditions at 17.9 m/s and at 6.7 m/s. The pressure varied from 28 kPa to 83 kPa throughout the test as different locations of the train went over the cell location (Fig. 8.18). These pressures are within the subgrade pressure limit of 140 kPa (AREMA 2008). The subgrade pressures that have the highest frequencies of occurrence are 62 kPa and 69 kPa.

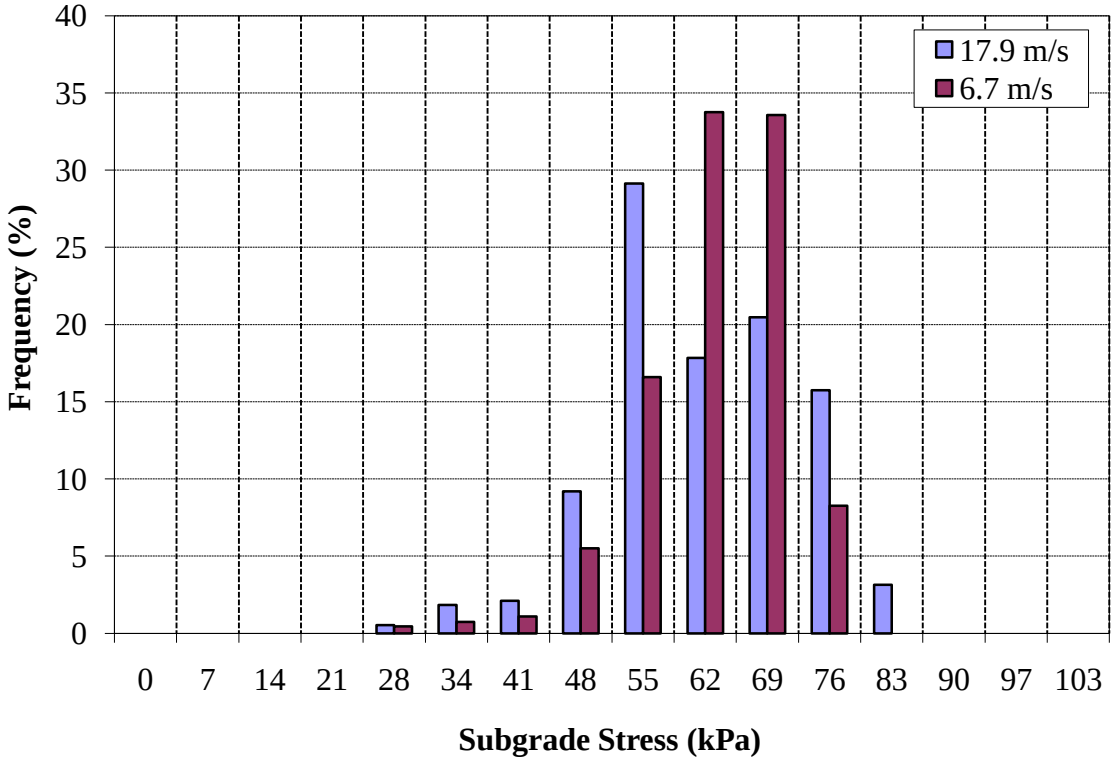

Figure 8.18 – Subgrade pressure in LTM under Tie 125

8.3 SOLUTION DESIGN

The design of the proposed solution was adapted from the original concept of installing varying length steel bars between the ties into the subgrade as previously discussed at the beginning of this section. The design parameters include the total number of steel bars needed, the depth of each steel bar, and the rate of depth decrease moving away from the abutment. These are site-specific parameters and depend on the soil conditions at the site.

The conditions at the LTM section, along with the base case measurements, provide some guidelines as to the design of the solution. For example, since the clay

layer is only 1.5 m thick, the steel bars do not have to be very much longer. Also, based on the length of influence found from the base case measurements, the total length of the solution along the track will equal 5 m. The steel bars will need to be between each tie as well since the clay is weak. To optimize the design given these guidelines, 4-D finite element simulations were conducted using LS-DYNA.

8.3.1 Numerical Simulations

To determine the number and exact depth of the steel bars, a 4-D finite element model of the LTM section was created with HyperMesh (Fig. 8.19). Simulations were then performed using LS-DYNA to optimize the design of the solution. The direction of travel for the truck model is from the LTM section to the control section. This direction was chosen because, from the parametric study results (Section 7), the track response is more severe for a train moving from a soft location to a stiff location. The velocity of the truck was set as 17.9 m/s since that is the speed at which tests are run at FAST.

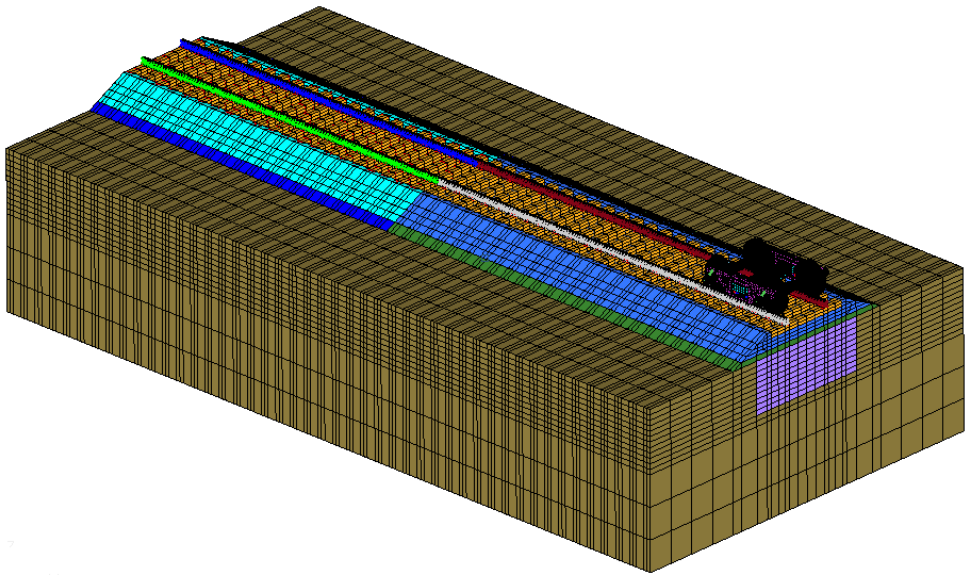

Figure 8.19 – Finite element model of the LTM section

8.3.1.1 Model Description

The same truck and track model previously used for the parametric study was used for the LTM simulations. The steel bars were modeled with standard steel properties: a density of 7850 kg/m^3 (0.49 kcf), a modulus of elasticity of 200,000 MPa (4.18x10^6 ksf), and a Poisson's ratio of 0.28. The track substructure was modeled based on the actual site conditions.

The material properties for the ballast, subballast, clay subgrade and the natural subgrade are given in Table 8.4. The modulus of elasticity (E) for the clay and silty sand were chosen based on the range of modulus values provided in Section 8.2.1.2. The shear modulus (G) and shear wave velocity were calculated according to Eq. 5.3 and Eq. 5.4, respectively.

Table 8.4 – Material properties for LTM numerical model

Material	ρ (kg/m^3)	E (MPa)	G (MPa)	v_s (m/s)	μ
Ballast	1630	150	58	188	0.3
Subballast	2173	80	30	117	0.35
Clay	2000	14	5	49	0.45
Natural Silty Sand	1874	83	31	128	0.35

Rayleigh damping was assumed for both the control section and the LTM section in the model and calculated according to Eq. 5.5. The α and β damping constants for the control section are 2.86 and 0.00049, respectively. The α and β damping constants for the LTM section are 2.42 and 0.00057, respectively.

8.3.1.2 Base Case Results

To determine the track response for the LTM section with no solution, a base case simulation was performed using LS-DYNA. First, to validate the model and ensure that the it represents the actual track conditions, the track modulus at various locations was found. This was accomplished by applying a nodal vertical force at the top of the track in the model and recording the vertical track displacement. The track modulus was then calculated according to BOEF theory (Eq. 2.4). The resulting track modulus profile for the numerical model is shown in Fig. 8.20. The profile closely matches the actual profile after 34 MGT of traffic which represents the maximum track modulus differential seen at the site.

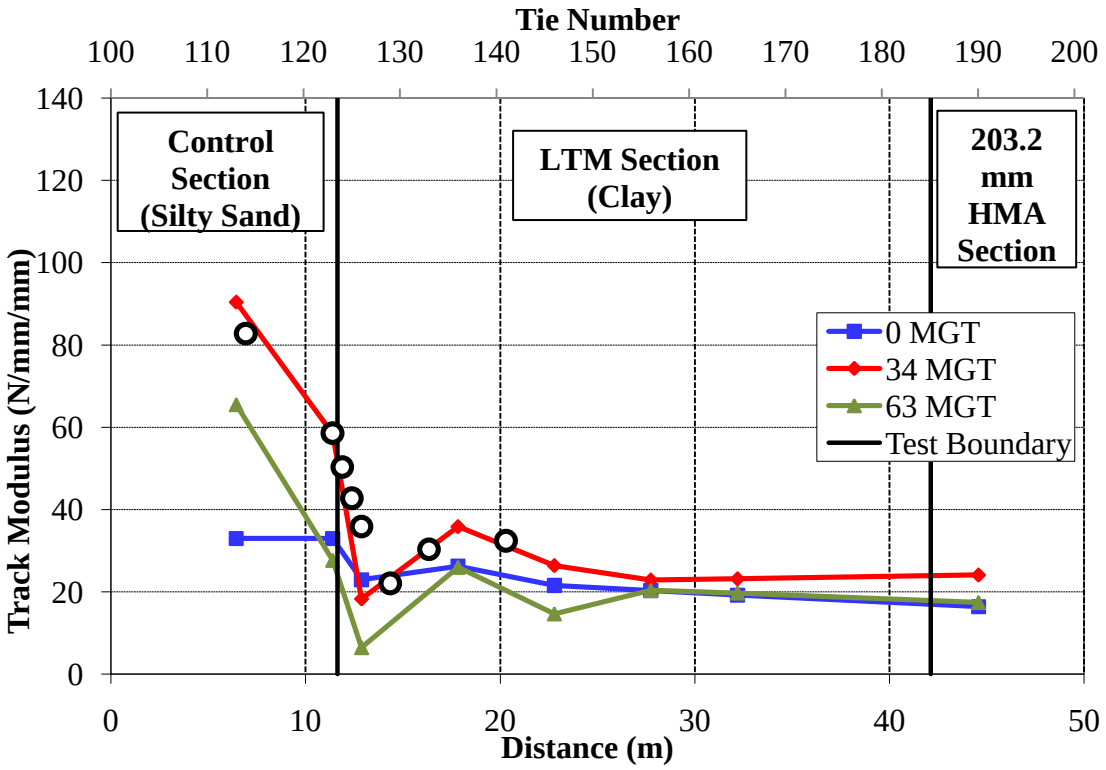

Figure 8.20 – Simulation track modulus compared to measured track modulus

Next, the simulations of a truck moving over the LTM section with no solution were conducted. The resulting wheel/rail forces indicate that no increased impact forces occur at the transition between the LTM section and the control section (Fig. 8.21). This agrees with the findings from the wheel loads measured in the base case field test. Since the measurements include significant rocking and rolling, a direct comparison cannot be made with the simulations though. The DLF for the base case is 1.01. It would initially appear that the LTM section would not cause problems, but the track deflection, ballast and subgrade pressures should be evaluated before coming to a conclusion.

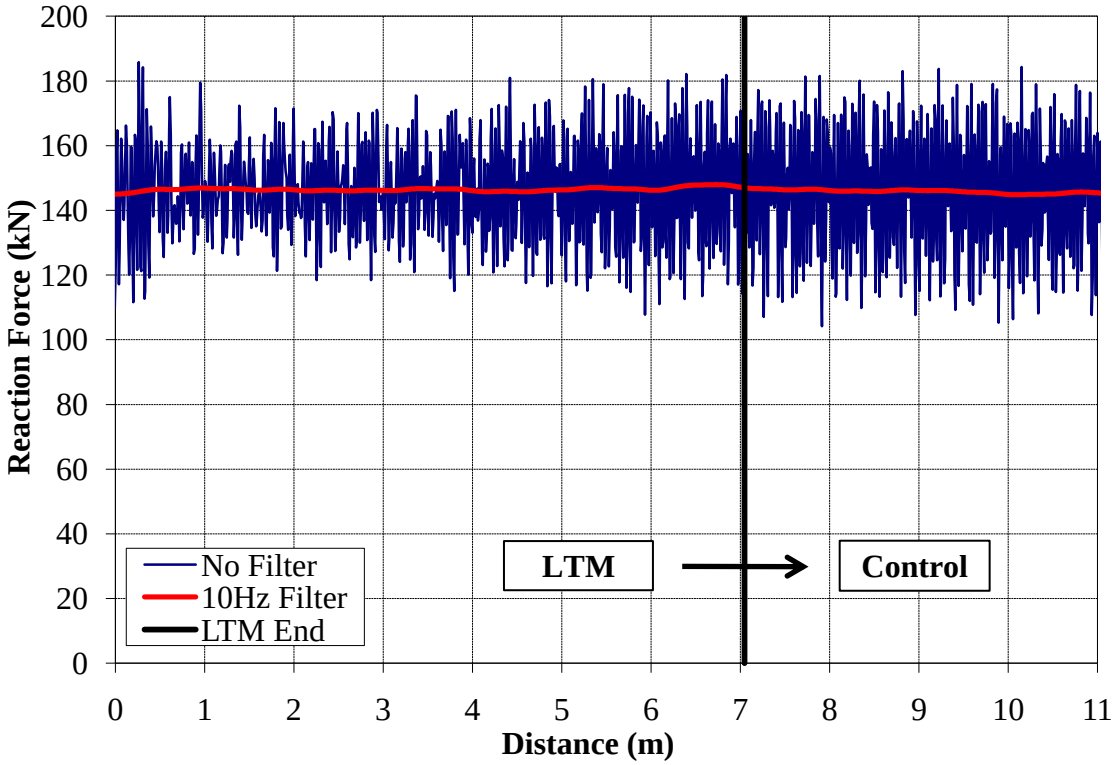

Figure 8.21 – Wheel/Rail forces at LTM section from numerical model (base case)

The track deflection under both the front and back axles is shown in Fig. 8.22. Even though no impact forces are seen, the track deflection is still deviated at the transition as seen with the bridge/approach simulations in Section 6. The main difference between this transition and a bridge/approach transition, however, is the fact that the silty sand of the control section can deform more than a rigid bridge abutment (Fig. 6.3c). This causes the deflected track profile to not be as severe as for a bridge/approach location. Also note that the track deflection is measured after one cycle in the simulation. The deflection and the slope of the deflected profile at the transition will increase with

increased number of cycles (or MGT). This will eventually lead to track degradation and a bump/dip.

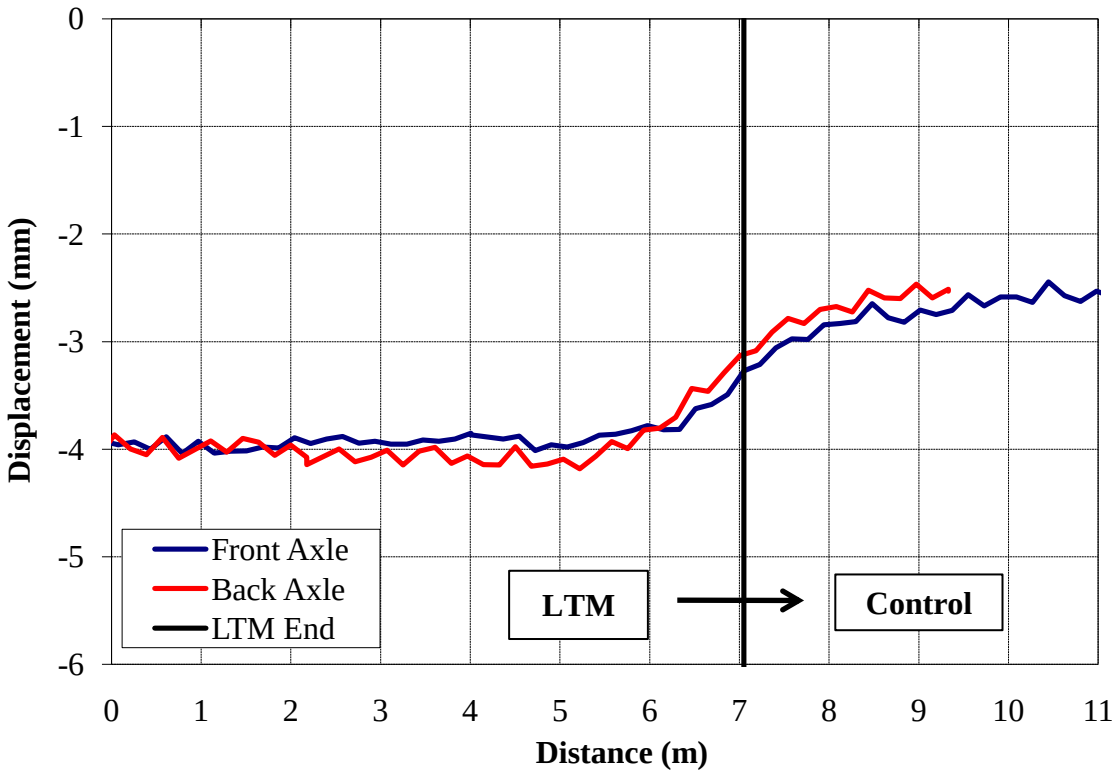

Figure 8.22 – Track deflection at LTM section from numerical model (base case)

The ballast and subgrade pressures for the base case LTM test are shown in Fig. 8.23 and Fig. 8.24, respectively. Remember that negative pressure values in the figures represent compression. The average ballast pressure on the LTM is around 240 kPa (compression). The ballast pressures slightly increase around the transition between the LTM and controls sections. The DBF for the base case is 1.50.

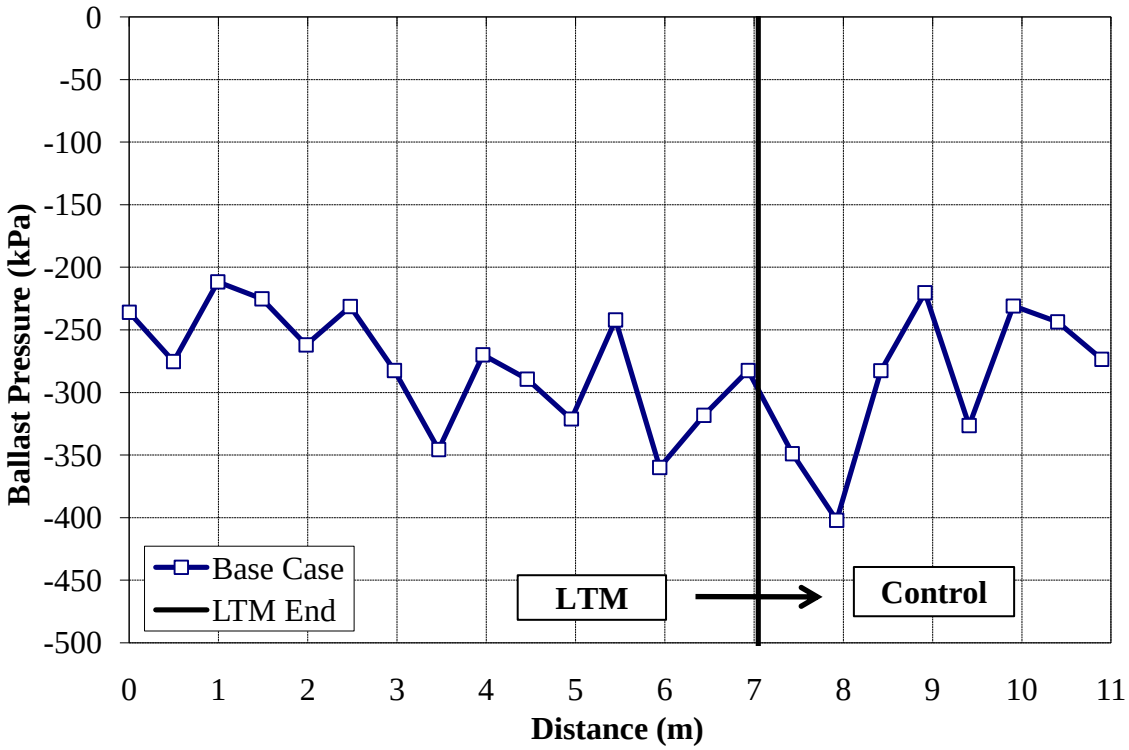

Figure 8.23 - Ballast pressure at LTM section from numerical model (base case)

The average subgrade pressure on the LTM is around 80 kPa (compression). The average subgrade pressure on the control section is higher than the average subgrade pressure on the LTM section. This is because the clay soil is much softer than the silty sand. The silty sand provides more confining pressure than the clay, leading to higher vertical pressures. The DSF on the LTM in this case is 1.21.

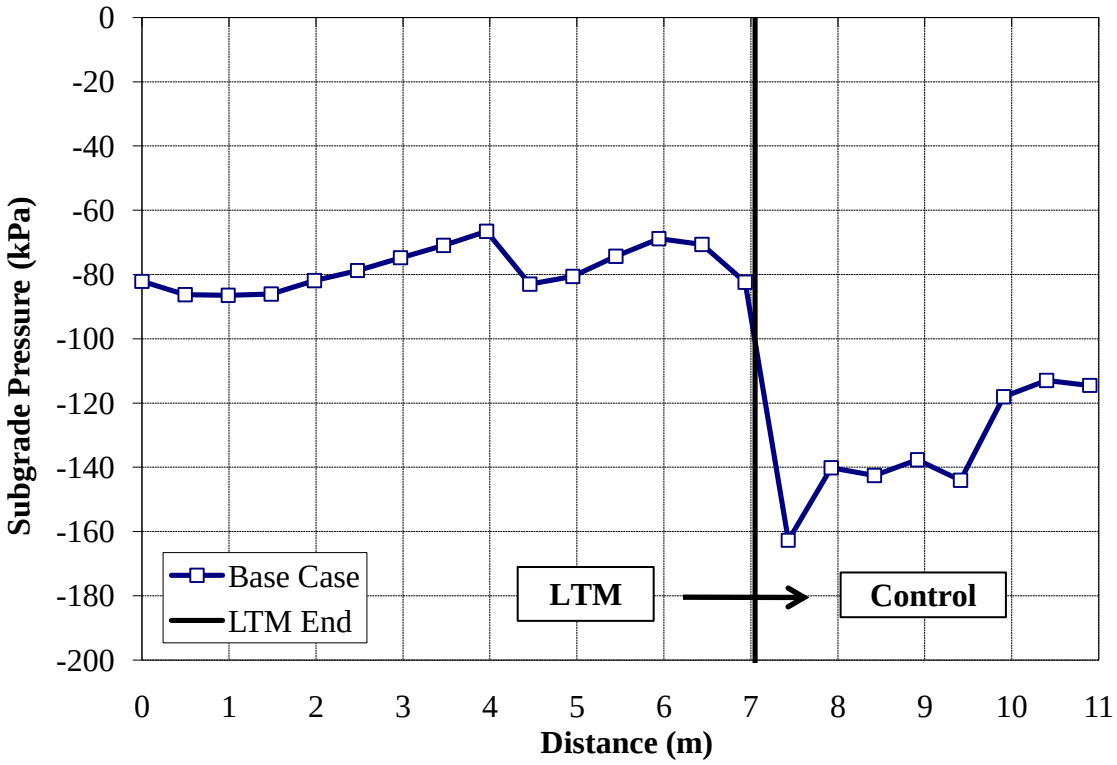

Figure 8.24 – Subgrade pressure at LTM section from numerical model (base case)

It is also important to note that at the location for Tie 125 (around 6 m in Fig. 8.24), the subgrade pressure is 69 kPa. The subgrade pressures measured at the same location with the pressure cells during the base case field test were around this value. The pressure with the maximum frequency (33.8 %) was 62 kPa. Very close behind, at a frequency of 33.6 %, was 69 kPa. The simulation results match the actual measured subgrade pressure which serves to validate the results of the model.

8.3.1.3 Design Alternatives

In addition to a base case simulation, where no solution is modeled, six design alternatives were simulated. All are fairly similar to each other with bar length, rate of bar length decrease, and total number of bars varying between each case. For all alternatives, however the total length of the solution along the track is equal to about 5 m. This was determined based on the length of influence found from the base case simulation.

The first (Design Alternative 1) looked at having all the steel bars uniform in length at 1.83 m (Fig. 8.25). The next alternative (Design Alternative 2) looked at linearly varying the length steel bars by decreasing the bar length between each tie by 152.4 mm with the longest bar 1.83 m (Fig. 9.26). Another alternative (Design Alternative 3) looked at having a nonlinear rate of bar length decrease where the longest bars of 1.83 m, 1.68 m and 1.52 m are repeated in the clay subgrade (Fig. 9.27). Similarly, an additional alternative (Design Alternative 4) also looked at having a nonlinear rate of bar length decrease and repeated bar lengths at the beginning of the solution, except the longest bar in this alternative is 2.1 m, not 1.83 m (Fig. 9.28). Another alternative (Design Alternative 5) is identical to Design Alternative 2 except there are 8 bars between each tie instead of 4 (Fig. 9.29). Finally, the last alternative (Design Alternative 6) is identical to Design Alternative 3 except that there are 8 bars between each tie instead of 4 (Fig. 9.30). For each alternative, the wheel/rail forces, track deflection, ballast and subgrade pressures were evaluated to optimize the design.

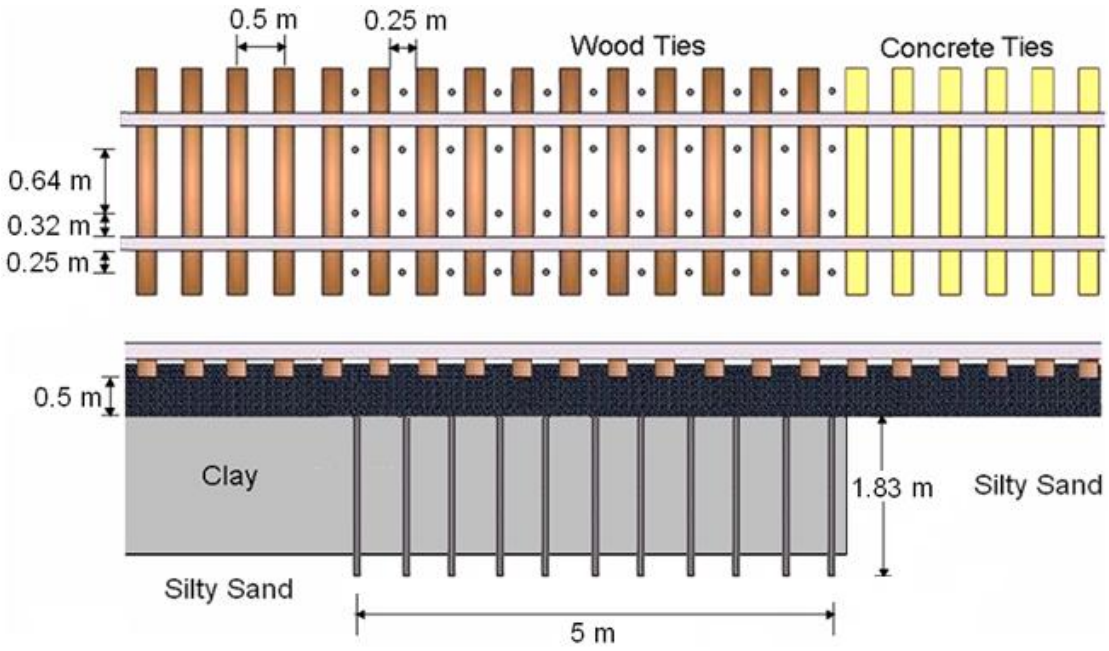

Figure 8.25 – Design Alternative 1: Uniform bar lengths with 1.83 m longest bar and 44 total bars

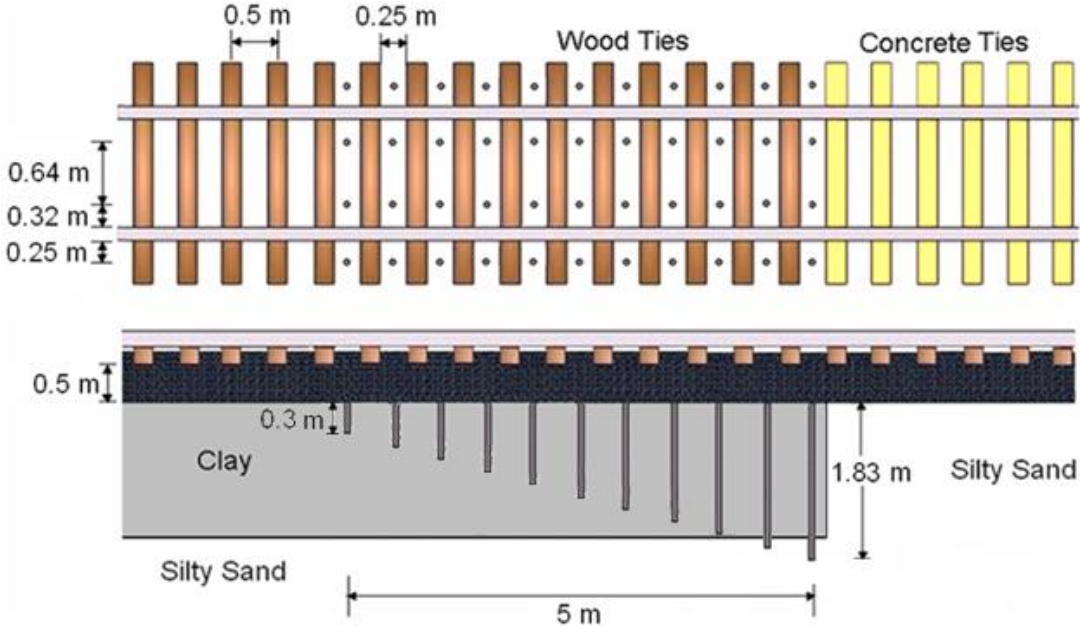

Figure 8.26 – Design Alternative 2: Equal bar length decrease with 1.83 m longest bar and 44 bars total

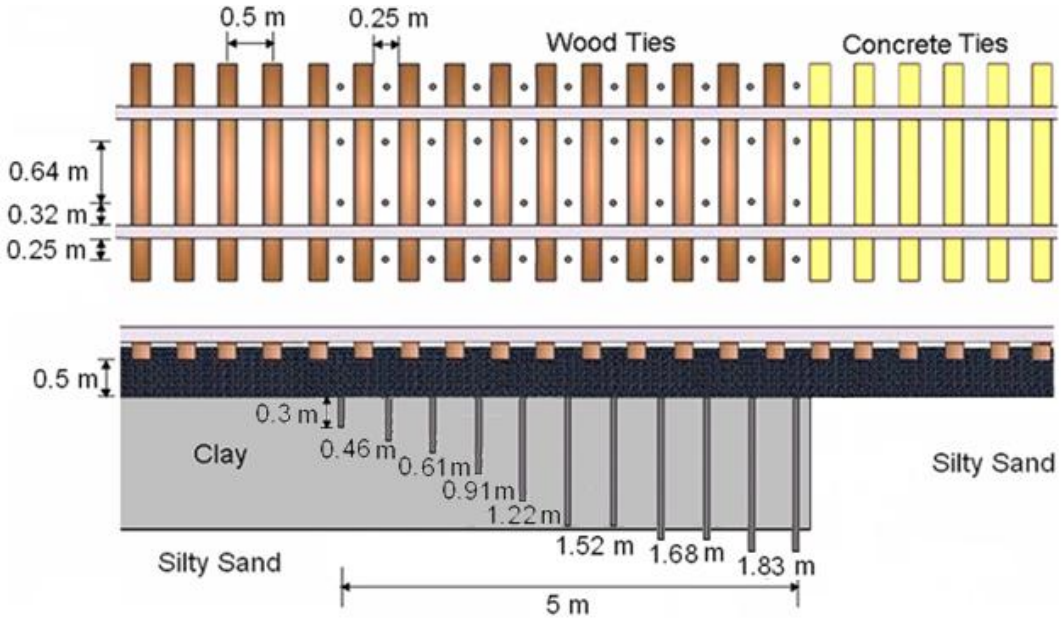

Figure 8.27 – Design Alternative 3: Unequal bar length decrease with 1.83 m longest bar and 44 total bars

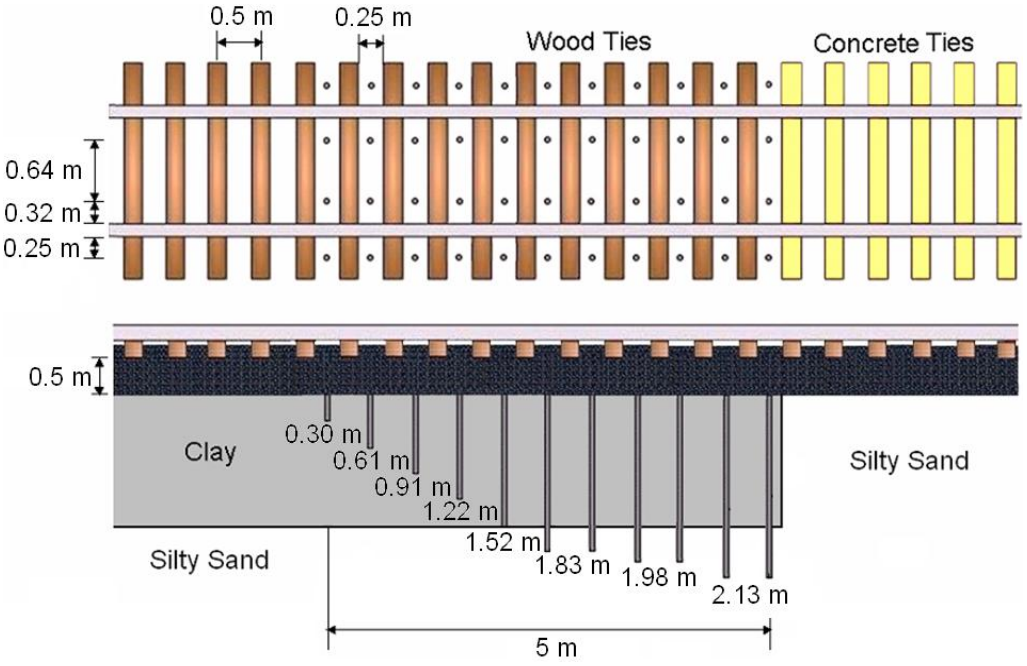

Figure 8.28 – Design Alternative 4: Unequal bar length decrease with 2.13 m longest bar and 44 total bars

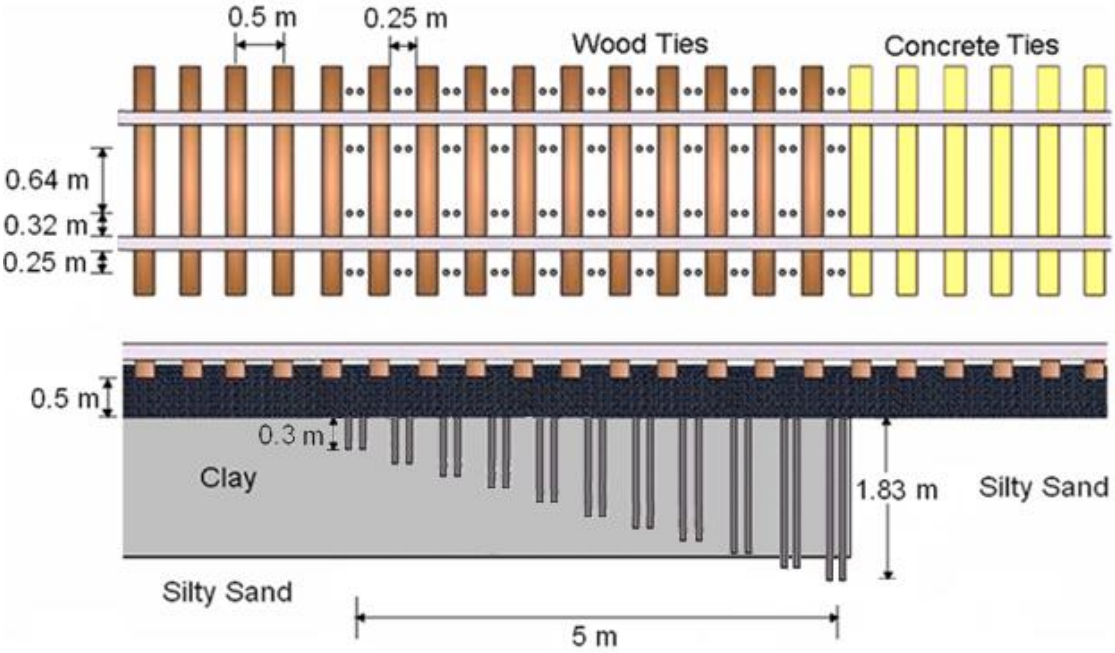

Figure 8.29 – Design Alternative 5: Equal bar length decrease with 1.83 m longest bar and 88 total bars

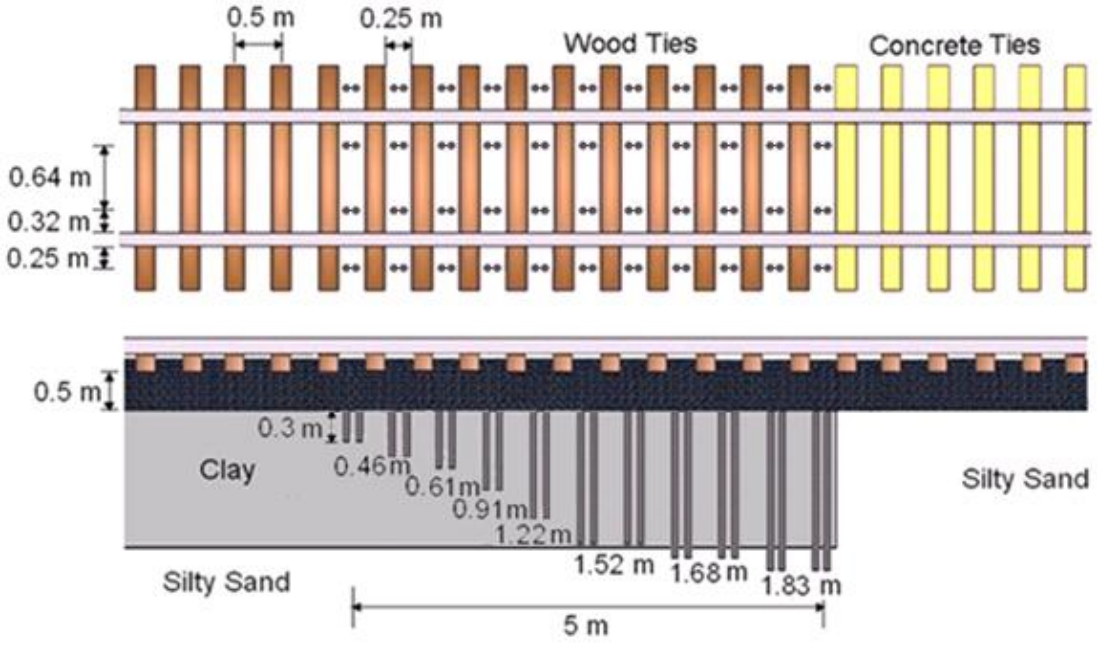

Figure 8.30 – Design Alternative 6: Unequal bar length decrease with 1.83 m longest bar and 88 total bars

8.3.1.4 Optimization Results

Each design alternative was simulated using LS-DYNA to evaluate the track response and determine an adequate prototype design. All of the design alternatives responded similarly to the base case in terms of wheel/rail forces (Fig. 8.31). The impact forces on the track are negligible and the DLF for each case (including the base case) is 1.01. The low DLF does not mean that there is no track response. The track deflection, ballast and subgrade pressures may be affected even if the impact forces are not.

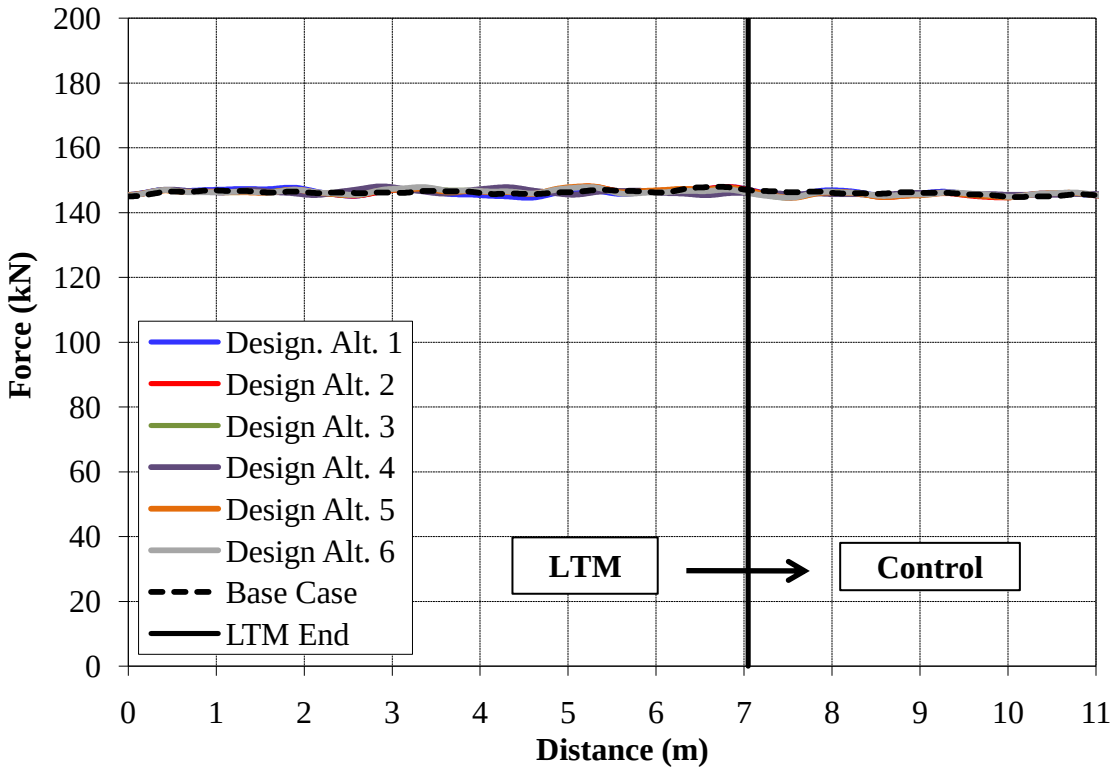

Figure 8.31 – 10 Hz wheel/rail force comparison for solution design alternatives at LTM section

In terms of track deflection, each alternative performs better than the base case (Fig. 8.32). The track deflection for Design Alternative 1 is similar to the base case except that the steep bump in the profile has been moved back further from the transition in the LTM section. This is expected because the solution consists of uniform bar lengths. An abrupt track modulus differential between the section with the solution and the rest of the LTM is then formed. The design alternatives with varying length bars cause a shallower slope to form in the track deflection profile. The best profile transition occurs with Design Alternative 4. The DDF is not defined for these cases as no increased track deflection from the average is seen.

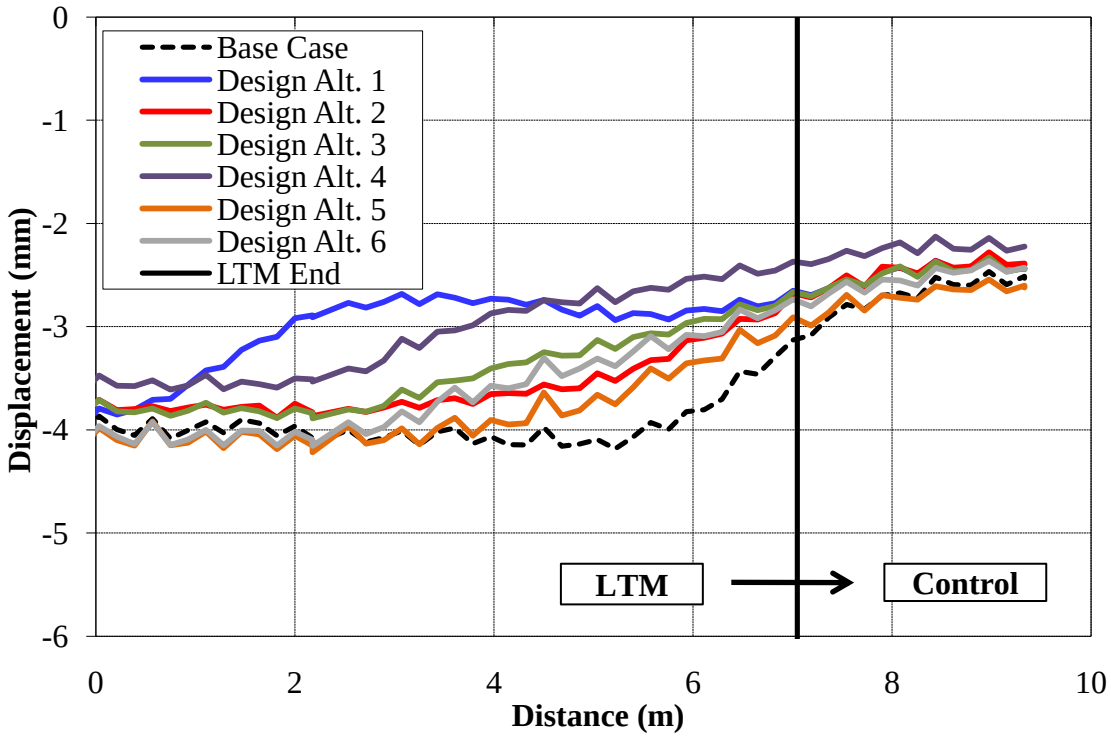

Figure 8.32 – Track deflection under the back axle comparison for solution design alternatives at LTM section

The ballast pressures for each design alternative are shown in Fig. 8.33. Based on the figure, there is not a significant difference between the design alternatives. The average ballast pressure on the LTM (with a solution) is around 325 kPa (compression). This is slightly higher than the average ballast pressure for the base case.

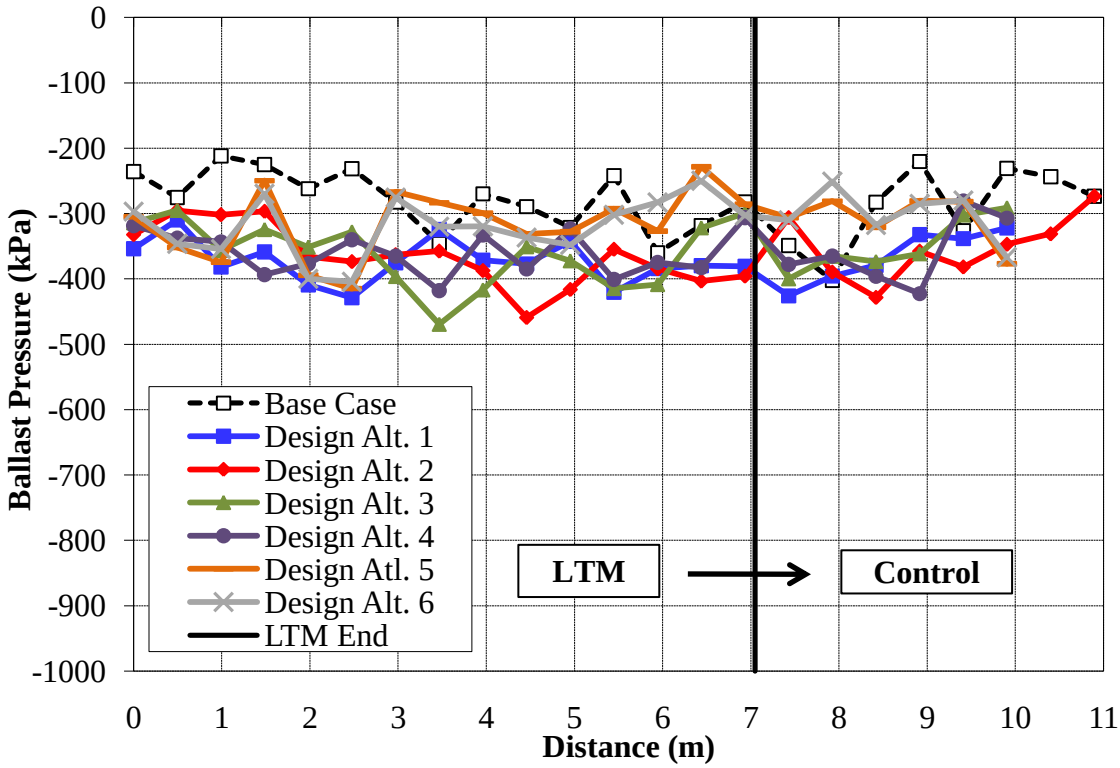

Figure 8.33 – Ballast pressure comparison for solution design alternatives at LTM section

The subgrade pressures are shown in Fig. 8.34. The average subgrade pressure on the LTM is about 80 kPa (compression). Across the length of the solution, the subgrade pressure actually reduces for each design alternative. This means that the steel bars are

taking on some of the subgrade stress. Again, the subgrade pressure on the LTM section is lower than the subgrade pressure on the control section. This is because the silty sand provides more confining pressure than the clay which leads to higher vertical pressures.

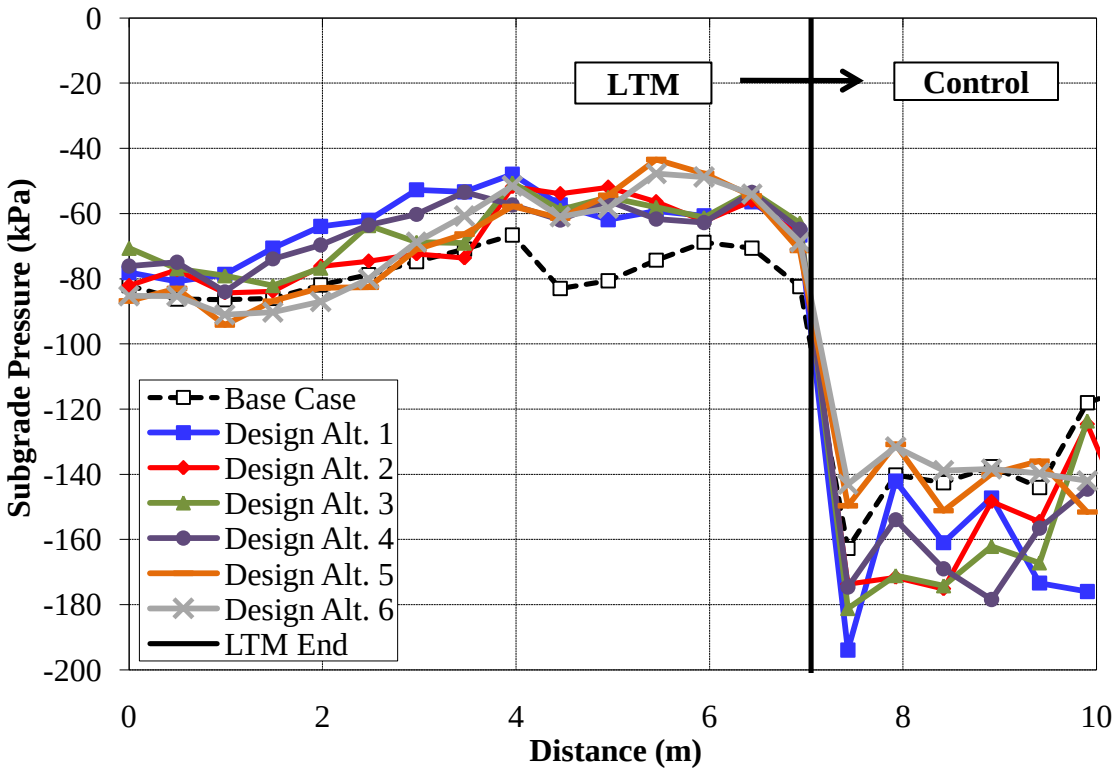

Figure 8.34 - Subgrade pressure comparison for solution design alternatives at LTM section

If directly comparing Fig. 8.34 to a bridge/approach location, the subgrade pressure on the control would be removed from the figure. Doing this shows a limitation of using the LTM section as a mock bridge/approach: the subgrade pressures are

increased at the transition rather than decreased. This works to minimize the bump that can form as opposed to at a bridge/approach location.

8.3.1.5 Summary

A summary of the results are found in Table 8.5. In all cases, the DLF, DBF did not exceed the threshold limits (AREMA 2008). As previously mentioned, the DLF is constant with or without a solution (Fig. 8.35). The design alternatives do reduce both the ballast and subgrade pressures from the base case situation though. The best case alternatives in terms of DBF are Design Alternatives 5 and 6 (Fig. 8.36). These alternatives consist of installing 8 bars between each tie instead of 4. They are the worst alternatives, however, for subgrade pressures (Fig. 8.37). The best case alternative in terms of DSF is Design Alternative 1, although Design Alternatives 1-4 are all very similar.

Table 8.5 – Design alternative summary

Design Alternative	DLF	DBF	DSF
1	1.01	1.32	1.01
2	1.01	1.41	1.05
3	1.01	1.44	1.03
4	1.01	1.29	1.05
5	1.01	1.28	1.18
6	1.01	1.24	1.14
Base Case	1.01	1.5	1.21

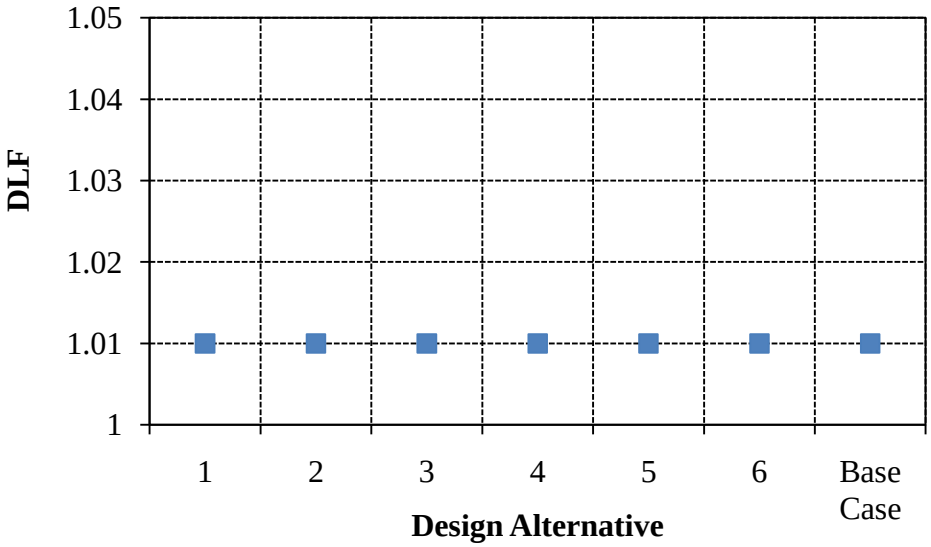

Figure 8.35 – DLF for track transition design alternatives

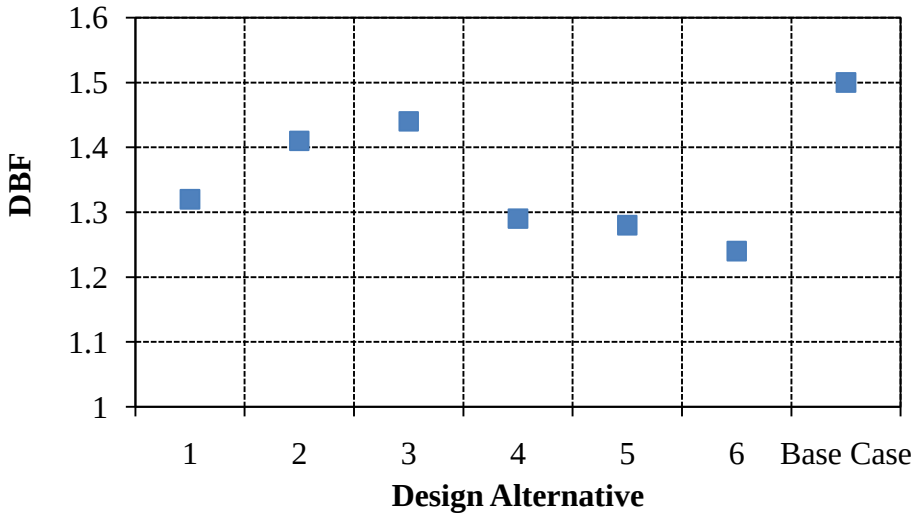

Figure 8.36 – DBF for track transition design alternatives

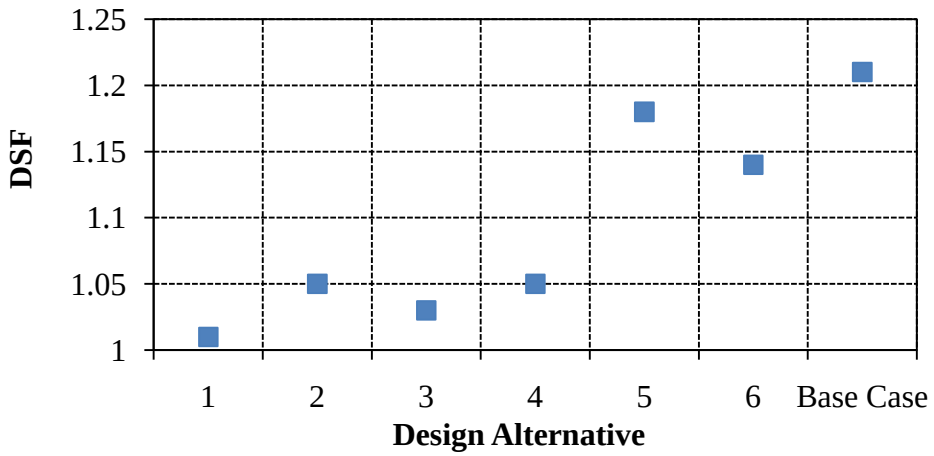

Figure 8.37 – DSF for track transition design alternatives

8.3.2 Recommended Solution

Based on the results from the numerical simulations (Table 8.5), the best design is Design Alternative 4 (Fig. 8.28, shown again below). Design Alternative 4 was chosen because it performed better all around when considering track deflection (Fig. 8.38), ballast pressures (Fig. 8.39) and subgrade pressures (Fig. 8.40). It also increased the track modulus on the LTM section and reduced the track modulus differential at the boundary (Fig. 8.41).

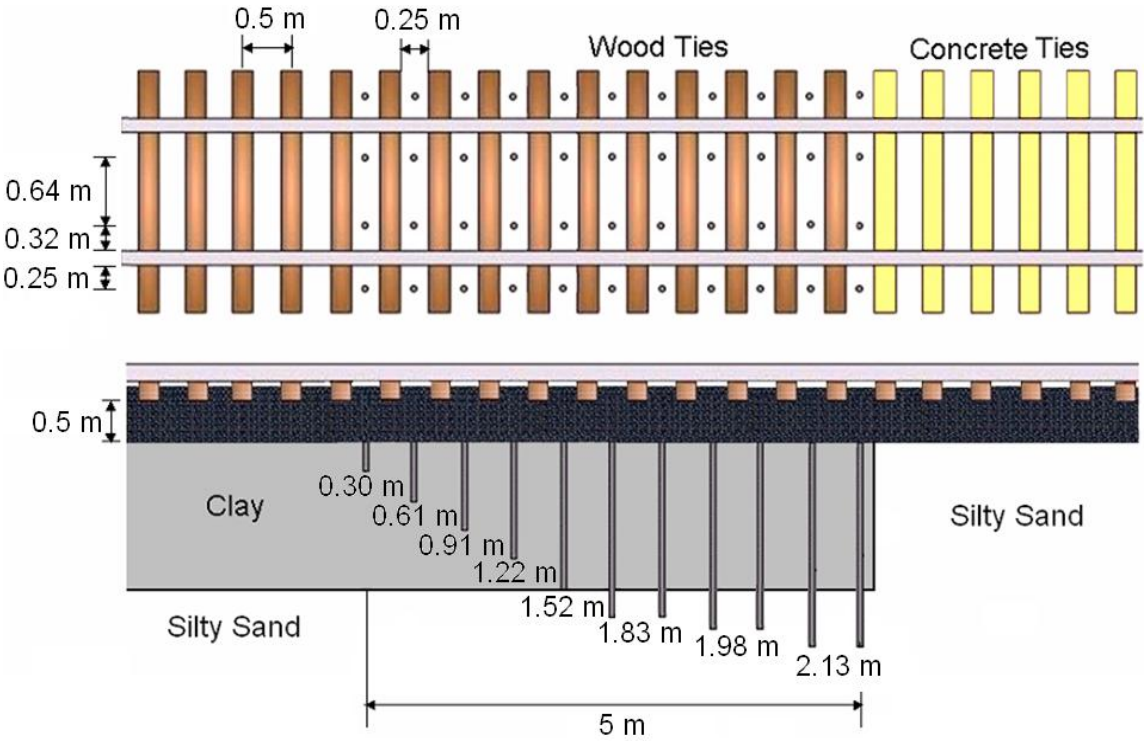

Figure 8.28 – Design Alternative 4: Unequal bar length decrease with 2.13 m longest bar and 44 total bars

This recommended solution involves placing four rows of varying length 1.375" diameter steel bars into the soft subgrade at the Low Track Modulus (LTM) section at FAST. The total length of the solution, measured as the center to center distance between the first and last bars, is 16.25 ft. The longest bars are 7 ft in length while the shortest bars are 1 ft in length. Four rows of each length will be installed: 2 inside the tracks and 2 outside of the tracks. The 2 bars inside the tracks are located 12.6" from the base of the rail and the center to center spacing of the 2 bars is 25.3". The 2 bars outside of the tracks are 9.9" from the base of the rail.

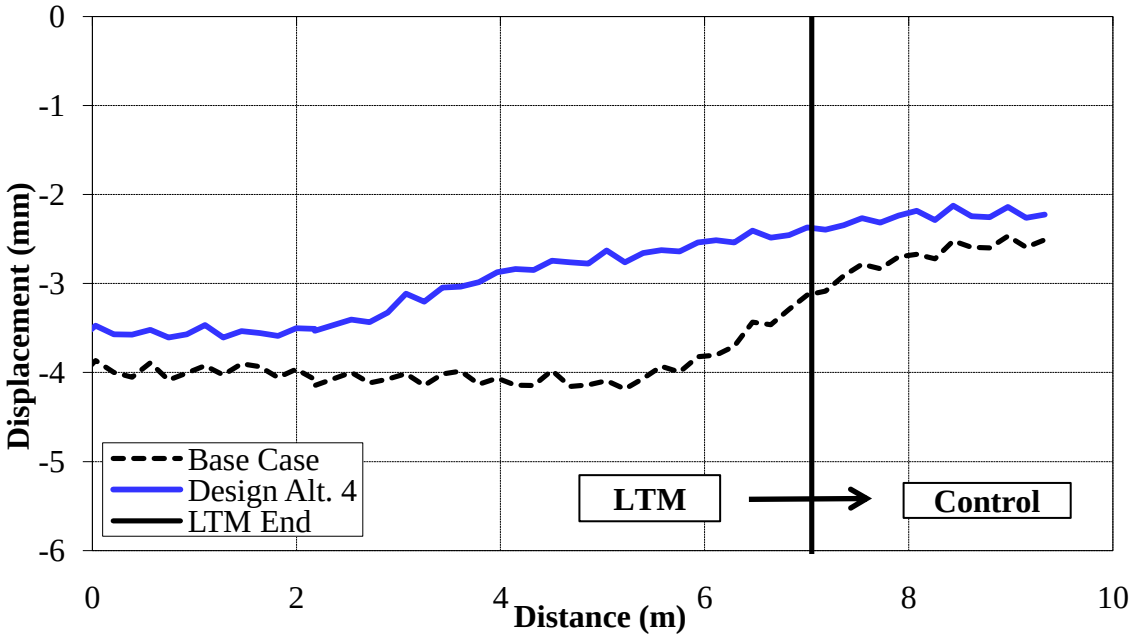

Figure 8.38 – Track deflection comparison for recommended solution design and base case simulation

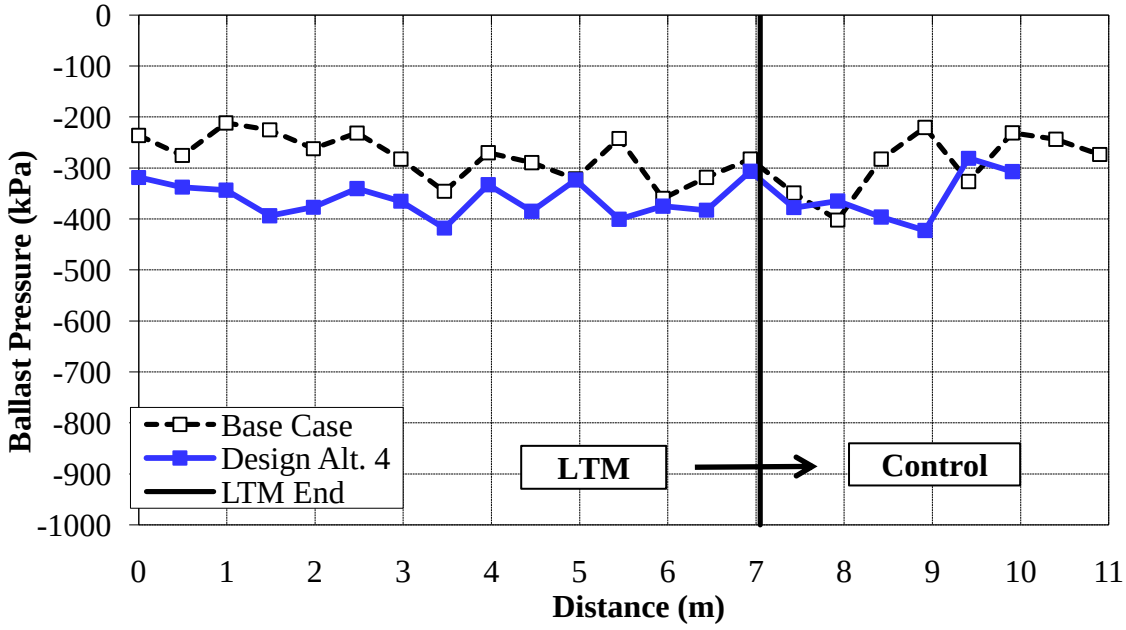

Figure 8.39 – Ballast pressure comparison for recommended solution design and base case simulation

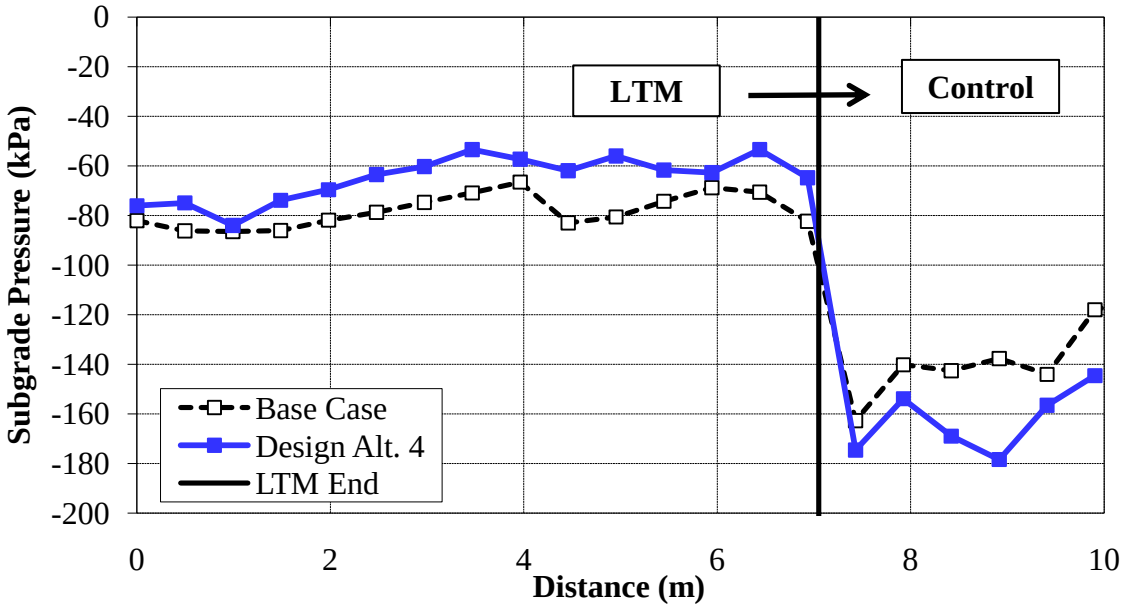

Figure 8.40- Subgrade pressure comparison for recommended solution design and base case simulation

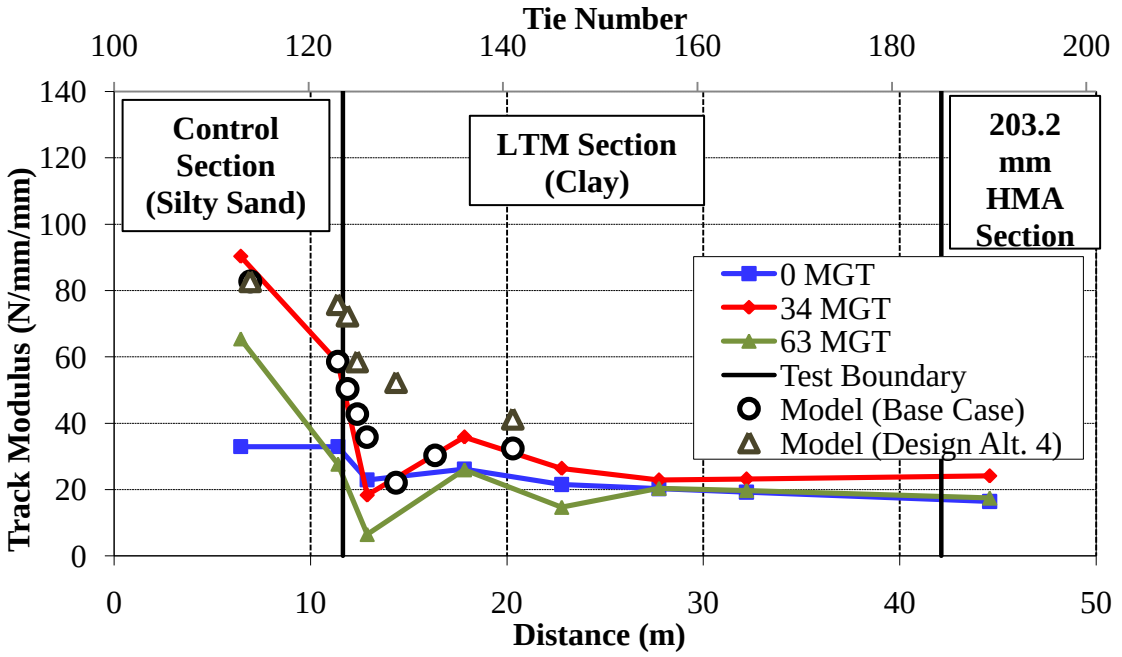

Figure 8.41 – Track modulus comparison for recommended solution design and base case simulation

Before field testing the recommended solution, the ultimate and allowable load capacity of the steel bars must be calculated and compared to actual values under traffic. The ultimate load capacity (Q_{ult}) is the sum of both skin friction (Q_f) and end bearing (Q_b) (Fig. 8.42). The allowable load capacity (Q_{allow}) is the ultimate load capacity divided by a factor of safety. A factor of safety of 3 was considered adequate for this analysis. The actual load on the bars must be less than the allowable load capacity to prevent failure.

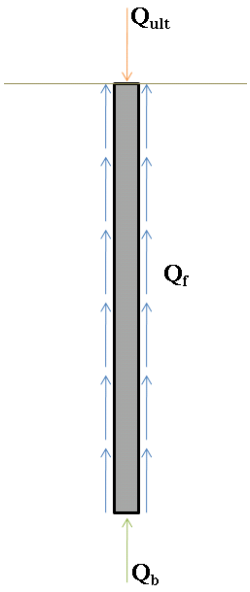

Figure 8.42 – Pile skin friction and end bearing

The skin friction was calculated according to the α-Method (Budhu 2000) for driven piles (Eq. 8.2).

$$Q_f = \alpha s_u \pi D L \tag{8.2}$$

where α is a coefficient, s_u is the undrained shear strength, D is the pile diameter and L is the pile length. The end bearing capacity was calculated using Eq. 8.3 (Budhu 2000).

$$Q_b = N_c s_u A_b \tag{8.3}$$

where N_c is a bearing capacity coefficient and A_b is the cross-sectional area of the pile base. Only one pile had to be evaluated in the design, the shortest pile, because it represented the worst-case scenario. If the shortest pile, which is founded only in the soft clay, has enough load capacity, then the rest of the longer piles will be adequate. To also be conservative, any pile group effects that may be present are neglected. The capacity of a single pile only is evaluated.

The skin friction for the shortest pile (0.30 m) is calculated as 950 N. This uses an α value of 0.93 (API 1984), a s_u value of 31 kPa (from laboratory tests), a pile diameter of 35 mm and a pile length of 0.30 m. The end bearing capacity is calculated as 268 N. This uses a N_c value of 9 (Skempton 1959), a s_u value of 31 kPa, and an A_b of 9.62 X 10^{-4} m^2. The ultimate load capacity is therefore 1218 N; the allowable load capacity is 406 N.

From the base case field results and the numerical simulations, the pressure at the top of the subgrade is around 69 kPa. Equating this as a force at the top of the steel bar, the force is 66.4 N. This maximum force is well below the allowable load capacity of 406 N.

8.4 DESIGN SOLUTION FIELD TEST

To validate the effectiveness of the proposed solution (Fig. 8.28) at the LTM section, a full-scale field is being conducted with the support of the AAR and the Transportation Technology Center, Inc. (TTCI). The base case for the test has previously been conducted (Section 9.2). Similar measurements will be obtained in the design solution field test to compare to the base case results.

8.4.1 Installation

Installation of the steel rods began on Monday, August 3, 2009 and commenced on Tuesday, August 4, 2009. The first row of bars in the solution was installed at the interface between the control section and the LTM. This location is between Tie No. 123 and Tie No. 124, or the concrete and wood ties in Fig. 8.43.

Figure 8.43 - Interface between control and LTM section at FAST

The steel rods are 1.375 in (35 mm) diameter Dywidag bars (Fig. 8.44). The bars were purchased by TTCI. The total 240 ft (73.15 m) length was divided into: 8 – 20 ft (6.10 m) bars, 4 – 18.5 ft (5.64 m) bars and 1 – 6 ft (1.83 m) bar. The total length of bars needed for the solution is 216 ft (65.83 m). The bars were cut to fit the recommended solution as follows:

1) The 4 - 18.5 ft (5.64 m) bars were cut into 4 – 7 ft (2.13 m) bars, 4 – 6.5 ft (1.98 m) bars and 4 – 5 ft (1.52 m) bars (0 ft remaining)
2) 4 of the 20 ft (6.10 m) bars can be cut into 4 – 7 ft (2.13 m) bars, 4 – 6 ft (1.83 m) bars, 4 – 4 ft (1.22 m) bars and 4 – 3 ft (0.91 m) bars (0 ft remaining)
3) 3 of the 20 ft (6.10 m) bars can be cut into 3 – 6.5 ft (1.98 m) bars, 3 – 6 ft (1.83 m) bars, 3 – 2 ft (0.61 m) bars, 3 – 1 ft (0.30 m) bars (4.5 ft/bar (1.37 m/bar) remaining – 13.5 ft (4.11 m) total)
4) 1 of the 20 ft (6.10 m) bars can be cut into 1 – 6.5 ft (1.98 m) bars, 1 – 2 ft (0.61 m) bars and 1 – 1 ft (0.30 m) bars (10.5 ft (3.20 m) remaining)
5) 1 of the 6 ft (1.83 m) bars can be used as is for one of the 6 ft (1.83 m) bars (0 ft remaining)

Figure 8.44 - Dywidag bars

To determine the ballast depth and measure the dimensions of a previously installed settlement rod, the ballast was removed between ties 127 and 128 (Fig. 8.45). The ballast depth was measured at 26 inches (0.66 m) from the top of the tie to the top of the subgrade. The plate at the end of the settlement rods was measured as having a width of 1 ft. The location of the steel rods had to therefore be modified between these ties only to avoid hitting the 4 settlement rods during installation (Fig. 8.46). The bars were placed about 9 in (0.23 m) from center of the settlement rods. This gives a clearance of 3 in (0.08 m) from the end of the settlement plate to the center of the steel bars.

Figure 8.45 –Ballast removal between Ties 127 and 128 at location of settlement rod

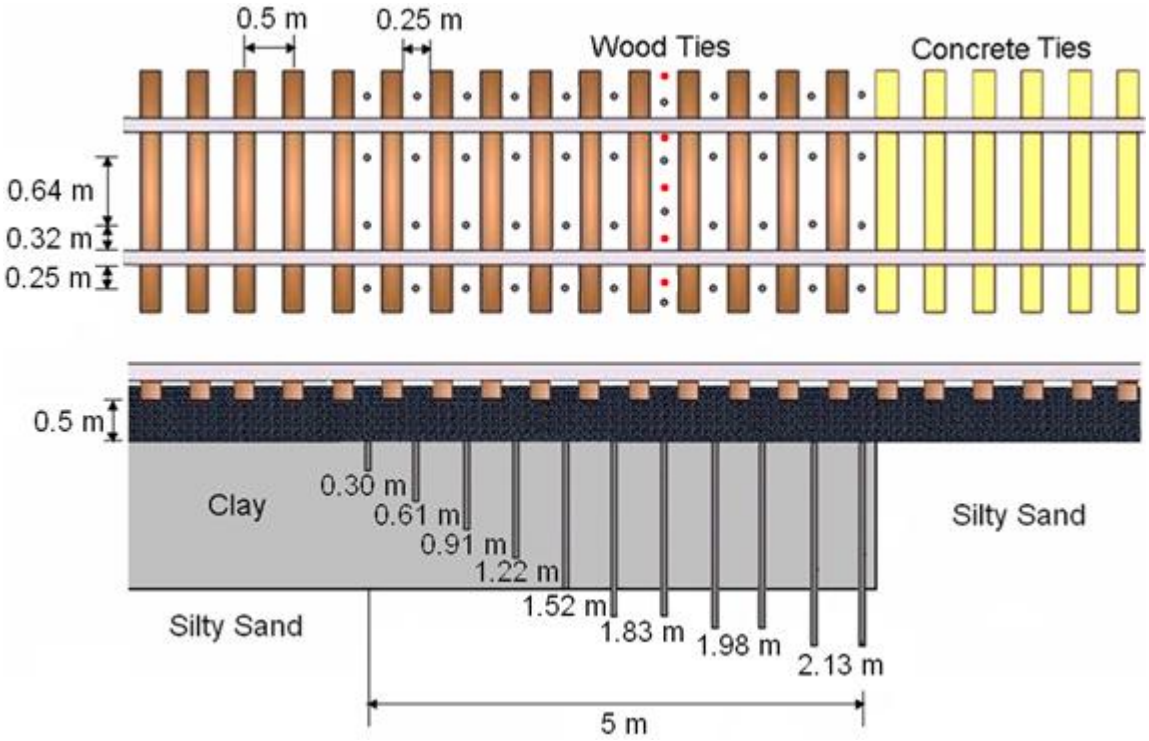

Figure 8.46 - Schematic of actual installation (settlement rods are in red)

The bars were then initially driven into the ballast using a small single-acting air hammer (Fig. 8.47). The hammer was held using a forklift and used an air pressure of around 100 psi (689.5 kPa). The contractors (Hayward Baker) did not have an adequate size drive rod to account for the 26 inches (0.66 m) of ballast, so the bars were only driven so that about 2-3 ft (0.61–0.91 m) of bar remained above the ballast while a longer drive rod was being machined by TTCI.

Figure 8.47 - Initial driving of the rods using an impact hammer

Once this occurred, the bars could be driven to depth. The small air hammer, however, did not have enough force to drive the bars deeper. The forklift was then used as an impromptu impact hammer to drive the bars (Fig. 8.48). This caused the weld in the drive rod to break. Another drive rod was then fashioned which included a small

casing to go over the head of the steel bar and a coupling to attach a vibratory hammer (Fig. 8.49). It is important that the casing surrounding the steel rods not be too long as this can cause the ballast to jam in between the casing and the rod. This, in turn, causes the rod to be pulled back up when the driving rod is removed after installation.

Figure 8.48 - Forklift used as impact hammer

Figure 8.49 - Drive rod to install the steel bars

Since the air hammer did not have enough force to drive the steel bars, a vibratory driver called “the torpedo” was used to successfully drive the bars through the ballast into the subgrade (Fig. 8.50 to Fig. 8.51). The air pressure was increased to about 110 psi (758.4 kPa) to operate the torpedo. The drive rod was pulled up after driving by tying a chain around the rod and using the forklift. The rod was hit with a hammer and twisted to ensure that the rod did not pull up the steel bar with it.

Figure 8.50 - Vibratory driver

Figure 8.51 – Vibratory driver used to install steel bars

In total, it took about 8-10 minutes to drive each bar through the ballast into the subgrade. For the 44 bars in this solution design, the total installation time is approximately 7 hours. With more powerful equipment, however, the total time can be reduced to no more than 4 hours. The next step is to re-level the track before traffic is allowed run over the track. A brief summary of the installation procedure is outlined below:

1) Steel bars were initially driven with a small air hammer. The hammer did not have enough force to fully drive the rods though.
2) A forklift was used as an impromptu impact hammer until the drive rod broke.

3) A vibratory hammer (the torpedo) was then used to finish driving the bars through the ballast into the subgrade.
4) The drive rod should include a small length cap to go around the top of the steel bars and a bar long enough to account for the ballast depth (Fig. 7). It is important that the casing surrounding the steel rods not be too long as this can cause the ballast to jam in between the casing and the rod.
5) Once the bar has been driven to depth, the drive rod should be pulled up and removed from the ground.

8.4.2 Cost

In total, the field test cost approximately $6000. The steel bars were $19.52 ($5.95/ft) per meter. A total of 73.15 m (240 ft) was purchased leading to a material cost of $1428. Delivery cost for the steel bars was $400. The installation was performed by a third party contractor, Hayward Baker. Mobilization costs were $1500 and pile installation was $1500/day. Less than 2 days was required to install the field test. This time length, and thus cost, can be significantly reduced in the future since the kinks and mistakes from the initial installation can be avoided.

9. CONCLUSIONS

9.1 SURVEY

The current views on the causes, problems and mitigation measures associated with the bump at the end of the bridge were found through a survey distributed across the world to various railroad companies and personnel (Section 4). From the survey, the current state of the problem for railroads was also discovered. A survey of this kind had not been previously performed.

Based on the survey responses, the bump/dip problem affects, on average, 51% of railroad bridges. The typical bump size ranges from 6.4 mm (¼") to 101.6 mm (4") with an average difference in elevation of 33 mm (1.3") along the rail profile. The horizontal length over which the bump occurs also varies, ranging from 1.2 m (4') to 15.2 m (50') with an average of approximately 5.2 m (17'). This leads to an average slope for current bumps equal to approximately 1:150. This slope is worse than the tolerable slope of 1:200 allowed for highway bridges (Briaud et al., 1997). It is also not acceptable according to those surveyed who defined a tolerable slope for railroad bridges as 1:253.

The annual cost of maintenance for the affected bridges of each company, including both internal and contracted, is estimated at $23 million total. The estimated annual cost from the survey is close to the figure of $26 million per year predicted in AAR's 2008 Strategic Research Initiatives (SRI) plan.

The most common factors leading to the bump, according to the survey respondents, are settlement of the fill, differential track modulus, poor surfacing, improper tamping and poor maintenance practices. The least common were lateral movement of the bridge abutment, settlement of the natural soil under the bridge abutment and poor construction specifications.

The cases where the problem appears to be worse are when the bridge is an open deck bridge, when the bridge is made of concrete and has concrete ties, when concrete approach ties are used and when wet conditions are present. The top three cases serve to stiffen up the track structure which can lead to increased impact loads. Conversely, the cases where the problem appears to be minimized are when the bridge is a ballasted deck bridge, when the bridge/approach location is well maintained and when there is good drainage.

The most common detection method is through visual inspection. Once detected, the most popular repair method is leveling by ballast tamping. The more expensive methods, such as improving the properties of the fill or natural soil under the fill, retrofitting with an approach slab, and mud jacking are less desirable for repair.

A standard design procedure across the industry has not been made to prevent or fix the bump/dip problem (rather than maintain it). Current practice concerning the bump varies among railroad companies. The most popular design measure is to simply have better cooperation between the track maintenance supervisor and the bridge maintenance supervisor. Another common design procedure for new bridges is to improve drainage

and avoid open deck bridges. The least used design procedure is to place the bridge abutment on spread footings.

The main conclusion from the survey is that differential settlement must be accommodated so that a tolerable ramp can develop as opposed to a steep bump. It seems as if the bump is unavoidable in the long-term. Solutions and factors to minimize the bump/dip that does form are necessary, however, to mitigate the problem.

9.2 PARAMETRIC STUDY

The results of this parametric study provide insight into the factors that are believed to contribute to the bump at the end of the railway bridge. This study found that abrupt track stiffness changes, as seen at a bridge/approach location, result in increased impact loads, track deflection, ballast pressures and subgrade pressures. While the response for a track stiffness change alone may not be unreasonable, adding a geometry change such as a bump or a dip to the track will cause the problem to be severe. This was demonstrated in Section 6.

After evaluating the reference cases for a track modulus change itself, with a bump and with a dip, the best and worst cases are found (Table 9.1). The results show that the track modulus change alone was the “best” case in terms of DLF, DBF, DSF and DDF. The dip profile, while producing higher dynamic loads than the other two cases, is actually less severe than the bump profile. This is important to recognize: a higher DLF does not necessarily mean the problem is worse. Other factors, such as track deflection, ballast and subgrade pressures, must also be considered. This was accomplished through

the ranking system developed in the last section (Section 7). By grouping the overall parametric study rankings for both the bump and the dip, a clearer picture of each varied parameter emerges.

Table 9.1 – Parametric study conclusion: reference cases

Case	Local Rank	Brief Description	DLF	DBF	DSF	DDF
27	1	No Slope @ 22.2 m/s	1.14	1.30	1.36	1.40
Ref. (Dip)	2	1:150 Dip @ 22.2 m/s	1.45	2.14	1.78	2.24
Ref. (Bump)	3	1:150 Bump @ 22.2 m/s	1.28	2.33	2.18	2.40

The first parameter varied was the train direction. The results indicate that going off of the bridge is better on the track system than going on to the bridge (Table 9.2 and Table 9.3). For the case of a train going on to the bridge, the train is traveling from a softer material (the approach) to a harder material (the bridge). Since the bridge is not as deformable as the approach, an impact will occur. For the case of a train moving off of the bridge, the train is traveling from a harder material (the bridge) to a softer material (the approach). The approach will tend to deform with the load rather causing any impact on the track to be less severe.

Table 9.2 – Parametric study conclusion: train direction (Bump)

Case	Global Rank	Local Rank	Brief Description	DLF	DBF	DSF	DDF
1	1	1	Direction: Off of Bridge	1.13	1.10	1.05	1.02
Ref.	20	2	Direction: On to Bridge	1.28	2.33	2.18	2.40

Table 9.3 - Parametric study conclusion: train direction (Dip)

Case	Global Rank	Local Rank	Brief Description	DLF	DBF	DSF	DDF
1	4	1	Direction: Off of Bridge	1.27	1.57	1.70	1.45
Ref.	20	2	Direction: On to Bridge	1.45	2.14	1.78	2.24

The results for velocity indicate that decreasing the velocity will reduce the effects due to a bump or a dip (Table 9.4 and Table 9.5, respectively). The trends for DLF, DDF, DBF and DSF for the bump and the dip are all fairly linear. The steepness of this trend is typically higher for the bump, however, than for the dip. This suggests that velocity is a bigger factor for a bump than for a dip. While the dip experiences higher DLFs than the bump, the opposite is largely true for DDF, DBF and DSF.

Therefore, to avoid large impacts on the track, trains should travel slowly over the bridge/approach location. This is often not feasible, however, as it could delay traffic considerably. In trouble locations, however, slow orders must be placed to limit the wheel/rail forces, track deflection, ballast and subgrade pressures.

Table 9.4 – Parametric study conclusions: train velocity (Bump)

Case	Global Rank	Local Rank	Brief Description	DLF	DBF	DSF	DDF
2	4	1	8.9 m/s	1.07	1.55	1.37	1.46
3	9	2	15.6 m/s	1.18	2.02	1.78	1.83
Ref.	20	3	22.2 m/s	1.28	2.33	2.18	2.40
4	45	4	33.5 m/s	1.55	3.15	3.43	3.45
5	49	5	44.7 m/s	1.66	3.56	4.05	4.07

Table 9.5 - Parametric study conclusions: train velocity (Dip)

Case	Global Rank	Local Rank	Brief Description	DLF	DBF	DSF	DDF
2	7	1	8.9 m/s	1.13	1.51	1.42	1.63
3	10	2	15.6 m/s	1.29	1.57	1.50	1.92
Ref.	20	3	22.2 m/s	1.45	2.14	1.78	2.24
4	35	4	33.5 m/s	1.54	1.80	1.58	2.26
5	41	5	44.7 m/s	1.72	2.28	1.84	2.43

An increase in the steepness of the slope for the bump leads to an increase in the DLF, DDF, DBF and DSF (Table 9.6). The slopes with equal length performed only slightly better than the same slopes with equal heights. This indicates that the height and length of the bump does not matter as much as the overall slope. Analysis of the results also suggests that if a slope is steep enough, the track geometry is more influential on impact forces than the change in track modulus.

Table 9.6 – Parametric study conclusions: bump slope

Case	Global Rank	Local Rank	Brief Description	DLF	DBF	DSF	DDF
26	2	1	No Slope @ 15.6 m/s	1.10	1.54	1.10	1.23
27	3	2	No Slope @ 22.2 m/s	1.14	1.30	1.36	1.40
2	4	3	1:150 @ 8.9 m/s	1.07	1.55	1.37	1.46
22	5	4	1:250 (Equal Height) @ 15.6 m/s	1.14	1.85	1.48	1.60
28	6	5	No Slope @ 33.5 m/s	1.22	1.61	1.41	1.33
18	7	6	1:200 (Equal Height) @ 15.6 m/s	1.15	1.85	1.70	1.76
29	8	7	No Slope @ 44.7 m/s	1.27	1.85	1.48	1.50
3	9	8	1:150 @ 15.6 m/s	1.18	2.02	1.78	1.83
23	11	9	1:250 (Equal Height) @ 22.2 m/s	1.20	1.80	1.95	2.10
9	12	10	1:250 (Equal Length)	1.22	1.82	2.04	1.98
19	14	11	1:200 (Equal Height) @ 22.2 m/s	1.23	2.19	2.07	2.20
8	15	12	1:200 (Equal Length)	1.24	1.82	2.19	2.16
14	18	13	1:100 (Equal Height) @ 15.6 m/s	1.25	2.28	2.32	2.12
Ref.	20	14	1:150 @ 22.2 m/s	1.28	2.33	2.18	2.40
10	28	15	1:50 (Equal Height) @ 15.6 m/s	1.32	2.10	2.52	2.43
24	39	16	1:250 (Equal Height) @ 33.5 m/s	1.35	2.76	2.58	2.68
20	40	17	1:200 (Equal Height) @ 33.5 m/s	1.44	2.99	2.82	2.44
15	41	18	1:100 (Equal Height) @ 22.2 m/s	1.40	2.67	2.75	2.88
7	42	19	1:100 (Equal Length)	1.35	2.82	2.94	2.93
11	43	20	1:50 (Equal Height) @ 22.2 m/s	1.45	3.54	3.05	3.24
25	44	21	1:250 (Equal Height) @ 44.7 m/s	1.50	4.29	2.88	2.92
4	45	22	1:150 @ 33.5 m/s	1.55	3.15	3.43	3.45
21	46	23	1:200 (Equal Height) @ 44.7 m/s	1.57	3.69	3.94	3.50
16	47	24	1:100 (Equal Height) @ 33.5 m/s	1.74	3.98	3.71	3.50
12	48	25	1:50 (Equal Height) @ 33.5 m/s	1.91	4.41	2.92	3.48

Table 9.6 Cont'd

Case	Global Rank	Local Rank	Brief Description	DLF	DBF	DSF	DDF
5	49	26	1:150 @ 44.7 m/s	1.66	3.56	4.05	4.07
6	50	27	1:50 (Equal Length)	1.56	4.29	4.16	4.60
17	51	28	1:100 (Equal Height) @ 44.7 m/s	2.00	4.17	4.99	3.54
13	52	29	1:50 (Equal Height) @ 44.7 m/s	2.17	4.61	3.29	4.57

The results are different for the dip (Table 9.7). While for each slope, the best cases are for slower velocities, there is a not a strong correlation with bump slope. While a general trend is visible between dip slopes with equal heights and the DLF, there is not a strong correlation for DDF, DBF and DSF. In fact, the profile of these are similar themselves, having a sinusoidal shape rather than a linear shape (Section 7).

Table 9.7 - Parametric study conclusions: dip slope

Case	Global Rank	Local Rank	Brief Description	DLF	DBF	DSF	DDF
26	1	1	No Slope @ 15.6 m/s	1.10	1.54	1.10	1.23
27	2	2	No Slope @ 22.2 m/s	1.14	1.30	1.36	1.29
28	3	3	No Slope @ 33.5 m/s	1.22	1.61	1.41	1.33
29	5	4	No Slope @ 44.7 m/s	1.27	1.85	1.48	1.50
14	6	5	1:100 (Equal Height) @ 15.6 m/s	1.16	1.34	1.38	1.37
2	7	6	1:150 @ 8.9 m/s	1.13	1.51	1.42	1.63
22	8	7	1:250 (Equal Height) @ 15.6 m/s	1.14	1.68	1.54	1.68
15	9	8	1:100 (Equal Height) @ 22.2 m/s	1.26	1.72	1.44	1.72
3	10	9	1:150 @ 15.6 m/s	1.29	1.57	1.50	1.92

Table 9.7 Cont'd

Case	Global Rank	Local Rank	Brief Description	DLF	DBF	DSF	DDF
18	11	10	1:200 (Equal Height) @ 15.6 m/s	1.20	1.80	1.66	1.96
9	12	11	1:250 (Equal Length)	1.39	1.67	1.65	1.88
8	13	12	1:200 (Equal Length)	1.45	1.64	1.67	2.06
16	17	13	1:100 (Equal Height) @ 33.5 m/s	1.48	2.32	1.47	1.80
Ref.	20	14	1:150 @ 22.2 m/s	1.45	2.14	1.78	2.24
23	22	15	1:250 (Equal Height) @ 22.2 m/s	1.21	2.19	1.91	2.38
10	32	16	1:50 (Equal Height) @ 15.6 m/s	1.53	2.07	1.84	1.76
17	34	17	1:100 (Equal Height) @ 44.7 m/s	1.76	2.01	1.67	1.84
4	35	18	1:150 @ 33.5 m/s	1.54	1.80	1.58	2.26
19	38	19	1:200 (Equal Height) @ 22.2 m/s	1.31	2.16	2.02	2.61
24	39	20	1:250 (Equal Height) @ 33.5 m/s	1.45	2.22	2.14	2.22
11	40	21	1:50 (Equal Height) @ 22.2 m/s	1.83	2.40	1.90	1.83
5	41	22	1:150 @ 44.7 m/s	1.72	2.28	1.84	2.43
20	43	23	1:200 (Equal Height) @ 33.5 m/s	1.56	2.67	2.27	2.22
25	45	24	1:250 (Equal Height) @ 44.7 m/s	1.52	2.25	2.38	2.39
12	48	25	1:50 (Equal Height) @ 33.5 m/s	1.96	2.66	2.51	1.66
21	49	26	1:200 (Equal Height) @ 44.7 m/s	1.70	2.21	2.46	3.16
7	50	27	1:100 (Equal Length)	1.75	2.01	2.61	2.83
13	51	28	1:50 (Equal Height) @ 44.7 m/s	1.92	2.90	3.00	2.12
6	52	29	1:50 (Equal Length)	2.28	3.23	2.81	3.74

As expected, the impact due to the track modulus change is greater for a soft soil with a low modulus than for a stiffer soil when a bump is present (Table 9.8). There is a

linear relationship between the soil modulus and the track modulus; a higher soil modulus leads to a higher track modulus. The stiffest soil will therefore reduce the track modulus differential between the bridge and the approach resulting in lower DLF, DDF and DSF values as compared to softer soils. There is not a strong correlation between the DBF and the soil modulus, however, suggesting that the maximum ballast pressure is not dependent on the modulus of the soil.

Table 9.8 – Parametric study conclusions: soil modulus (Bump)

Case	Global Rank	Local Rank	Brief Description	DLF	DBF	DSF	DDF
32	10	1	100 MPa Soil Modulus	1.18	2.40	1.80	2.29
31	21	2	50 MPa Soil Modulus	1.18	2.72	2.10	2.50
30	26	3	20 MPa Soil Modulus	1.30	2.31	2.20	2.54

Again, the results for the dip are slightly different than for the bump (Table 9.9). While the best case is for the strongest soil (100 MPa), the worst case is not for the weakest soil (20 MPa), While the DLF and DSF are the highest for the weakest soil, the DBF and DDF are the lowest. Note that the maximum displacement is still largest for the case having a soil modulus of 20 MPa though and will still cause more problems than the cases with higher soil moduli.

Table 9.9 - Parametric study conclusions: soil modulus (Dip)

Case	Global Rank	Local Rank	Brief Description	DLF	DBF	DSF	DDF
32	16	1	100 MPa Soil Modulus	1.35	2.06	1.72	2.19
30	18	2	20 MPa Soil Modulus	1.44	1.89	1.78	2.04
31	36	3	50 MPa Soil Modulus	1.41	2.08	1.75	2.41

The results indicate that approach tie material does not play a major role on the wheel/rail forces (Table 9.10 and Table 9.11). It does, however, affect the track deflection, ballast and subgrade pressures. Wood ties performed the best when considering all four types of responses. Adding rubber pads under the rail seats on the approach is the worst case. This is because the rubber pads make the approach softer when the problem is that the approach is already too soft.

Table 9.10 – Parametric study conclusion: approach tie material (Bump)

Case	Global Rank	Local Rank	Brief Description	DLF	DBF	DSF	DDF
Ref.	20	Ref.	Wood Ties	1.28	2.33	2.18	2.40
33	25	33	Concrete Ties	1.28	2.54	2.09	2.50
34	32	38	Plastic Ties	1.30	2.85	2.47	2.55
38	33	34	Concrete Ties with Rubber Tie Pads	1.31	2.30	2.89	2.84
37	34	37	Wood Ties with Rubber Tie Pads	1.31	2.45	2.92	2.84
35	36	35	Concrete Ties with Rubber Rail Seat Pads	1.42	3.44	2.96	2.14
36	37	36	Wood Ties with Rubber Rail Seat Pads	1.42	3.44	2.96	2.16

Table 9.11 - Parametric study conclusion: approach tie material (Dip)

Case	Global Rank	Local Rank	Brief Description	DLF	DBF	DSF	DDF
Ref.	20	1	Wood Ties	1.45	2.14	1.78	2.24
33	21	2	Concrete Ties	1.46	1.88	1.81	2.28
34	25	3	Plastic Ties	1.46	2.24	1.91	2.35
38	32	4	Concrete Ties with Rubber Tie Pads	1.31	2.30	2.89	2.84
37	44	5	Wood Ties with Rubber Tie Pads	1.58	1.89	2.41	2.38
35	46	6	Concrete Ties with Rubber Rail Seat Pads	1.57	2.51	2.28	2.51
36	47	7	Wood Ties with Rubber Rail Seat Pads	1.57	2.83	2.23	2.54

Unlike for approach ties, the bridge tie material does not seem to have a large influence on the DLF, DDF, DBF or DSF (Table 9.12 and Table 9.13). This is because the bridge tie material does not significantly affect the track modulus of the bridge. Since each simulation case models similar track modulus differentials, the track response for each case is also similar. This is also because the tie material of the approach, where the problem occurs, is unchanged in each simulation. Adding rubber rail seat pads does slightly reduce the DLF, but the DBF, DSF and DDF response is similar to bare ties.

Table 9.12 – Parametric study conclusion: bridge tie material (Bump)

Case	Global Rank	Local Rank	Brief Description	DLF	DBF	DSF	DDF
41	16	1	Wood Ties with Rubber Rail Seat Pads	1.20	2.33	2.13	2.35
42	17	2	Concrete Ties with Rubber Rail Seat Pads	1.20	2.35	2.15	2.38
Ref.	20	3	Wood Ties	1.28	2.33	2.18	2.40
40	22	4	Plastic Ties	1.28	2.32	2.28	2.50
39	27	5	Concrete Ties	1.28	2.41	2.24	2.53

Table 9.13 - Parametric study conclusion: bridge tie material (Dip)

Case	Global Rank	Local Rank	Brief Description	DLF	DBF	DSF	DDF
42	19	1	Concrete Ties with Rubber Rail Seat Pads	1.41	2.08	1.72	2.48
Ref.	20	2	Wood Ties	1.45	2.14	1.78	2.24
41	24	3	Wood Ties with Rubber Rail Seat Pads	1.42	2.11	1.80	2.48
40	23	4	Plastic Ties	1.46	2.17	1.75	2.37
39	26	5	Concrete Ties	1.46	2.21	1.82	2.39

The results for the bump indicate that a ballast deck bridge with a ballast mat performs the best while the open deck bridge performs the worst (Table 9.14). This is likely because adding a ballast mat reduces the track modulus for the ballasted deck bridge. While it reduces the DLF and the DDF, the DBF and DSF are increased because of the lower track modulus. Overall, however, adding a ballast mat is recommended.

Table 9.14 – Parametric study conclusion: bridge deck type (Bump)

Case	Global Rank	Local Rank	Brief Description	DLF	DBF	DSF	DDF
44	23	1	Ballast Deck Bridge with a Ballast Mat	1.17	2.08	2.36	2.12
43	30	2	Ballast Deck Bridge	1.22	1.62	2.30	2.46
Ref.	20	3	Open Deck Bridge	1.28	2.33	2.18	2.40

The results for bridge deck type are slightly different for the dip (Table 9.15). The best case is the ballast deck bridge while the worst case is still the open deck bridge. Adding a ballast mat to the ballast deck bridge does not make a big difference in the track response for the dip. The DLF, DDF, DBF and DSF are all very close to the values for the ballast deck alone. A ballast mat is still recommended for ballast deck bridges with a dip on the approach embankment.

Table 9.15 - Parametric study conclusion: bridge deck type (Dip)

Case	Global Rank	Local Rank	Brief Description	DLF	DBF	DSF	DDF
43	14	1	Ballast Deck Bridge	1.34	1.62	1.51	1.96
44	15	2	Ballast Deck Bridge with a Ballast Mat	1.33	1.62	1.56	1.98
Ref.	20	3	Open Deck Bridge	1.45	2.14	1.78	2.24

Overall, larger ballast thicknesses are better than smaller ballast thicknesses when a bump is present (Table 9.16). While there is a not a significant difference in terms of DLF, the DDF, DBF and DSF are all smaller for larger ballast thicknesses. This

is because a thicker ballast layer will stiffen the track structure and help dissipate pressures.

Table 9.16 – Parametric study conclusion: ballast thickness (Bump)

Case	Global Rank	Local Rank	Brief Description	DLF	DBF	DSF	DDF
48	13	1	406.4 mm Ballast Thickness	1.28	2.12	2.04	2.14
47	19	2	304.8 mm Ballast Thickness	1.25	2.48	2.07	2.33
Ref.	20	3	254 mm Ballast Thickness	1.28	2.33	2.18	2.40
46	24	4	203.2 mm Ballast Thickness	1.26	2.49	2.28	2.38
45	38	5	152.4 mm Ballast Thickness	1.31	2.88	2.50	2.87

The same ballast thickness results for the bump are generally true when a dip is present. The best case, however, is for the middle ballast thickness simulated. This is because the DLF is just under the 1.5 tolerable limit while the DLF for the other ballast thicknesses, except for 203.2 mm, is just over the limit. This means that these cases had more exceedances than the reference case and were therefore ranked lower. The ballast thickness of 203.2 mm had an equal amount of exceedances to the majority of cases, but the DSF was slightly greater than tolerable, not the DLF.

Table 9.17 - Parametric study conclusion: ballast thickness (Dip)

Case	Global Rank	Local Rank	Brief Description	DLF	DBF	DSF	DDF
Ref.	20	1	254 mm Ballast Thickness	1.45	2.14	1.78	2.24
48	27	2	406.4 mm Ballast Thickness	1.52	1.74	1.44	1.81
47	30	3	304.8 mm Ballast Thickness	1.52	1.87	1.60	2.00
46	31	4	203.2 mm Ballast Thickness	1.49	1.60	2.03	1.93
45	33	5	152.4 mm Ballast Thickness	1.51	2.16	1.73	1.88

The results indicate that when a bump is present, increasing the approach tie leads to a worse track response (Table 9.18). The results are slightly scattered however, as the worst case is for the smallest tie length. The results are even more scattered when the dip is present (Table 9.19). This is because there is a weak correlation between the approach tie length and the DLF, DDF, DBF and DSF for both the bump and the dip. This suggests that the change in pressure and track response due to increasing tie lengths is negligible compared to the other factors present.

Table 9.18 – Parametric study conclusion: approach tie length (Bump)

Case	Global Rank	Local Rank	Brief Description	DLF	DBF	DSF	DDF
Ref.	20	1	2.6 m Approach Tie Length	1.28	2.33	2.18	2.40
50	29	2	3.0 m Approach Tie Length	1.31	2.39	2.25	2.68
51	31	3	3.6 m Approach Tie Length	1.31	2.38	2.33	2.70
49	35	4	2.1 m Approach Tie Length	1.31	2.50	2.41	2.70

Table 9.19 - Parametric study conclusion: approach tie length (Dip)

Case	Global Rank	Local Rank	Brief Description	DLF	DBF	DSF	DDF
Ref.	20	1	2.6 m Approach Tie Length	1.45	2.14	1.78	2.24
51	28	2	3.6 m Approach Tie Length	1.50	1.68	1.90	1.82
50	29	3	3 m Approach Tie Length	1.50	1.73	1.86	1.84
49	37	4	2.1 m Approach Tie Length	1.52	1.94	1.79	2.14

Currently there are no guidelines to account for the bump/dip problem. Equations, such as the AREMA (2008) formula for the dynamic load factor on open track (Eq. 2.14) and the AREMA (2008) equations for bridge impact, are provided in order to design for an overall impact load. They are not made to estimate the dynamic load resulting from a specific geometry change such as a bump or a dip at the end of the railway bridge. In fact, the impact due to the bump can be much larger than that calculated using the AREMA forumla. For example, for a 1:50 dip slope (1.14^{o}) at 22.2 m/s (50 mph), the DLF is 2.28. The AREMA formula (Eq. 2.14), however, predicts the DLF as approximately 1.46. This difference can cause the track to significantly deteriorate faster than expected thus increasing maintenance costs.

A tolerable slope for the bump is also not defined. The industry survey conducted in this research concluded at a 1:250 slope was considered tolerable. Based on the 4-D simulations, this slope is reasonable for the entire velocity range tested based on the DLF. If looking at the subgrade pressures and the DSF, instead, the tolerable slope was

1:750 for a velocity of 44.7 m/s. To allow for a steeper slope, while keeping subgrade pressures within tolerable limits, the velocity must be reduced. In this case, to reach a slope of 1:250, the velocity must be reduced from 44.7 m/s to 22.2 m/s, or about half the speed.

9.3 DESIGN SOLUTION

While the bump may never be eliminated, it can be designed for in order to reduce track degradation and maintenance. To minimize the response at the transition, solutions to the problem must relieve both stiffness and settlement issues. After evaluating the current mitigation methods (Section 3), it is clear that there are a number of solutions for new bridge construction that are performing well: approach slabs, bridge approach support piling, stone columns and HMA underlayment. The solutions are not as feasible for existing bridges though.

A new solution is proposed in this dissertation for approach embankments with soft subgrades at existing bridges. The proposed solution for the bump/dip problem involves installing varying length steel bars between the ties into the subgrade (Fig. 8.1, shown again below). These pile-like elements will strength and stiffen the subgrade. The tops of the bars will begin directly underneath the ballast so as not to interfere with any future ballast tamping activities. The steel bars can be vibro-driven into place without removing any of the track structure.

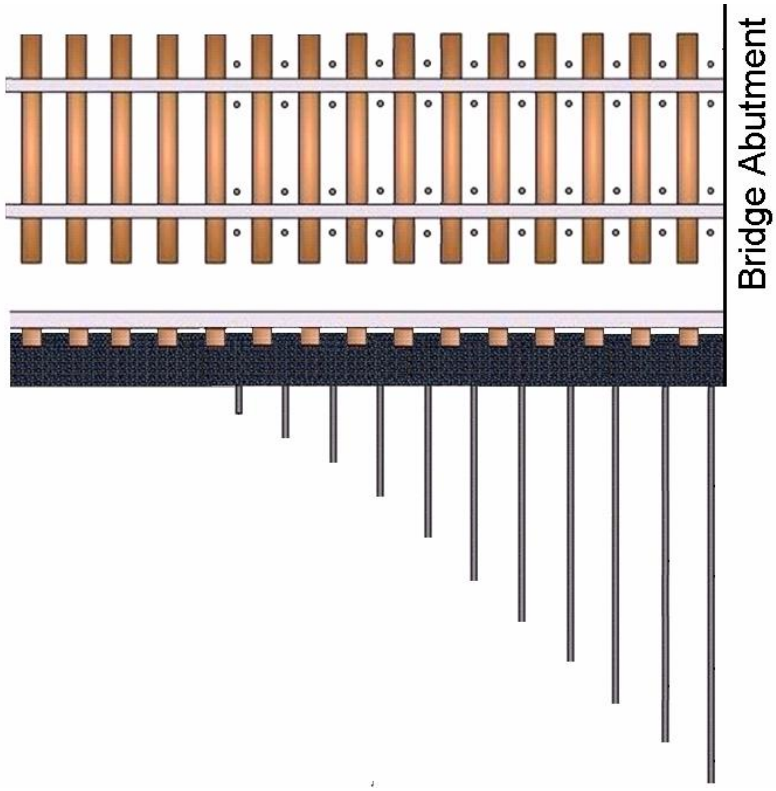

Figure 8.1 – Proposed solution sketch

To validate the effectiveness of the proposed solution at minimizing the bump at the end of the railway bridge, a full-scale field is being conducted with the support of the AAR and the Transportation Technology Center, Inc. (TTCI). Numerical simulations using LS-DYNA optimized the design of the solution for this test site. Base case tests at the site indicate that a dip has formed. The success of the solution will therefore depend on how well the solution prevents or minimizes the formation of that dip. While numerical simulations indicate that the solution will reduce subgrade pressures and minimize track deflection, the full-scale field test will validate the conclusion.

9.4 FUTURE RELATED RESEARCH

There are a number of possible avenues for continued research within this topic of the bump at the end of the railway bridge. For one, the field tests to evaluate the proposed design solution are ongoing. Track modulus, wheel/rail forces, track settlement, subgrade settlement and subgrade pressures are all being measured to study and determine the viability of the solution.

Another area involves continuing the numerical simulations for the bump/d problem. The model created in this study to simulate the problem used an elastic soil model for the ballast, subballast and soil, but these materials are only elastic under small strains. Applying constitutive models will allow for a more thorough investigation of the permanent settlement of the soil leading to bump/dip formation. Since LS-DYNA supports constitutive models, the 4-D model created for this analysis can be used.

The proposed solution to minimize the bump/dip problem is mainly applicable to soft subgrades. Some bump/dip problems are not a result of subgrade issues though. The bump/dip can also occur as a result of ballast degradation due to increased loads and ballast pressures. Research into prevention of ballast degradation should continue in order to solve this important problem that affects more than the bump at the end of the railway bridge.

This study also did not evaluate the effect of the bump on vehicle dynamics. A simple truck model was created for this study since the focus was more on the track structure and substructure. A more advanced truck model could be combined with this model to investigate the effects of the bump problem on the vehicle.

REFERENCES

Association of American Railroads (AAR). (2005). *Field manual of the AAR interchange rules*, Rule 41, AAR, Washington, DC, 268-325.

AAR. (2008). "Overview of America's freight railroads." *Railroads: The Vital Link to North America's Economic Future, Policy and Economics Department*, AAR.

Ahlbeck, D.R. (1980). "An investigation of impact loads due to wheel flats and rail joints." *80-WA/RT-1*, American Society of Mechanical Engineers.

Alva-Hurtado, J.E. and Selig, E.T. (1981). "Permanent strain behavior of railroad ballast." *Proceedings of the 10th International Conference on Soil Mechanics and Foundation Engineering*, Stockholm, Sweden, 1, 543-546.

American Petroleum Institute (API). (1984). *Recommended practice for planning, designing and constructing fixed off-shore platforms*, API, Washington, DC.

American Railway Engineering and Maintenance-of-Way Association (AREMA). (2008). *Manual for railway engineering*. AREMA, Washington, DC.

Arnold, R., Lu, S., Hogan, C., Farritor, S., Fateh, M., and El-Sibaie, M. (2006). "Measurement of vertical track modulus from a moving railcar." *Proceedings of the AREMA 2006 Annual Conference*, Louisville, KY, <http://www.arema.org/eseries/scriptcontent/custom/e_arema/library/2006_Conference_Proceedings/017.pdf> (October 30, 2009).

American Structural Foundries (ASF). (Date Unknown). "Freight car truck design." *User's Guide*, ASF652, obtained from Stan Gurule in March 2007.

Bakeer, R.M., Shutt, M.A., Zhong, J., Das, S.C., and Morvant, M. (2005). "Performance of pile-supported bridge approach slabs." *Journal of Bridge Engineering*, 10 (2), ASCE, 228-237.

Banimahd, M. and Woodward, P.K. (2007). "3-Dimensional finite element modelling of railway transitions." *Proceedings of 9th International Conference on Railway Engineering*, London, <http://www.xitrack.com/paper5.pdf> (October 30, 2009).

Blader, F.B., Elkins, J.A., Wilson, N.G., and Klauser, P.E. (1989). "Development and validation of a general railroad vehicle dynamics simulation (NUCARS)." *Proceedings of the 1989 IEEE/ASME Joint Railroad Conference*, Philadelphia, PA, 39-46.

Bleakley, S.S. (2006). "Time frequency analysis of railway wagon body accelerations for a low-power autonomous device." M.Eng Thesis, Central Queensland University.

Briaud, J.-L., James, R.W., and Hoffman, S.B. (1997). "Settlement of bridge approaches (The bump at the end of the bridge)." *NCHRP, Synthesis of Highway Practice 234*, Transportation Research Board, Washington, D.C.

Budhu, M. 2000. *Soil mechanics & foundations*. John Wiley & Sons, New York.

Cai, Z., Raymond, G.P., and Bathurst, R.J. (1994). "Estimate of static track modulus using elastic foundation models." *Transportation Research Record 1470*, National Academy Press, Washington, DC, 65-72.

Chang, C.S., Adegoke, C.W., and Selig, E.T. (1980). "The GEOTRACK model for railroad track performance." *Journal of Geotechnical Engineering Division*, ASCE, 106 (GT11), 1201-1218.

Choros, J., Adams, G.G., (1979), "Steadily moving load on an elastic beam resting on a tensionless Winkler foundation," *Journal of Applied Mechanics – Transactions of the ASME*, 46 (1), 175-180.

Dahlberg, T. (2001). "Some railroad settlement models – a critical review." *Proceedings of the Institution of Mechanical Engineers*, 215 (F), 289-300.

Das, B.M. (1998). *Principles of foundation engineering*, CL-Engineering, New York.

Davis, D.D., Otter, D., Dingqing, L., and Satya, S. (2003). "Bridge approach performance in revenue service." *Railway Track & Structures*, 99 (12), 18-20.

Davis, D.D., Anaya, R., Chrismer, S.M., and Smith, L. (2007). "Development of a differential settlement model for design and maintenance of track transitions." *Technology Digest*, TD-07-002.

Davis, D.D. and Plotkin, D. (2009). "Track settlement at bridge approaches," *Railway Track & Structures*, 105 (2), 33-38.

Dupont, B. and Allen, D.L. (2002). *Movements and settlements of highway bridge approaches*, Kentucky Transportation Center, Lexington, KY.

Ebersohn, W. and Selig, E.T. (1994). "Track modulus on a heavy haul line." *Transportation Research Record 1470*, 73-83.

Elkins, J.A., Klauser, P.E. and Blader, F.B. (1990). "Applications using NUCARS: A general purpose rail vehicle dynamics simulation." *Proceedings of the 2nd International*

Conference on Computer Aided Design, Manufacture and Operation in the Railway and other Advanced Mass Transit Systems, Rome, Italy, 147-161.

Farritor, S. (2006). "Real-time measurement of track modulus from a moving car." *Final Report*, U.S. Department of Transportation, FRA, Washington, DC.

FEA Information, Inc. (2006). LS-DYNA Applications, <http://www.ls-dyna.com> (Feb. 6, 2006).

Filonenko-Borodich, M.M. (1940). "Some approximate theories of elastic foundation." *Uchenyie Zapiski Moskovskogo Gosudarstuennogo Universiteta Mekhanika*, Moscow, 46, 3-18 (in Russian).

Federal Railroad Administration (FRA). (1993). "Estimated railroad bridge population from the FRA bridge safety survey of 1992-93, bridge carrying railroad tracks," <http://www.fra.dot.gov/downloads/safety/bridges.pdf> (May 5, 2009).

FRA. (2003). "Passenger equipment safety standards." *FRA Regulations*, Title 49, CFR Part 238, Department of Transportation, 63 (119), Washington DC.

Frederick, C.O. (1978). "The effect of wheel and rail irregularities on the track." *1st International Heavy Haul Conferenc*e, Institution of Engineers, Perth, Australia, Paper G2.

Frederick, C.O., Round, D.J., (1985), "Vertical track loading," *Track Technology: Proceedings of a Conference*, University of Nottingham, UK, Thomas Telford Ltd., 135-149.

Frýba, L. (1999). *Vibration of solids and structures under moving loads*. Thomas Telford, London.

GeMeiner, W., Davis, D. (2002). "Performance evaluation of alternative bridge approach designs." Design of Track Structures for Bridges and Bridge Approaches Workshop, Transportation Research Board, Washington DC.

Hallquist, J.O. (2006). LS-DYNA theory manual. Livermore Software Technology Corporation, <http://www.lstc.com/pdf/ls-dyna_theory_manual_2006.pdf> (Feb. 6, 2006).

Hay, W.W. (1982). *Railroad engineering, second edition*, John Wiley & Sons, New York.

Helwany, S.M.B., Wu, J.T.H. and Froessl, B. (2003). "GRS bridge abutments – an effective means to alleviate bridge approach settlement." *Geotextiles and Geomebranes*, 21 (3), 177-196.

Hetényi, M. (1946). *Beams on elastic foundations*, University of Michigan Press, Ann Arbor, MI.

Hoppe, E.J. (1999). *Guidelines for the use, design, and construction of bridge approach slabs*, Virginia Transportation Research Council, Charlottesville, VA.

Huang, Y.H., Lin, C., Deng, X. and Rose, J. (1984). *KENTRACK, A computer program for hot-mix asphalt and conventional ballast railway trackbeds*, Asphalt Institute, Lexington, KY.

Hunt, H.E.M. and Newland, D.E. (1996). "The effect of variable foundation properties on railway-track vibration." *Proceedings of the 4th International Congress on Sound and Vibration*, St. Petersburg, Russia, 1065-1072.

Hunt, H.E.M. (1997). "Settlement of railway track near bridge abutments." *Proceedings of the Institution of Civil Engineers*, Transportation, 123, Thomas Telford, 68-73.

Indraratna, B., Khabbaz, H., Salim, W., Christie, D. (2006). "Geotechnical properties of ballast and the role of geosynthetics in rail track stabilization." *Ground Improvement*, 10 (3), 91-101.

Iwnicki, S., ed. (1999). "The Manchester benchmarks for rail vehicle simulation." *Supplement to Vehicle Systems Dynamics*, 31, Swets & Zeitlinger B.V., Lisse, The Netherlands.

Iwnicki, S., ed. (2006). *Handbook of railway vehicle dynamics*, CRC Press, Boca Raton, FL.

Jenkins, H.H., Stephenson, J.E., Clayton, G.A., Morland, G.W., and Lyon, D. (1974). "The effect of track and vehicle parameters on wheel/rail vertical dynamic forces." *Rail Engineering Journal*, 3 (1), 2-16.

Jenks, C.W. (2006). "Design of track transitions." *Research Results Digest 79*, Transit Cooperative Research Program, Transportation Research Board, Washington DC.

Kalker, J.J. (1990). *Three-dimensional elastic bodies in rolling contact* (*Solid Mechanics and its Applications*), Springer, New York, NY.

Kalker, J.J. (1979). "Survey of wheel-rail rolling contact theory." *Vehicle System Dynamics*, 5, 317-358.

Kerr, A.D. (2002). "The determination of the track modulus k for the standard track analysis." *2002 AREMA Annual Conference*, Washington, DC, <http://www.arema.org/eseries/scriptcontent/custom/e_arema/library/2002_Conference_Proceedings/00010.pdf>.

Kerr, A.D., Shenton, H.W., (1985), "On the reduced area method for calculating the vertical track modulus," *American Railway Engineering Association Bulletin*, 86 (703), 416-429.

Knothe, K. and Grassie, S.L. "Modelling of railway track and vehicle/track interaction at high frequencies." *Vehicle System Dynamics*, 22, 209-262.

LDS. (2003). "Understanding FFT windows." *Application Note*, ANO 14, LDS-Group, Wallingford, CT.

Lee, M.L. and Chiu, W.K. (2005). "A comparative study on impact force prediction on a railway track-like structure." *Structural Health Monitoring*, 4 (4), 355-376.

Lei, X., and Mao, L. (2004). "Dynamic response analyses of vehicle and track coupled system on track transition of conventional high speed railway." *Journal of Sound and Vibration*, 271, 1133-1146.

Li, D., Read, D. and Chrismer, S. (1997). "Effects of heavy axle loads on soft-subgrade performance" *Technology Digest*, TD-97-020, July.

Li, D. (2000). "FAST load and subgrade environment." Presentation slides obtained from the author in July 2008, TTCI/AAR.

Li, D., Rose, J. and LoPresti, J. (2001). "Test of hot-mix asphalt trackbed over soft subgrade under heavy axle loads." *Technology Digest*, TD-01-009, April.

Li, D., Smith, L., Doe, B., Otter, D. and Uppal, S. (2003). "Study of bridge approach and track transition degradation - factors and mitigation." *Contract DTFR53-01-H-00305*, Federal Railroad Administration Washington, DC.

Li, D., Thompson, R., Marquez, P. and Kalay, S. 2004a. "Development and implementation of a continuous vertical track-support testing technique." *Transportation Research Record*, 1863, 68-73.

Li, D., Thompson, R. and Kalay, S. 2004b. "Update of TTCI's research in track condition testing and inspection," *Proceedings of AREMA 2004 Annual Conference*, Nashville,TN,<http://www.arema.org/eseries/scriptcontent/custom/e_arema/library/2004_Conference_Proceedings/00059.pdf> (October 30, 2009).

Li, D. and Davis, D. (2005). "Transition of railroad bridge approaches." *Journal of Geotechnical and Geoenvironmental Engineering*, 131 (11), 1392-1398.

Lim, W.L. (2004). "Mechanics of railway ballast behaviour." Ph.D. Thesis, University of Nottingham, UK.

Long, J.H., Olson, S.M., Stark, T.D. and Samara, E.A. (1998). "Differential movement at embankment-bridge structure interface in Illinois." *Transportation Research Record*, 1633, 53-60.

LoPresti, J. and Li, D. (2005). "Long-term performance of hot-mix asphalt over soft subgrade at FAST." *Technology Digest*, TD-05-035, December.

LS-DYNA, (2007), Description of LS-DYNA, <http://www.lstc.com/lsdyna.htm> (Jan. 7, 2007).

Livermore Software Technology Corporation (LSTC). (2007). LS-DYNA keyword user's manual, 1 (971), <http://www.lstc.com/pdf/ls-dyna_971_manual_k.pdf> (Jan. 7, 2007).

Lu, S. and Xuejun, D. (1998). "Dynamic analysis to infinite beam under a moving line load with uniform velocity." *Journal of Applied Mathematics and Mechanics*, English Edition, 19 (4), 367-373.

Lu, S., Hogan, C., Minert, B., Arnold, R., Farritor, S., GeMeiner, W. and Clark, W. (2007). "Exception criteria in vertical track deflection modulus." *Proceedings of ASME/IEEE Joint Rail Conference & Internal Combustion Engine Spring Technical Conference*, Pueblo, CO, 191-198.

Lu, S. (2008). "Real-time vertical track deflection measurement system." Ph.D. Dissertation, University of Nebraska, Lincoln.

Lundgren, L.R. and Martin, G.C. (1970). "A simulation of ballast support and the modulus of track elasticity." *Civil Engineering Studies*, Transportation Series No. 4, University of Illinois, Urbana, IL.

Lundqvist, A., Larsson, R. and Dahlberg, T. (2006). "Influence of railway track stiffness variations on wheel/rail contact force." *Workshop on Tracks for High-Speed Railways*, Porto, Portugal.

Mahmood, I.U. (1990). Evaluation of causes of bridge approach settlement and development of settlement prediction models. Ph.D. Thesis, University of Oklahoma, Norman.

Miller, G.A., The, S.Y., Li, D. and Zaman, M.M. (2000). "Cyclic shear strength of soft railroad subgrade." *Journal of Geotechnical and Geoenvironmental Engineering*, 126 (2), 139-147.

Namura, A. and Suzuki, T. (2007). "Evaluation of countermeasures against differential settlement at track transitions." *Quarterly Report of RTRI*, 48 (3), 176-182.

Norman, C., Farritor, S., Arnold, R. and Elias, S.E.G. (2003). "Preliminary design of a system to measure track modulus from a moving railcar," *Railway Engineering 2003,* <http://www.engineering.unl.edu/research/robots/publicationdocs/Railway_Engineering_2003_Farritor.pdf> (October 30, 2009).

Norman, C., Farritor, S., Arnold, R., Elias, S.E.G., Fateh, M. and El-Sibaie, M. (2004). "Design of a system to measure track modulus from a moving railcar." *Proceedings of the 2004 AREMA National Conference*, Nashville, TN, <http://www.arema.org/eseries/scriptcontent/custom/e_arema/library/2004_Conference_Proceedings/00015.pdf> (October 30, 2009).

NUCARS. (2009). "About NUCARS." <http://www.aar.com/nucars/index.asp> (May 5, 2009).

Oldknow, K. and Reiff, R. (2006). *Use of dynamic rail deflection as a means of determining changes in top of rail friction*, FRA, Washington, DC.

Plotkin, D., Davis, D.D., Gurule, S. and Chrismer, S.M. (2006). "Track transitions and the effects of track stiffness." *Proceedings of the AREMA 2006 Annual Conference*, Louisville, KY.

Plotkin, D. and Davis, D.D. (2008). *Bridge approaches and track stiffness*, FRA, Washington DC.

Pasternak, P.L. (1954). "On a new method of analysis of an elastic foundation by means of two foundation constants." *Gosudarstvennoe Izdatelstvo Literaturi po Stroitelstuve i Arkhitekture* (in Russian).

Raymond, G.P. (1977). "Ballast production control." Lecture Notes, Queens University, Australia,<http://civil.queensu.ca/people/faculty/raymond/Notes/845RailCourseNotes/7B-CONTR.pdf> (October 30, 2009).

Raymond, G.P. (1978). "Design for railroad ballast and subgrade support." *Journal of the Geotechnical Engineering Division*, ASCE, 104 (GT1), 45-60.

Read, D., Chrismer, S., Ebersohn, W. and Selig, E. (1994). "Track modulus measurements at the Pueblo soft subgrade Site." *Transportation Research Record 1470*, 55-64.

Read, D. and Li, D. (1995). "Subballast considerations for heavy axle load trackage." *Technology Digest*, TD95-028, December.

Redden, J.W.P., Selig, E.T. and Zaremsbki, A.M. (2002). "Stiff track modulus considerations: Stiff track modulus considerations, particularly where track is supported by a concrete floor, have to be factored into Alameda Corridor work – stiff railroad track surface work – Statistical Data Included." *Railway Track and Structures*, 98 (2), 21-23.

Reid, W.M. and Buchanan, N.W. (1984). "Bridge approach support piling." *Proceedings of the International Conference on Advances in Piling and Group Treatment for Foundations*, London, Thomas Telford, 267-274.

Reiff, R. and Sasaoka, C. (2003). "HAL revenue service monitoring." *TRB Workshop on Advance in Track Design, Construction and Maintenance,* <http://www.trbrail.com/pdfs/LTK/Session1TedSussman/Sess1Pres32Rev1TRB%202004%20main%20section%20rev%201-8.pdf> (October 30, 2009).

Ribeiro, C.A., Calçada, R. and Delgado, R. (2008). "Dynamic analysis of transition zones of high speed railway lines." *Proceedings of Noise and Vibration on High Speed Railways,* Porto, Portugal.

Robnett, Q.L., Thompson, M.R., Knutson, R.M. and Tayabji, S.D. (1975). "Development of a structural model and materials valuation procedures." *Report No. DOT-FRA-30038*, Ballast and Foundation Materials Research Program, University of Illinois, Urbana, IL.

Rose, J.G. and Konduri, K.C. (2006). "KENTRACK – A railway trackbed structural design program." *Proceedings of the 2006 AREMA Annual Conference*, Louisville, KY, <http://www.arema.org/eseries/scriptcontent/custom/e_arema/library/2006_Conference_Proceedings/015.pdf> (October 30, 2009).

Sasaoka, C.D. and Davis, D.D. (2005). "Implementing track transition solutions for heavy axle load service." *Proceedings of the AREMA 2005 Annual Conference*, Chicago, IL,<http://www.arema.org/eseries/scriptcontent/custom/e_arema/library/2005_Conference_Proceedings/00024.pdf> (October 30, 2009).

Sasaoka, C.D. (2006). "Track transition designs for heavy-axle-load service." *Railway Track & Structures*, 102 (4), 15-18.

Schneider, P.D. (2006). "Crossties: the tie that binds." *Trains Magazine*, May, < http://www.trains.com/trn/default.aspx?c=a&id=236> (October 30, 2009).

Selig, E.T. and Li, D. (1994). "Track modulus: its meaning and factors influencing it." *Transportation Research Record 1470*, National Academy Press, Washington, D.C., 47-54.

Selig, E.T., Waters, J.M. (1994). *Track geotechnology and substructure management*. Thomas Telford, London.

Seo, J. (2003). "The bump at the end of the bridge: An investigation." Ph.D dissertation, Texas A&M University, College Station.

Seo, J., Ha, H. and Briaud, J.-L. (2002). "Investigation of settlement at bridge approach slab expansion joint." *Technical Report 0-4142-2*, Texas Transportation Institute, College Station.

Shu, X. and Wilson, N. (2006). "NUCARS wheel/rail contact models and simulation results for FRA LD benchmark." *Report on FRA LD Benchmark Study*, Volpe National Transportation Systems Center.

Singh, S.P., Davis, D.D., Guillen, D. and Williams, D. (2004). *Reducing the adverse effects of wheel impacts on special trackwork foundations*, U.S. Department of Transportation, Federal Railroad Administration.

Skempton, A.W. (1959). "Cast-in-situ bored piles in London clay." *Geotechnique*, 9 (4), 153-173.

Solomon, B. (2006). *Working on the railroad*, Voyageur Press, St. Paul, MN.

Stark, T.D., Olson, S.M. and Long, J.H. (1995). "Differential movement at the embankment/structure interface – mitigation and rehabilitation," *Final Report*, Project IAB-H1, FY93, Illinois Transportation Research Center, Illinois DOT.

Steele, C.R. (1967). "The finite beam with a moving load." *Journal of Applied Mechanics*, 35 (4), 111-119.

Stewart, H.E. and Selig, E.T. (1982). "Predicted and measured resilient response of track," *Journal of the Geotechnical Engineering Division*, 108 (GT11), 1423-1442.

Stratman, B., Liu, Y. and Mahadevan, S. (2007). "Structural health monitoring of railroad wheels using wheel impact load detectors." *Journal of Failure Analysis and Prevention*, 7, 218-225.

Sun, L. (2001). "Closed-form representation of beam response to moving line loads." *Journal of Applied Mechanics*, Brief Notes, 68, 348-350.

Sun, Y.Q., Dhanasekar, M., and Roach, D. (2003). "A three-dimensional model for the lateral and vertical dynamics of wagon-track systems." *Proceedings Institution of Mechanical Engineers*, 217, Part F.

Sussman, T.R. and Selig, E.T. (1998). *Track component contributions to track stiffness*. E.T. Selig, Inc., Amherst, MA.

Talbot, A.N. (1918). "Stresses in railroad track," *Proceedings of the AREA, First Progress Report*, Reports of the Special Committee on Stresses in Railroad Track. 19, 873-1062.

Tanahashi, H. (2007). "Pasternak model formulation of elastic displacements in the case of a rigid circular foundation." *Journal of Asian Architecture and Building Engineering*, 6 (1), 167-173.

Terzaghi, K. (1943). *Theoretical soil mechanics*. John Wiley & Sons, New York.

Thompson, R. and Li, D. (2002). "Automated vertical track strength testing using TTCI's track loading vehicle." *Technology Digest*, TD-02-002.

Timoshenko, S. (1926). "Method of analysis of statical and dynamical stress in rail." *Proceedings of the 2nd International Conference for Applied Mechanics*, Zurich, 407-418.

Vlasov, V.Z. and Leont'ev, N.N. (1966). "Beams, plates and shells on elastic foundations." *Israel Program for Scientific Translations*, Jerusalem (Translated from Russian; original Russian version published in 1960).

Wahls, H.E. (1990). "Design and construction of bridge approaches." *NCHRP, Synthesis of Highway Practice 159*, Transportation Research Board, Washington, DC.

Wanek, M. (2006). "Special trackwork by design." *Railway Track and Structures*, 102 (7), 18-20.

Winkler, E. (1867). Die lehre von der elasticitaet und Festigkeit. H. Dominicus, Prague (in German).

Wu, T.X. and Thompson, D.J. (2001). "Vibration analysis of railway track with multiple wheels on the rail." *Journal of Sound and Vibration*, 239, 69-97.

Zarembski, A.M. and Choros, J. (1980). "On the measurement and calculation of vertical track modulus." *Proceedings American Railway Engineering Association*, 81, 156-173.

Zarembski, A.M. (1989a). "Distribution of vertical wheel loads: ballast and subgrade." Research Paper, Railway Tie Association, 71-72.

Zarembski, A.M. (1989b). "Track modulus characteristics." *Research Paper*, Railway Tie Association, 61-62.

Zarembski, A.M. (1989c). "Track modulus vs. track structure." *Research Paper*, Railway Tie Association, 59-60.

Zarembski, A.M. (1989d). "Track stiffness and impact." *Research Paper*, Railway Tie Association, 61-62.

Zarembski, A.M. and Bell, J.G. (2002). "Limiting the effects of high-speed dynamic forces on track structure: New method for evaluating equipment." *TR News 222*, Transportation Research Record.

Zhai, W.M., Cai, C.B., Wang, Q.C., Lu, Z.W. and Wu, X.S. (2001). "Dynamic effects of vehicles on tracks in the case of raising train speeds." *Proceedings of the Institution of Mechanical Engineers*, 215 (F), 125-135.

APPENDIX A

SURVEY QUESTIONNAIRE

TEXAS A&M UNIVERSITY

THE BUMP AT THE END OF A RAILWAY BRIDGE

QUESTIONNAIRE

Name of Respondent : _____

Title : _____

Company : _____

Phone No. : _____

Fax No. : _____

E-mail Address : _____

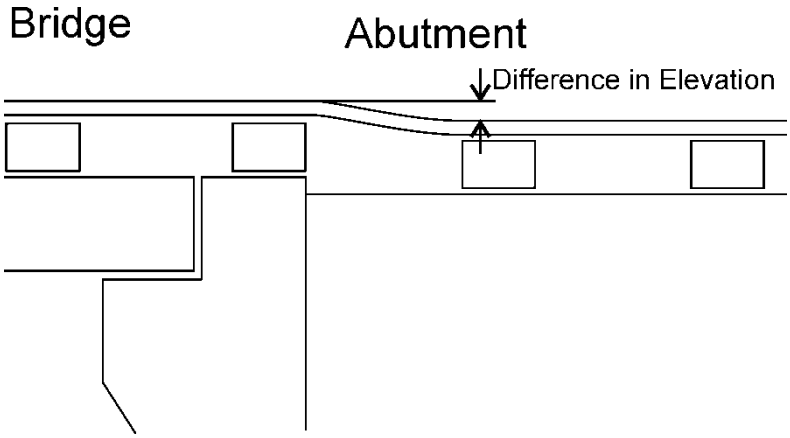

The objective of this survey is to collect data and opinions on the problem of the bump at the end of the railway bridge. This is part of a project sponsored by the Association of American Railroads. The bump is defined as the vertical difference in elevation which occurs at the interface between the railway bridge and the embankment.

1. How many bridges are you responsible for? _____

2. Have you encountered the problem of the bump at the end of the bridge? Please estimate the percentage of bridges that are affected by this condition:

   □ 0% □ 10% □ 20% □ 30% □ 40% □ 50% □ OTHER ___%

3. What is your estimate of the total maintenance cost per year on your railway for this problem including both internal and contracted maintenance?

   Estimated Total Maintenance Cost (per year): $_____
   Estimated Total Maintenance Cost (per million gross tons (MGT)) $_____

4. Among the bridges that are affected by the bump at the end of the bridge, what percentages have the following characteristics? If information is not available, please estimate.

a) Bridge Deck

Open Deck	____%
Ballasted deck	____%
Total	100 %

b) Approach Slab

Rigid (concrete) slab	____%
Flexible (asphalt) slab	____%
No approach slab	____%
Unknown	____%
Total	100 %

c) Bridge Deck

Shallow foundation (eg: spread footing)	____%
Deep foundation (eg: piles)	____%
Unknown	____%
Total	100 %

d) Skew

No skew	____%
Back of abutment skewed	____%
Skewed, back of abutment perpendicular to track in area under ties	____%
Skewed, unknown	____%
Total	100 %

e) Soil Used as Compacted Fill

Clay	_____%
Silt	_____%
Sand	_____%
Stabilized soil	_____%
Unknown	_____%
Total	100%

f) Foundation Soil

Clay	_____%
Silt	_____%
Sand	_____%
Unknown	_____%
Total	100%

g) Height of Approach Embankment

Less than 10 ft high	_____%
Greater than 10 ft high	_____%
Unknown	_____%
Total	100%

5. What is the typical bump size (difference in elevation) along the rail profile? _____

6. Over what horizontal longitudinal length does the bump typically occur along the rail profile?_____

7. How would you define a tolerable bump along the rail profile?

_____

_____

8. In your opinion, what is a tolerable slope for the bump along the rail profile? _____

9. What is the typical axle load of
   a) a freight railcar? _____
   b) a passenger car? _____
   c) a locomotive? _____

10. What methods do you use to detect the problem and how often do you use the methods?
    Please use the following scale: 1=often, 2=sometimes, 3=rarely, 4=not at all

    a) Visual inspection _____
    b) Ridability (subjective) _____
    c) Ridability (quantitative) _____
    d) Complaints from user _____
    e) Track geometry evaluation car _____
    f) Ride quality accelerometers _____
    g) Non-destructive tests (NDT) _____
    Please explain the test(s) used:

    _____

    h) Other; if other, please explain:

    _____

11. What are the common causes of the bump problems for your bridges?
    Please rank using: 1=most common, 2=frequent, 3=may be a factor, 4=never a factor

    a) Settlement of fill _____
    b) Loss of fill by erosion _____
    c) Poor drainage _____
    d) Poor fill material _____
    e) Settlement of natural soil under the fill _____
    f) Settlement of natural soil under the bridge abutment _____
    g) Too rigid a bridge foundation _____
    h) Differential settlement between bridge and fill _____
    i) Poor construction specifications _____

j) Poor construction practices _____
k) Lateral movement of the bridge abutment _____
l) Bridge type _____
m) Abutment type _____
n) Poor joints _____
o) Temperature cycle _____
p) Dynamic impact of cars _____
q) Poor compaction of ballast on fill _____
r) Other. If other, please explain: _____

12. In what cases does the problem appear to be worse? **Please comment:**

_____
_____

13. In what cases does the problem appear to be minimized? **Please comment:**

_____
_____

14. Are there any areas of the country which are worse than others?

□ YES □ NO If YES, please explain:

_____
_____

15. How and when do you decide to perform maintenance on a bridge or approach with this problem?

_____
_____

16. Does someone try to find the exact cause of the problem for a given bridge?

□ YES □ NO

17. What method do you use to repair the problem and how often do you use these methods?

Please use the following scale: 1=often, 2=sometimes, 3=rarely, 4=not at all

____ leveling by ballast tamping
____ mud jacking

____ drainage improvements
____ improve the properties of the fill (ex: grouting)
____ improve the properties of the natural soil under the fill
____ eliminate rail joints from the transition area
____ retrofit with an approach slab
____ remove and replace approach slab
____ OTHER, please explain below:

_____
_____

18. At what range of speeds do trains typically travel over bridges?
    Freight trains _____
    Passenger trains _____

19. Can you track any accidents back to the bridge bump problem?
    □ YES □ NO If YES, please describe below:
    _____

20. Is there anything your organization is doing from a procedural or managerial standpoint to improve or decrease the problem of the bridge bump?

    □ YES □ NO If YES, please describe below:
    _____
    _____

21. What can one do at the design stage to decrease the magnitude and frequency of the problem, and how important is each recommendation?

    Please rank by using: 1=most important, 2=important, 3=not very important, 4=not used
    ____ specify better backfill
    ____ use more rigorous compaction specifications
    ____allow for more settlement under the bridge abutment
    ____ place the bridge abutment on spread footings
    ____ design the bridge abutment and approach fill so they settle by approximately the same amount
    ____ better cooperation between the track maintenance supervisor and bridge maintenance supervisor
    ____ use a properly-designed approach slab
    ____ improve drainage provisions
    ____ design better joint at bridge-embankment connection
    ____ avoid open deck bridges
    ____ confine the approach fill parallel to track retaining walls

____ OTHER, please explain below:

_____

22. a) What can be done at the construction stage to decrease the problem and how important is each recommendation?

    Please rank by using: 1=most important, 2=important, 3=not very important, 4=not used
    ____ better compaction control of the fill
    ____ waiting period after the fill construction prior to pacing the abutment
    ____ install rubber pads under ties on bridge
    ____ install rubbed pads under ties on fill
    ____ improved abutment design
    ____ other unique or innovative methods to handle the problem

    b) If you are using unique or innovative methods or designs to handle the problem, please explain below:
    _____
    _____

    c) Would you be willing to share specifications or drawings pertaining to your solutions if requested?

    □ YES □ NO

23. Has your organization performed or sponsored any research, development, or training efforts in this area?

    □ YES □ NO If YES, please briefly describe these efforts and enclose copies of any available reports:

24. What research would help in minimizing the problem?

    _____
    _____

25. What organizations lead the way when it comes to avoiding or solving this problem?
    _____
    _____

26. Please list any other comments you might have regarding the bump at the end of the bridge.
    _____
    _____

APPENDIX B

SURVEY RESPONSES

As part of this project, a survey was sent out to various railway professionals around the world. A total of 22 questionnaires were distributed and 14 were returned with answers. The following companies are represented within this survey:

- Austrian Railways (AR)
- Canadian National (CN)
- Canadian Pacific Railway (CPR)
- FRA
- Norfolk Southern (NS)
- Queensland Rail (QR)
- TTCI
- Savage Industries/CANAC (SI/CANAC)
- Union Pacific (UP)

A summary of the survey is as follows:

1. How many bridges are you responsible for?
    - Average = 5,233 bridges
    - Low = 0 for Savage Industries/CANAC Consultant and for FRA
    - High = 17,842 for Union Pacific

2. Have you encountered the problem of the bump at the end of the bridge? Estimate the % of bridges affected by the bump.
    - Yes, Average = 51%

3. Estimate total maintenance cost on your railway for this problem including both internal and contracted maintenance:
    - Per year (Average): $2.55 million (Low = $300, High = $20 million)
    - Per MGT (Average): $6,042 (Low = $25, High = $18,000)

4. Among the bridges that are affected by the bump at the end of the bridge, what percentages have the following characteristics?
    - Bridge Deck
        1) Open deck: 69.5%
        2) Ballasted deck: 30.5%
    - Approach Slab
        1) Rigid (concrete) slab: 2.46%
        2) Flexible (asphalt) slab: 0.27%
        3) No approach slab: 97.08%
        4) Unknown: 0.19%
    - Type of foundation
        1) Shallow foundation (e.g. Spread footing): 19%
        2) Deep foundation (e.g. Piles): 78%

3) Unknown: 3%

- Skew
  1) No skew: 83%
  2) Back of abutment skewed: 10%
  3) Skewed, back of abutment perpendicular to track in area under ties: 6%
  4) Skewed, unknown: 1%
- Soil used as compacted fill
  1) Clay: 4%
  2) Silt: 3%
  3) Sand: 6%
  4) Stabilized soil: 13%
  5) Unknown: 74%
- Foundation soil
  1) Clay: 12%
  2) Silt: 5%
  3) Sand: 4%
  4) Unknown: 79%
- Height of approach embankment
  1) Less than or equal to 10 ft high: 56.55%
  2) Greater than 10 ft high: 43%
  3) Unknown: 0.45%

5. What is the typical bump size (difference in elevation) along the rail profile?
    - Average = 1.3”
    - Range = 1/4” – 4”

6. Over what horizontal length does the bump typically occur along the rail profile?
    - Average = 17.3’
    - Range = 4’ – 50’

7. How would you define a tolerable bump along the rail profile?
    - Average = 0.67”
    - Range = 0” – 3.25”
    - FRA 216.63 defines max runoff as 1.5” in 31’ and max deviation from the uniform profile as 2” in 62’

8. What is a tolerable slope for the bump along the rail profile?
    - Average: 1:253 (≈ 0.4%)
    - Range: 1:100 – 1:1333

9. What is the typical axle load of:
    - A freight railcar: 61.6 kips (average)
    - A passenger car: 32.7 kips (average)
    - A locomotive: 59.5 kips (average)

10. What methods do you use to detect the problem and how often do you use the methods?

→ 1 = often, 2 = sometimes, 3 = rarely, 4 = not at all

- Visual inspection: 1.1 (average)
- Ridability (subjective): 2.3 (average)
- Ridability (quantitative): 3.0 (average)
- Complaints from user: 2.2 (average)
- Track geometry evaluation car: 1.9 (average)
- Ride quality accelerometers: 3.6 (average)
- Non-destructive tests (NDT): 3.8 (average)
- Others:
  1) Measure track stiffness
  2) Use survey equipment to establish uniform profile

11. What are the common causes of the bump problems for your bridges?

→ 1 = most common, 2 = frequent, 3 = may be a factor, 4 = never a factor

- Settlement of fill: 1.9 (average)
- Loss of fill by erosion: 2.9 (average)
- Poor drainage: 2.2 (average)
- Poor fill material: 2.7 (average)
- Settlement of natural soil under the fill: 2.9 (average)
- Settlement of natural soil under the bridge abutment: 3.5 (average)

- Too rigid a bridge foundation: 3.0 (average)
- Differential settlement between bridge and fill: 2.4 (average)
- Poor construction specifications: 3.4 (average)
- Poor construction practices: 3.1 (average)
- Lateral movement of the bridge abutment: 3.7 (average)
- Bridge type: 2.6 (average)
- Abutment type: 2.9 (average)
- Poor joints: 2.6 (average)
- Temperature cycle: 3.1 (average)
- Dynamic impact of cars: 2.2 (average)
- Poor compaction of ballast on fill: 2.4 (average)
- Others:
    1) Poor surfacing
    2) Poor maintenance practices by bridge and track forces
    3) Not tamping approaches properly
    4) Difference in track modulus at transition between the bridge and approach structures

12. In what cases does the problem appear to be worse?

- Open deck bridges
- Concrete bridges with concrete ties
- Concrete approach ties

- With wet conditions
- With rail joints on/near bridge end
- Poor drainage
- Poor ballast condition
- Poor track tie condition
- Poor bridge bearing condition
- Bottom of grades with poor rail anchor patterns
- Where guardrail prohibits tamping
- In areas of little maintenance
- Settlement of fill
- Heavy haul
- Lack of ballast retainers

13. In what cases does the problem appear to be minimized?

- Ballast deck bridges
- Well maintained
- Good drainage
- Closely spaced approach ties
- Where tamping can be conducted through approach to bridge and across bridge
- Longer bridge approach ties in transition zone
- L-wall type ballast retainers

- Mild climate
- Good stabilized soil used as compacted fill
- Concrete as fill
- Where relieving slabs have been installed
- Concrete slabs

14. Are there any areas of the country which are worse than others? Yes:
    - >50 MGT routes regardless of geographic location
    - Southern, Midwest, and Northwest climates where annual rainfall is high and freeze thaw cycles occur
    - Areas where maintenance efforts are reduced due to traffic levels
    - Areas with poor quality, clay based formations

15. How and when do you decide to perform maintenance on a bridge or approach with a bump problem?
    - TTCI: FRA Safety & TTC/FAST Maintenance Limits and feedback from train crew - they go over the same spot 100+ times/day
    - UP: When ride quality deteriorates, when ties start to crush, or a condition is detected by bridge and track inspectors, geometry cars, or reports of poor ride from train crews;
    - NS: Track maintenance people decide
    - CPR: Following visual inspections and track geometry car runs

- CN: Following visual inspection, geometry car test results, and/or complaints
- AR: Due to information from inspection
- QR: Requirement is determined by visual inspection of the "hole" at the bridge end or when an exceedance is reported by track geometry car

16. Does someone try to find the exact cause of the problem for a given bridge?

    Typically, yes.

17. What method do you use to repair the problem and how often do you use these methods?

    → 1 = often, 2 = sometimes, 3 = rarely, 4 = not at all

    - Leveling by ballast tamping: 1.0 (average)
    - Mud jacking: 3.9 (average)
    - Drainage improvements: 2.1 (average)
    - Improve the properties of the fill (eg. Grouting): 3.7 (average)
    - Improve the properties of the natural soil under the fill: 3.6 (average)
    - Eliminate rail joints from the transition area: 1.5 (average)
    - Retrofit with an approach slab: 3.5 (average)
    - Remove and replace approach slab: 4.0 (average)
    - Others: 1.7 (average)

1) Track surfacing with a conventional RR track tamper
2) Retrofit track on bridge to match approach stiffness
3) Dig out mud, replace track ties and ballast
4) Install transition ties (longer bridge approach ties) to provide greater bearing area

18. At what range of speeds do trains typically travel over bridges:

- Freight trains: 0 mph – 79 mph (Average = 50 mph)
- Passenger trains: 25 mph – 100 mph (Average = 65 mph)

19. Can you track any accidents back to the bump problem?

- No

20. Is there anything your organization is doing to improve or decrease the problem? What?

- TTCI: Research and testing
- UP: Installation of VTI equipment (vertical accelerometers) in locomotives on select corridors and identifying locations that need repair by investigating locations that are detected by these ride indicator, modifying details for guardrail installations to allow tamping up to backwall, and eliminating joints on and/or near bridges

- AREMA: AREMA Committee 7 (Timber Structures) is working on the bump problem
- NS: We use 10' ties off open deck bridge ends (Typically, ties range from 8’ to 9’ in length)
- CPR: Track crews tamp low bridge approaches typically when track geometry data indicates "bump" greater than 5/8"
- CN: Better understanding of problem, improved inspection practice, and installation of L-walls to retain ballast
- QR: Ensure track resurfacing gangs lift and pack sleepers away from the bridge approaches

21. What can one do at the design stage to decrease the magnitude and frequency of the problem and how important is each recommendation?

→ 1 = most important, 2 = important, 3 = not very important, 4 = not used

- Specify better backfill: 1.8 (average)
- Use more rigorous compaction specifications: 1.8 (average)
- Allow for more settlement under the bridge abutment: 3.4 (average)
- Place the bridge abutment on spread footings: 3.6 (average)
- Design the bridge abutment and approach fill so they settle by approximately the same amount: 3.2 (average)
- Better cooperation between the track maintenance supervisor and bridge maintenance supervisor: 1.3 (average)

- Use a properly designed approach slab: 2.7 (average)
- Improve drainage provisions: 1.5 (average)
- Design better joint at bridge-embankment connection: 2.3 (average)
- Avoid open deck bridges: 1.6 (average)
- Confine approach fill parallel to track retaining walls: 2.2 (average)
- Others: 2.0 (average)
    1) Avoid skew, particularly for open deck bridges.

22. What can be done at the construction stage to decrease the problem and how important is each recommendation:

→ 1 = most important, 2 = important, 3 = not very important, 4 = not used

- Better compaction control of the fill: 1.5 (average)
- Waiting period after the fill construction prior to placing the abutment: 2.9 (average)
- Install rubber pads under ties on bridge: 2.5 (average)
- Install rubber pads under ties on fill: 3.4 (average)
- Improved abutment design: 2.7 (average)
- Others: 2.2 (average)
    1) Geo-piers (stone columns) proved effective in one test installation (TTCI)
    2) Longer bridge approach transition ties to improve bearing
    3) Prevent ballast runoff at approaches by installing L-walls

4) Reducing sleeper spacing
5) Reducing ballast depth with a layer of Geogrid

23. Has your organization performed or sponsored any research, development, or training efforts in this area?

- All yes except CPR, Austrian Railways, and Queensland Rail

24. What research would help in minimizing the problem?

- Design track for a maintainable ramp (not a bump)
- Actual tests to determine thresholds both that can be physically measured by inspector/geometry car and allowable vertical accelerations such as the VTI system being used now on Critical Coal routes on the UP
- Comprehensive research with different combinations of backfill conditions and different methods of stabilizing backfill soils
- Additional research is needed to develop the true forces that are impacting the bridge structure with low approaches in order to justify the changes in maintenance practices or develop other corrective action items
- Research into means of minimizing track structure stiffness variation from approach track to track on open deck bridges
- Slab construction, winy walls, fill compaction

25. What organizations lead the way when it comes to avoiding or solving this problem?

    - AAR/TTCI
    - AREMA
    - UIC
    - Russia?

26. Please list any other comments you might have regarding the bump at the end of the bridge.

    - What is needed: Accommodation of differential settlement - We need a ramp, not a bump.
    - With new construction, the bump seems unavoidable. RR bridges are almost always built on pile foundations that do not settle. But new track construction in areas with wet moist soil will be subject to consolidation over a prolonged period as tonnage accumulates
    - If drainage issues are addressed, and methods devised to provide a consistent modulus across this transition, most of the issues could be easily addressed.
    - New specifications for approach slabs would be of great benefit, however, the major problem facing the maintenance engineer today is to address all of the structures that have bumps with no work scheduled.

- Solution related to addressing various factors that promote bridge approach sag such as stabilizing slope and eliminating loss of ballast, installation of good ballast on adequately compacted and well drained soil, greater distribution of traffic loads on longer ties and elimination of abrupt changes in track modulus, etc.
- Need a tamper capable of working up to the bridge abutment
- QR uses a guard rail and splay rail design off the ends of ballasted bridges to minimize risks from derailment. The design is intended to redirect derailed wheels onto the sleepers so a derailed wheelset does not go over the side of the bridge. This design involves two extra rails fastened to the sleepers between the running rails. The extra track stiffness from this design probably helps with the transition at the end.

Estimated Costs

The following are responses to questions 1, 2, and 3

Company	Number of Bridges	Percent Affected	No. Affected Bridges	Est. Annual Maint. Cost	Est. Maint. Cost per MGT
TTCI	4	75%	3	$300	$25
TTCI	3			$10,000	$100
UP	3,490	75%	2,618	$25,000 - $50,000	
UP	17,842	40%	7,137	$20,000,000	$18,000
UP	3813	50%	1,907	$150,000 - $200,000	
UP	300+	50%	150+	$100,000	
UP	7,240	10%	724		
FRA		80%		$575/approach	
NS	10,801	50%	5,401		
CPR	2,300	40%	920	$1,500,000	
CN	8,000	50%	4,000		
SI/CANAC		50%			
AR	6000	10%	600	$1,000,000	
QR	3000	80%	2400	$120,000	
TOTAL	62,793		25,858	$22,942,800	
AVERAGE	5,233	51%	2,351	$2,549,200	$6,042

Characteristics of Bridges Affected by the Bump Problem

The following are responses to question 4, about the percentages of bridges affected by the bump problem with the following characteristics

	Bridge Deck		Approach Slab				Type of Foundation		
Company	Open	Ballasted	Rigid	Flexible	None	Unknown	Shallow	Deep	Unknown
TTCI	33%	67%	0%	0%	100%	0%	0%	100%	0%
TTCI	33%	67%	0%	0%	100%	0%	0%	100%	0%
UP	95%	5%	0%	0%	100%	0%	0%	100%	0%
UP	75%	25%	0%	0%	100%	0%	15%	85%	0%
UP	90%	10%	0%	2.5%	95%	2.5%	10%	90%	0%
UP	80%	20%	5%	0%	95%	0%	25%	75%	0%
UP	83%	17%	0%	0%	100%	0%	15%	75%	10%
FRA			0%	0%	100%	0%			
NS	90%	10%	0%	0%	100%	0%			
CPR	85%	15%	0%	0%	100%	0%	10%	90%	0%
CN	70%	30%	5%	0%	95%	0%	40%	40%	20%
SI/CANAC									
AR	40%	60%	2%	1%	97%	0%	75%	25%	0%
QR	60%	40%	20%	0%	80%	0%			
AVERAGE	69.5%	30.5%	2.46%	0.27%	97.08%	0.19%	19.0%	78.0%	3.0%

	Skew				Height of Approach Embankment		
Company	No skew	Back of abutment skewed	Skewed, back of abutment ⊥ to track in area under ties	Skewed, Unknown	≤ 10'	> 10'	Unknown
TTCI	100%	0%	0%	0%	67%	33%	0%
TTCI	100%	0%	0%	0%			
UP	95%	3%	0%	2%	50%	50%	0%
UP	90%	5%	5%	0%	60%	40%	0%
UP	90%	5%	0%	5%	50%	50%	0%
UP	40%	20%	40%	0%			
UP	95%	0%	0%	5%	70%	30%	0%
FRA					95%	5%	0%
NS	50%	40%	10%	0%	30%	70%	0%
CPR	90%	0%	10%	0%	10%	90%	0%
CN	85%	15%	0%	0%	70%	25%	5%
SI/CANAC							
AR	80%	20%	0%	0%	70%	30%	0%
QR					50%	50%	0%
AVERAGE	83%	10%	6%	1%	56.55%	43.00%	0.45%

	Soil used as compacted fill					Foundation Soil			
Company	Clay	Silt	Sand	Stabilized Soil	Unknown	Clay	Silt	Sand	Unknown
TTCI	0%	0%	0%	0%	100%	0%	0%	0%	100%
TTCI UP	0%	0%	0%	0%	100%	0%	0%	0%	100%
UP	10%	8%	5%	2%	75%	10%	10%	5%	75%
UP	20%	0%	5%	0%	75%	25%	0%	25%	50%
UP	10%	0%	50%	25%	15%	70%	30%	0%	0%
UP	0%	0%	0%	0%	100%	0%	0%	0%	100%
FRA	0%	0%	0%	0%	100%	0%	0%	0%	100%
NS	0%	0%	0%	0%	100%	0%	0%	0%	100%
CPR	0%	0%	0%	0%	100%	0%	0%	0%	100%
CN	5%	20%	5%	20%	50%	10%	10%	10%	70%
SI/CANAC AR QR	0%	0%	0%	100%	0%	20%	5%	5%	70%
AVERAGE	4%	3%	6%	13%	74%	12%	5%	4%	79%

Bump Size and Tolerable Slope

The following are responses to questions 5, 6, 7, and 8

Company	Typical Bump Size	Horizontal Length Bump Occurs Along	Tolerable Bump Size	Tolerable Slope
TTCI	Varies	Varies		Varies
TTCI	3/4"	40'		1:240
UP	1.5" - 3"	5' - 10'	< 1"	1:360
UP	1" - 3"	5' - 20'	1/2" - 3.25"	1:744
UP	1" - 2"	10' - 20'		1:105
UP	1" - 4"	20'	< 1"	1:600
UP	3/4"	4'		1:240
FRA	3/4" - 1.5"	5' - 6.7'	0"	
NS	2"	20'	0"	
CPR	1/4" - 3/4"	10' - 20'	< 1/4"	1:1920
CN	1/2" - 3/4"	10'	1/2" - 3/4"	1:100
SI/CANAC	Varies	≤ 50'		
AR	2 cm	2.5 m		1:3333
QR	10mm - 15mm	4m - 6m	15mm	1:200
RANGE	1/4" - 4"	4' - 50'	0" - 3.25"	1:100 - 1:3333
AVERAGE	1.3"	17.3'	0.67"	1:253

Typical Axle Loads

The following are responses to question 9

Company	Freight Railcar	Passenger Car	Locomotive
TTCI	79 kips		68 kips
TTCI	39 kips	25 kips	33 kips
UP	70 kips		60 kips
UP	72 kips	50 kips	70 kips
UP	71.5 kips		68 kips
UP			
UP			
FRA	71.5 kips - 78.75 kips		
NS			
CPR	70 kips		70 kips
CN	71.5 kips	25 kips	67 kips
SI/CANAC	15 kips - 74 kips	30 kips	66 kips
AR	20 tonnes - 22.5 tonnes	10 tonnes - 15 tonnes	24.5 tonnes
QR	15 tonnes - 20 tonnes	15 tonnes - 20 tonnes	15 tonnes - 20 tonnes
AVERAGE	61.6 kips	32.7 kips	59.5 kips

Inspection and Detection Methods

The following are responses to question 10

(Low values are most common; high values are least common)

Company	Visual Inspection	Ridability (Subjective)	Ridability (Quantitative)	Complaints from User
TTCI	1	1	3	4
TTCI	1	1	2	1
UP	1	4	4	2
UP	1	2	2	1
UP	1	3	2	2
UP	1	1	4	2
UP	1	2	2	1
FRA	1	4	4	1
NS	1	1	1	3
CPR	1	4	4	4
CN	1	2	3	2
SI/CANAC	2	2	4	1
AR	1	3	3	4
QR	1	2	4	3
AVERAGE	1.1	2.3	3.0	2.2

Company	Track Geometry Evaluation Car	Ride Quality Accelerometers	NDT	Other
TTCI	2	3	2	
TTCI	2	3	3	Measure Track Stiffness
UP	3	4	4	
UP	2	3	4	Survey Equipment
UP	2	2	4	
UP	2	4	4	
UP	2	4	4	
FRA	4	4	4	
NS	1	3	4	
CPR	1	4	4	
CN	1	4		
SI/CANAC	1	4	4	
AR	1	4	4	
QR	2	4	4	
AVERAGE	1.9	3.6	3.8	

Common Causes of the Bump Problem

The following are responses to question 11

(Low values are most common; high values are least common)

Company	Setl of Fill	Loss of Fill	Poor Drain	Poor Fill Mat	Setl Under Fill	Setl Under Abut	Too Rigid Found	Diff Setl	Poor Const Spec	Poor Const Pract	Lat Mvmt of Abut	Brid Type
TTCI	2	4	4	4	3	4	1	2	3	3	4	3
TTCI	1	4	4	4	4	4	4	1	4	4	4	4
UP	3	3	1	3	3	3	3	3	4	3	4	3
UP	2	3	1	1	2	3	3	1	3	3	3	2
UP	3	3	1	3	3	3	3	3	4	3	4	2
UP	2	3	2	2	4	4	2	4	4	4	4	2
UP	2	3	2	2	2	3	4	2	3	3	4	2
FRA	1	1	3	3	4	4	4	2	2	2	4	2
NS	1	4	1	3	2	3	4	3	3	3	3	3
CPR	3	4	3	3	3	4	2	1	3	3	4	2
CN	2	3	3	3	3	3	1	2	4	3	3	3
SI/CANAC	3	2	2	3	3	4	4	2	3	3	3	3
AR	1	3	3	3	3	3	3	3	4	3	4	3
QR	1	1	1	1	1	4	4	4	4	4	4	
AVERAGE	1.9	2.9	2.2	2.7	2.9	3.5	3.0	2.4	3.4	3.1	3.7	2.6

Company	Abut Type	Poor Joints	Temp Cycle	Dyn Impact of Cars	Poor Comp of Ballast on Fill	Other
TTCI	3	2	4	3	3	
TTCI	4	3	3	3	3	
UP	3	2	3	2	2	
UP	2	2	3	2	3	
UP	3	2	3	2	2	
UP	3	1	3	1	1	
UP	3	4	3	2	2	
FRA	2	2	4	3		Poor maint prac by brid & trck forces, not tamp apprch prop
NS	3	3	3	3	3	Poor surfacing
CPR	3	4	4	2	2	
CN	3	2	2	3	3	
SI/CANAC	3	3	1	1	2	Diff in trck mod at trans btwn brid & app struct
AR	3	4	4	3	4	
QR				1	1	
AVERAGE	2.9	2.6	3.1	2.2	2.4	

Comments Related to Causes of Bumps

The following are responses to questions 12, 13, and 14

Worst Cases:	Concrete bridges with concrete ties
Minimized Cases:	Softer ties (timber, ties with pads) -- Compaction and consolidation of the approach backfill -- Broad gentle embankment slopes -- Good quality backfill -- Good drainage -- Lack of rainfall
Worst Cases:	Wet conditions -- Rail joints on bridge
Minimized Cases:	Design lift tamping -- Lower stiffness track on bridge
Worst Cases:	Poor drainage -- Poor ballast condition -- Poor track tie condition -- Poor bridge bearing condition -- Occasionally, poor rail or joint conditions -- Bottom of grades with poor rail anchor patterns
Minimized Cases:	Good drainage -- Good ballast -- Good track ties -- Good bearings -- Good rail and anchors
Worst Locations:	H.A.L. and > 50 MGT routes, regardless of geographic location
Worst Cases:	Areas of little track maintenace -- Concrete approach ties -- Poor drained ballast sections -- Rail joints near bridge end
Minimized Cases:	Ballast deck bridge ends -- Well maintained track structure -- Well drained ballast sections --Bridge approaches with closely spaced track ties (< 22")
Worst Locations:	Southern, Midwest, and Northwest climates where annual rainfall is high and freeze thaw cycles occur
Worst Cases:	Areas where pumping occurrs due to poor drainage -- Rail joints at end of bridge -- Where guardrail prohibits tamping
Minimized Cases:	Ballast deck bridges w/o guardrail -- Guardrail details so that tamping can be done up to backwall
Worst Locations:	Areas where moisture is abundant -- Areas w/hard winters causing problems at spring thaw
Worst Cases:	Solid structures with approaches on fills
Minimized Cases:	Ballast Deck Bridges
Worst Locations:	Northern climates where freeze/thaw cycles occur -- Type and frequency of traffic are factors
Worst Cases:	Areas of little maintenance -- Concrete approach ties
Minimized Cases:	Well maintained -- Good drainage -- Closely spaced approach ties
Worst Cases:	Areas of little maintenance
Worst Locations:	Where proper maintenance is not followed
Worst Cases:	Poor drainage
Minimized Cases:	Good drainage -- Good maintenance -- Ballast deck bridges
Worst Cases:	Open deck bridges
Minimized Cases:	Ballasted deck bridges - Ability for track machinery to tamp and compact through approach to bridge and across bridge
Worst Locations:	Areas where maintenace efforts are reduced due to traffic levels
Worst Cases:	Reduced shoulder width -- Poor ballast -- Lack of ballast retainers
Minimized Cases:	Longer bridge approach ties in transition zone -- L-wall type ballast retainers
Worst Locations:	Areas where poor soil conditions and drainage exist
Worst Cases:	Where ballast is poor and scant -- Climate is wet and there is a lot of frost
Minimized Cases:	Where ballast is ample and of good quality -- fill material is adequate -- Fill wide enough -- Climate is mild and dry
Worst Locations:	The worst areas are those with damp climates -- Worst of all are permafrost locations where the bridge itself heaves, even if founded on piles
Worst Cases:	Settlement of fill
Minimized Cases:	Good stabilized soil used as compacted fil -- concrete as fill -- concrete slab
Worst Cases:	Heavy haul
Minimized Cases:	Where relieving slabs have been installed
Worst Locations:	Areas with poor quality, clay based formations

Comments Related to Detection and Maintenance

The following are responses to questions 15 and 16

How and when maintained:	FRA Safety & TTC/FAST Maintenance Limits -- Feedback from train crew
Try to find problem?	Yes
How and when maintained:	When we start to crush ties or timber -- Drive bearings into the foundation
Try to find problem?	Yes
How and when maintained:	When ride quality deteriorates -- Condition is detected by bridge and track inspectors, geometry cars, or reports of poor ride from train crews
Try to find problem?	Yes
How and when maintained:	When ride becomes an issue -- When ties at end of bridge, both on bridge and approach, are becoming damaged (crushed) or will not hold spikes or maintain line
Try to find problem?	Yes
How and when maintained:	When it affects train speeds and rideablity
Try to find problem?	No
How and when maintained:	Reports from geometry car, bridge inspector, track inspector
Try to find problem?	No
How and when maintained:	Track maintenance people decide
Try to find problem?	Yes
How and when maintained:	Following visual inspections and track geometry car runs
Try to find problem?	Yes
How and when maintained:	Following visual inspection, geometry car test results, and/or complaints
Try to find problem?	Sometimes
How and when maintained:	Local decision -- Track geometry car -- FRA track safety limits
Try to find problem?	Rarely, unless it is unusally bad and is causing operating problems
How and when maintained:	Due to information from inspection
Try to find problem?	Yes
How and when maintained:	Typical treatment is tamping -- Requirement is determined by visual inspection of the “hole” at the bridge end or when an excedance is reported by track geometry car
Try to find problem?	No

Common Repair Methods

The following are responses to question 17

(Low values are most common; high values are least common)

Company	Ballast Tamp	Mud Jack	Drain Imprvmt	Fill Imprvmt	Soil Imprvmt	Elim Rail Joints	Retrofit w/App Slab	Remove/ Replace App Slab	Other
TTCI									1
TTCI	1	4	3	4	4	1	4	4	1
UP	1	4	1	4	3	1	4	4	1
UP	1	4	2	4	4	1	4	4	
UP	1	4	2	4	4	1	3	4	
UP	1	4	3	4	4	1	3	4	
UP	1	4	3	4	4	1	4	4	
FRA									
NS	1		2	3	4	2	4		
CPR	1	3	2	3	4	1	4	4	
CN	1								1
SI/CANAC	1	4	2	3	4	2	4	4	2
AR	1	4	2	4	4	4	4	4	4
QR	1	4	1	4	1	1	1		
AVERAGE	1.0	3.9	2.1	3.7	3.6	1.5	3.5	4.0	1.7

Train Speeds Over Bridges

The following are responses to question 18

Company	Freight Trains	Passenger Trains
TTCI	40 mph	
TTCI	40 mph	40 mph
UP	60 mph	70 mph
UP	70 mph	79 mph
UP	60 mph	70 mph
UP	50 - 70 mph	70 mph
UP	60 mph	70 mph
FRA	0 - 79 mph	
NS	50 mph	70 mph
CPR	25 mph	
CN	25 - 65 mph	25 - 100 mph
SI/CANAC		
AR	60 - 120 km/h	80 - 160 km/h
QR	40 - 100 km/h	40 - 100 km/h
RANGE	0 - 79 mph	25 - 100 mph
AVERAGE	50 mph	65 mph

Organizational Methods to Reduce Problem

The following are responses to questions 19 and 20

Company	Accidents Related to Bump Problem?	Improvements/Methods to Decrease the Bump Problem
TTCI	NO	Research and testing
TTCI	NO	
UP	NO	Geometry car -- Rolling stock sensors to measure g-forces on equipment -- Inspection findings and reports
UP	NO	Installation of VTI equipment (vertical accelerometers) in locomotives on select corridors -- Identifying locations that need repair as detected by these ride indicators
UP	NO	Equipping engines to detect significant ride issues -- Modifying details for guardrail installations to allow tamping up to backwall -- Eliminating joints on and/or near bridges
UP	NO	Vigilant Track inspection and reporting -- Regular surfacing of track structure
UP	NO	Installation of vertical accelerometers to certain locomotives to start identifying locations needing repair
FRA		AREMA Committee 7 (Timber Structures) is working on the problem
NS	NO	Use 10' ties off open deck bridge ends
CPR	NO	Track crews tamp low bridge approaches typically when track geometry data indicates "bump" greater than 5/8"
CN	NO	Better understanding of problem -- Improved inspection practice -- Installation of L-walls to retain ballast
SI/CANAC		
AR	NO	
QR	NO	Ensure track resurfacing gangs lift and pack sleepers away from the bridge approaches

Common Design Procedures to Reduce Bump Problem

The following are responses to question 21

(Low values are most common; high values are least common)

Company	Spec Better Backfill	Use More Compact	Allow More Setl	Sprd Footgs	Design for Setl	Better Coop
TTCI	2	2	4	4	4	2
TTCI					1	
UP	2	2	3	3	2	1
UP	1	1	4	4	4	1
UP	2	2	3	3	2	1
UP	2	1	3	3	4	1
UP	2	2	3	3	3	1
FRA						
NS	2	2	3	4	4	2
CPR	2	2	3	4	4	1
CN	2	2	3	3	4	2
SI/CANAC	2	2	4	4	4	1
AR	1	2	4	4	2	2
QR	2	2	4	4	4	1
AVERAGE	1.8	1.8	3.4	3.6	3.2	1.3

Company	Use App Slab	Impr Drain	Better Joints	Avoid Open Deck	Confine App Fill	Other
TTCI		2	3		2	2
TTCI			2		2	
UP	3	1	1	1	2	
UP	2	2	2	1	2	
UP	2	1	1	1	2	
UP	2	1	2	2	3	
UP	2	2	2	1	2	
FRA						
NS	4	1		2	4	
CPR	4	2	3	1	1	
CN	4	2	4	2	2	
SI/CANAC	4	2	2	2	3	
AR	2	1	2	3	2	
QR	1	1	4	2	2	
AVERAGE	2.7	1.5	2.3	1.6	2.2	2.0

Common Construction Controls to Reduce Bump Problem

The following are responses to question 22

(Low values are most common; high values are least common)

Company	Better Compact Control	Waiting Period	Rubber Pads On Bridge	Rubber Pads on Fill	Impr Abut Design	Other
TTCI	1	3	2	4	2	2
TTCI	2	4	3		2	
UP	1	2	3	3	3	2
UP	1	3	2	3	2	
UP	1	4	2	2	3	2
UP	1	2	1	4	3	2
UP	2	3	2	3	2	
FRA						
NS	1	3	2	4	3	
CPR	1	4	4	4	2	
CN	2	3	2	4	3	1
SI/CANAC	2	2	2	3	3	
AR	2	3	3	3	3	4
QR	2	2	4	4	4	
AVERAGE	1.5	2.9	2.5	3.4	2.7	2.2

Comments Related to Repair, Design, and Construction

The following are responses to questions 17, 21, and 22

Other methods to repair bump problem:	Track surfacing with a conventional RR track tamper
Other design procedures:	Avoid skew, particularly for open deck bridges -- This leads to ties partially supported on the bridge, partially on the embankment -- It also lengthens the distance that is difficult or impossible to surface using conventional tamping machines.
Other construction controls:	Geo-piers (stone columns) proved effective in one test installation
Other methods to repair bump problem:	Lift approaches -- Retrofit track on bridge to match approach stiffness
Other methods to repair bump problem:	Dig out mud, replace track ties and ballast
Other methods to repair bump problem:	Install transition ties (longer bridge approach ties) to provide greater bearing area
Other construction controls:	Longer bridge approach transition ties to improve bearing -- Prevent ballast runoff at approaches by installing L-walls
Other methods to repair bump problem:	Install bridge approach ties as per AREMA Plan 913-02
Other design procedures:	Reducing sleeper spacing and reducing ballast depth with a layer of Geogrid have been used with only marginal success -- Greatest success from the use of relieving slabs

Comments Related to Research and Leading Organizations

The following are responses to questions 24, 25, and 26

Leading organizations:	AAR/TTCI and their affiliated lab universities
Miscellaneous Comments:	With new construction, the bump seems unavoidable -- RR bridges are almost always built on pile foundations that do not settle, but new track construction in areas with wet, moist soil will be subject to consolidation over a prolonged period as tonnage accumulates
Research Suggestions:	Designing track for a mantainable ramp
Miscellaneous Comments:	Accommodate for differential settlement -- We need a ramp, not a bump
Research Suggestions:	Actual tests to determine thresholds both that can be physically measured by inspector/geometry car and by allowable vertical accelerations such as the VTI system being used now on Critical Coal routes on the UP
Leading organizations:	TTCI
Research Suggestions:	Need comprehensive research with different combinations of backfill conditions and different methods of stabilizing backfill soils
Miscellaneous Comments:	If drainage issues are addressed, and methods devised to provide a consistent modulus across this transition, most of the issues could be easily addressed
Leading organizations:	AREMA
Research Suggestions:	Additional research is needed to develop the true forces that are impacting the bridge structure with low approaches to justify changes in maintenance practices or develop other corrective action items
Leading organizations:	AREMA
Miscellaneous Comments:	New specifications for approach slabs would be of great benefit, however, the major problem facing the maint. engr. today is to address all of the structures that have bumps with no work scheduled.
Research Suggestions:	Research into means of minimizing track structure stiffness variation from approach track to track on open deck bridges
Leading organizations:	AAR/TTCI
Research Suggestions:	Testing of various materials that could provide a decreasing track modulus at the end of the bridge equivalent to that off the bridge
Leading organizations:	AAR/TTCI
Miscellaneous Comments:	Solution related to addressing various factors that promote bridge approach sag such as stabilizing slope and eliminating loss of ballast, installation of good ballast on adequately compacted and well drained soil, greater distribution of traffic loads on longer ties, and elimination of abrupt changes in track modulus, etc. -- Need a tamper capable of working up to the bridge abutment
Leading organizations:	The only large failway system I know that copes with track settlement and frost action on a large scale is that in Russia, but I don't know if the Russians are any more successful in dealing with it on a practical bassis than we are
Miscellaneous Comments:	It seems that bumps at the ends of bridges are like the weather, everybody talks about them but nobody does anything about them
Research Suggestions:	Slab construction -- Winy walls -- Fill compaction
Leading organizations:	UIC
Research Suggestions:	The problem appears to be related to differential stiffness, particularly when moving from transom top bridge to ballasted formation -- Research into track designs that help transition stiffness may be beneficial
Leading organizations:	Unknown, but suggest organizations that have a uniform track structure from formation to bridges (e.g. ballasted track or slab track have less of a problem compared with ballasted track to open deck bridges)
Miscellaneous Comments:	QR uses a guard rail and splay rail design off the ends of ballasted bridges to minimise risks from derailment -- The design is intended to redirect derailed wheels onto the sleepers so a derailed wheelset does not go over the side of the bridge -- This design involves two extra rails fastened to the sleepers between the running rails -- The extra track stiffness from this design probably helps with the transition at the bridge end

APPENDIX C

MATLAB FFT CODE

```
%Jennifer Nicks - 2009
%FFT on simulation signals
clear all
close all
%%%%%%%%%%%%%%%%%%%%%%%%%%%%%%%%%%%%%%%%%%%%%%%%%%%%%%%%%%%%%%%%%%%%%%%%%%%%%%%
%%%%

ForceSignal;    %Calls the m-file with input data from simulations(x)
Fs=2000;        %Samping rate - Data at every 0.0005 seconds = 2000 Hz
N=length(x);    %The number of data points in x
window=hann(N); %Define the Hanning window
x2=x-mean(x);
x1=x2.*window';


T=N/Fs;             %Total length of time for the input signal

%Takes the FFT of the signal:
X=abs(fft(x1,N))/N;  %Normalize the data

figure
%Plot the signal
plot((1:N)/Fs,x,(1:N)/Fs,x1)
hold on
figure
plot((1:N)*Fs/N,X(1:N))

%%%%%%%%%%%%%%%%%%%%%%%%%%%%%%%%%%%%%%%%%%%%%%%%%%%%%%%%%%%%%%%%%%%%%%%%%%%%%%%
%%%%
```

APPENDIX D

TRACK RESPONSE PLOTS: TRACK MODULUS TRANSITION

No Slope – Reference Case 361

No Slope – Off Of 363

No Slope – 15.6 m/s (35 mph) 365

No Slope – 33.5 m/s (75 mph) 367

No Slope – 44.7 m/s (100 mph) 369

No Slope – 10^3 Cycles 371

No Slope – 10^6 Cycles 373

No Slope – 10^9 Cycles 375

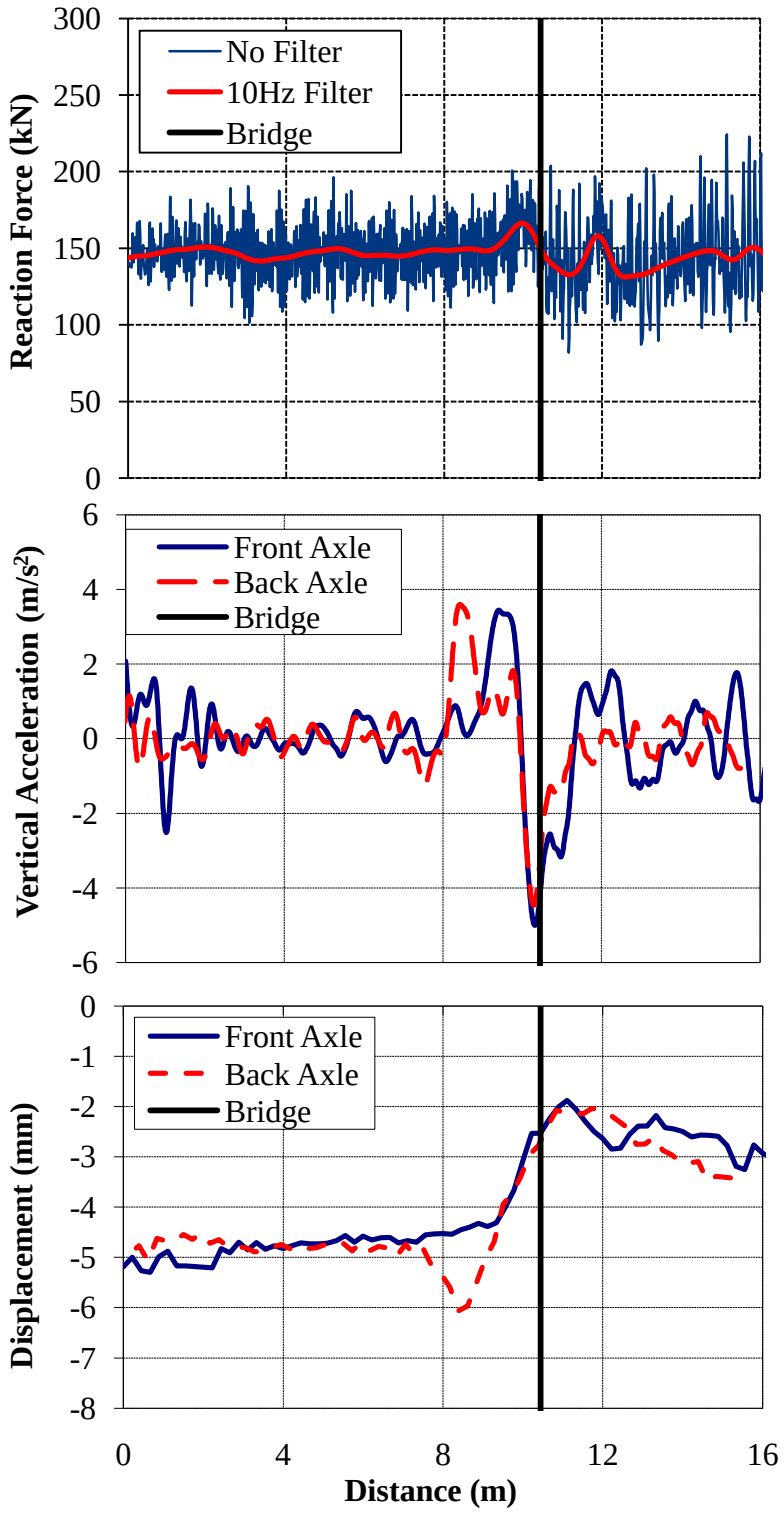

Figure D.1 - (a) Wheel/Rail forces (b) Axle accelerations and (c) Track deflection for No Slope at a bridge/approach location (v = 22.2 m/s)

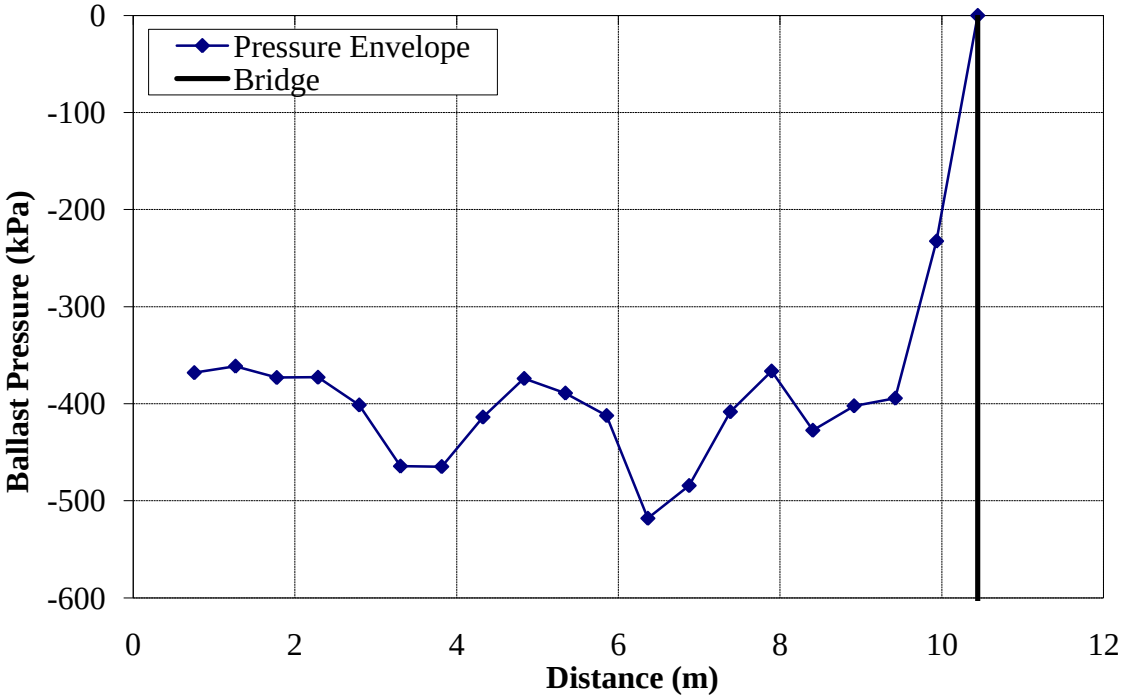

Figure D.2 - Ballast pressure for no slope at bridge/approach location (v = 22.2 m/s)

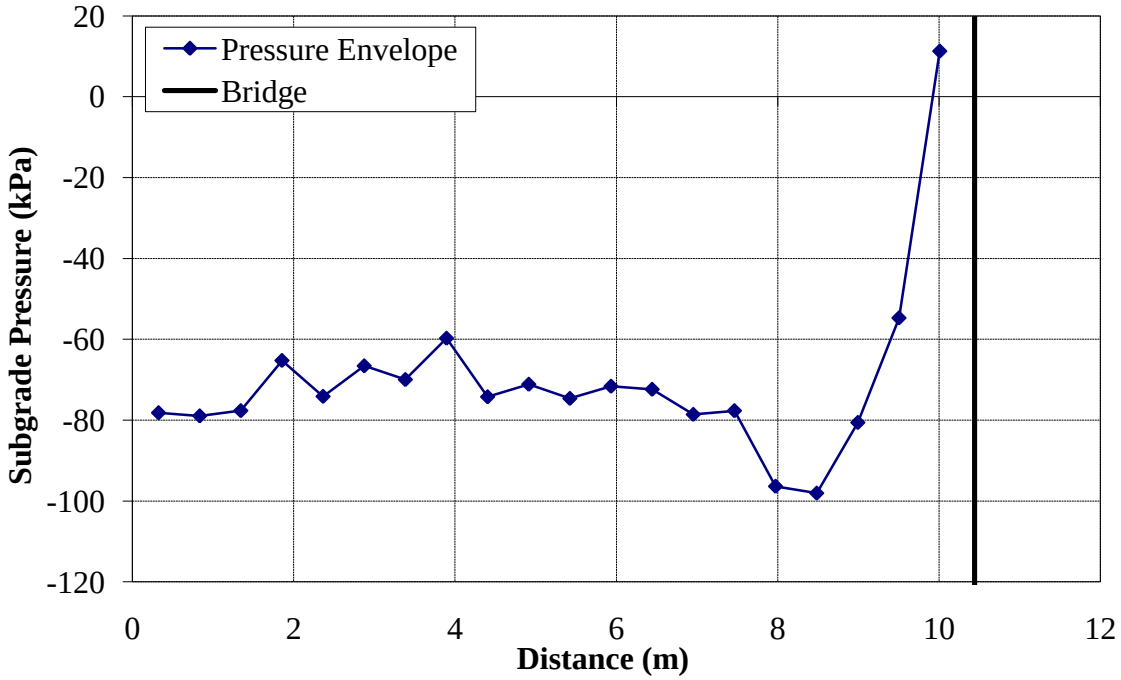

Figure D.3 - Subgrade pressure for no slope at bridge/approach location (v = 22.2 m/s)

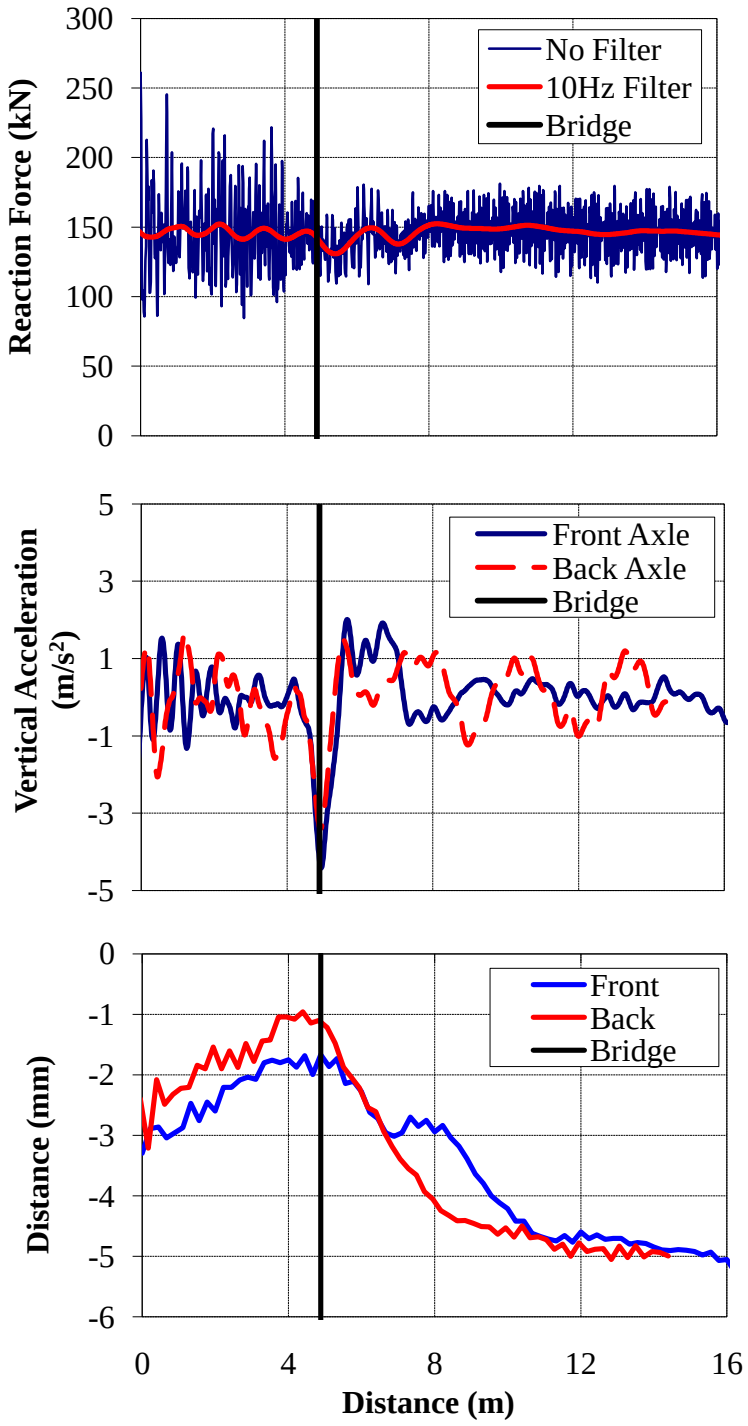

Figure D.4 - (a) Wheel/Rail Forces (b) Axle Accelerations and (c) Track Deflection due to a Truck Moving Off of the Bridge with No Slope at a Bridge/Approach Location (v = 22.2 m/s)

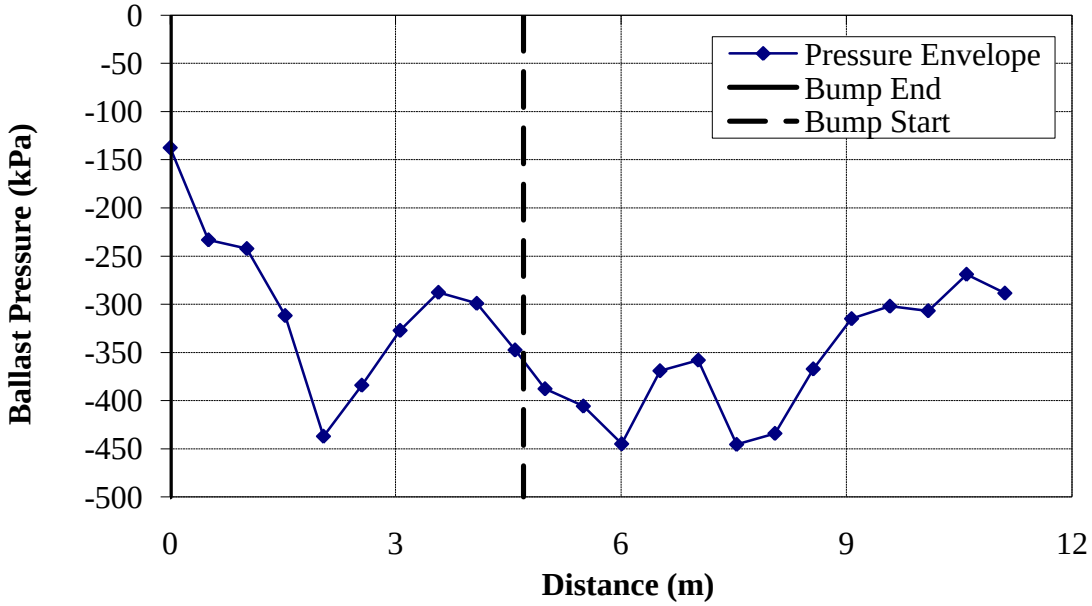

Figure D.5 – Ballast pressures due to a Truck Moving Off of the Bridge with a Stiffness Change Alone at a Bridge/Approach Location (v = 22.2 m/s)

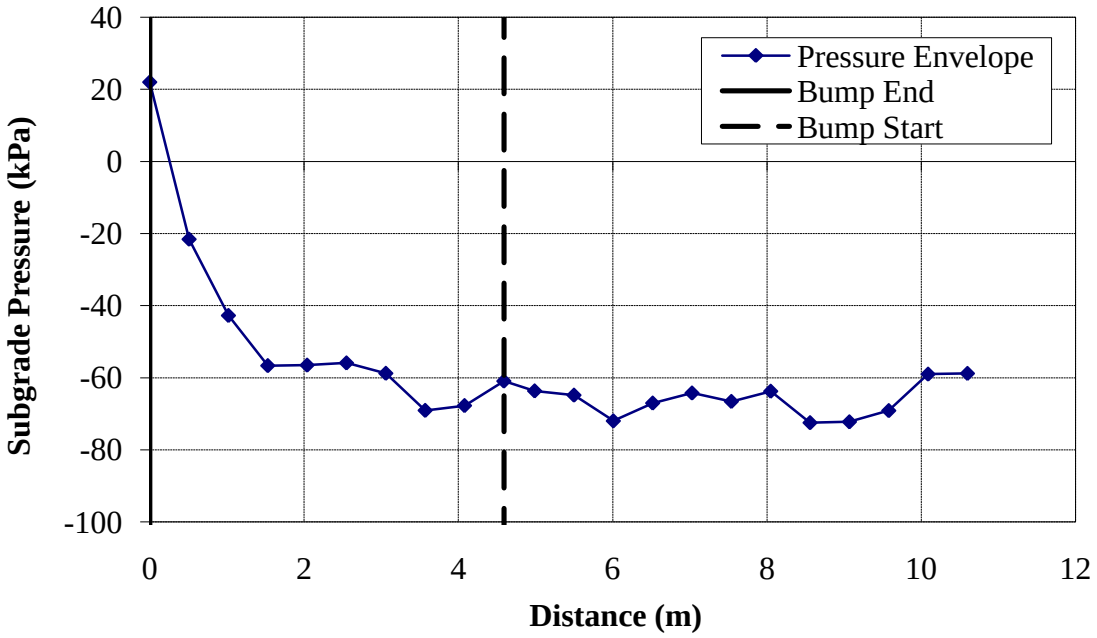

Figure D.6 - Subgrade pressures due to a Truck Moving Off of the Bridge with a Stiffness Change Alone at a Bridge/Approach Location (v = 22.2 m/s)

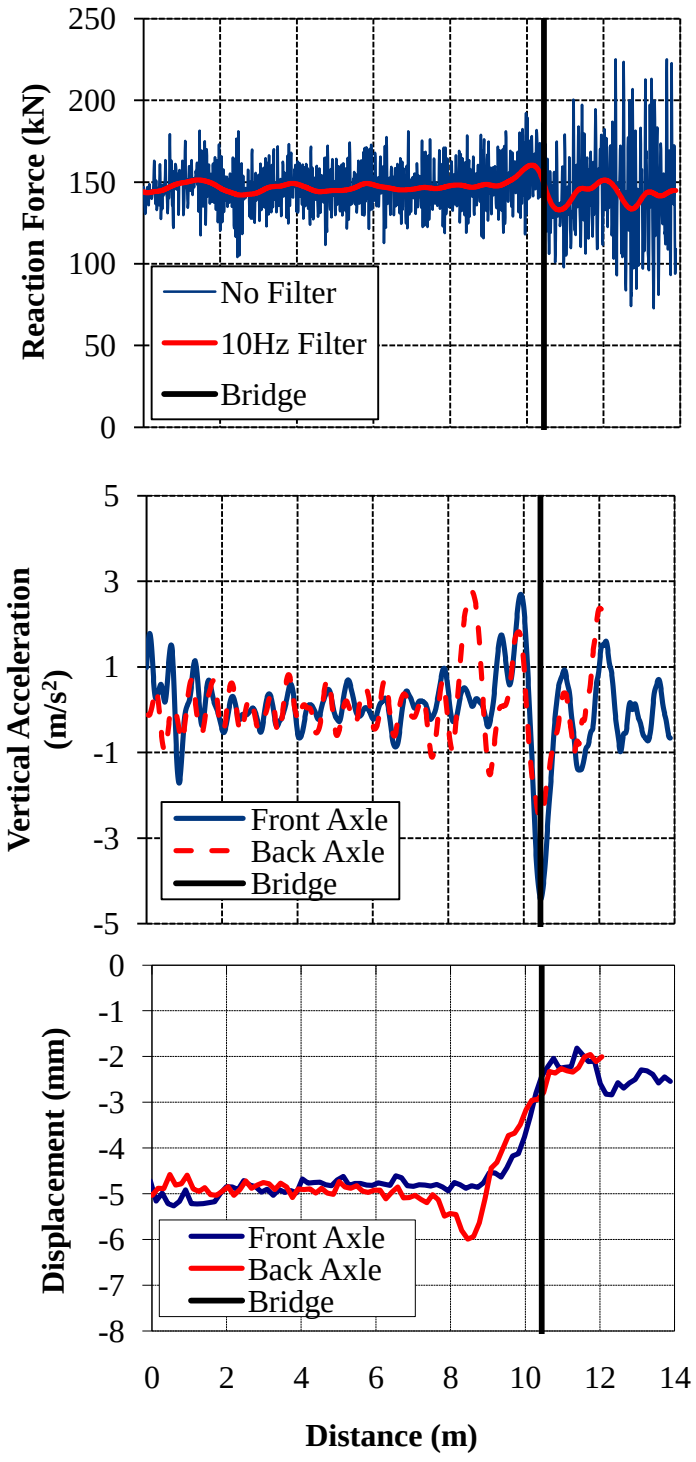

Figure D.7 - (a) Wheel/Rail Forces (b) Axle Accelerations and (c) Track Deflection due to a Stiffness Change Alone at a Bridge/Approach Location (v = 15.6 m/s)

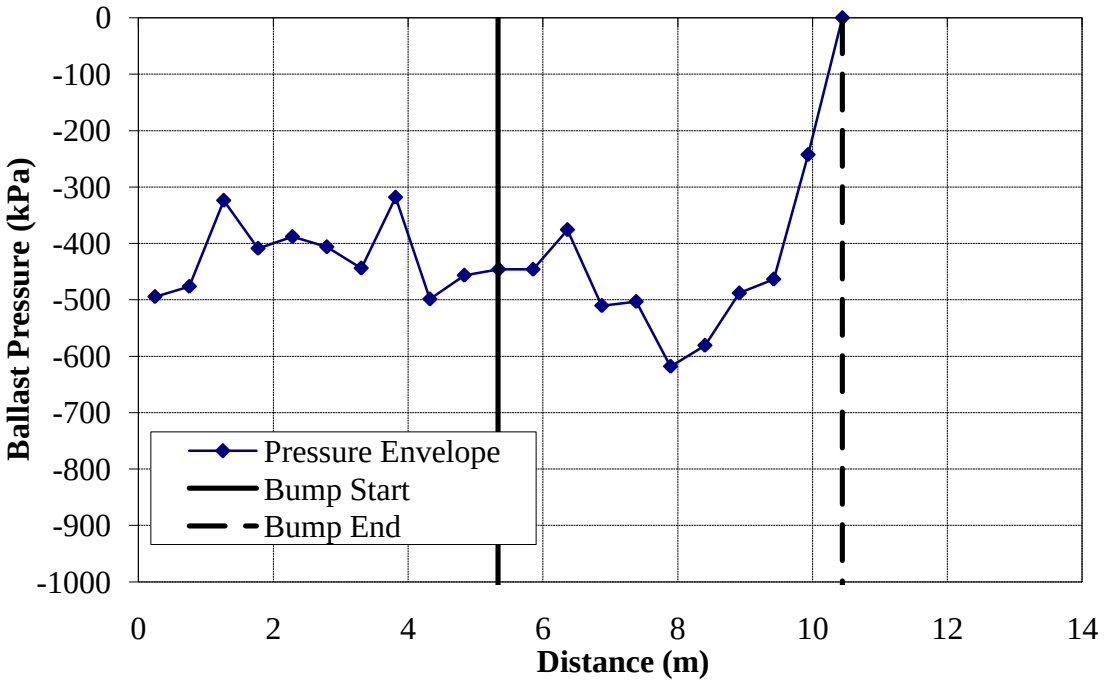

Figure D.8 – Ballast pressures due to a Stiffness Change Alone at a Bridge/Approach Location (v = 15.6 m/s)

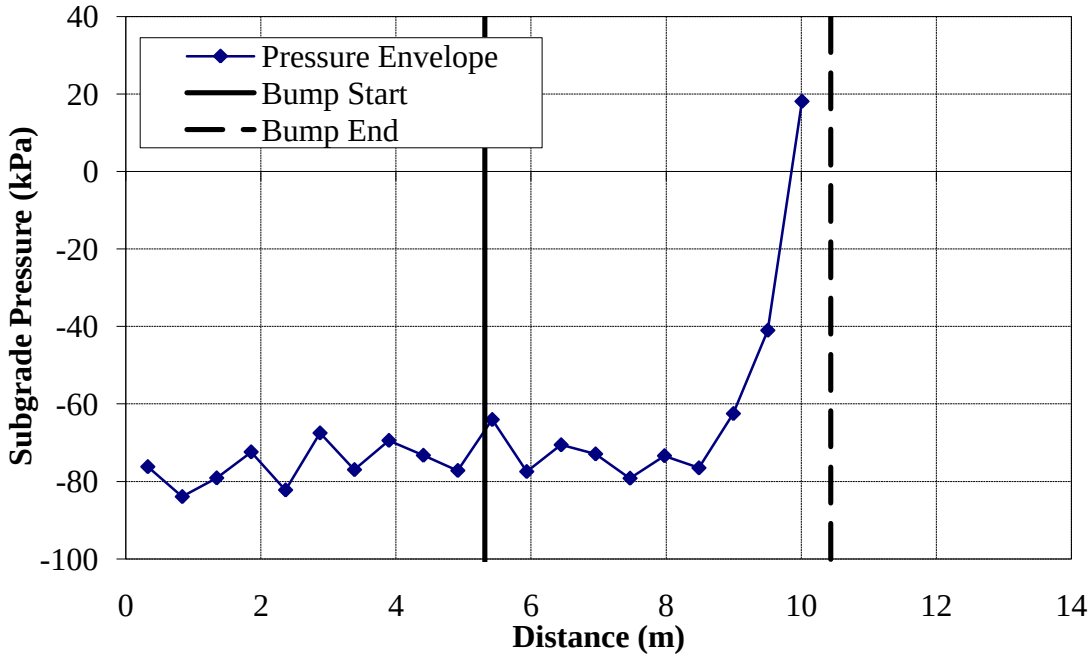

Figure D.9 - Subgrade pressures due to a Stiffness Change Alone at a Bridge/Approach Location (v = 15.6 m/s)

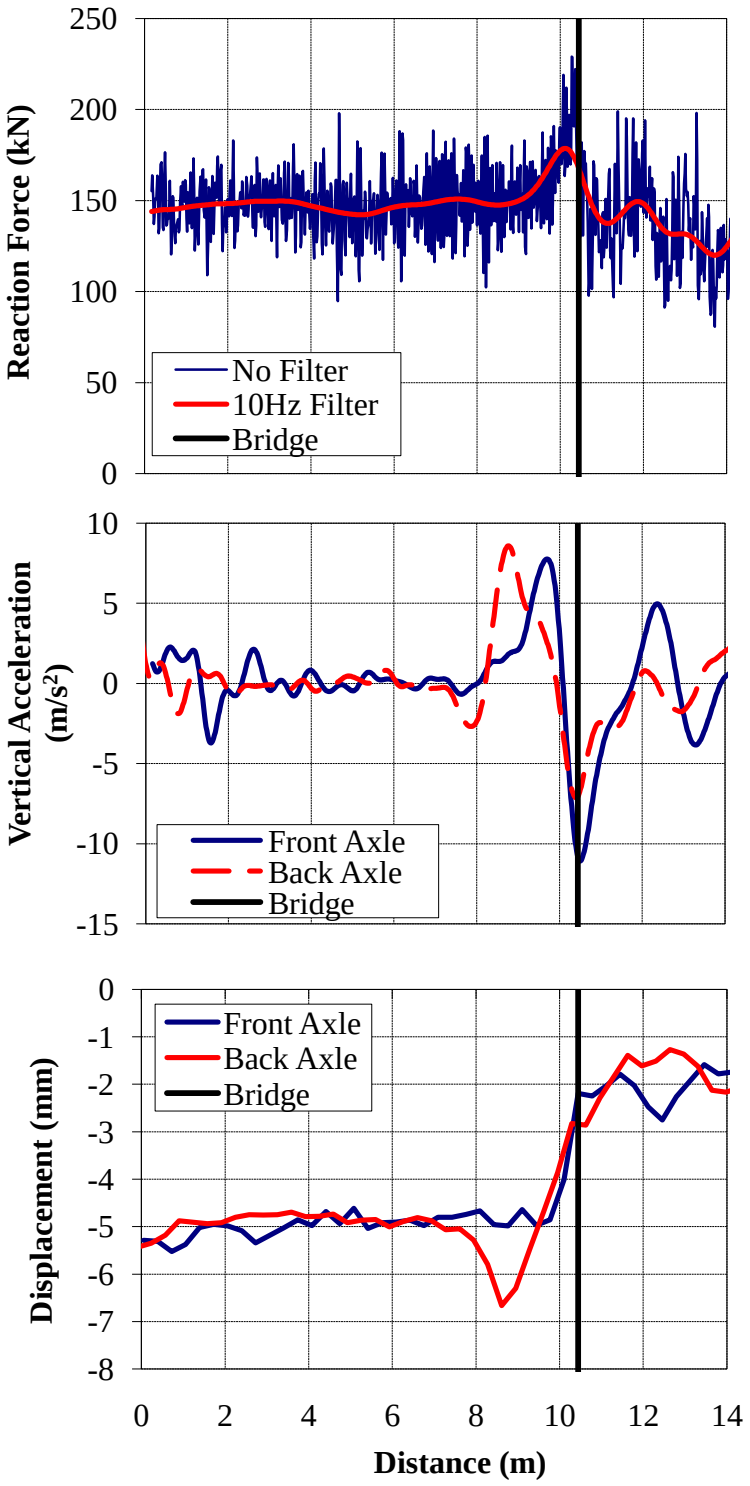

Figure D.10 – (a) Wheel/Rail Forces (b) Axle Accelerations and (c) Track Deflection due to a Stiffness Change Alone at a Bridge/Approach Location (v = 33.5 m/s)

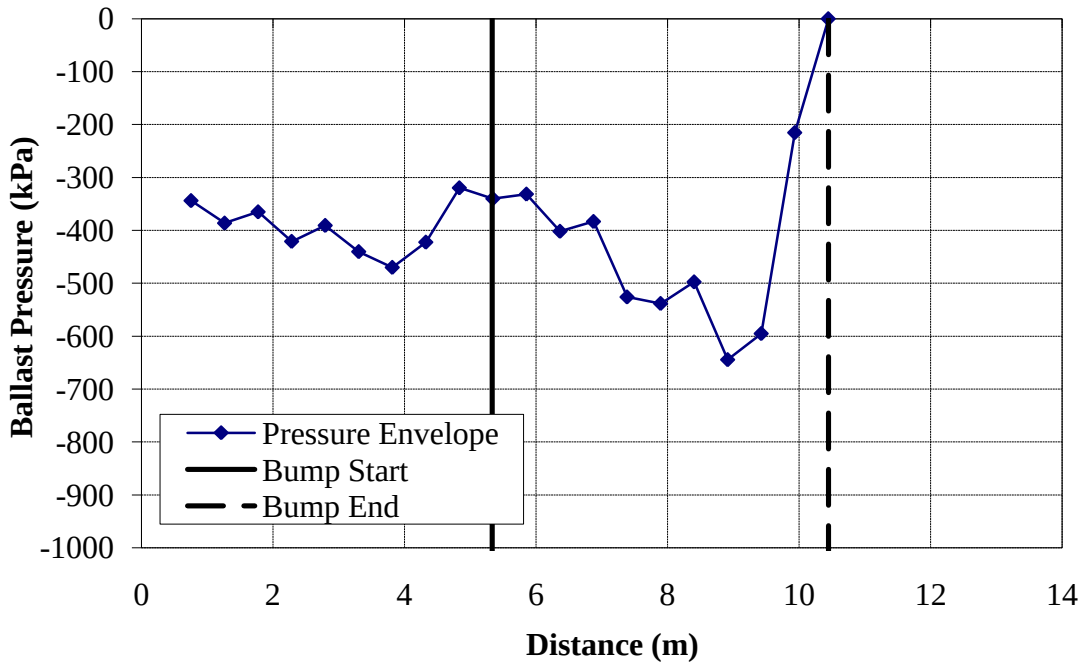

Figure D.11 – Ballast pressures due to a Stiffness Change Alone at a Bridge/Approach Location (v = 33.5 m/s)

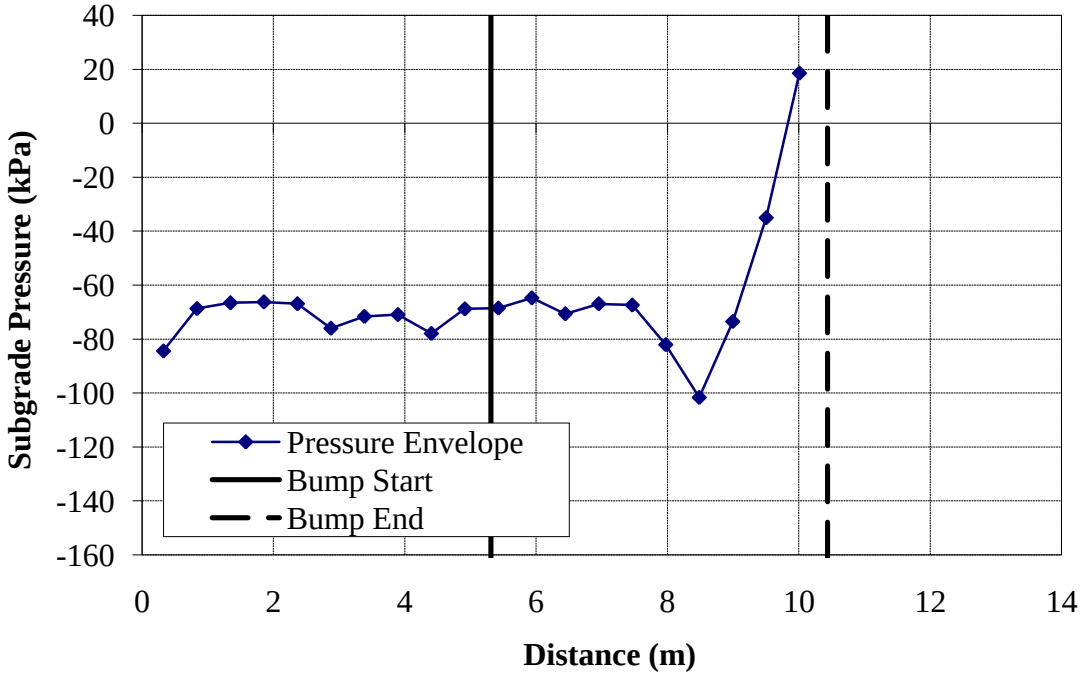

Figure D.12 - Subgrade pressures due to a Stiffness Change Alone at a Bridge/Approach Location (v = 33.5 m/s)

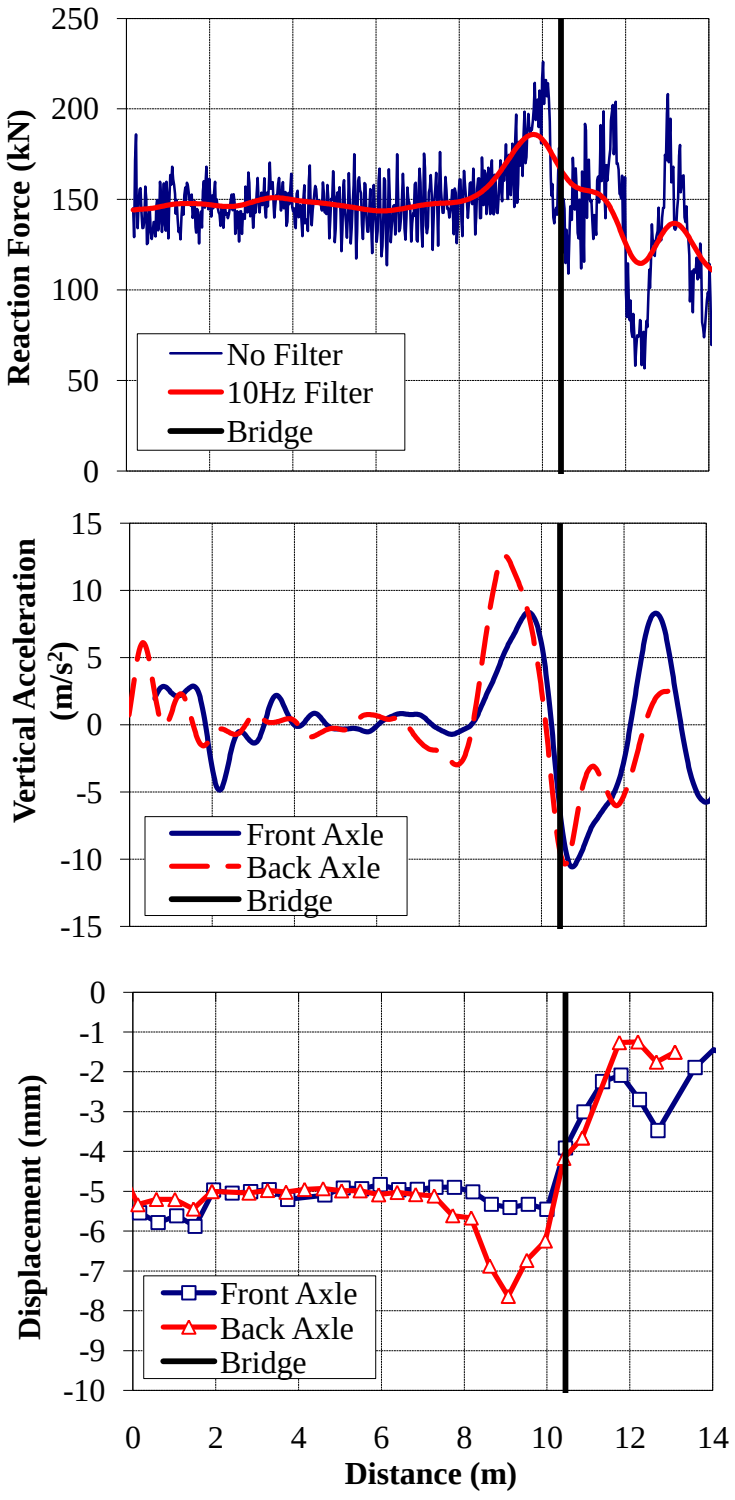

Figure D.13 - (a) Wheel/Rail Forces (b) Axle Accelerations and (c) Track Deflection due to a Stiffness Change Alone at a Bridge/Approach Location (v = 44.7 m/s)

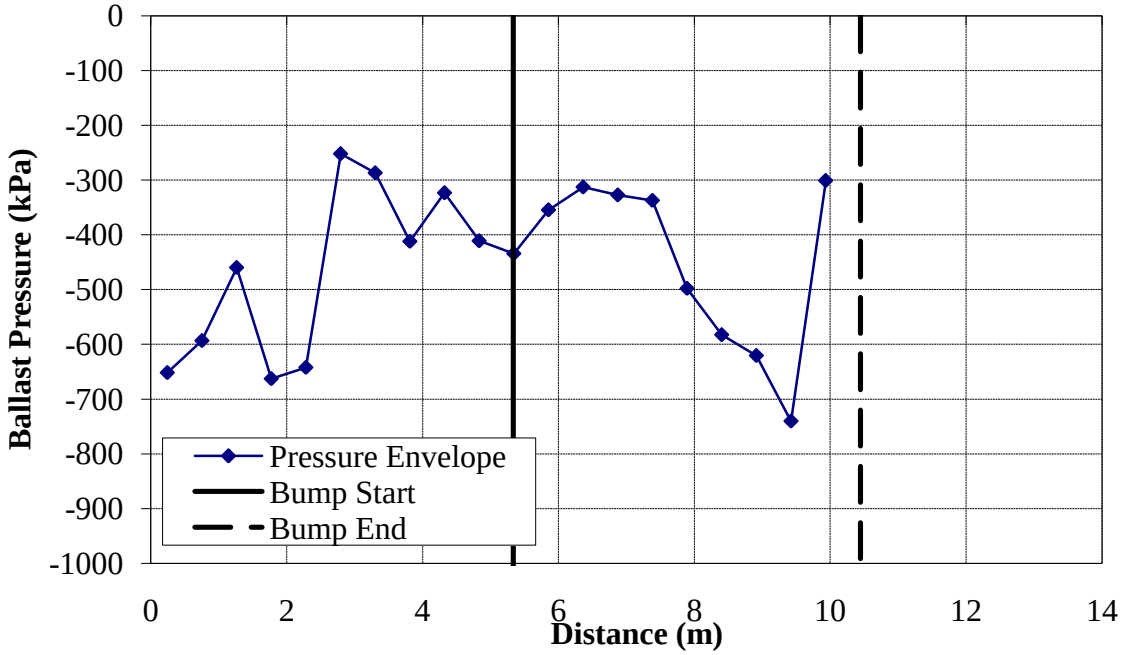

Figure D.14 – Ballast pressures due to a Stiffness Change Alone at a Bridge/Approach Location (v = 44.7 m/s)

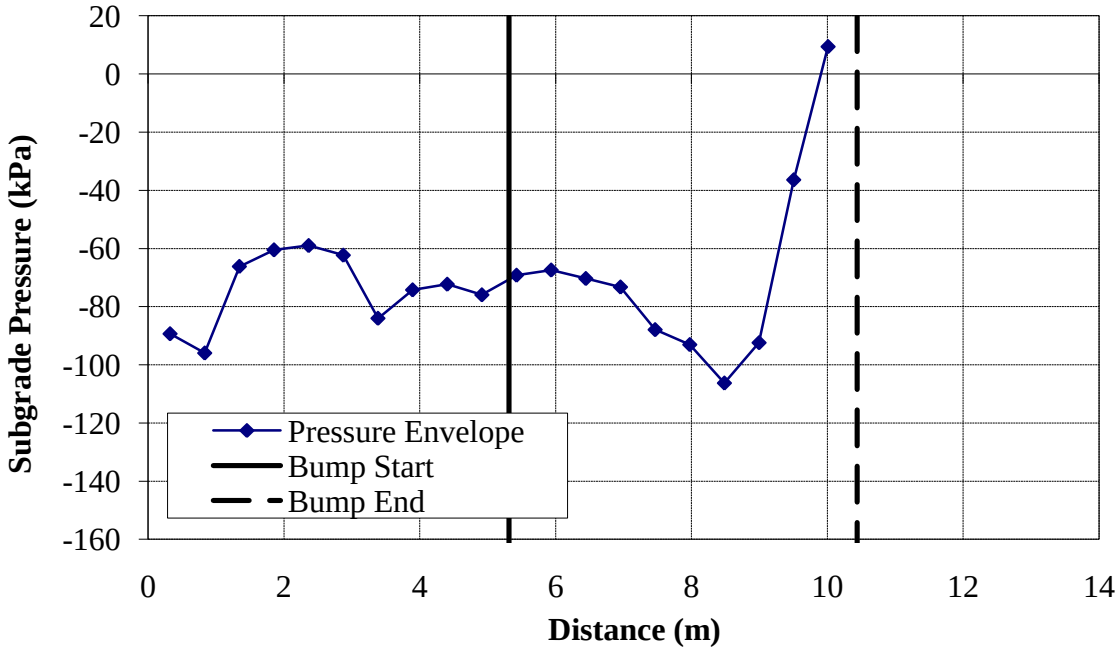

Figure D.15 - Subgrade pressures due to a Stiffness Change Alone at a Bridge/Approach Location (v = 44.7 m/s)

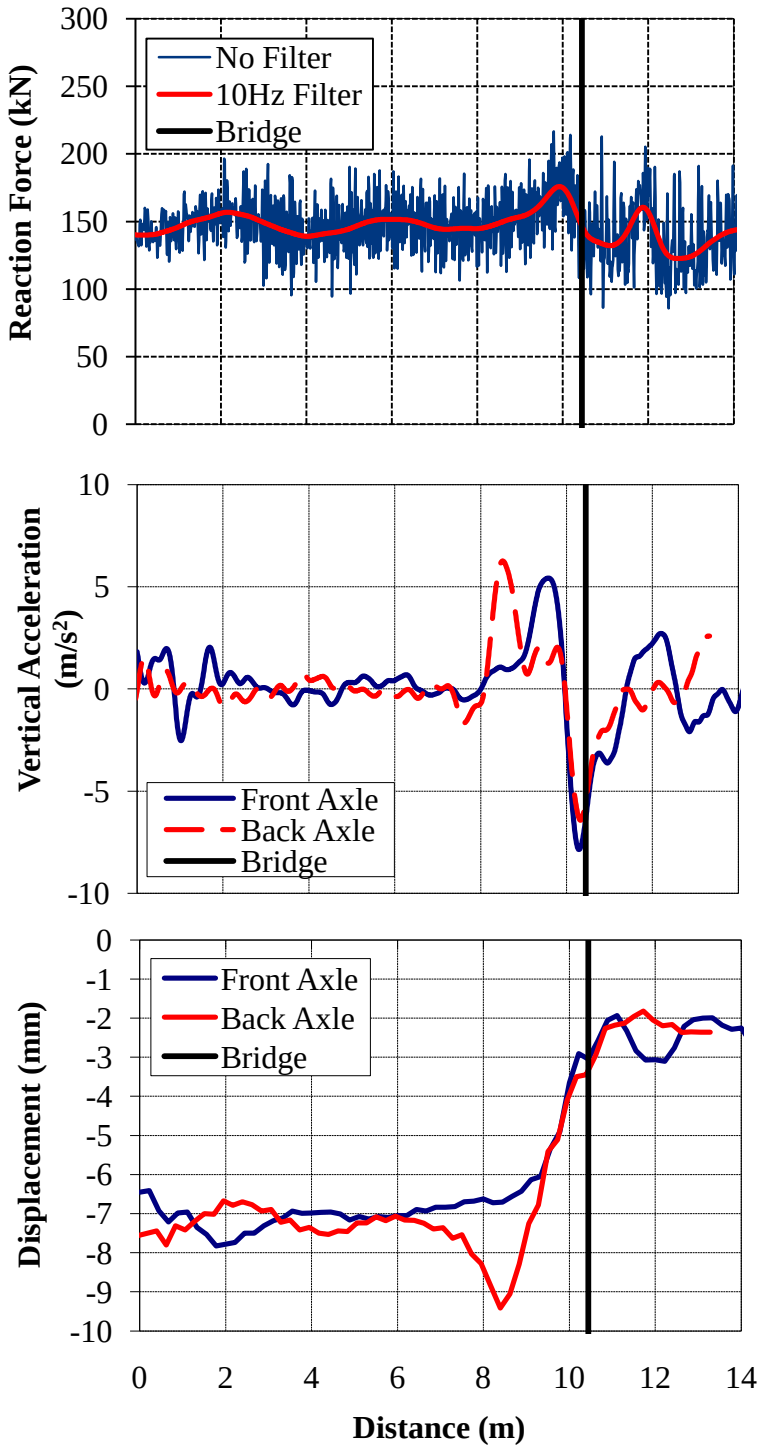

Figure D.16 - (a) Wheel/Rail Forces (b) Axle Accelerations and (c) Track Deflection due to a Stiffness Change Alone at a Bridge/Approach Location after 1,000 Cycles (v = 22.2 m/s)

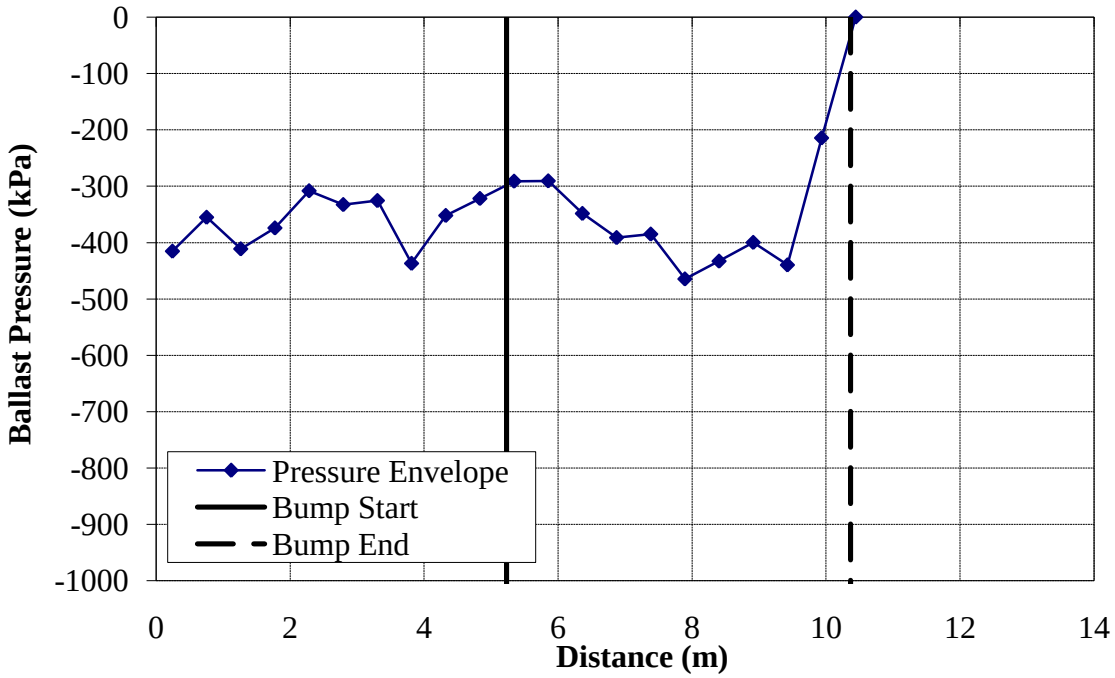

Figure D.17 – Ballast pressures due to a Stiffness Change Alone at a Bridge/Approach Location after 1,000 Cycles (v = 22.2 m/s)

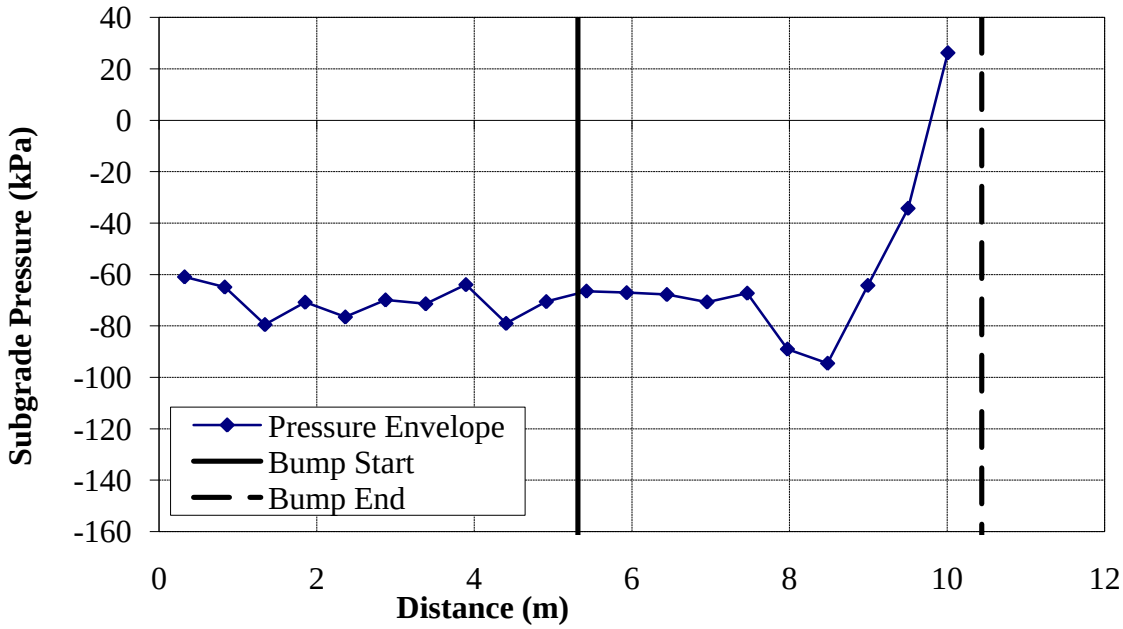

Figure D.18 - Subgrade pressures due to a Stiffness Change Alone at a Bridge/Approach Location after 1,000 Cycles (v = 22.2 m/s)

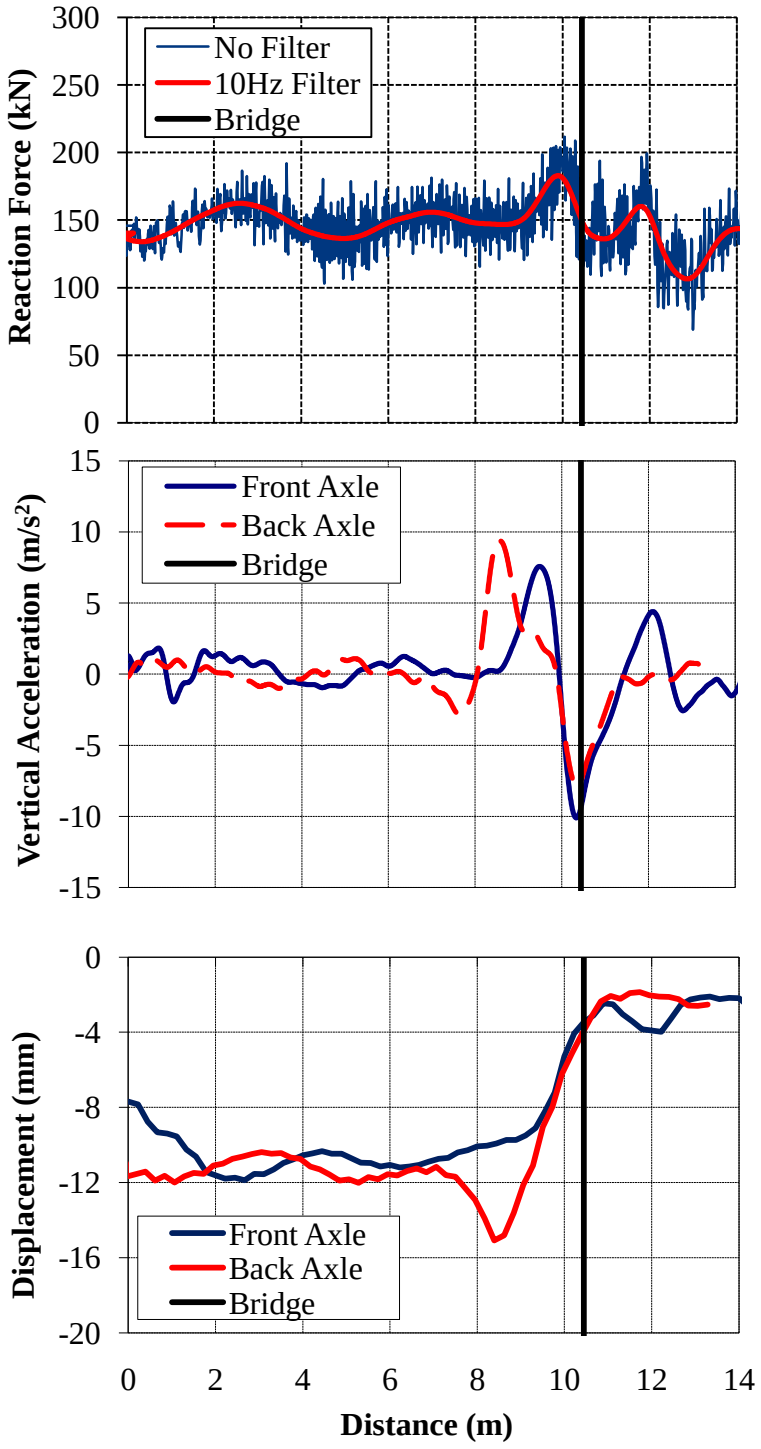

Figure D.19 - (a) Wheel/Rail Forces (b) Axle Accelerations and (c) Track Deflection due to a Stiffness Change Alone at a Bridge/Approach Location after 1,000,000 Cycles (v = 22.2 m/s)

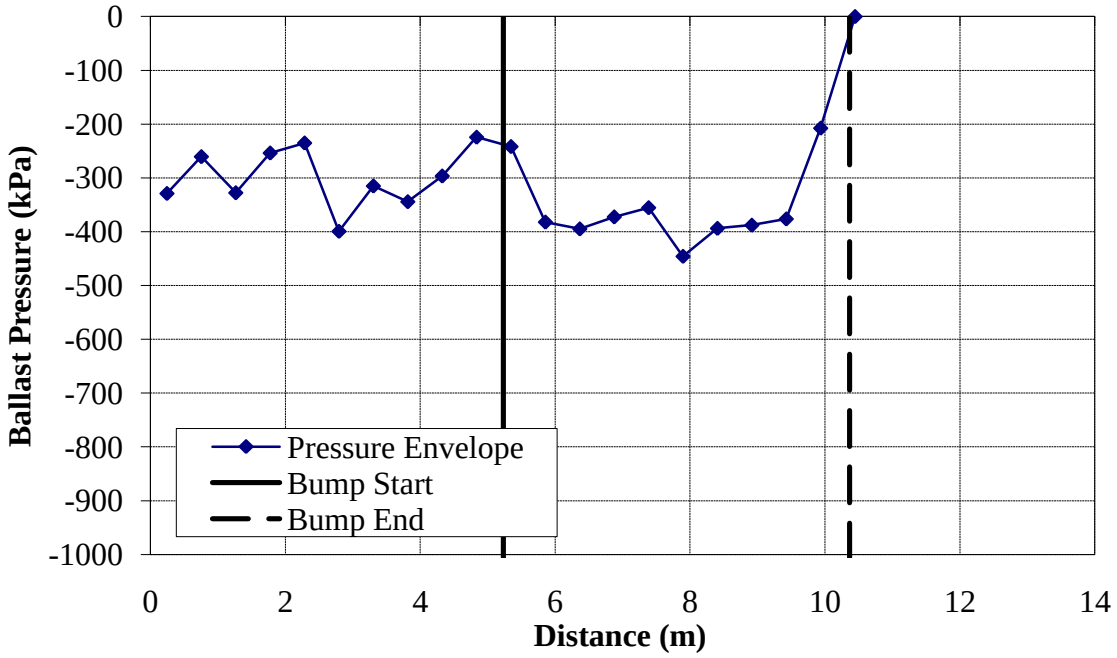

Figure D.2018 – Ballast pressures due to a Stiffness Change Alone at a Bridge/Approach Location after 1,000,000 Cycles (v = 22.2 m/s)

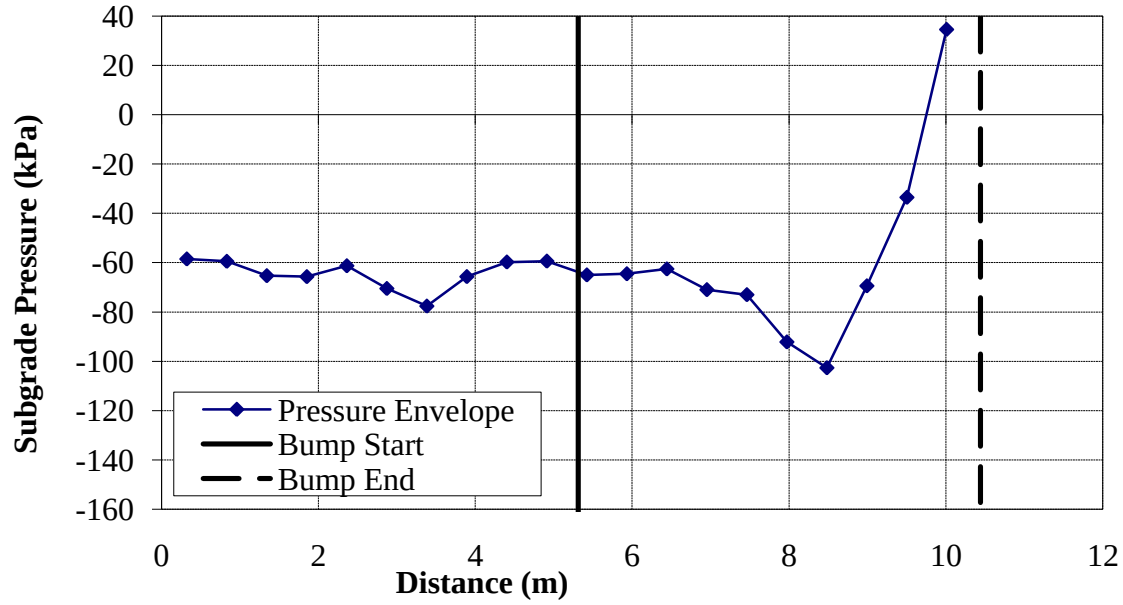

Figure D.21 - Subgrade pressures due to a Stiffness Change Alone at a Bridge/Approach Location after 1,000,000 Cycles (v = 22.2 m/s)

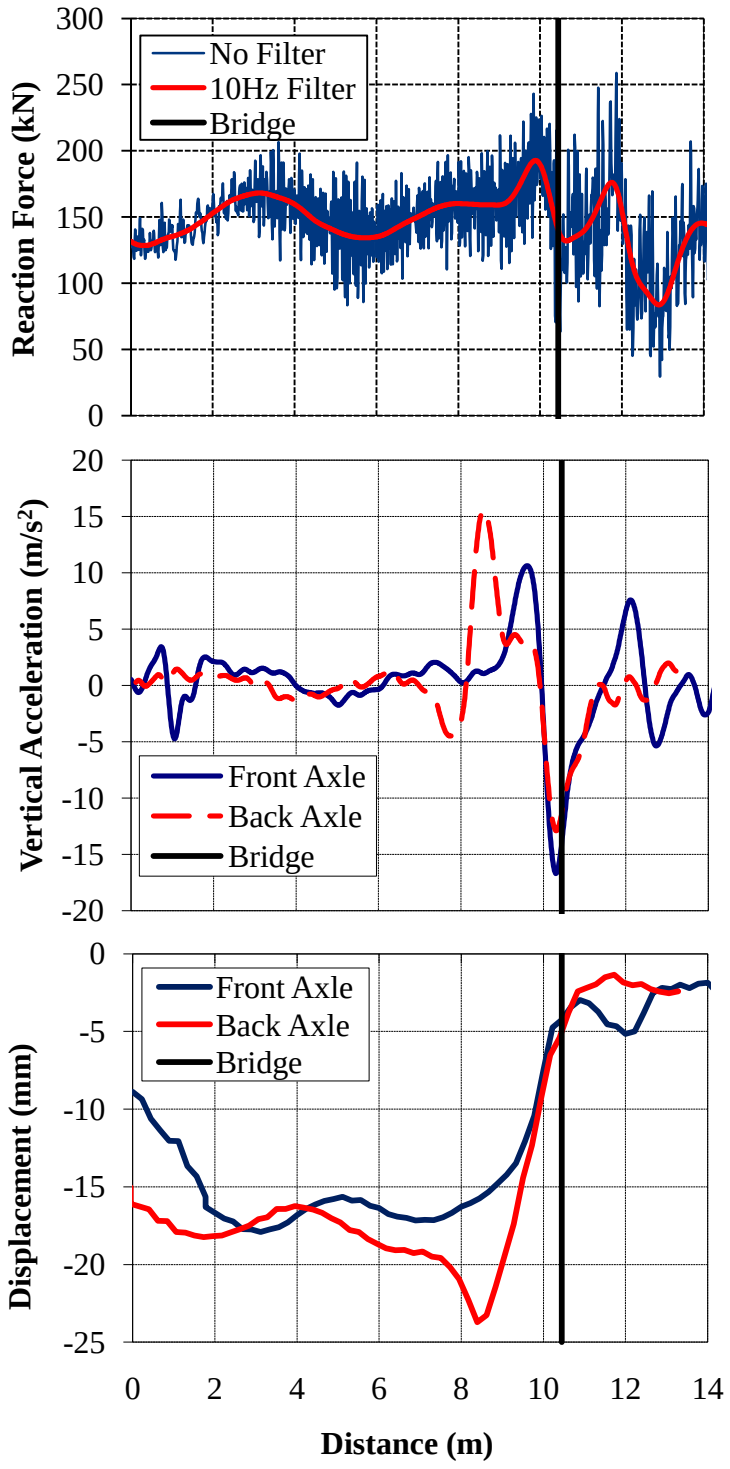

Figure D.22 - (a) Wheel/Rail Forces (b) Axle Accelerations and (c) Track Deflection due to a Stiffness Change Alone at a Bridge/Approach Location after 1,000,000,000 Cycles (v = 22.2 m/s)

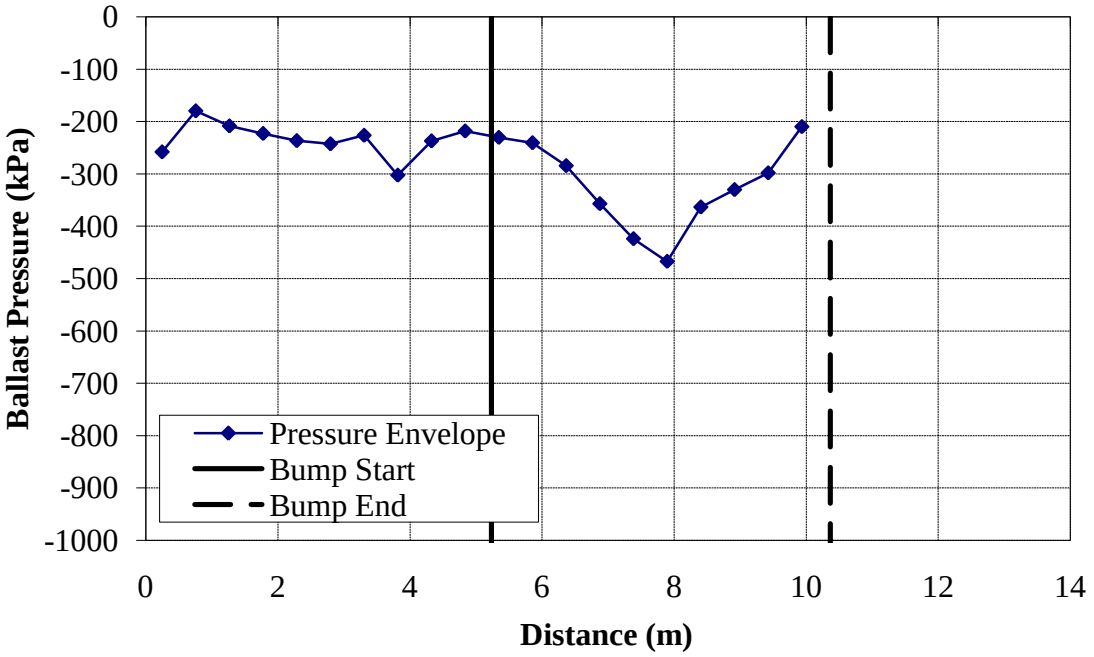

Figure D.23 – Ballast pressures due to a Stiffness Change Alone at a Bridge/Approach Location after 1,000,000,000 Cycles (v = 22.2 m/s)

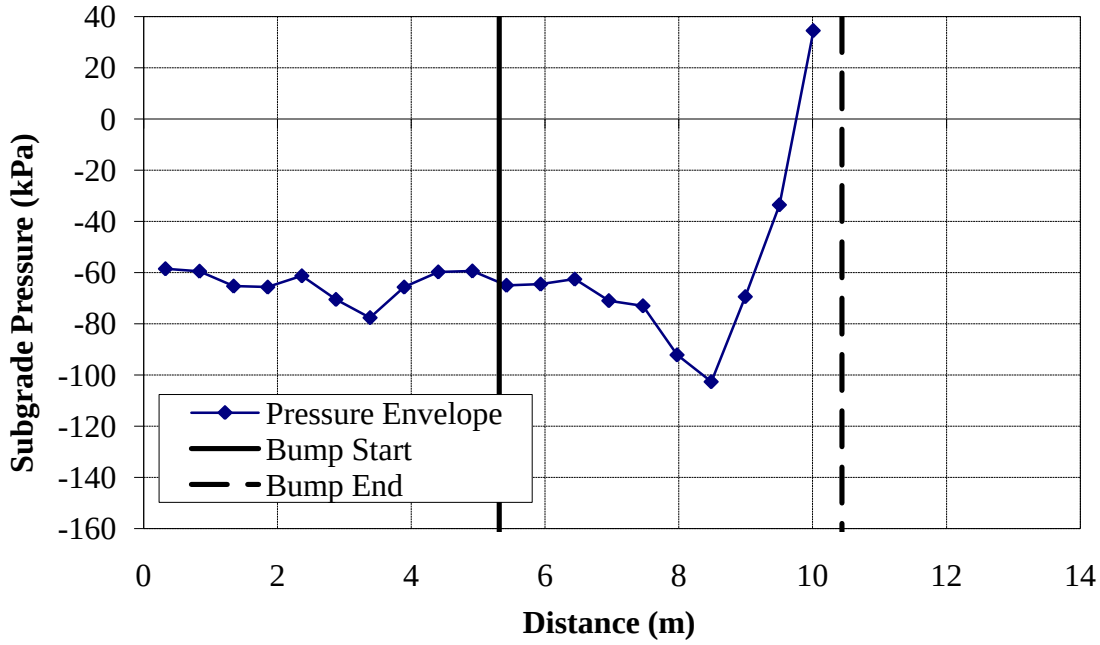

Figure D.24 - Subgrade pressures due to a Stiffness Change Alone at a Bridge/Approach Location after 1,000,000,000 Cycles (v = 22.2 m/s)

APPENDIX E

TRACK RESPONSE PLOTS: BUMP

Bump – Reference Case 380

Bump – Off Of 382

Bump – 8.9 m/s (20 mph)..... 384

Bump – 15.6 m/s (35 mph)..... 386

Bump – 33.5 m/s (75 mph)..... 388

Bump – 44.7 m/s (100 mph)..... 390

Bump – 1:50 slope (Equal Length) 392

Bump – 1:100 slope (Equal Length) 394

Bump – 1:200 slope (Equal Length) 396

Bump – 1:250 slope (Equal Length) 398

Bump – 1:50 slope (Equal Height)..... 400

Bump – 1:100 slope (Equal Height)..... 402

Bump – 1:200 slope (Equal Height)..... 404

Bump – 1:250 slope (Equal Height)..... 406

Bump – 1:50 slope (Equal Height, 15.6 m/s) 408

Bump – 1:50 slope (Equal Height, 33.5 m/s) 410

Bump – 1:50 slope (Equal Height, 44.7 m/s) 412

Bump – 1:100 slope (Equal Height, 15.6 m/s) 414

Bump – 1:100 slope (Equal Height, 33.5 m/s) 416

Bump – 1:100 slope (Equal Height, 44.7 m/s) 418
Bump – 1:200 slope (Equal Height, 15.6 m/s) 420
Bump – 1:200 slope (Equal Height, 33.5 m/s) 422
Bump – 1:200 slope (Equal Height, 44.7 m/s) 424
Bump – 1:250 slope (Equal Height, 15.6 m/s) 426
Bump – 1:250 slope (Equal Height, 33.5 m/s) 428
Bump – 1:250 slope (Equal Height, 44.7 m/s) 430
Bump – 20 MPa Fill 432
Bump – 50 MPa Fill 434
Bump – 100 MPa Fill 436
Bump – Concrete Approach Ties 438
Bump – Plastic Approach Ties 440
Bump – Wood Approach Ties with Rubber Rail Seat Pads 442
Bump – Concrete Approach Ties with Rubber Rail Seat Pads 444
Bump – Wood Approach Ties with Rubber Tie Pads 446
Bump – Concrete Approach Ties with Rubber Tie Pads 448
Bump – Concrete Bridge Ties 450
Bump – Plastic Bridge Ties 452
Bump – Wood Bridge Ties with Rubber Rail Seat Pads 454
Bump – Concrete Bridge Ties with Rubber Rail Seat Pads 456
Bump – Ballast Deck Bridge 458
Bump – Ballast Deck Bridge with Ballast Mat 460

Bump – 152.4 mm Ballast Thickness 462

Bump – 203.2 mm Ballast Thickness 464

Bump – 304.8 mm Ballast Thickness 466

Bump – 406.4 mm Ballast Thickness 468

Bump – 2.1 m Tie Length 470

Bump – 3.0 m Tie Length 472

Bump – 3.6 m Tie Length 474

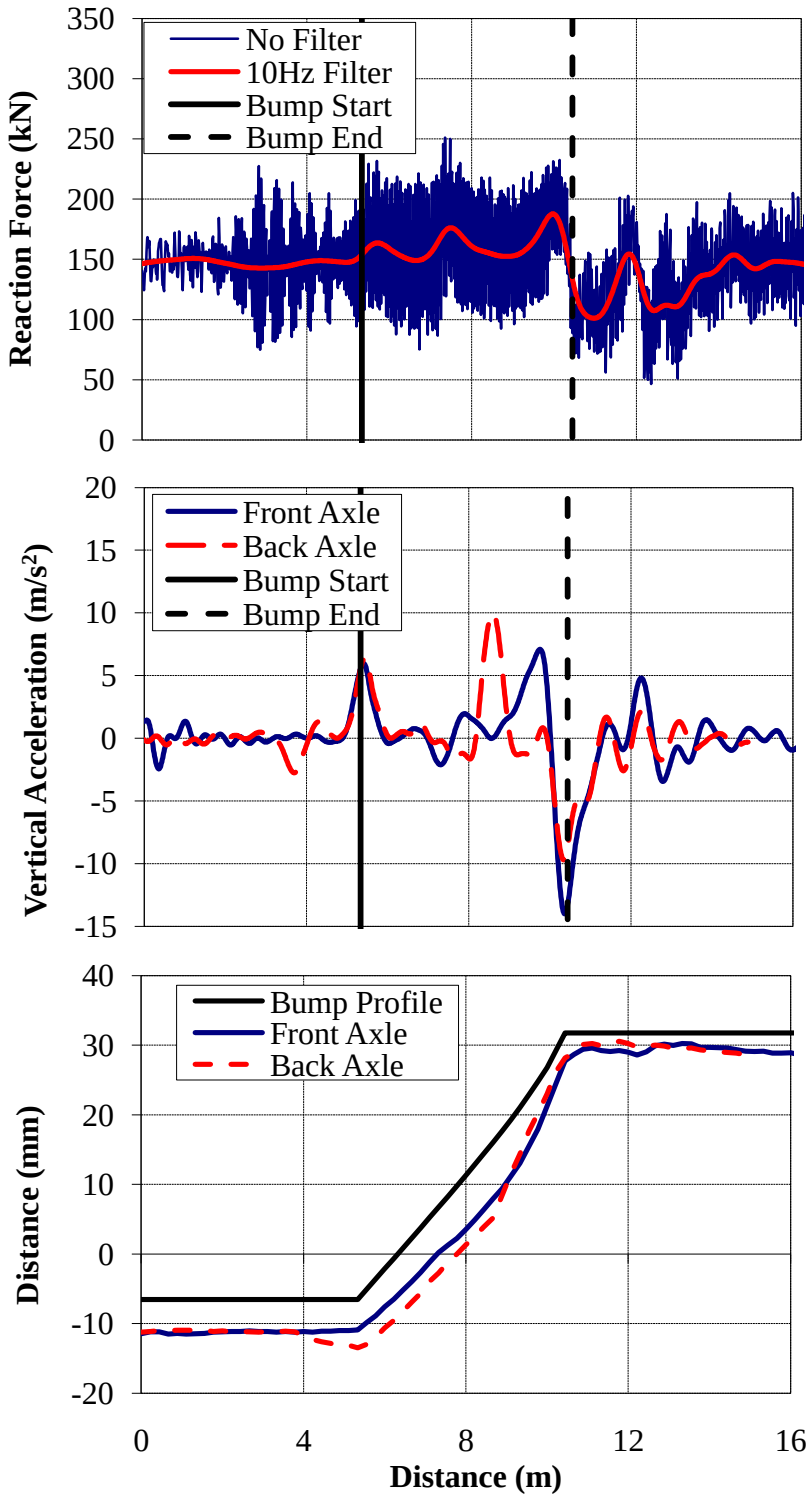

Figure E.1 - (a) Wheel/Rail Forces (b) Axle Accelerations and (c) Track Deflection due to a 1:150 Bump at a Bridge/Approach Location (v = 22.2 m/s)

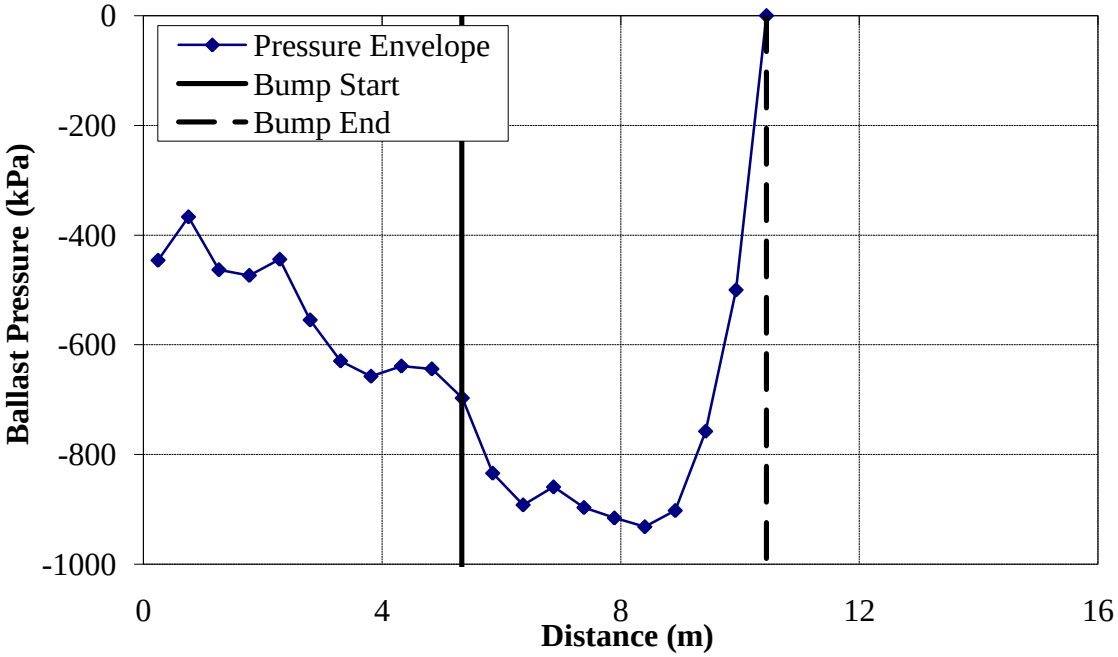

Figure E.2 - Ballast Pressure Resulting from a 1:150 Bump at a Bridge/Approach Location (v = 22.2 m/s)

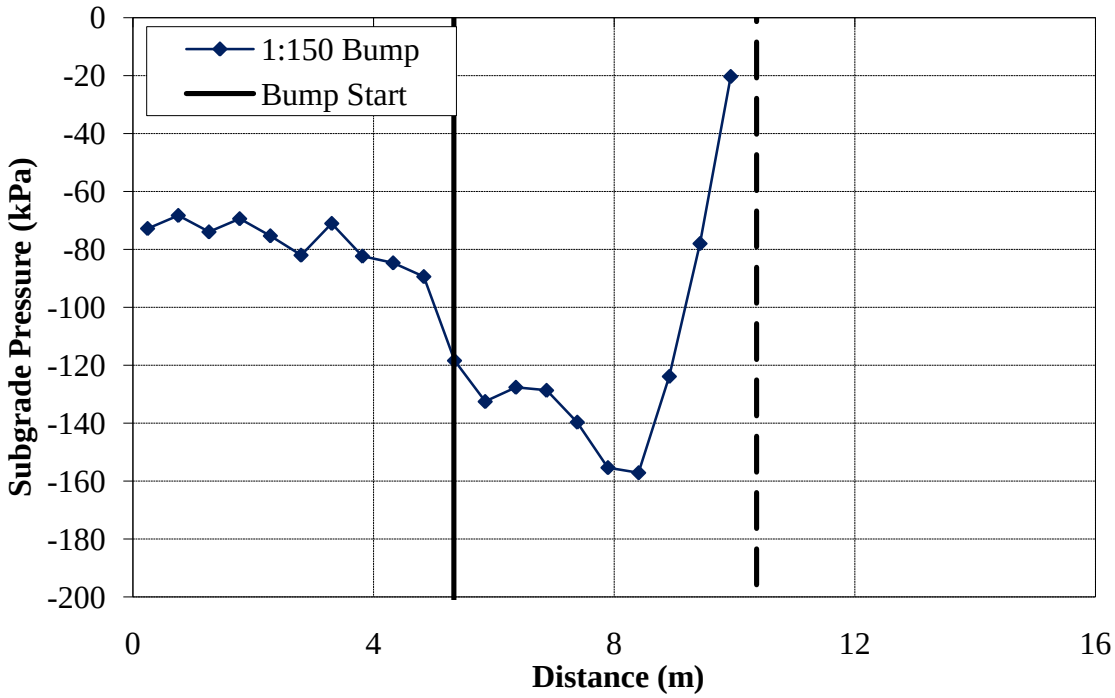

Figure E.3 - Subgrade Pressure Resulting from a 1:150 Bump at a Bridge/Approach Location (v = 22.2 m/s)

Figure E.4 - (a) Wheel/Rail Forces (b) Axle Accelerations and (c) Track Deflection due to moving off of the bridge on to an approach embankment with a 1:150 Bump v = 22.2 m/s)

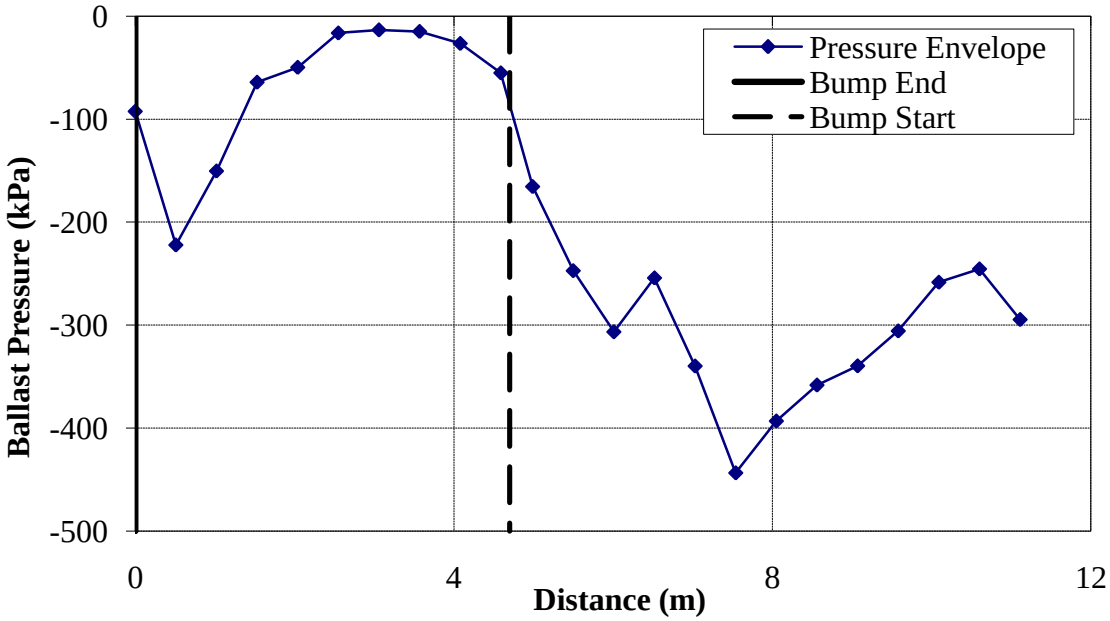

Figure E.5 - Ballast Pressure Resulting from Moving off of a Bridge on to a 1:150 Bump (v = 22.2 m/s)

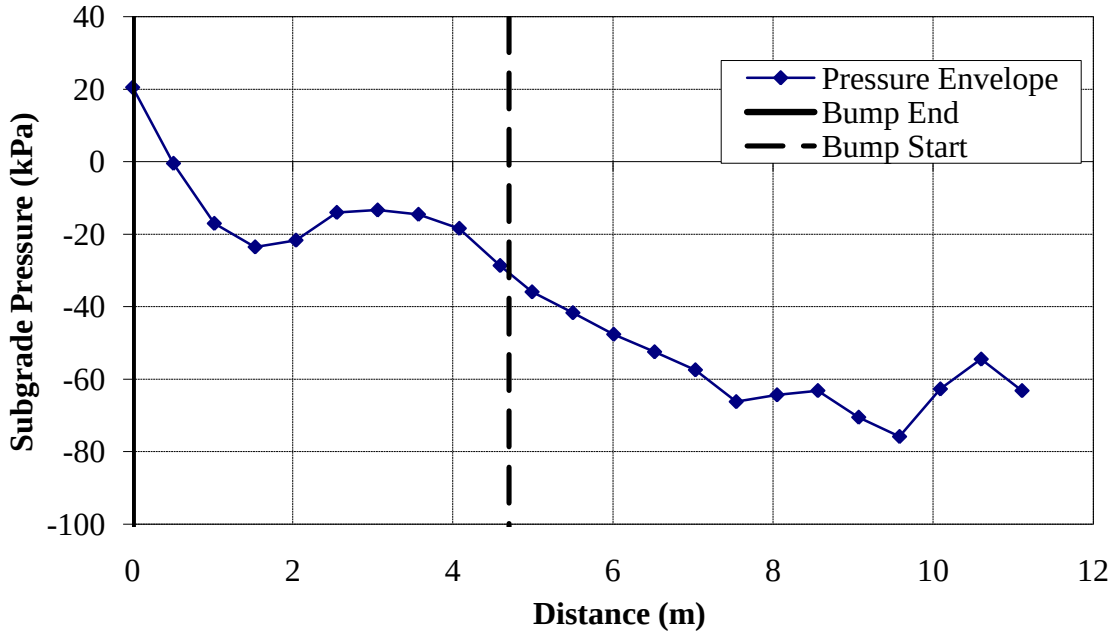

Figure E.6 - Subgrade Pressure Resulting from Moving off of a Bridge on to a 1:150 Bump (v = 22.2 m/s)

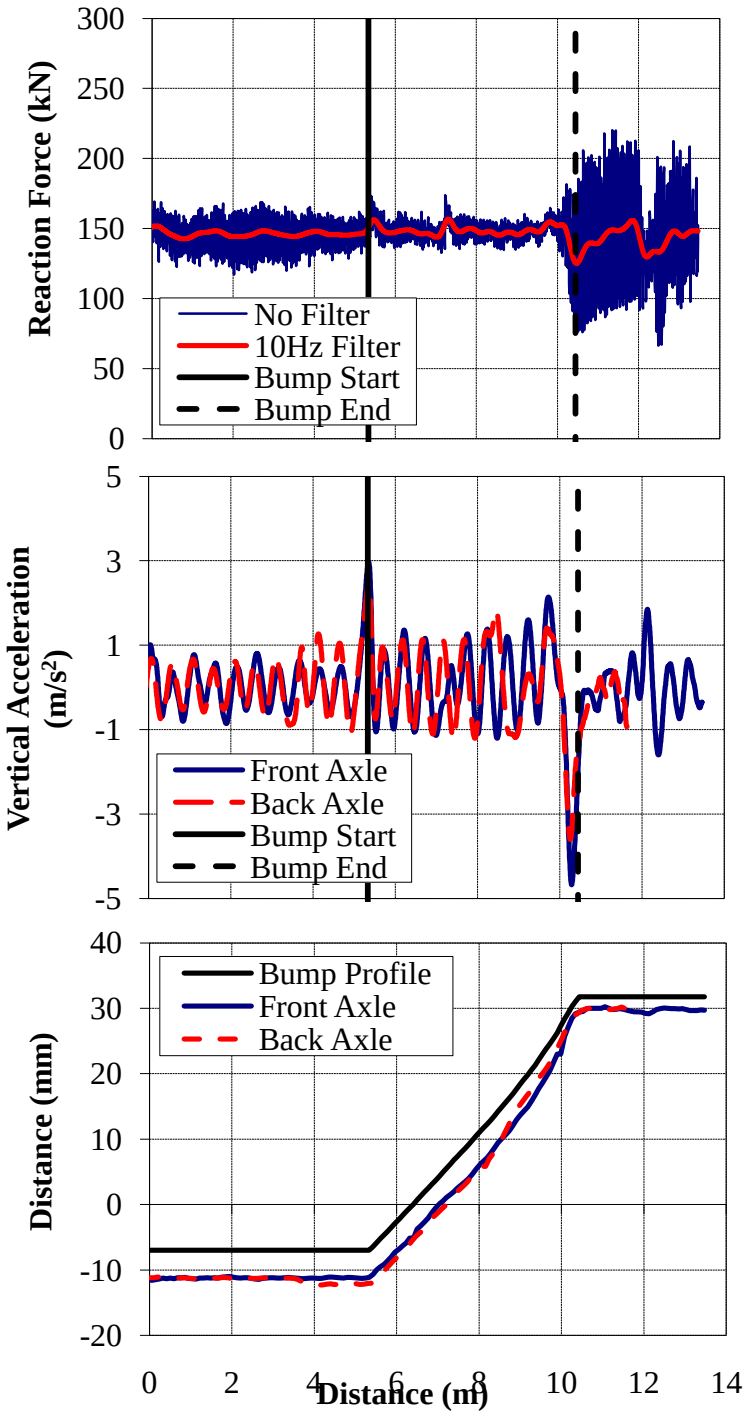

Figure E.7 - (a) Wheel/Rail Forces (b) Axle Accelerations and (c) Track Deflection for a truck moving at 8.9 m/s over a 1:150 Bump on to the bridge

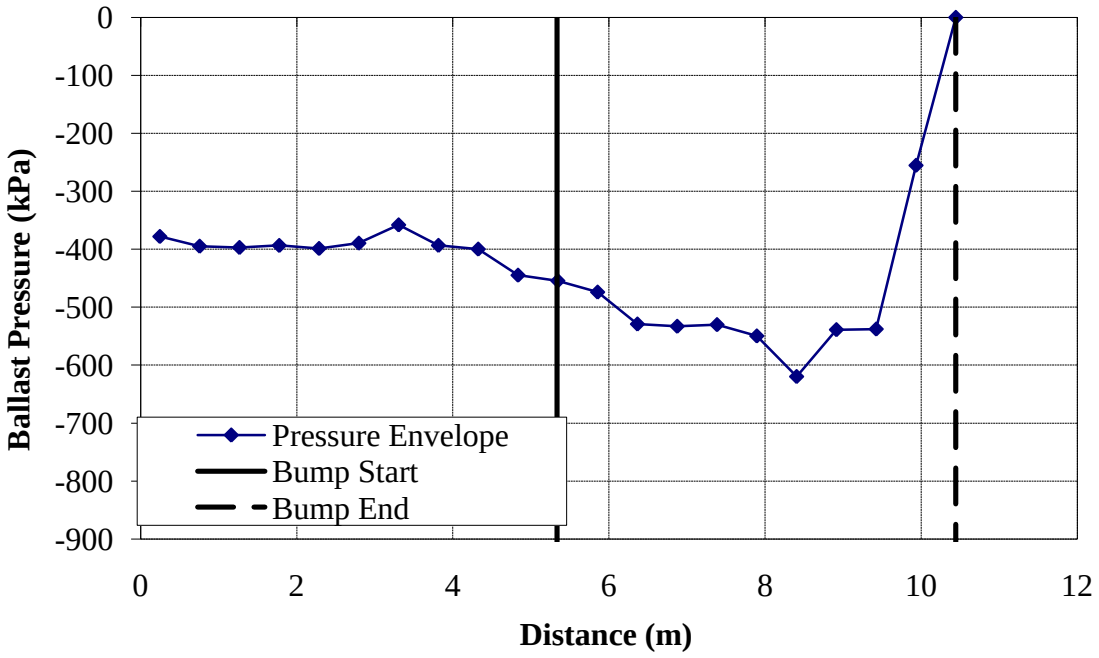

Figure E.8 – Ballast pressures for a truck moving at 8.9 m/s over a 1:150 bump on to the bridge

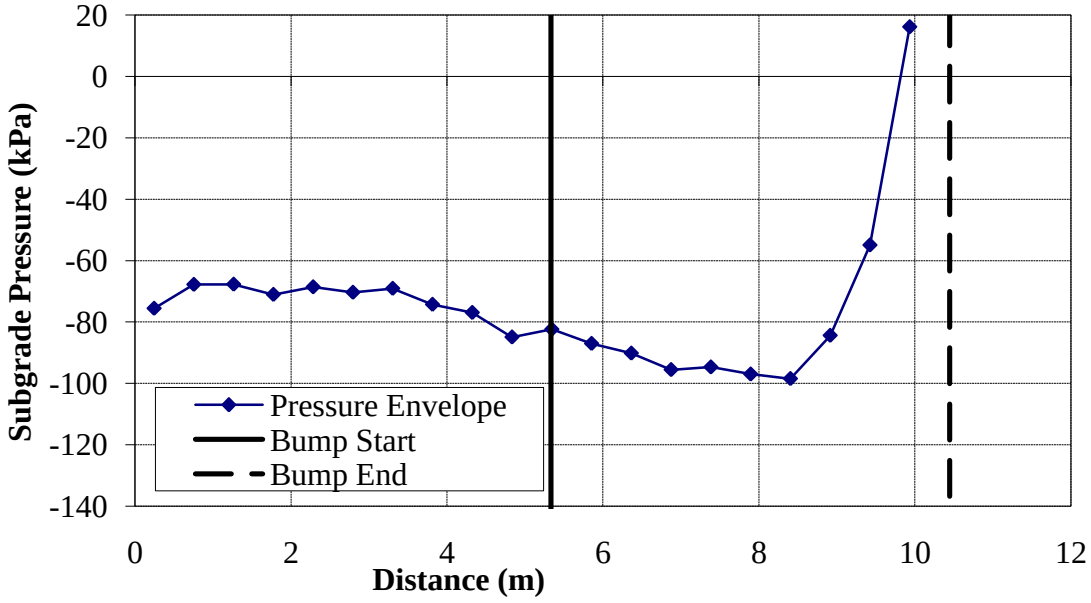

Figure E.9 - Subgrade pressures for a truck moving at 8.9 m/s over a 1:150 bump on to the bridge

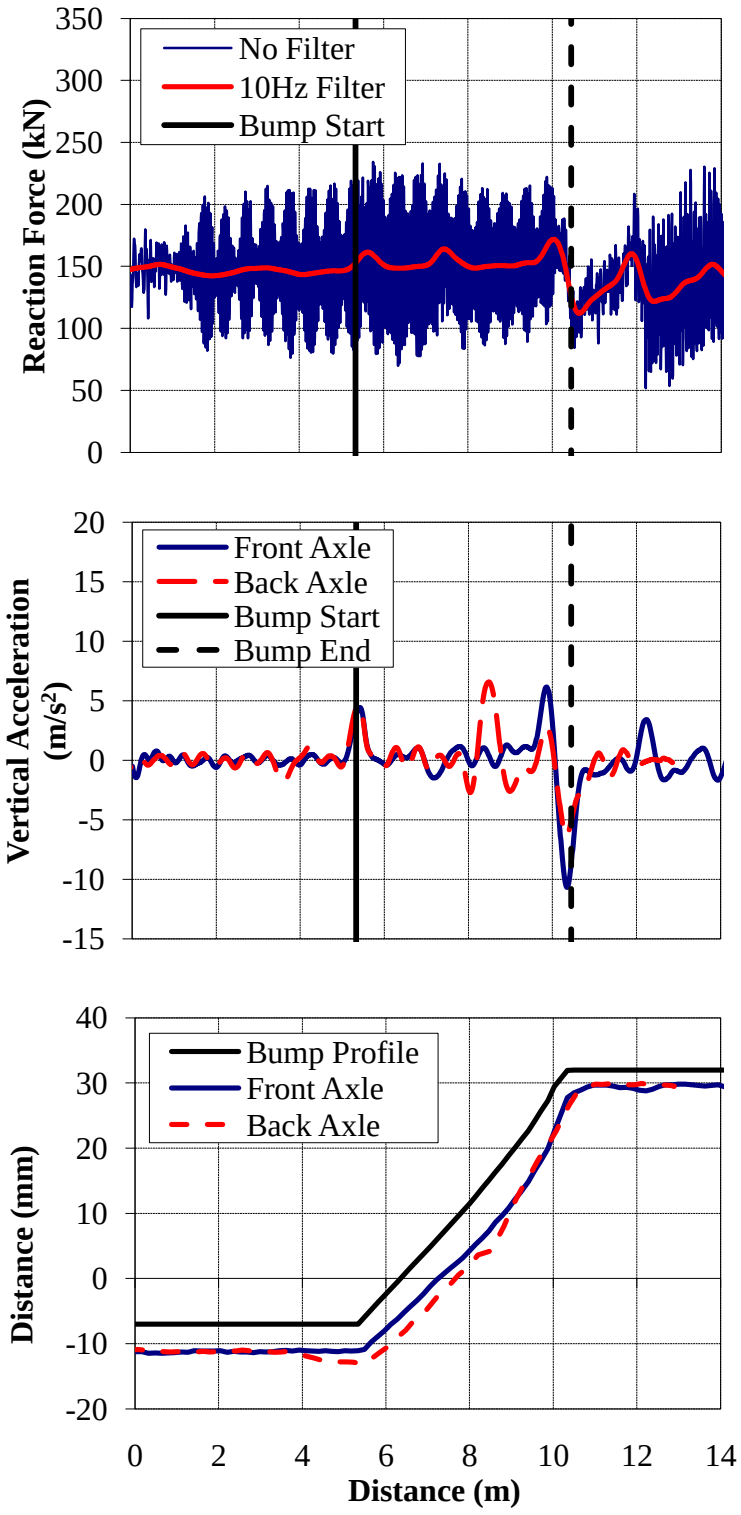

Figure E.10 - (a) Wheel/Rail Forces (b) Axle Accelerations and (c) Track Deflection for a truck moving at 15.6 m/s over a 1:150 Bump on to the bridge

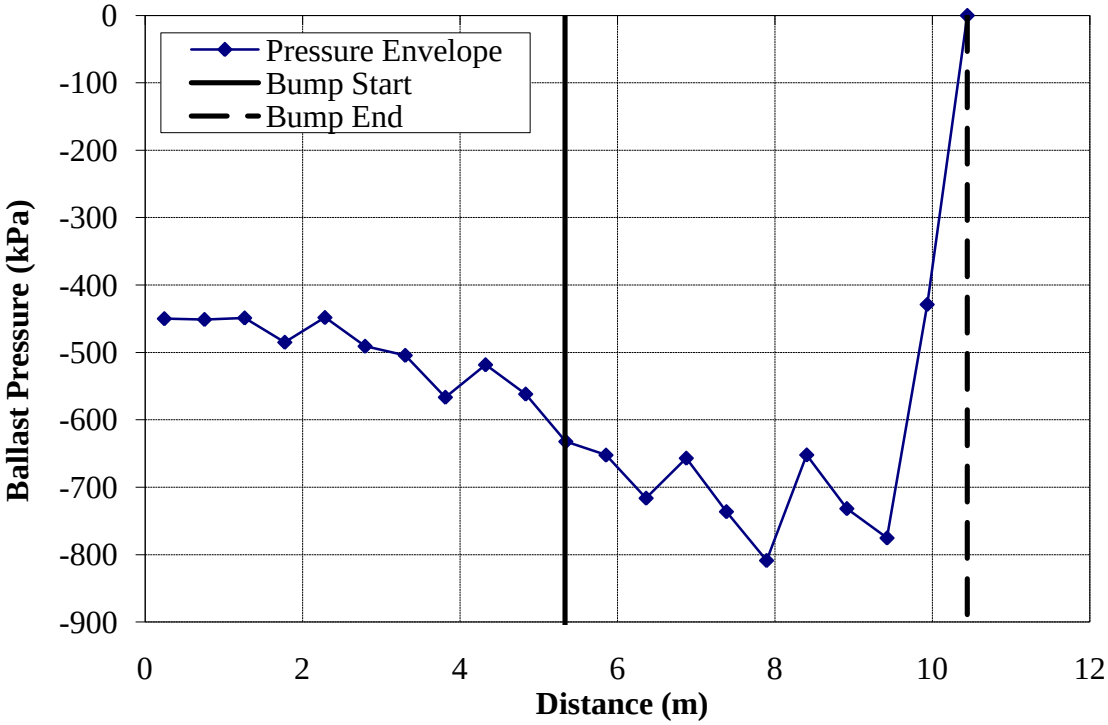

Figure E.11 - Ballast pressures for a truck moving at 15.6 m/s over a 1:150 bump on to the bridge

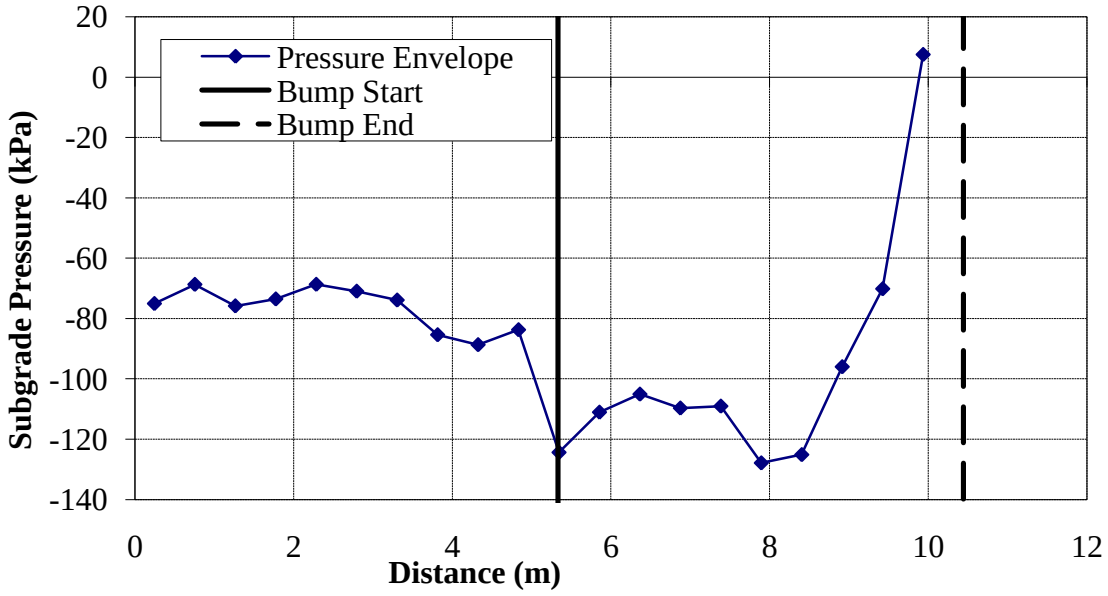

Figure E.12 – Subgrade pressures for a truck moving at 15.6 m/s over a 1:150 bump on to the bridge

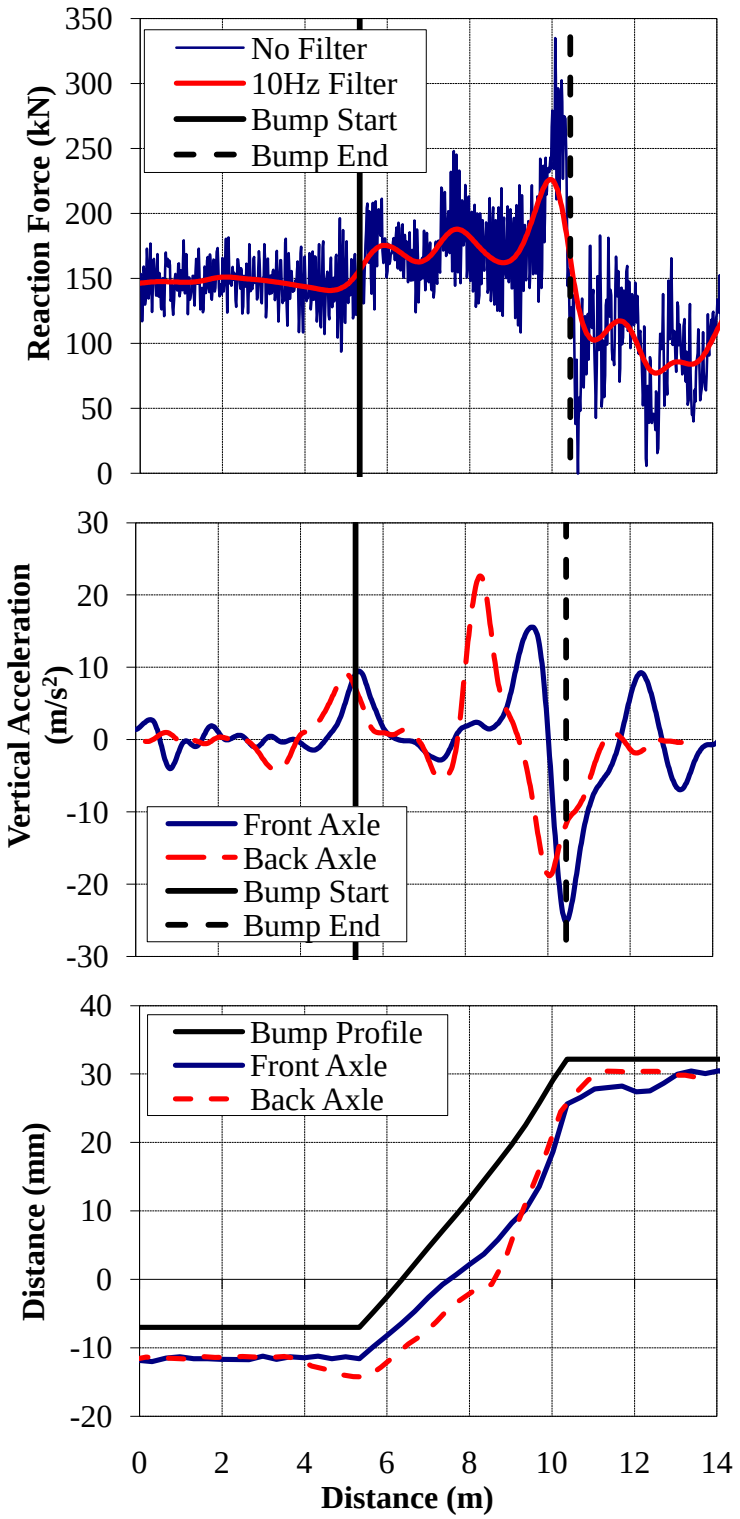

Figure E.13 - (a) Wheel/Rail Forces (b) Axle Accelerations and (c) Track Deflection for a truck moving at 33.5 m/s over a 1:150 Bump on to the bridge

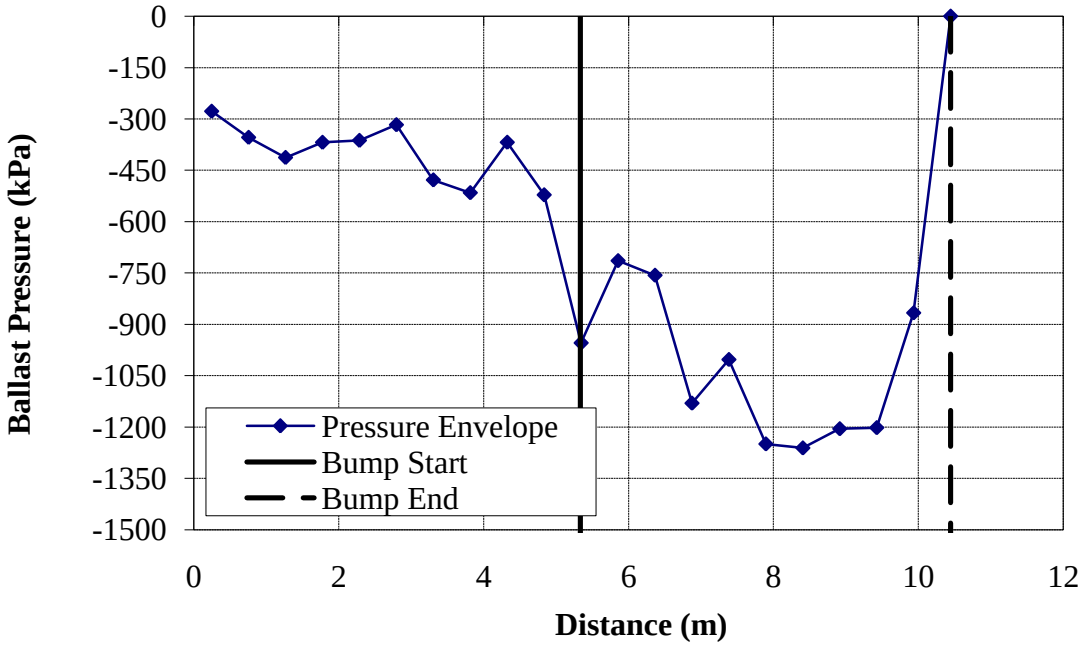

Figure E.14 - Ballast pressures for a truck moving at 33.5 m/s over a 1:150 bump on to the bridge

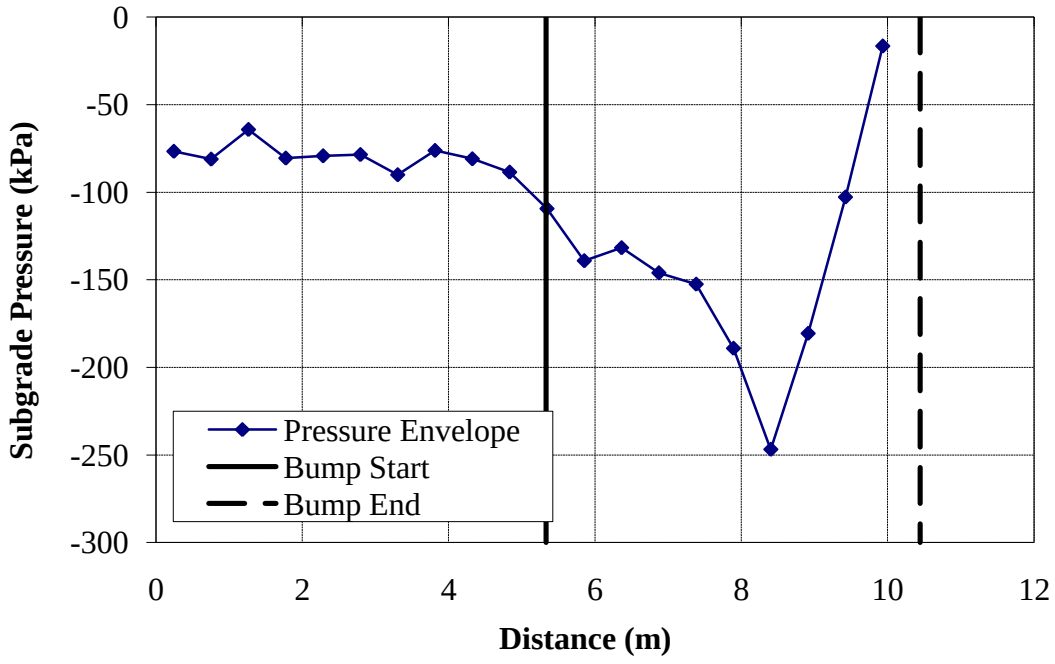

Figure E.15 - Subgrade pressures for a truck moving at 33.5 m/s over a 1:150 bump on to the bridge

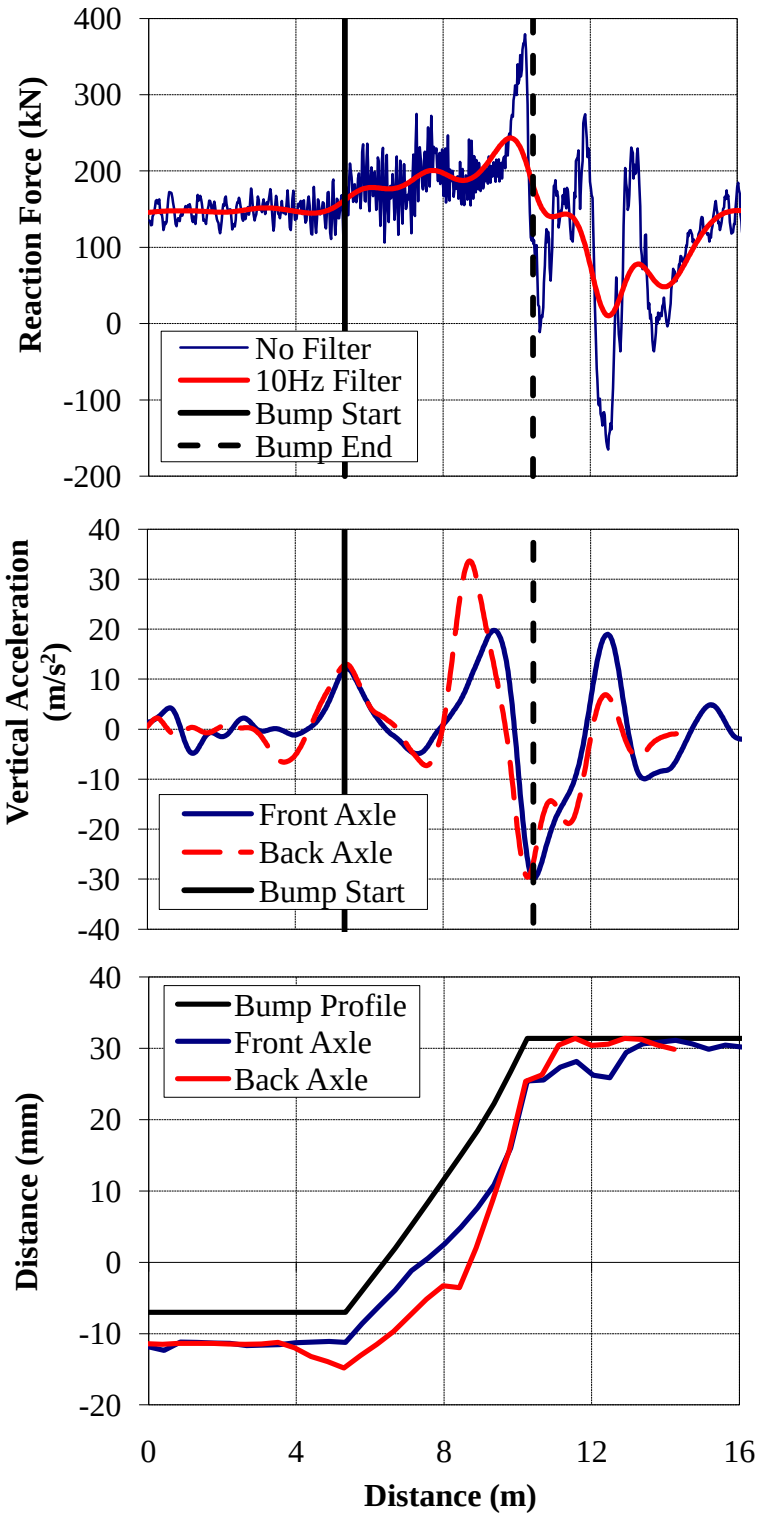

Figure E.16 - (a) Wheel/Rail Forces (b) Axle Accelerations and (c) Track Deflection for a truck moving at 44.7 m/s over a 1:150 Bump on to the bridge

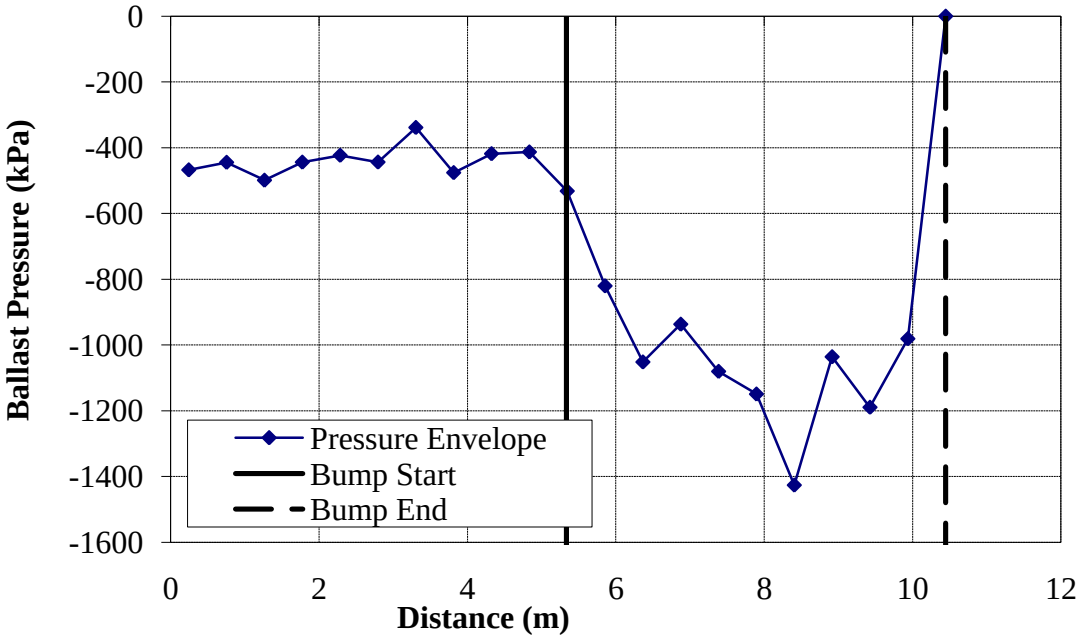

Figure E.17 - Ballast pressures for a truck moving at 44.7 m/s over a 1:150 bump on to the bridge

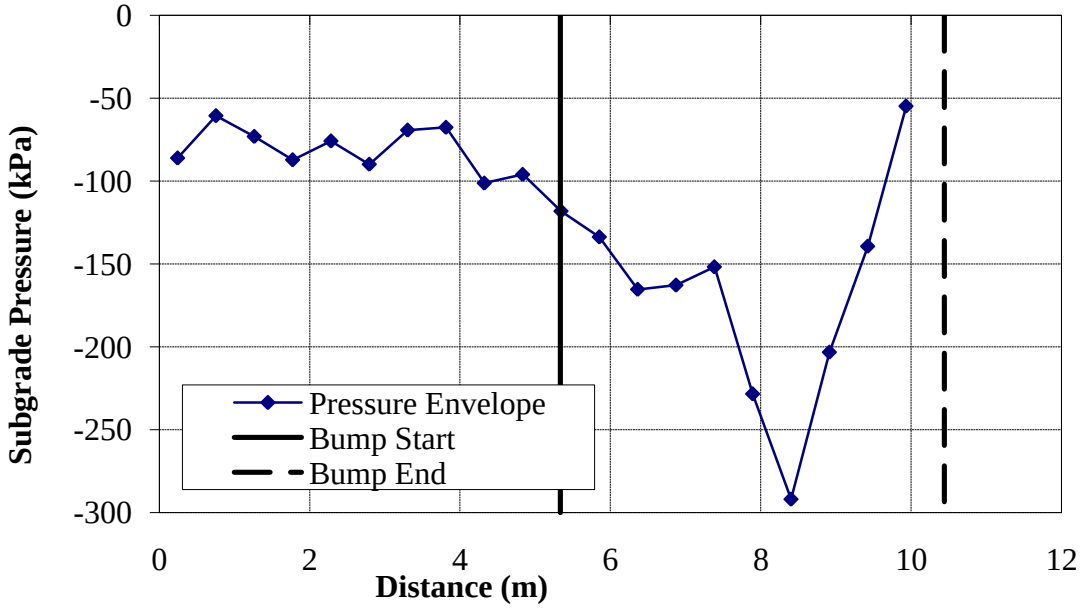

Figure E.18 - Subgrade pressures for a truck moving at 44.7m/s over a 1:150 bump on to the bridge

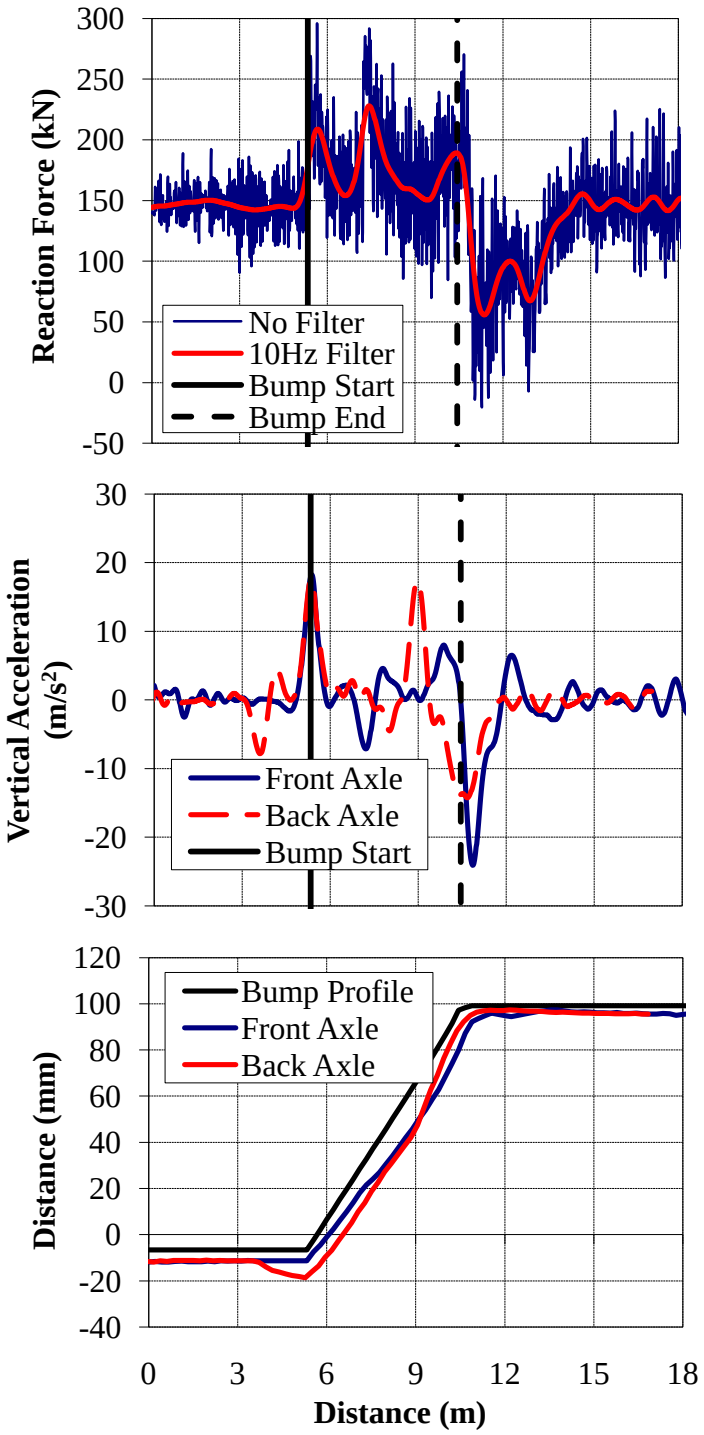

Figure E.19 - (a) Wheel/Rail Forces (b) Axle Accelerations and (c) Track Deflection due to a 1: 50 Bump (Equal Length, v = 22.2 m/s)

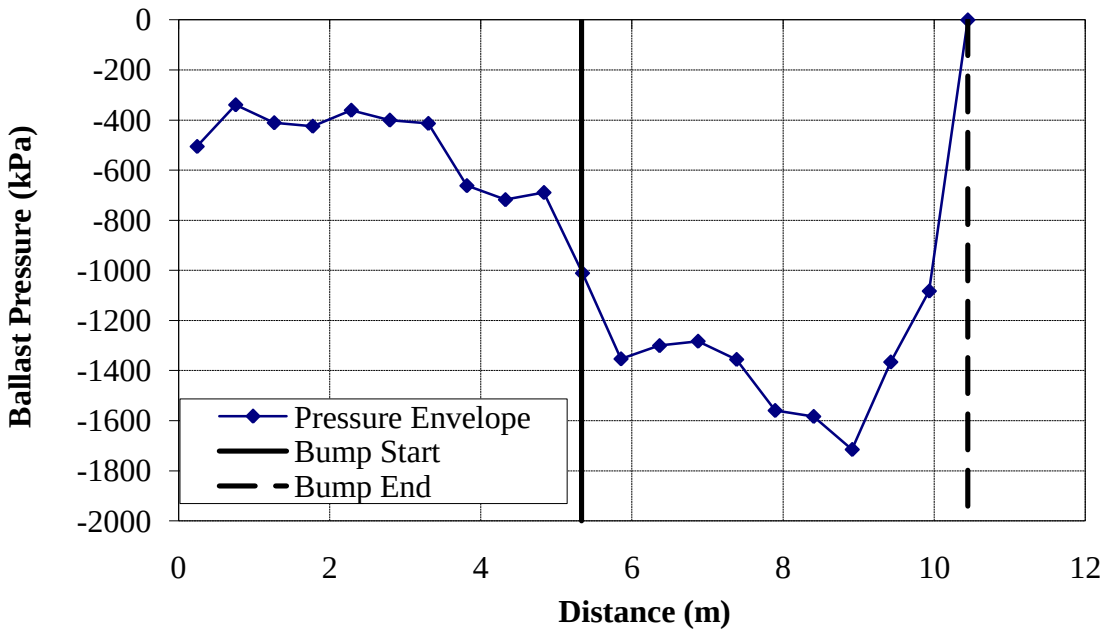

Figure E.20 – Ballast Pressure Resulting from a 1:50 Bump (Equal Length, v = 22.2 m/s)

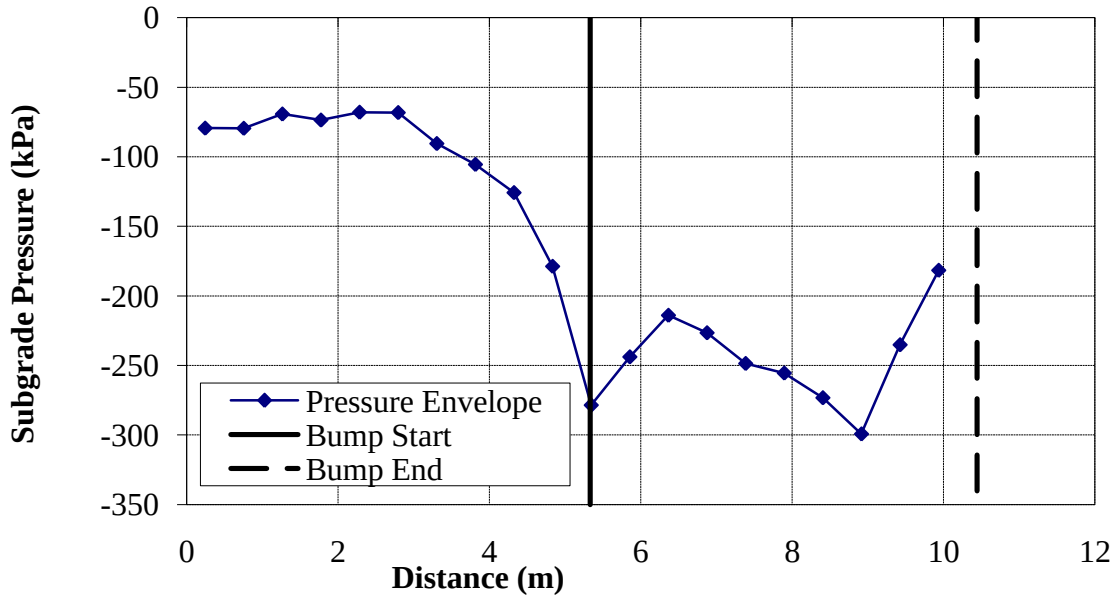

Figure E.21 - Subgrade Pressure Resulting from a 1:50 Bump (Equal Length, v = 22.2 m/s)

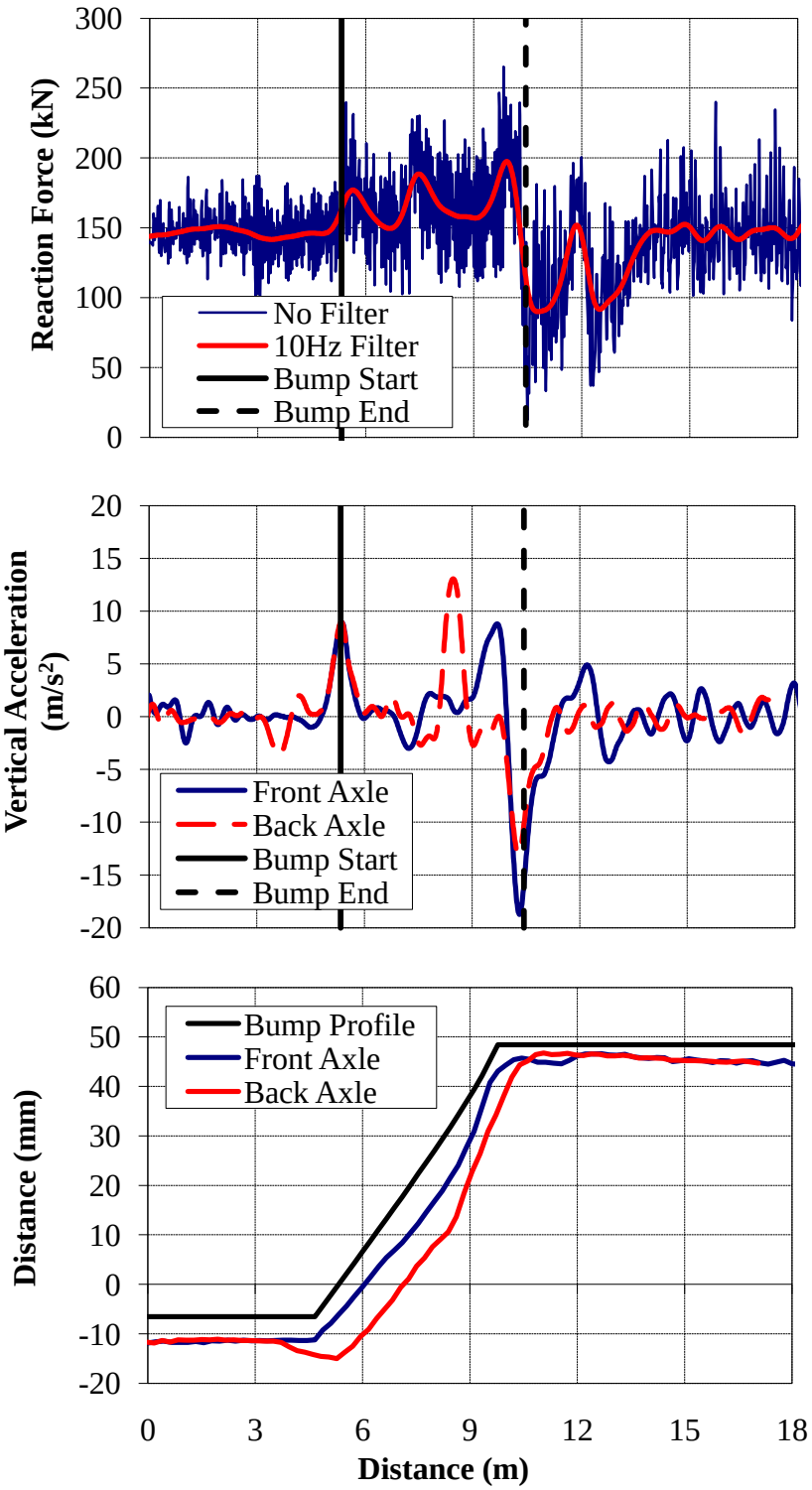

Figure E.22 - (a) Wheel/Rail Forces (b) Axle Accelerations and (c) Track Deflection due to a 1:100 Bump (Equal Length, v = 22.2 m/s)

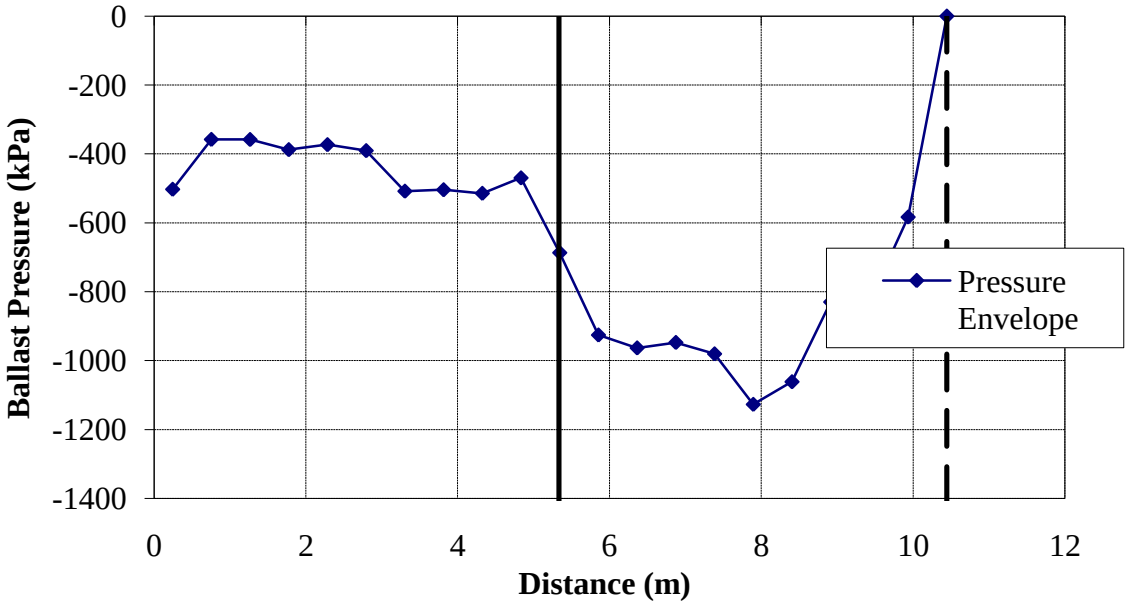

Figure E.23 – Ballast Pressure Resulting from a 1:100 Bump (Equal Length, v = 22.2 m/s)

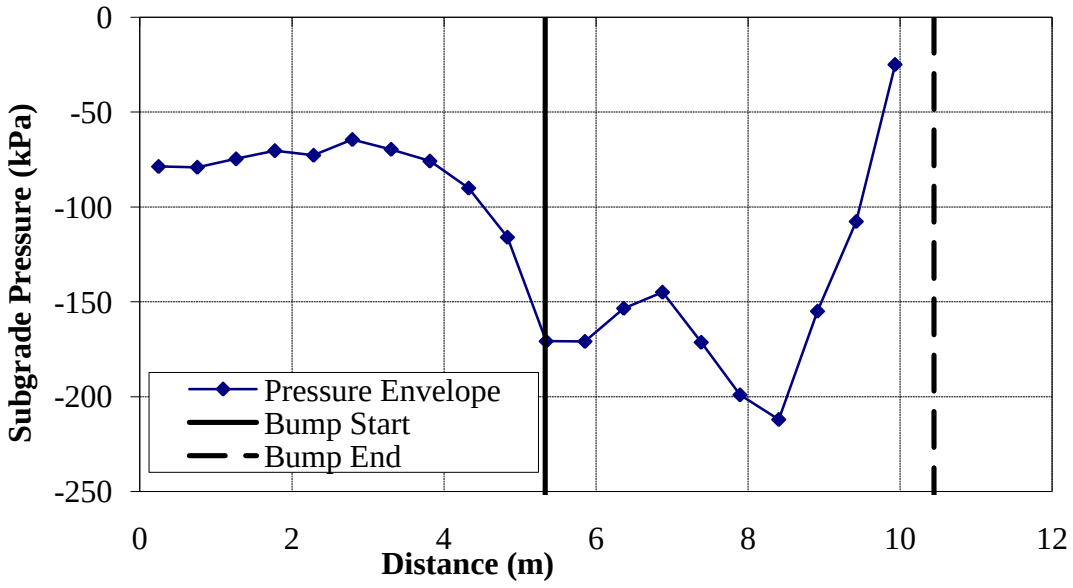

Figure E.24 - Subgrade Pressure Resulting from a 1:100 Bump (Equal Length, v = 22.2 m/s)

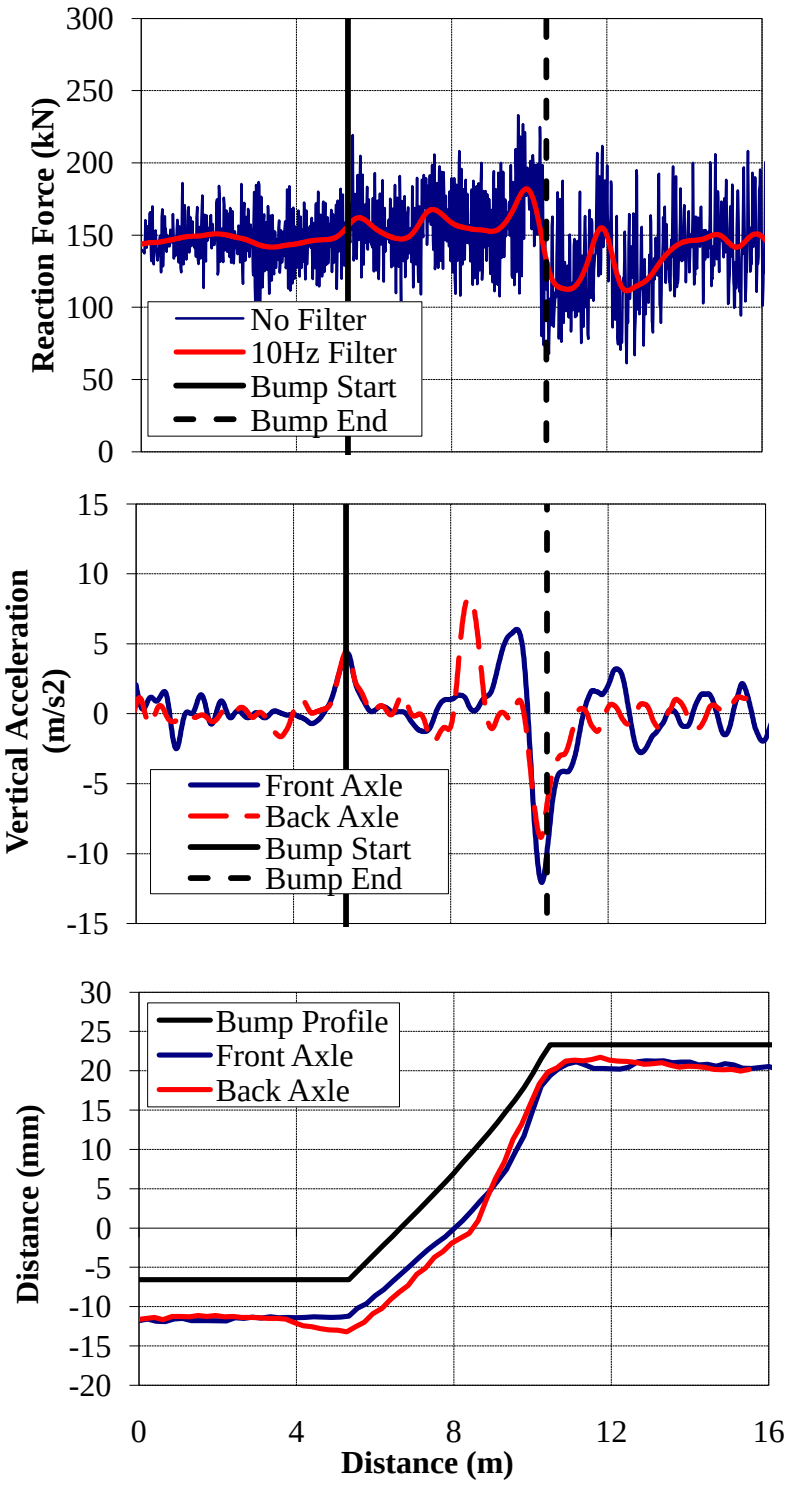

Figure E.25 - (a) Wheel/Rail Forces (b) Axle Accelerations and (c) Track Deflection due to a 1:200 Bump (Equal Length, v = 22.2 m/s)

Figure E.26 – Ballast Pressure Resulting from a 1:200 Bump (Equal Length, v = 22.2 m/s)

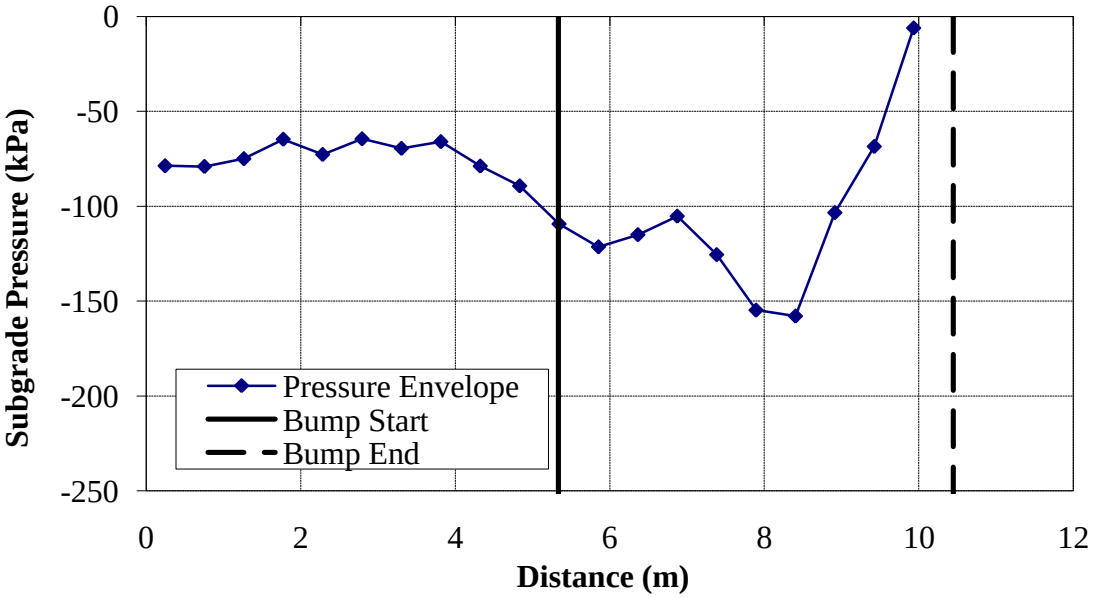

Figure E.27 - Subgrade Pressure Resulting from a 1:200 Bump (Equal Length, v = 22.2 m/s)

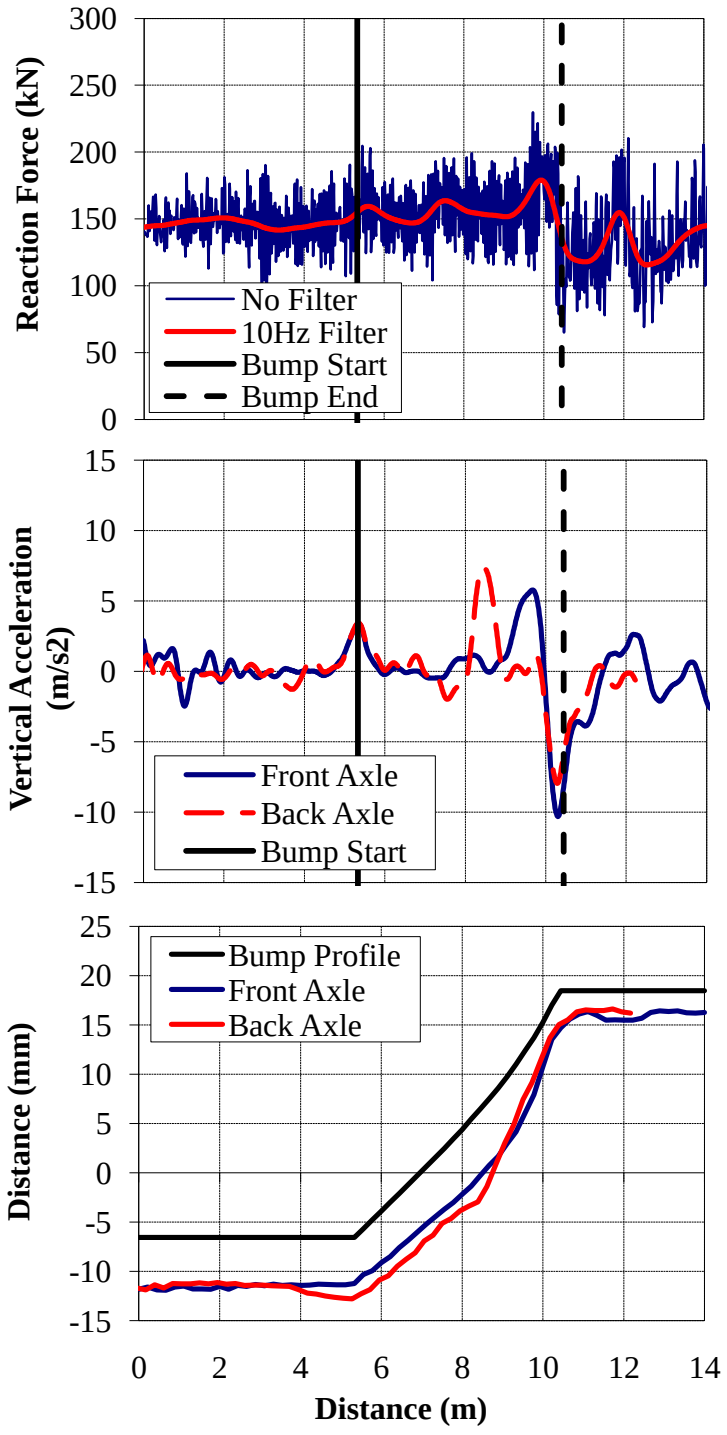

Figure E.28 - (a) Wheel/Rail Forces (b) Axle Accelerations and (c) Track Deflection due to a 1:250 Bump (Equal Length, v = 22.2 m/s)

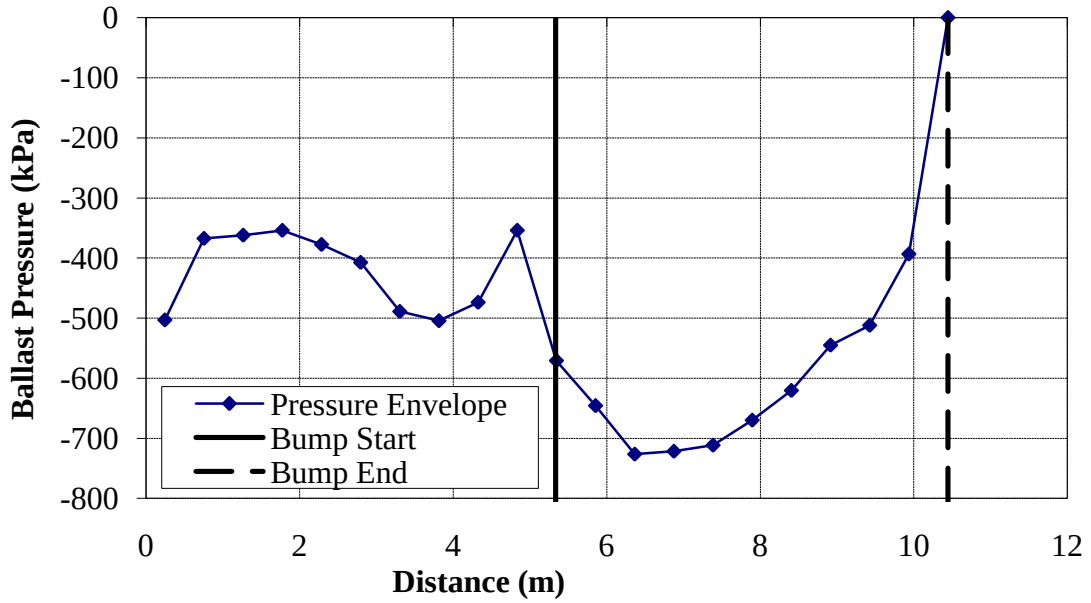

Figure E.29 – Ballast Pressure Resulting from a 1:250 Bump (Equal Length, v = 22.2 m/s)

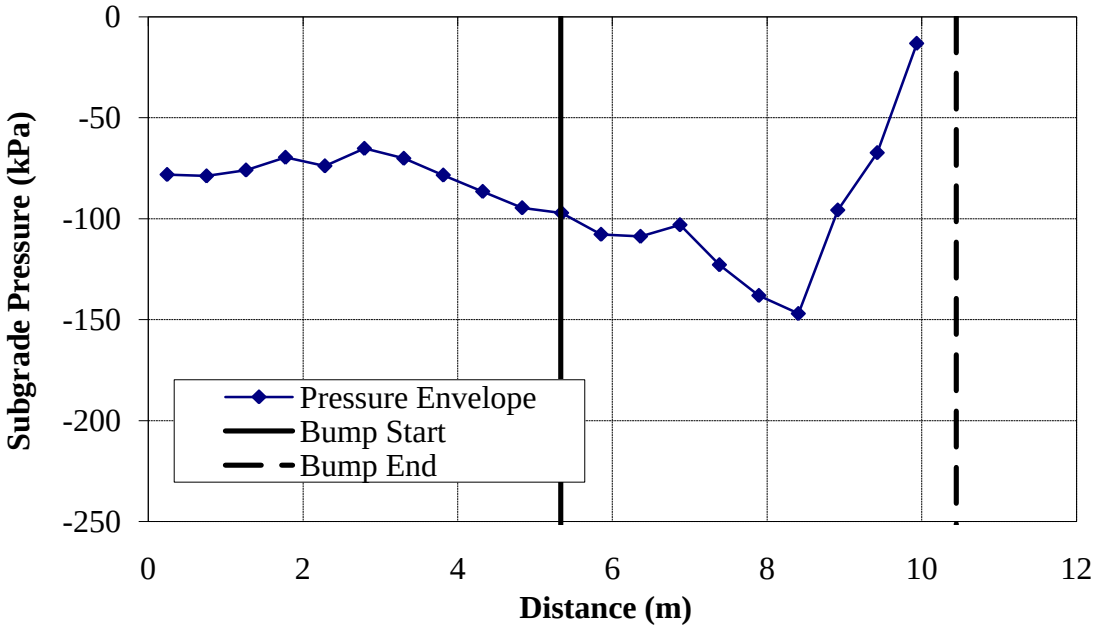

Figure E.30 - Subgrade Pressure Resulting from a 1:250 Bump (Equal Length, v = 22.2 m/s)

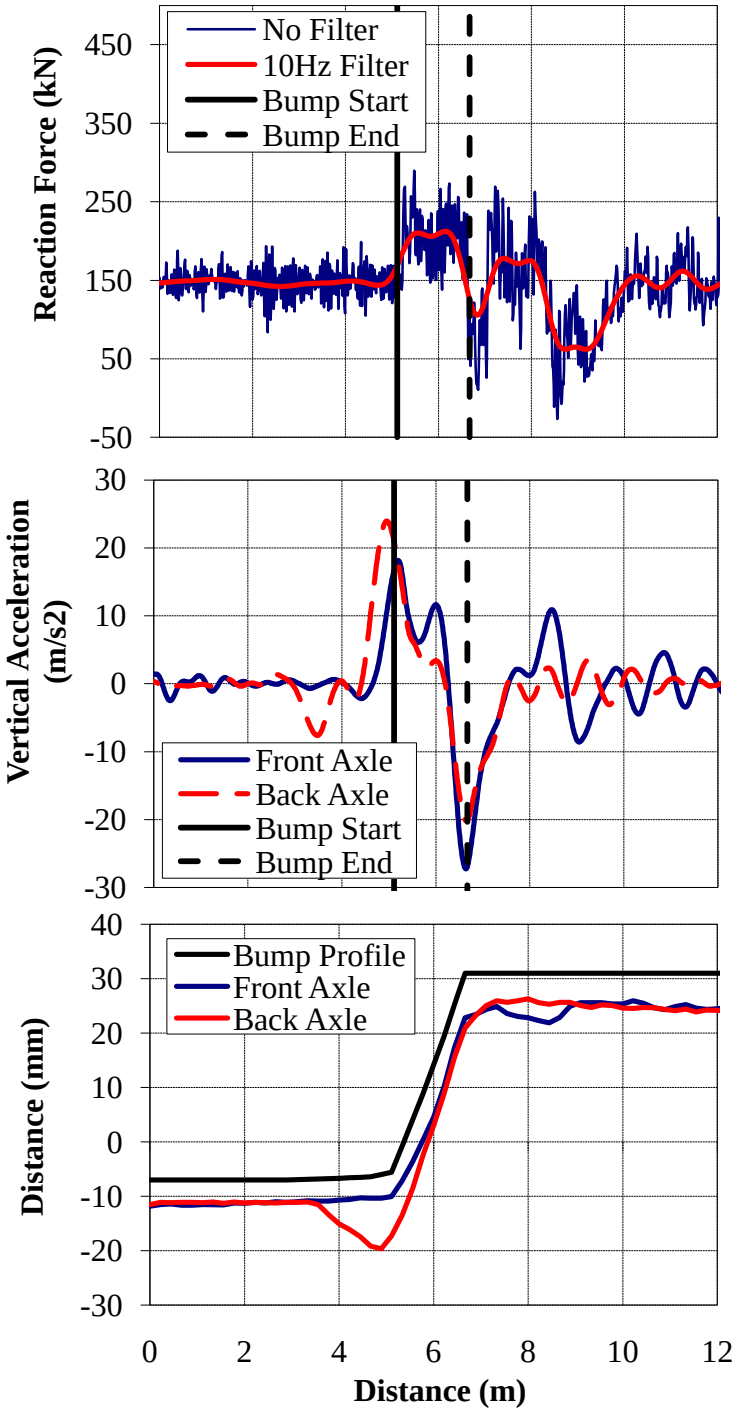

Figure E.31 - (a) Wheel/Rail Forces (b) Axle Accelerations and (c) Track Deflection due to a 1:50 Bump (Equal Height, v = 22.2 m/s)

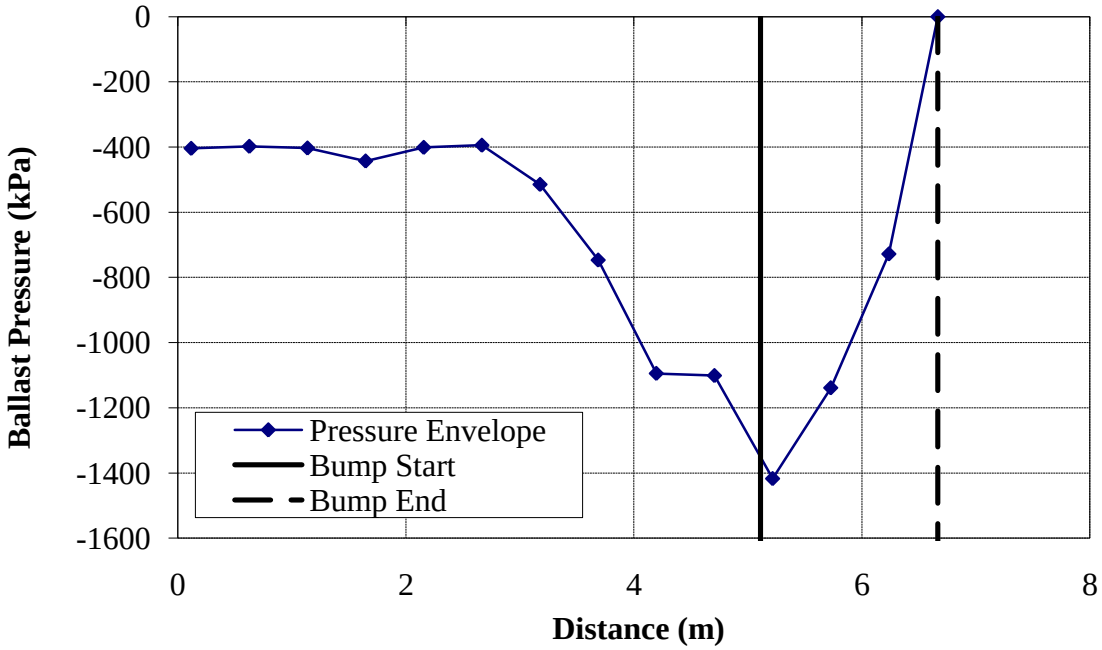

Figure E.32 – Ballast Pressure Resulting from a 1: 50 Bump (Equal Height, v = 22.2 m/s)

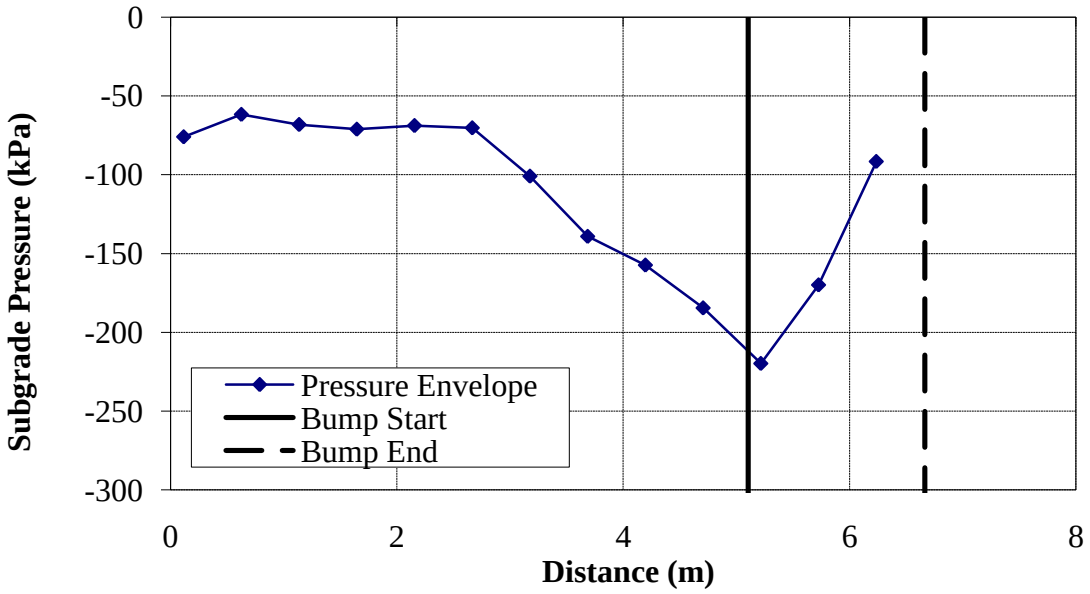

Figure E.33 - Subgrade Pressure Resulting from a 1:50 Bump (Equal Height, v = 22.2 m/s)

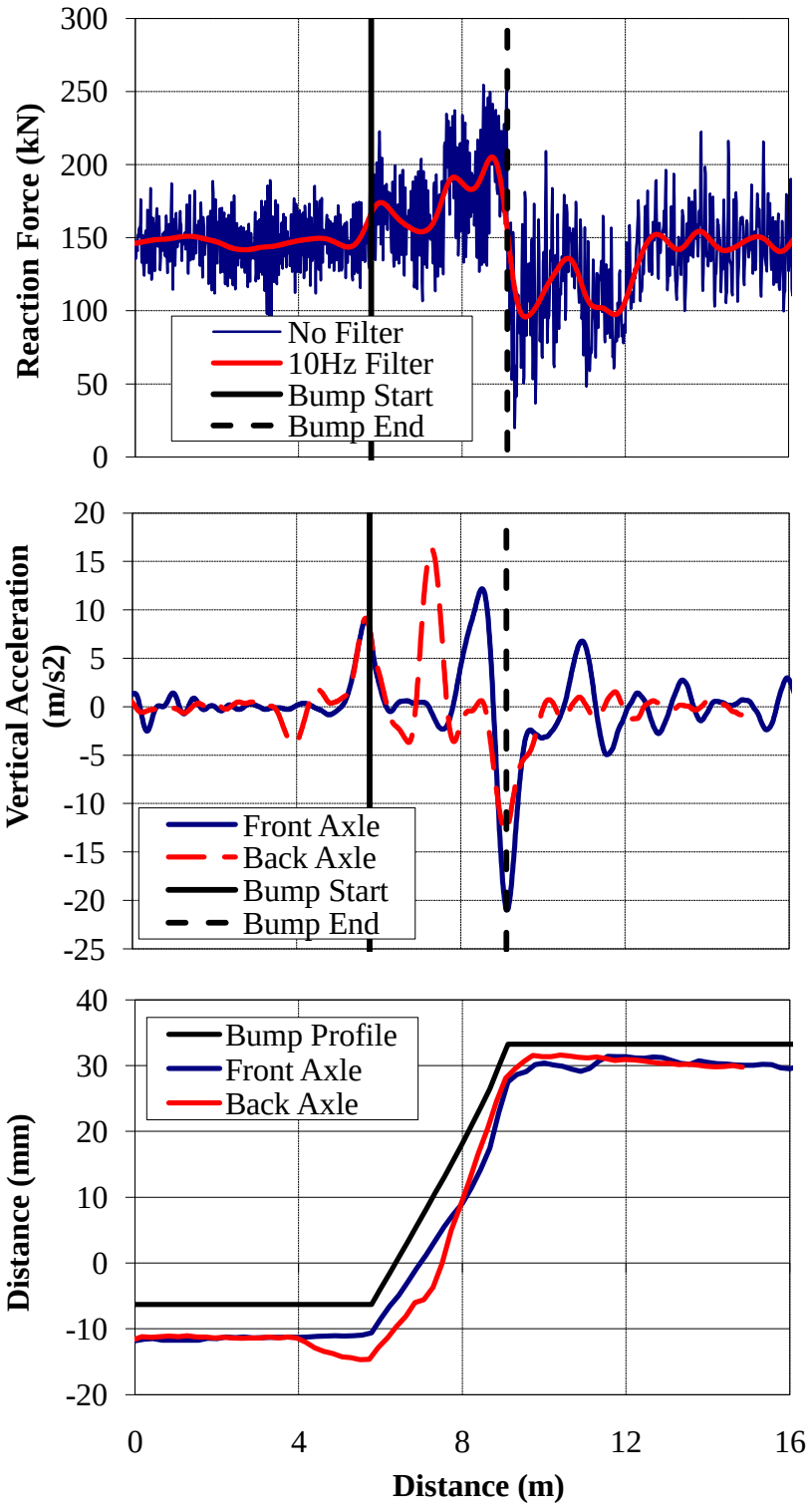

Figure E.34 - (a) Wheel/Rail Forces (b) Axle Accelerations and (c) Track Deflection due to a 1:100 Bump (Equal Height, v = 22.2 m/s)

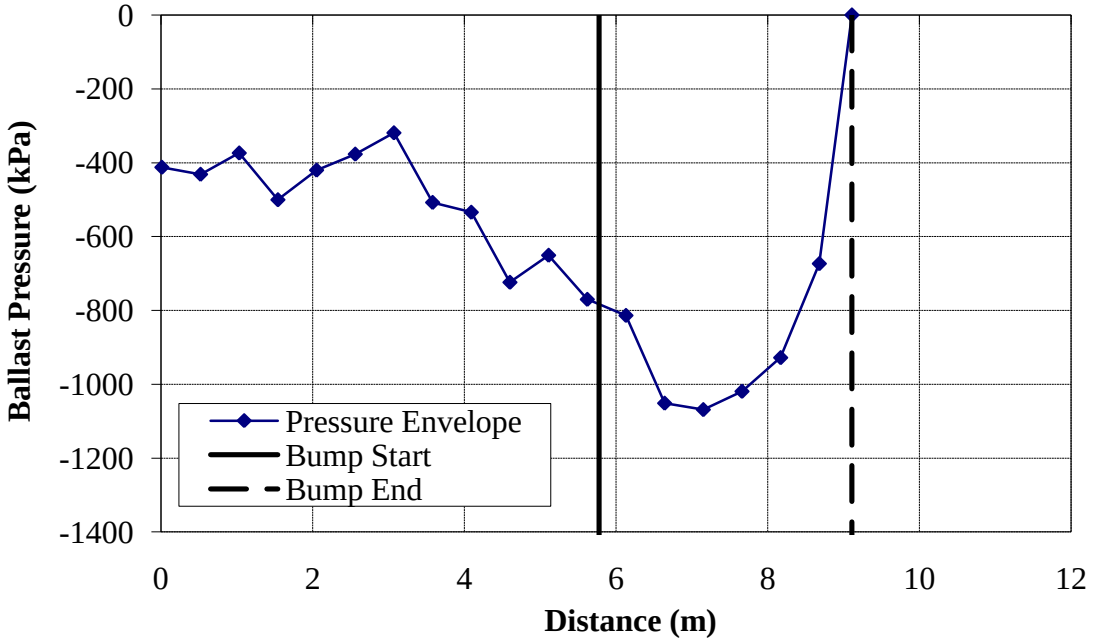

Figure E.35 – Ballast Pressure Resulting from a 1:100 Bump (Equal Height, v = 22.2 m/s)

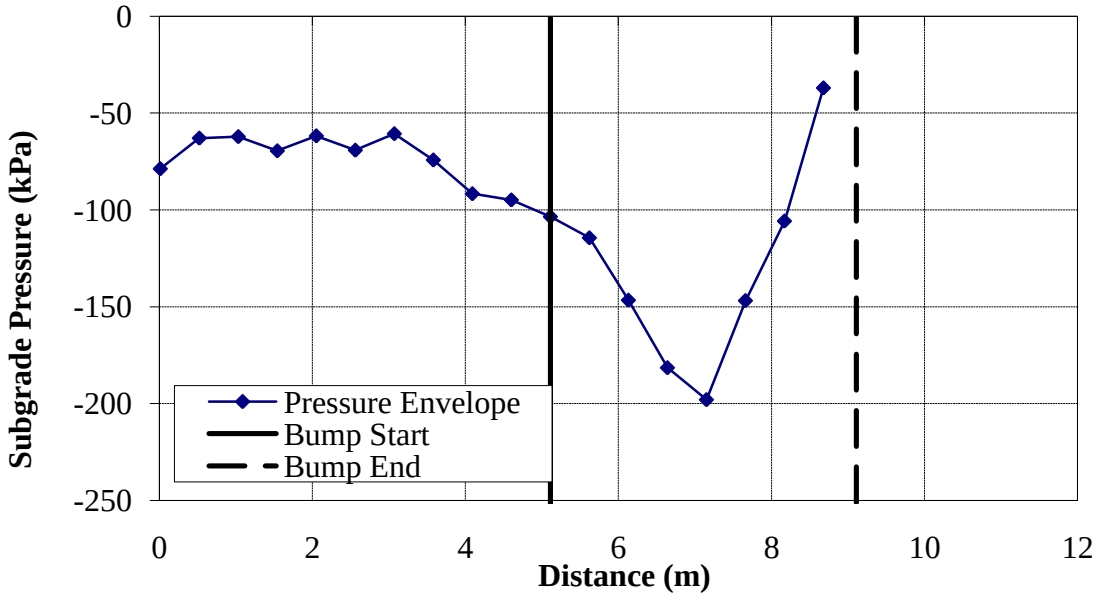

Figure E.36 - Subgrade Pressure Resulting from a 1:100 Bump (Equal Height, v = 22.2 m/s)

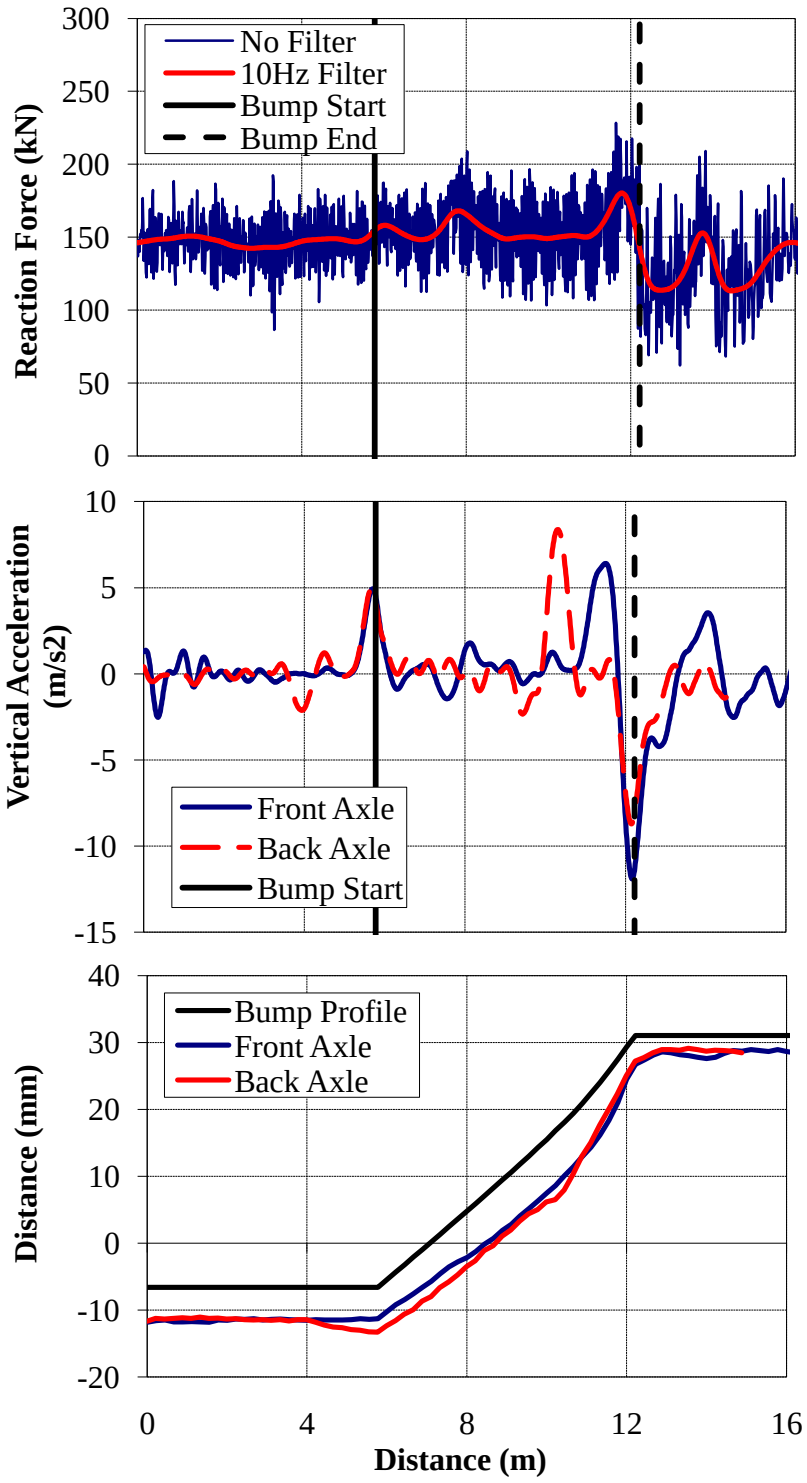

Figure E.37 - (a) Wheel/Rail Forces (b) Axle Accelerations and (c) Track Deflection due to a 1:200 Bump (Equal Height, v = 22.2 m/s)

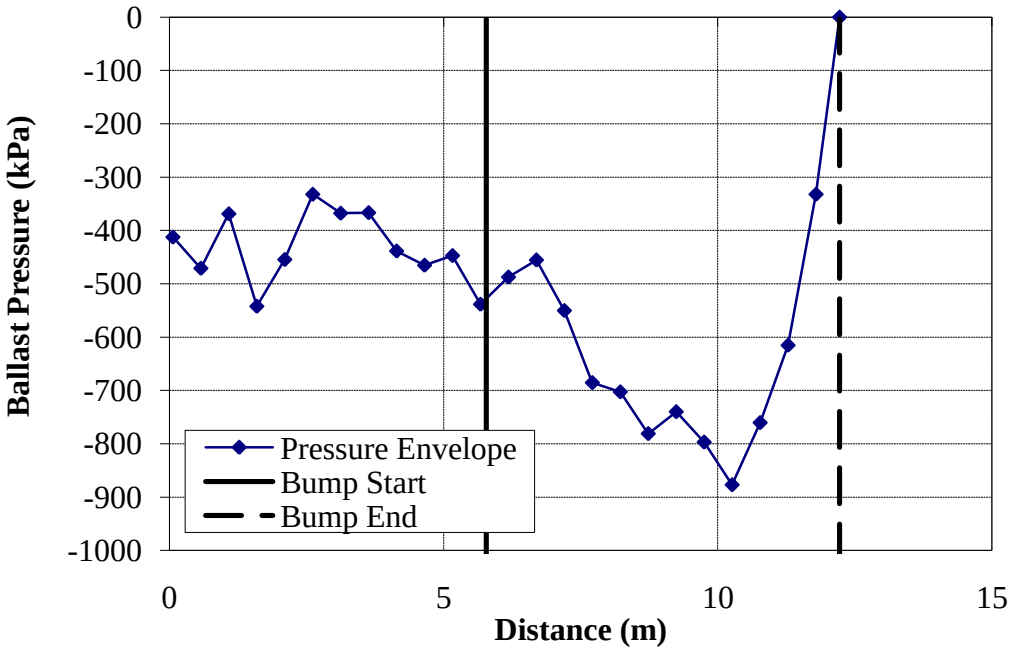

Figure E.38 – Ballast Pressure Resulting from a 1:200 Bump (Equal Height, v = 22.2 m/s)

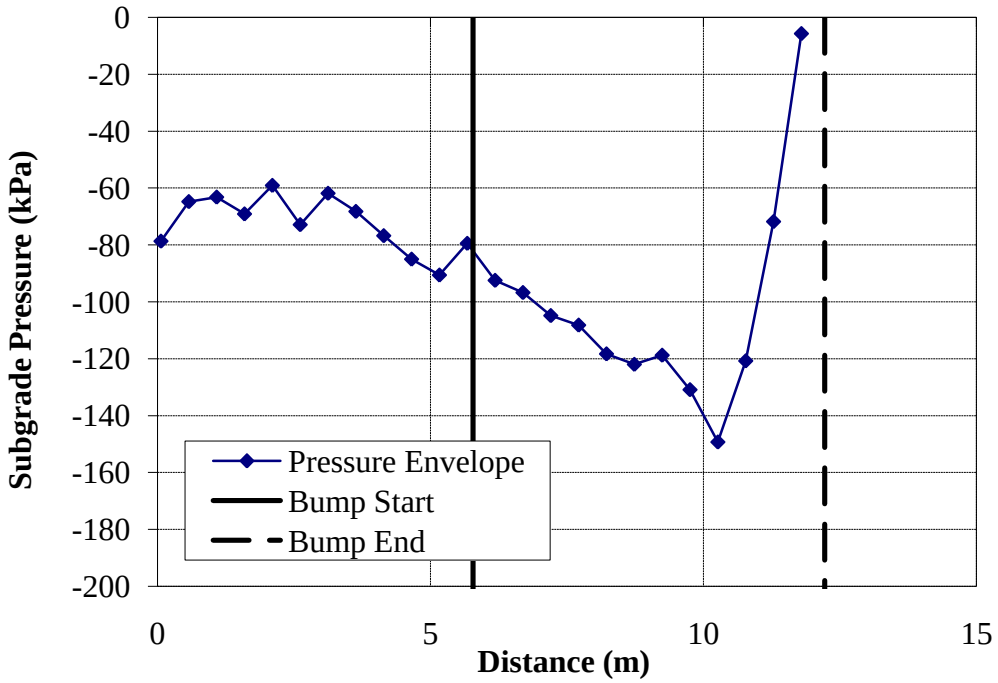

Figure E.39 - Subgrade Pressure Resulting from a 1:200 Bump (Equal Height, v = 22.2 m/s)

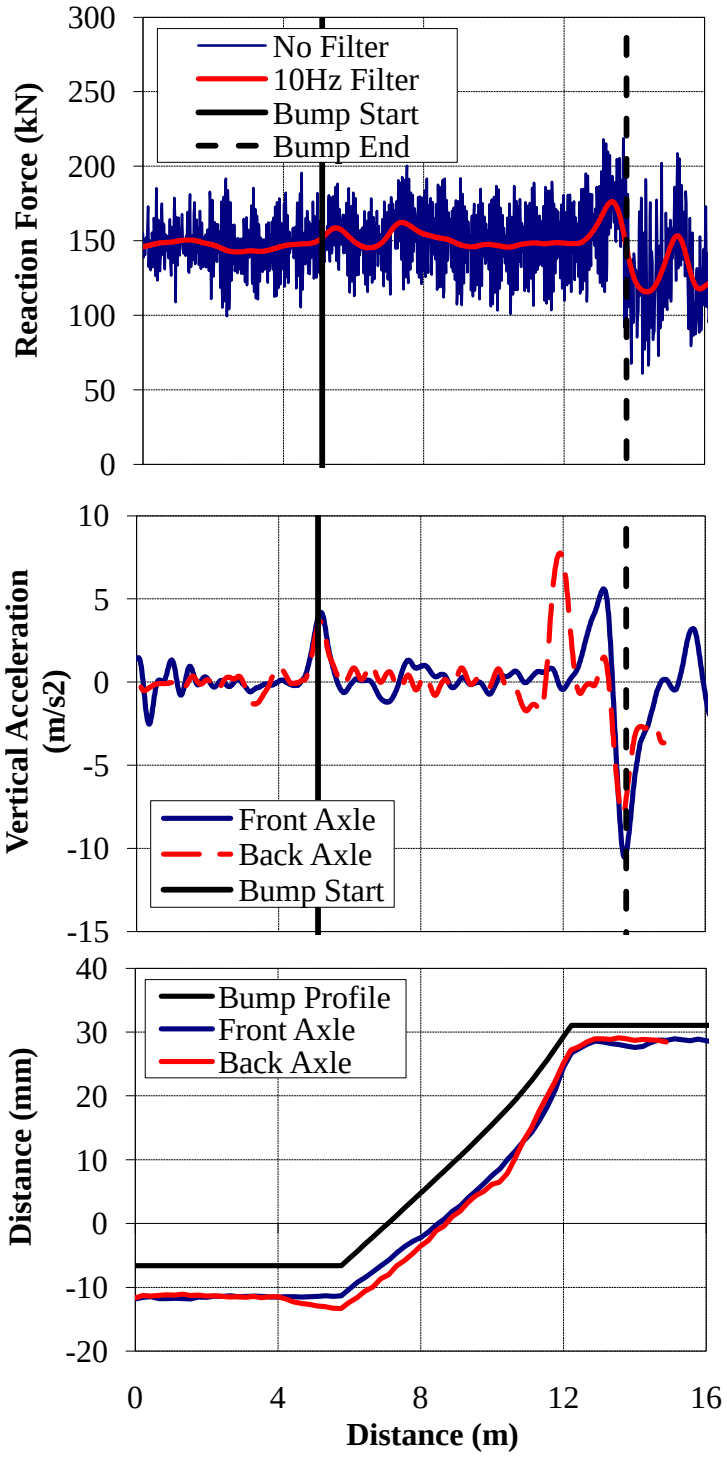

Figure E.40 - (a) Wheel/Rail Forces (b) Axle Accelerations and (c) Track Deflection due to a 1:250 Bump (Equal Height, v = 22.2 m/s)

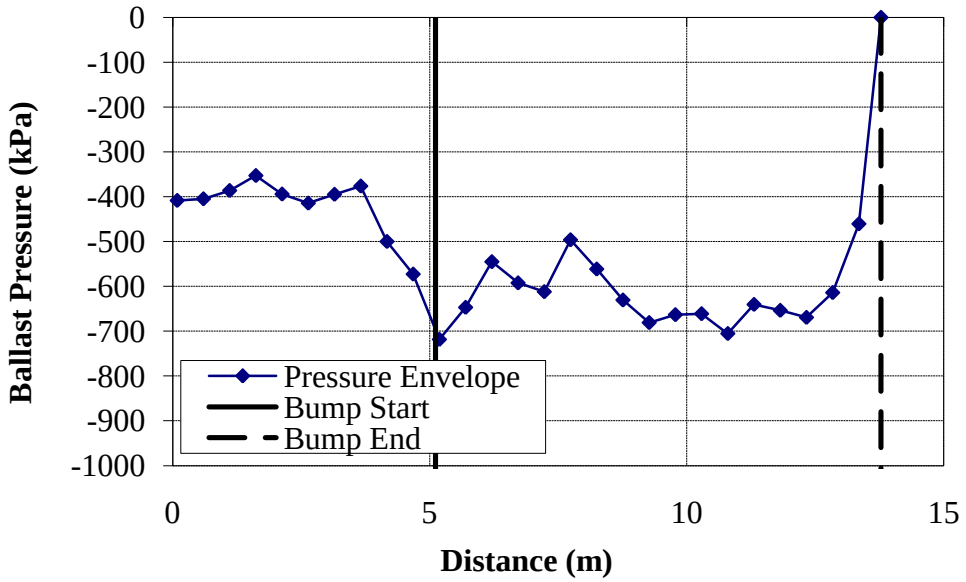

Figure E.41 – Ballast Pressure Resulting from a 1:250 Bump (Equal Height, v = 22.2 m/s)

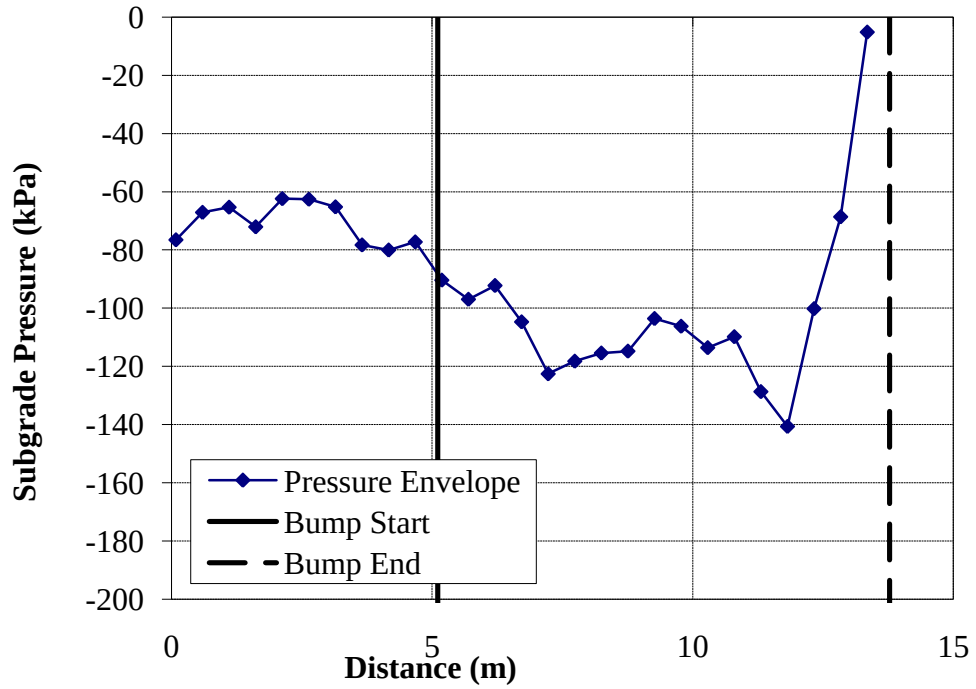

Figure E.42 - Subgrade Pressure Resulting from a 1:250 Bump (Equal Height, v = 22.2 m/s)

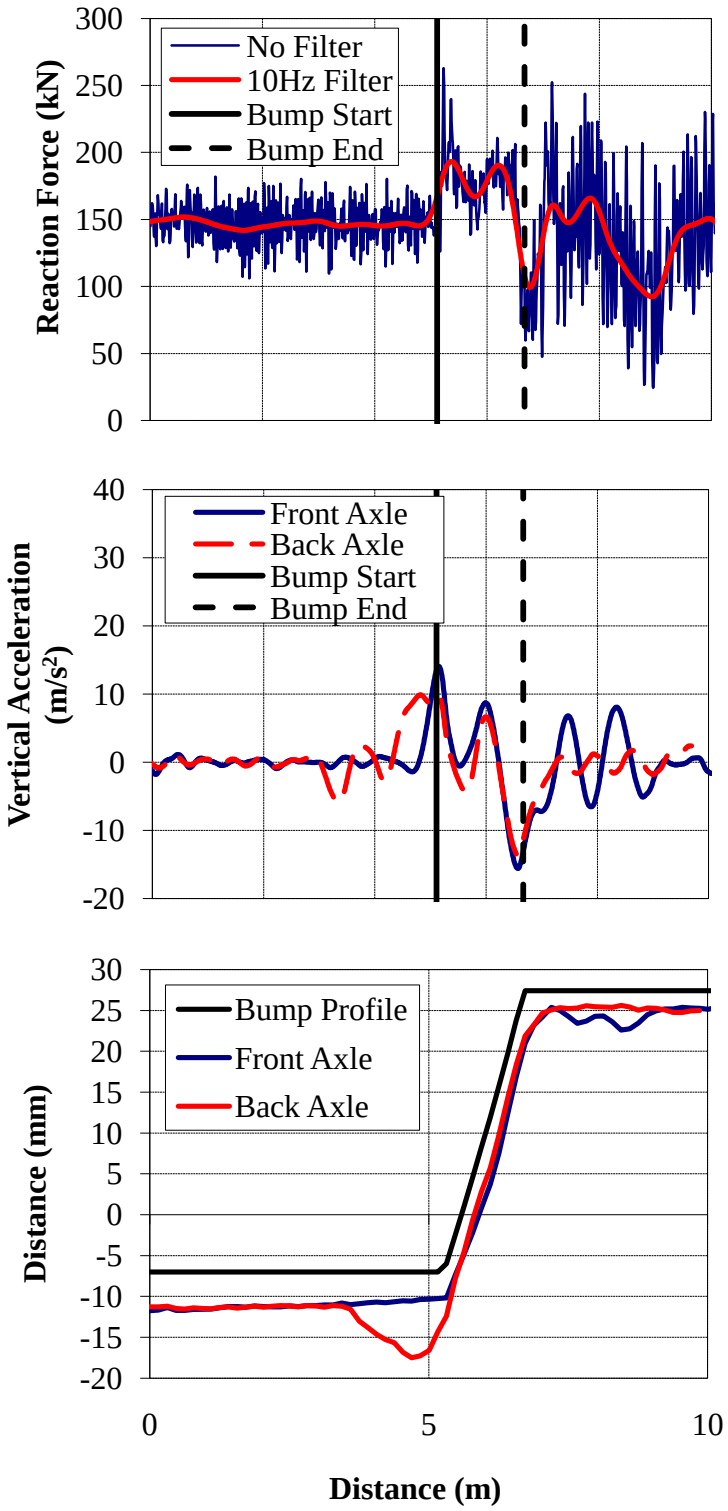

Figure E.43 - (a) Wheel/Rail Forces (b) Axle Accelerations and (c) Track Deflection due to a 1:50 Bump (Equal Height, v = 15.6 m/s)

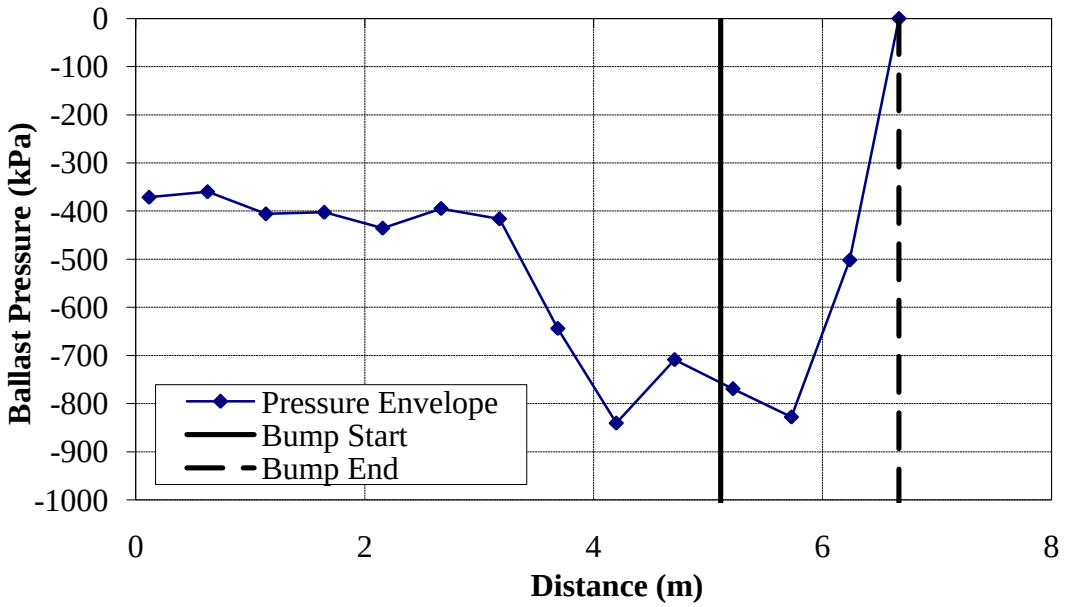

Figure E.44 – Ballast Pressure Resulting from a 1:50 Bump (Equal Height, v = 15.6 m/s)

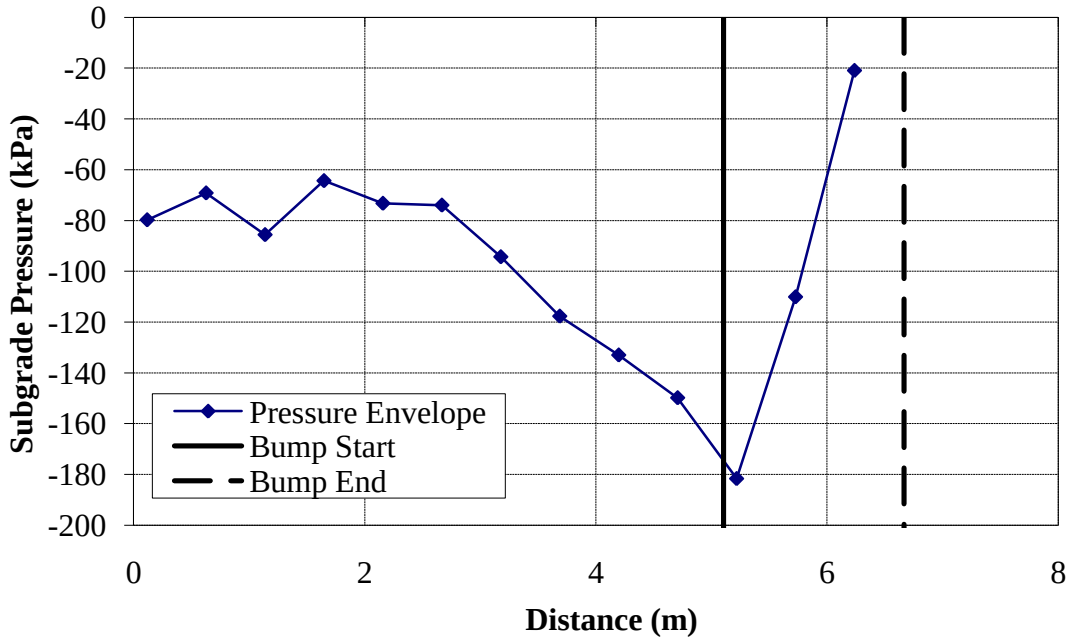

Figure E.45 - Subgrade Pressure Resulting from a 1:50 Bump (Equal Height, v = 15.6 m/s)

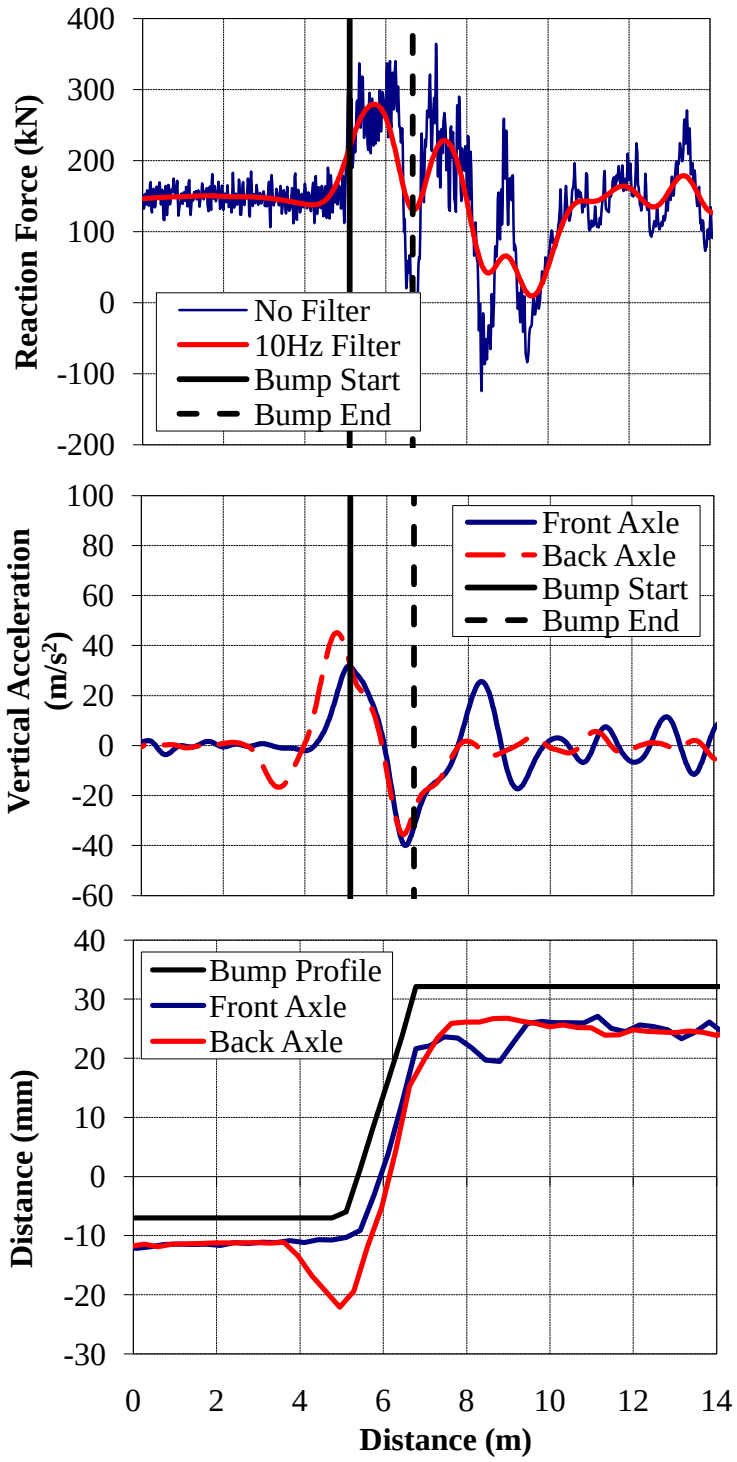

Figure E.46 - (a) Wheel/Rail Forces (b) Axle Accelerations and (c) Track Deflection due to a 1:50 Bump (Equal Height, v = 33.5 m/s)

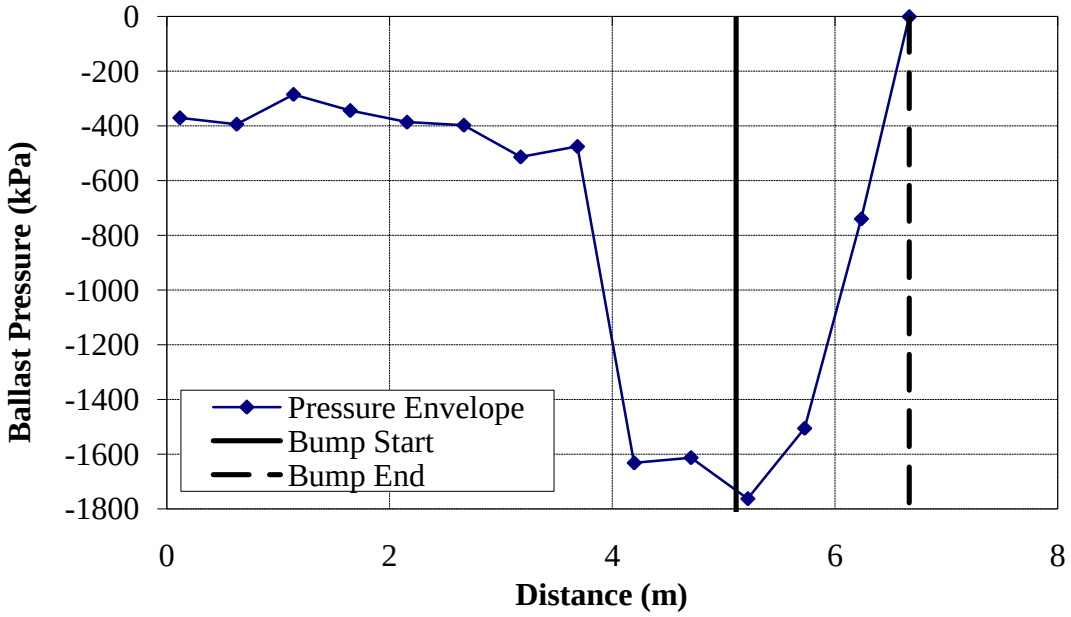

Figure E.47 – Ballast Pressure Resulting from a 1:50 Bump (Equal Height, v = 33.5 m/s)

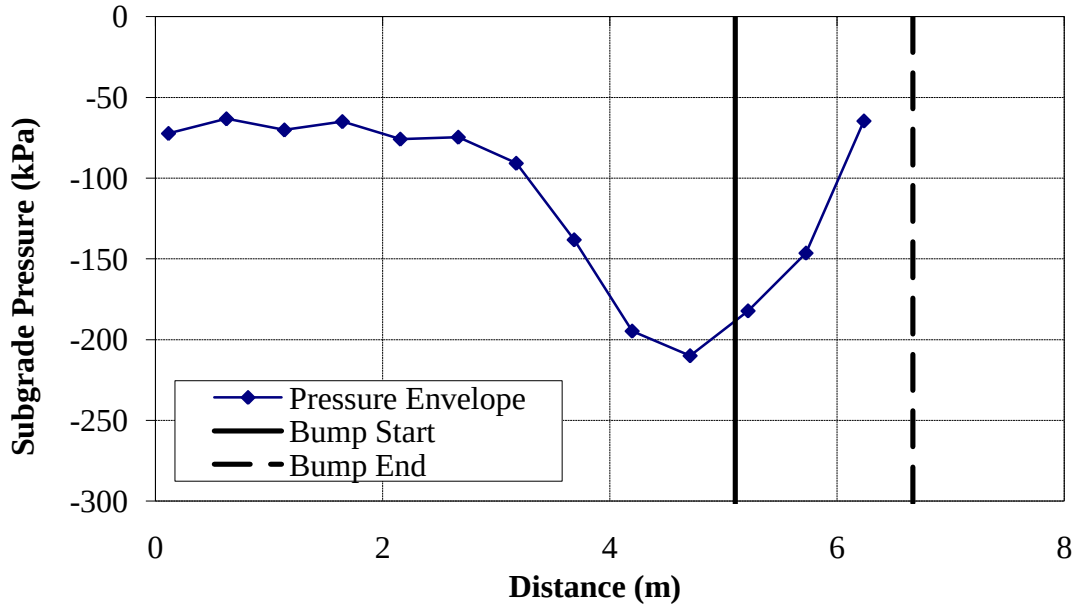

Figure E.48 - Subgrade Pressure Resulting from 1:50 Bump (Equal Height, v = 33.5 m/s)

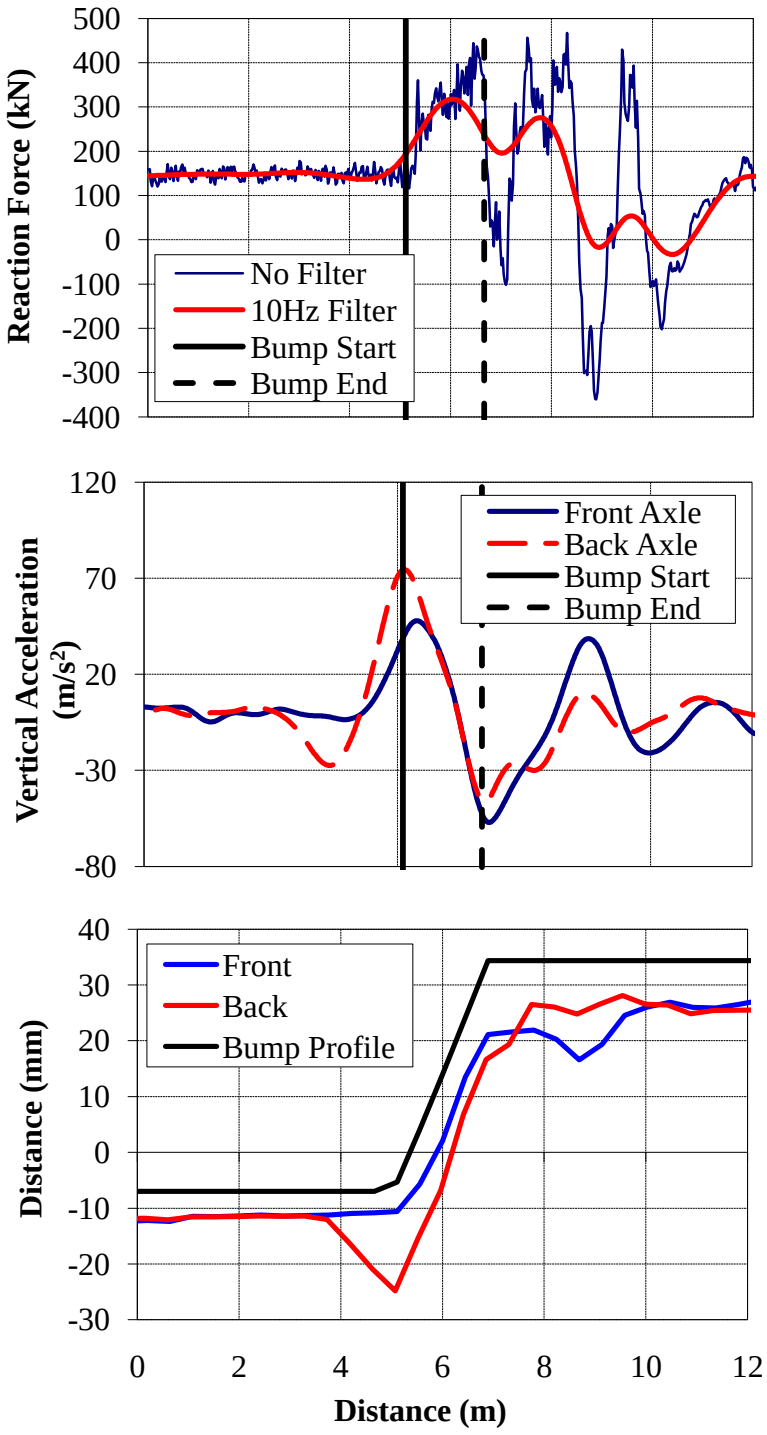

Figure E.49 - (a) Wheel/Rail Forces (b) Axle Accelerations and (c) Track Deflection due to a 1:50 Bump (Equal Height, v = 44.7 m/s)

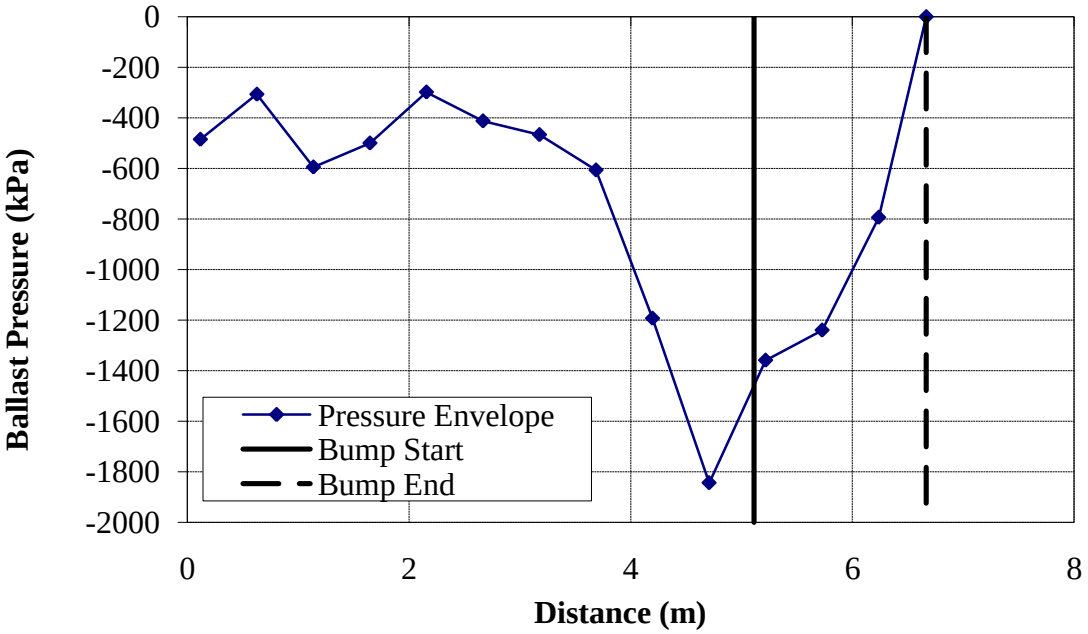

Figure E.50 – Ballast Pressure Resulting from a 1:50 Bump (Equal Height, v = 44.7 m/s)

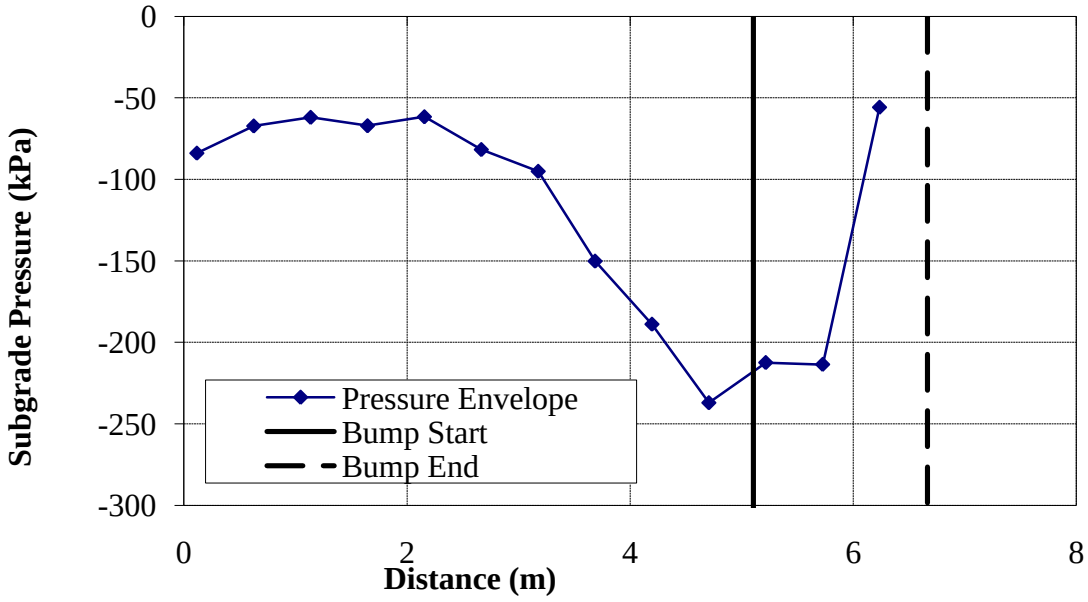

Figure E.51 - Subgrade Pressure Resulting from a 1:50 Bump (Equal Height, v = 44.7 m/s)

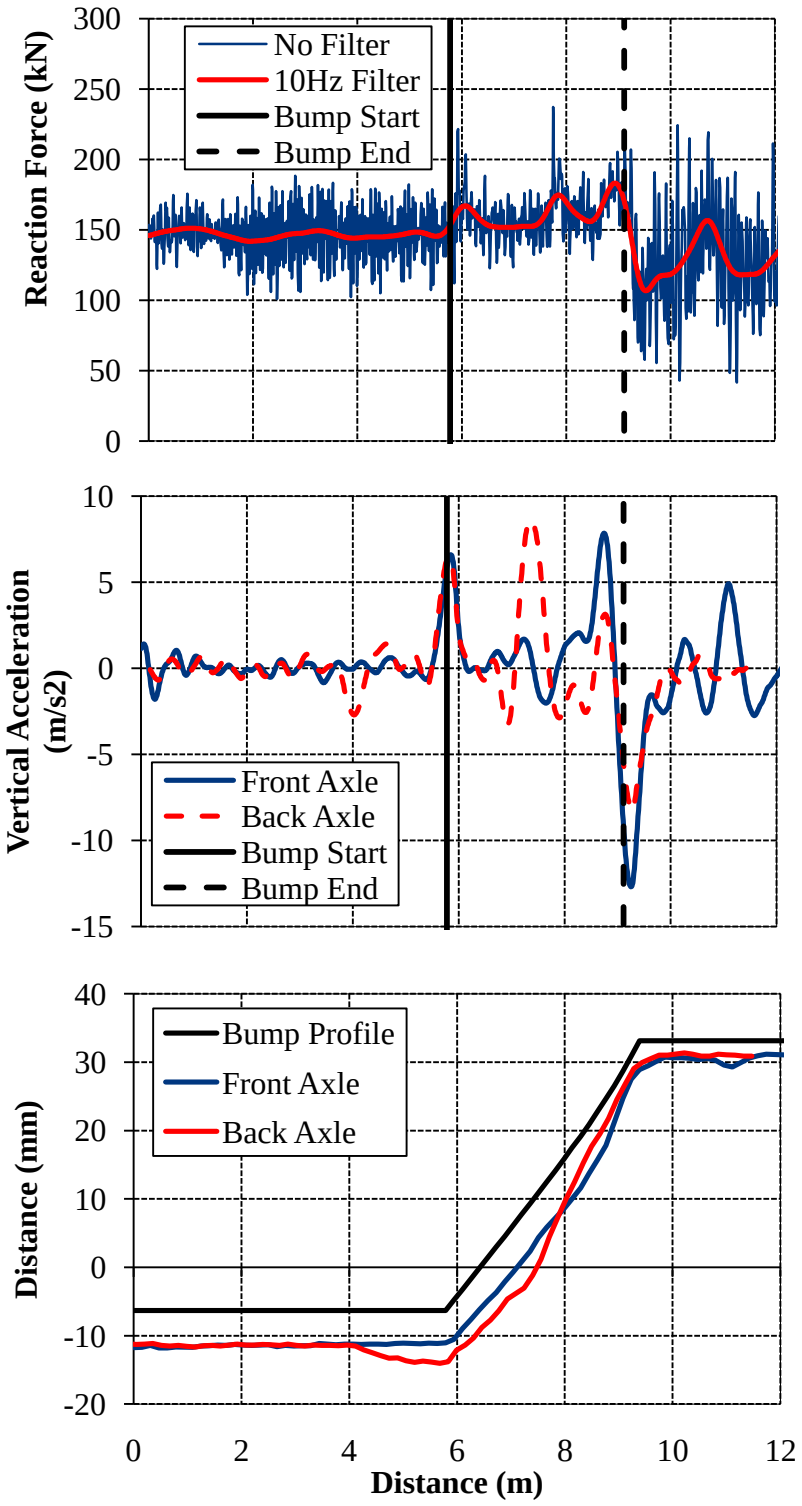

Figure E.52 - (a) Wheel/Rail Forces (b) Axle Accelerations and (c) Track Deflection due to a 1:100 Bump (Equal Height, v = 15.6 m/s)

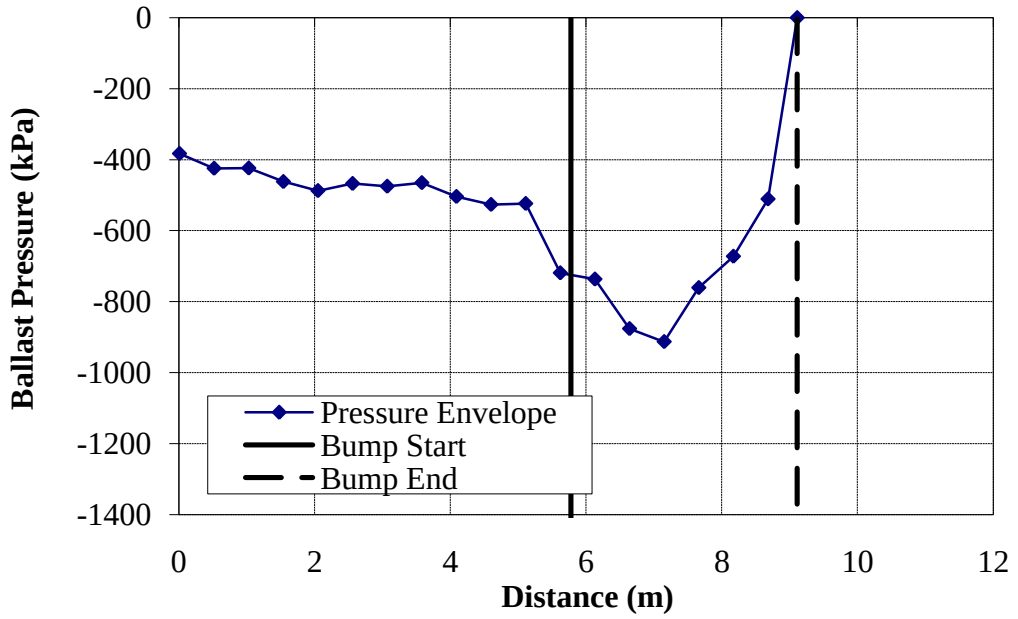

Figure E.19 - Ballast Pressure Resulting from a 1:100 Bump (Equal Height, v = 15.6 m/s)

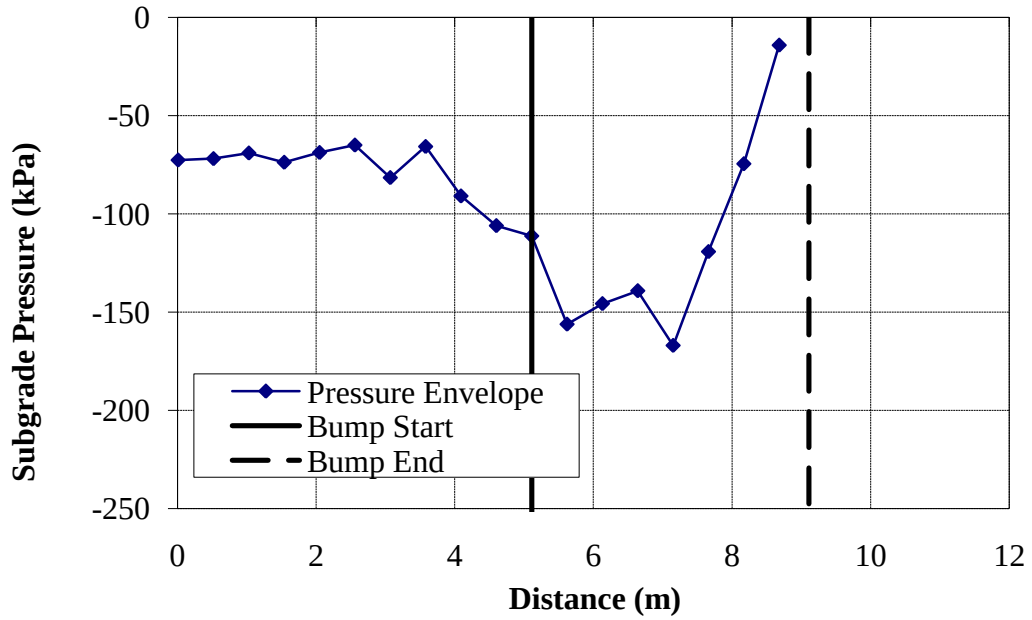

Figure E.54 - Subgrade Pressure Resulting from a 1:100 Bump (Equal Height, v = 15.6 m/s)

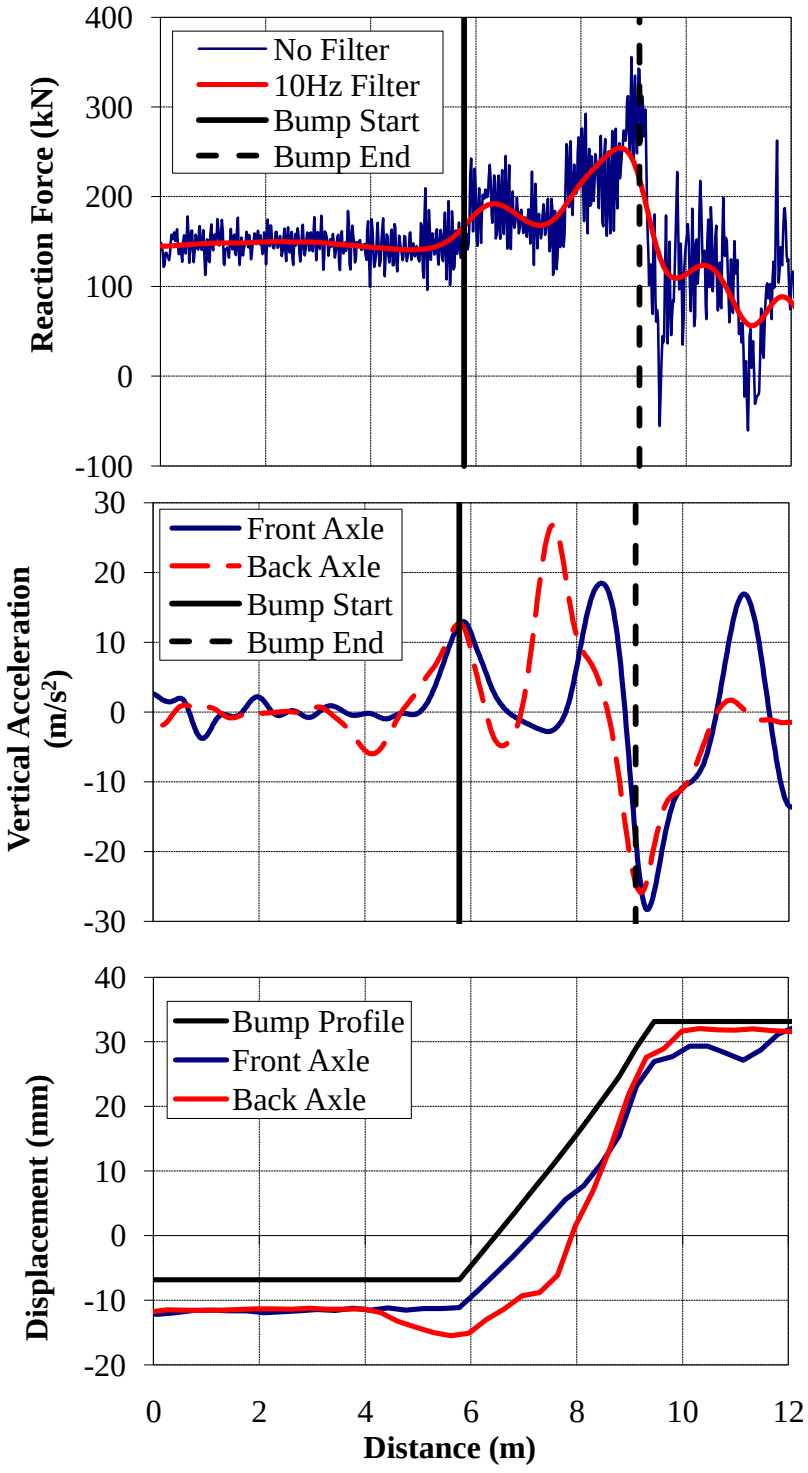

Figure E.55 - (a) Wheel/Rail Forces (b) Axle Accelerations and (c) Track Deflection due to a 1:100 Bump (Equal Height, v = 33.5 m/s)

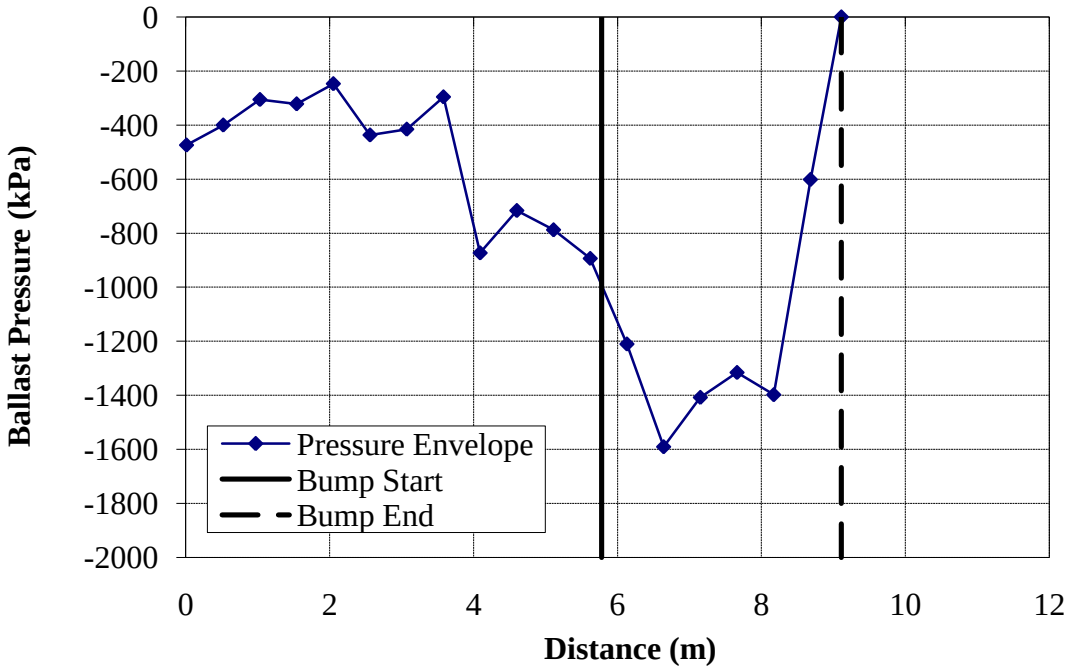

Figure E.56 - Ballast Pressure Resulting from a 1:100 Bump (Equal Height, v = 33.5 m/s)

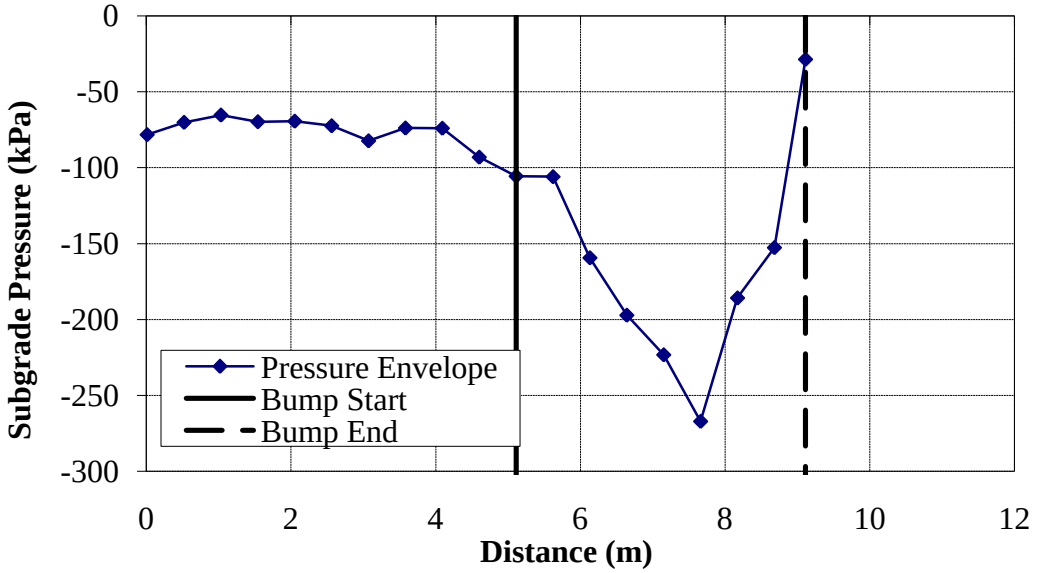

Figure E.57 - Subgrade Pressure Resulting from a 1:100 Bump (Equal Height, v = 33.5 m/s)

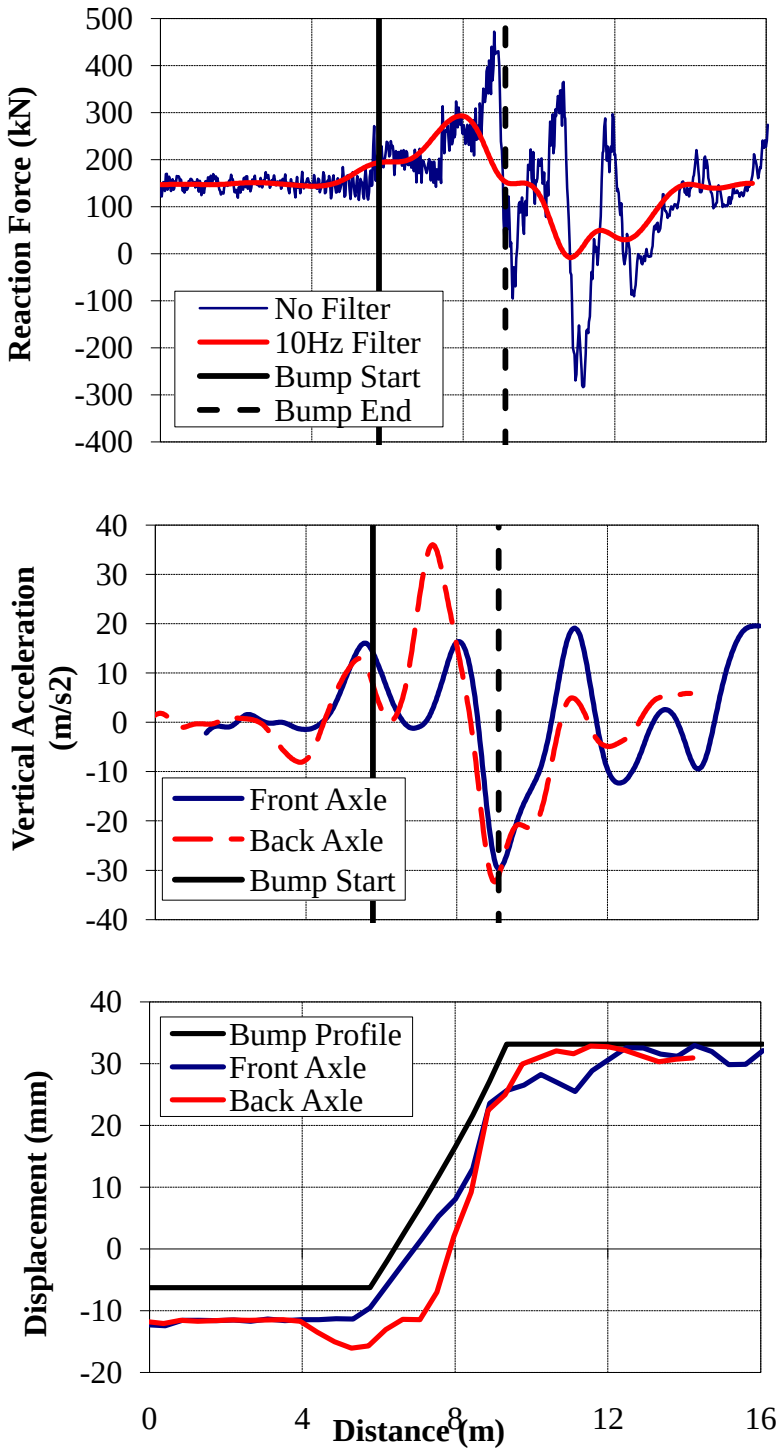

Figure E.58 - (a) Wheel/Rail Forces (b) Axle Accelerations and (c) Track Deflection due to a 1:100 Bump (Equal Height, v = 44.7 m/s)

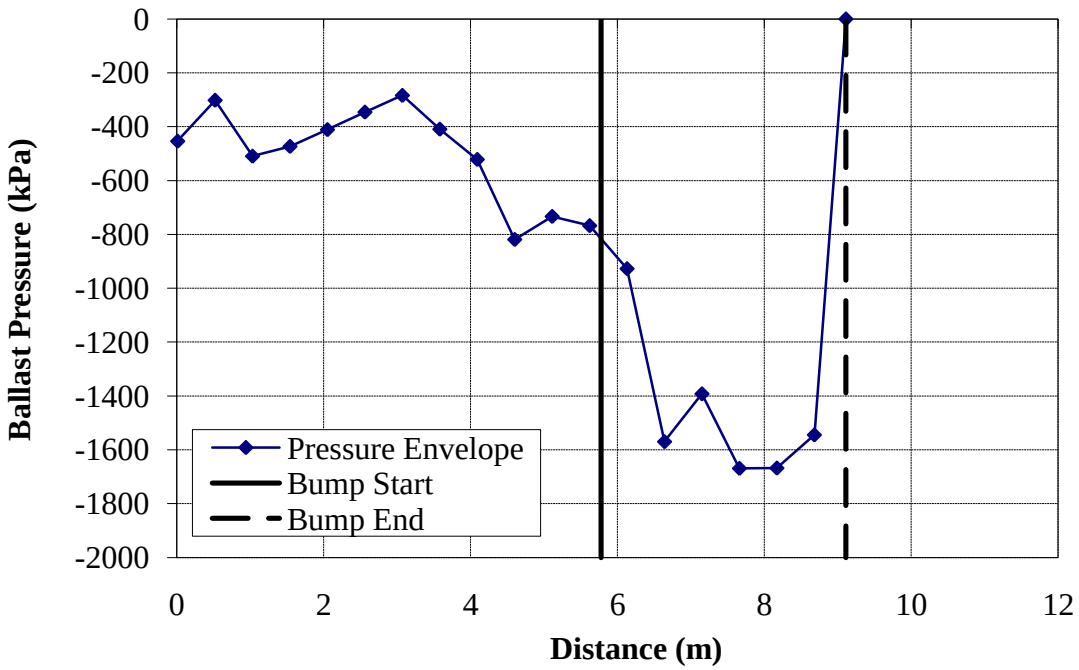

Figure E.59 – Ballast Pressure Resulting from a 1:100 Bump (Equal Height, v = 44.7 m/s)

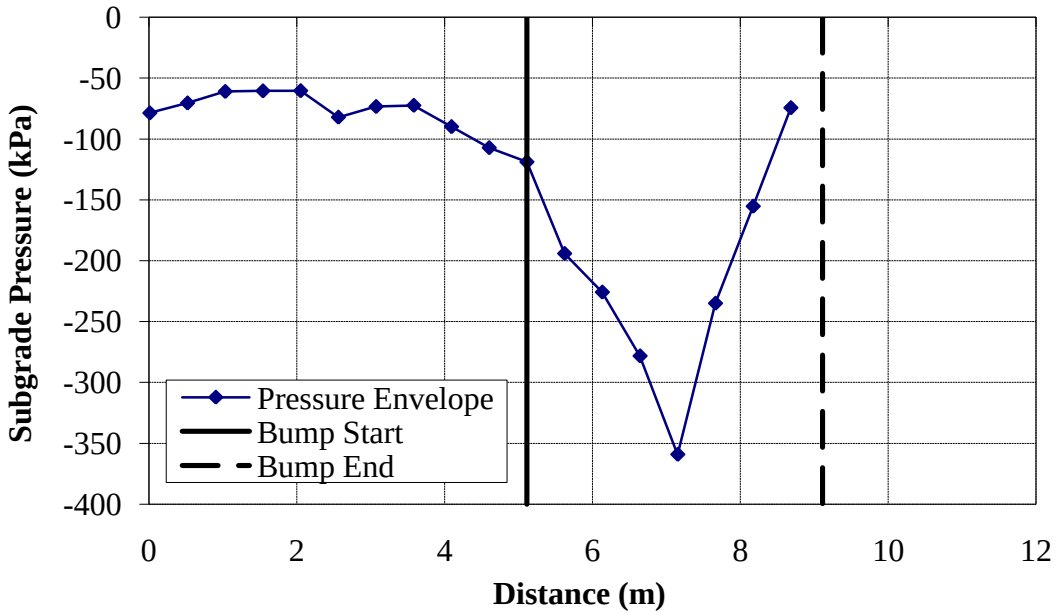

Figure E.60 - Subgrade Pressure Resulting from a 1:100 Bump (Equal Height, v = 44.7 m/s)

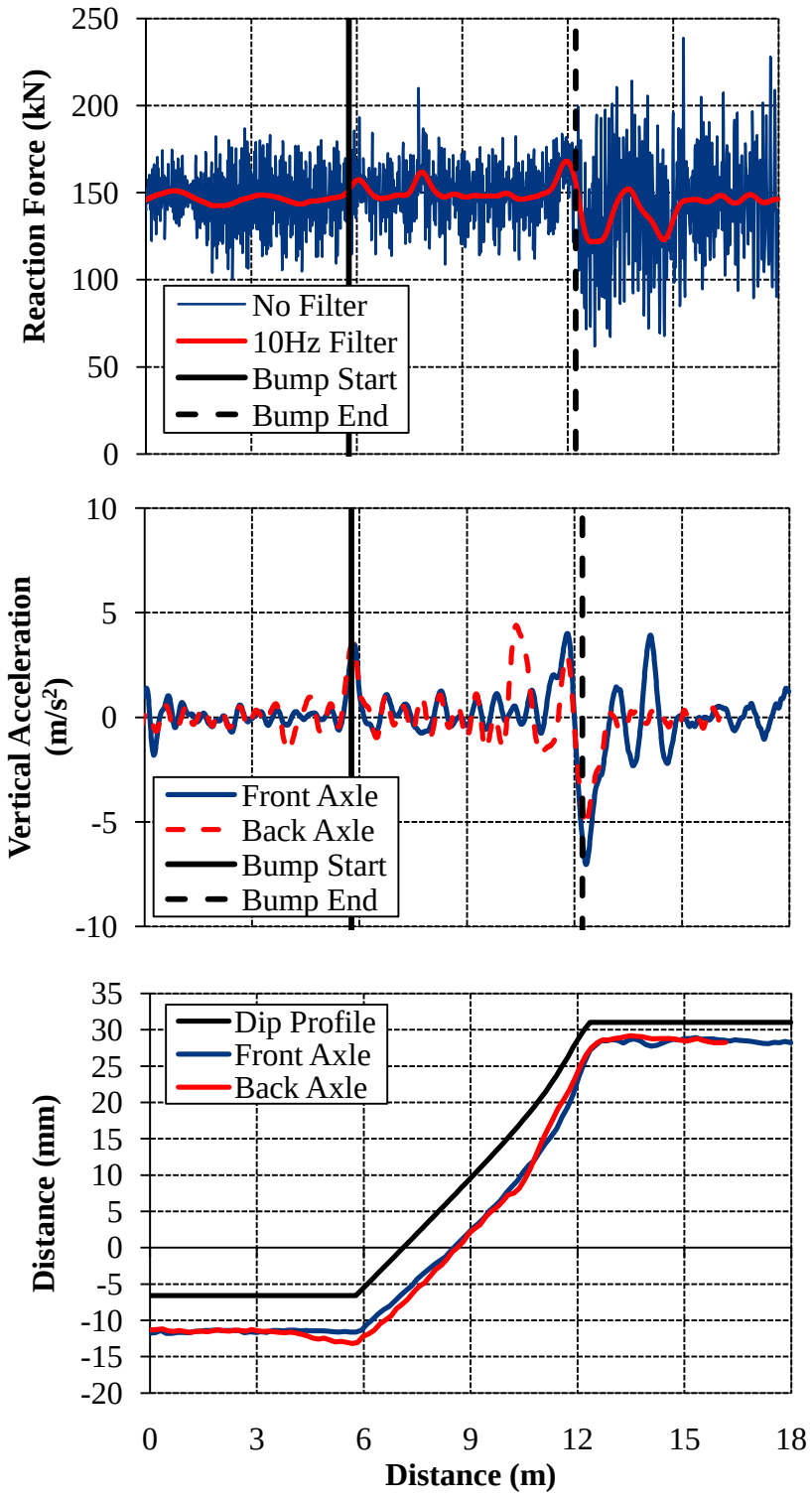

Figure E.61 - (a) Wheel/Rail Forces (b) Axle Accelerations and (c) Track Deflection due to a 1:200 Bump (Equal Height, v = 15.6 m/s)

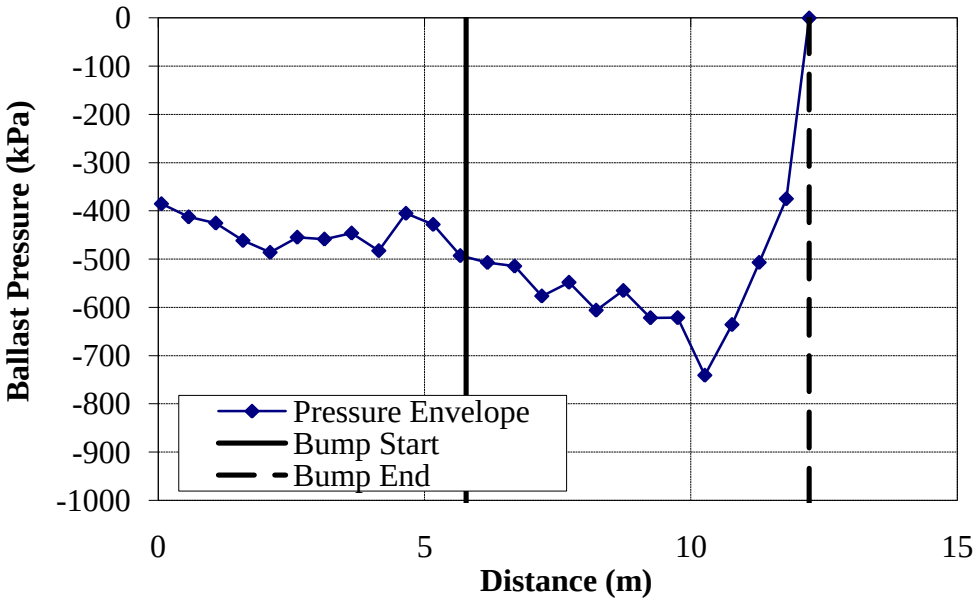

Figure E.62 –Ballast Pressure Resulting from a 1:200 Bump (Equal Height, v = 15.6 m/s)

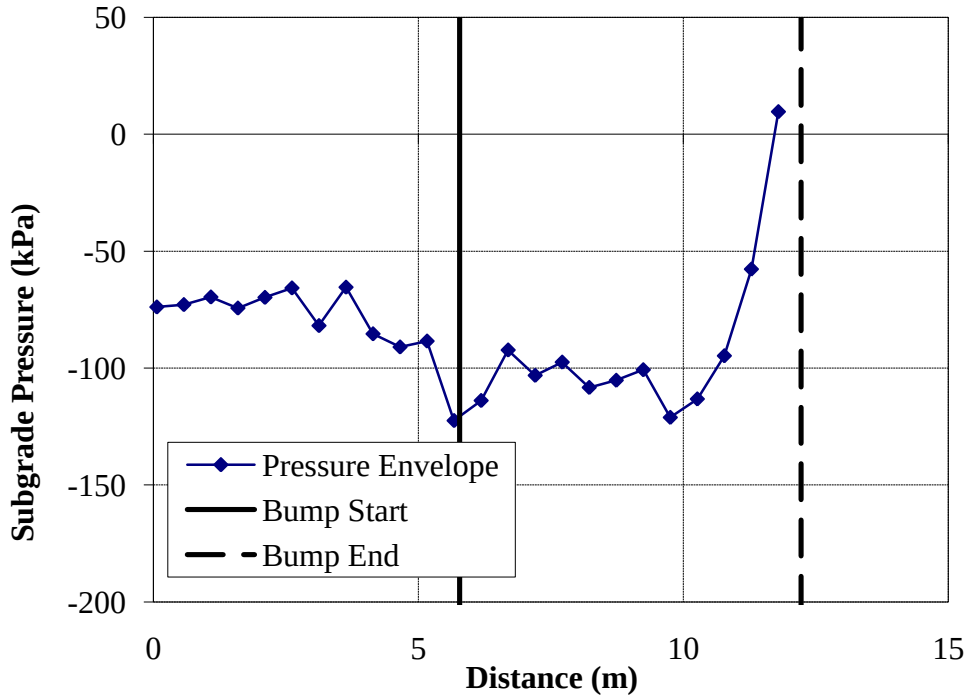

Figure E.63 - Subgrade Pressure Resulting from a 1:200 Bump (Equal Height, v = 15.6 m/s)

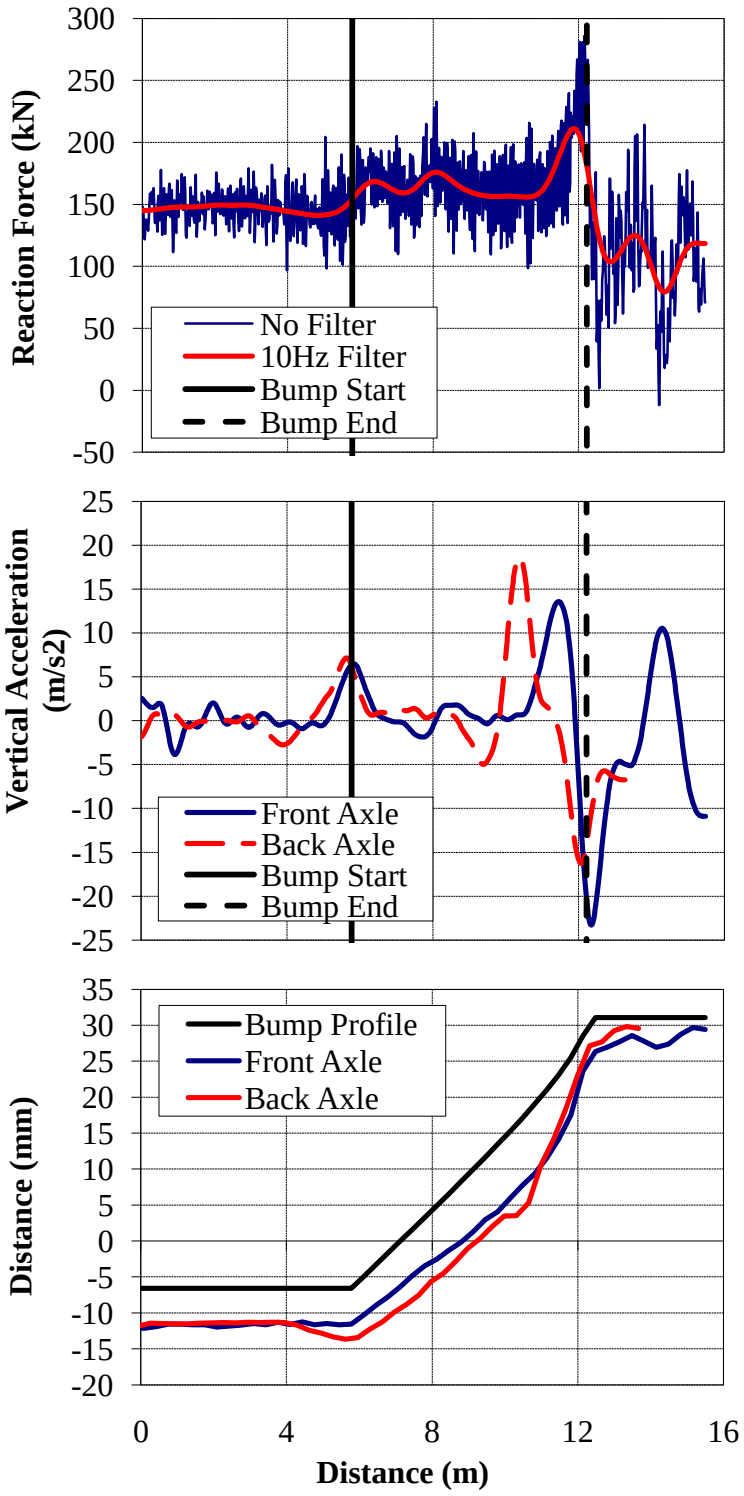

Figure E.64 - (a) Wheel/Rail Forces (b) Axle Accelerations and (c) Track Deflection due to a 1:200 Bump (Equal Height, v = 33.5 m/s)

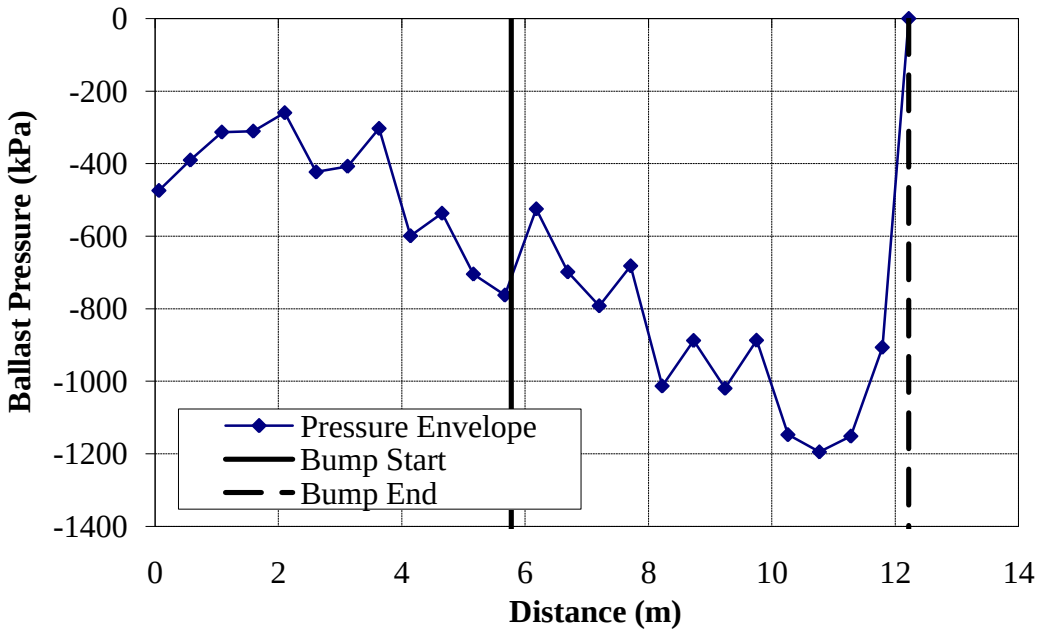

Figure E.65 – Ballast Pressure Resulting from a 1:200 Bump (Equal Height, v = 33.5 m/s)

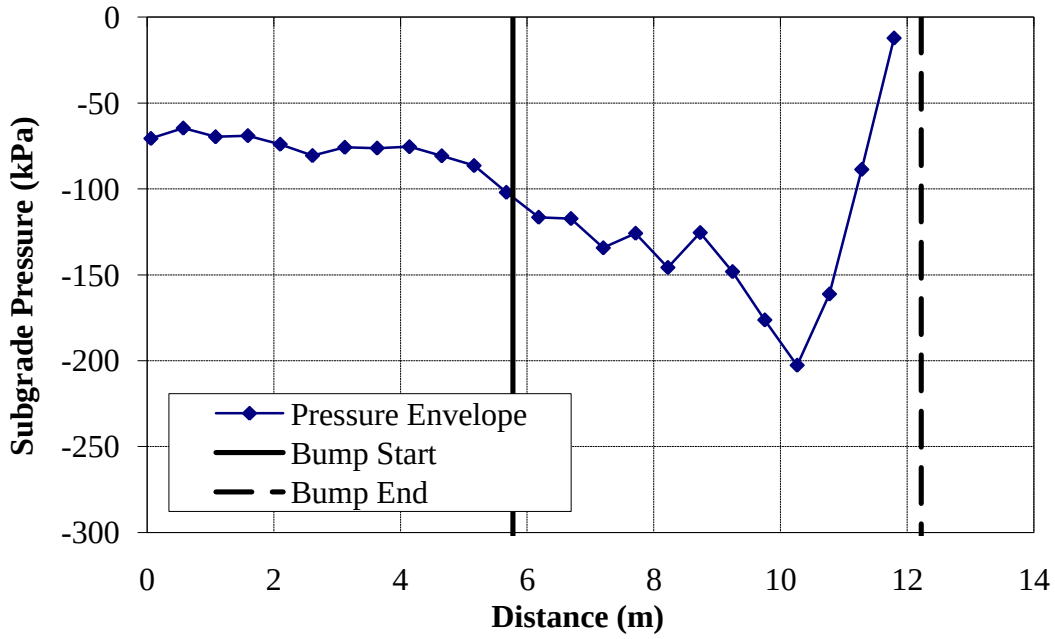

Figure E.66 - Subgrade Pressure Resulting from a 1:200 Bump (Equal Height, v = 33.5 m/s)

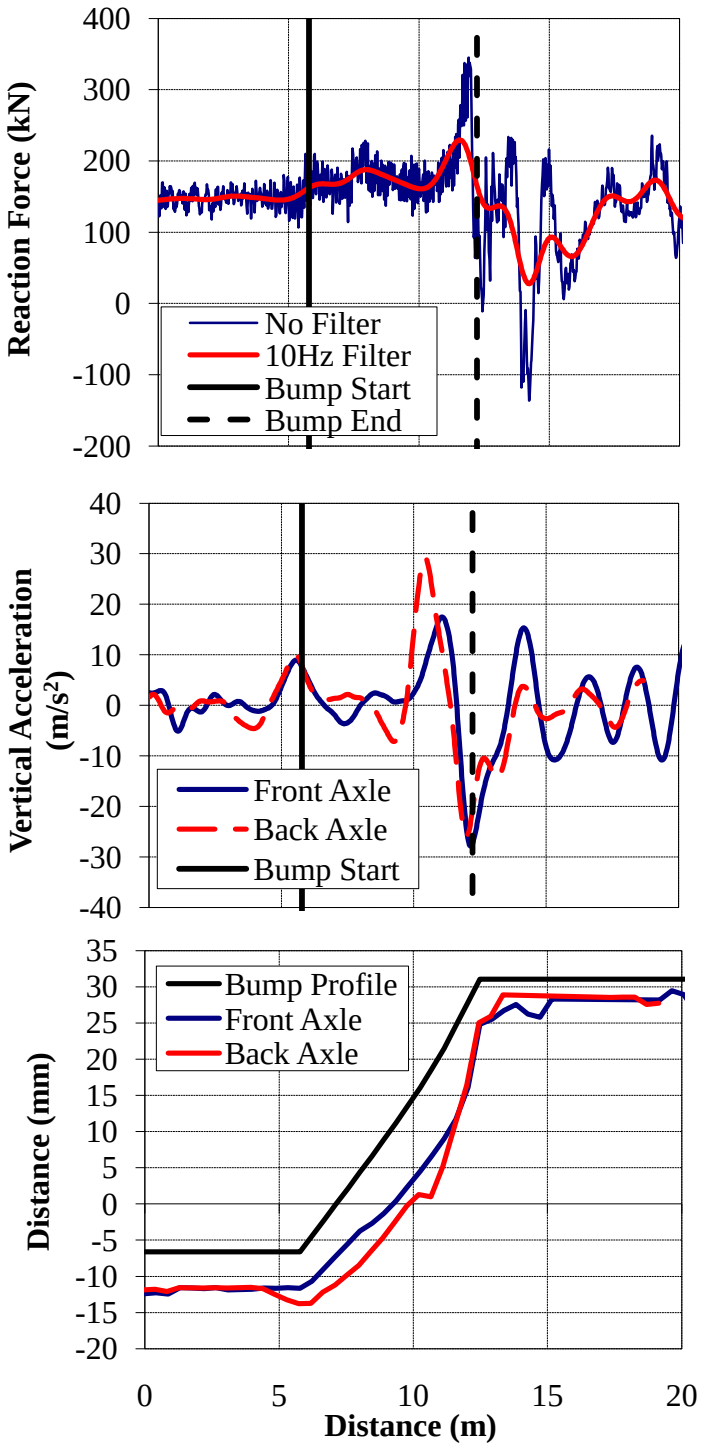

Figure E.67 - (a) Wheel/Rail Forces (b) Axle Accelerations and (c) Track Deflection due to a 1:200 Bump (Equal Height, v = 44.7 m/s)

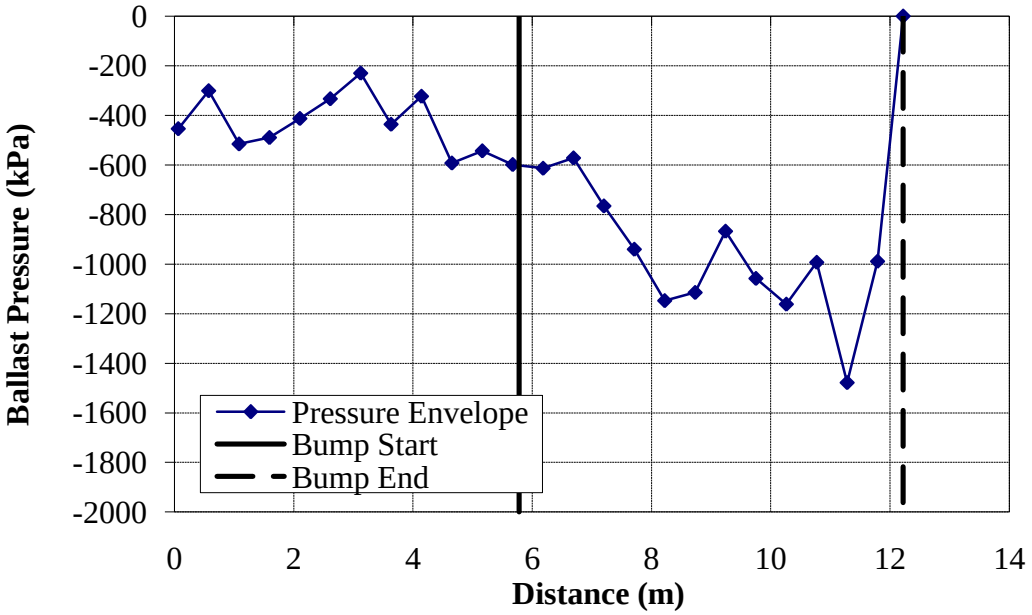

Figure E.68 – Ballast Pressure Resulting from a 1:200 Bump (Equal Height, v = 44.7 m/s)

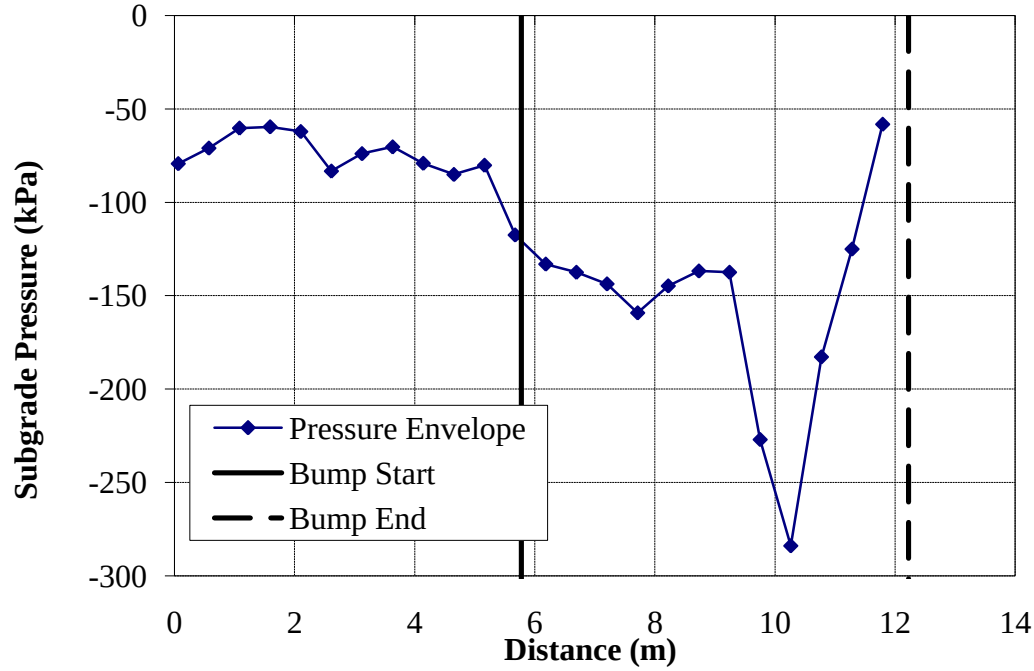

Figure E.69 - Subgrade Pressure Resulting from a 1:200 Bump (Equal Height, v = 44.7 m/s)

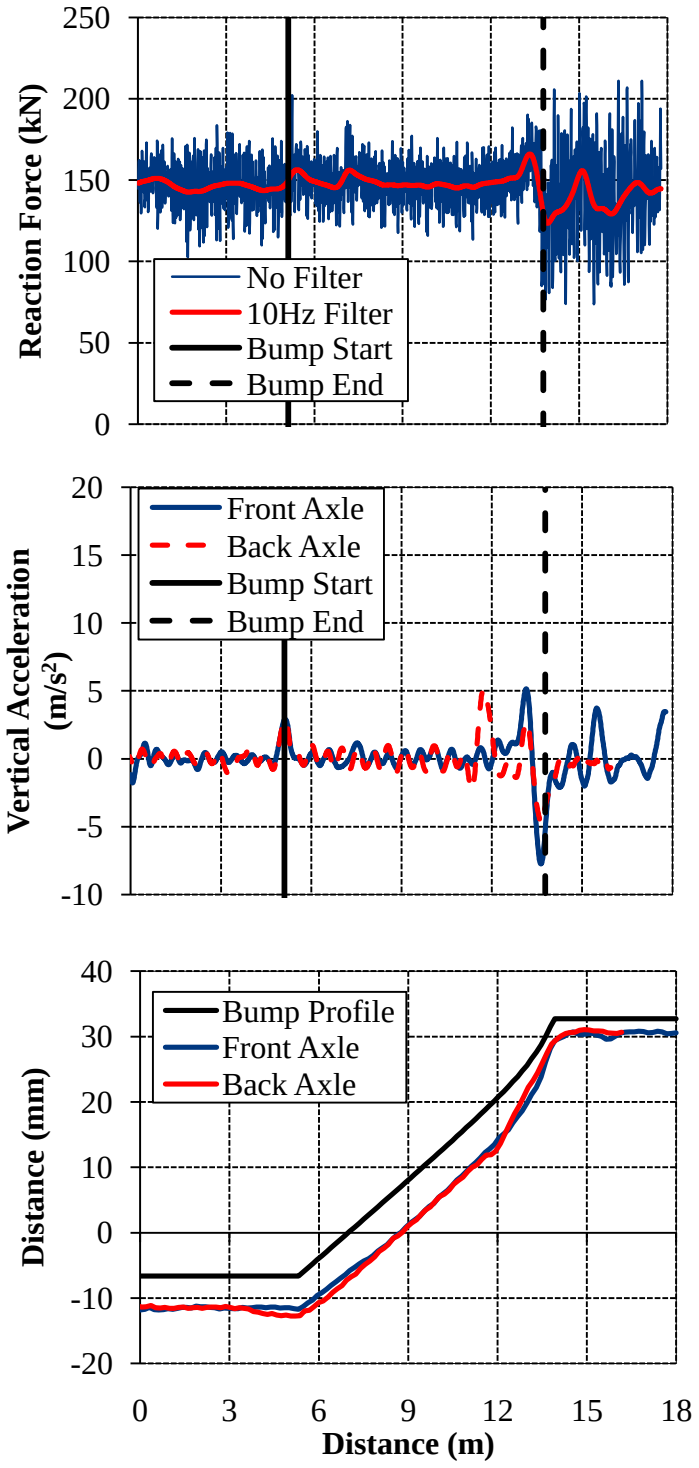

Figure E.70 - (a) Wheel/Rail Forces (b) Axle Accelerations and (c) Track Deflection due to a 1:250 Bump (Equal Height, v = 15.6 m/s)

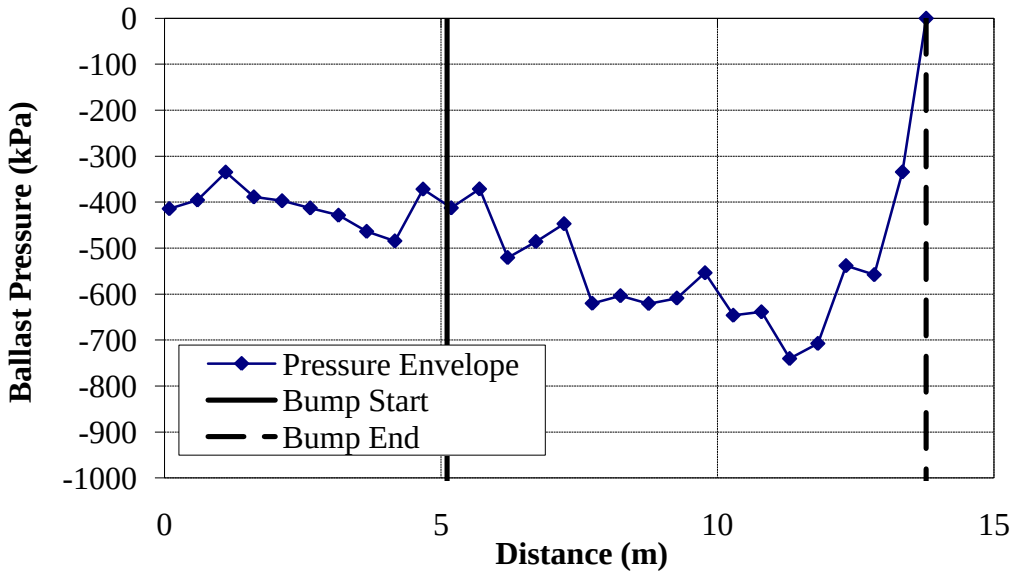

Figure E.71 – Ballast Pressure Resulting from a 1:250 Bump (Equal Height, v = 15.6 m/s)

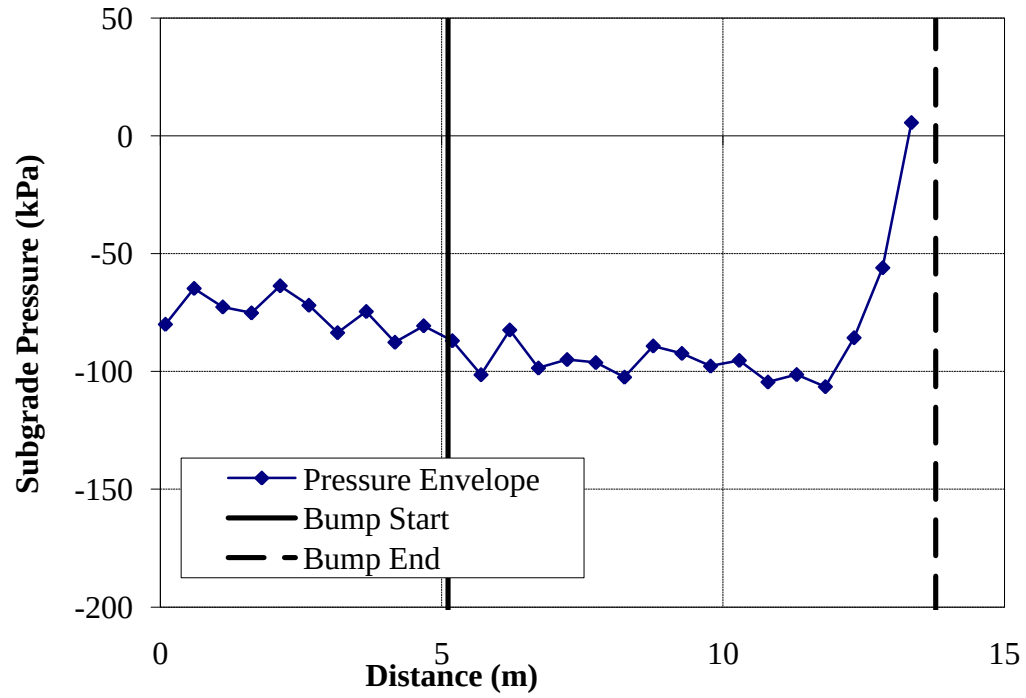

Figure E.72 - Subgrade Pressure Resulting from a 1:250 Bump (Equal Height, v = 15.6 m/s)

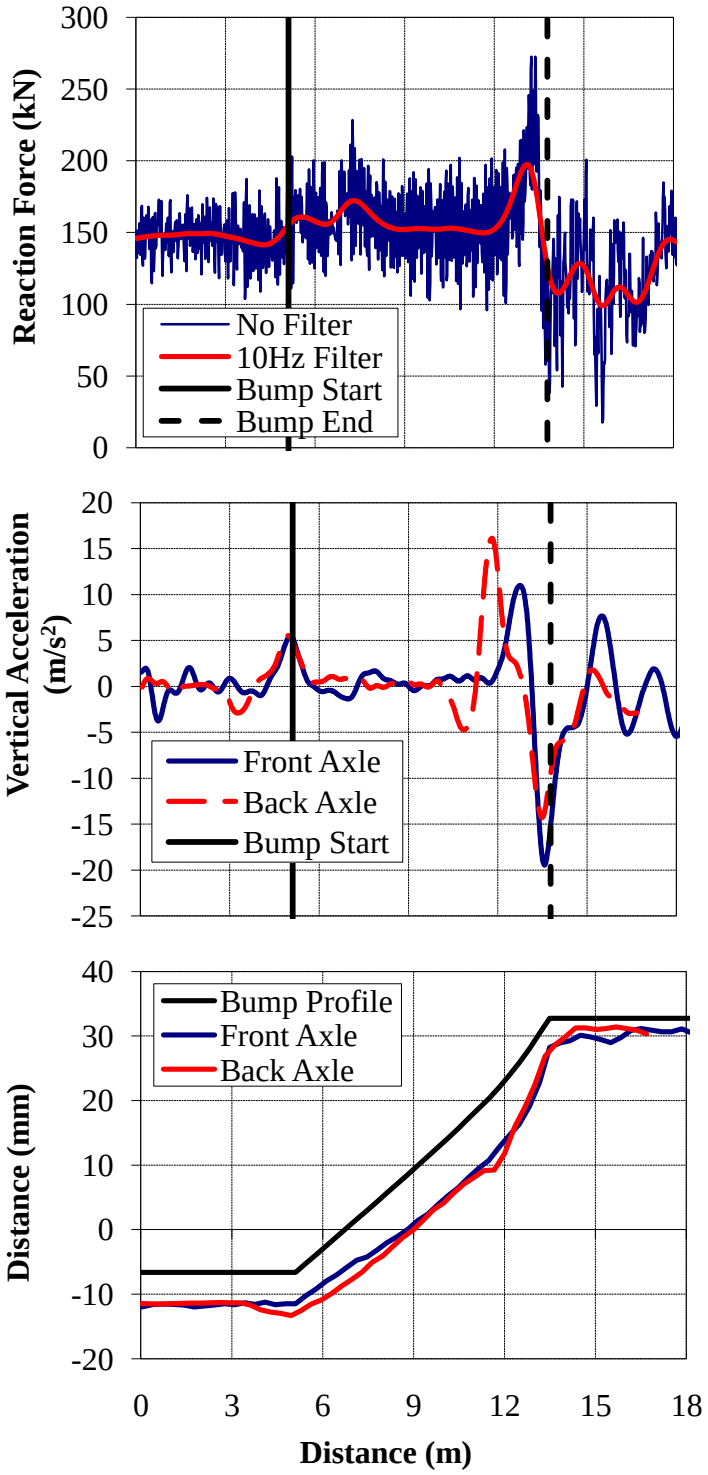

Figure E.73 - (a) Wheel/Rail Forces (b) Axle Accelerations and (c) Track Deflection due to a 1:250 Bump (Equal Height, v = 33.5 m/s)

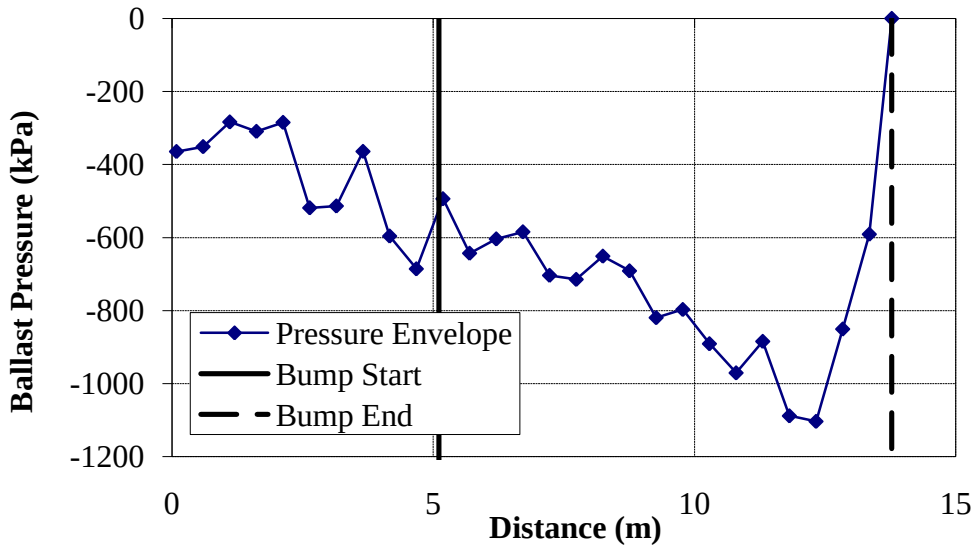

Figure E.74 – Ballast Pressure Resulting from a 1:250 Bump (Equal Height, v = 33.5 m/s)

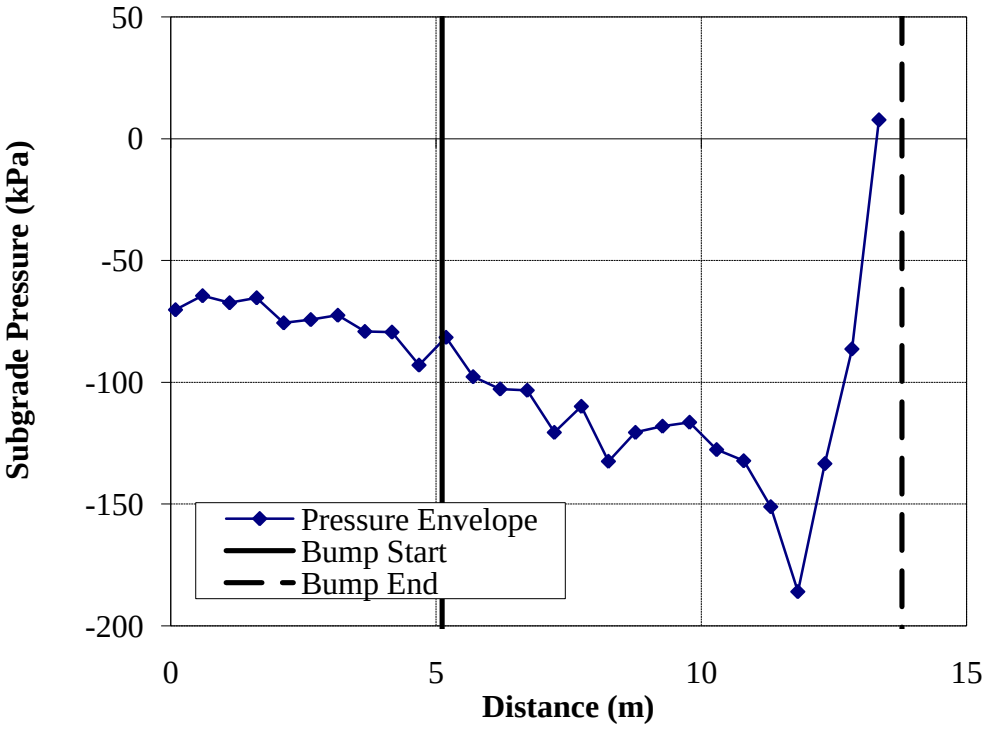

Figure E.75 - Subgrade Pressure Resulting from a 1:250 Bump (Equal Height, v = 33.5 m/s)

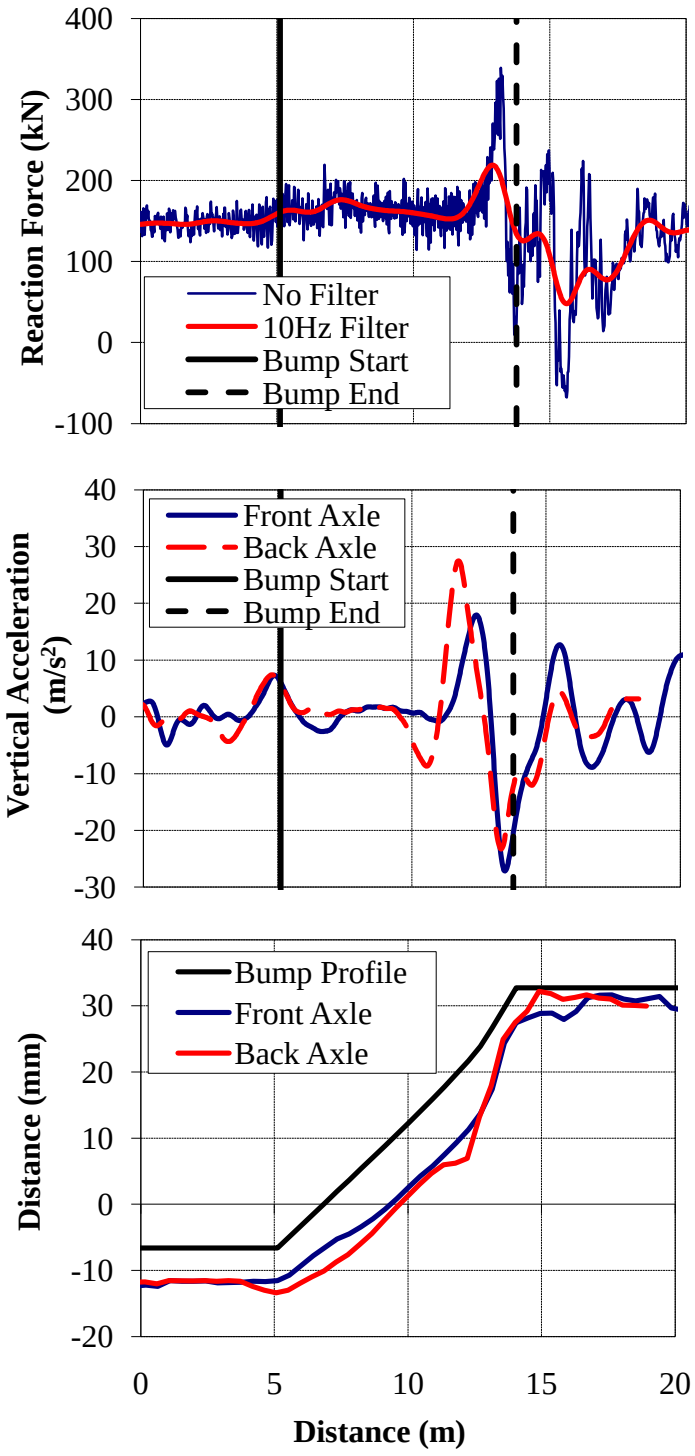

Figure E.76 - (a) Wheel/Rail Forces (b) Axle Accelerations and (c) Track Deflection due to a 1:250 Bump (Equal Height, v = 44.7 m/s)

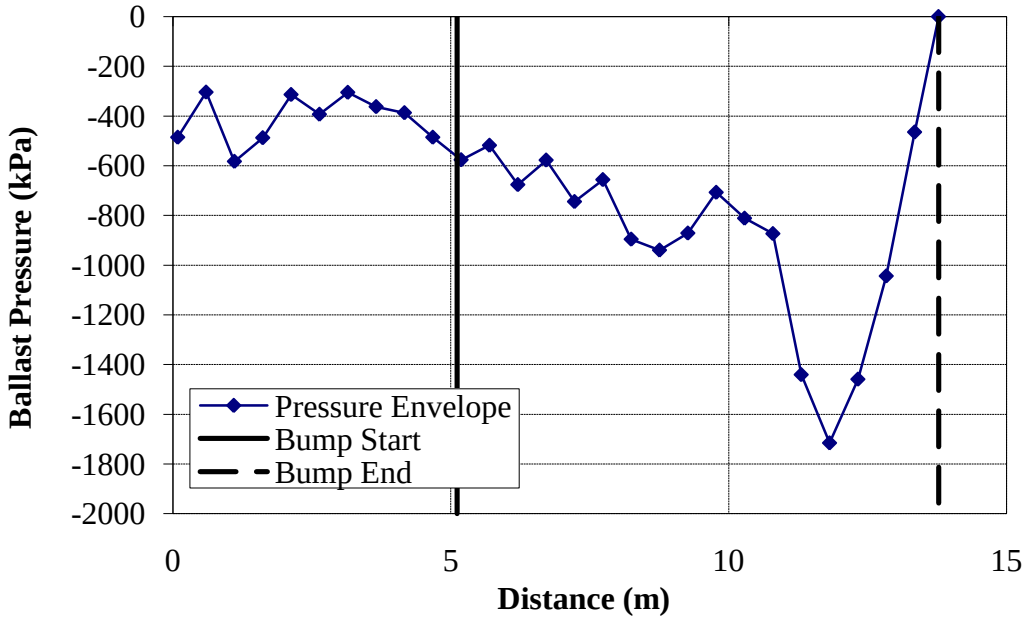

Figure E.77 – Ballast Pressure Resulting from a 1:250 Bump (Equal Height, v = 44.7 m/s)

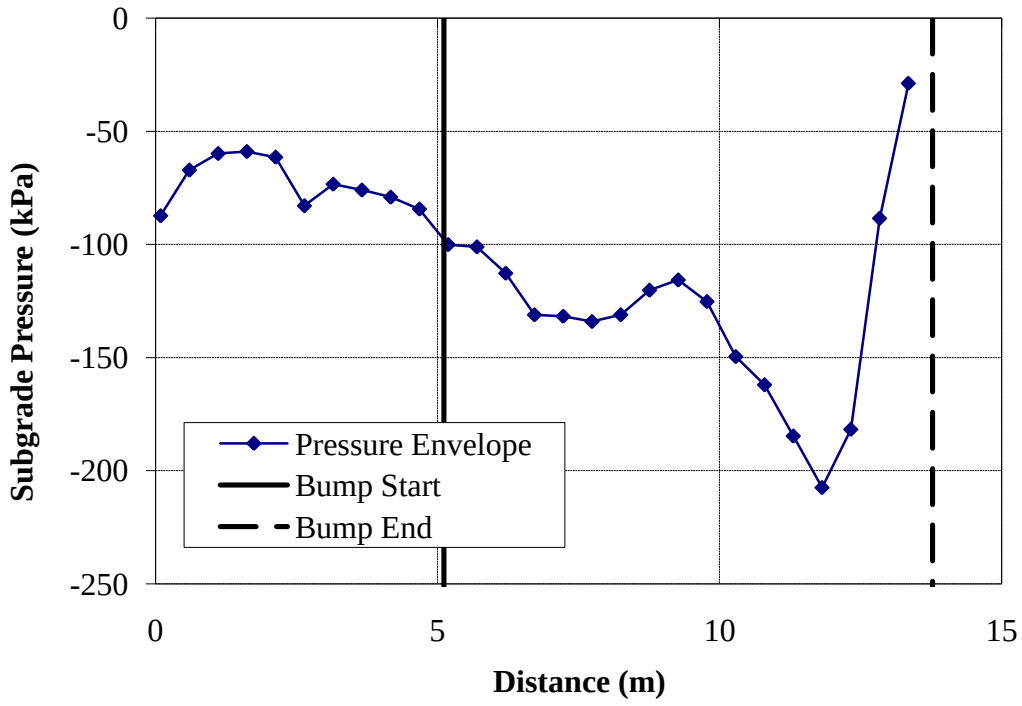

Figure E.78 - Subgrade Pressure Resulting from a 1:250 Bump (Equal Height, v = 44.7 m/s)

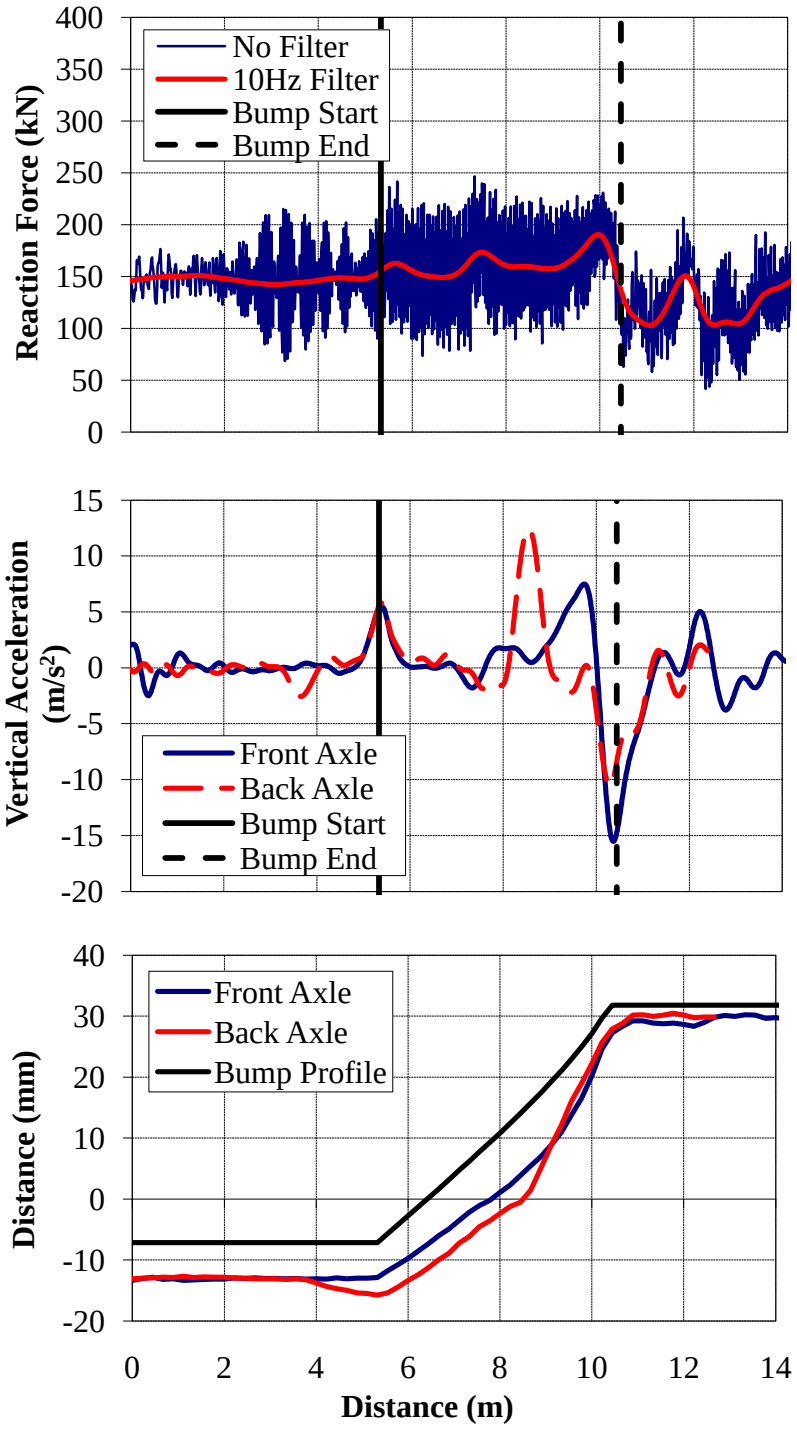

Figure E.79 - (a) Wheel/Rail Forces (b) Axle Accelerations and (c) Track Deflection due to a 1:150 Bump (20 MPa Fill and Subgrade Modulus, v = 22.2 m/s)

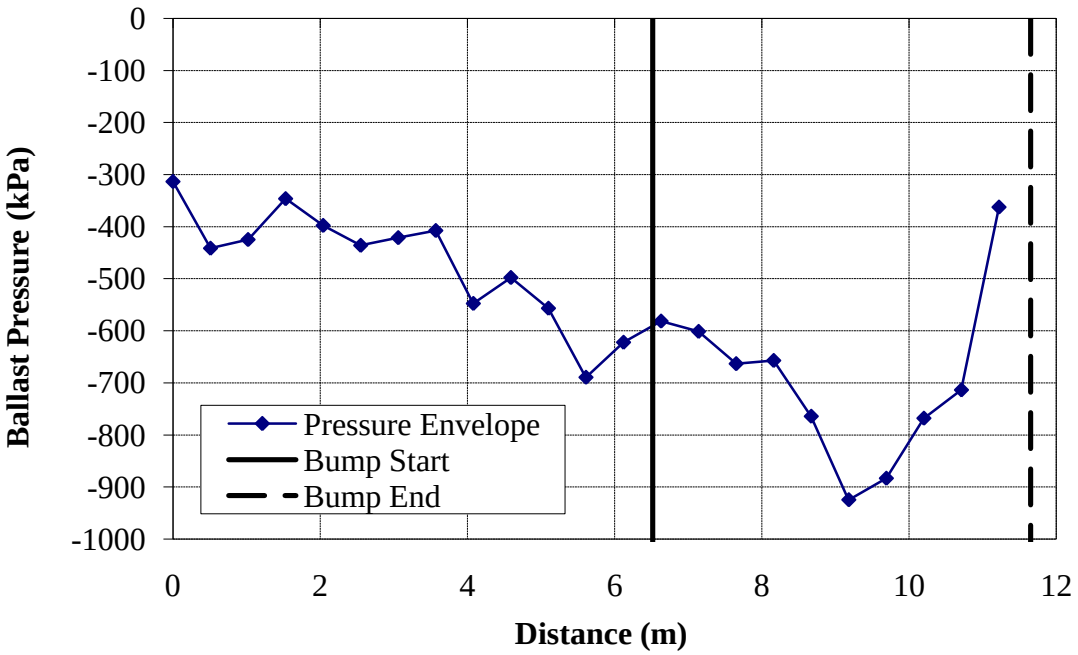

Figure E.80 – Ballast Pressure Resulting from a 1:150 Bump (20 MPa Fill and Subgrade Modulus, v = 22.2 m/s)

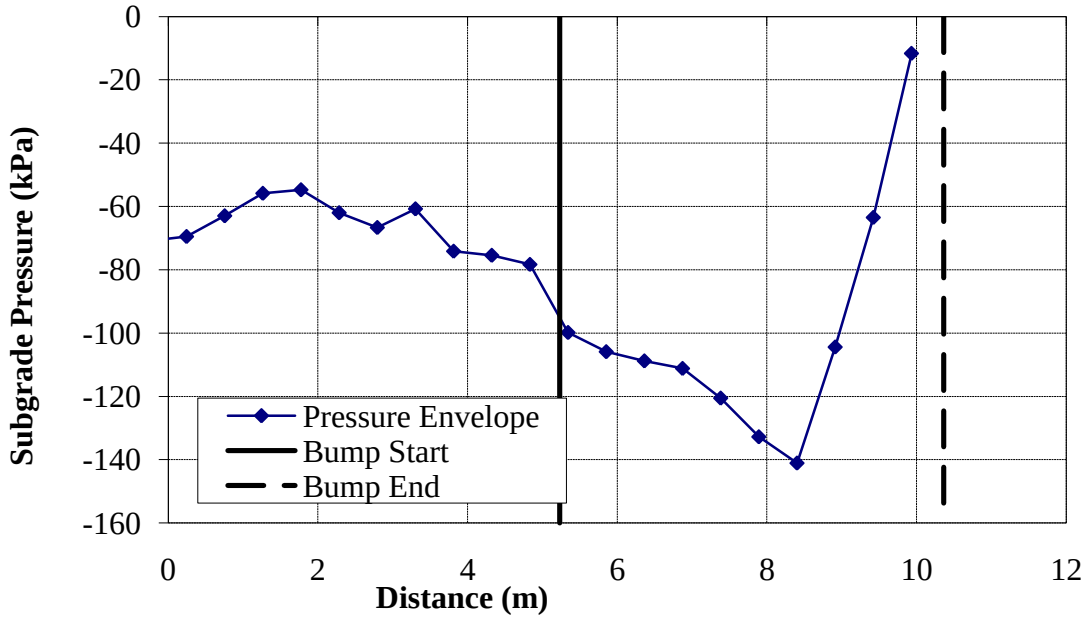

Figure E.81 - Subgrade Pressure Resulting from a 1:150 Bump (20 MPa Fill and Subgrade Modulus, v = 22.2 m/s)

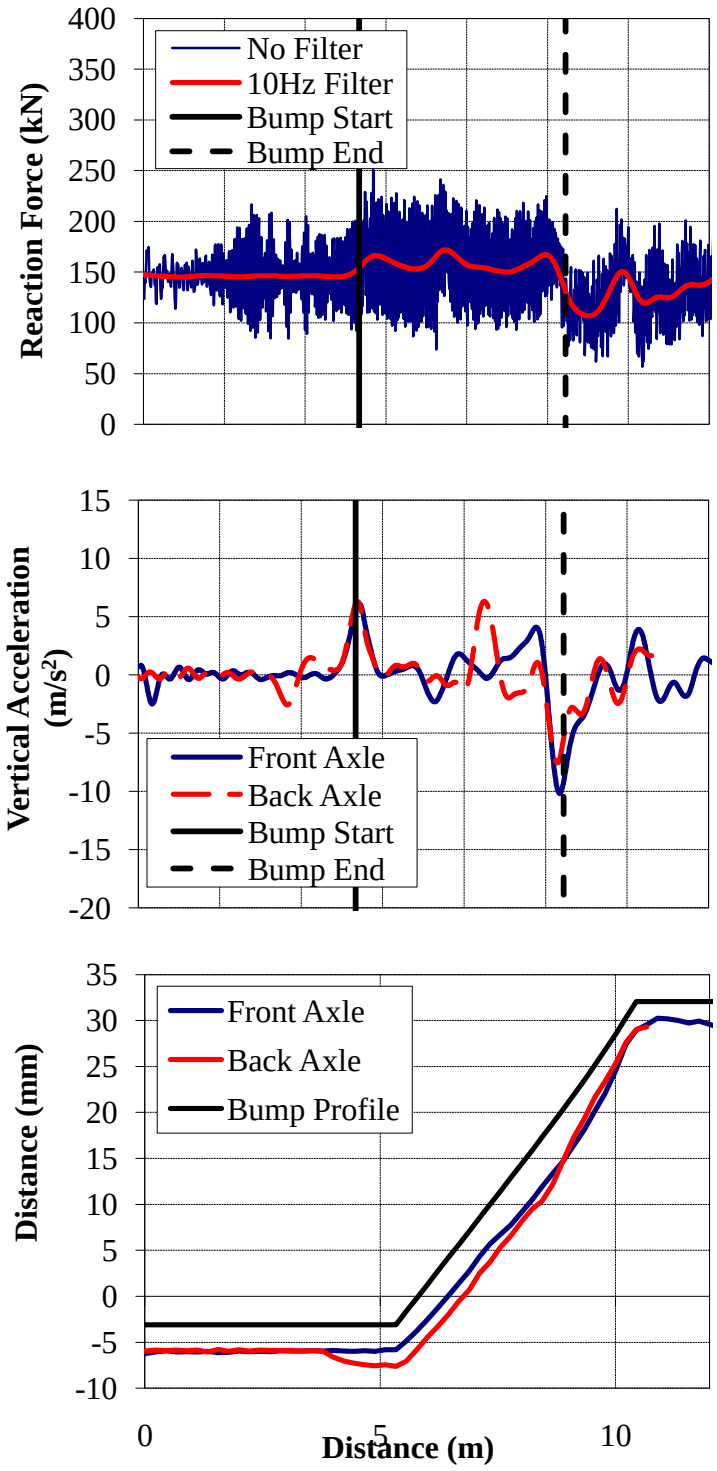

Figure E.82 - (a) Wheel/Rail Forces (b) Axle Accelerations and (c) Track Deflection due to a 1:150 Bump (50 MPa Fill and Subgrade Modulus, v = 22.2 m/s)

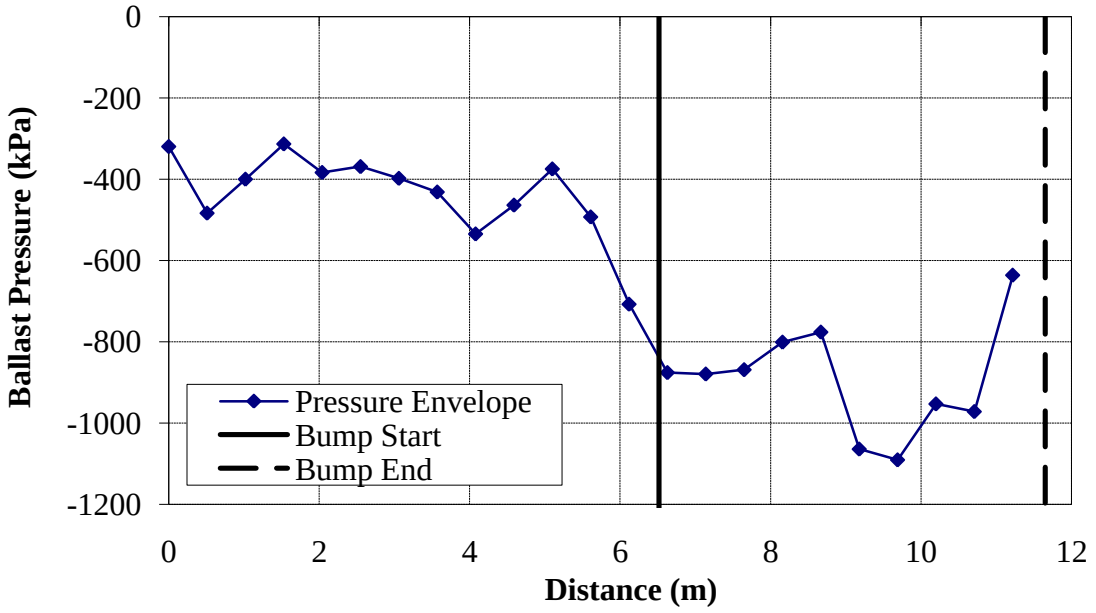

Figure E.83 – Ballast Pressure Resulting from a 1:150 Bump (50 MPa Fill and Subgrade Modulus, v = 22.2 m/s)

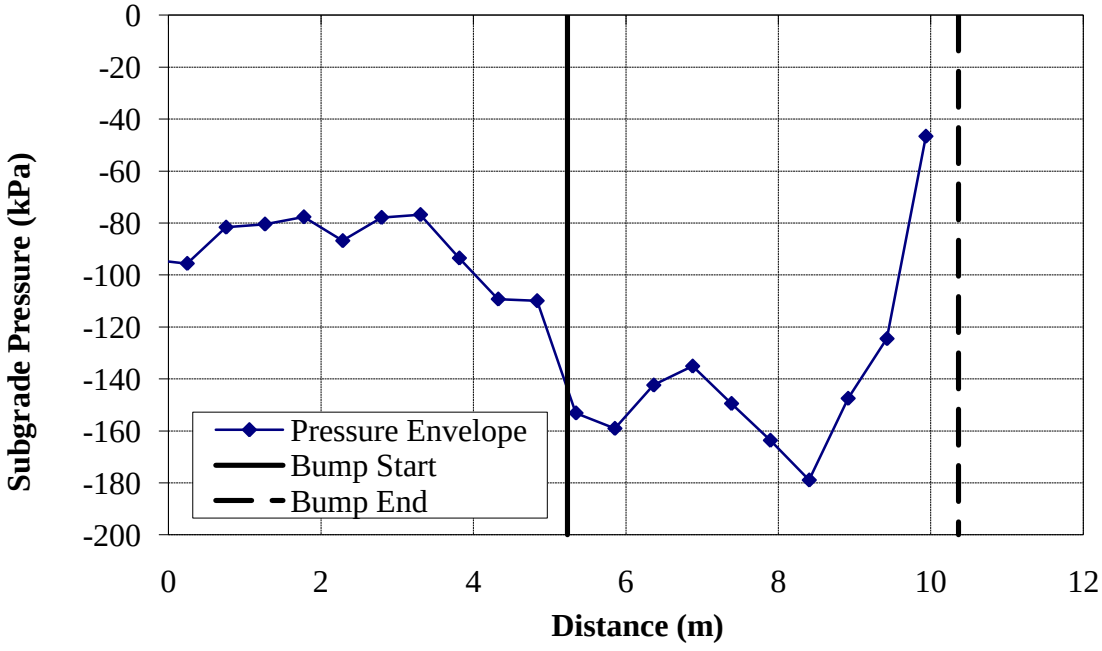

Figure E.84 - Subgrade Pressure Resulting from a 1:150 Bump (50 MPa Fill and Subgrade Modulus, v = 22.2 m/s)

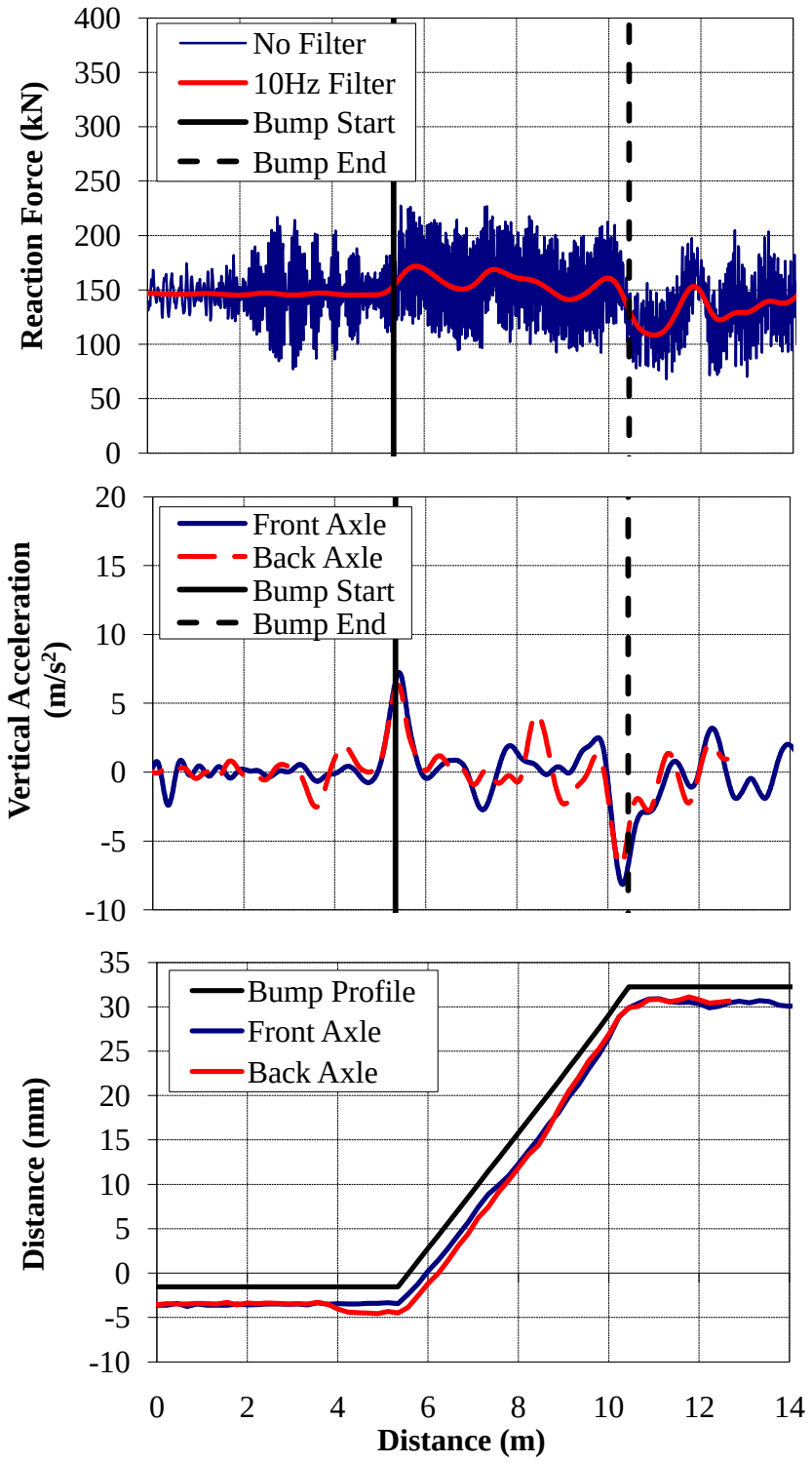

Figure E.85 - (a) Wheel/Rail Forces (b) Axle Accelerations and (c) Track Deflection due to a 1:150 Bump (100 MPa Fill and Subgrade Modulus, v = 22.2 m/s)

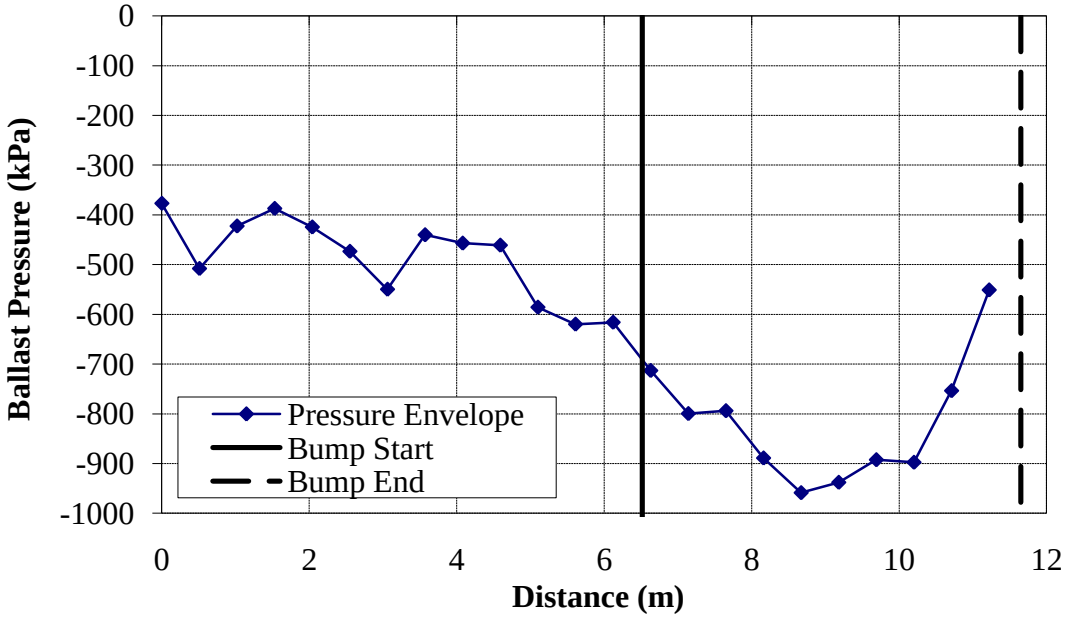

Figure E.86 – Ballast Pressure Resulting from a 1:150 Bump (100 MPa Fill and Subgrade Modulus, v = 22.2 m/s)

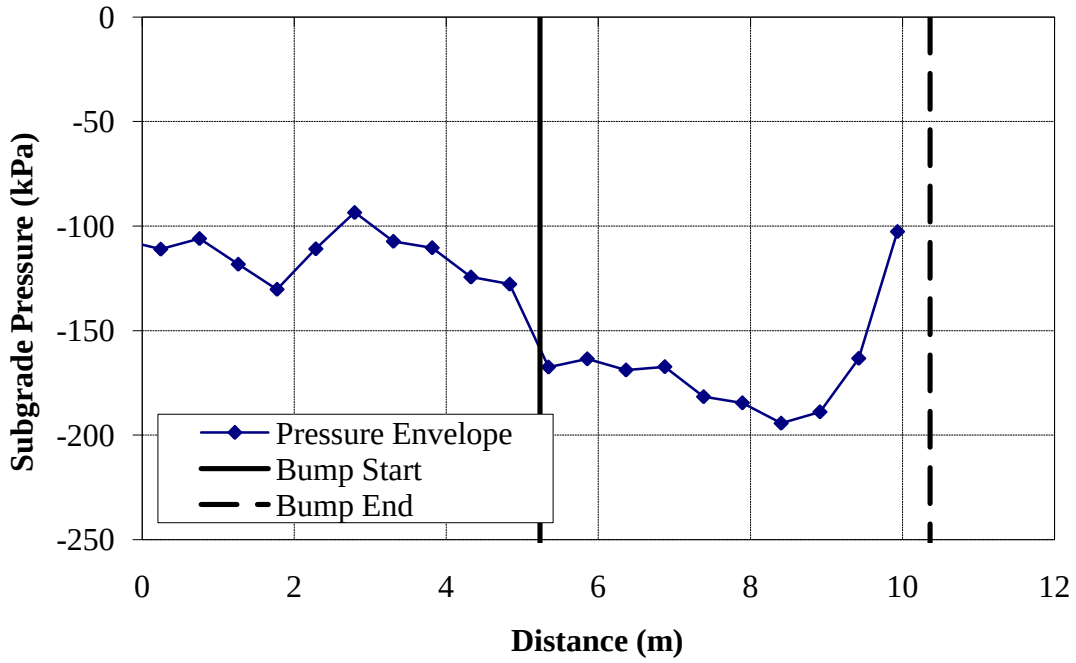

Figure E.87 - Subgrade Pressure Resulting from a 1:150 Bump (100 MPa Fill and Subgrade Modulus, v = 22.2 m/s)

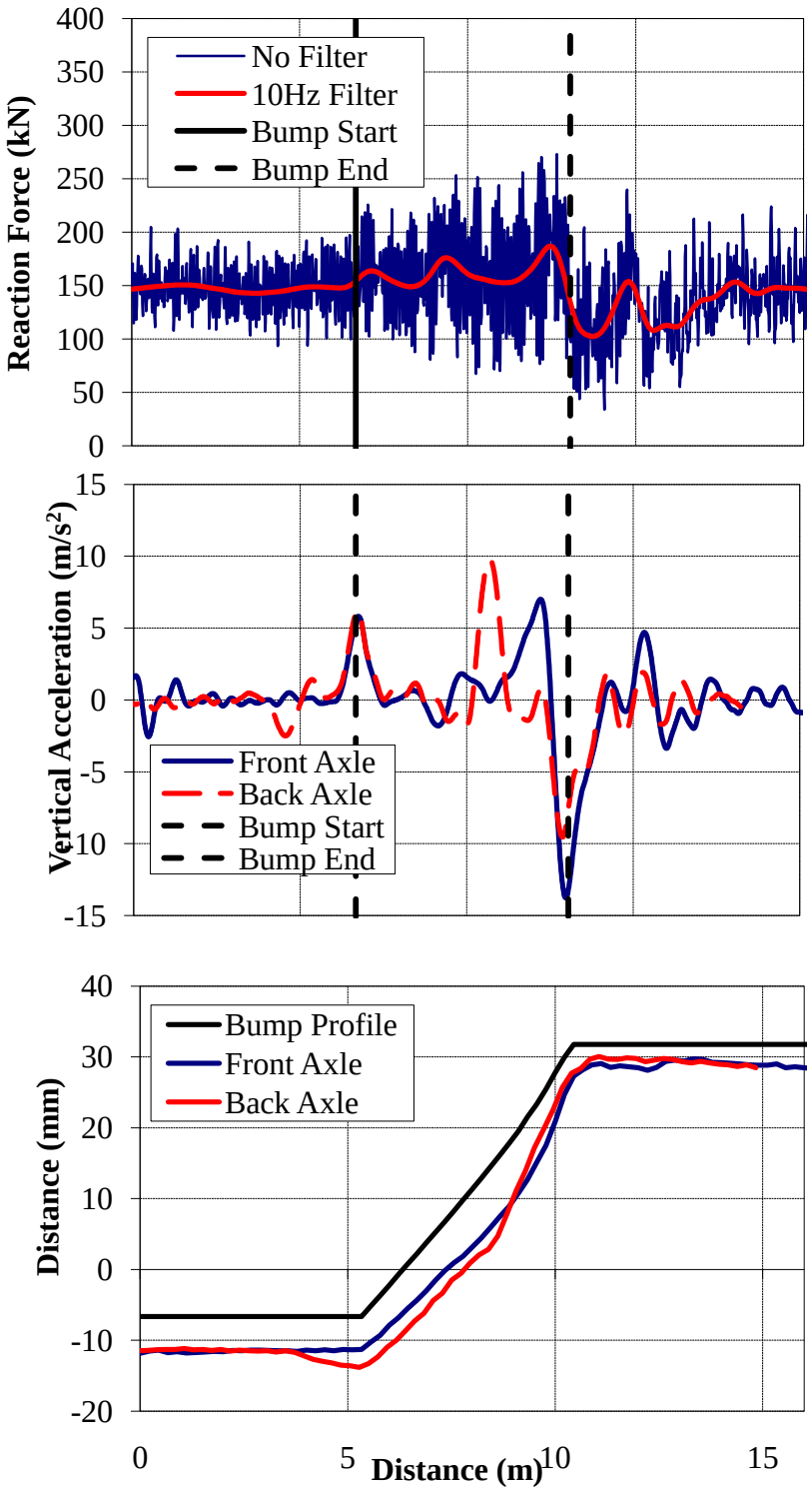

Figure E.88 - (a) Wheel/Rail Forces (b) Axle Accelerations and (c) Track Deflection due to a 1:150 Bump with Concrete Approach Ties (v = 22.2 m/s)

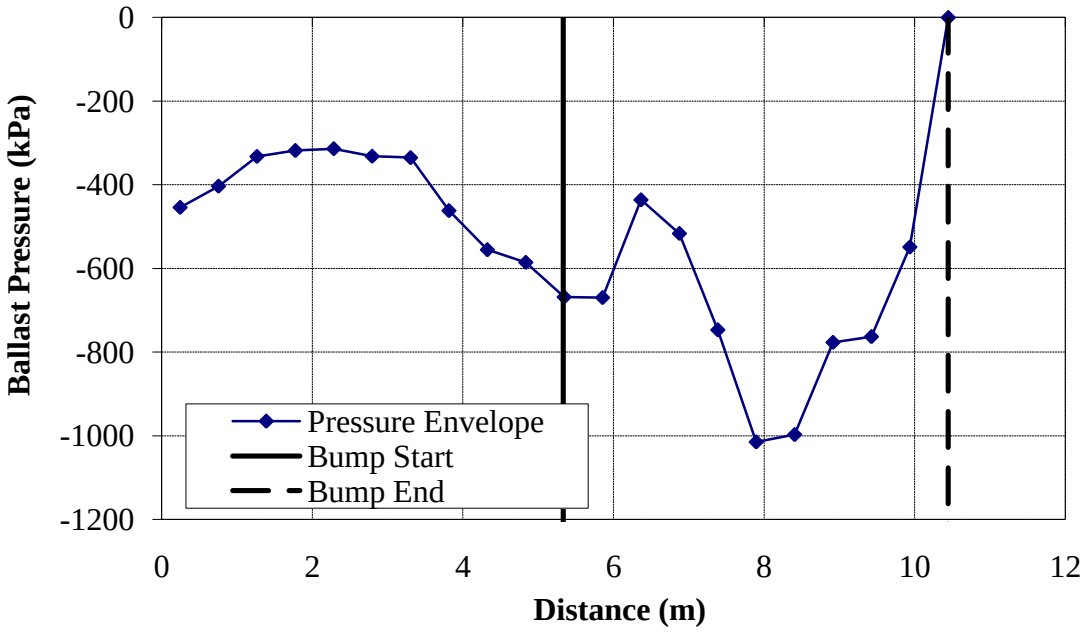

Figure E.89 –Ballast Pressure Resulting from a 1:150 Bump with Concrete Approach Ties (v = 22.2 m/s)

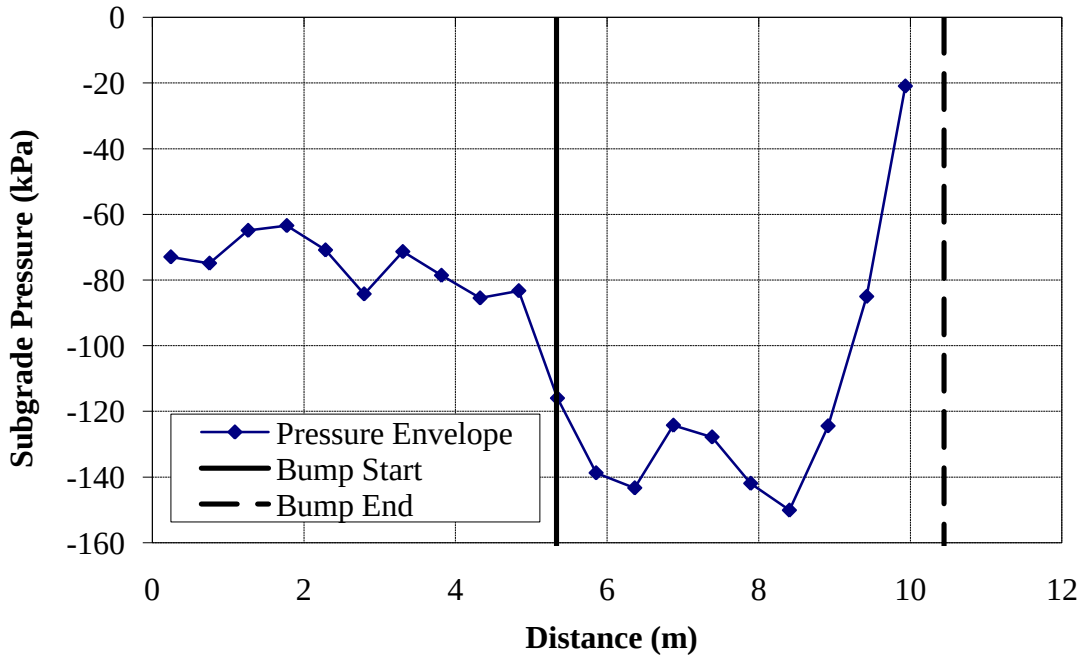

Figure E.90 - Subgrade Pressure Resulting from a 1:150 Bump with Concrete Approach Ties (v = 22.2 m/s)

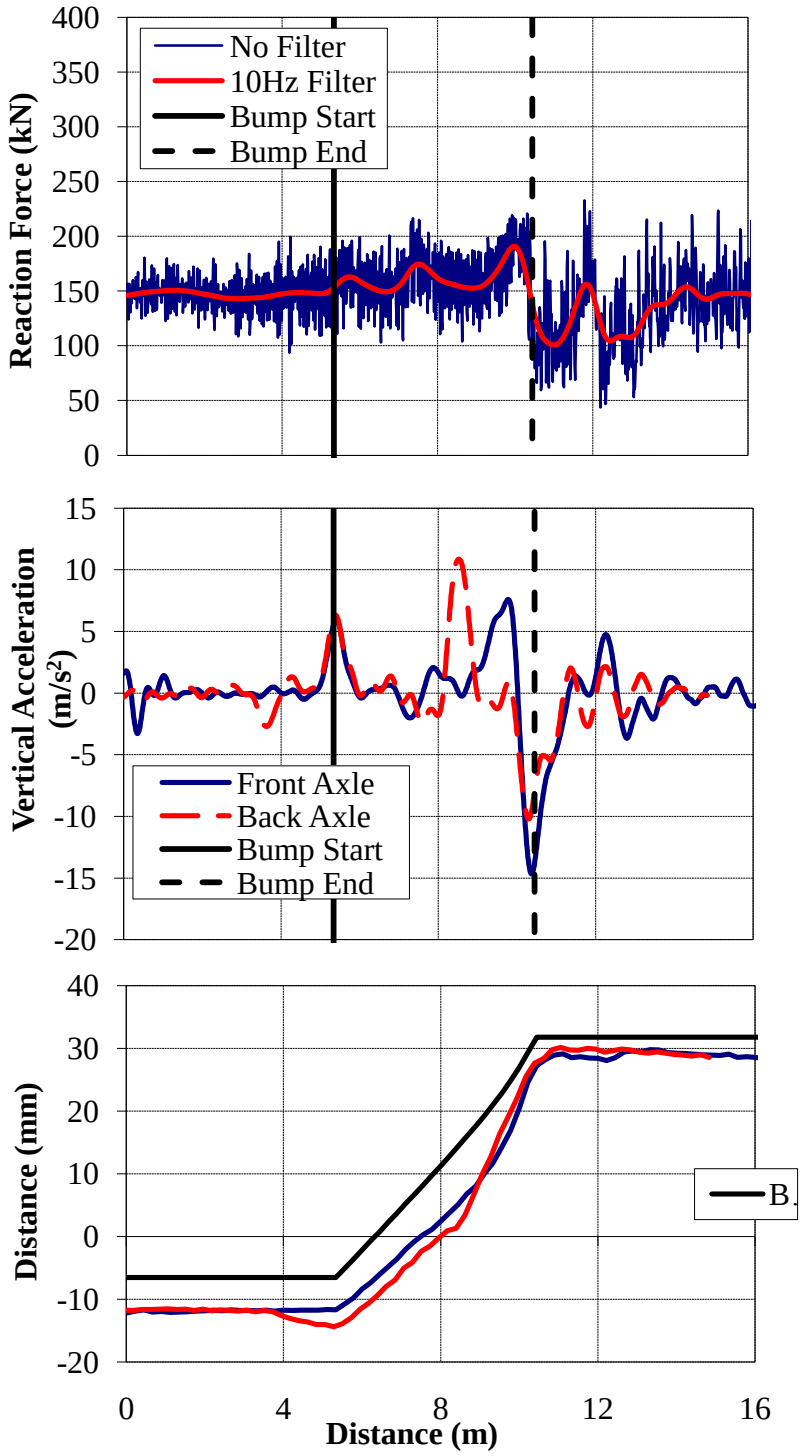

Figure E.91 - (a) Wheel/Rail Forces (b) Axle Accelerations and (c) Track Deflection due to a 1:150 Bump with Plastic Approach Ties (v = 22.2 m/s)

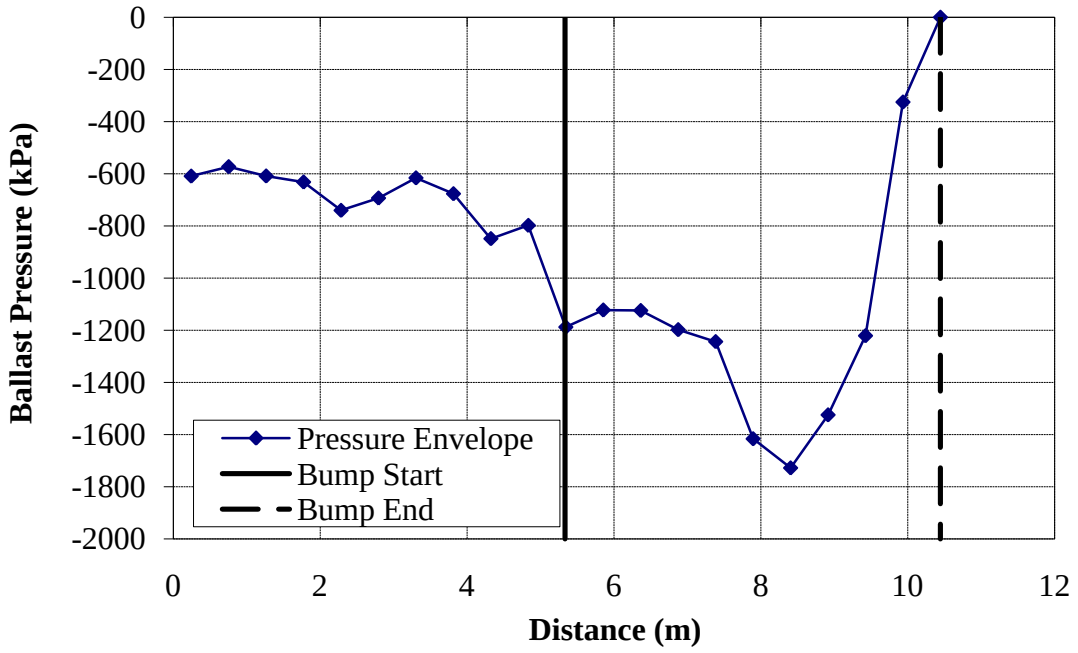

Figure E.92 – Ballast Pressure Resulting from a 1:150 Bump with Plastic Approach Ties (v = 22.2 m/s)

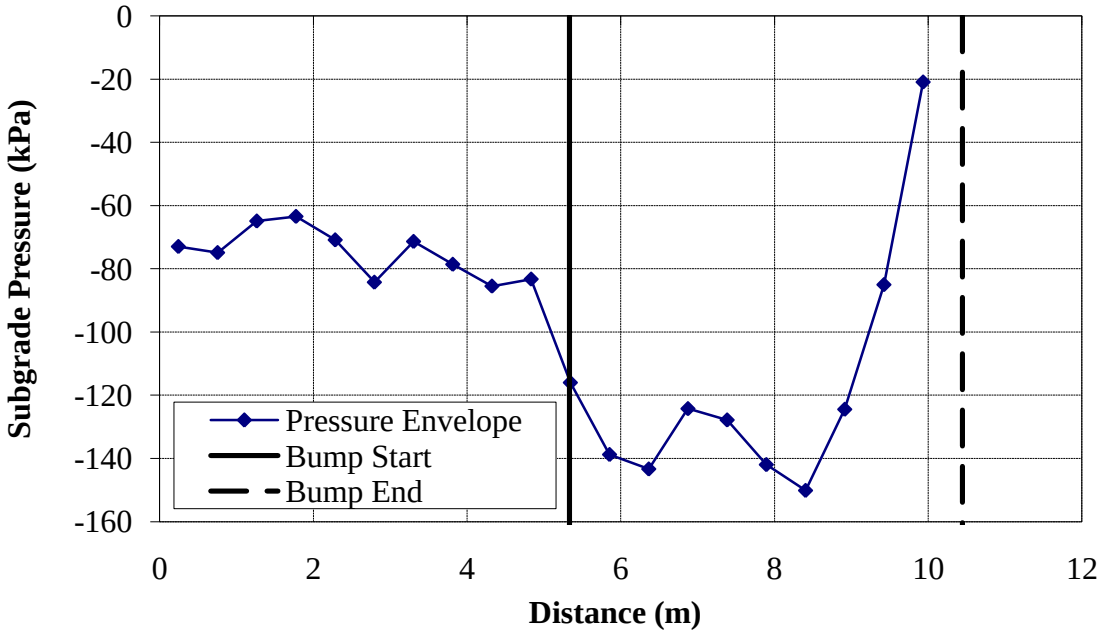

Figure E.93 - Subgrade Pressure Resulting from a 1:150 Bump with Plastic Approach Ties (v = 22.2 m/s)

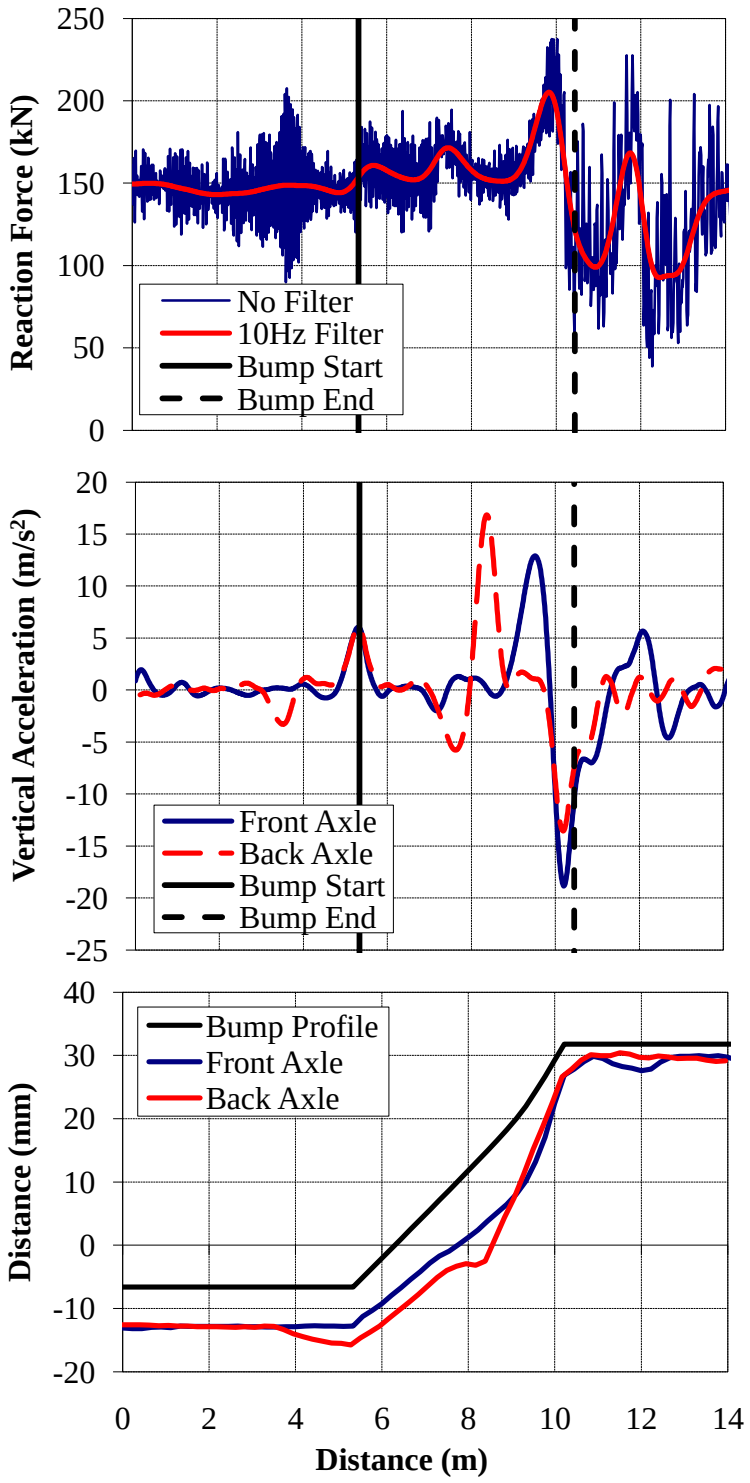

Figure E.94 - (a) Wheel/Rail Forces (b) Axle Accelerations and (c) Track Deflection due to a 1:150 Bump with Wood Approach Ties and Rubber Rail Seat Pads (v = 22.2 m/s)

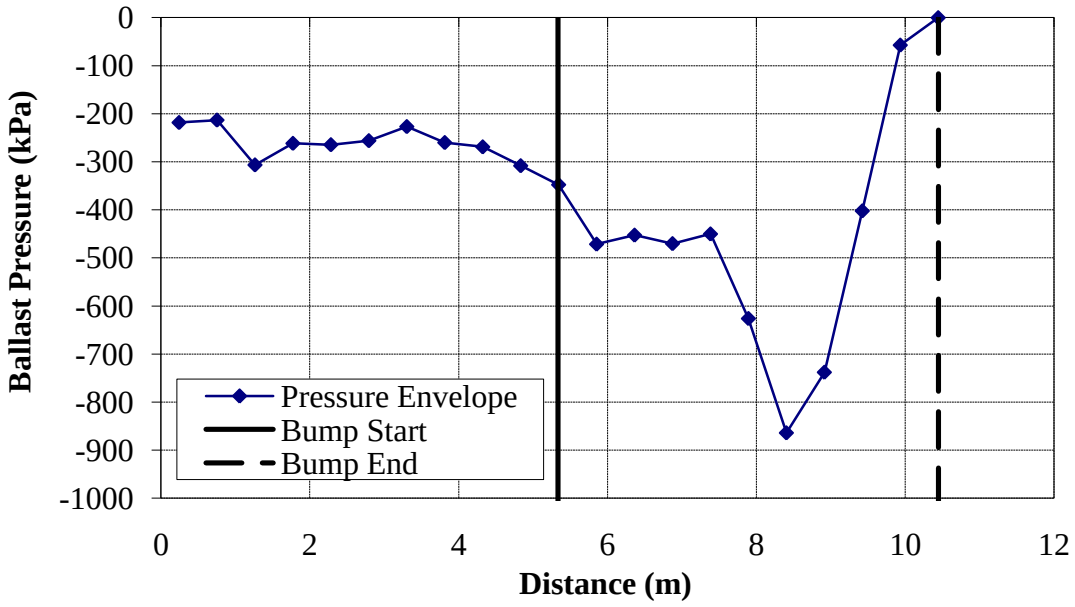

Figure E.95 –Ballast Pressure Resulting from a 1:150 Bump with Wood Approach Ties and Rubber Rail Seat Pads (v = 22.2 m/s)

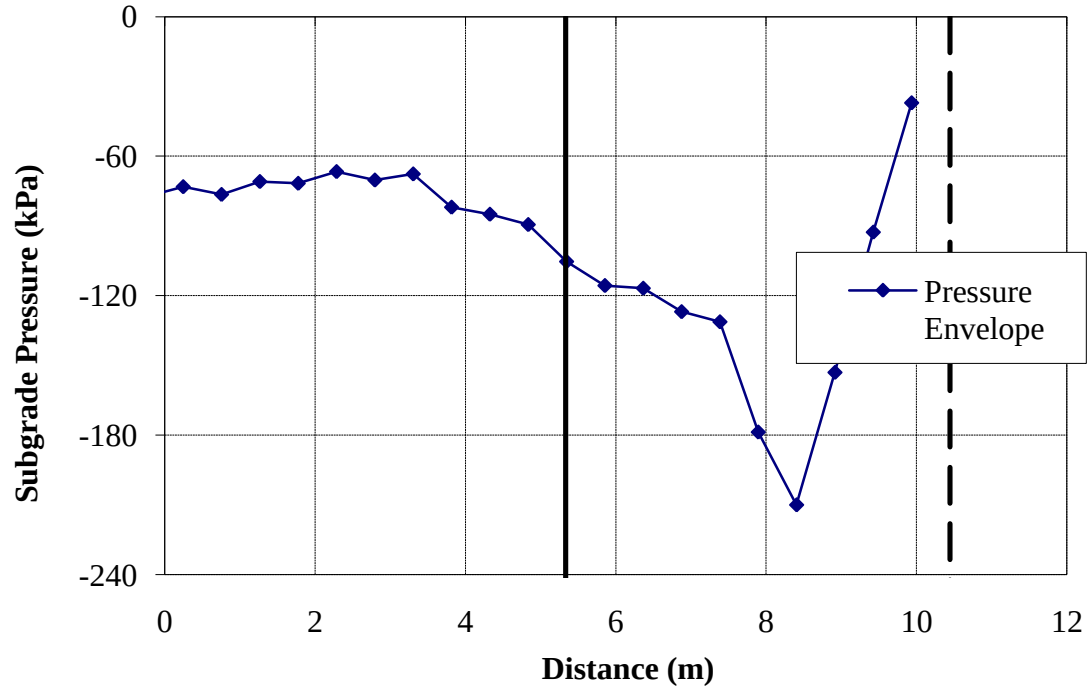

Figure E.96 - Subgrade Pressure Resulting from a 1:150 Bump with Wood Approach Ties and Rubber Rail Seat Pads (v = 22.2 m/s)

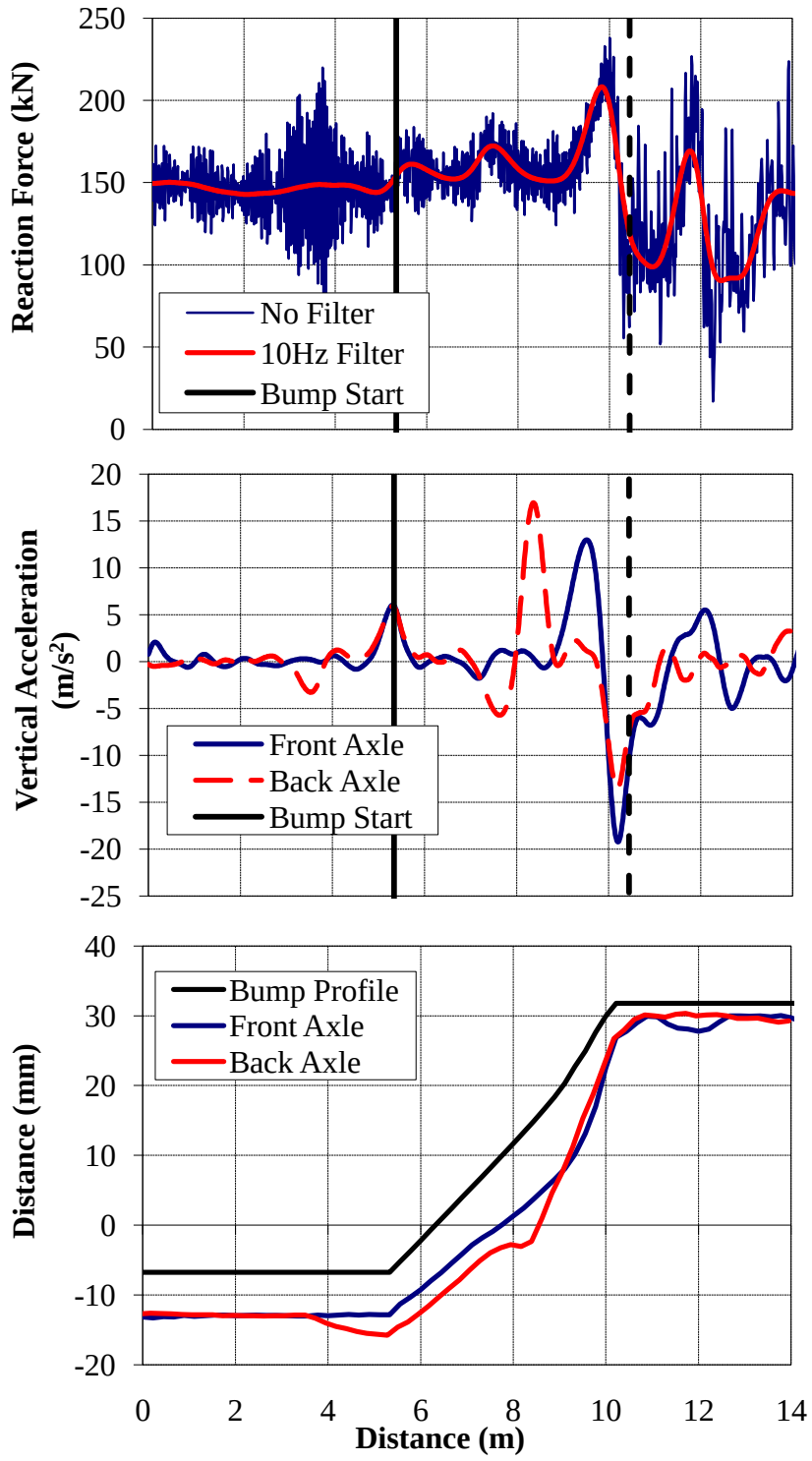

Figure E.97 - (a) Wheel/Rail Forces (b) Axle Accelerations and (c) Track Deflection due to a 1:150 Bump with Concrete Approach Ties and Rubber Rail Seat Pads (v = 22.2 m/s)

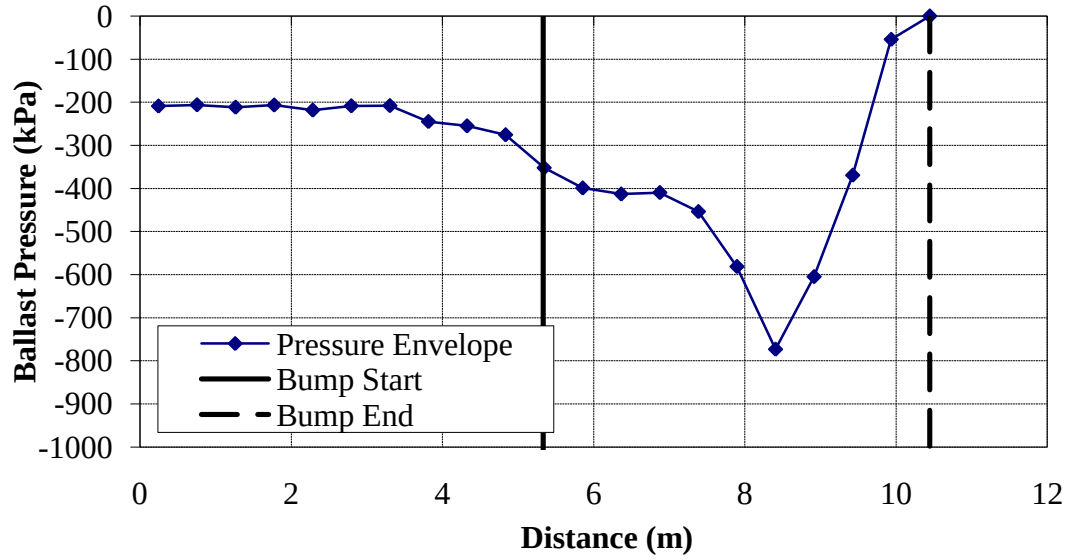

Figure E.98 – Ballast Pressure Resulting from a 1:150 Bump with Concrete Approach Ties and Rubber Rail Seat Pads (v = 22.2 m/s)

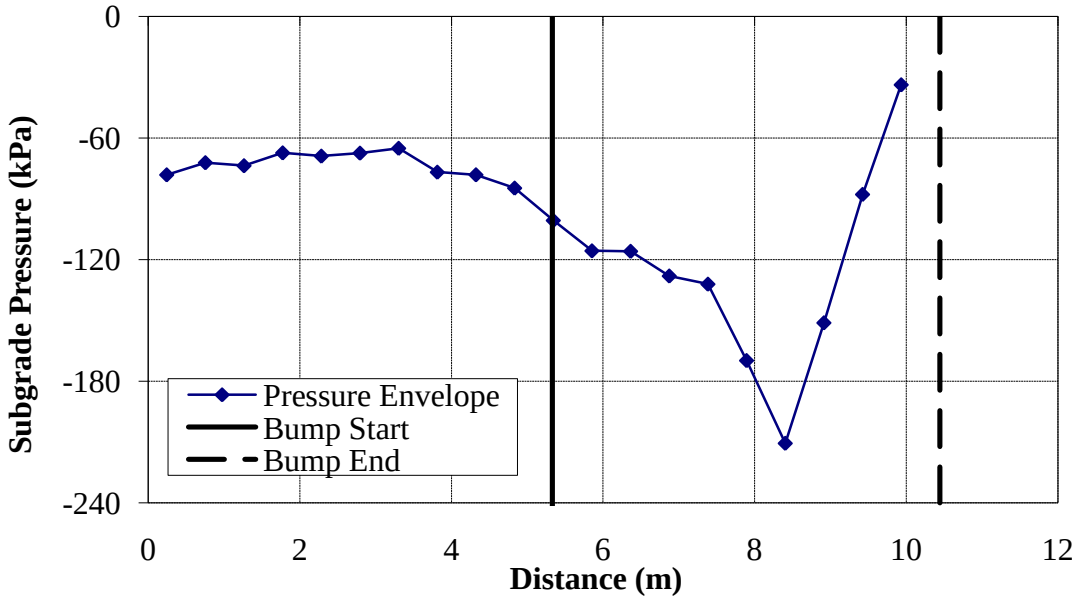

Figure E.99 - Subgrade Pressure Resulting from a 1:150 Bump with Concrete Approach Ties and Rubber Rail Seat Pads (v = 22.2 m/s)

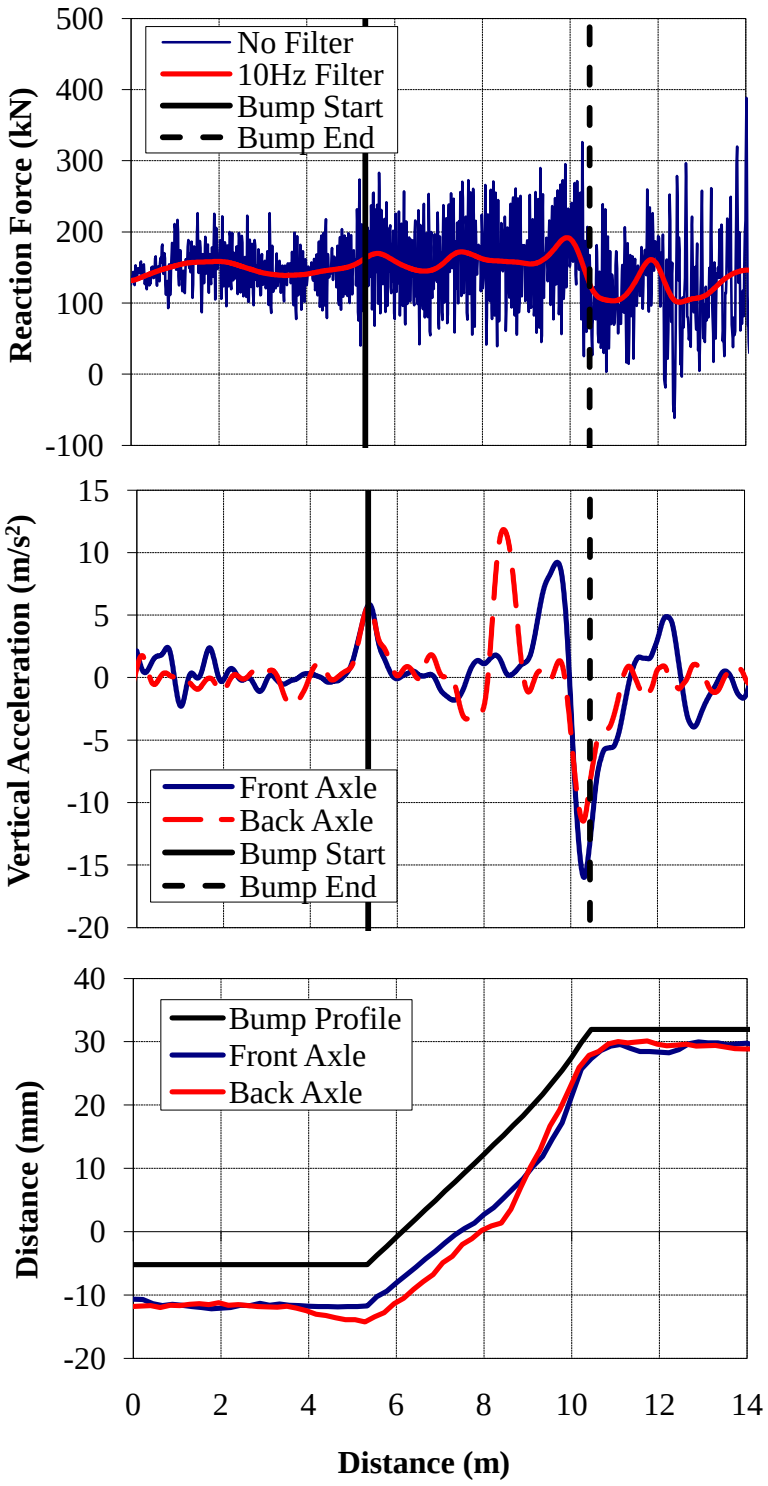

Figure E.100 - (a) Wheel/Rail Forces (b) Axle Accelerations and (c) Track Deflection due to a 1:150 Bump with Wood Approach Ties and Rubber Tie Pads (v = 22.2 m/s)

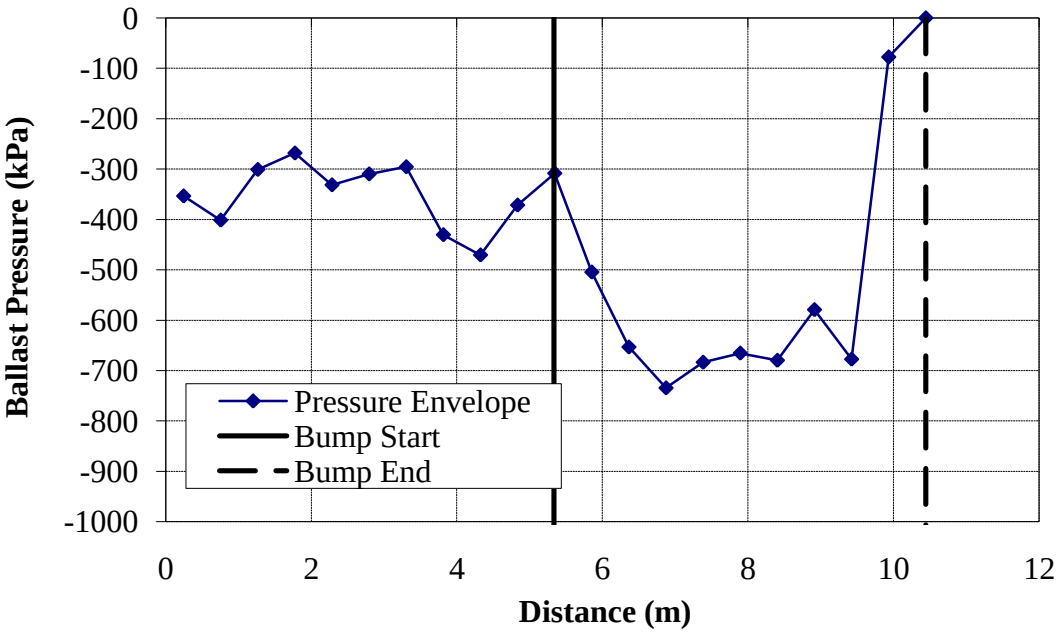

Figure E.101 – Ballast Pressure Resulting from a 1:150 Bump with Wood Approach Ties and Rubber Tie Pads (v = 22.2 m/s)

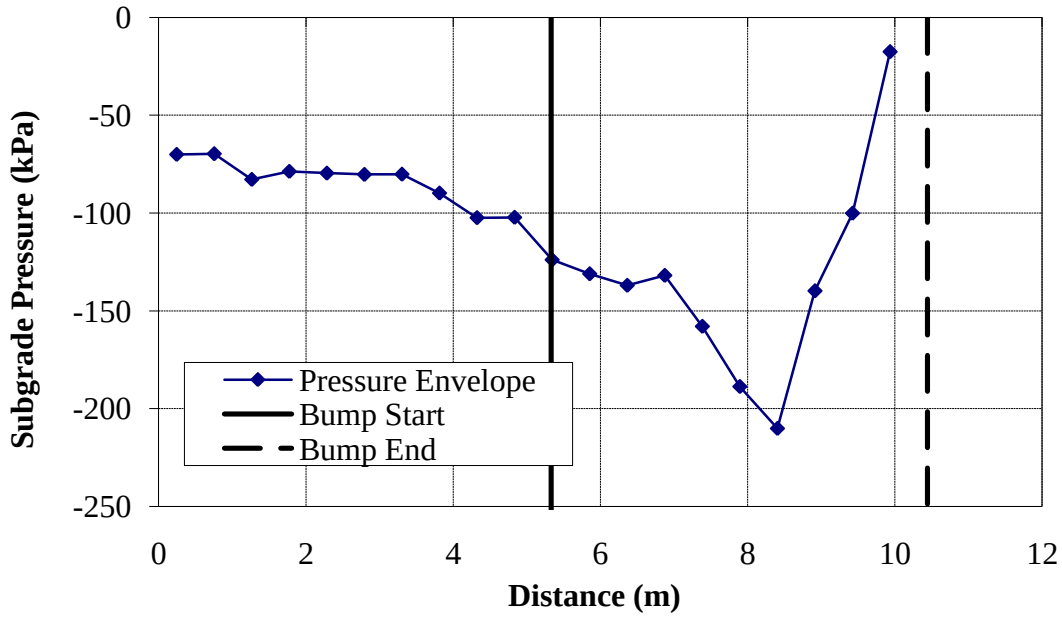

Figure E.102 - Subgrade Pressure Resulting from a 1:150 Bump with Wood Approach Ties and Rubber Tie Pads (v = 22.2 m/s)

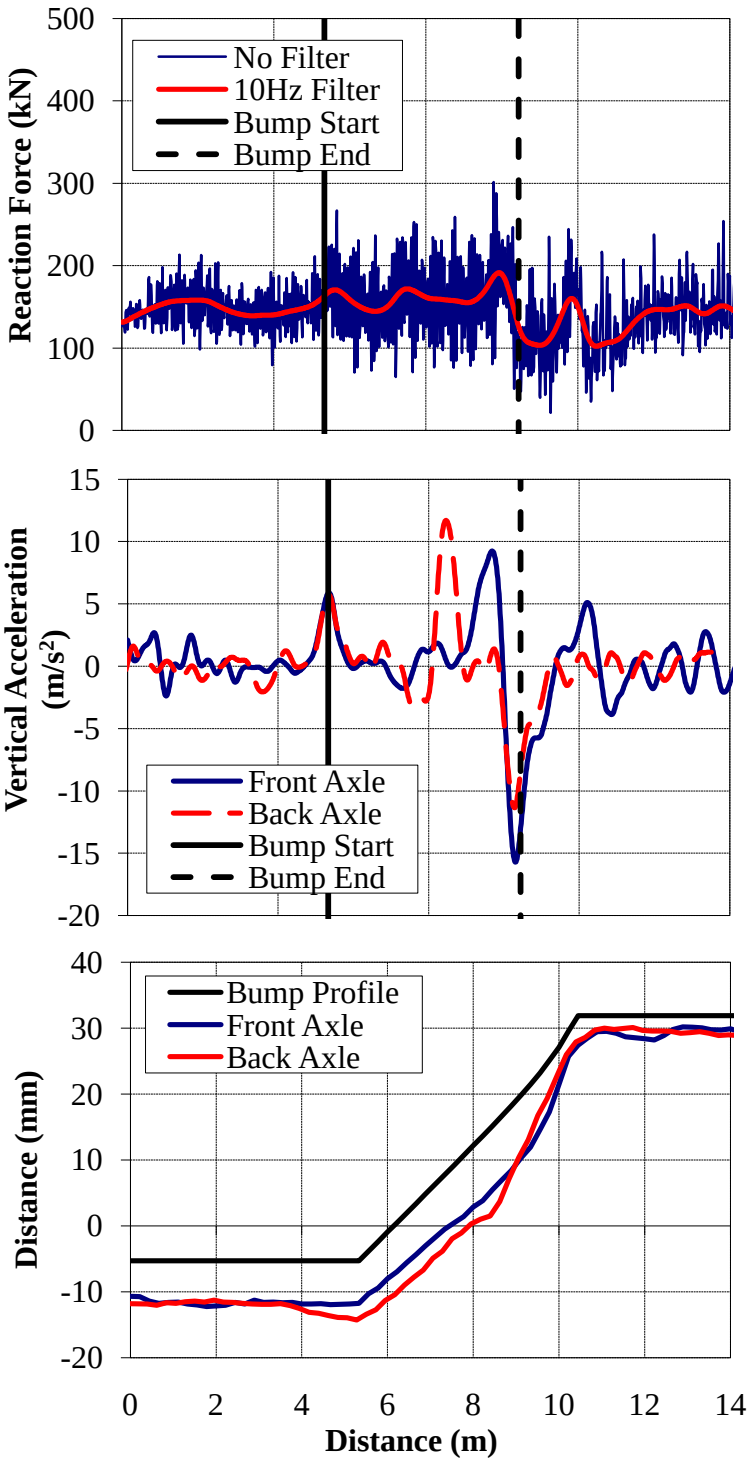

Figure E.103 - (a) Wheel/Rail Forces (b) Axle Accelerations and (c) Track Deflection due to a 1:150 Bump with Concrete Approach Ties and Rubber Tie Pads (v = 22.2 m/s)

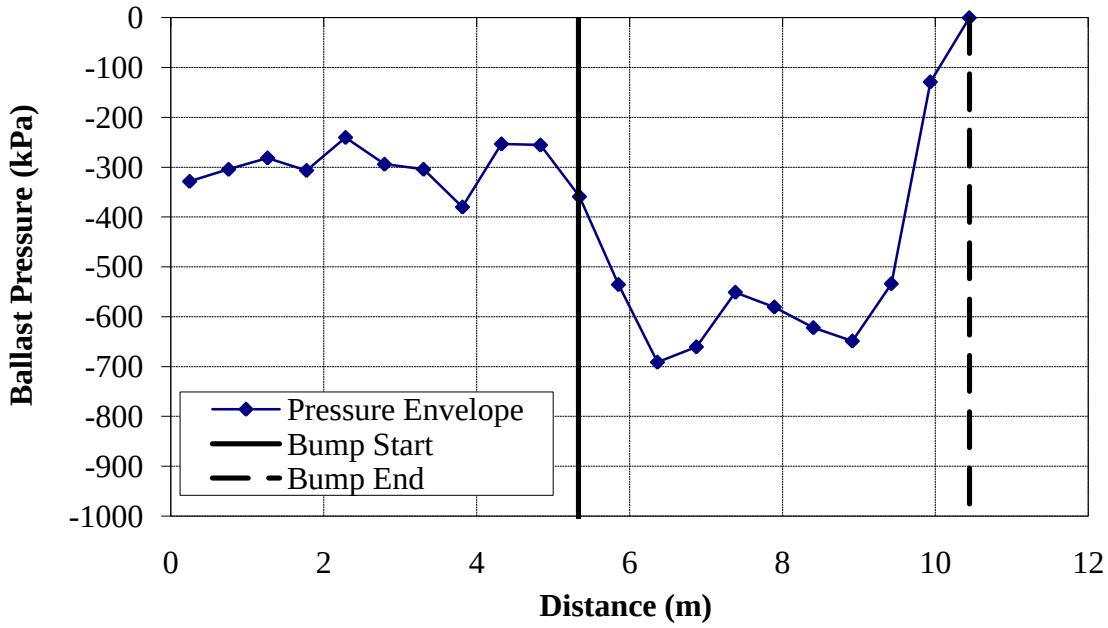

Figure E.104 – Ballast Pressure Resulting from a 1:150 Bump with Concrete Approach Ties and Rubber Tie Pads (v = 22.2 m/s)

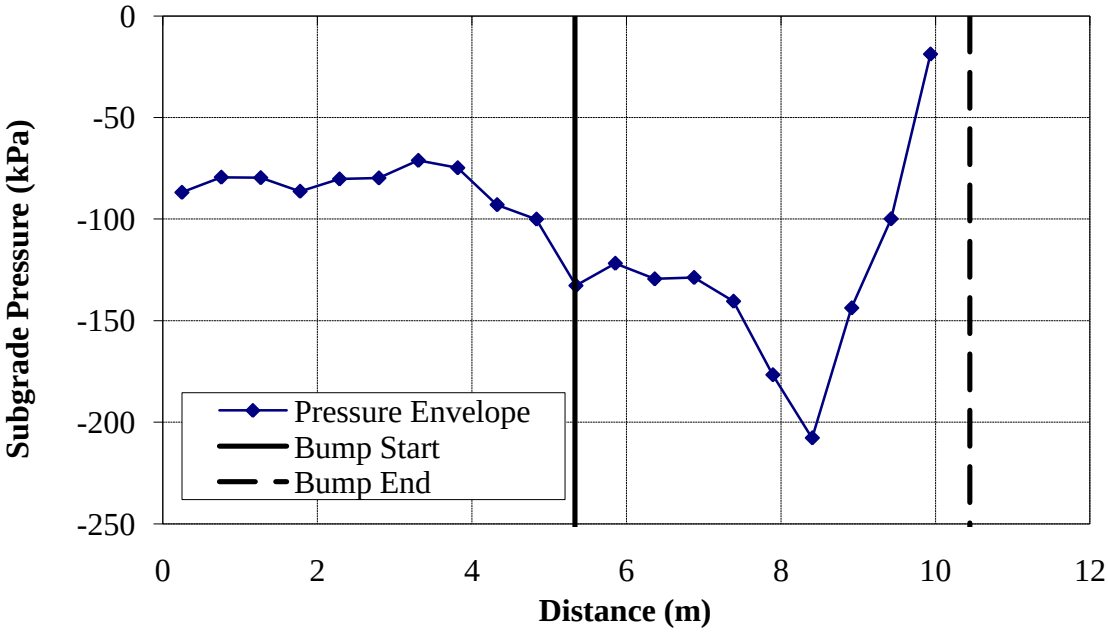

Figure E.105 - Subgrade Pressure Resulting from a 1:150 Bump with Concrete Approach Ties and Rubber Tie Pads (v = 22.2 m/s)

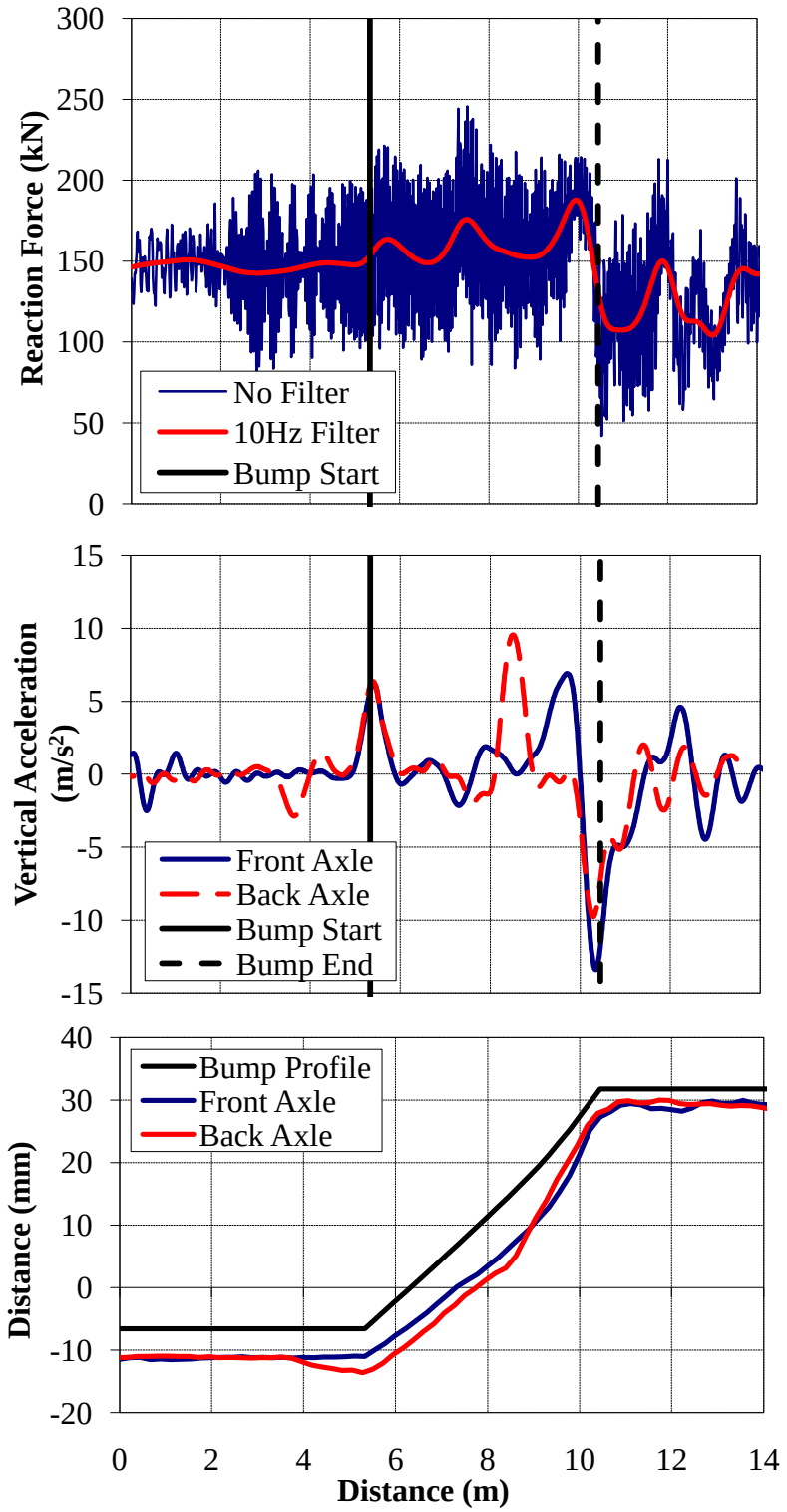

Figure E.106 - (a) Wheel/Rail Forces (b) Axle Accelerations and (c) Track Deflection due to a 1:150 bump with concrete bridge ties (v = 22.2 m/s)

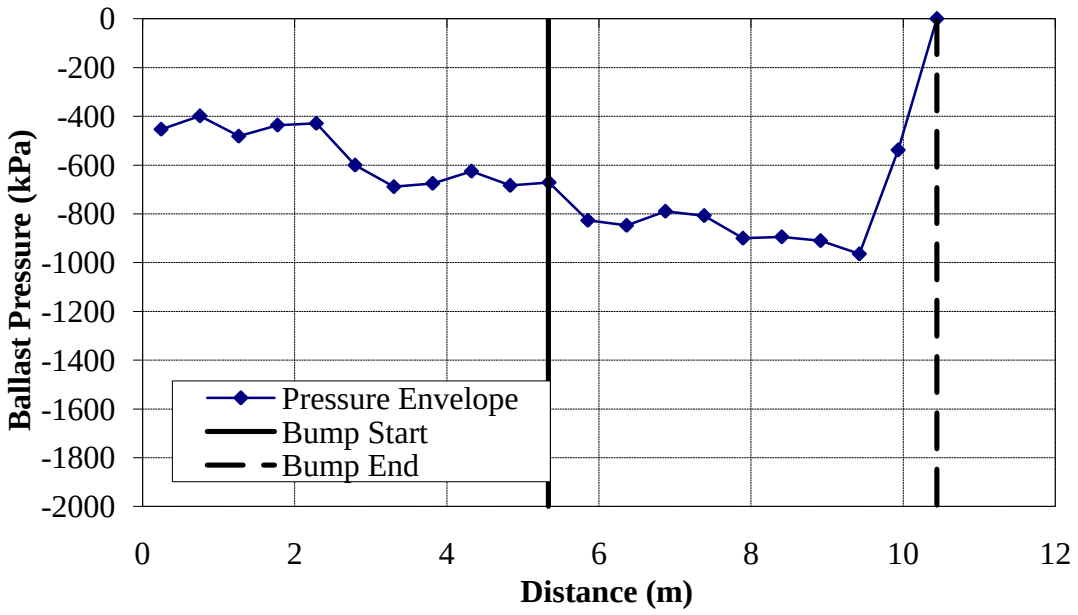

Figure E.107 – Ballast Pressure Resulting from a 1:150 bump with concrete bridge ties (v = 22.2 m/s)

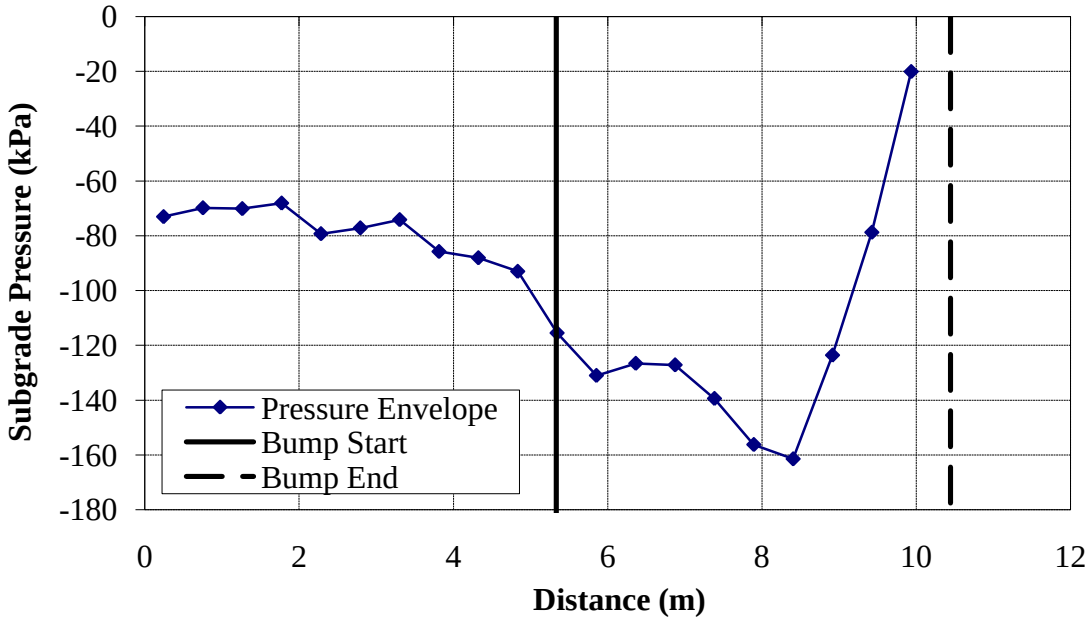

Figure E.108 - Subgrade Pressure Resulting from a 1:150 bump with concrete bridge ties (v = 22.2 m/s)

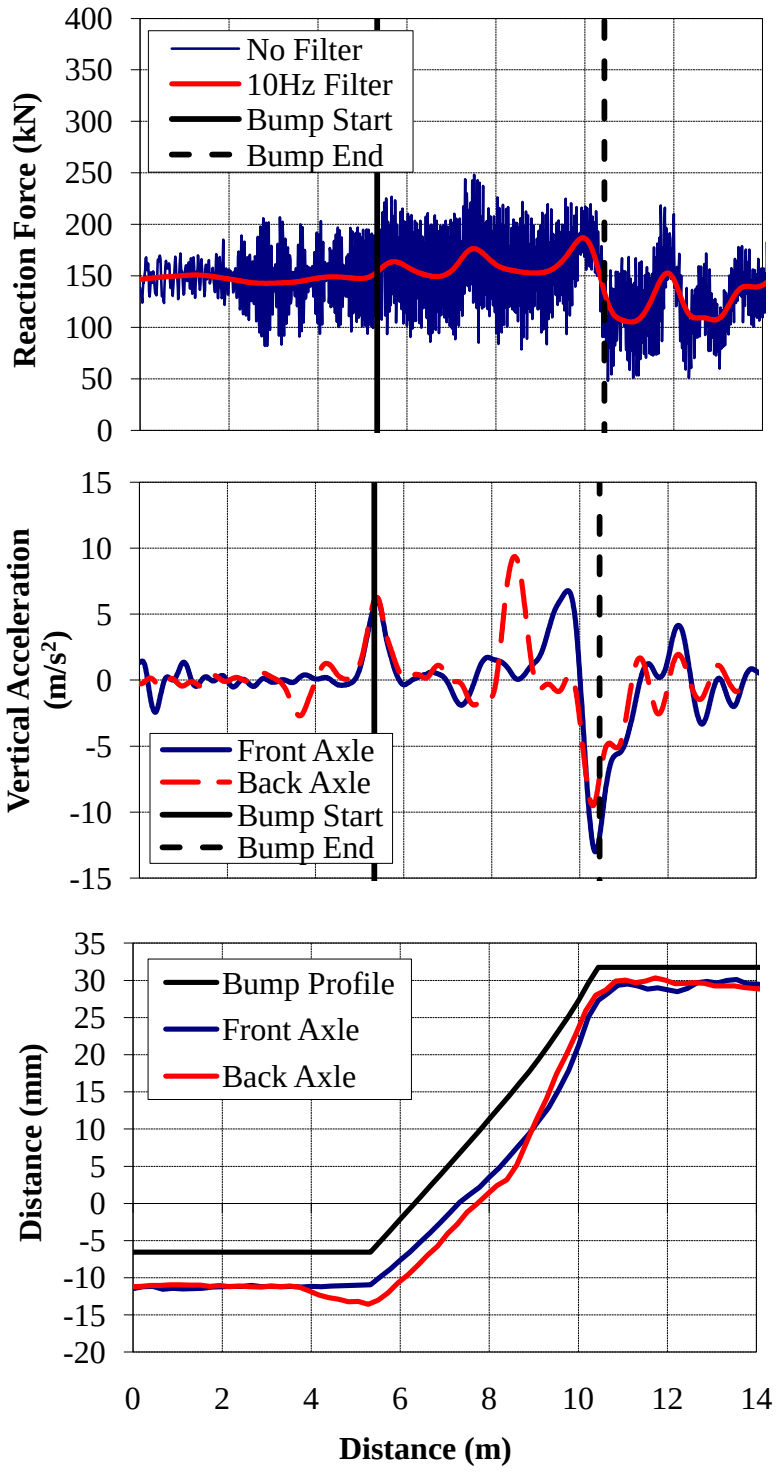

Figure E.109 - (a) Wheel/Rail Forces (b) Axle Accelerations and (c) Track Deflection due to a 1:150 bump with plastic bridge ties (v = 22.2 m/s)

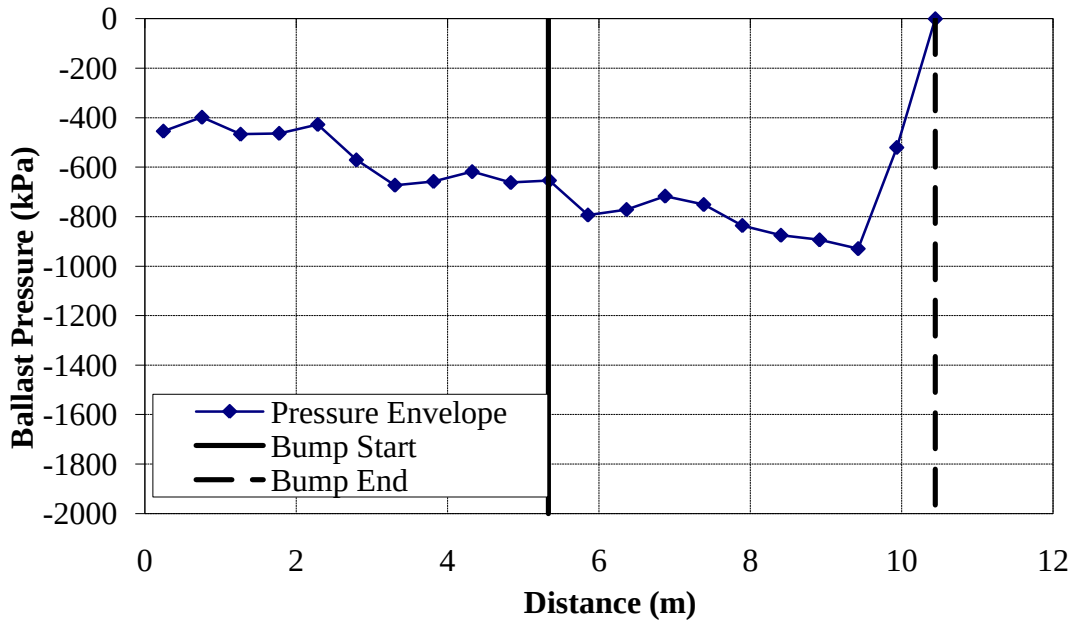

Figure E.110 – Ballast Pressure resulting from a 1:150 bump with plastic bridge ties (v = 22.2 m/s)

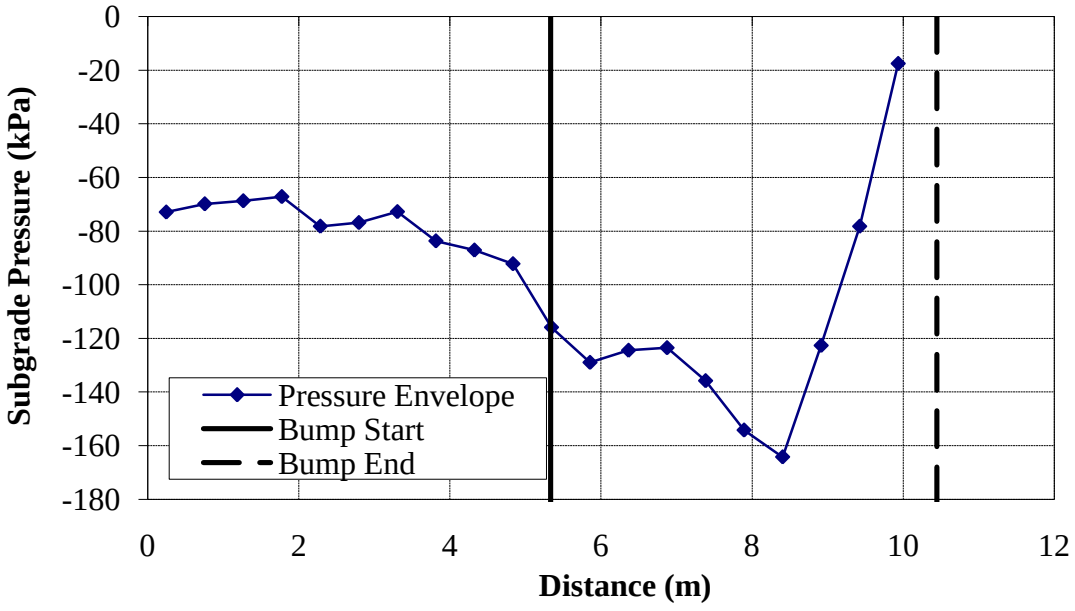

Figure E.111 - Subgrade Pressure resulting from a 1:150 bump with plastic bridge ties (v = 22.2 m/s)

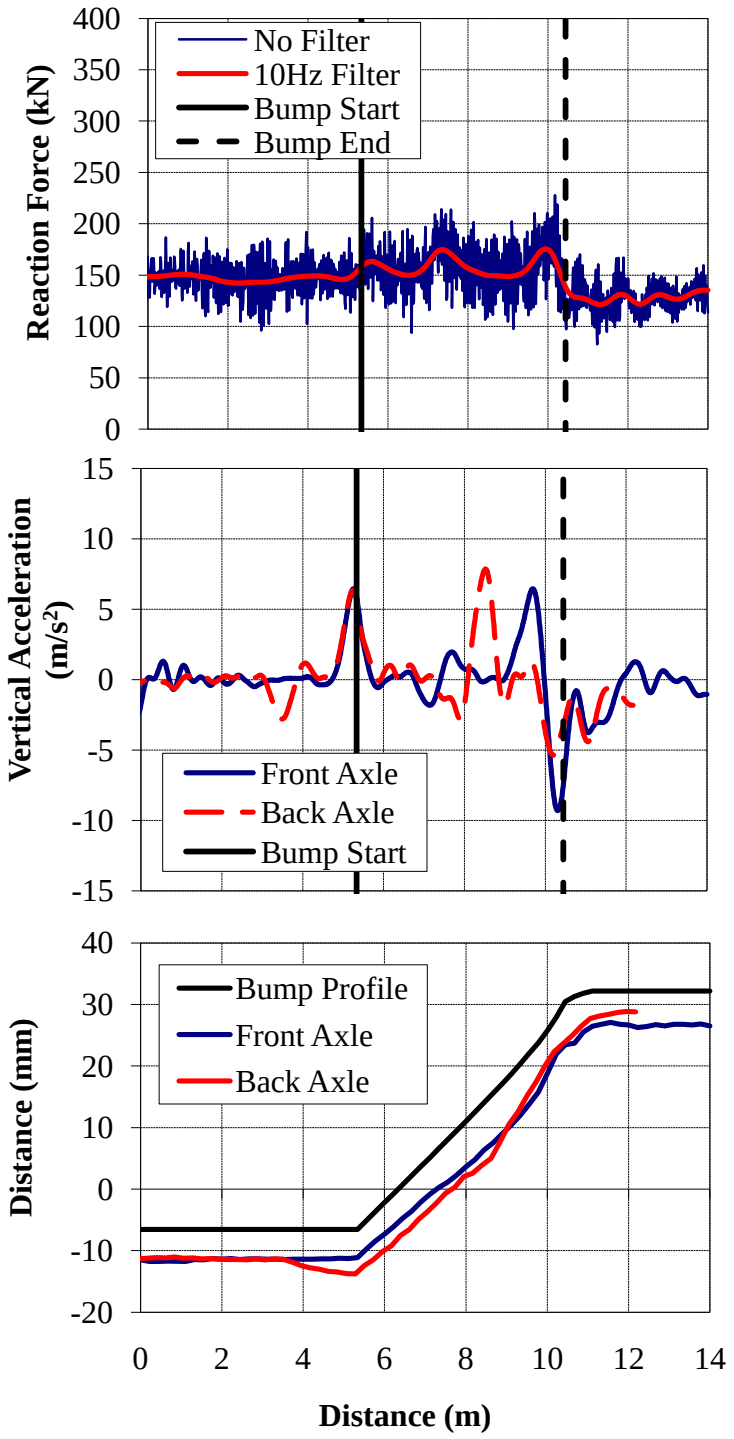

Figure E.112 - (a) Wheel/Rail Forces (b) Axle Accelerations and (c) Track Deflection due to a 1:150 bump with wood bridge ties and rubber rail seat pads (v = 22.2 m/s)

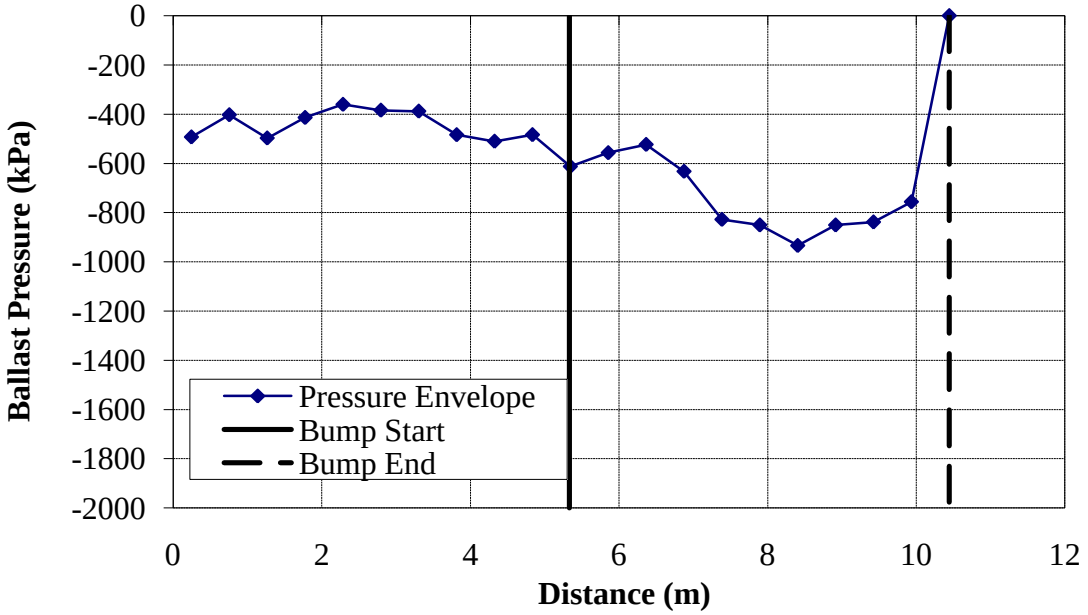

Figure E.113 – Ballast pressures due to a 1:150 bump with wood bridge ties and rubber rail seat pads (v = 22.2 m/s)

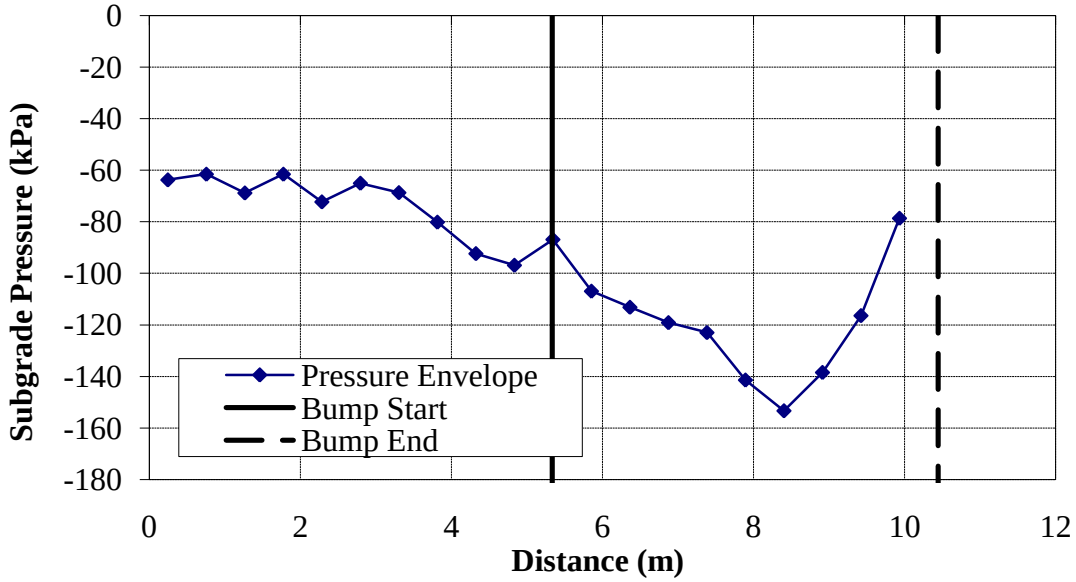

Figure E.114 - Subgrade pressures due to a 1:150 bump with wood bridge ties and rubber rail seat pads (v = 22.2 m/s)

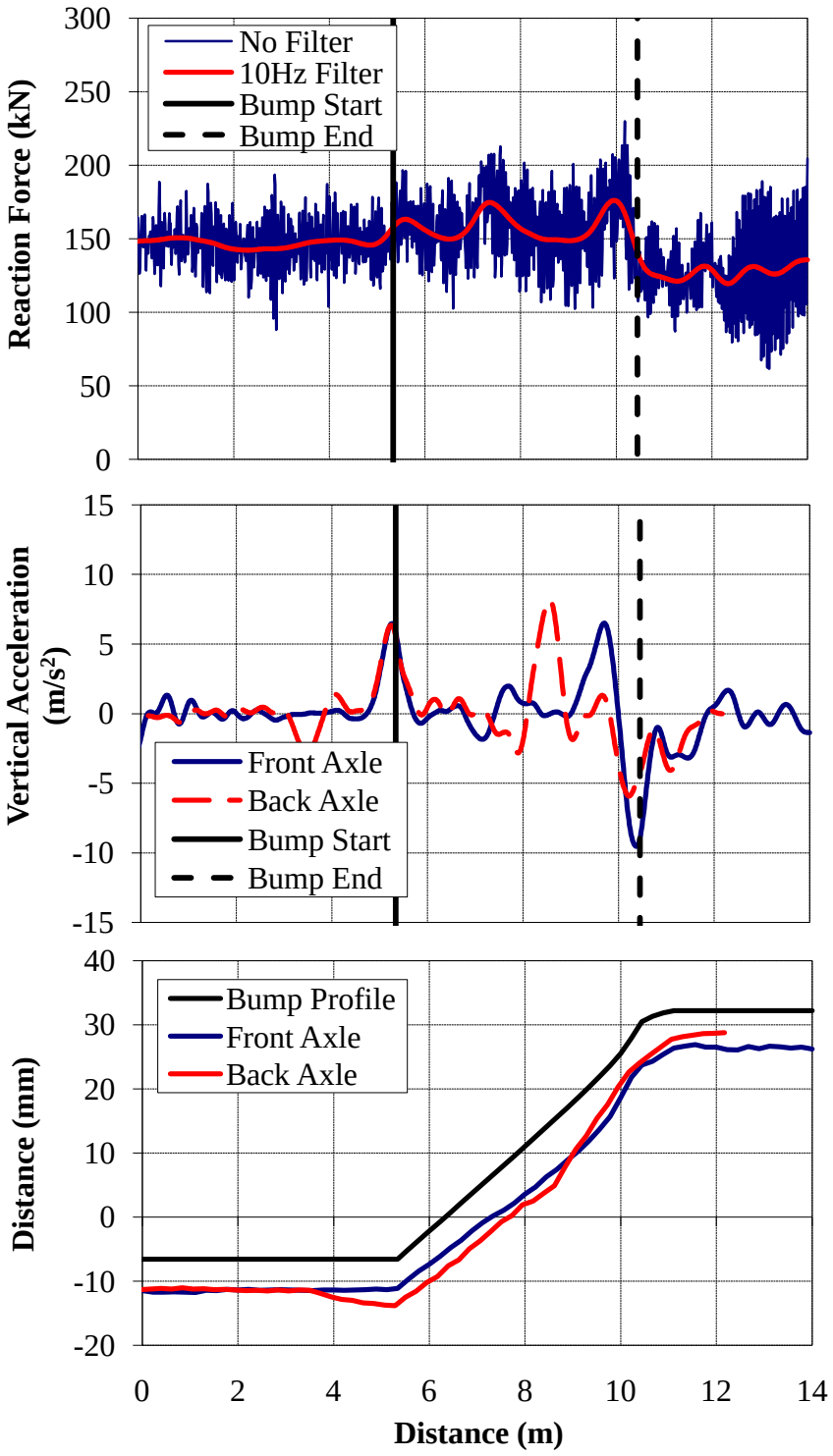

Figure E.115 - (a) Wheel/Rail Forces (b) Axle Accelerations and (c) Track Deflection due to a 1:150 bump with concrete bridge ties and rubber rail seat pads (v = 22.2 m/s)

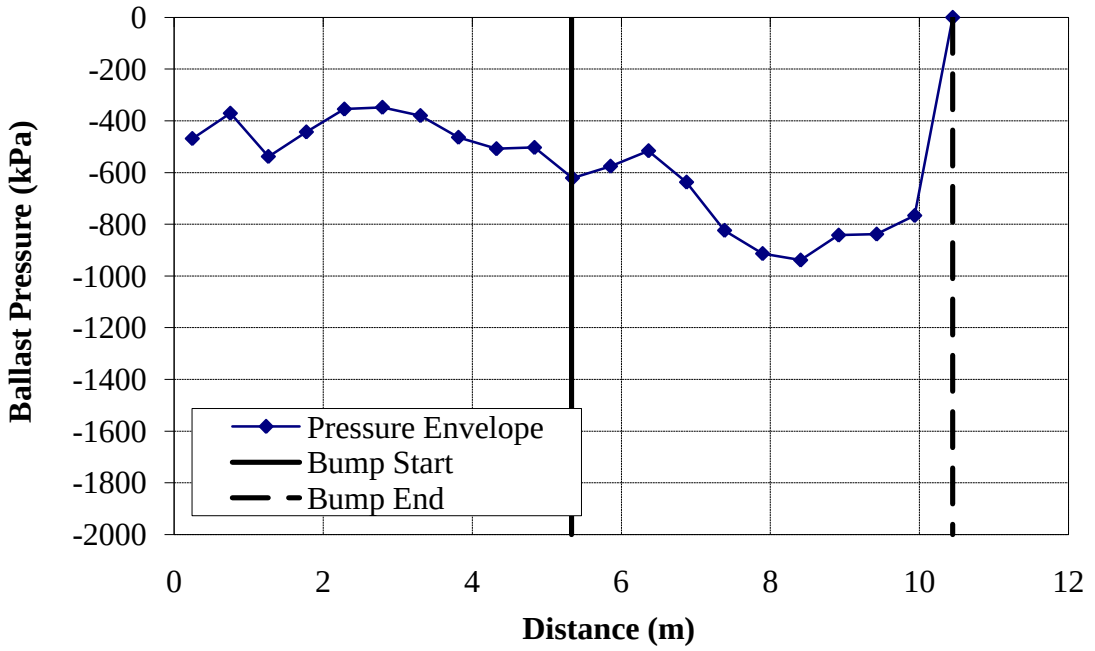

Figure E.116 – Ballast pressures due to a 1:150 bump with concrete bridge ties and rubber rail seat pads (v = 22.2 m/s)

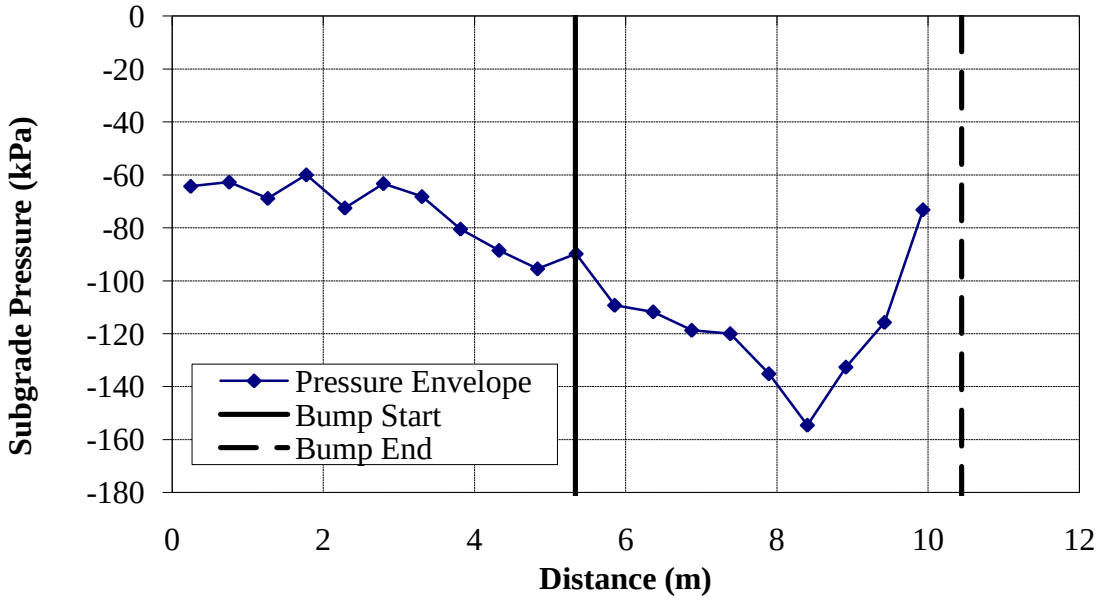

Figure E.117 - Subgrade pressures due to a 1:150 bump with concrete bridge ties and rubber rail seat pads (v = 22.2 m/s)

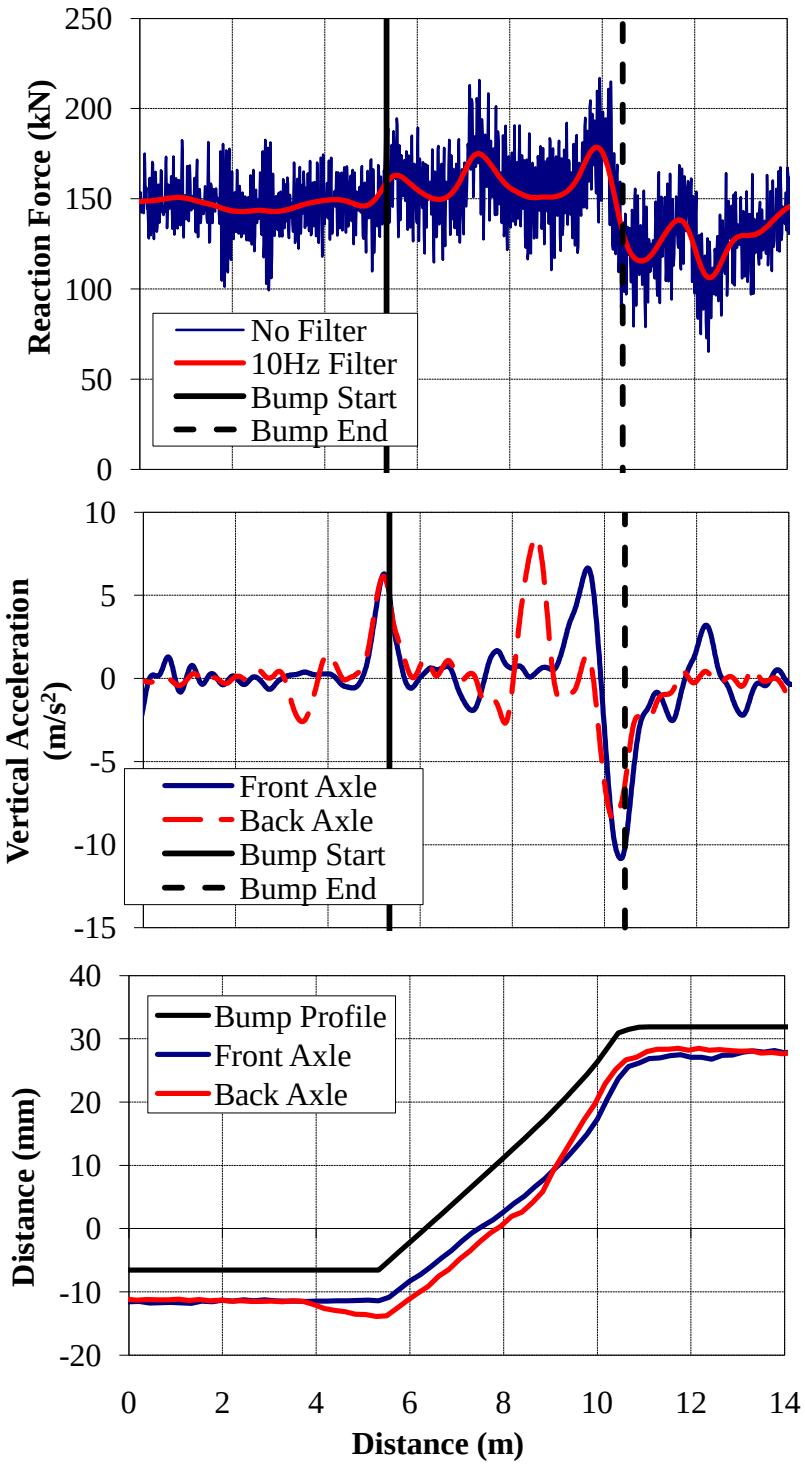

Figure E.118 - (a) Wheel/Rail Forces (b) Axle Accelerations and (c) Track Deflection due to a 1:150 bump on to a Ballast Deck Bridge (v = 22.2 m/s)

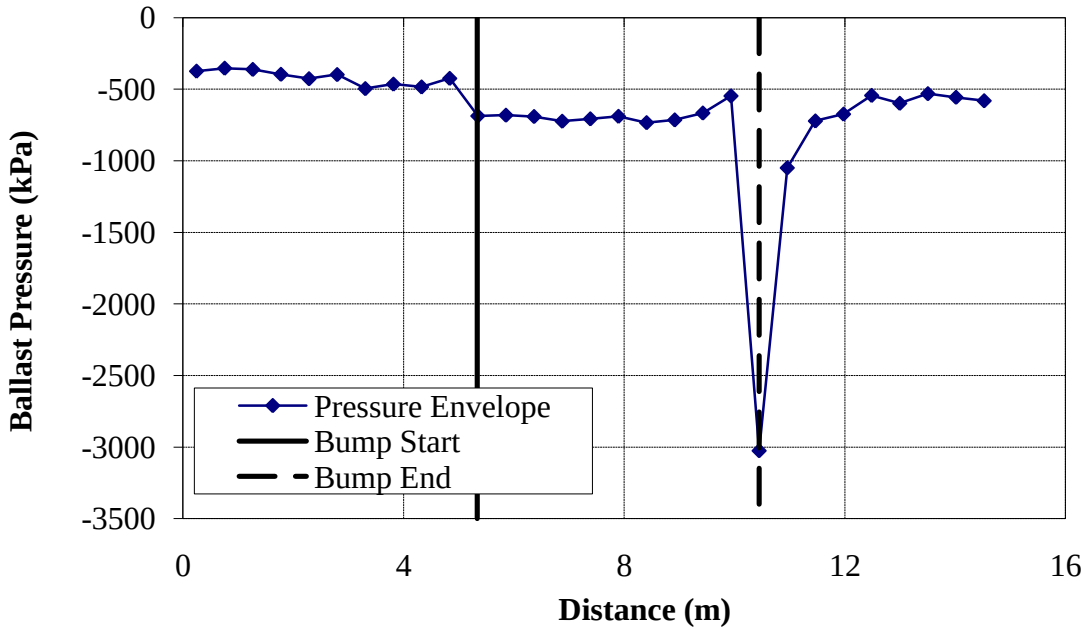

Figure E.119 – Ballast pressure due to a 1:150 bump on to a Ballast Deck Bridge (v = 22.2 m/s)

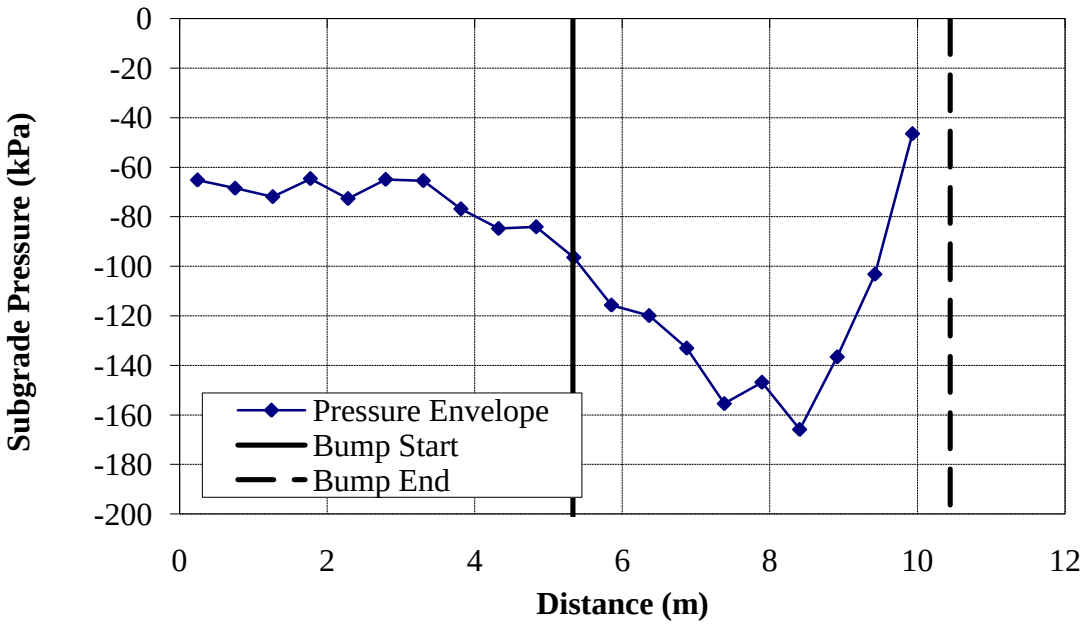

Figure E.120 - Subgrade pressure due to a 1:150 bump on to a Ballast Deck Bridge (v = 22.2 m/s)

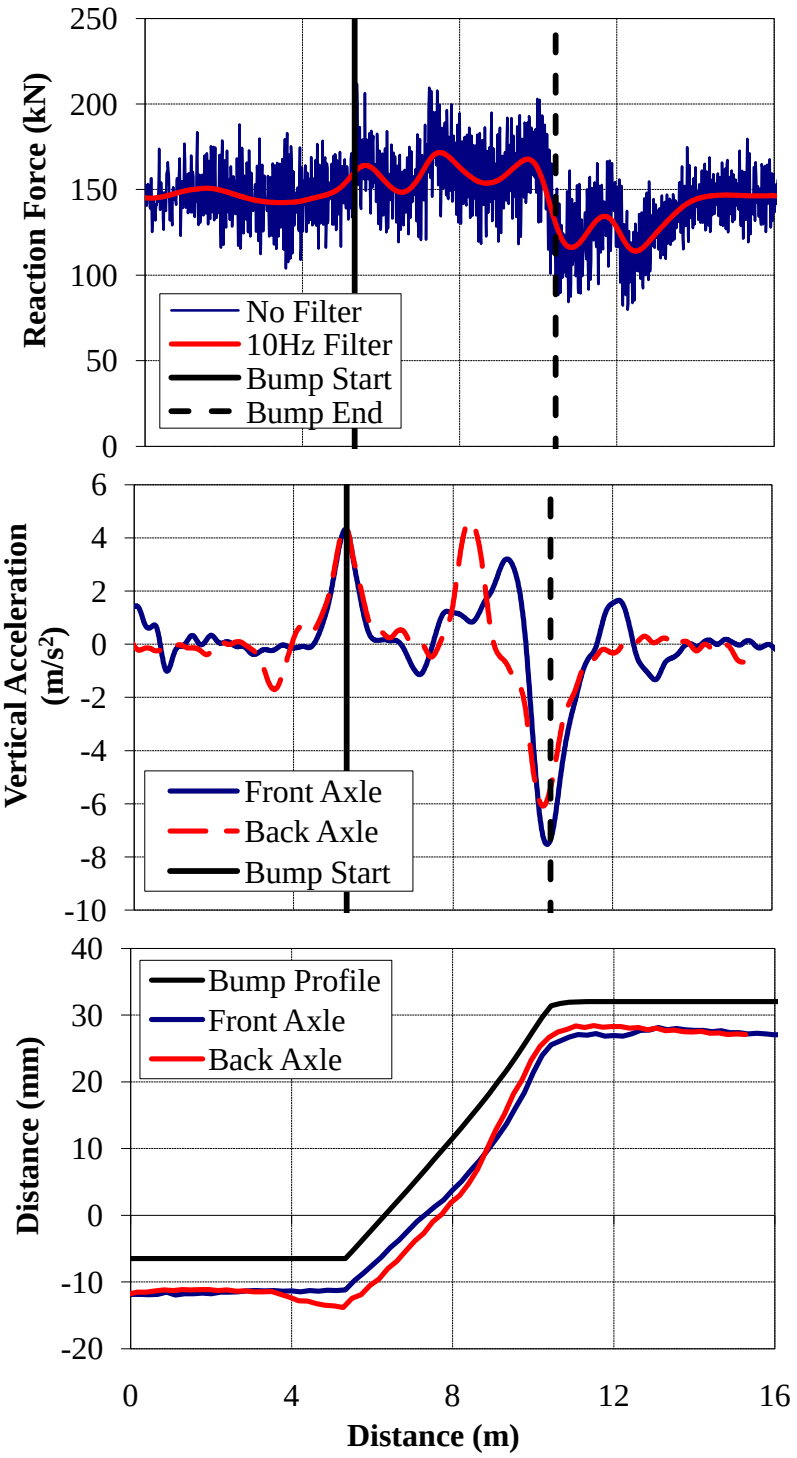

Figure E.121 - (a) Wheel/Rail Forces (b) Axle Accelerations and (c) Track Deflection due to a 1:150 bump on to a Ballast Deck Bridge with a Ballast Mat (v = 22.2 m/s)

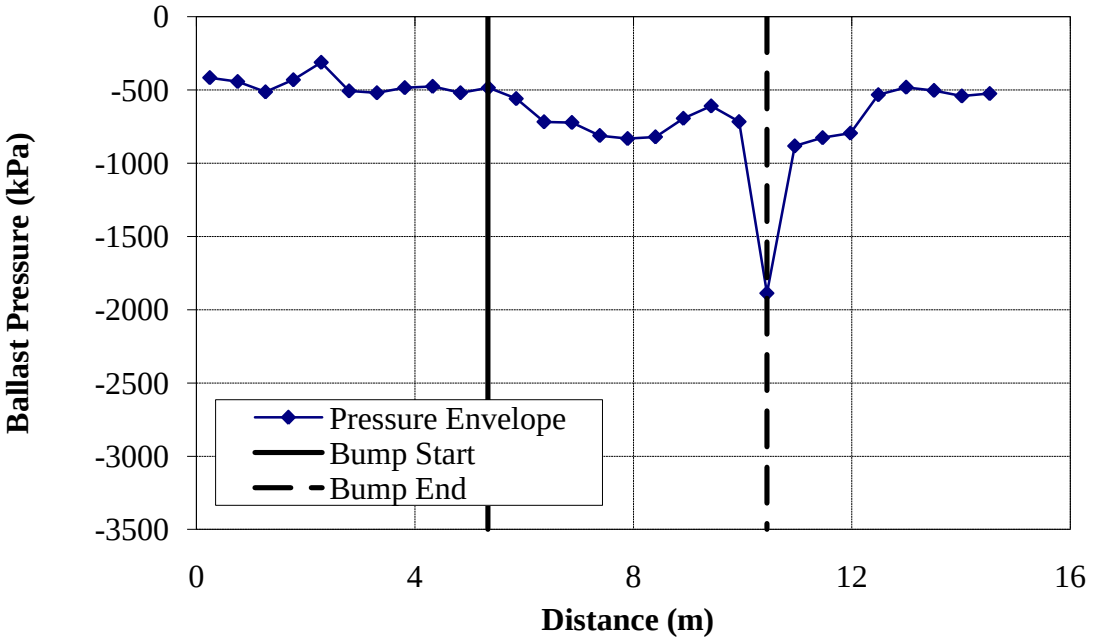

Figure E.122 – Ballast pressure due to a 1:150 bump on to a Ballast Deck Bridge with a Ballast Mat (v = 22.2 m/s)

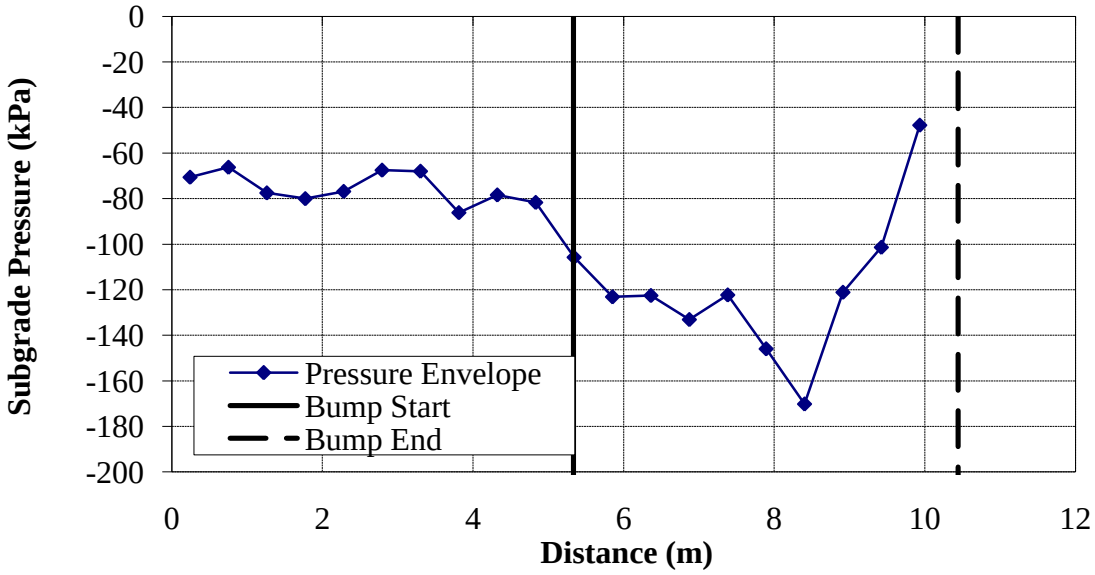

Figure E.123 - Subgrade pressure due to a 1:150 bump on to a Ballast Deck Bridge with a Ballast Mat (v = 22.2 m/s)

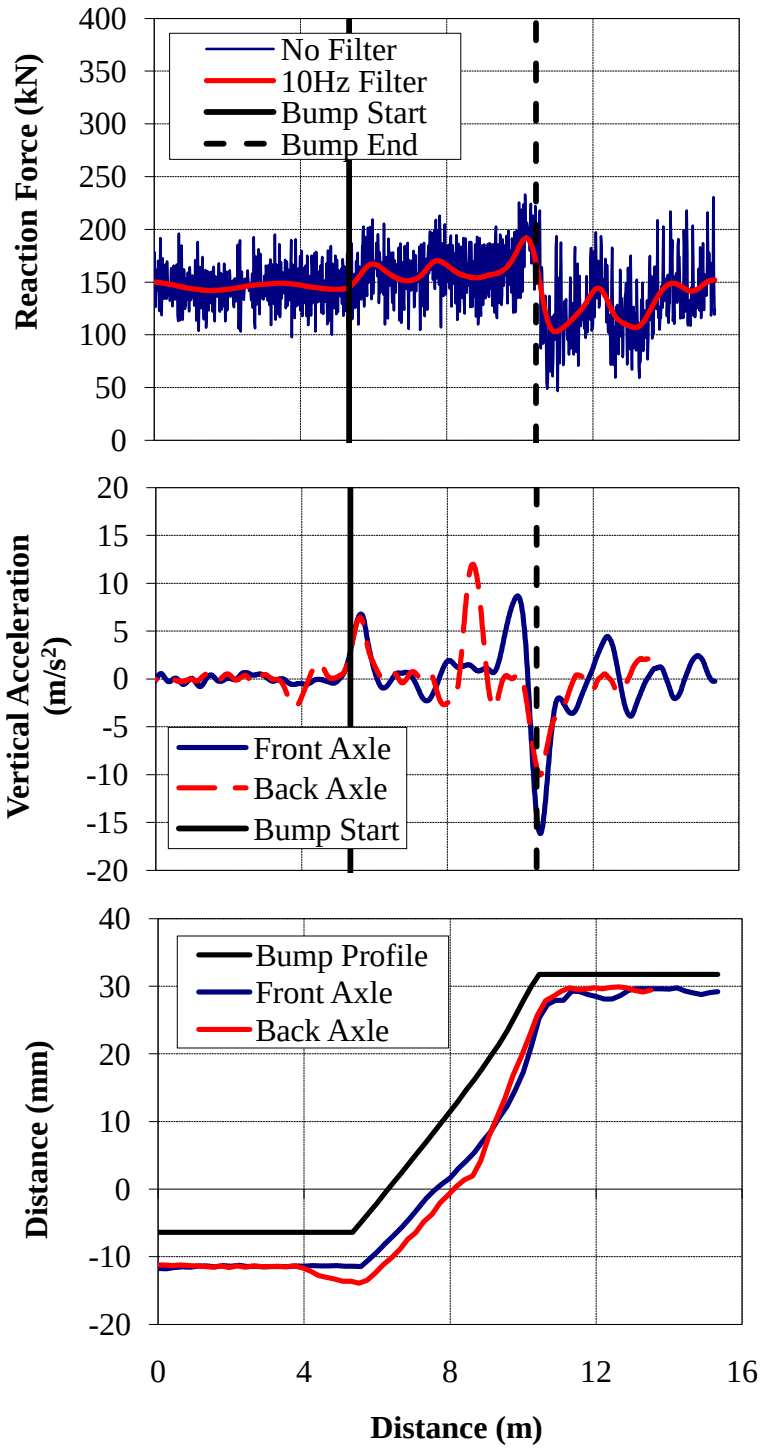

Figure E.124 - (a) Wheel/Rail Forces (b) Axle Accelerations and (c) Track Deflection due to a 1:150 bump with 152.4 mm thick ballast (v = 22.2 m/s)

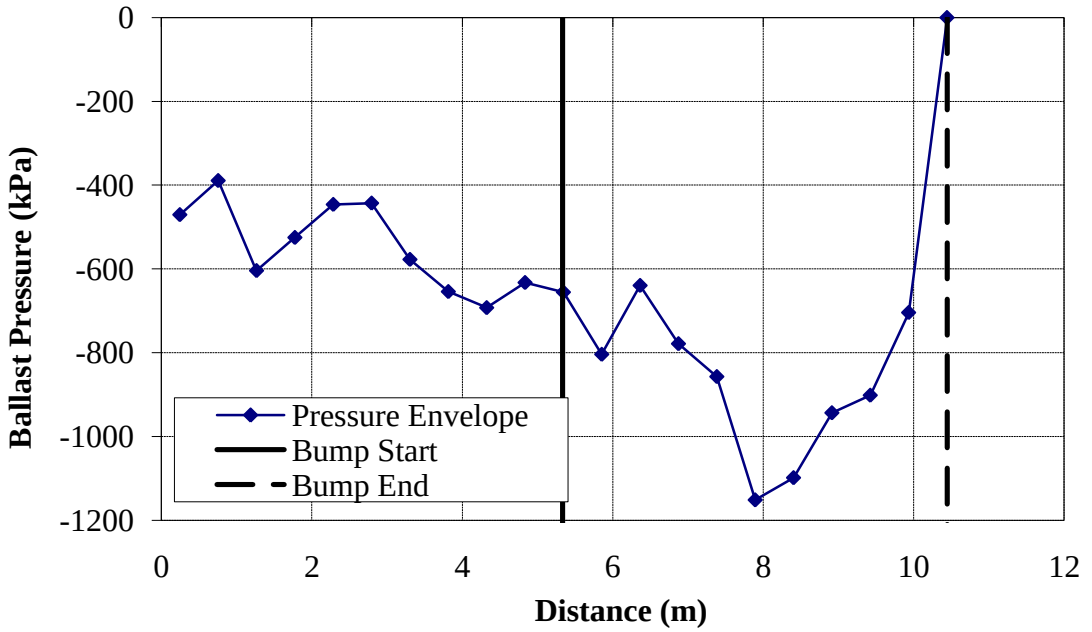

Figure E.125 – Ballast pressure due to a 1:150 bump with 152.4 mm thick ballast (v = 22.2 m/s)

Figure E.126 – Subgrade pressure due to a 1:150 bump with 152.4 mm thick ballast (v = 22.2 m/s)

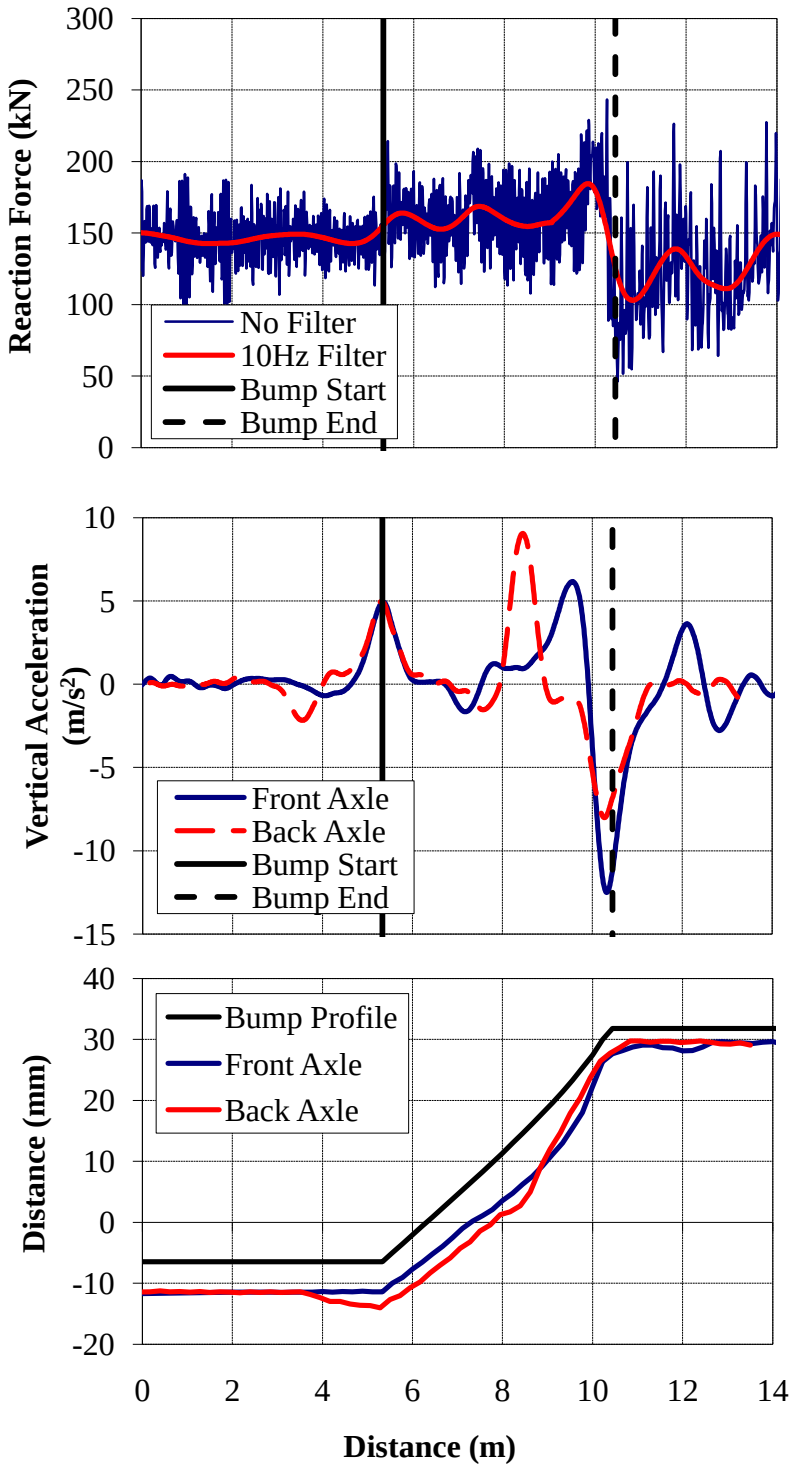

Figure E.127 - (a) Wheel/Rail Forces (b) Axle Accelerations and (c) Track Deflection due to a 1:150 bump with 203.2 mm thick ballast (v = 22.2 m/s)

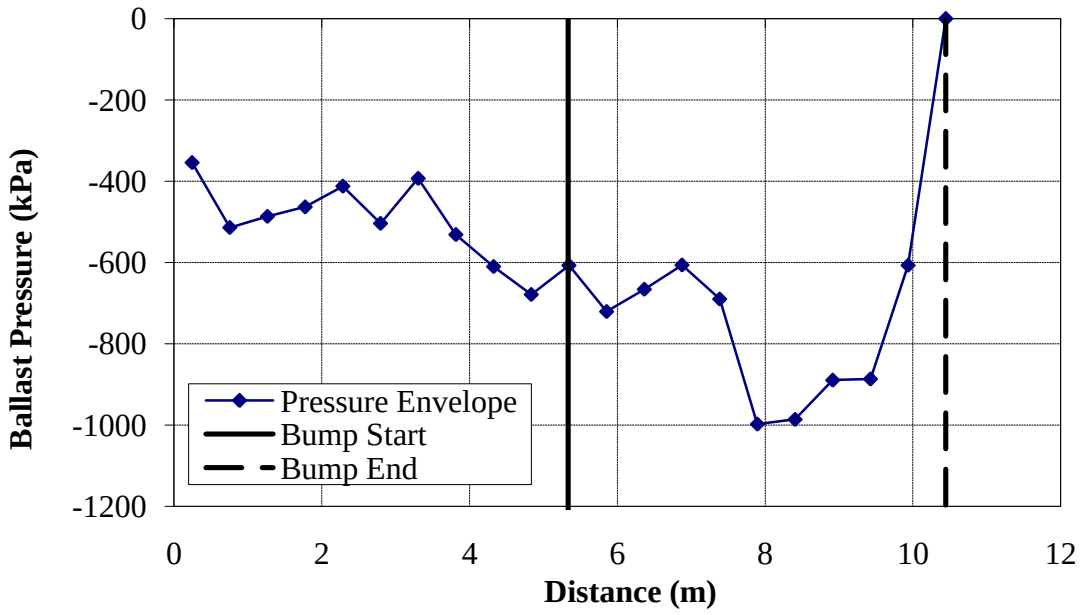

Figure E.128 – Ballast pressure due to a 1:150 bump with 203.2 mm thick ballast (v = 22.2 m/s)

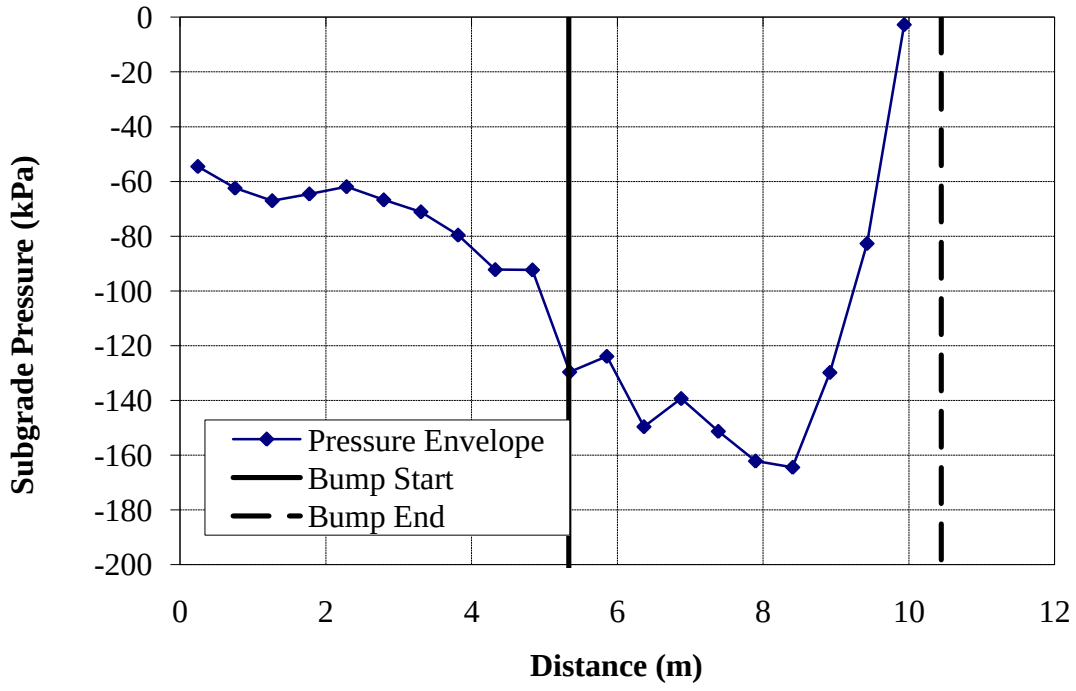

Figure E.129 - Subgrade pressure due to a 1:150 bump with 203.2 mm thick ballast (v = 22.2 m/s)

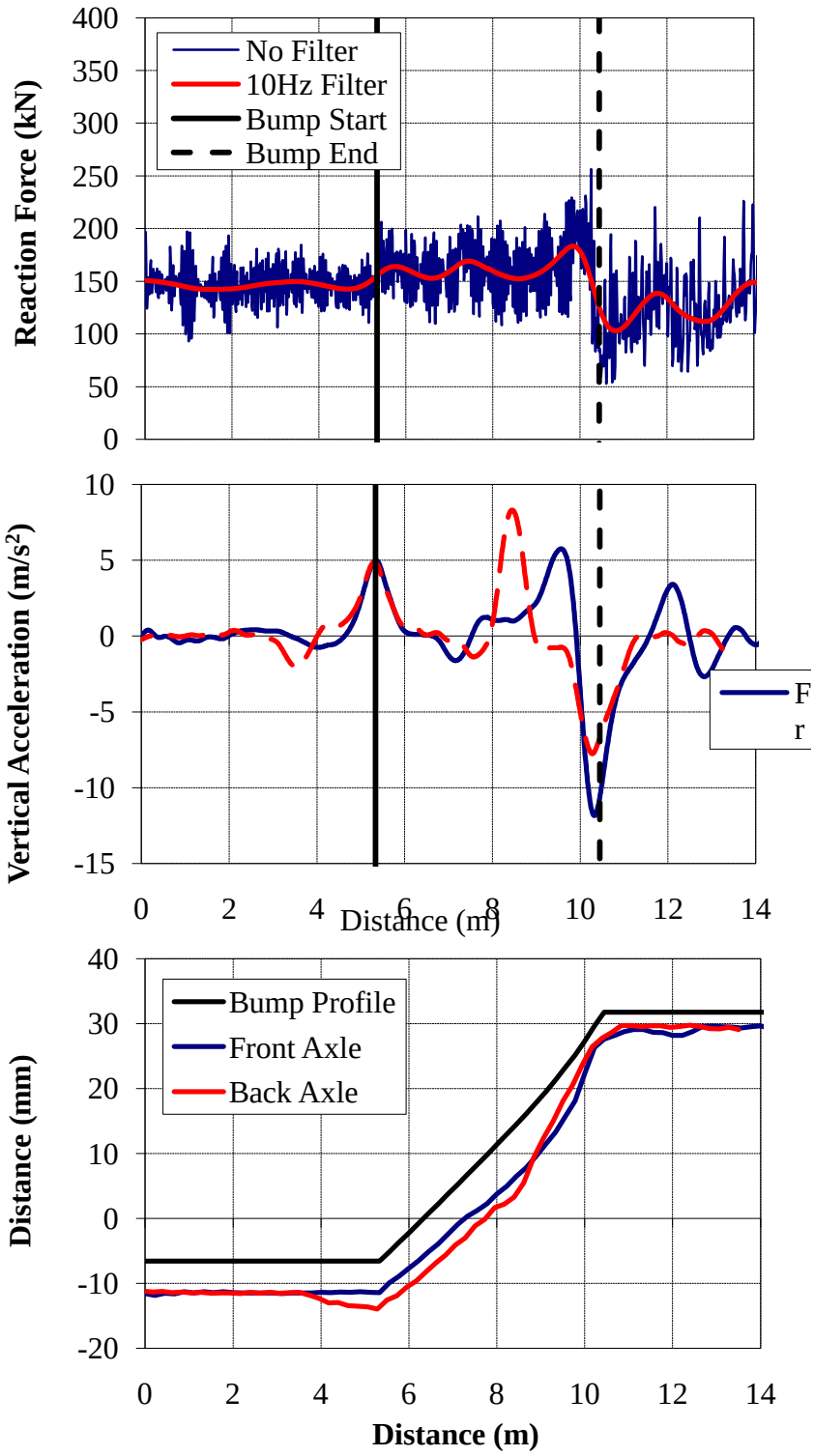

Figure E.130 - (a) Wheel/Rail Forces (b) Axle Accelerations and (c) Track Deflection due to a 1:150 bump with 304.8 mm thick ballast (v = 22.2 m/s)

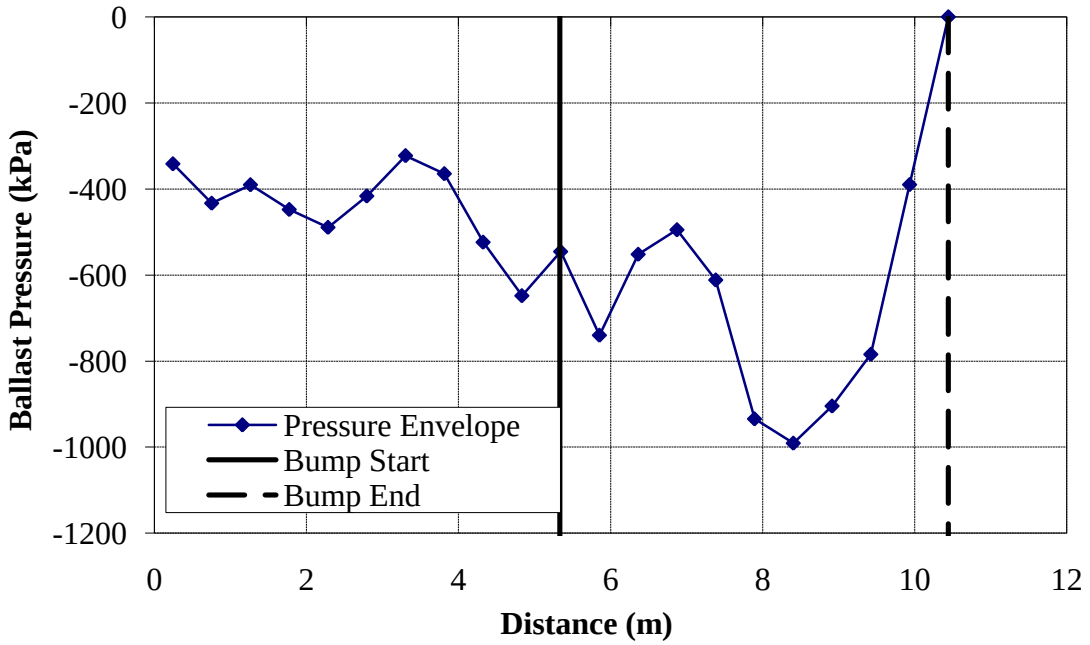

Figure E.131 – Ballast pressure due to a 1:150 bump with 304.8 mm thick ballast (v = 22.2 m/s)

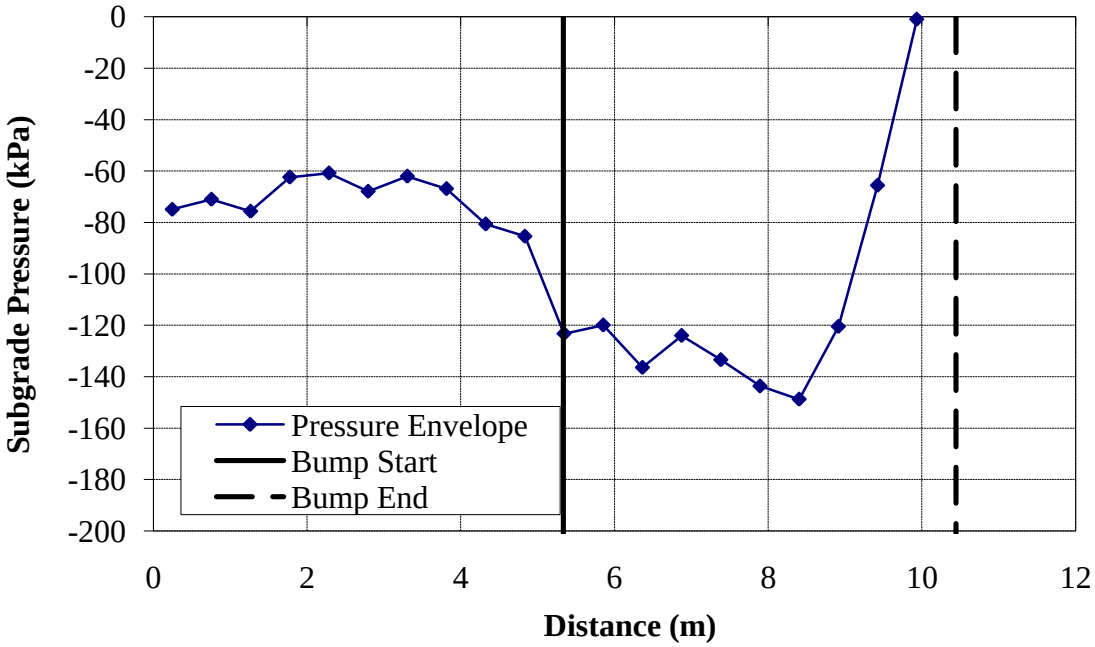

Figure E.132 - Subgrade pressure due to a 1:150 bump with 304.8 mm thick ballast (v = 22.2 m/s)

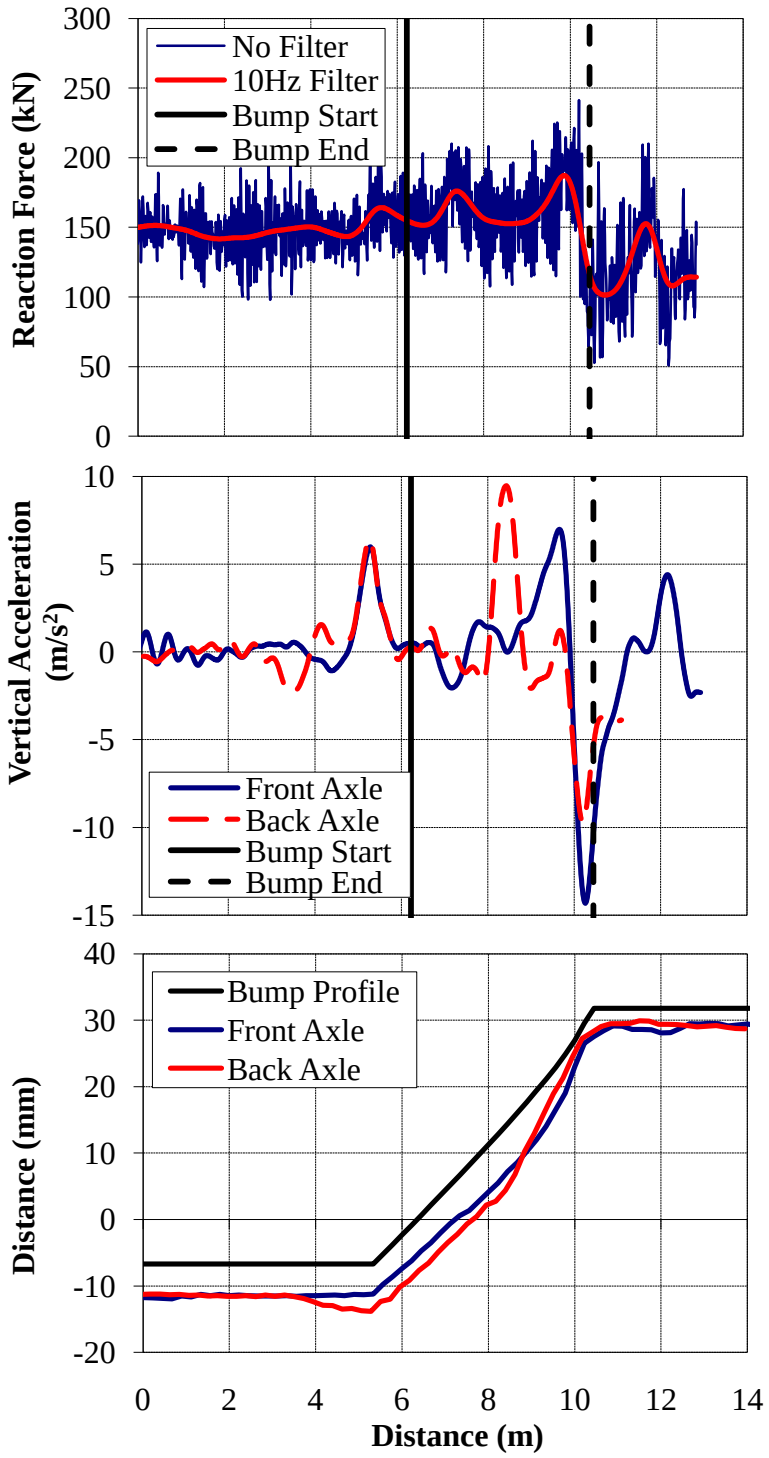

Figure E.133 - (a) Wheel/Rail Forces (b) Axle Accelerations and (c) Track Deflection due to a 1:150 bump with 406.4 mm thick ballast (v = 22.2 m/s)

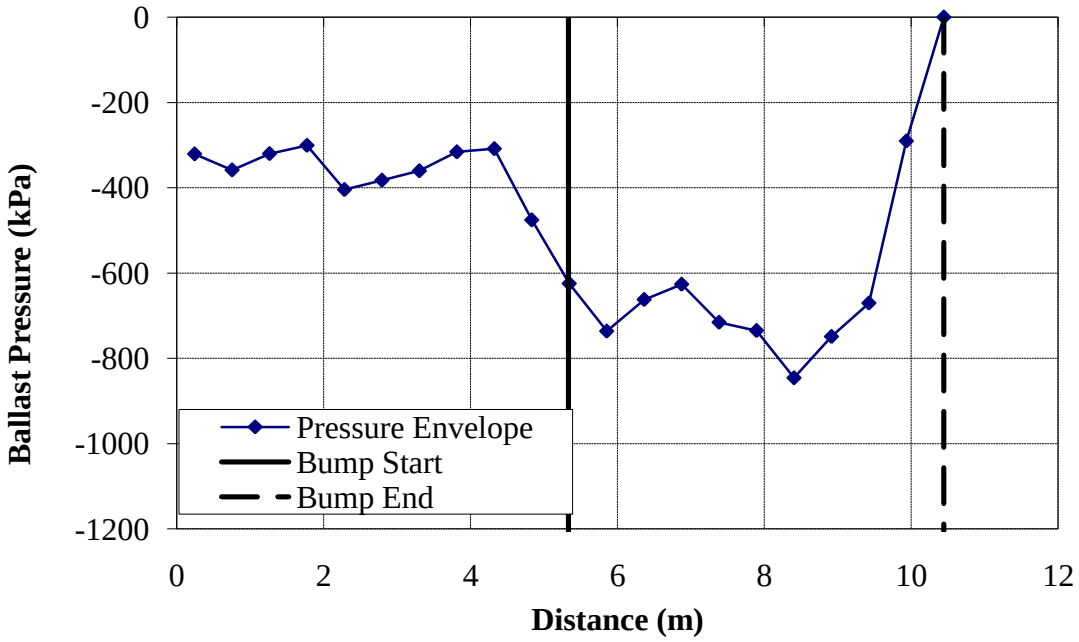

Figure E.134 – Ballast pressure due to a 1:150 bump with 406.4 mm thick ballast (v = 22.2 m/s)

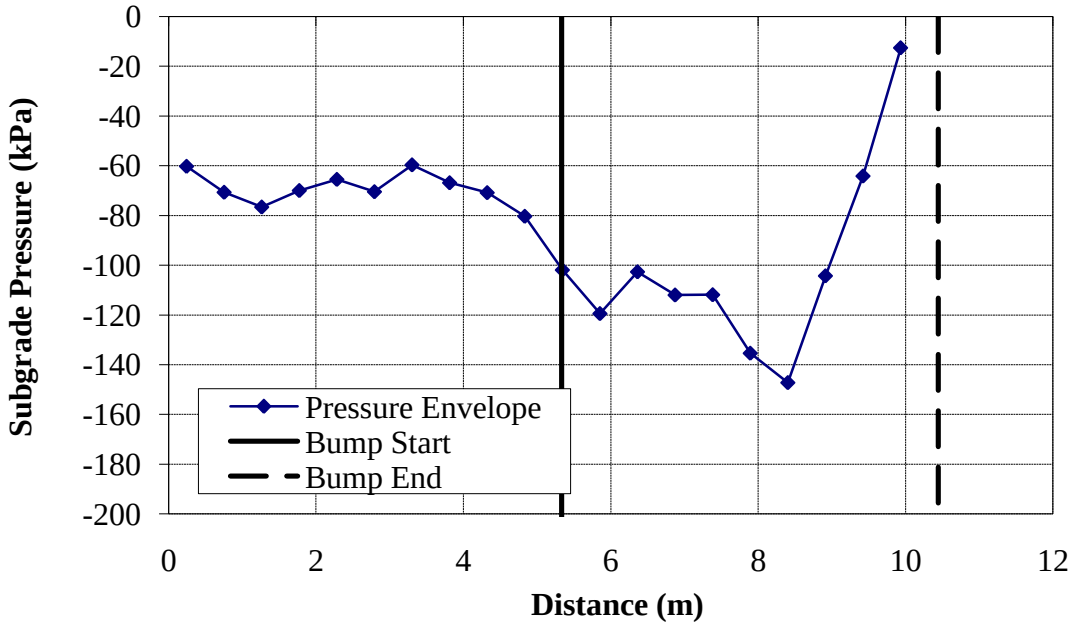

Figure E.135 - Subgrade pressure due to a 1:150 bump with 406.4 mm thick ballast (v = 22.2 m/s)

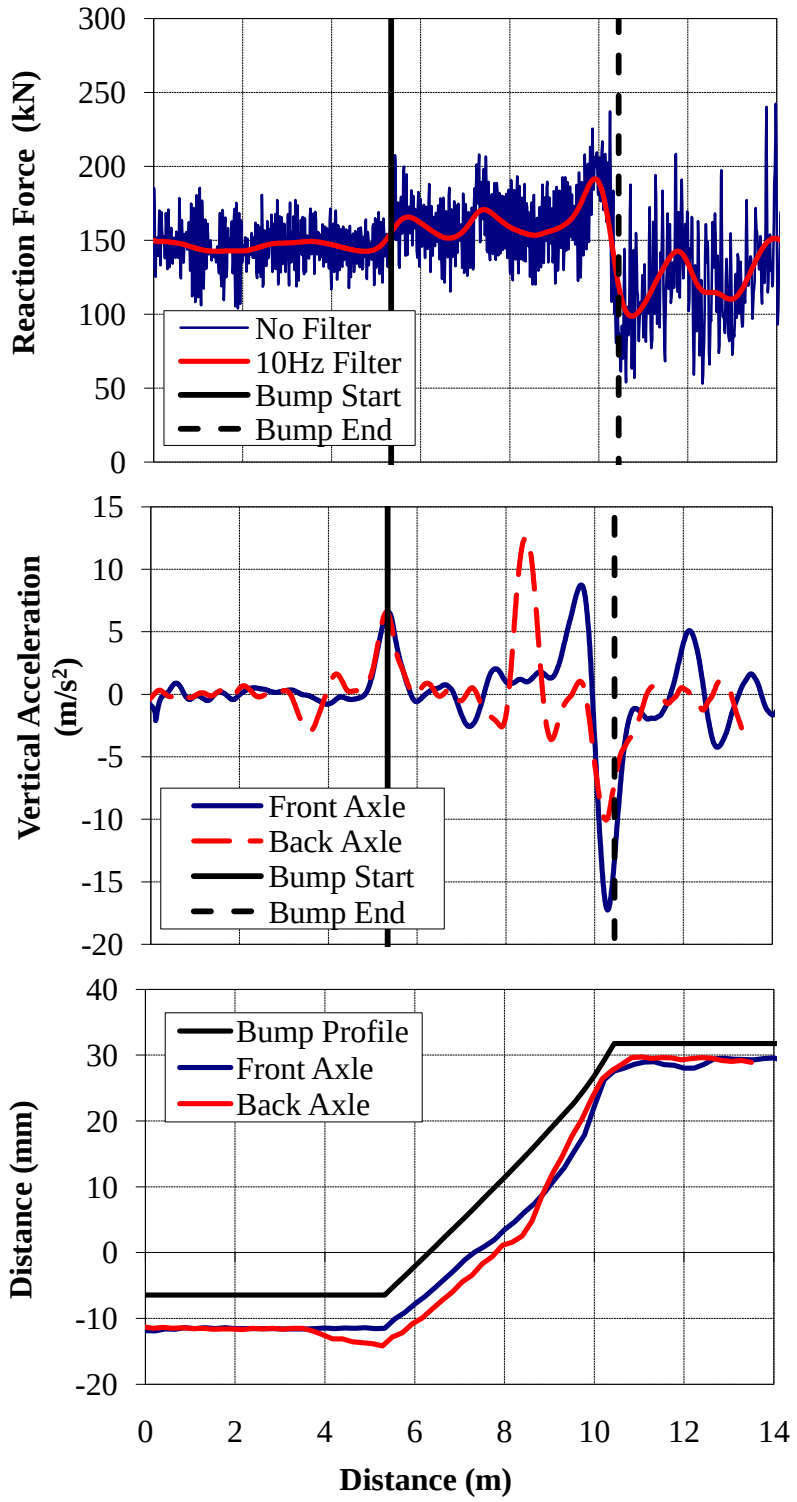

Figure E.136 - (a) Wheel/Rail Forces (b) Axle Accelerations and (c) Track Deflection due to a 1:150 bump with 2.1 m tie lengths (v = 22.2 m/s)

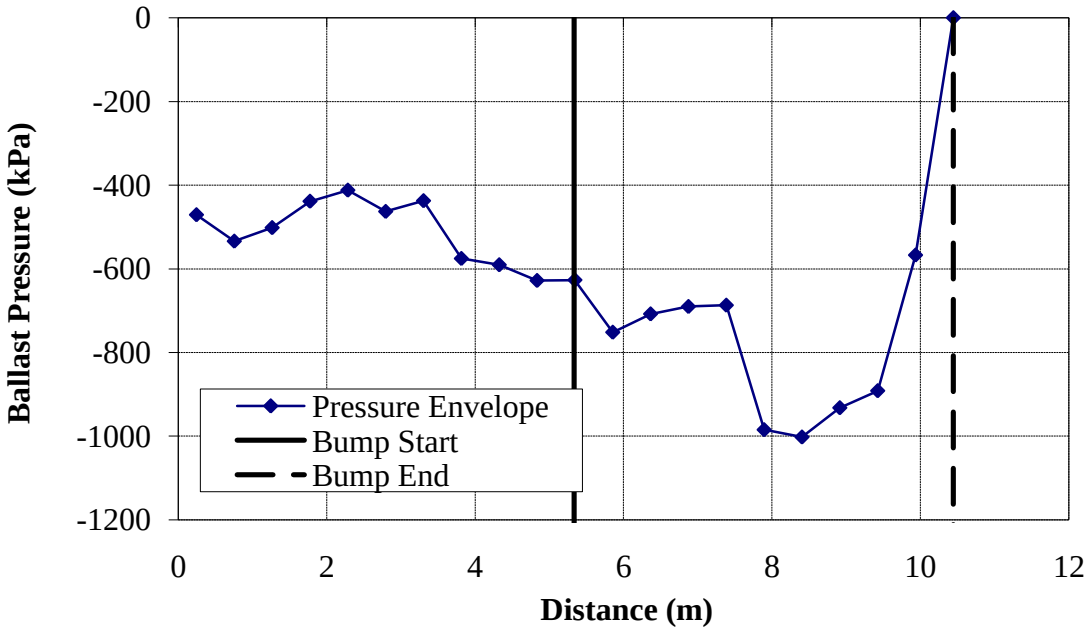

Figure E.137 – Ballast pressure due to a 1:150 bump with 2.1 m tie lengths (v = 22.2 m/s)

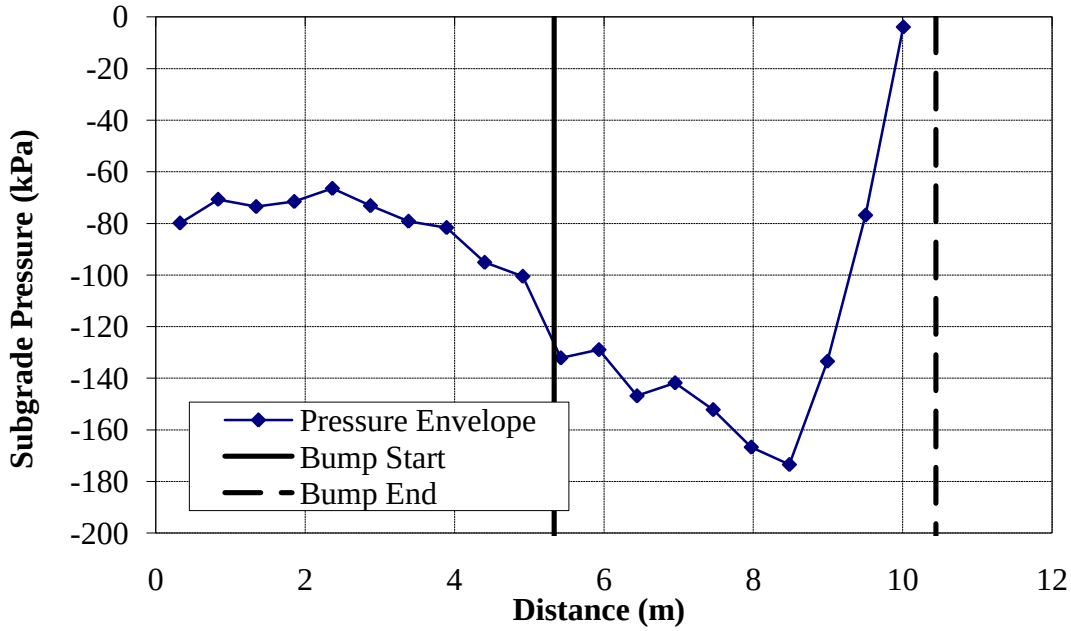

Figure E.138 - Subgrade pressure due to a 1:150 bump with 2.1 m tie lengths (v = 22.2 m/s)

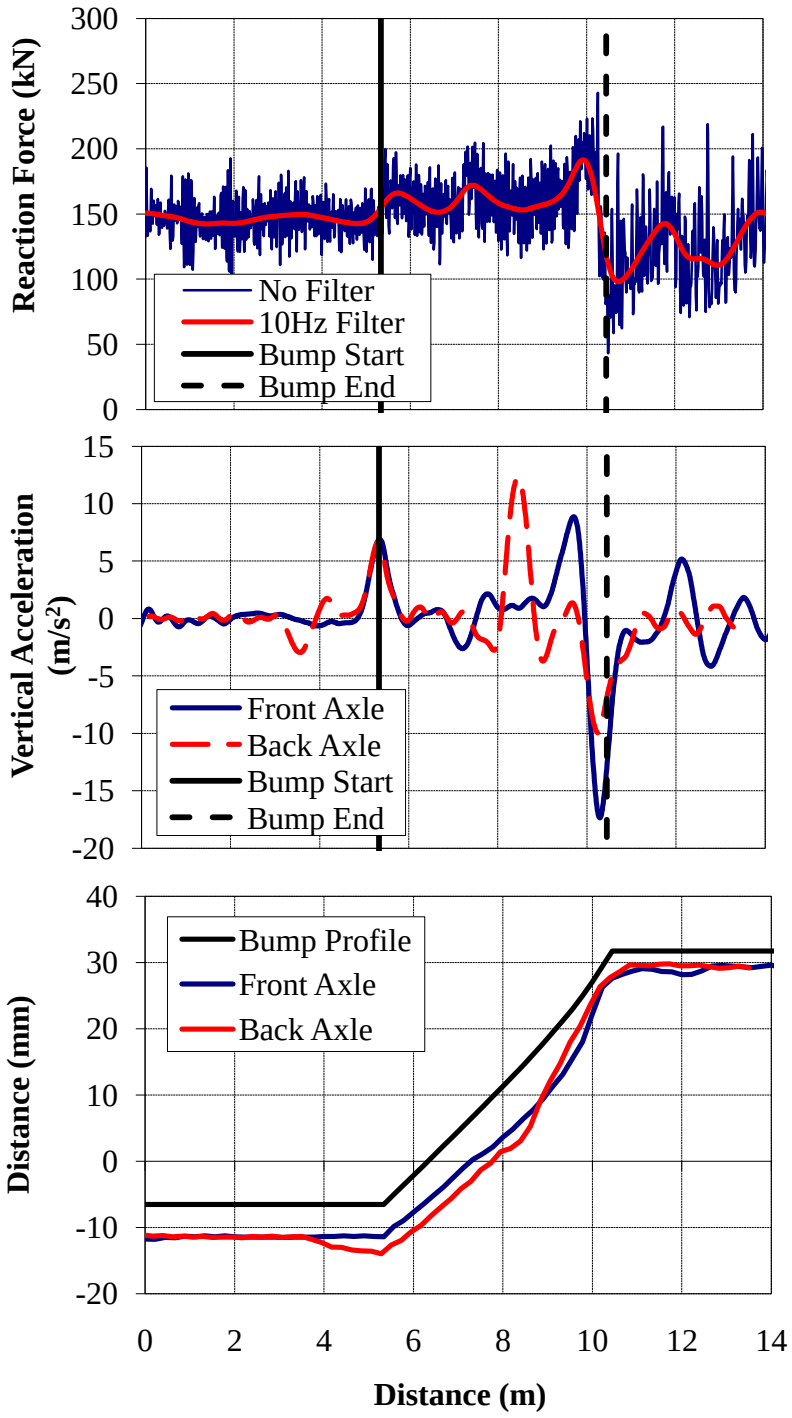

Figure E.139 - (a) Wheel/Rail Forces (b) Axle Accelerations and (c) Track Deflection due to a 1:150 bump with 3.0 m tie lengths (v = 22.2 m/s)

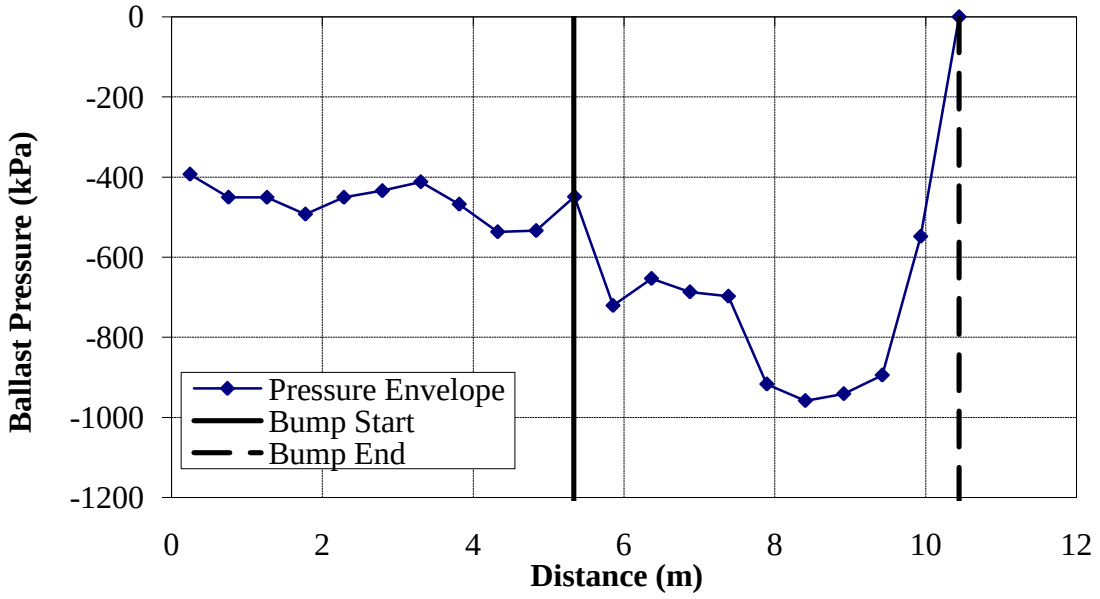

Figure E.140 – Ballast pressure due to a 1:150 bump with 3.0 m tie lengths (v = 22.2 m/s)

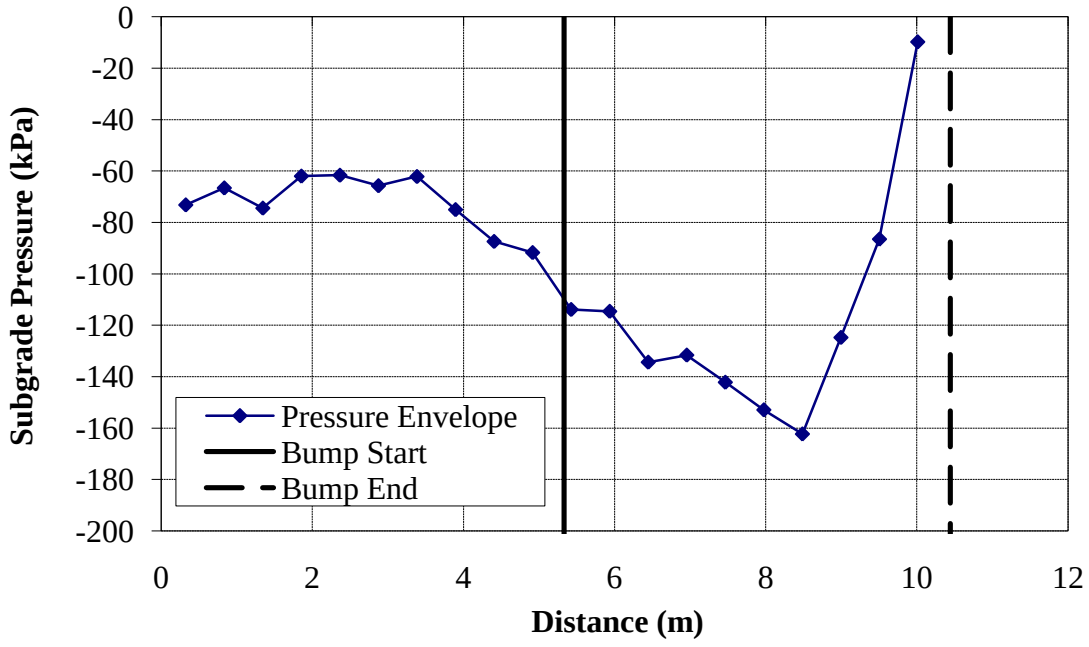

Figure E.141 - Subgrade pressure due to a 1:150 bump with 3.0 m tie lengths (v = 22.2 m/s)

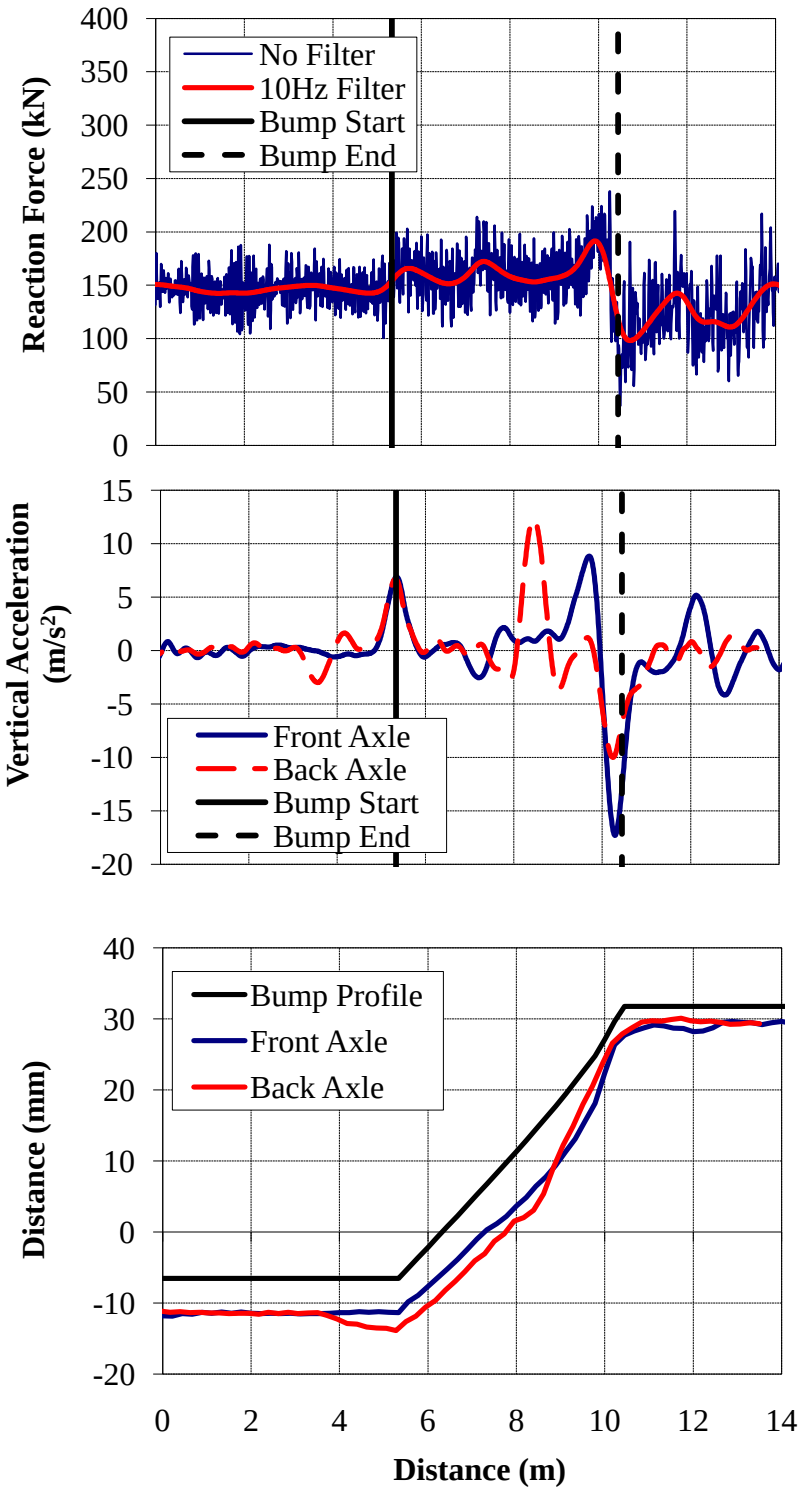

Figure E.142 - (a) Wheel/Rail Forces (b) Axle Accelerations and (c) Track Deflection due to a 1:150 bump with 3.6 m tie lengths (v = 22.2 m/s)

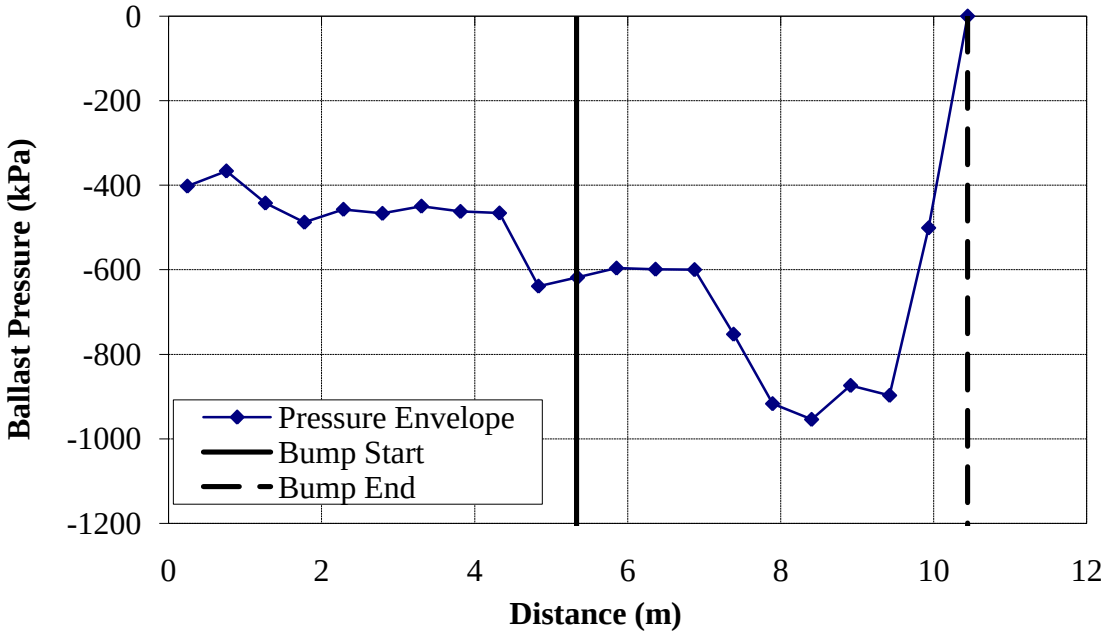

Figure E.143 –Ballast pressure due to a 1:150 bump with 3.6 m tie lengths (v = 22.2 m/s)

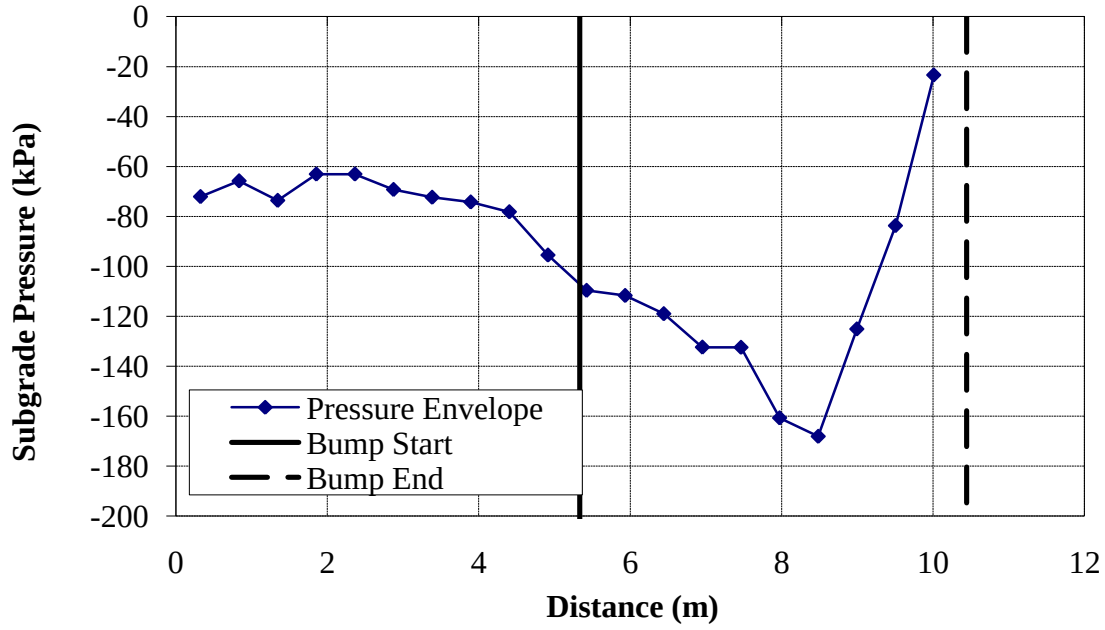

Figure E.144 - Subgrade pressure due to a 1:150 bump with 3.6 m tie lengths (v = 22.2 m/s)

APPENDIX F

TRACK RESPONSE PLOTS: DIP

Dip – Reference Case 479

Dip – Off Of 481

Dip – 8.9 m/s (20 mph) 483

Dip – 15.6 m/s (35 mph) 485

Dip – 33.5 m/s (75 mph) 487

Dip – 44.7 m/s (100 mph) 489

Dip – 1:50 slope (Equal Length) 491

Dip – 1:100 slope (Equal Length) 493

Dip – 1:200 slope (Equal Length) 495

Dip – 1:250 slope (Equal Length) 497

Dip – 1:50 slope (Equal Height) 499

Dip – 1:100 slope (Equal Height) 501

Dip – 1:200 slope (Equal Height) 503

Dip – 1:250 slope (Equal Height) 505

Dip – 1:50 slope (Equal Height, 15.6 m/s) 507

Dip – 1:50 slope (Equal Height, 33.5 m/s) 509

Dip – 1:50 slope (Equal Height, 44.7 m/s) 511

Dip – 1:100 slope (Equal Height, 15.6 m/s) 513

Dip – 1:100 slope (Equal Height, 33.5 m/s) 515

Dip – 1:100 slope (Equal Height, 44.7 m/s) 517

Dip – 1:200 slope (Equal Height, 15.6 m/s) 519
Dip – 1:200 slope (Equal Height, 33.5 m/s) 521
Dip – 1:200 slope (Equal Height, 44.7 m/s) 523
Dip – 1:250 slope (Equal Height, 15.6 m/s) 525
Dip – 1:250 slope (Equal Height, 33.5 m/s) 527
Dip – 1:250 slope (Equal Height, 44.7 m/s) 529
Dip – 20 MPa Fill 531
Dip – 50 MPa Fill 533
Dip – 100 MPa Fill 535
Dip – Concrete Approach Ties 537
Dip – Plastic Approach Ties 539
Dip – Wood Approach Ties with Rubber Rail Seat Pads 541
Dip – Concrete Approach Ties with Rubber Rail Seat Pads 543
Dip – Wood Approach Ties with Rubber Tie Pads 545
Dip – Concrete Approach Ties with Rubber Tie Pads 547
Dip – Concrete Bridge Ties 549
Dip – Plastic Bridge Ties 551
Dip – Wood Bridge Ties with Rubber Rail Seat Pads 553
Dip – Concrete Bridge Ties with Rubber Rail Seat Pads 555
Dip – Ballast Deck Bridge 557
Dip – Ballast Deck Bridge with Ballast Mat 559
Dip – 152.4 mm Ballast Thickness 561

Dip – 203.2 mm Ballast Thickness 563

Dip – 304.8 mm Ballast Thickness 565

Dip – 406.4 mm Ballast Thickness 567

Dip – 2.1 m Tie Length 569

Dip – 3.0 m Tie Length 571

Dip – 3.6 m Tie Length 573

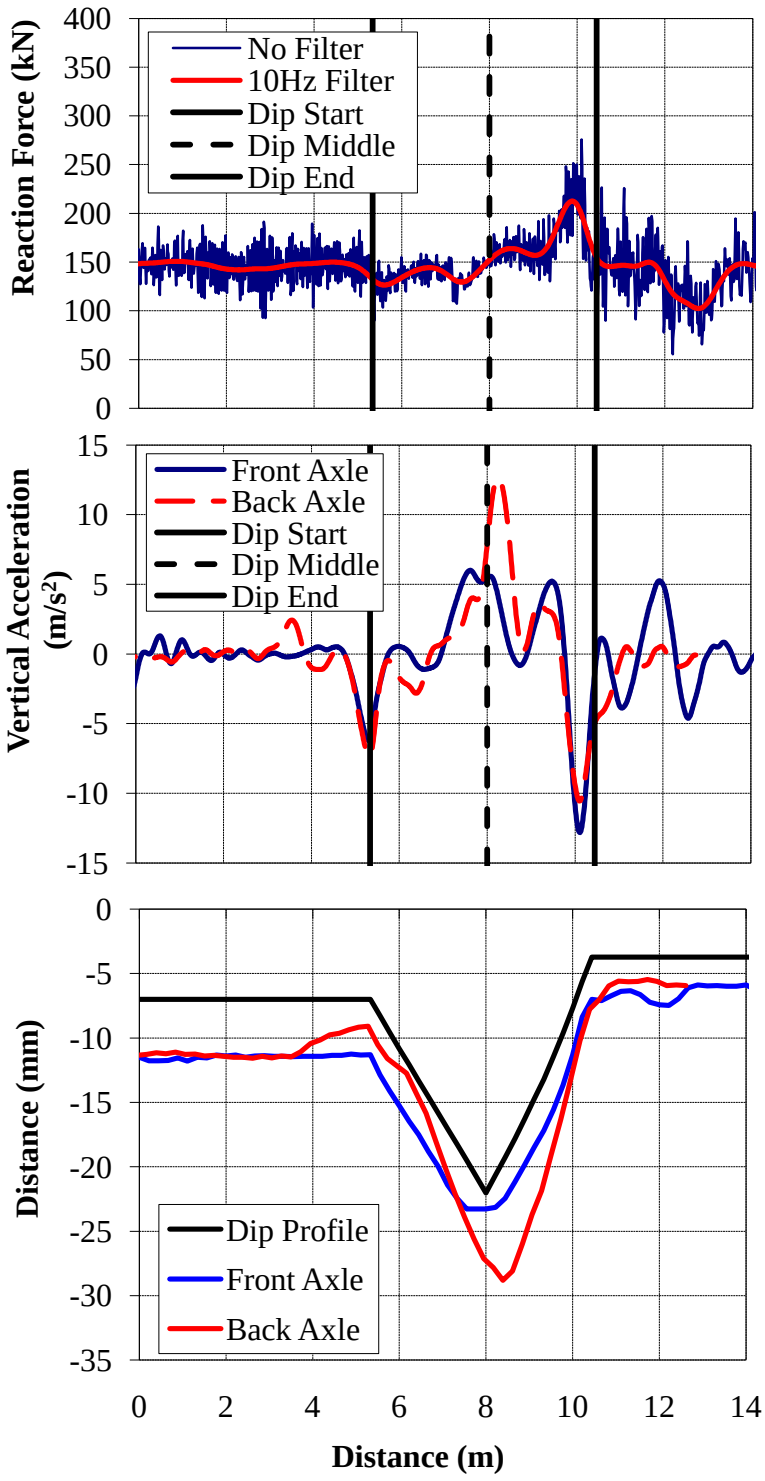

Figure F.1 - (a) Wheel/Rail Forces (b) Axle Accelerations and (c) Track Deflection due to a 1:150 Dip at a Bridge/Approach Location (v = 22.2 m/s)

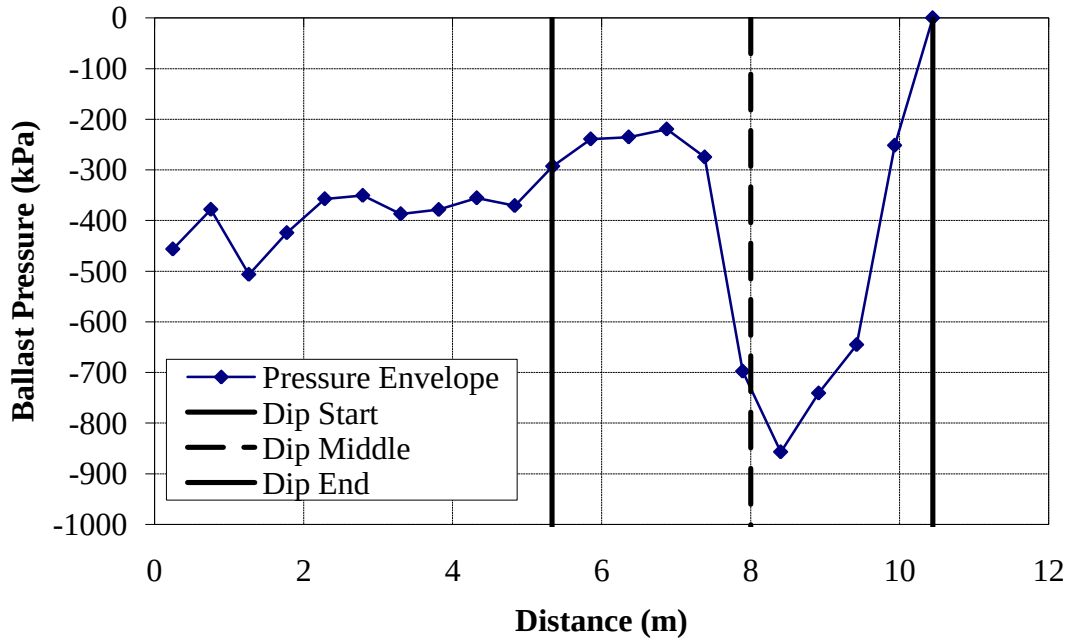

Figure F.2 – Ballast pressures due to a 1:150 Dip at a Bridge/Approach Location (v = 22.2 m/s)

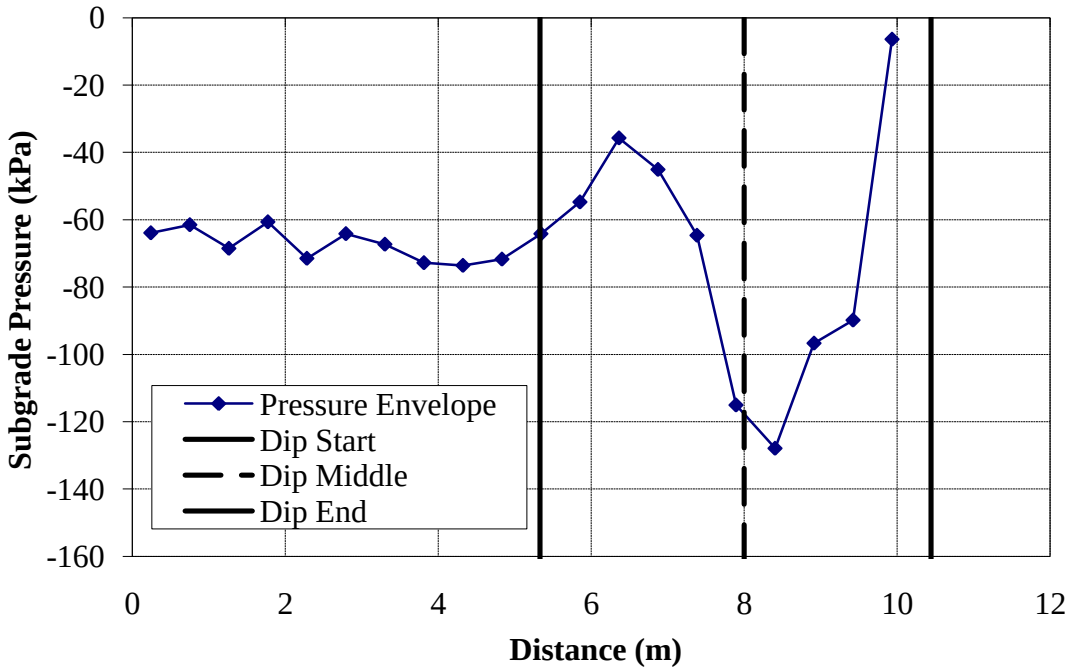

Figure F.3 - Subgrade pressures due to a 1:150 Dip at a Bridge/Approach Location (v = 22.2 m/s)

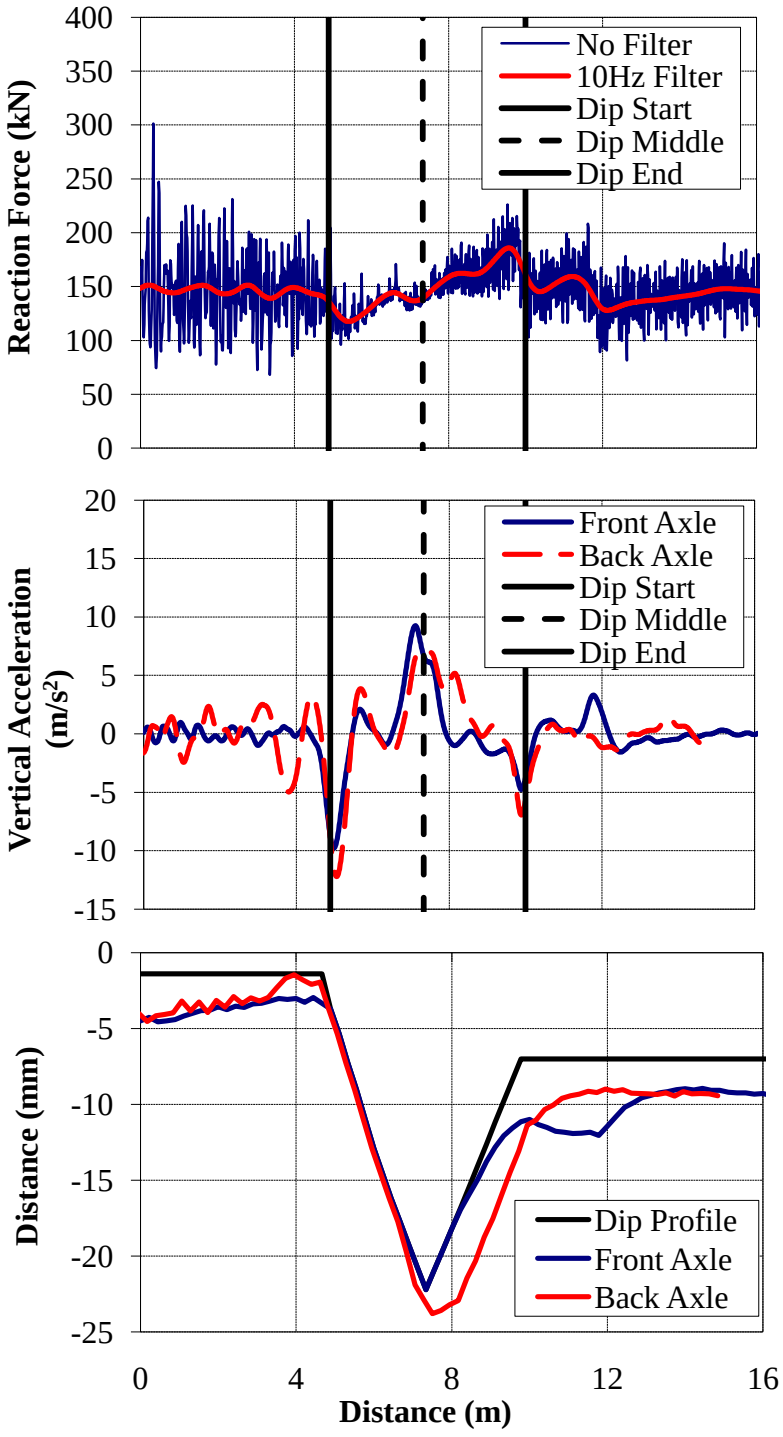

Figure F.4 - (a) Wheel/Rail Forces (b) Axle Accelerations and (c) Track Deflection due to a truck moving off of the bridge onto an approach embankment with a 1:150 Dip (v = 22.2 m/s)

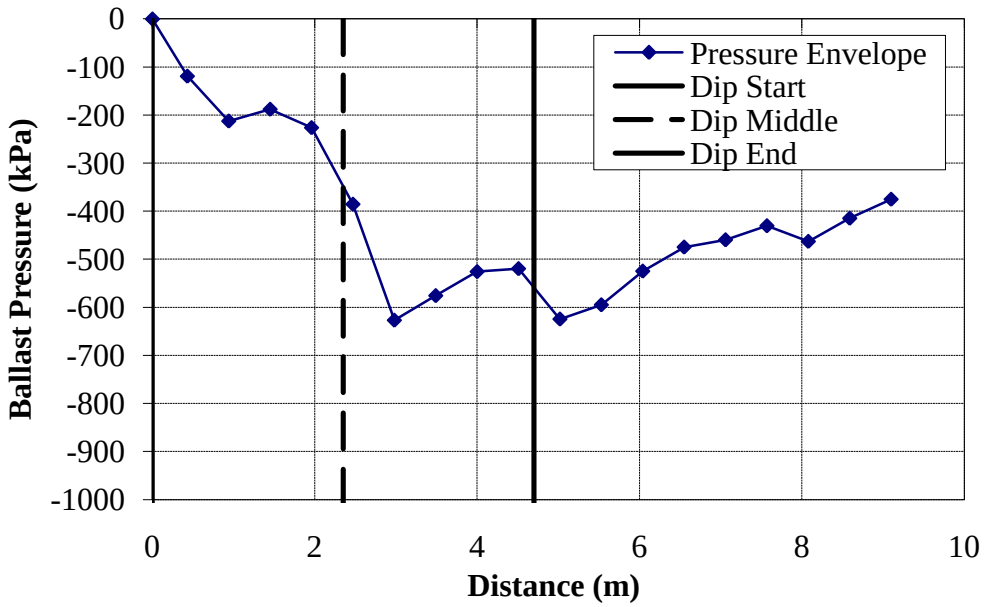

Figure F.5 – Ballast pressures due to a truck moving off of the bridge onto an approach embankment with a 1:150 Dip (v = 22.2 m/s)

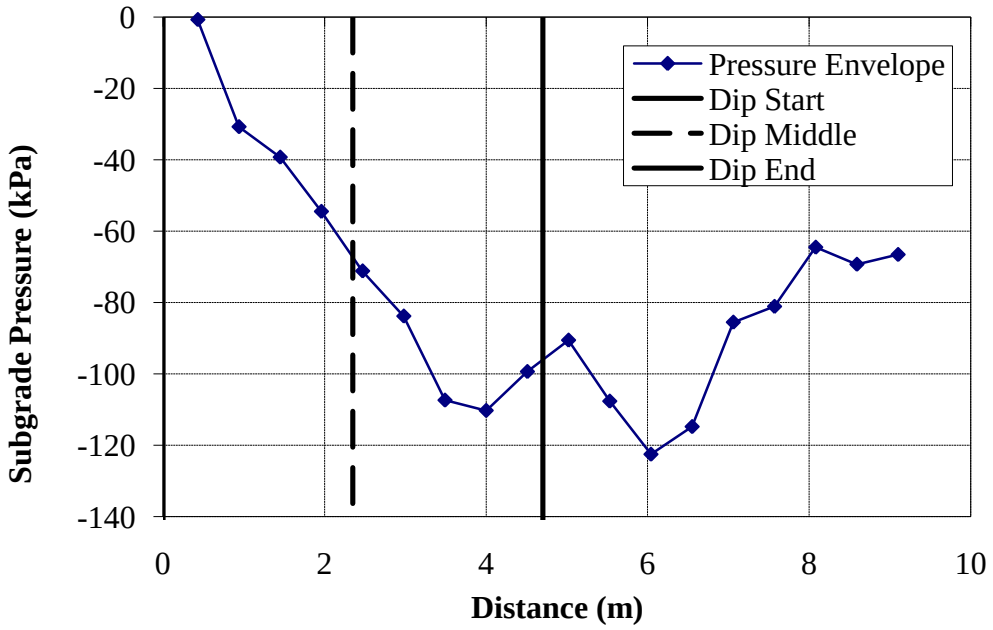

Figure F.6 - Ballast pressures due to a truck moving off of the bridge onto an approach embankment with a 1:150 Dip (v = 22.2 m/s)

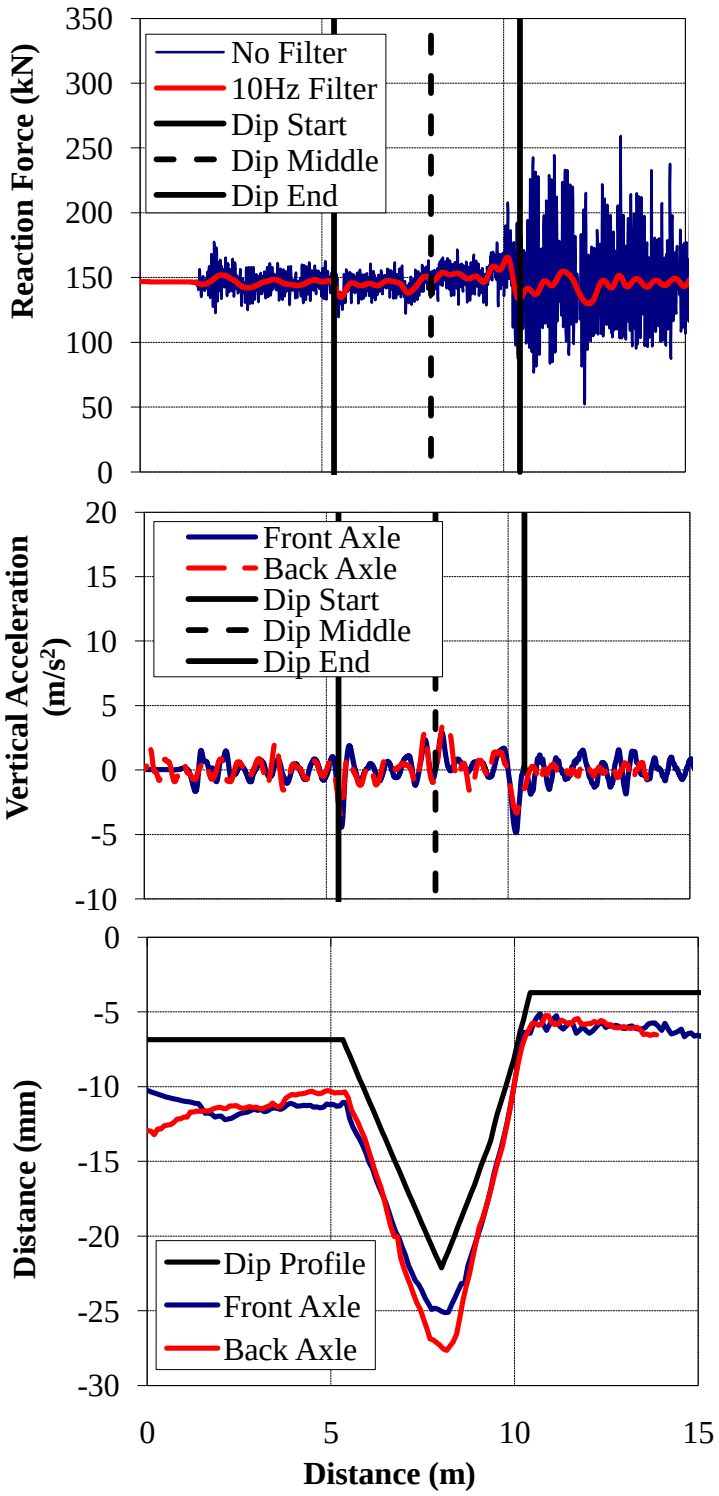

Figure F.7 - (a) Wheel/Rail Forces (b) Axle Accelerations and (c) Track Deflection due to a 1:150 Dip at a Bridge/Approach Location (v = 8.9 m/s)

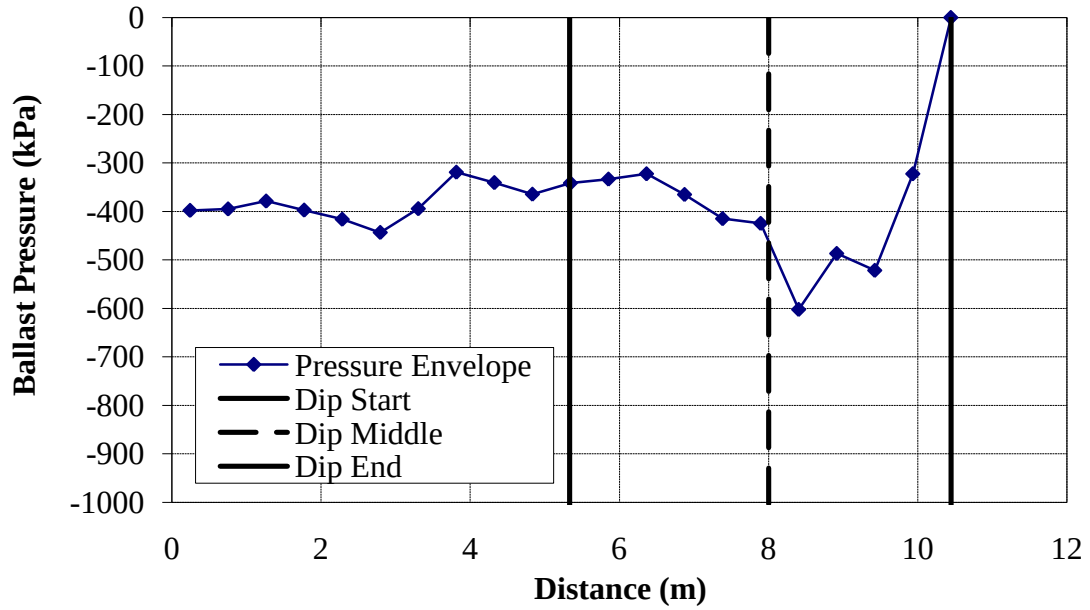

Figure F.8 – Ballast pressures due to a 1:150 Dip at a Bridge/Approach Location (v = 8.9 m/s)

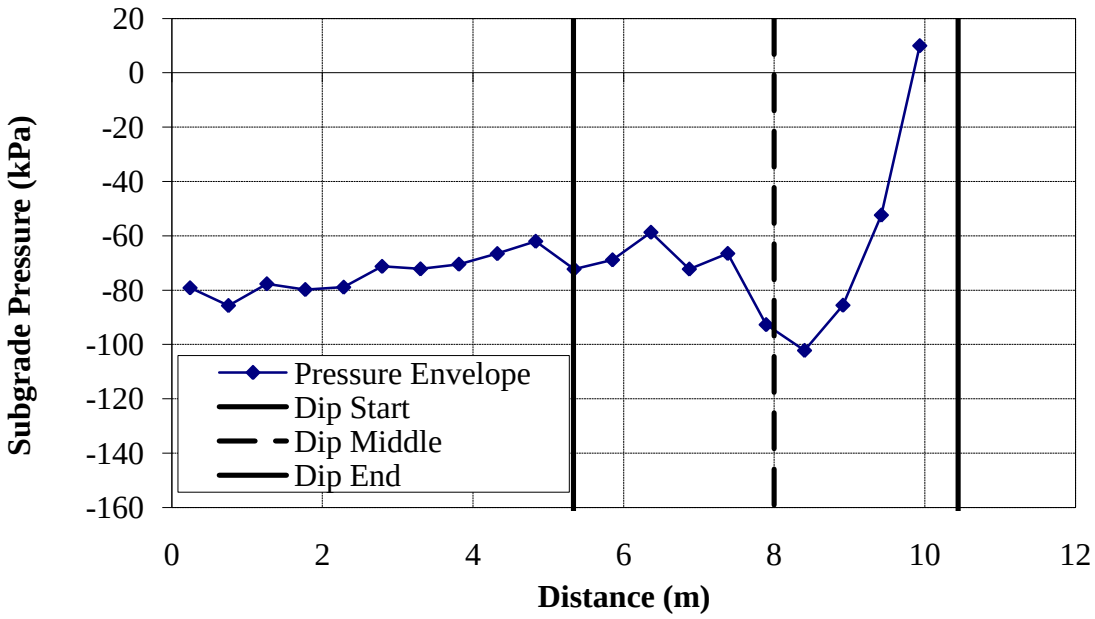

Figure F.9 - Subgrade pressures due to a 1:150 Dip at a Bridge/Approach Location (v = 8.9 m/s)

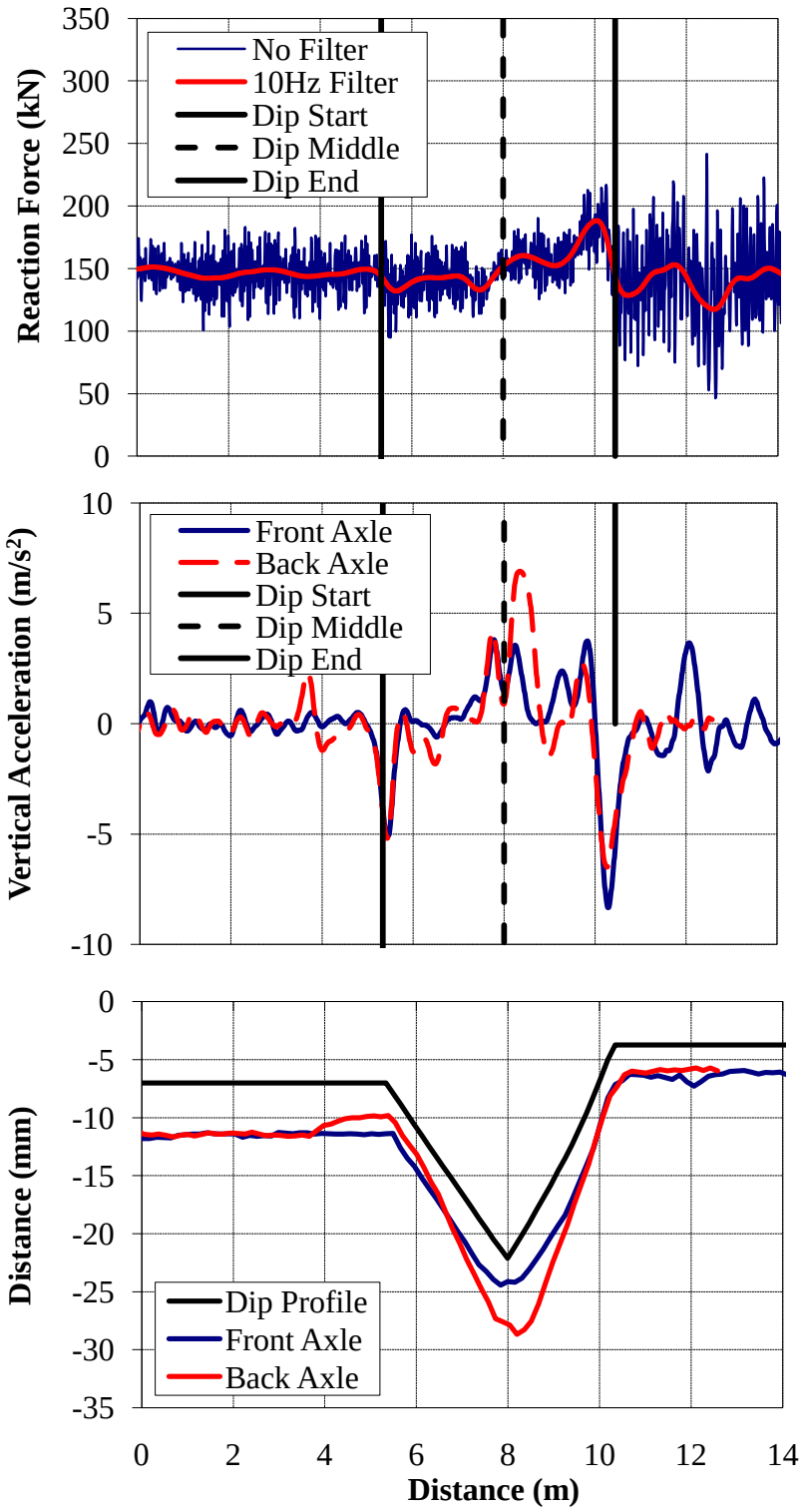

Figure F.10 - (a) Wheel/Rail Forces (b) Axle Accelerations and (c) Track Deflection due to a 1:150 Dip at a Bridge/Approach Location (v = 15.6 m/s)

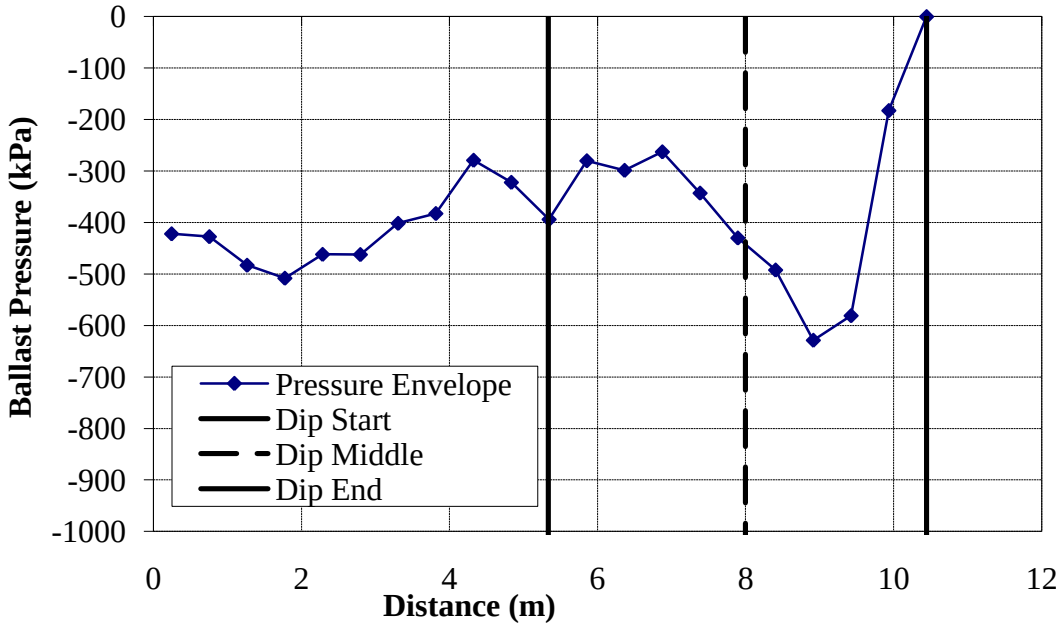

Figure F.11 – Ballast pressures due to a 1:150 Dip at a Bridge/Approach Location (v = 15.6 m/s)

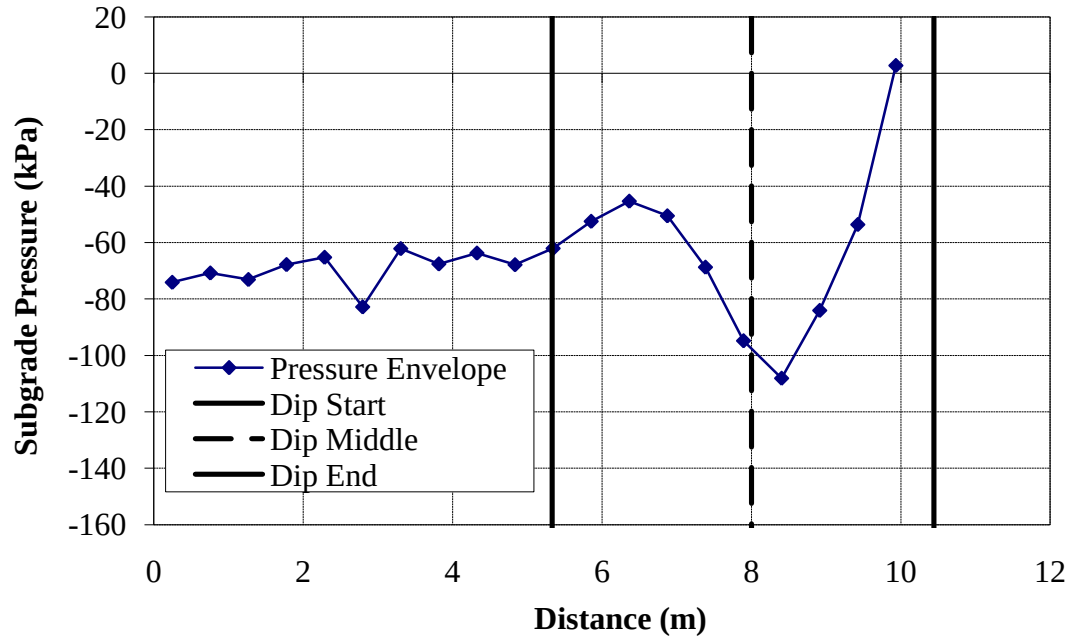

Figure F.12 - Subgrade pressures due to a 1:150 Dip at a Bridge/Approach Location (v = 15.6 m/s)

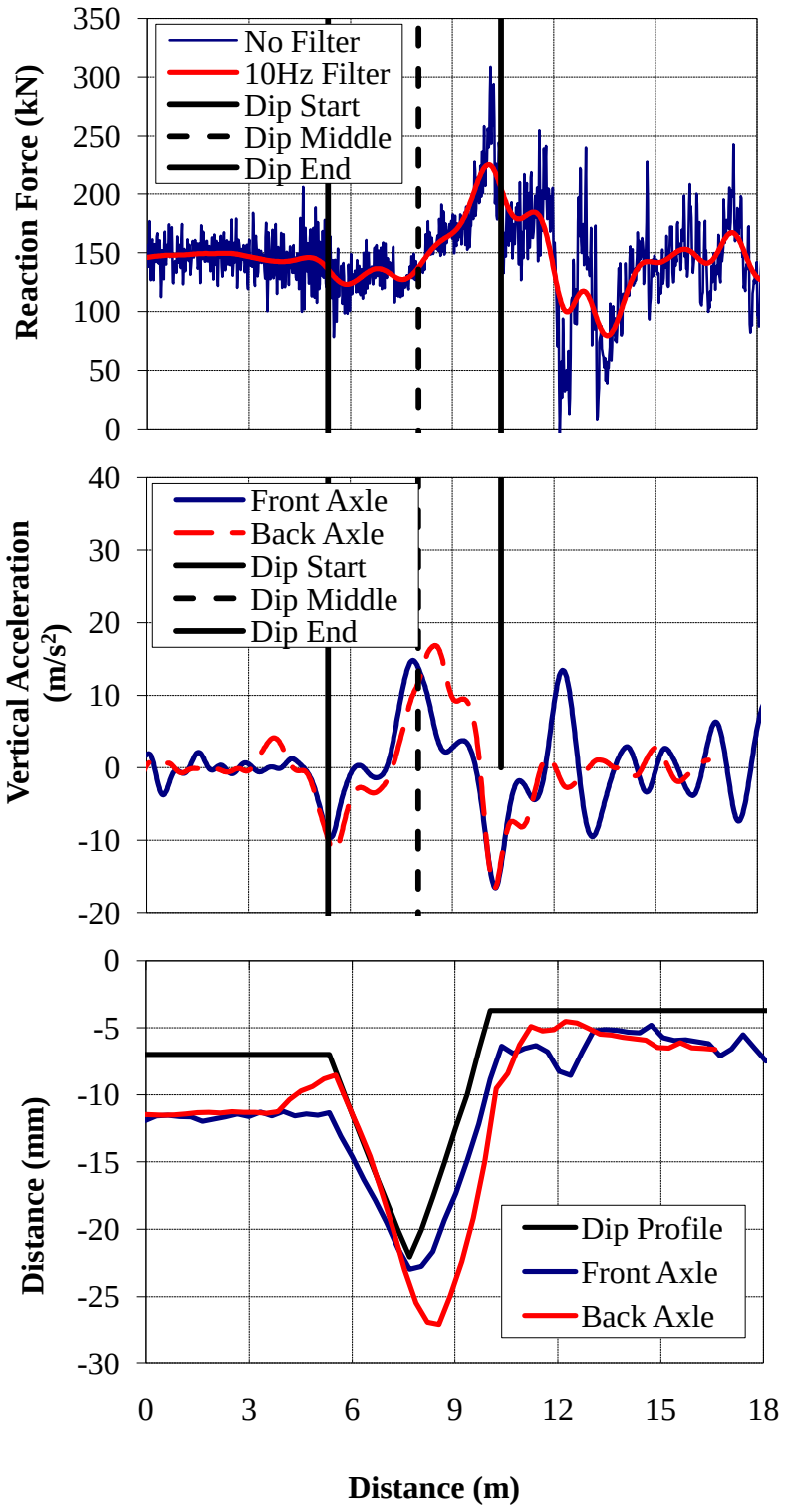

Figure F.13 - (a) Wheel/Rail Forces (b) Axle Accelerations and (c) Track Deflection due to a 1:150 Dip at a Bridge/Approach Location (v = 33.5 m/s)

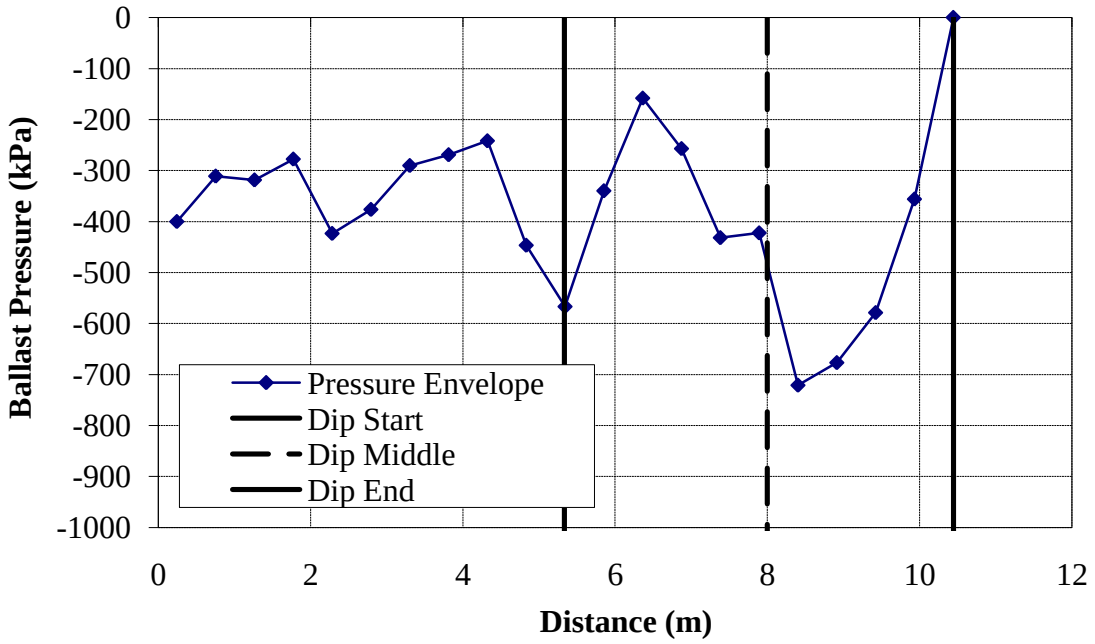

Figure F.14 – Ballast pressures due to a 1:150 Dip at a Bridge/Approach Location (v = 33.5 m/s)

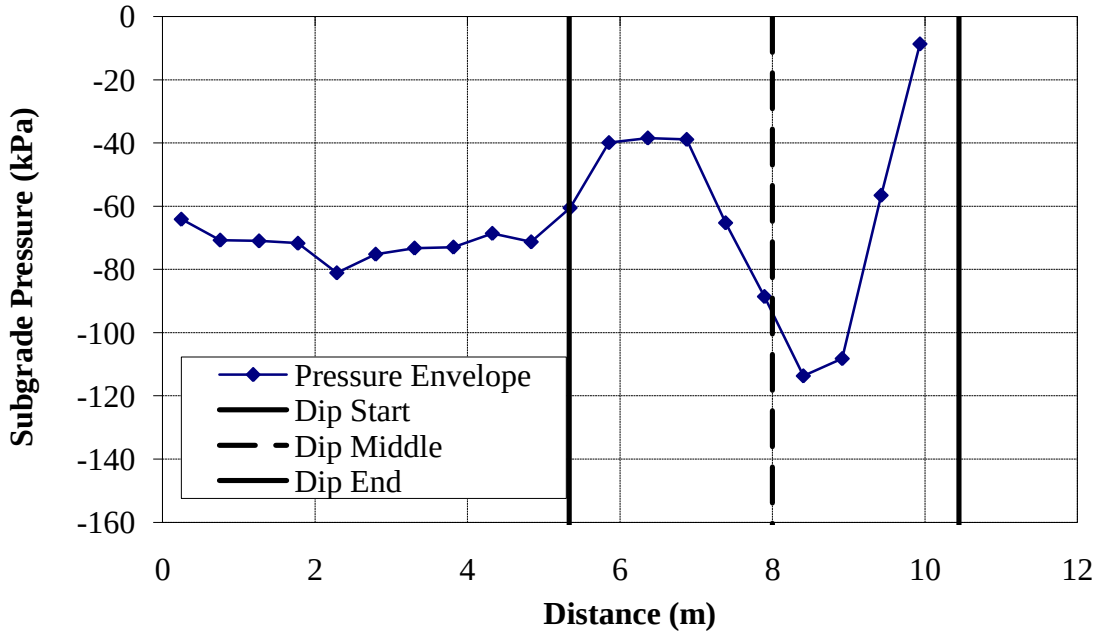

Figure F.15 - Subgrade pressures due to a 1:150 Dip at a Bridge/Approach Location (v = 33.5 m/s)

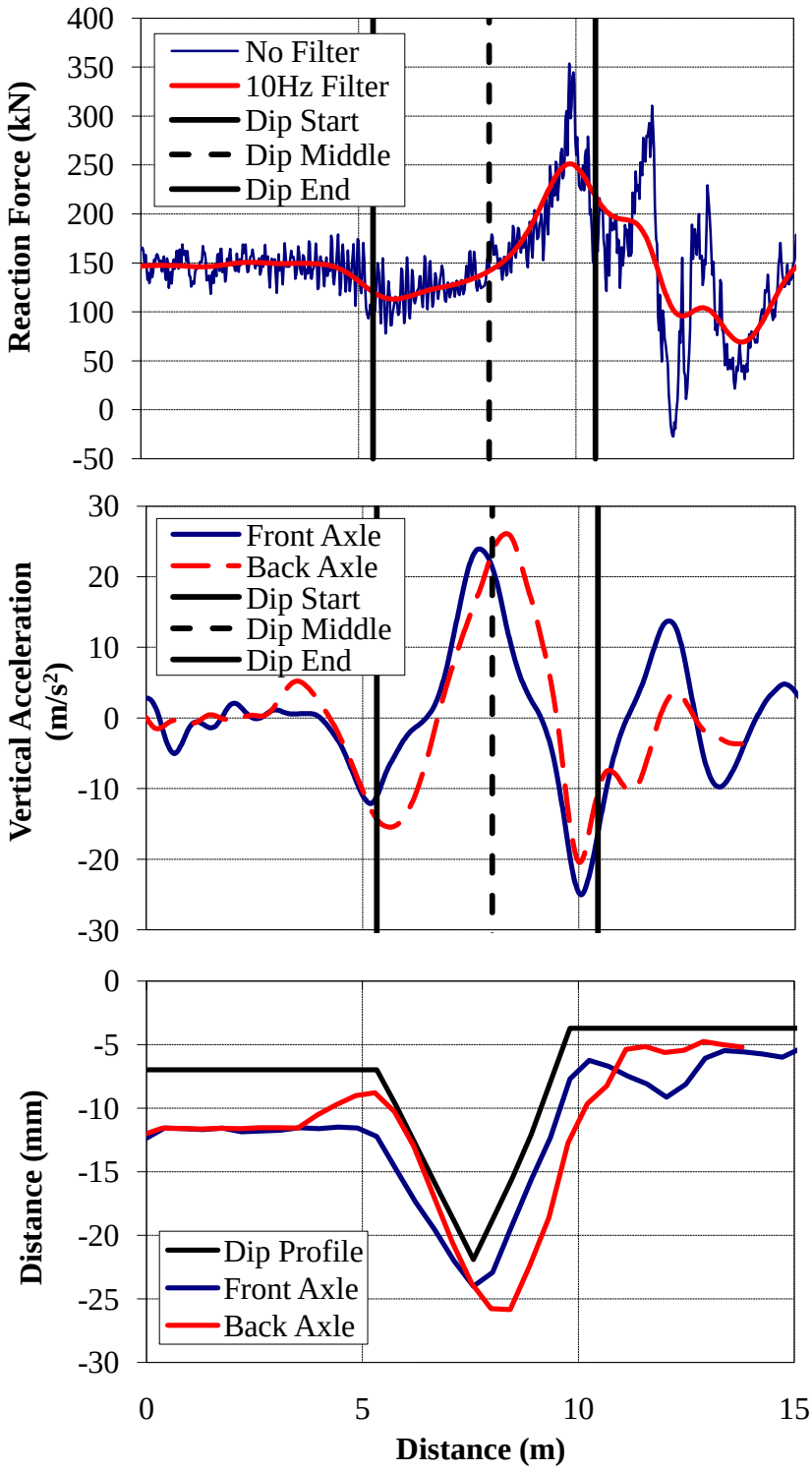

Figure F.16 - (a) Wheel/Rail Forces (b) Axle Accelerations and (c) Track Deflection due to a 1:150 Dip at a Bridge/Approach Location (v = 44.7 m/s)

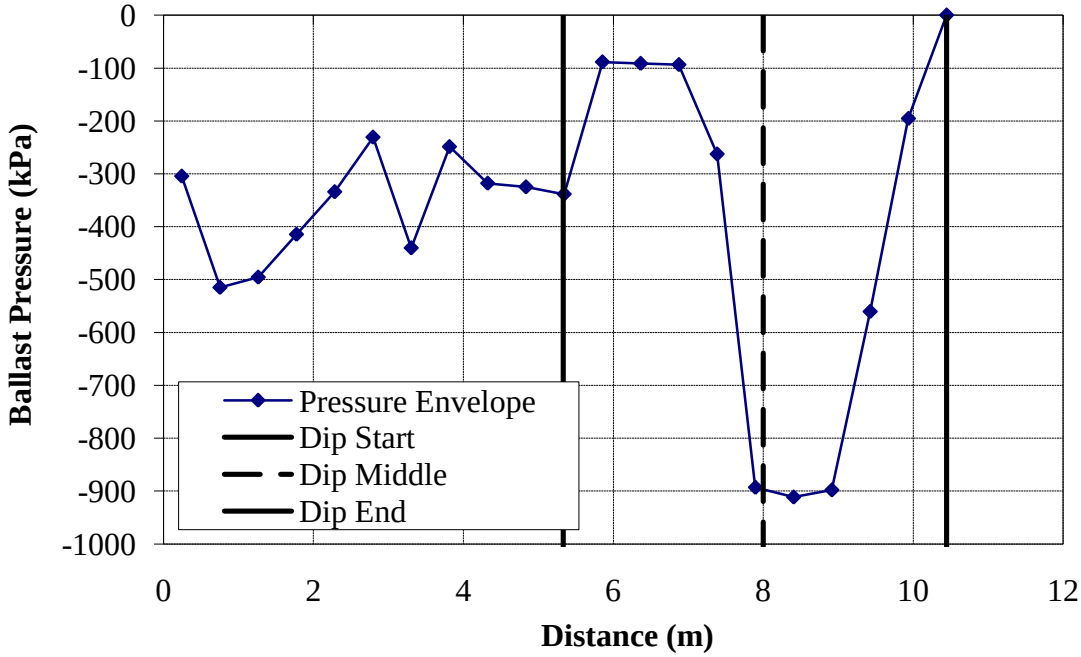

Figure F.17 – Ballast pressures due to a 1:150 Dip at a Bridge/Approach Location (v = 44.7 m/s)

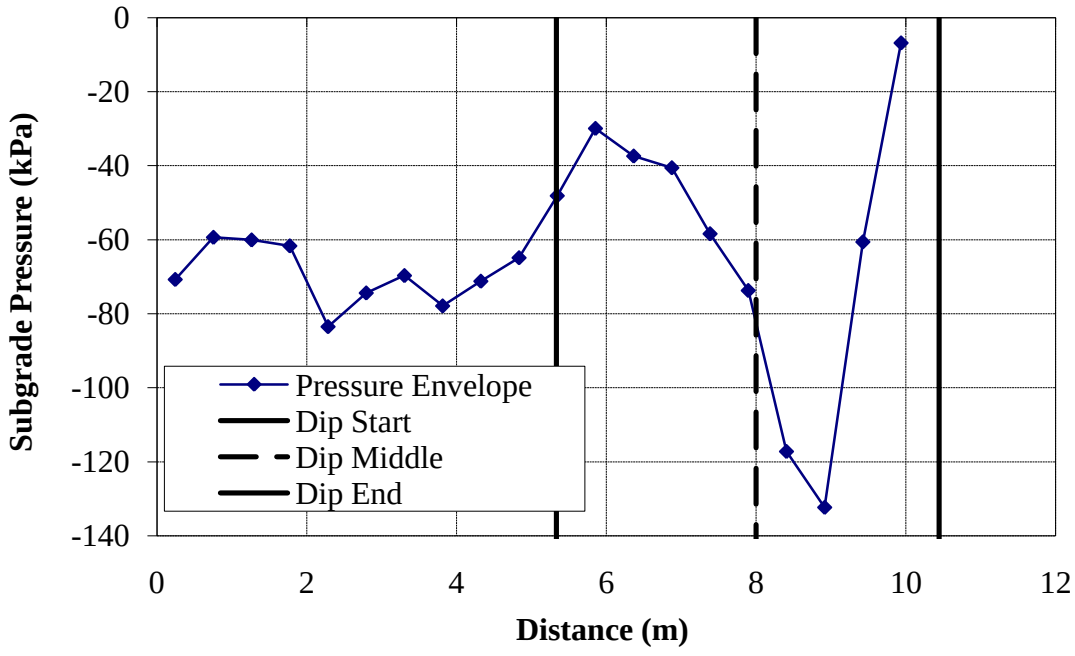

Figure F.18 - Subgrade pressures due to a 1:150 Dip at a Bridge/Approach Location (v = 44.7 m/s)

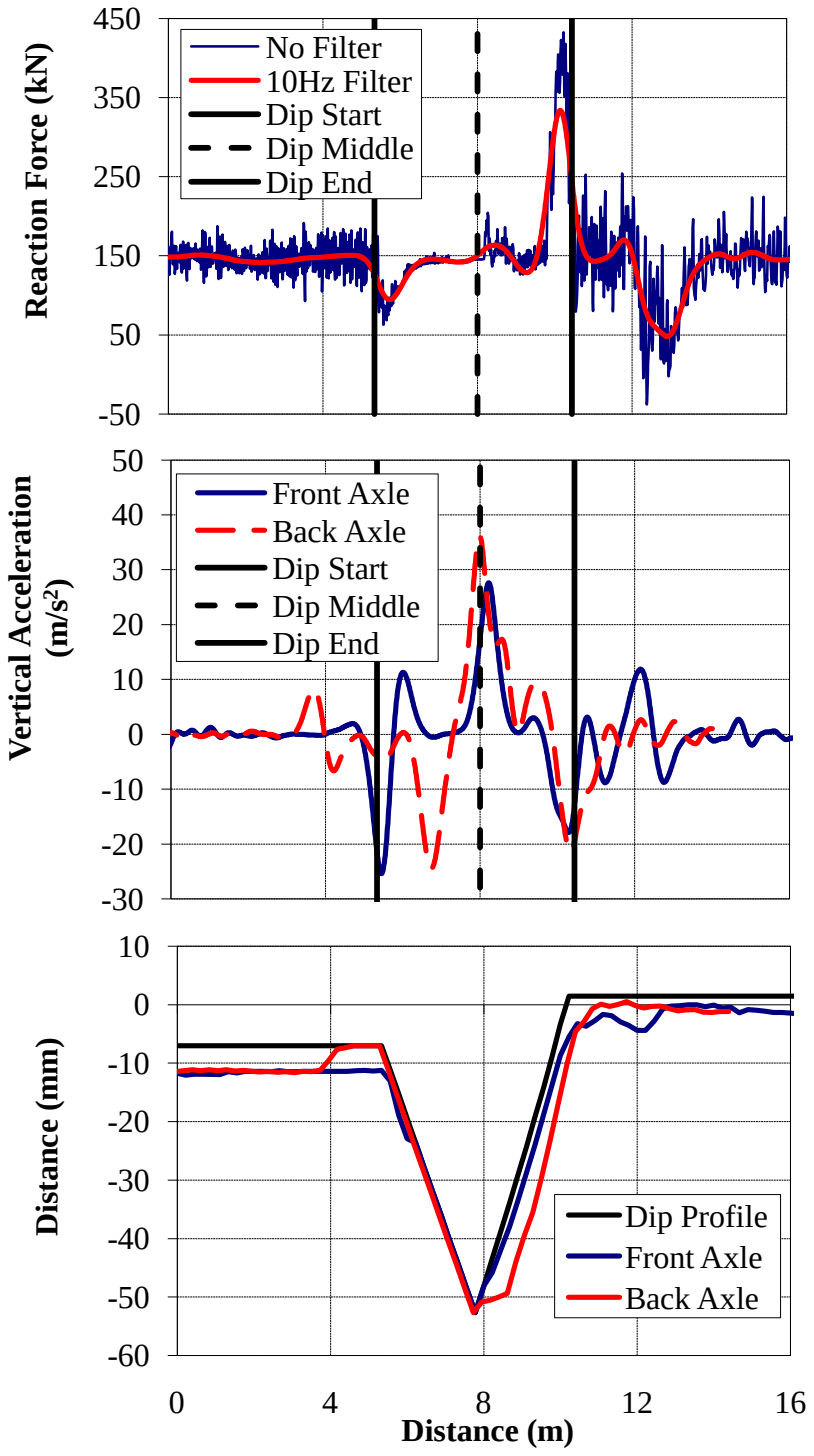

Figure F.19 - (a) Wheel/Rail Forces (b) Axle Accelerations and (c) Track Deflection due to a 1:50 Dip at a Bridge/Approach Location (Equal Lengths, v = 22.2 m/s)

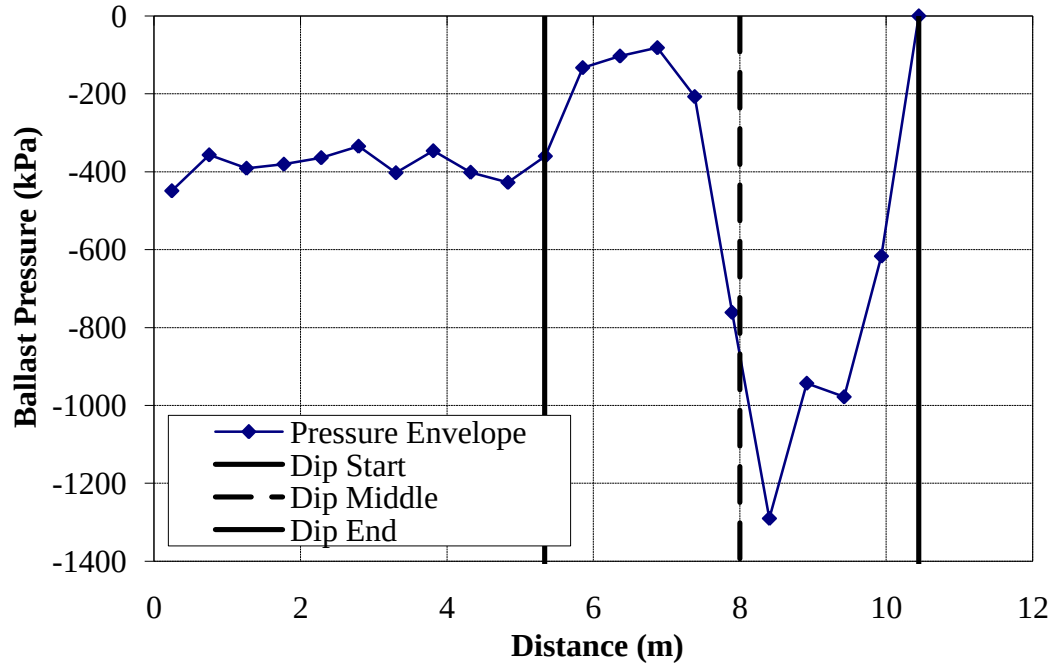

Figure F.20 – Ballast pressures due to a 1:50 Dip at a Bridge/Approach Location (Equal Lengths, v = 22.2 m/s)

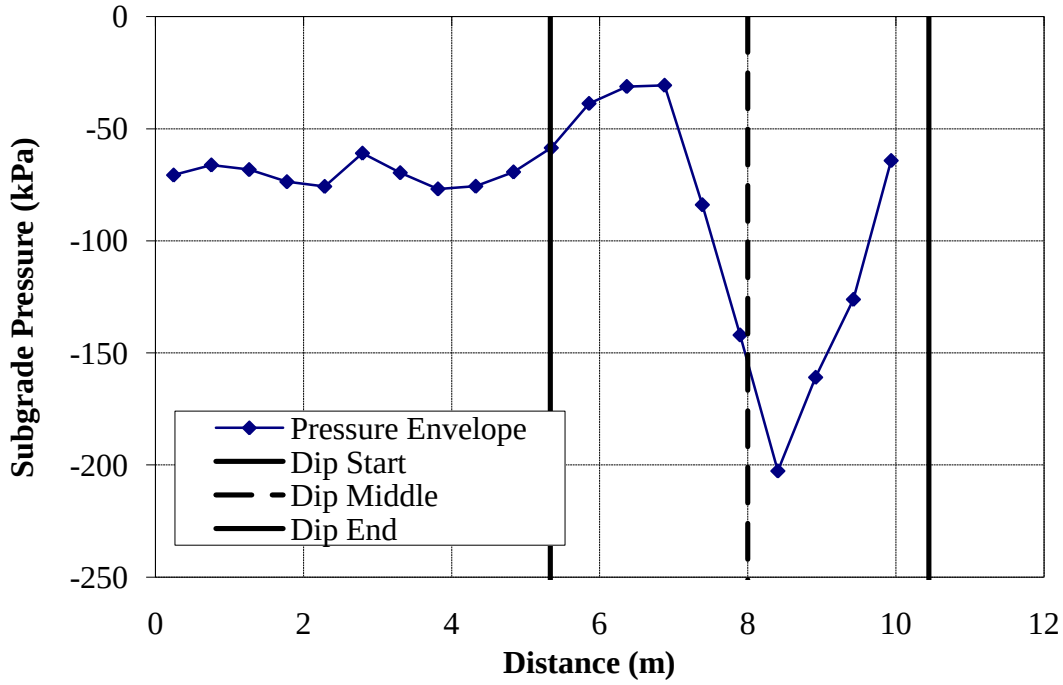

Figure F.21 – Subgrade pressures due to a 1:50 Dip at a Bridge/Approach Location (Equal Lengths, v = 22.2 m/s)

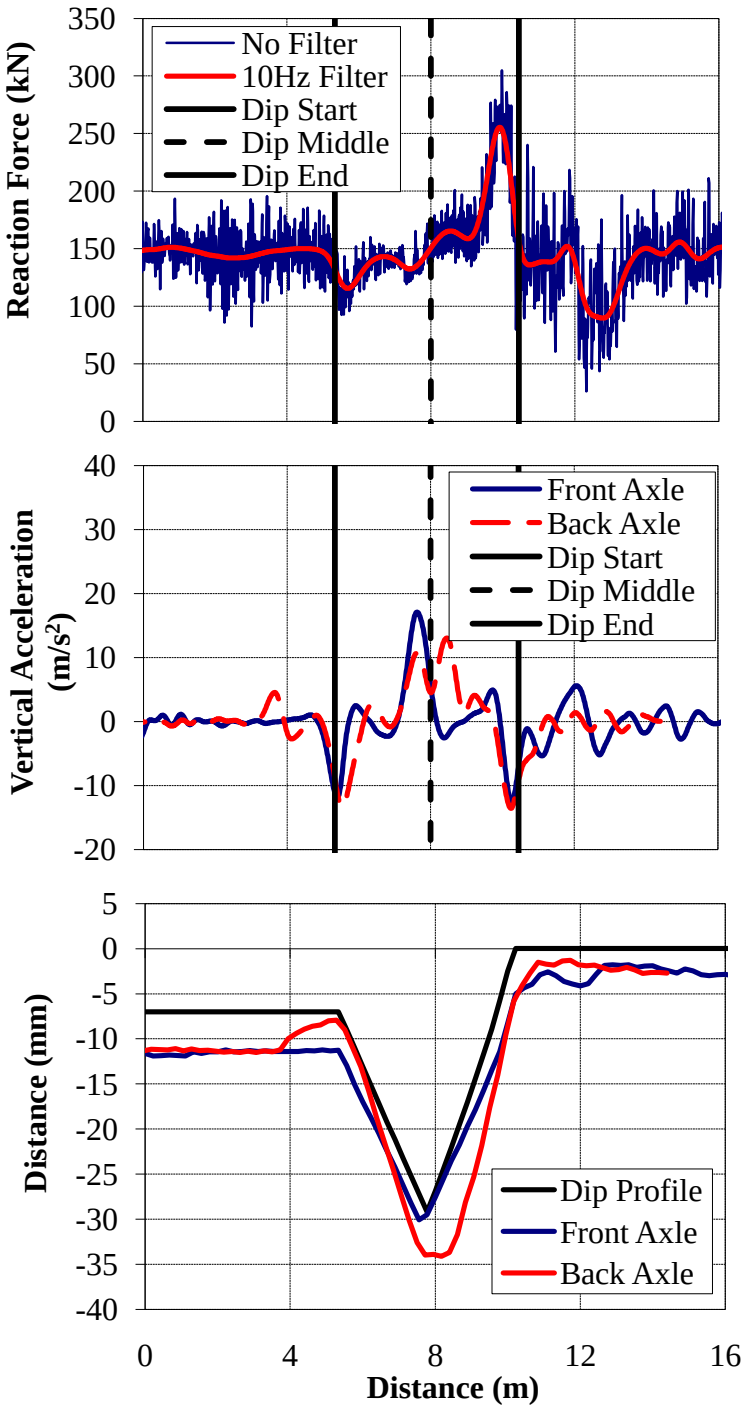

Figure F.22 - (a) Wheel/Rail Forces (b) Axle Accelerations and (c) Track Deflection due to a 1:100 Dip at a Bridge/Approach Location (Equal Lengths, v = 22.2 m/s)

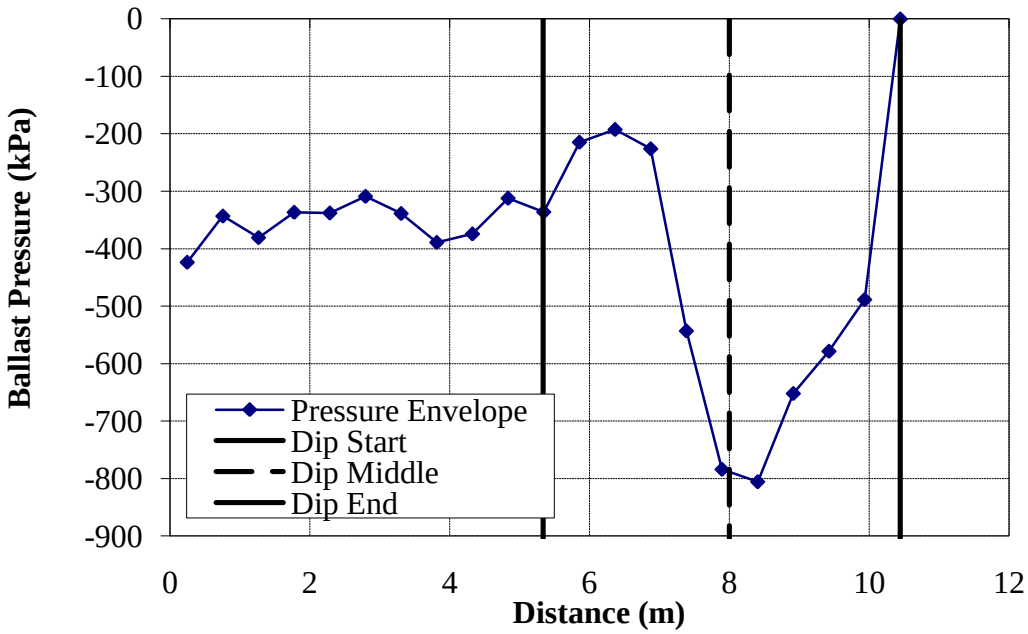

Figure F.23 – Ballast pressures due to a 1:100 Dip at a Bridge/Approach Location (Equal Lengths, v = 22.2 m/s)

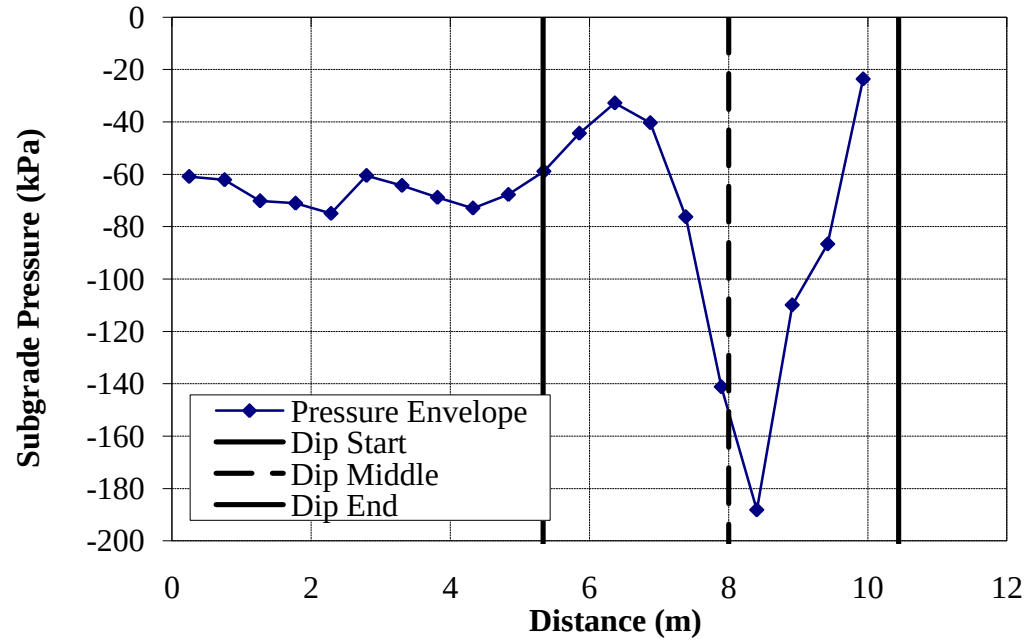

Figure F.24 - Subgrade pressures due to a 1:100 Dip at a Bridge/Approach Location (Equal Lengths, v = 22.2 m/s)

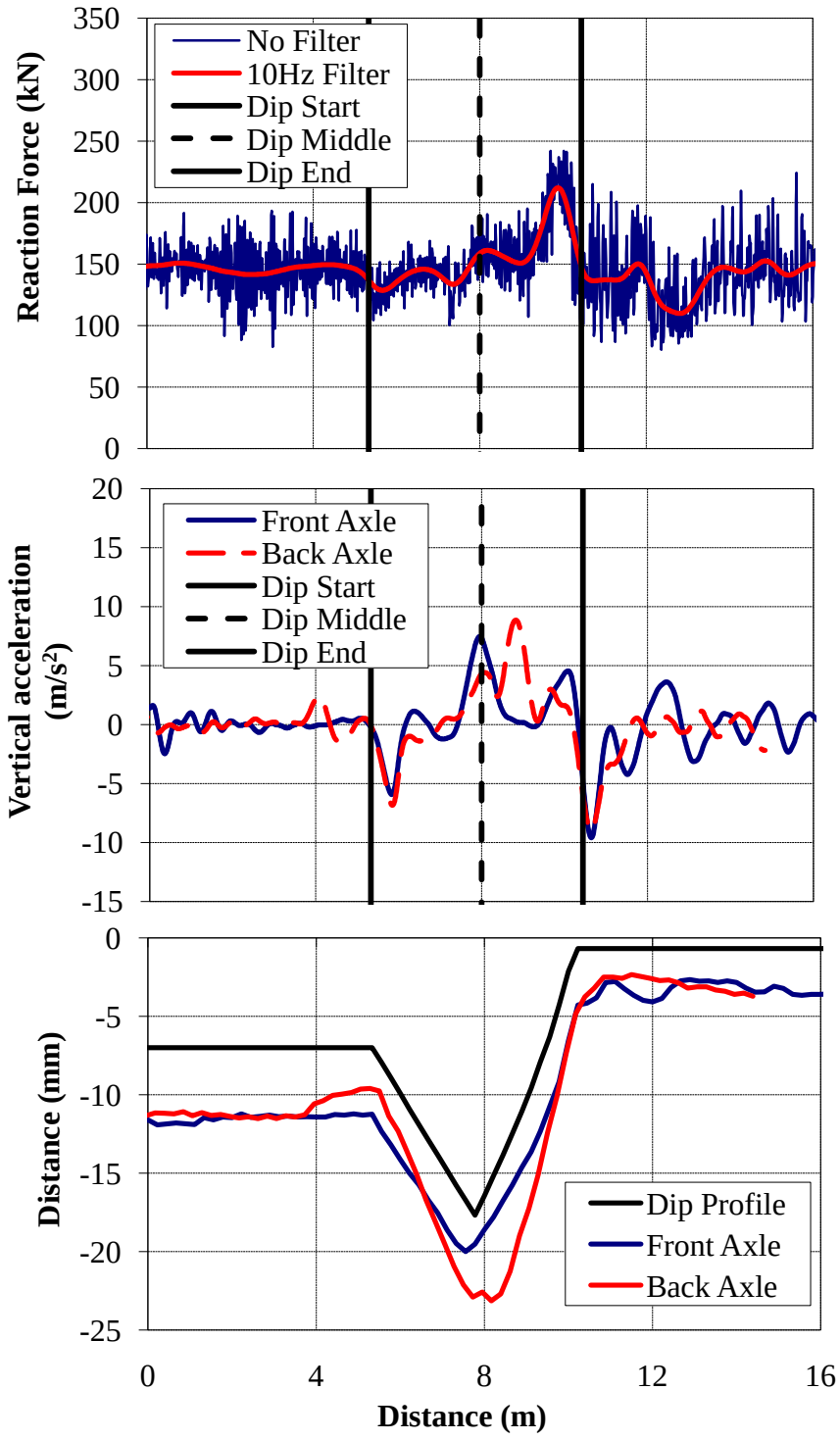

Figure F.25 - (a) Wheel/Rail Forces (b) Axle Accelerations and (c) Track Deflection due to a 1:200 Dip at a Bridge/Approach Location (Equal Lengths, v = 22.2 m/s)

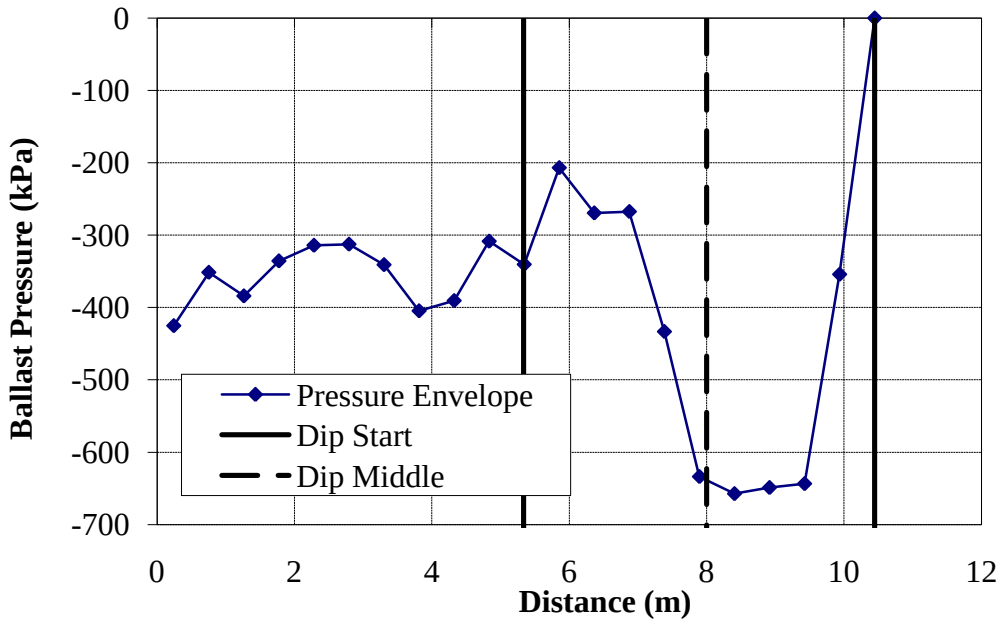

Figure F.26 – Ballast pressures due to a 1:200 Dip at a Bridge/Approach Location (Equal Lengths, v = 22.2 m/s)

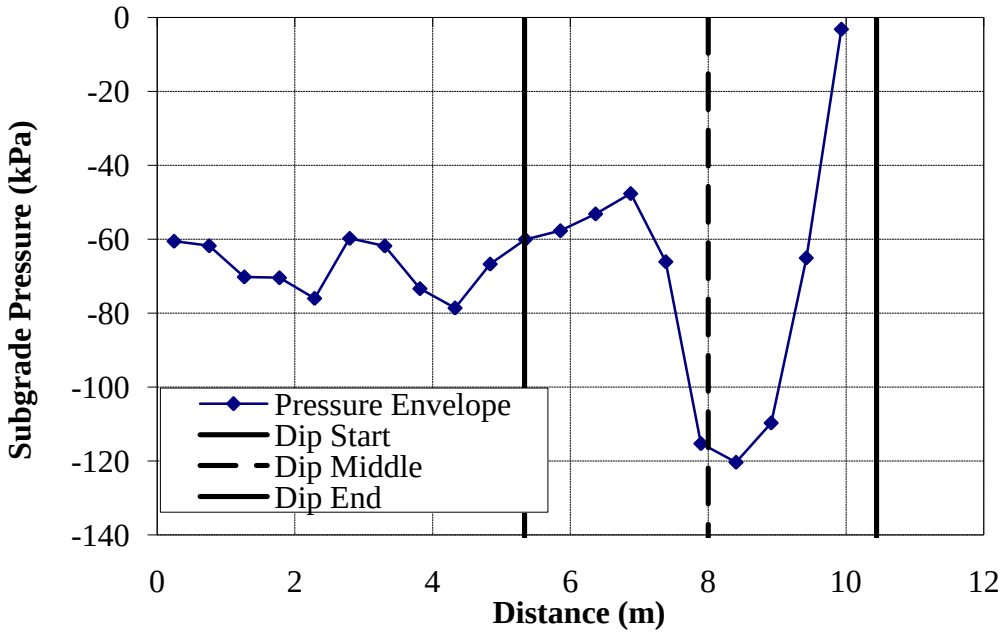

Figure F.27 - Subgrade pressures due to a 1:200 Dip at a Bridge/Approach Location (Equal Lengths, v = 22.2 m/s)

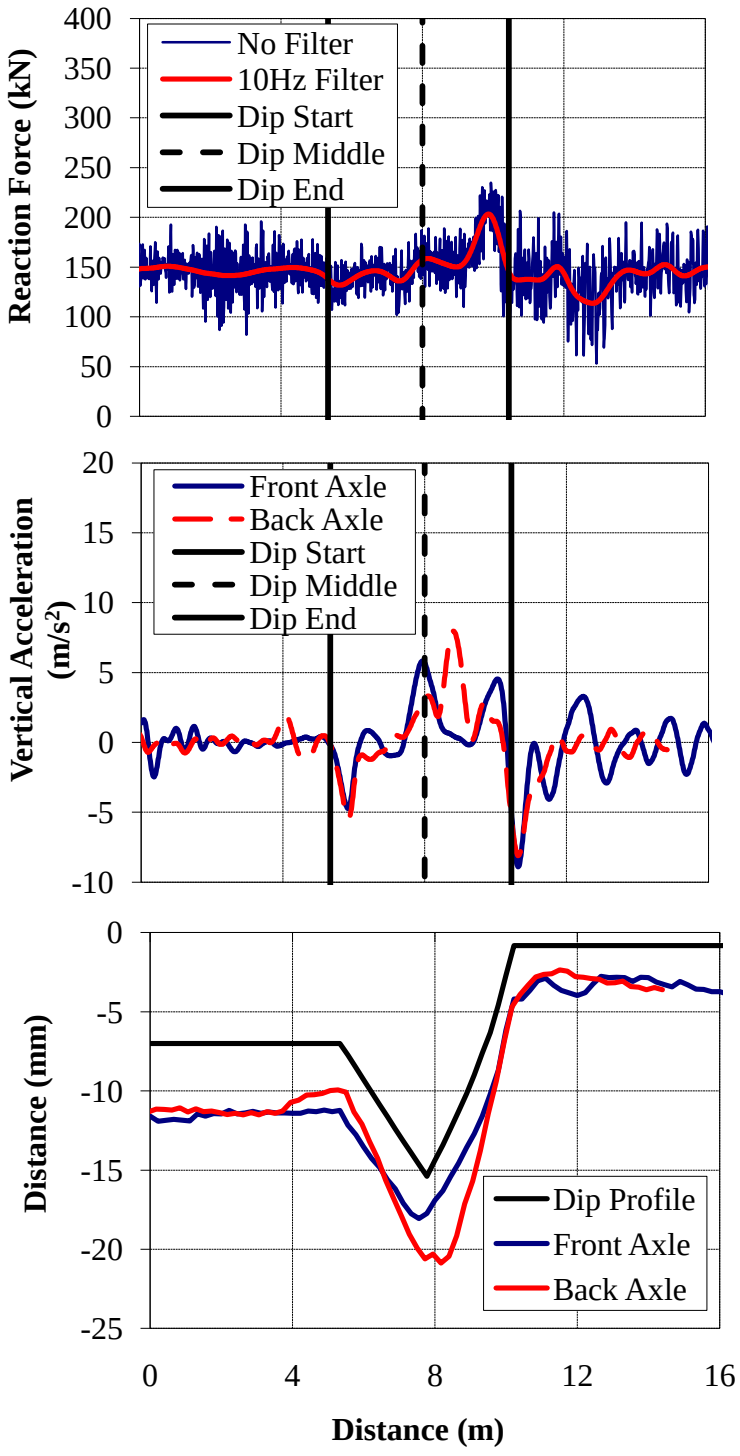

Figure F.28 - (a) Wheel/Rail Forces (b) Axle Accelerations and (c) Track Deflection due to a 1:250 Dip at a Bridge/Approach Location (Equal Lengths, v = 22.2 m/s)

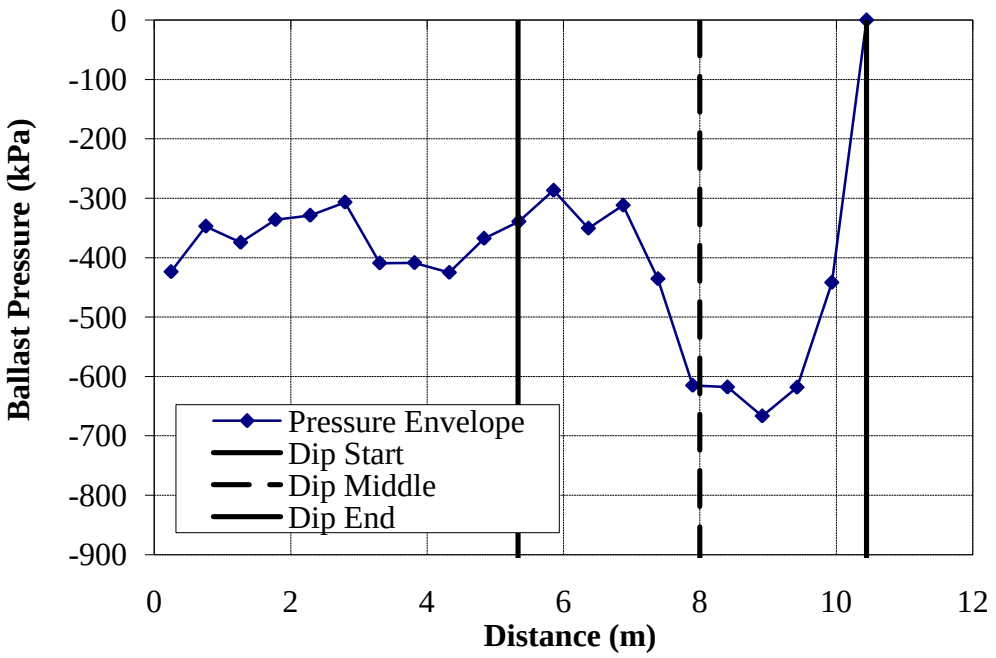

Figure F.29 – Ballast pressures due to a 1:250 Dip at a Bridge/Approach Location (Equal Lengths, v = 22.2 m/s)

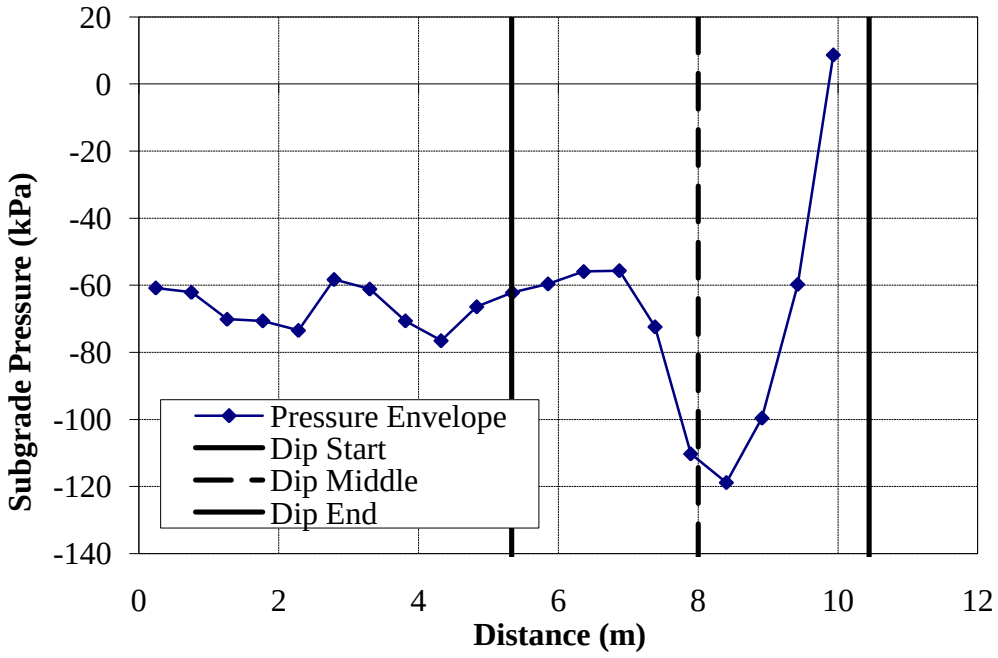

Figure F.30 - Subgrade pressures due to a 1:250 Dip at a Bridge/Approach Location (Equal Lengths, v = 22.2 m/s)

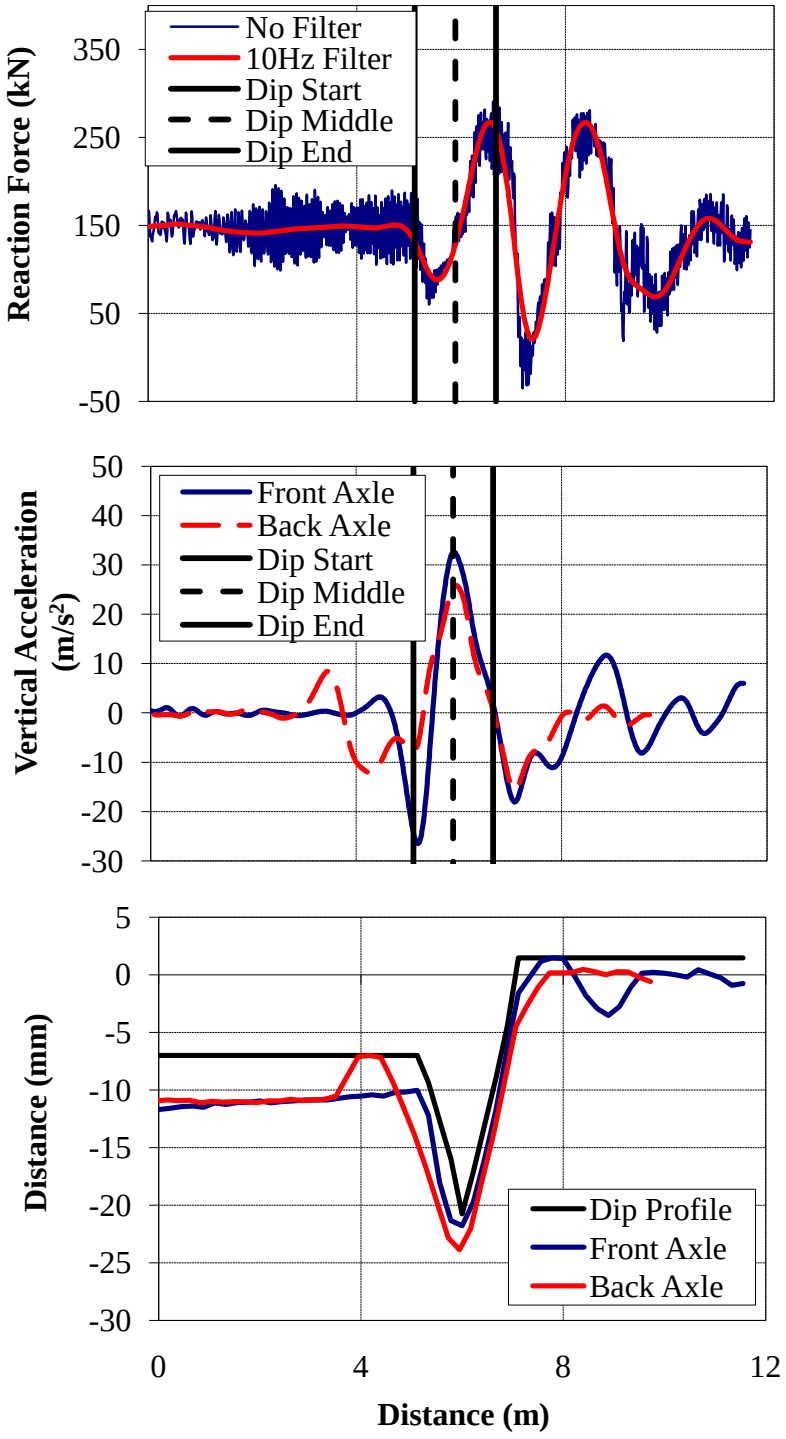

Figure F.31 - (a) Wheel/Rail Forces (b) Axle Accelerations and (c) Track Deflection due to a 1:50 Dip at a Bridge/Approach Location (Equal Height, v = 22.2 m/s)

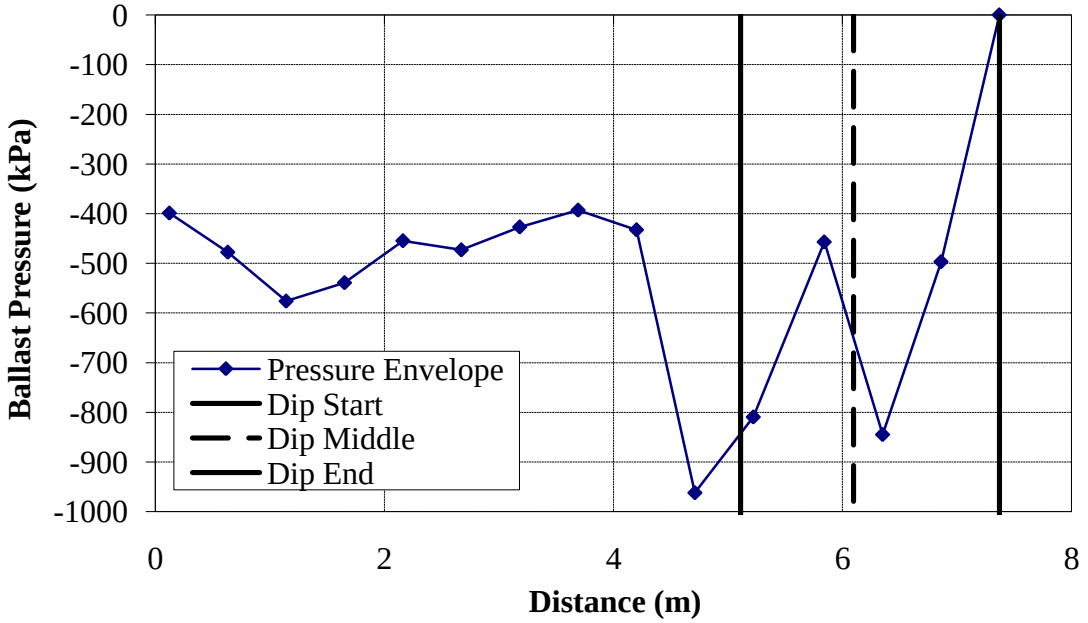

Figure F.32 – Ballast pressures due to a 1:50 Dip at a Bridge/Approach Location (Equal Height, v = 22.2 m/s)

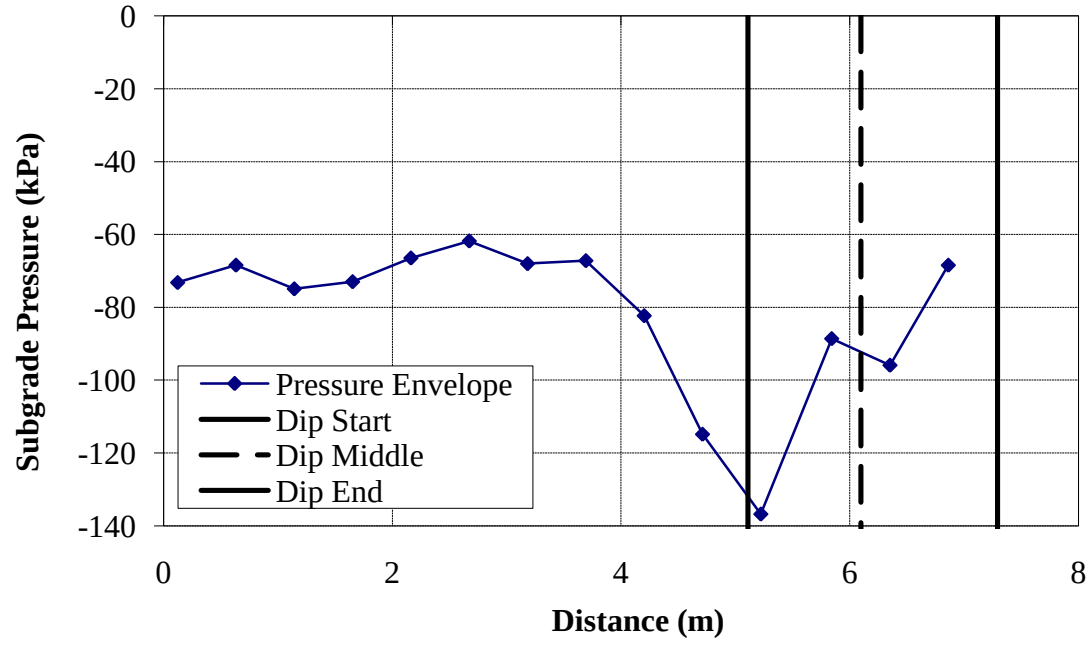

Figure F.33 - Subgrade pressures due to a 1:50 Dip at a Bridge/Approach Location (Equal Height, v = 22.2 m/s)

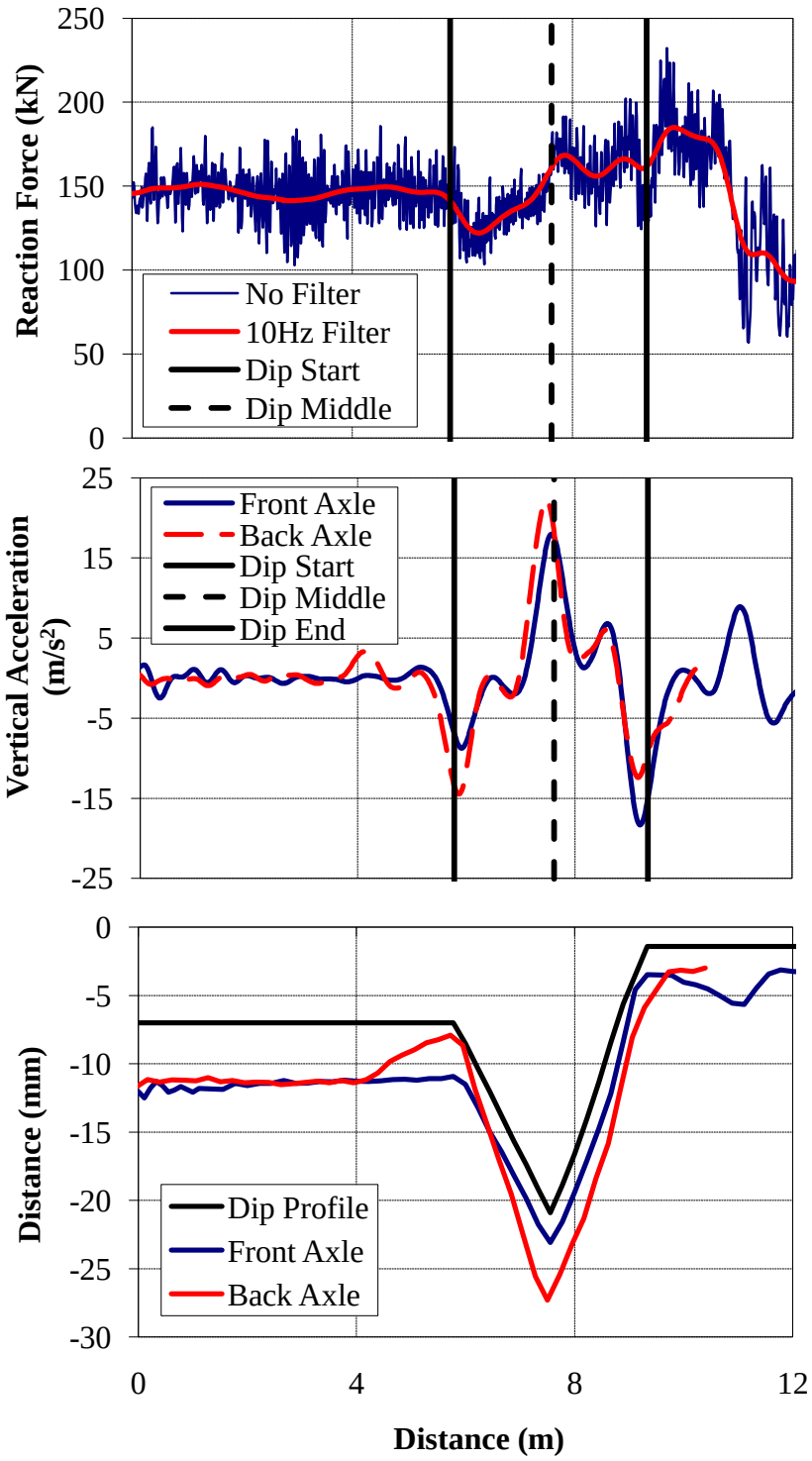

Figure F.34 - (a) Wheel/Rail Forces (b) Axle Accelerations and (c) Track Deflection due to a 1:100 Dip at a Bridge/Approach Location (Equal Height, v = 22.2 m/s)

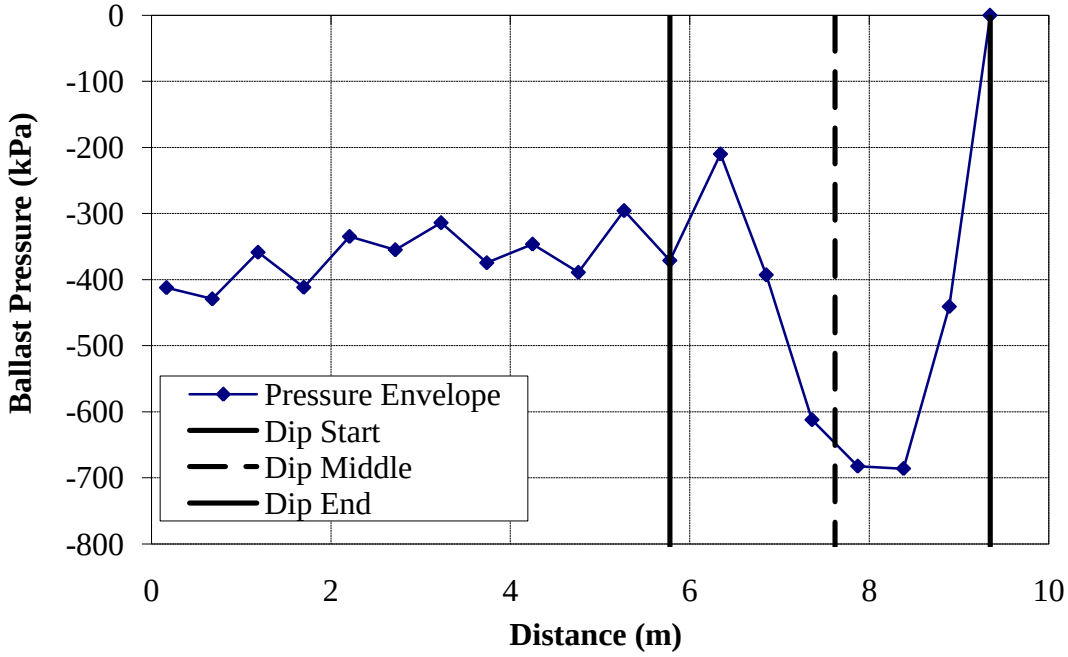

Figure F.35 – Ballast pressures due to a 1:100 Dip at a Bridge/Approach Location (Equal Height, v = 22.2 m/s)

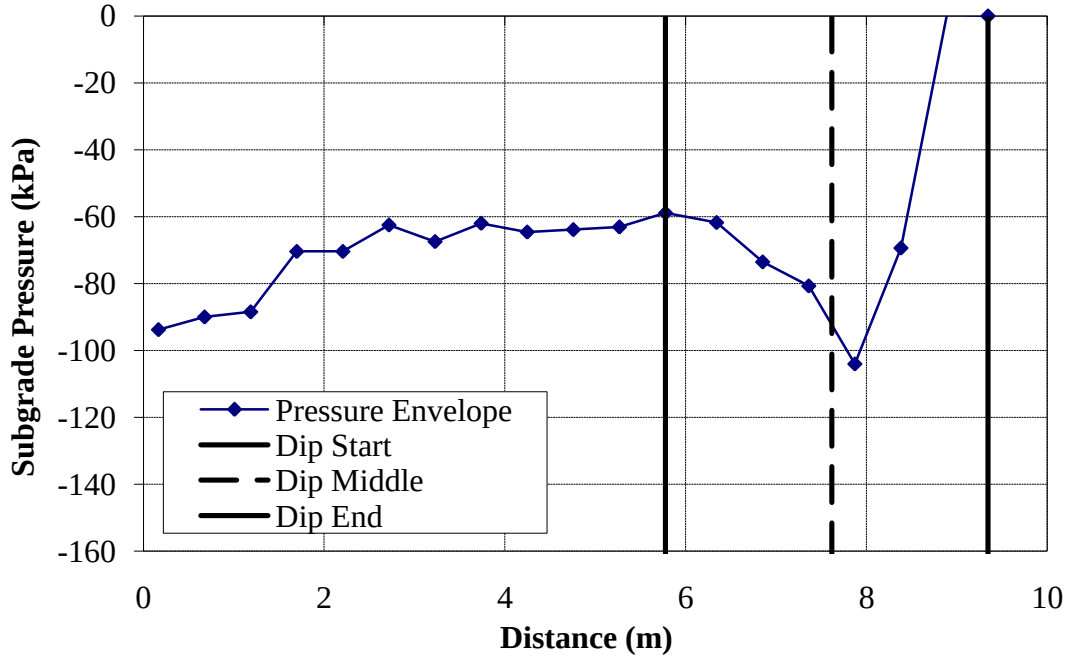

Figure F.36 - Subgrade pressures due to a 1:100 Dip at a Bridge/Approach Location (Equal Height, v = 22.2 m/s)

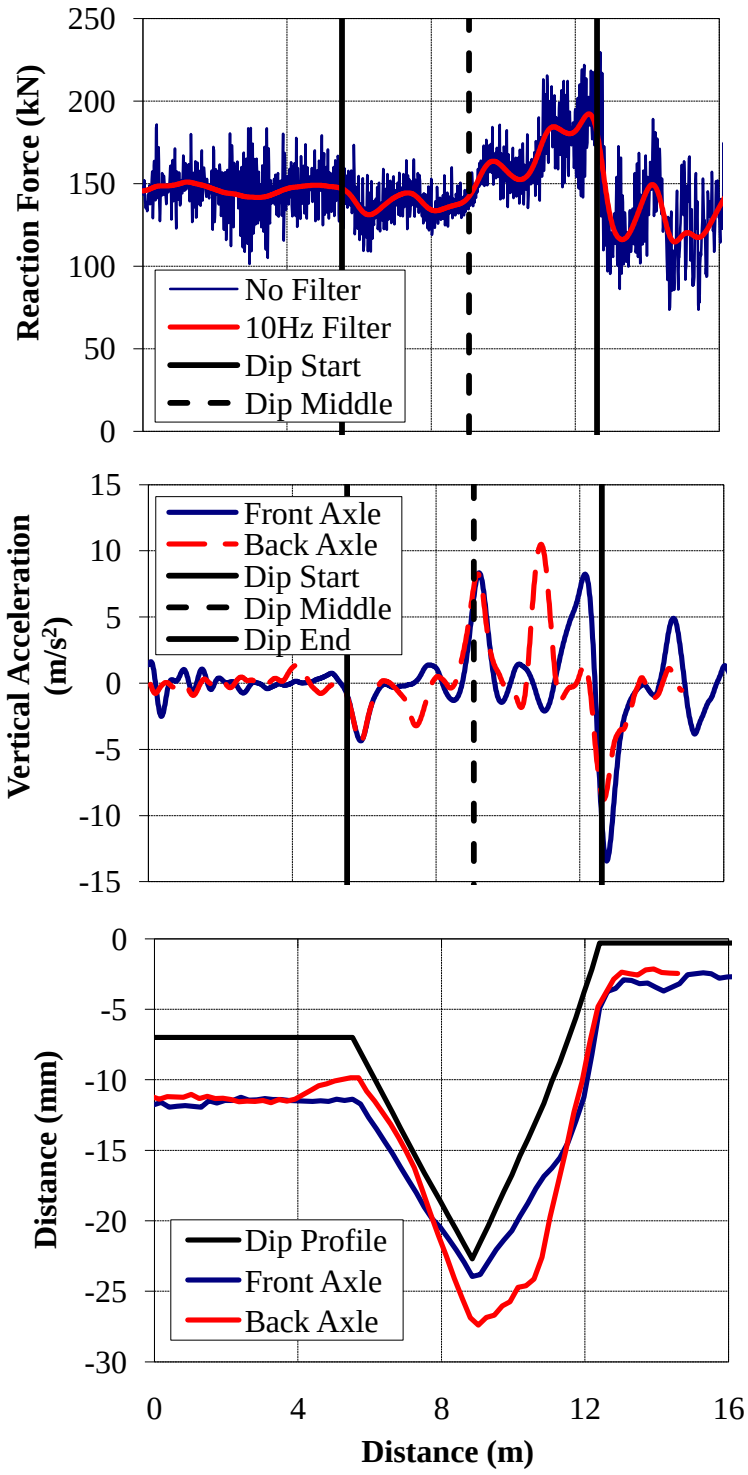

Figure F.37 - (a) Wheel/Rail Forces (b) Axle Accelerations and (c) Track Deflection due to a 1:200 Dip at a Bridge/Approach Location (Equal Height, v = 22.2 m/s)

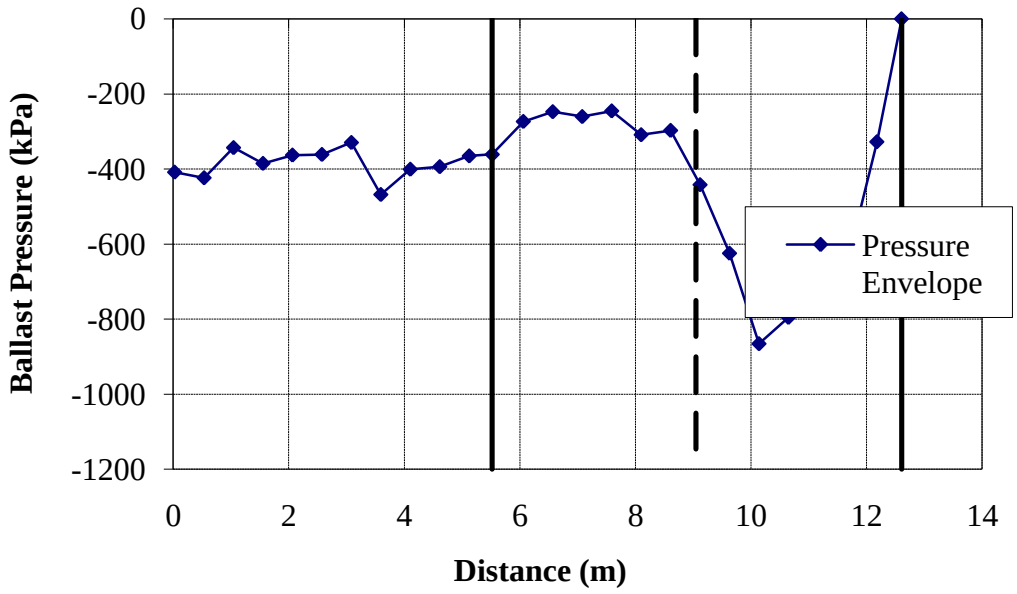

Figure F.38 – Ballast pressures due to a 1:200 Dip at a Bridge/Approach Location (Equal Height, v = 22.2 m/s)

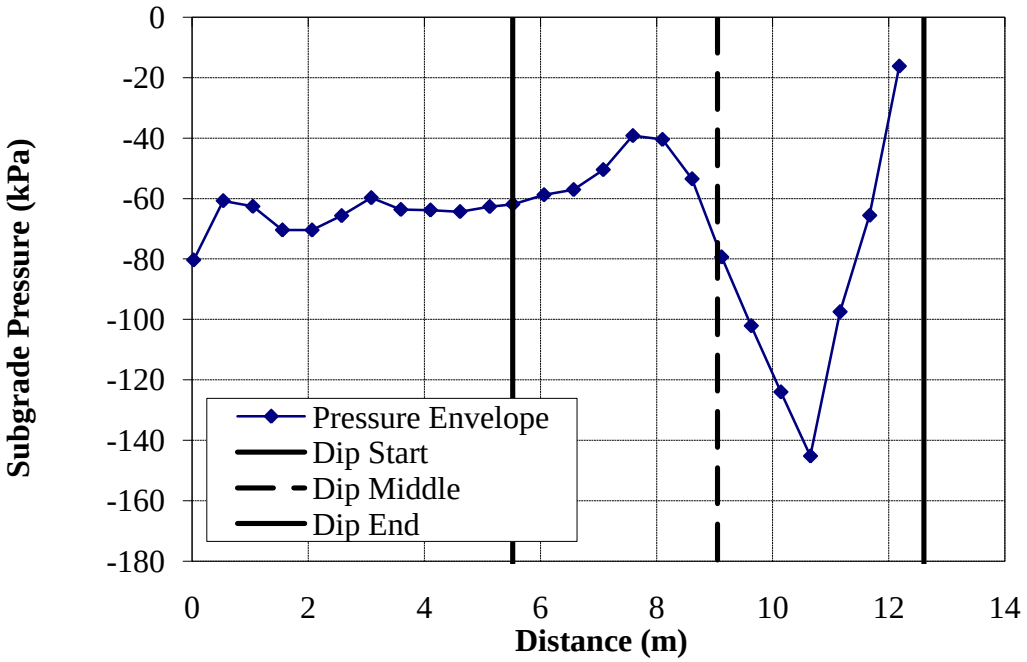

Figure F.39 - Subgrade pressures due to a 1:200 Dip at a Bridge/Approach Location (Equal Height, v = 22.2 m/s)

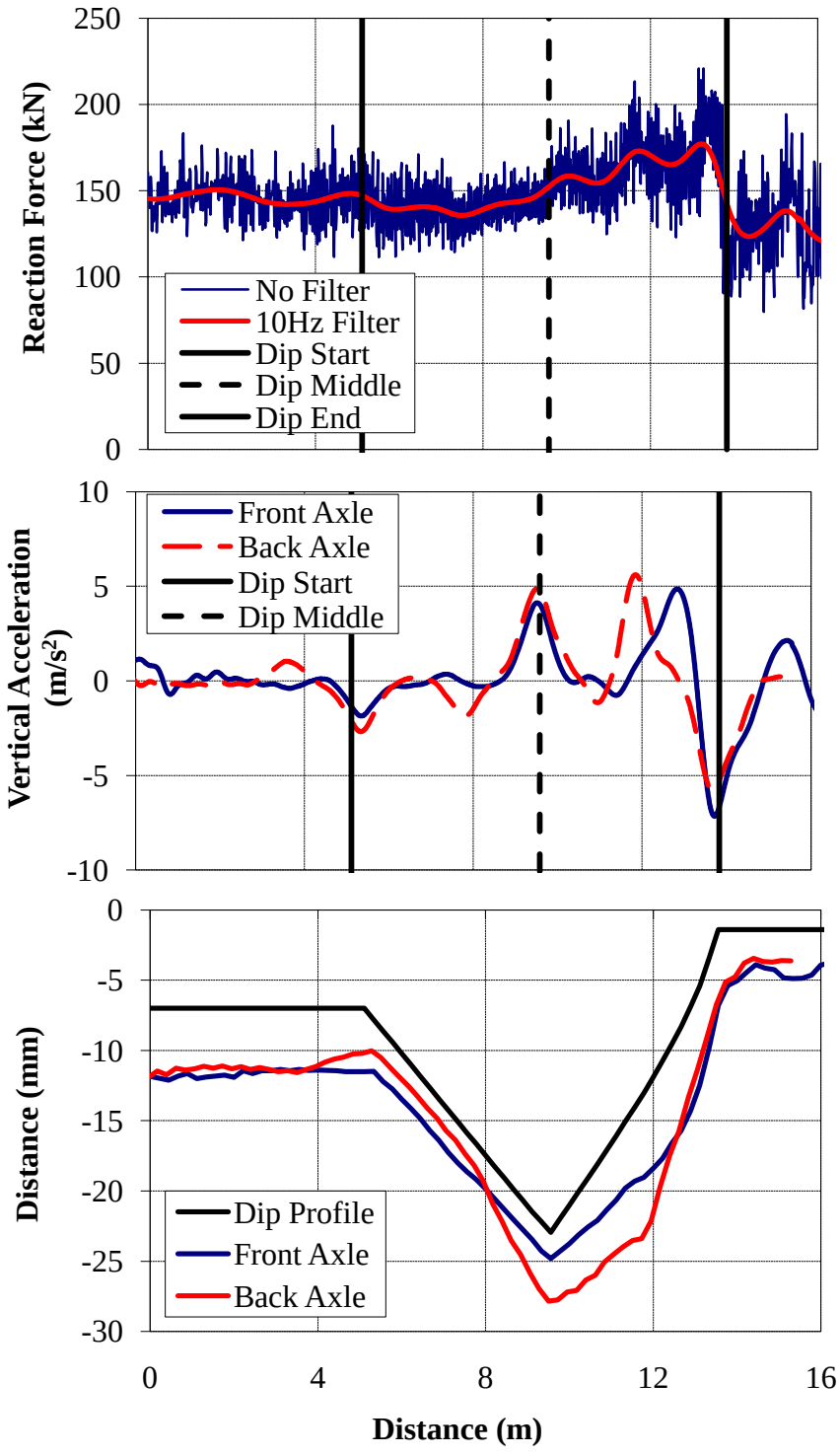

Figure F.40 - (a) Wheel/Rail Forces (b) Axle Accelerations and (c) Track Deflection due to a 1:250 Dip at a Bridge/Approach Location (Equal Height, v = 22.2 m/s)

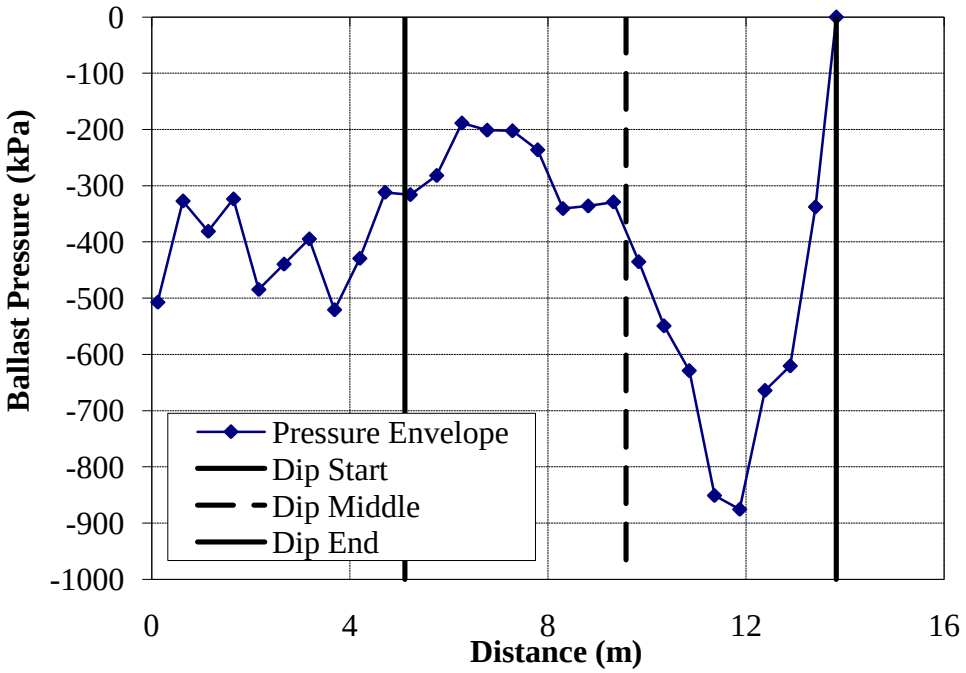

Figure F.41 - Ballast pressures due to a 1:250 Dip at a Bridge/Approach Location (Equal Height, v = 22.2 m/s)

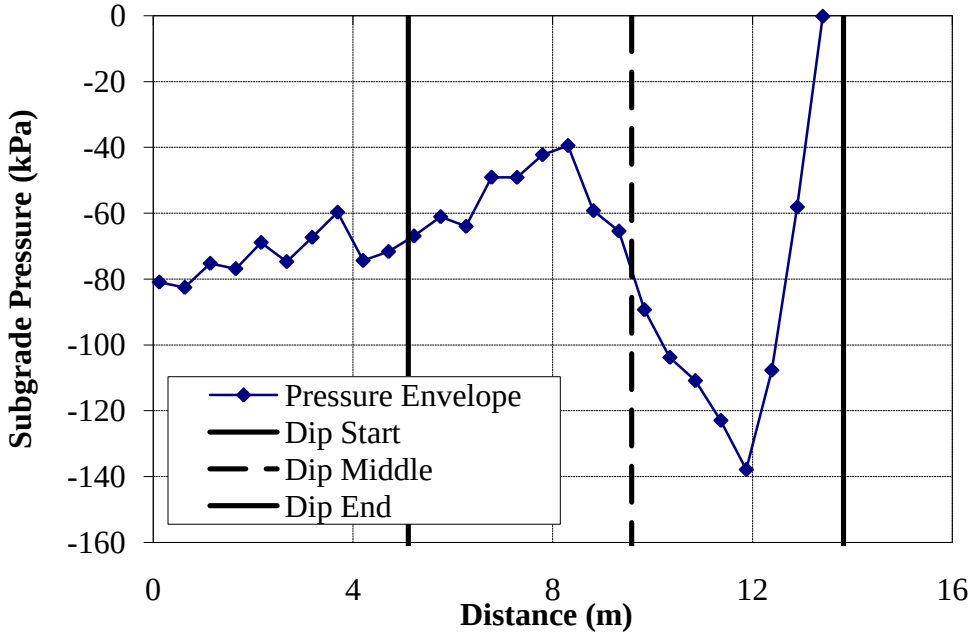

Figure F.42 - Subgrade pressures due to a 1:250 Dip at a Bridge/Approach Location (Equal Height, v = 22.2 m/s)

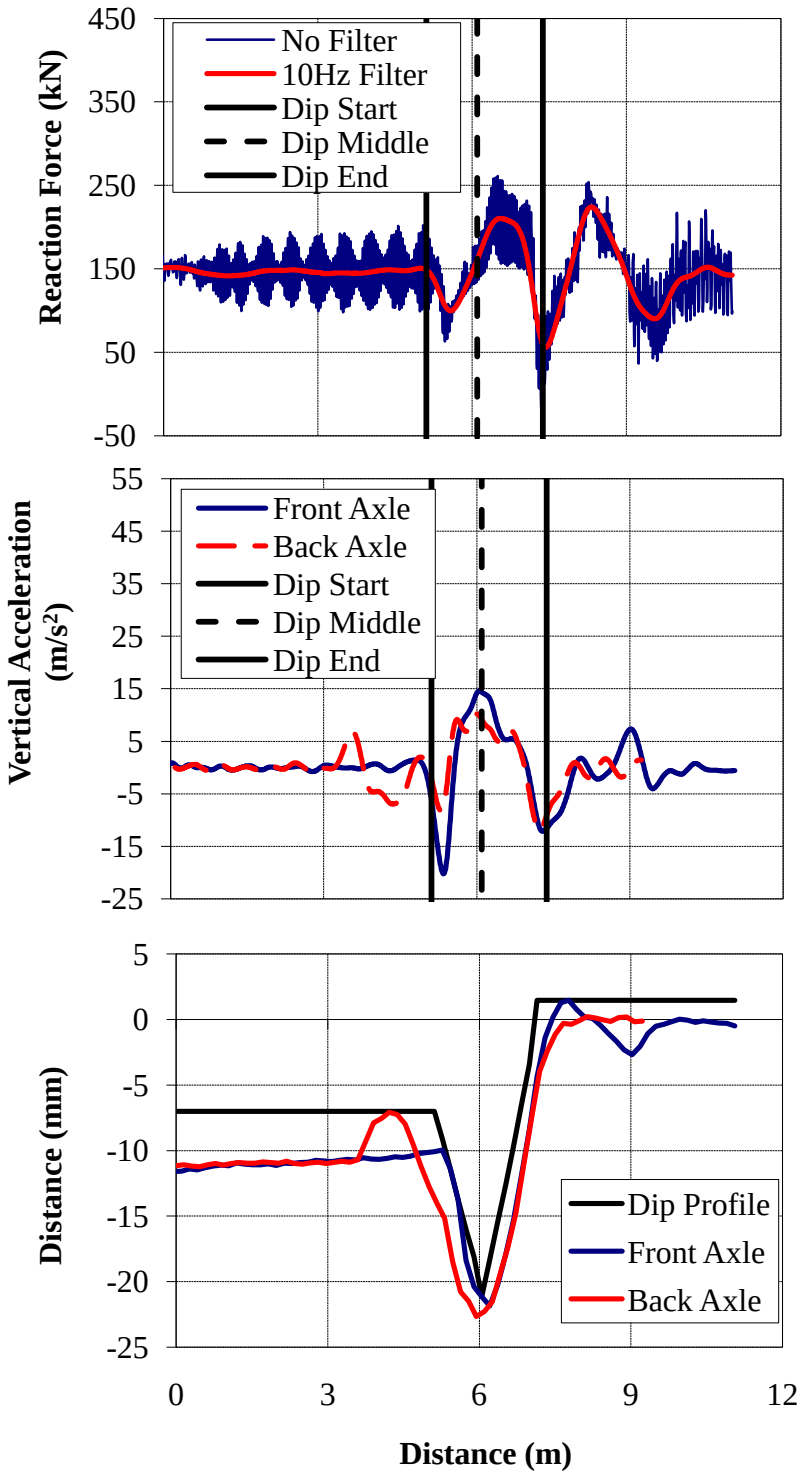

Figure F.43 - (a) Wheel/Rail Forces (b) Axle Accelerations and (c) Track Deflection due to a 1:50 Dip at a Bridge/Approach Location (Equal Height, v = 15.6 m/s)

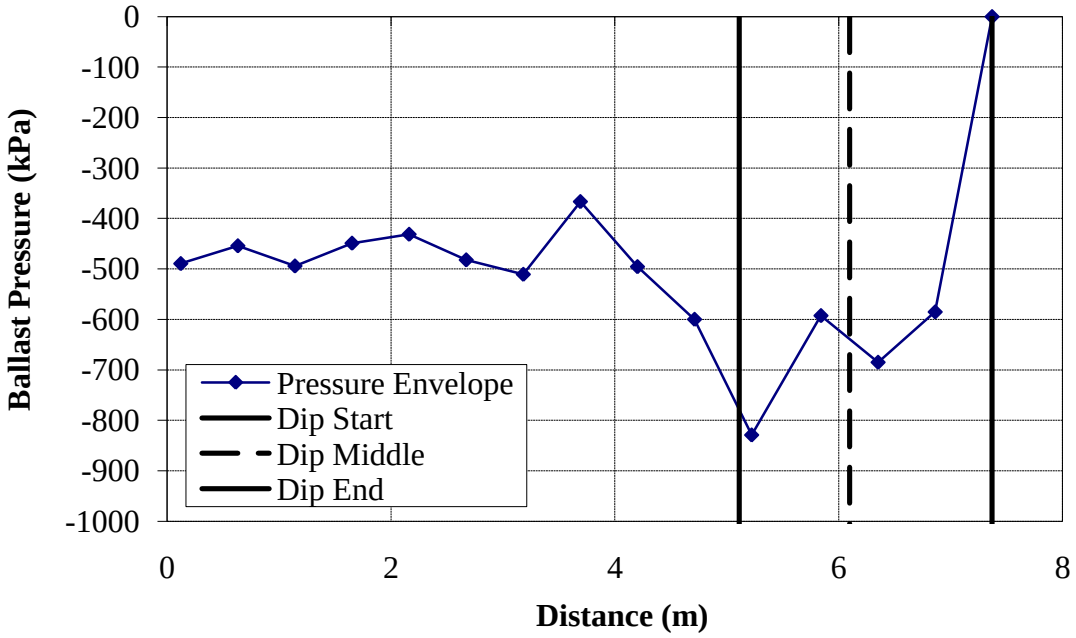

Figure F.44 – Ballast pressures due to a 1:50 Dip at a Bridge/Approach Location (Equal Height, v = 15.6 m/s)

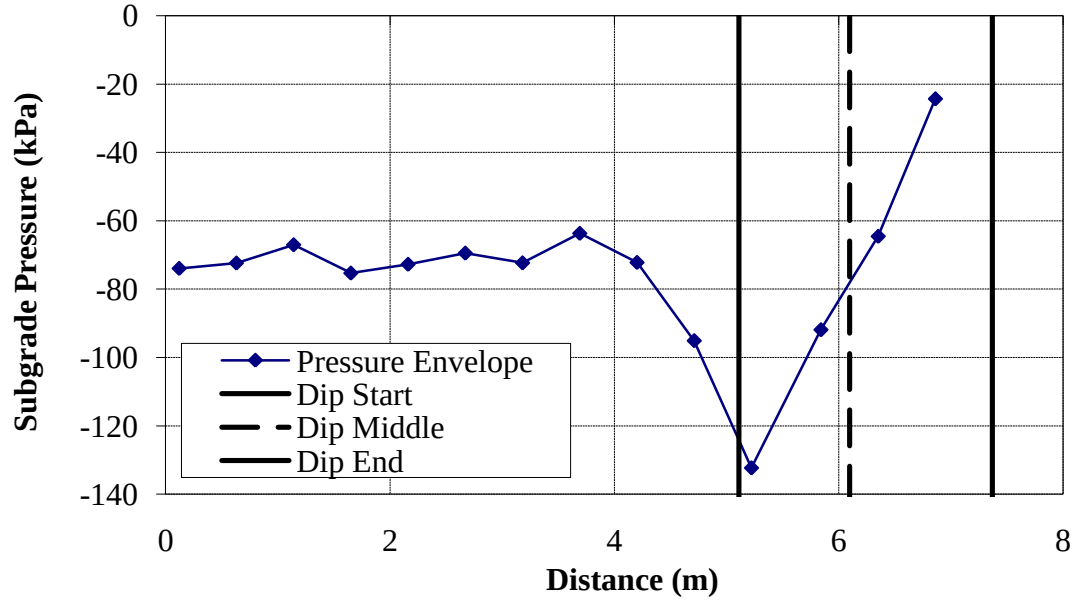

Figure F.45 - Subgrade pressures due to a 1:50 Dip at a Bridge/Approach Location (Equal Height, v = 15.6 m/s)

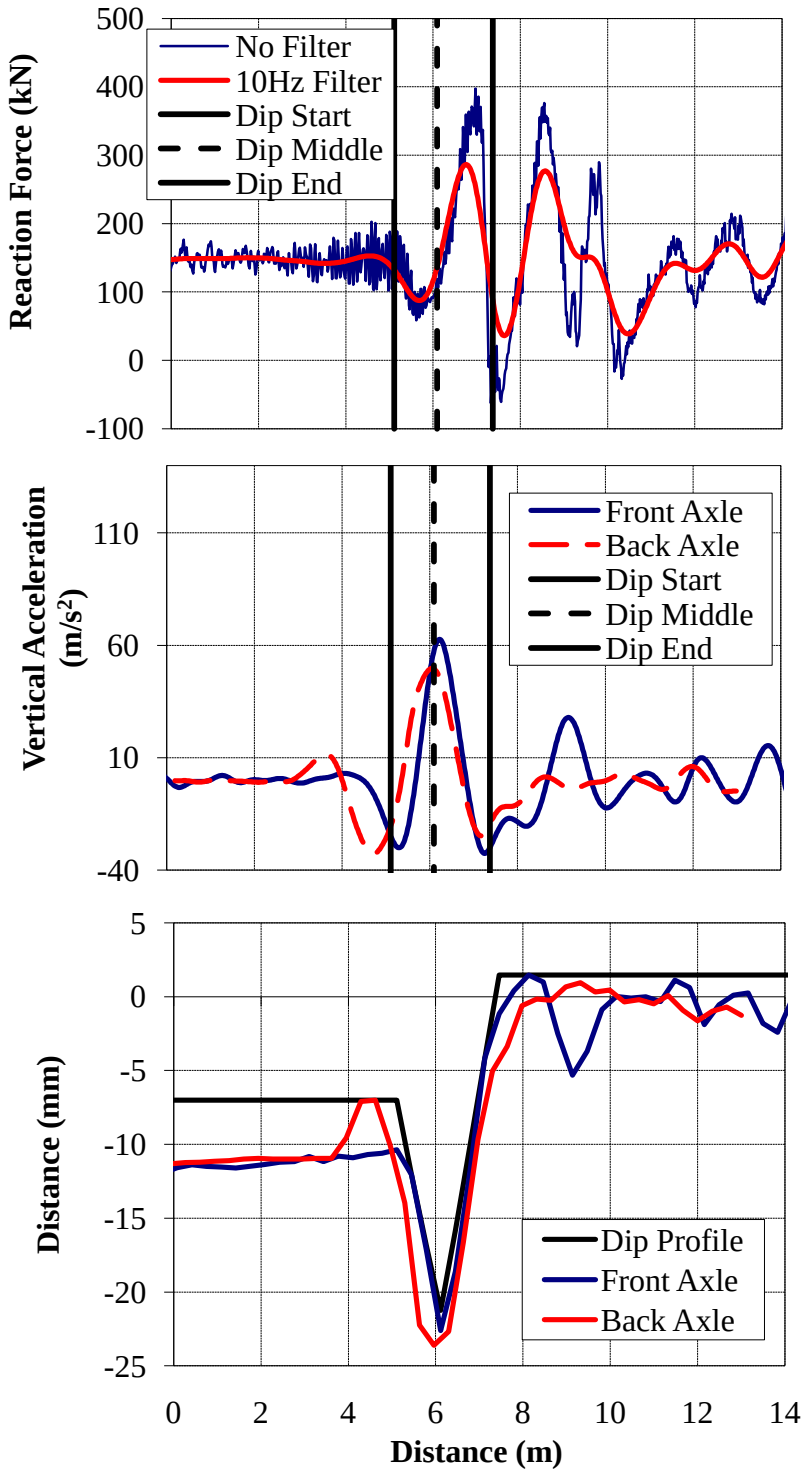

Figure F.46 - (a) Wheel/Rail Forces (b) Axle Accelerations and (c) Track Deflection due to a 1:50 Dip at a Bridge/Approach Location (Equal Height, v = 33.5 m/s)

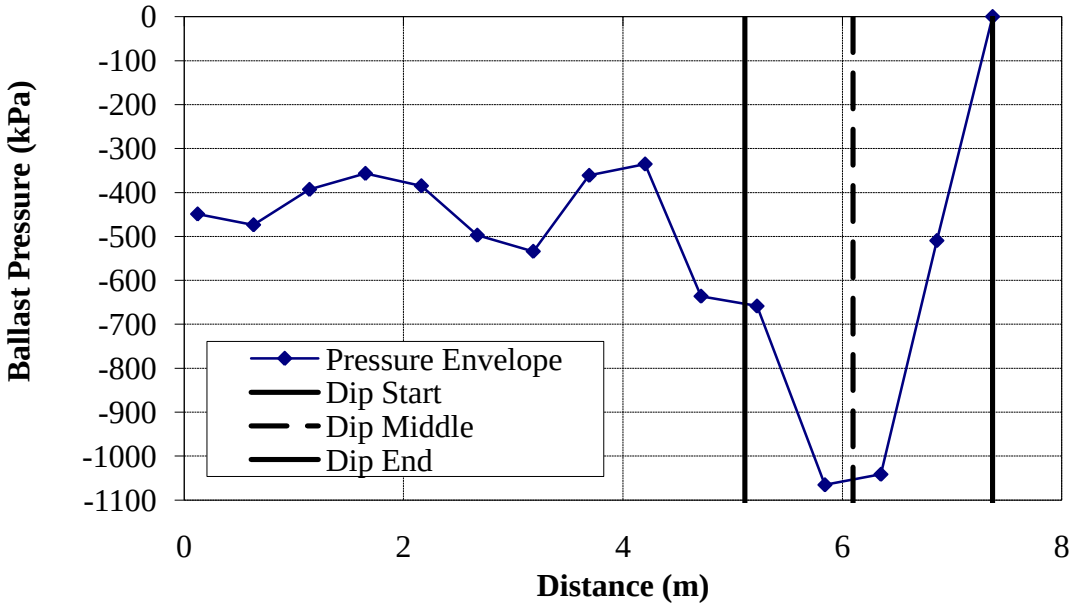

Figure F.47 – Ballast pressures due to a 1:50 Dip at a Bridge/Approach Location (Equal Height, v = 33.5 m/s)

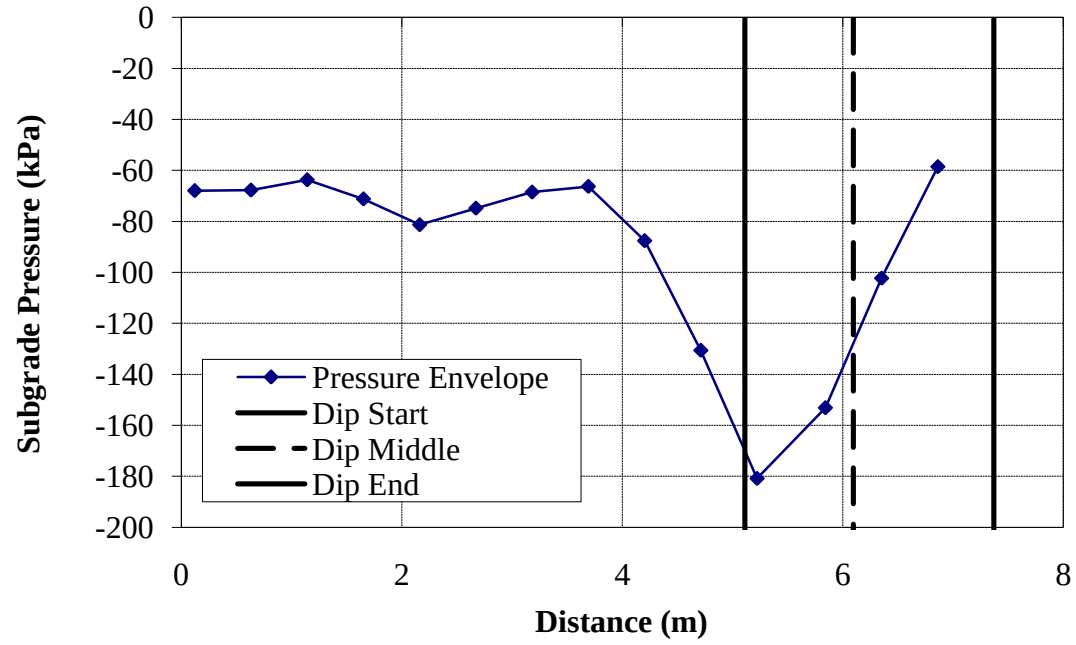

Figure F.48 - Subgrade pressures due to a 1:50 Dip at a Bridge/Approach Location (Equal Height, v = 33.5 m/s)

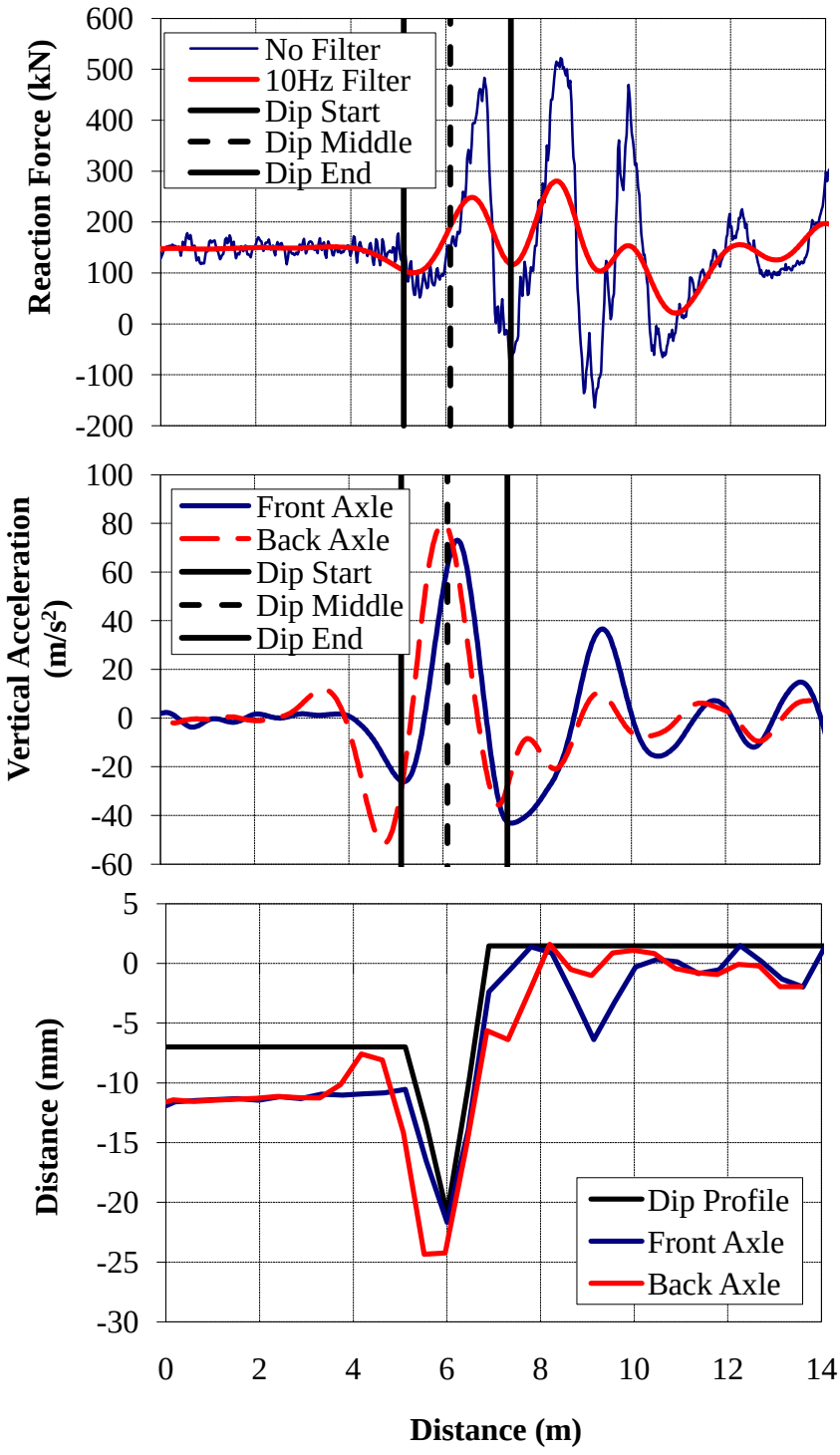

Figure F.49 - (a) Wheel/Rail Forces (b) Axle Accelerations and (c) Track Deflection due to a 1:50 Dip at a Bridge/Approach Location (Equal Height, v = 44.7 m/s)

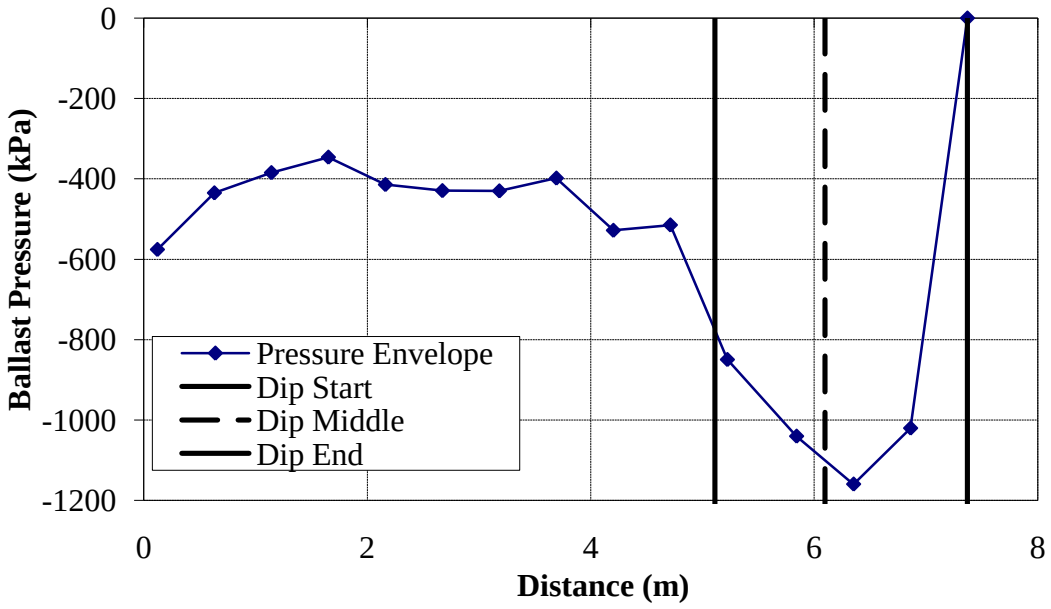

Figure F.50 – Ballast pressures due to a 1:50 Dip at a Bridge/Approach Location (Equal Height, v = 44.7 m/s)

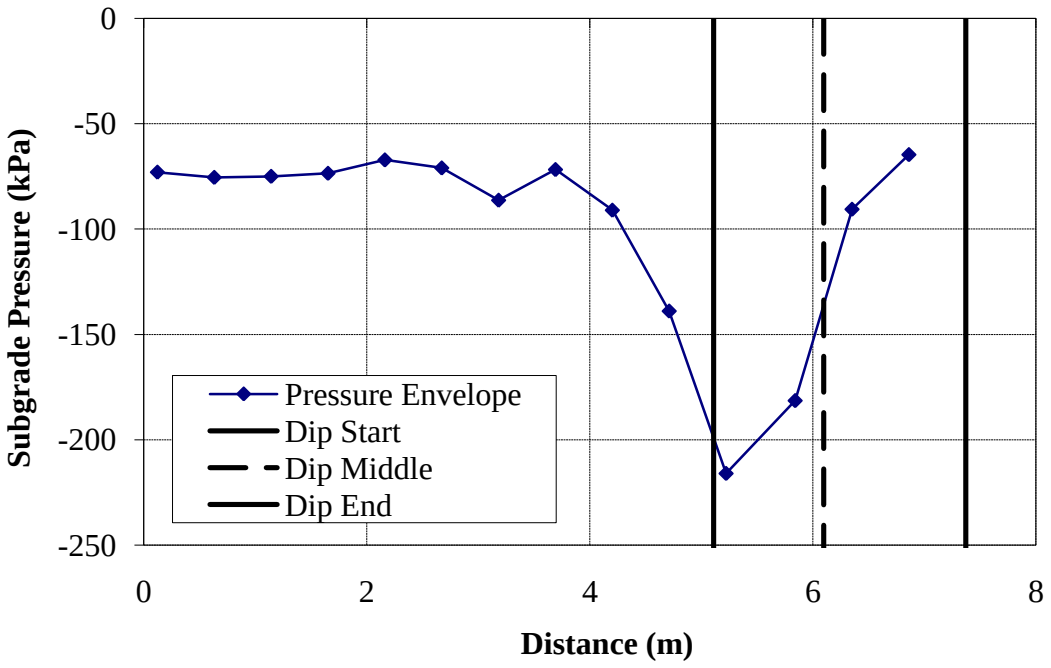

Figure F.51 - Subgrade pressures due to a 1:50 Dip at a Bridge/Approach Location (Equal Height, v = 44.7 m/s)

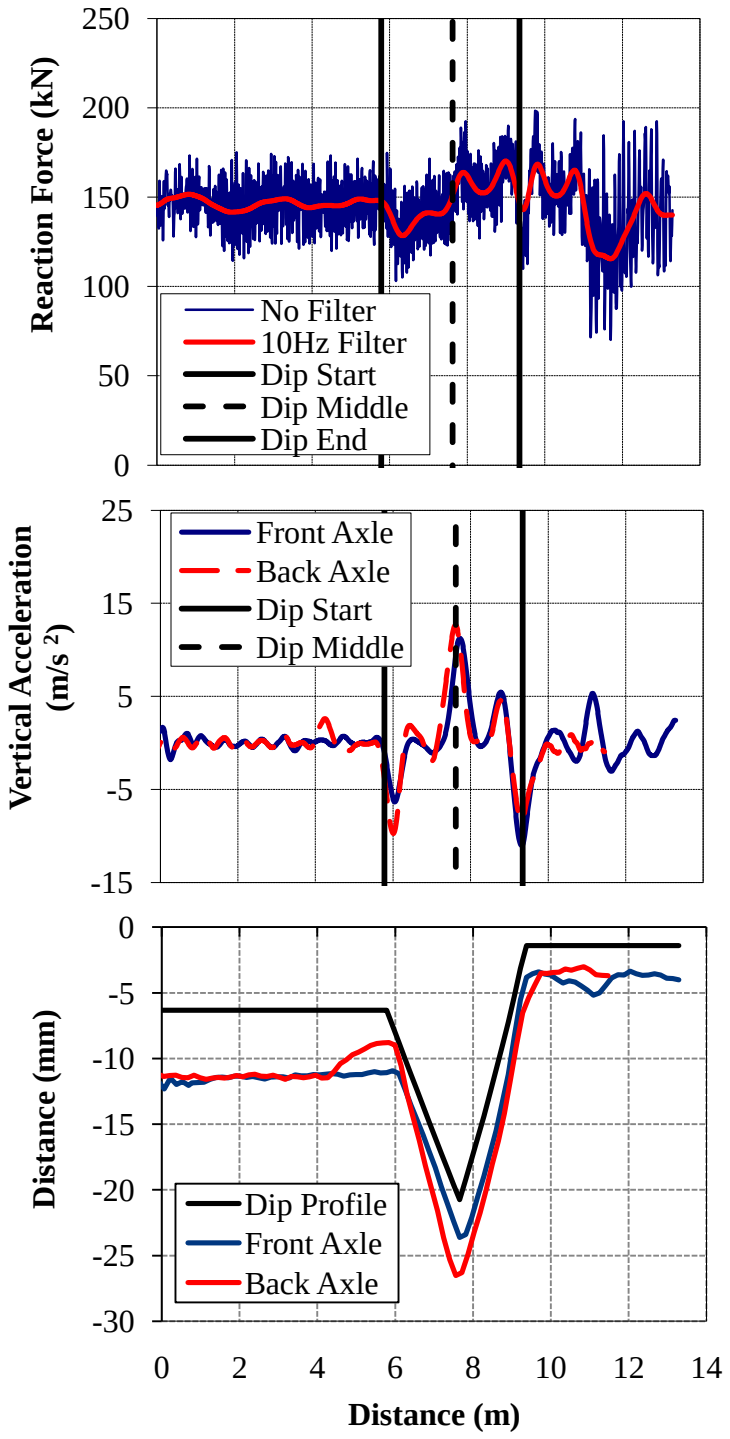

Figure F.52 – (a) Wheel/Rail Forces (b) Axle Accelerations and (c) Track Deflection due to a 1:100 Dip at a Bridge/Approach Location (Equal Height, v = 15.6 m/s)

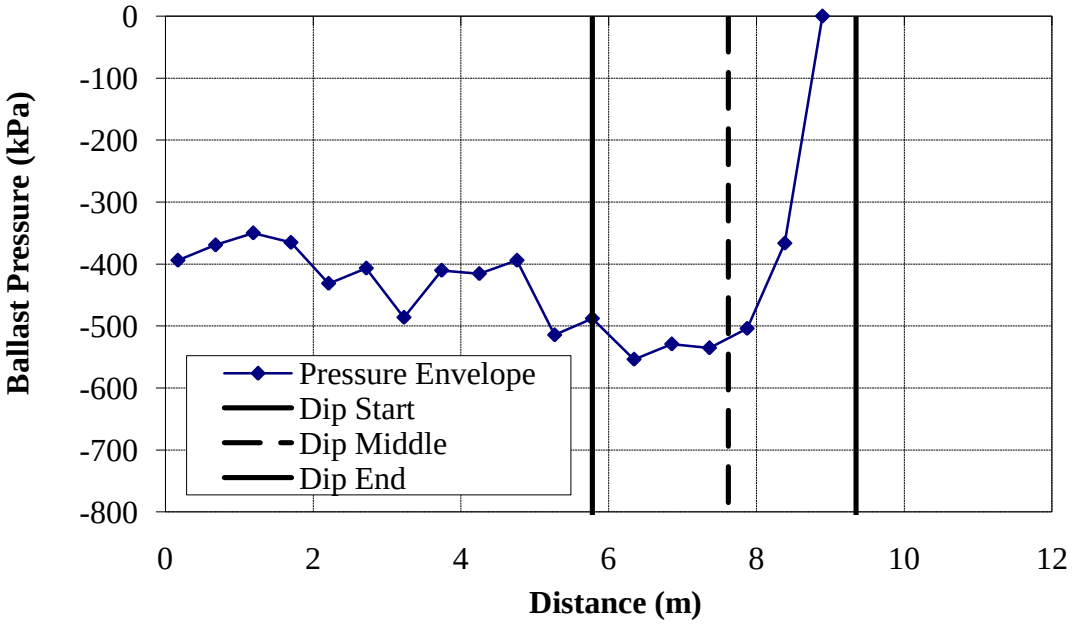

Figure F.53 – Ballast pressures due to a 1:100 Dip at a Bridge/Approach Location (Equal Height, v = 15.6 m/s)

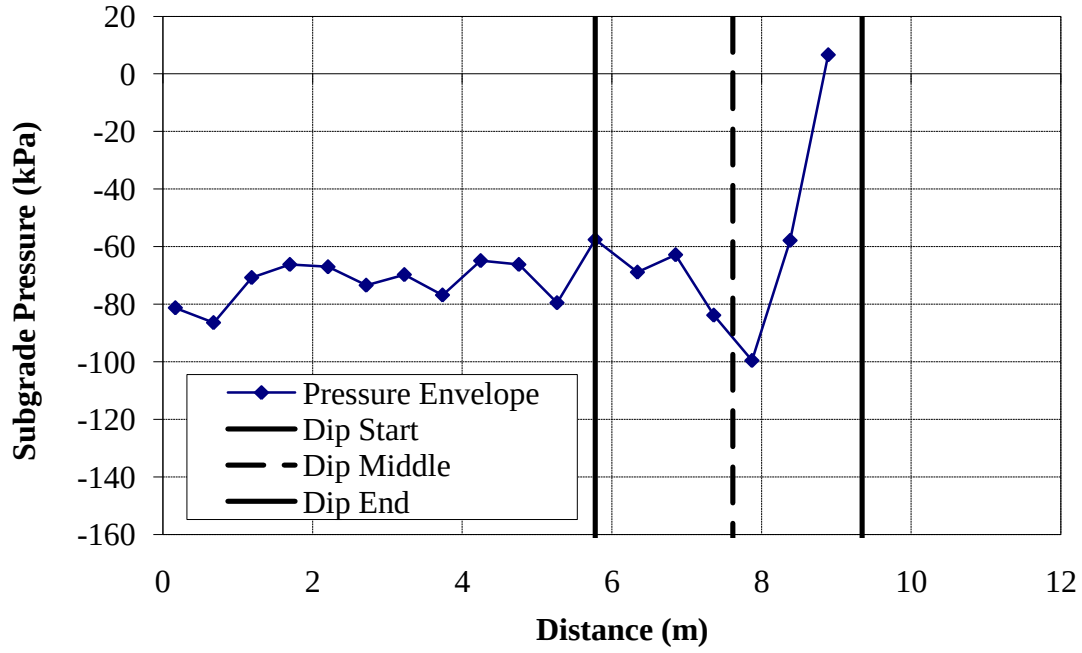

Figure F.54 - Subgrade pressures due to a 1:100 Dip at a Bridge/Approach Location (Equal Height, v = 15.6 m/s)

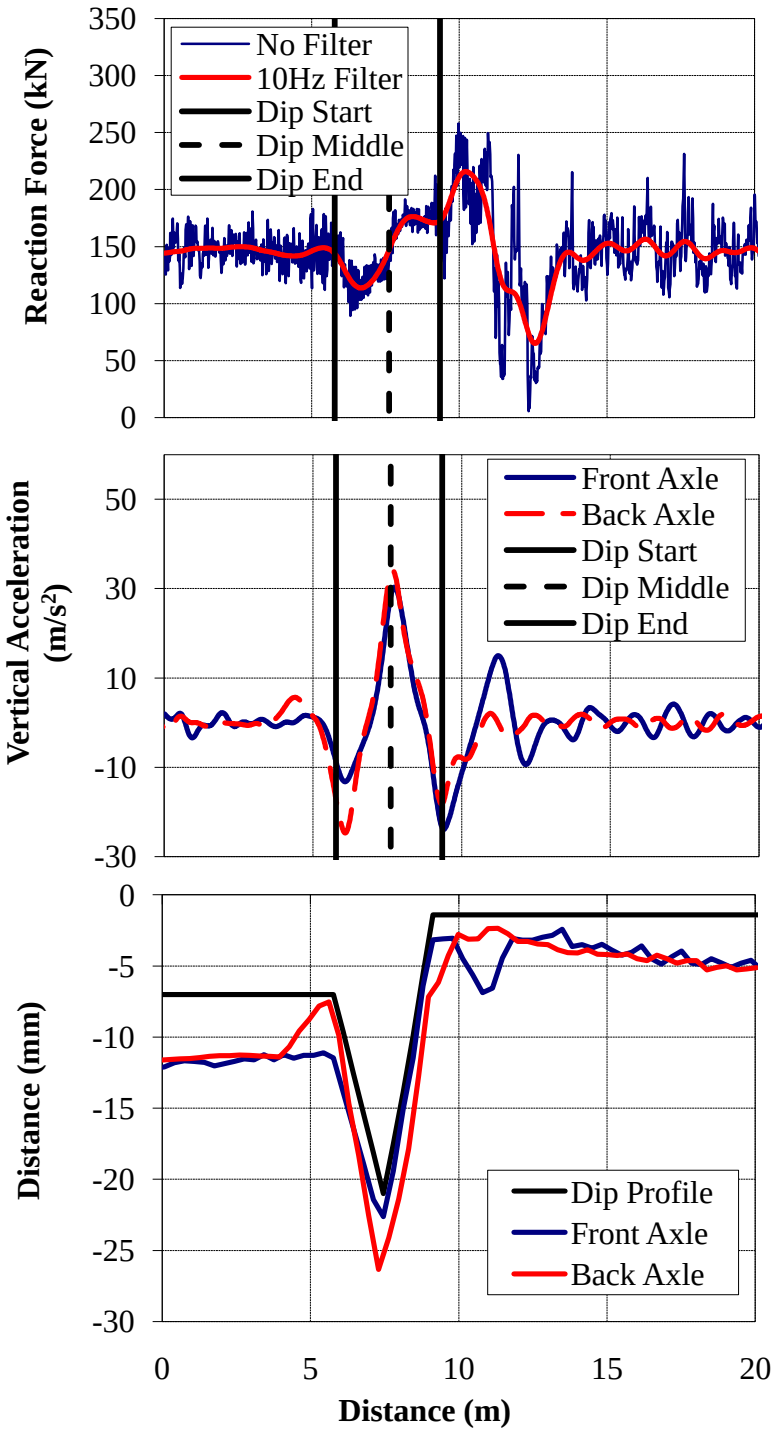

Figure F.55 - (a) Wheel/Rail Forces (b) Axle Accelerations and (c) Track Deflection due to a 1:100 Dip at a Bridge/Approach Location (Equal Height, v = 33.5 m/s)

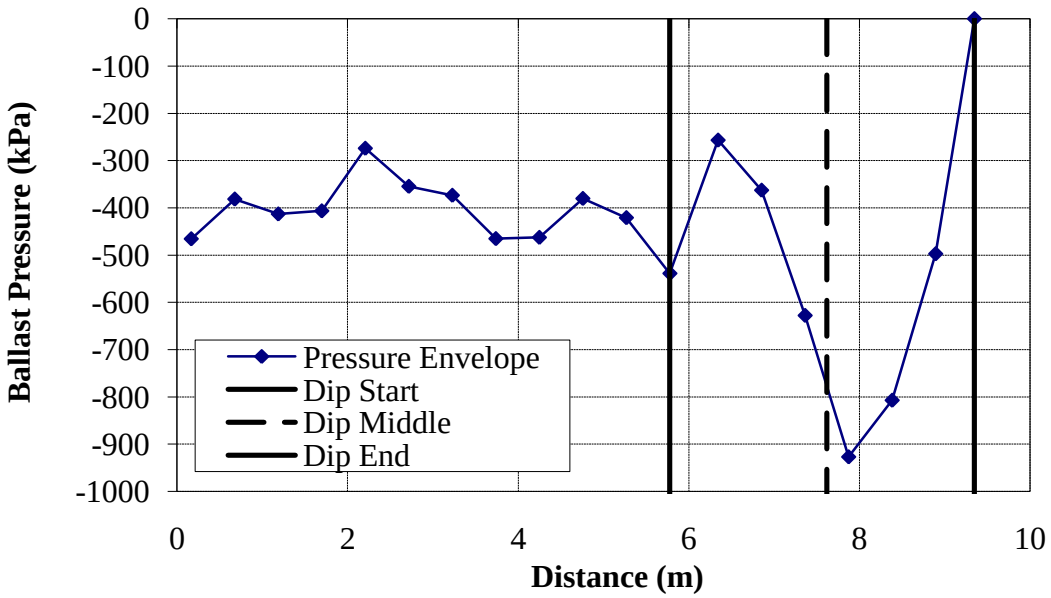

Figure F.56 – Ballast pressures due to a 1:100 Dip at a Bridge/Approach Location (Equal Height, v = 33.5 m/s)

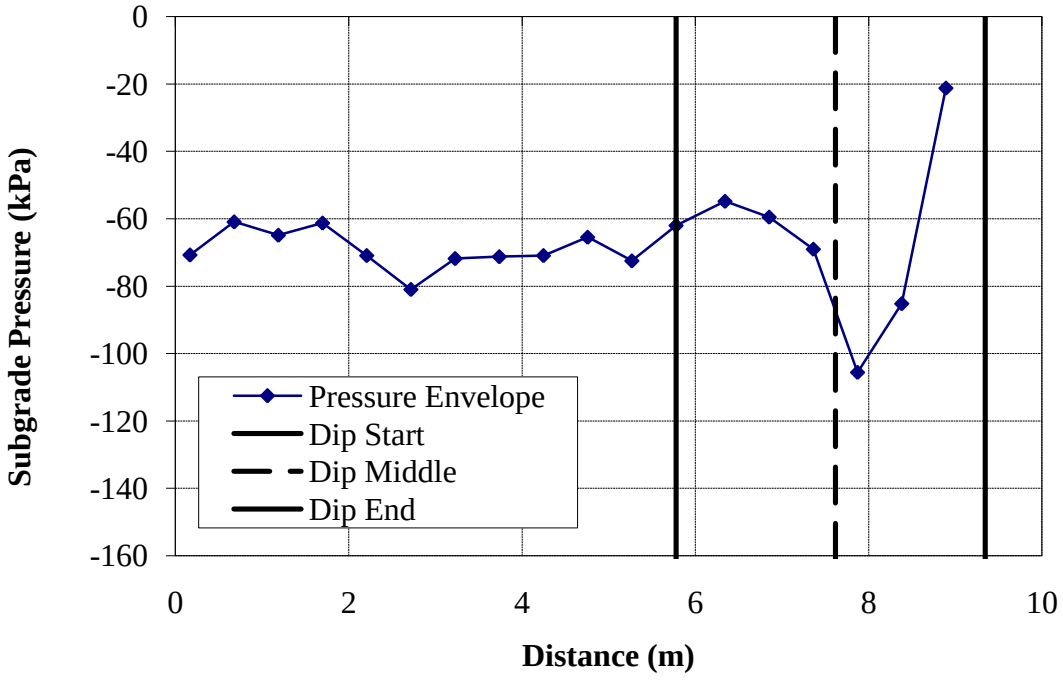

Figure F.57 - Subgrade pressures due to a 1:100 Dip at a Bridge/Approach Location (Equal Height, v = 33.5 m/s)

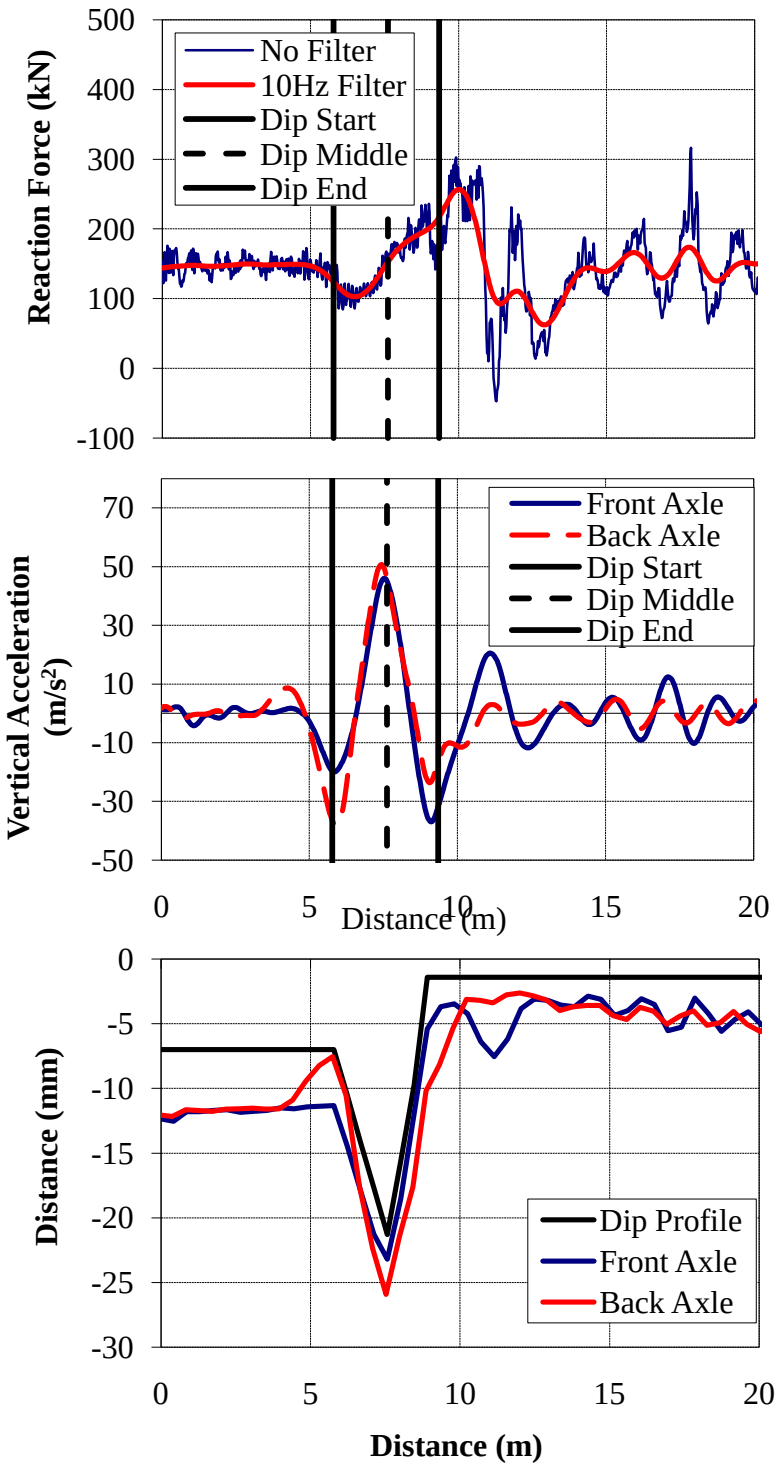

Figure F.58 - (a) Wheel/Rail Forces (b) Axle Accelerations and (c) Track Deflection due to a 1:100 Dip at a Bridge/Approach Location (Equal Height, v = 44.7 m/s)

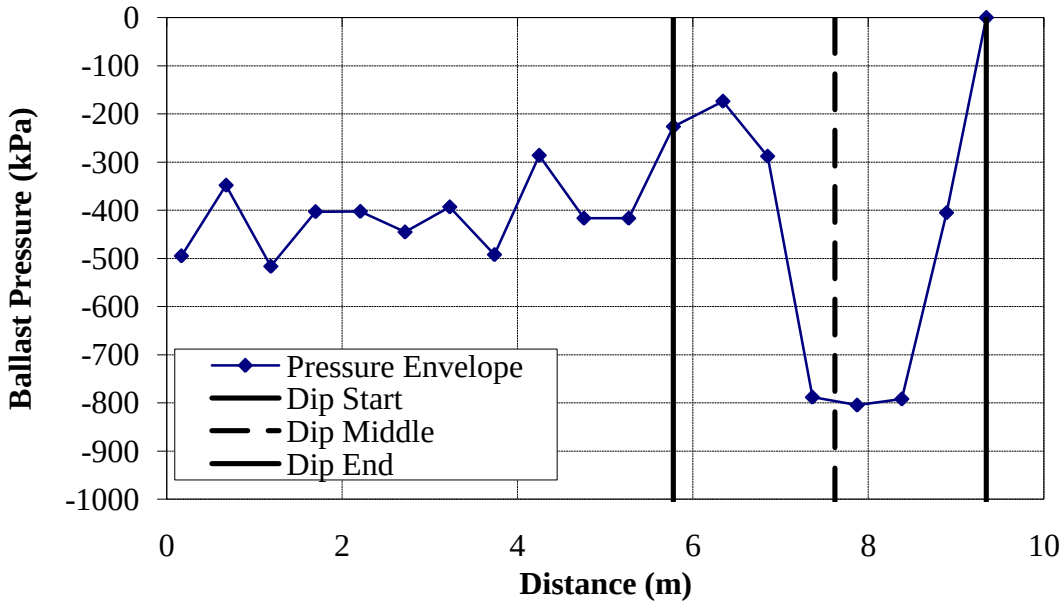

Figure F.59 - Ballast pressures due to a 1:100 Dip at a Bridge/Approach Location (Equal Height, v = 44.7 m/s)

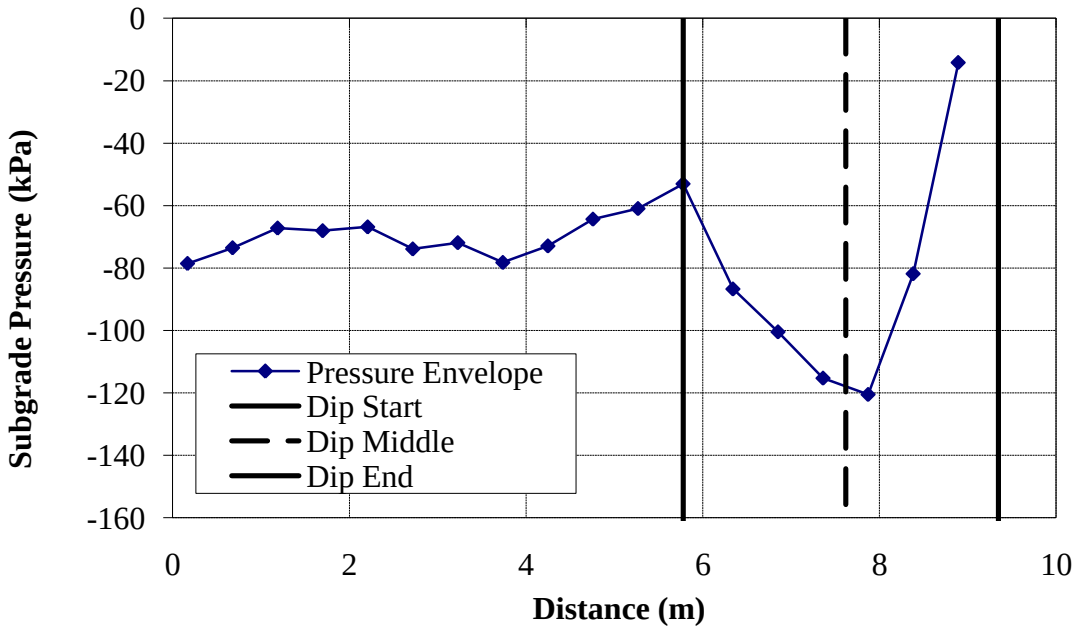

Figure F.60 - Subgrade pressures due to a 1:100 Dip at a Bridge/Approach Location (Equal Height, v = 44.7 m/s)

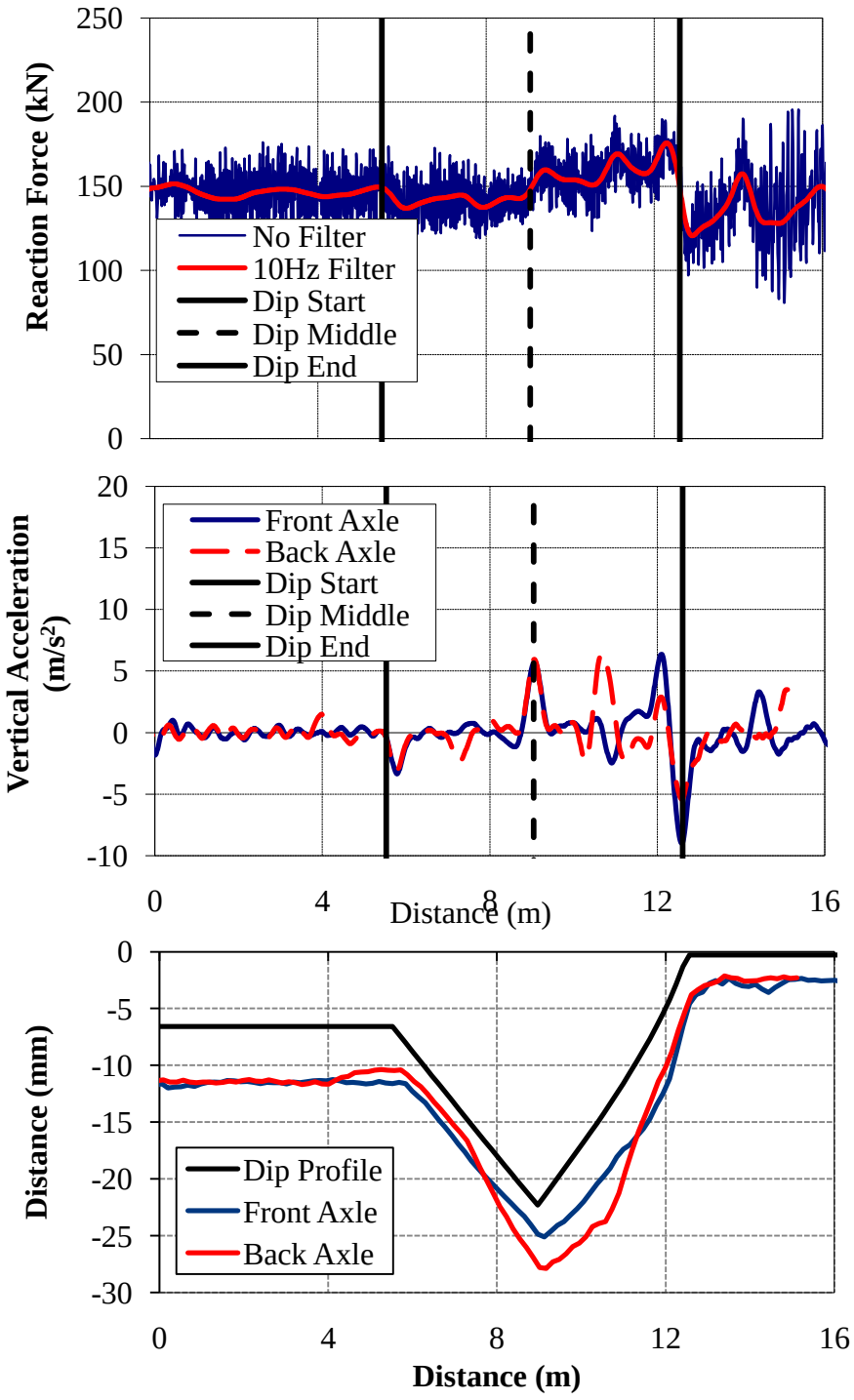

Figure F.61 - (a) Wheel/Rail Forces (b) Axle Accelerations and (c) Track Deflection due to a 1:200 Dip at a Bridge/Approach Location (Equal Height, v = 15.6 m/s)

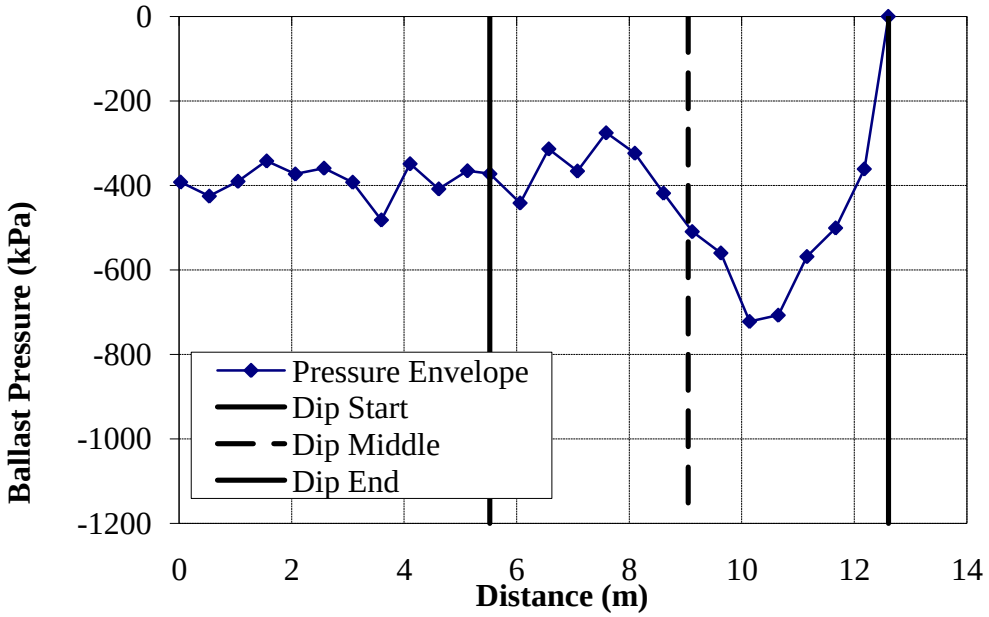

Figure F.62 – Ballast pressures due to a 1:200 Dip at a Bridge/Approach Location (Equal Height, v = 15.6 m/s)

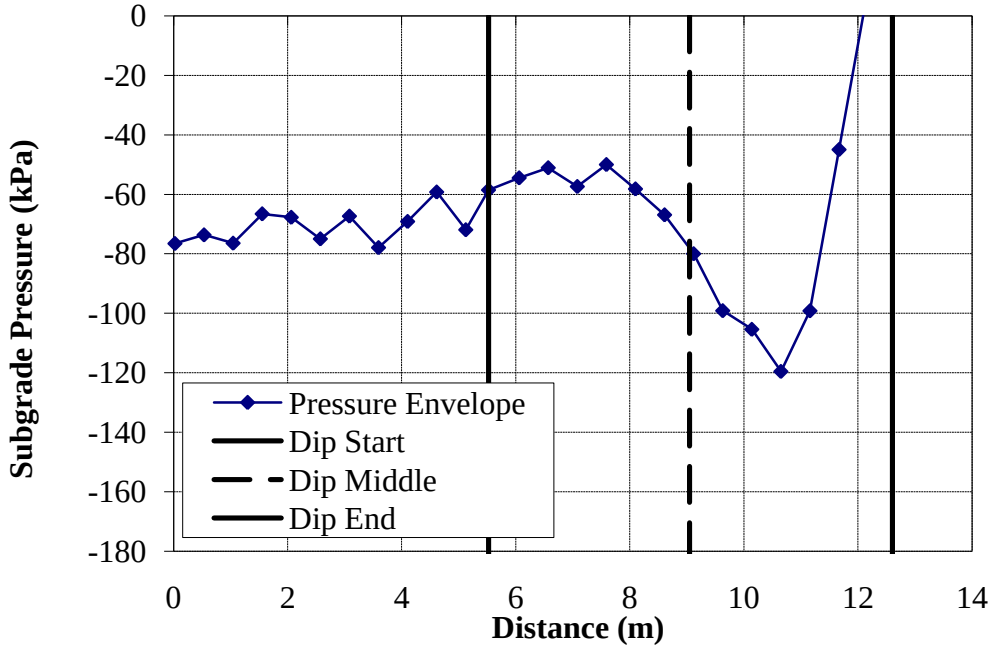

Figure F.63 - Subgrade pressures due to a 1:200 Dip at a Bridge/Approach Location (Equal Height, v = 15.6 m/s)

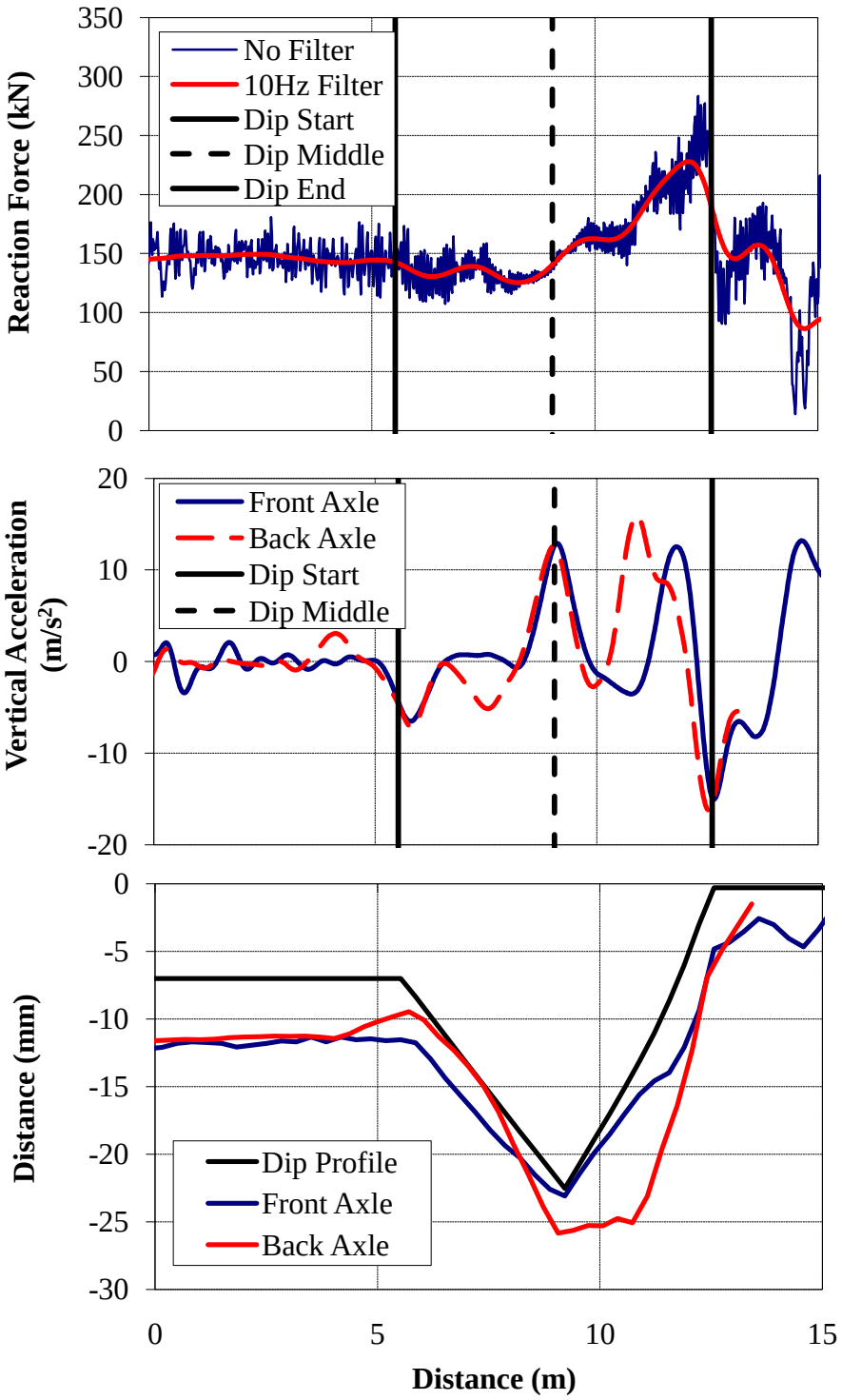

Figure F.64 - (a) Wheel/Rail Forces (b) Axle Accelerations and (c) Track Deflection due to a 1:200 Dip at a Bridge/Approach Location (Equal Height, v = 33.5 m/s)

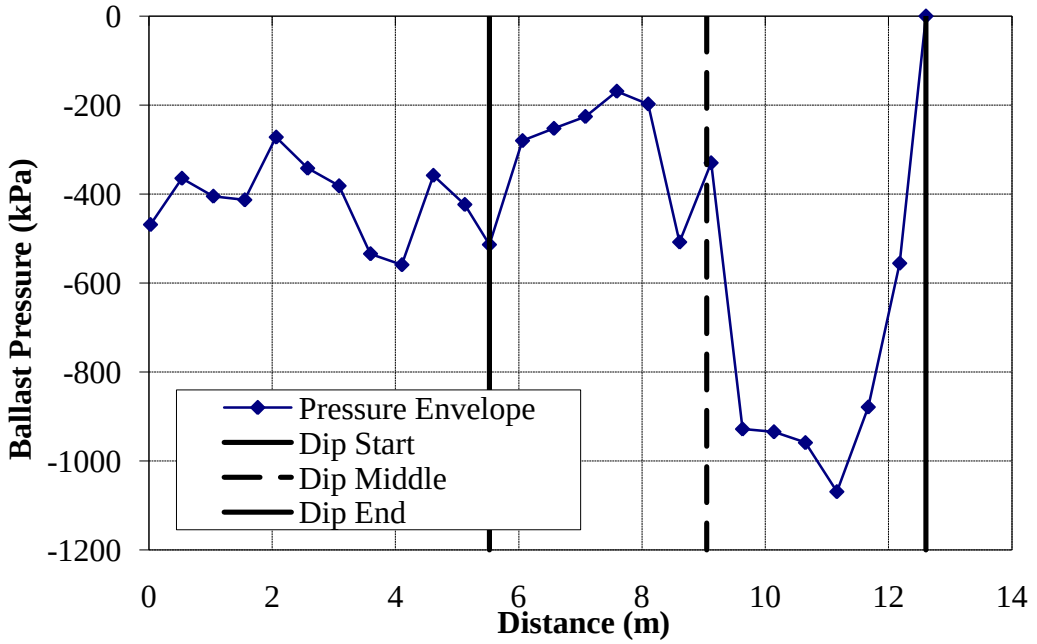

Figure F.65 – Ballast pressures due to a 1:200 Dip at a Bridge/Approach Location (Equal Height, v = 33.5 m/s)

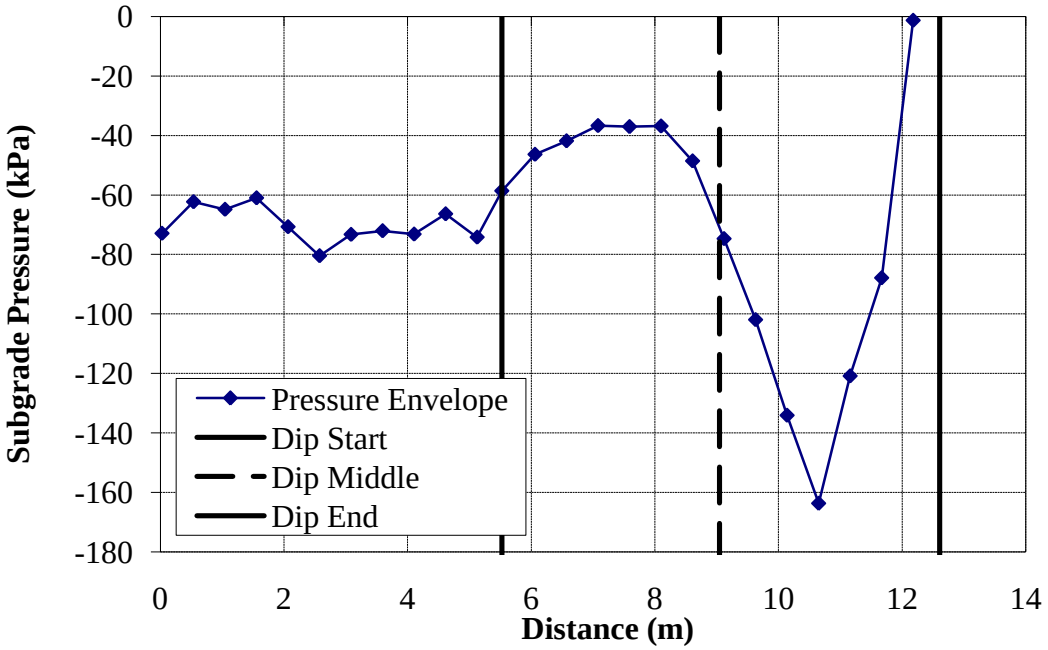

Figure F.66 - Subgrade pressures due to a 1:200 Dip at a Bridge/Approach Location (Equal Height, v = 33.5 m/s)

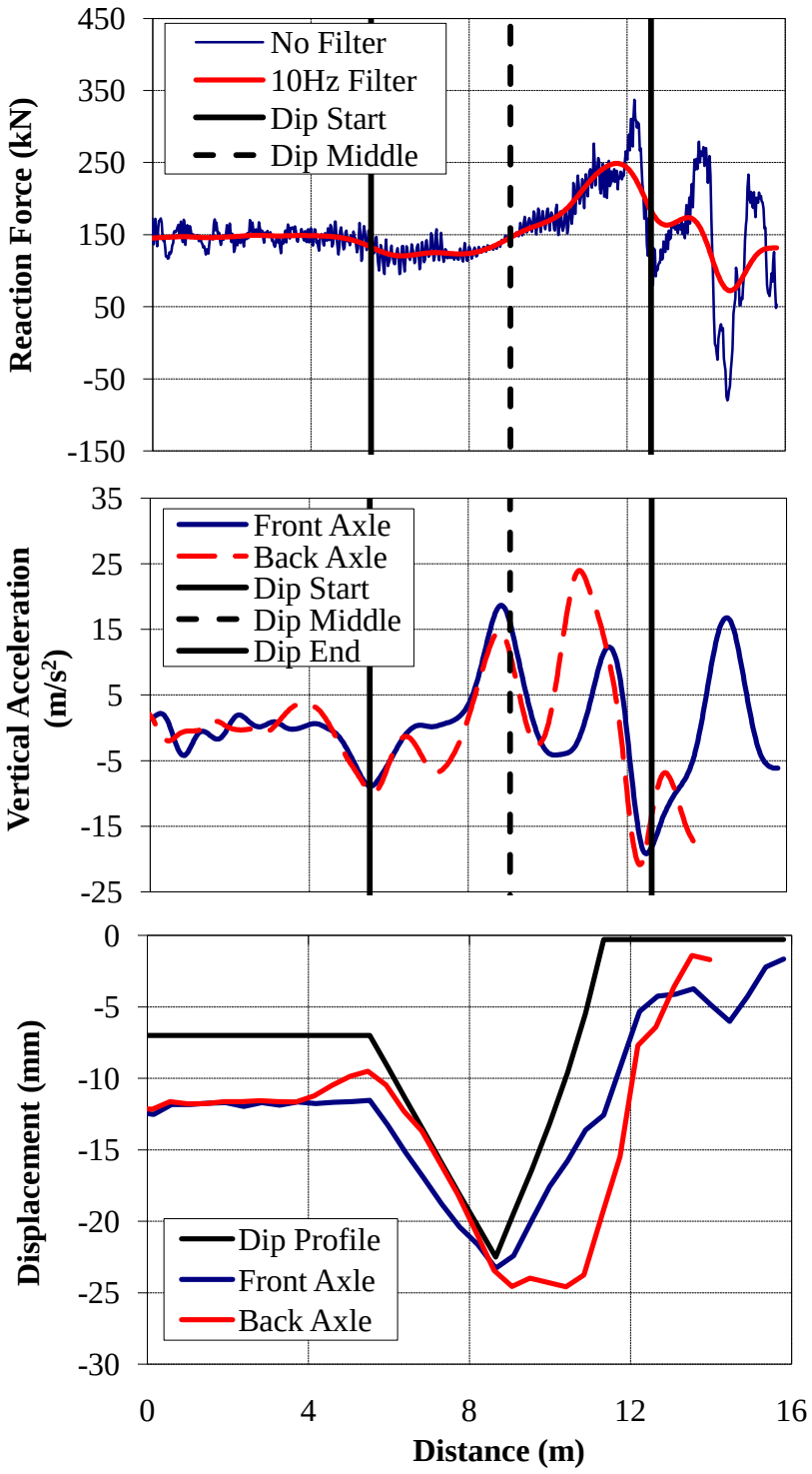

Figure F.67 - (a) Wheel/Rail Forces (b) Axle Accelerations and (c) Track Deflection due to a 1:200 Dip at a Bridge/Approach Location (Equal Height, v = 44.7 m/s)

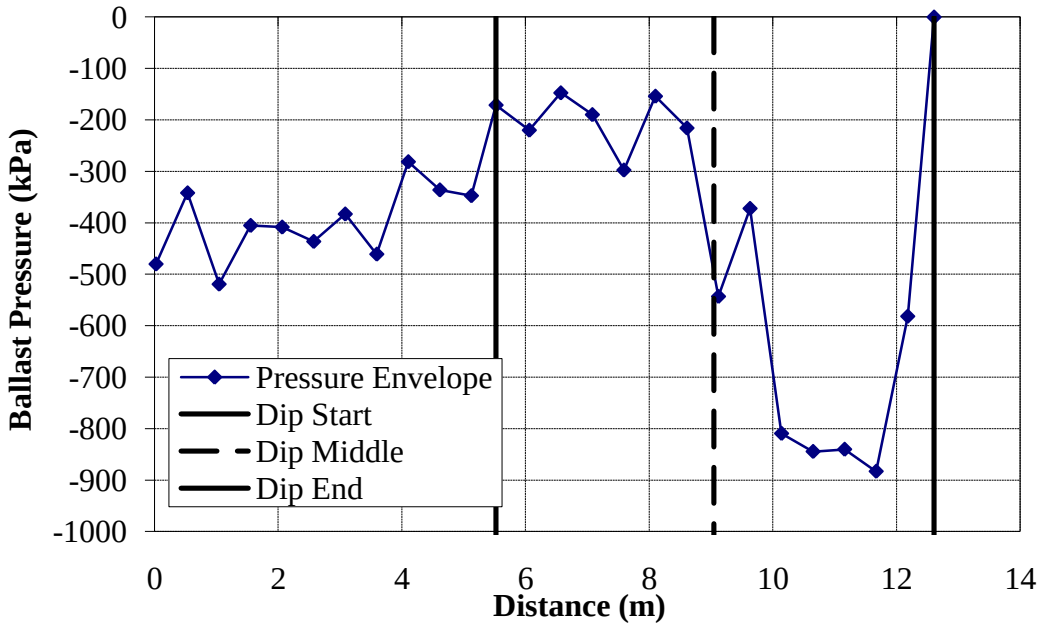

Figure F.68 – Ballast pressures due to a 1:200 Dip at a Bridge/Approach Location (Equal Height, v = 44.7 m/s)

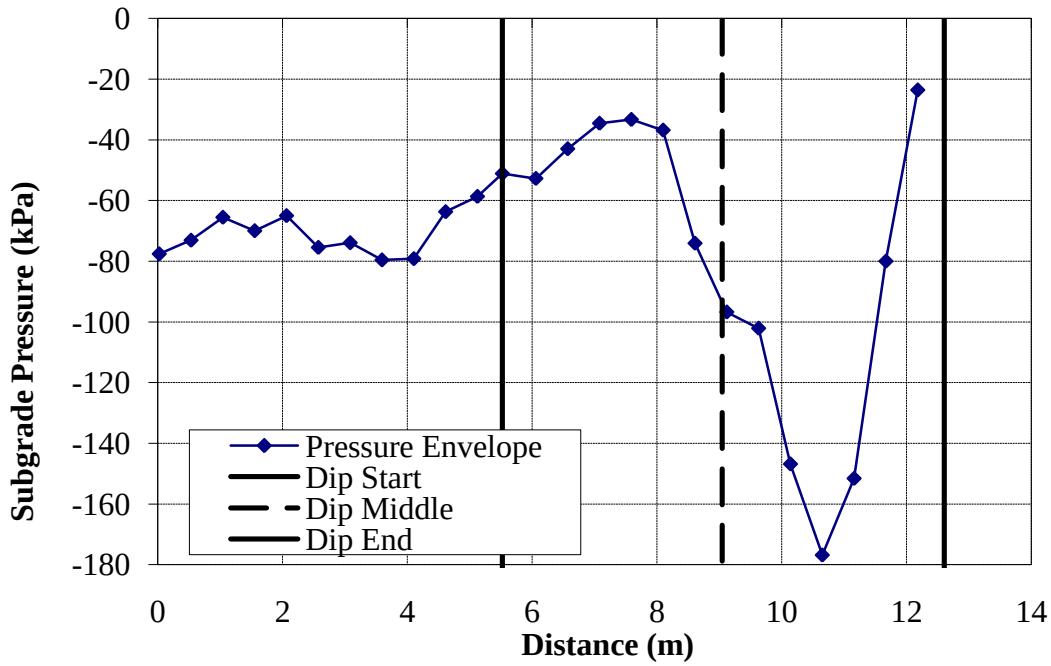

Figure F.69 - Subgrade pressures due to a 1:200 Dip at a Bridge/Approach Location (Equal Height, v = 44.7 m/s)

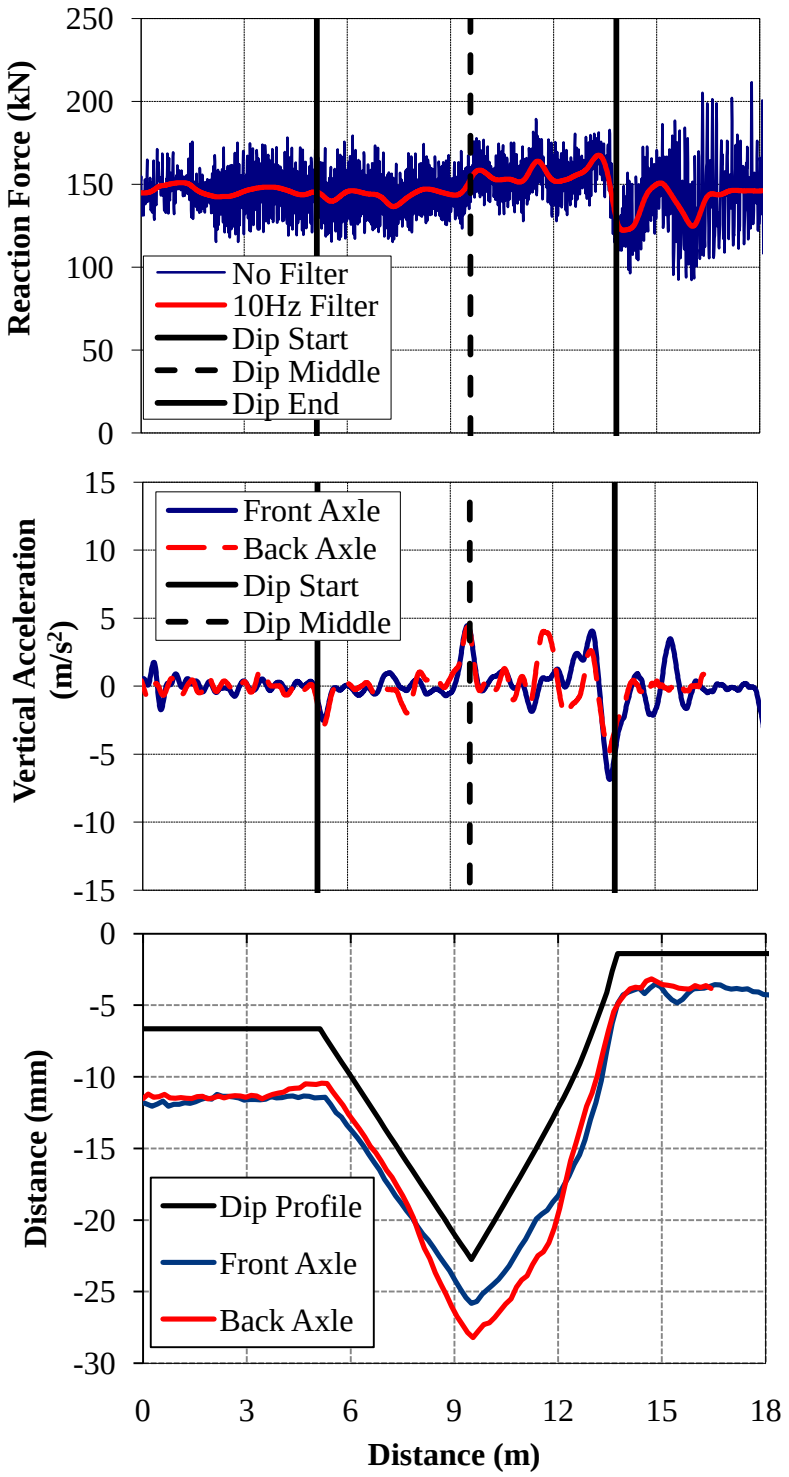

Figure F.70 - (a) Wheel/Rail Forces (b) Axle Accelerations and (c) Track Deflection due to a 1:250 Dip at a Bridge/Approach Location (Equal Height, v = 15.6 m/s)

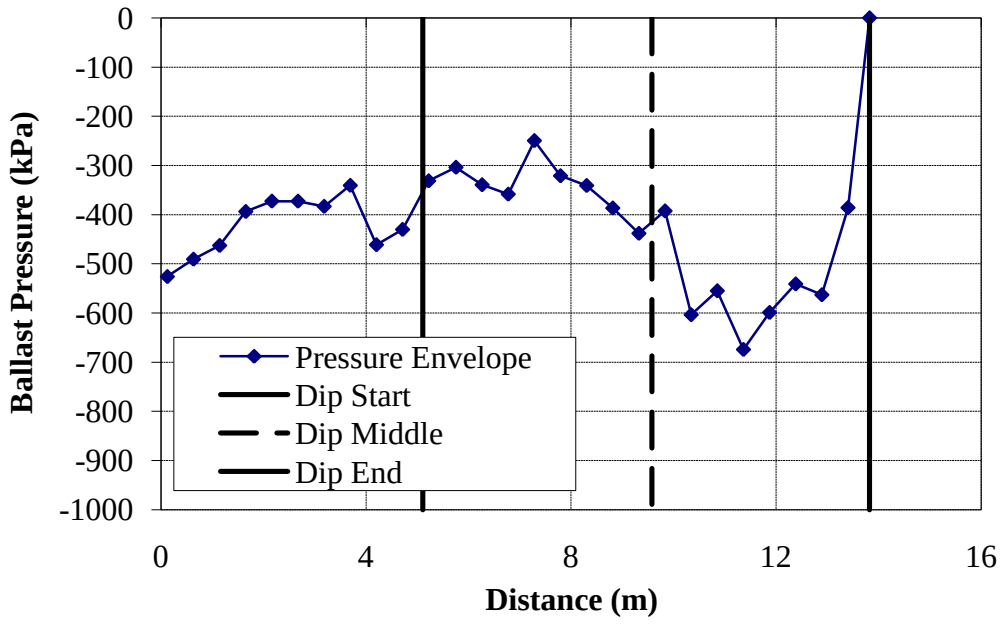

Figure F.71 – Ballast pressures due to a 1:250 Dip at a Bridge/Approach Location (Equal Height, v = 15.6 m/s)

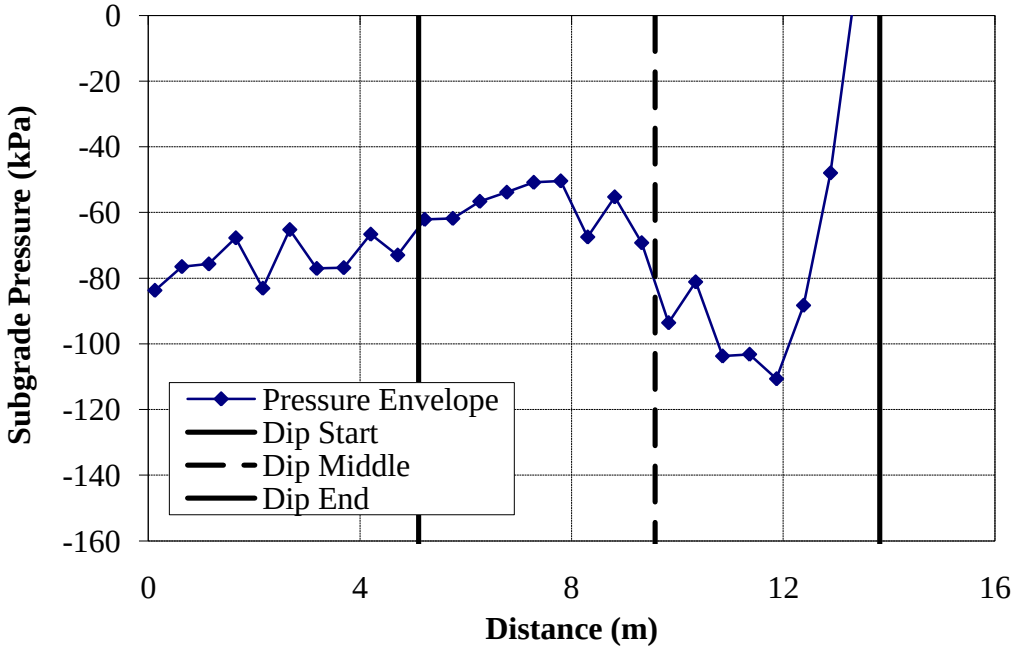

Figure F.72 - Subgrade pressures due to a 1:250 Dip at a Bridge/Approach Location (Equal Height, v = 15.6 m/s)

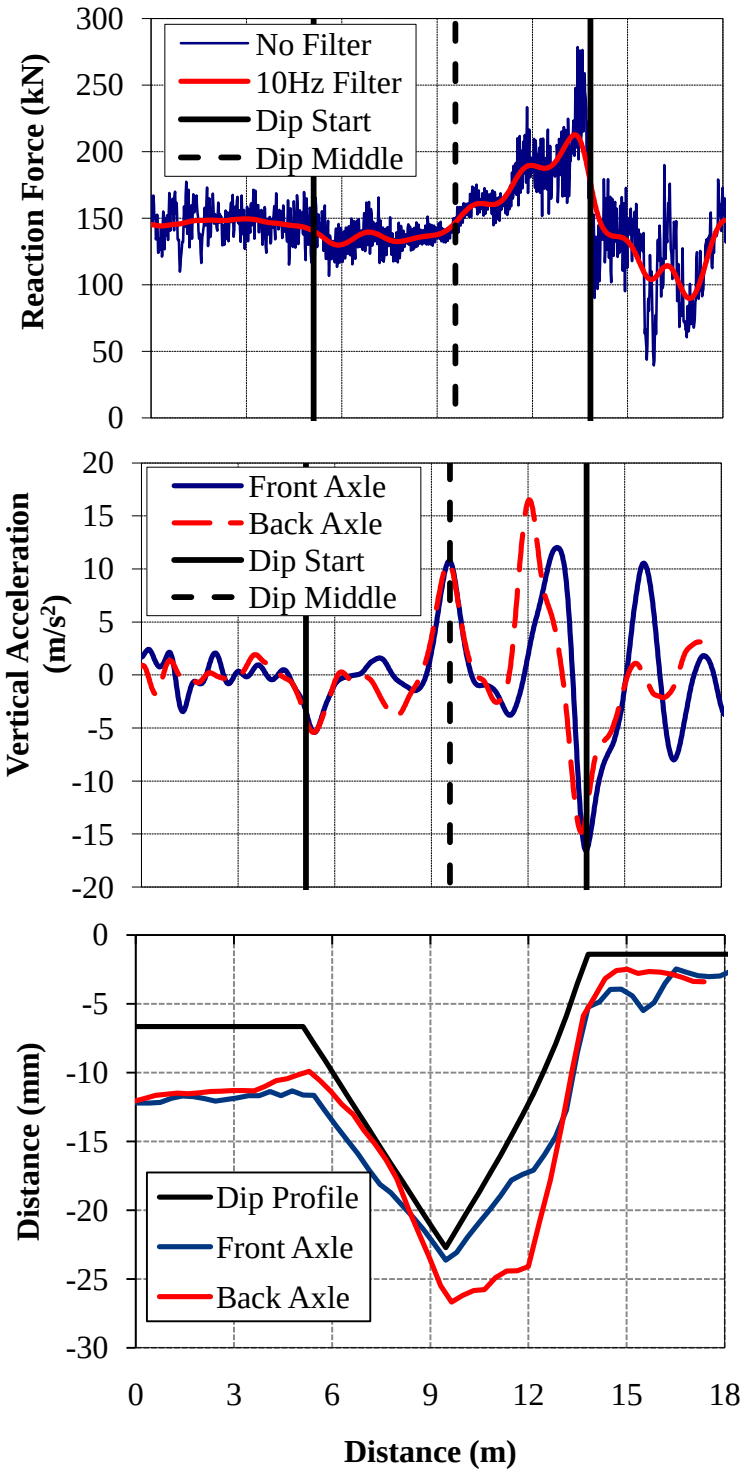

Figure F.73 - (a) Wheel/Rail Forces (b) Axle Accelerations and (c) Track Deflection due to a 1:250 Dip at a Bridge/Approach Location (Equal Height, v = 33.5 m/s)

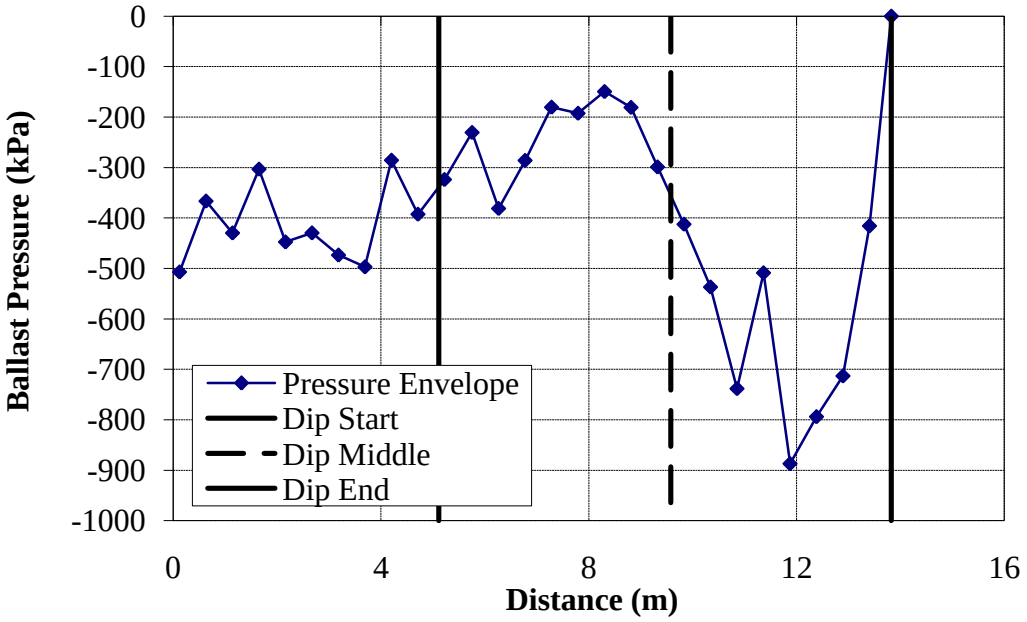

Figure F.74 – Ballast pressures due to a 1:250 Dip at a Bridge/Approach Location (Equal Height, v = 33.5 m/s)

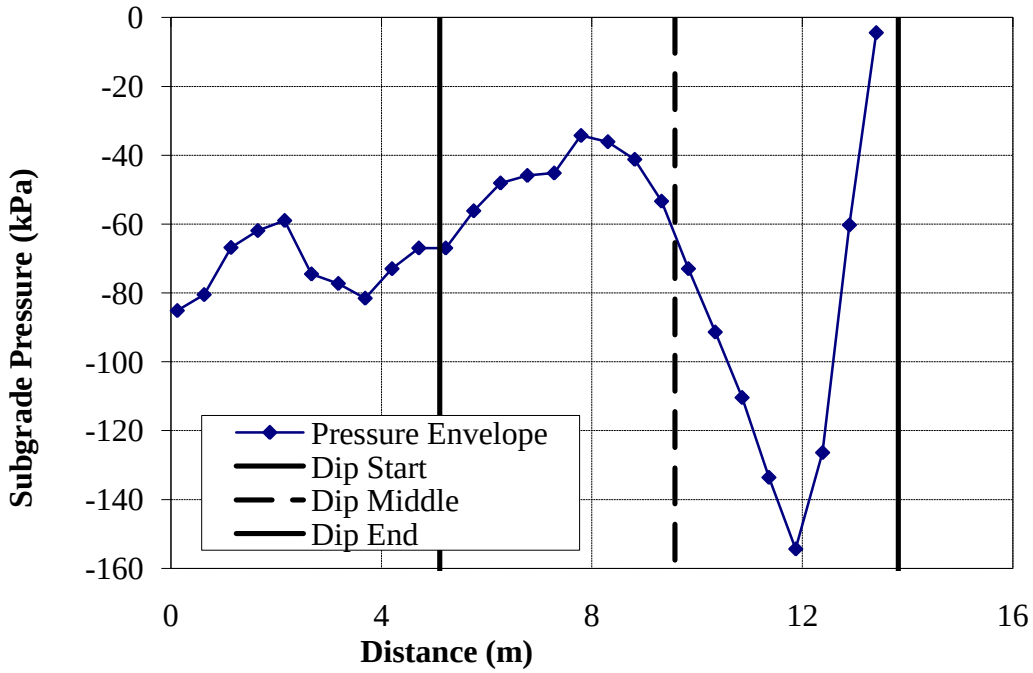

Figure F.75 - Subgrade pressures due to a 1:250 Dip at a Bridge/Approach Location (Equal Height, v = 33.5 m/s)

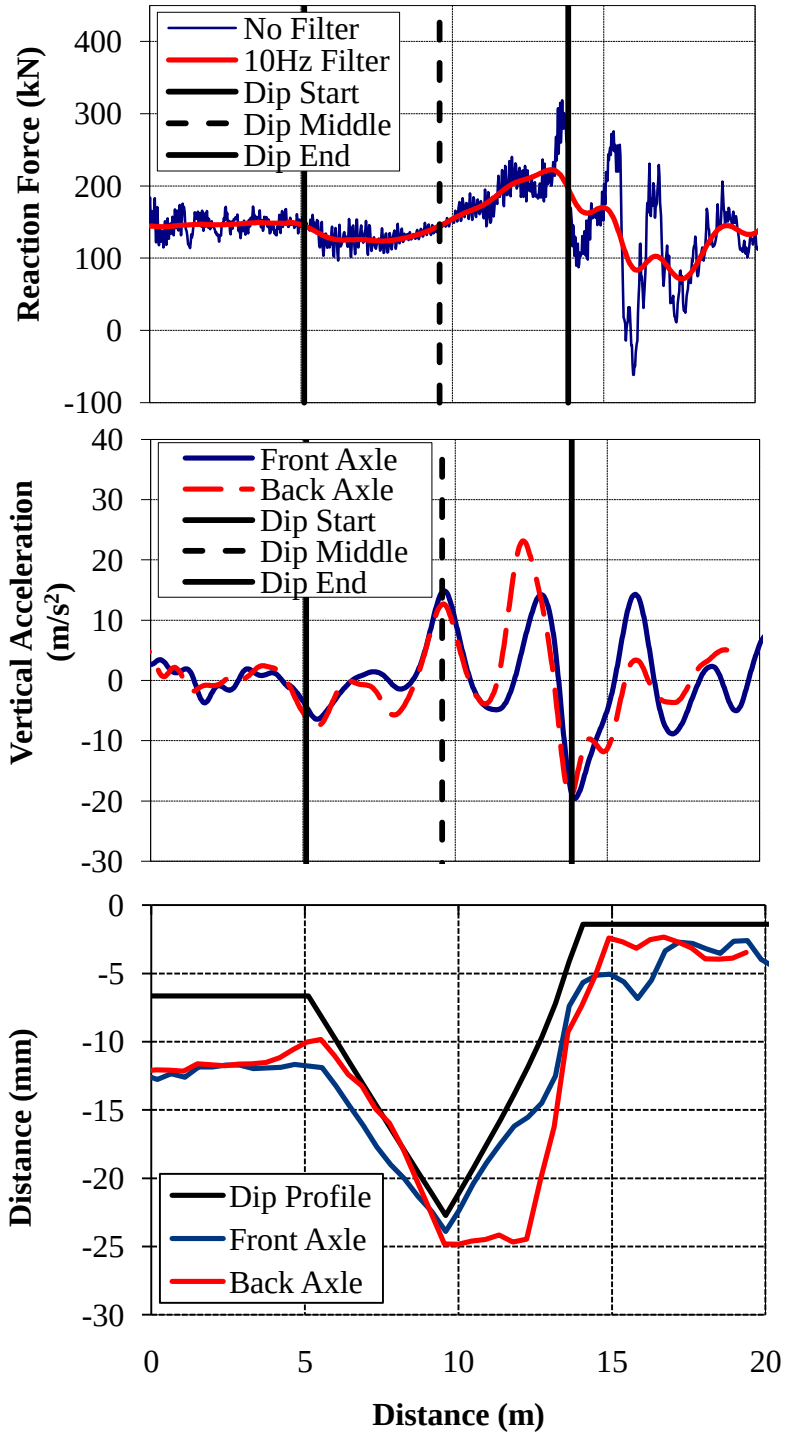

Figure F.76 - (a) Wheel/Rail Forces (b) Axle Accelerations and (c) Track Deflection due to a 1:250 Dip at a Bridge/Approach Location (Equal Height, v = 44.7 m/s)

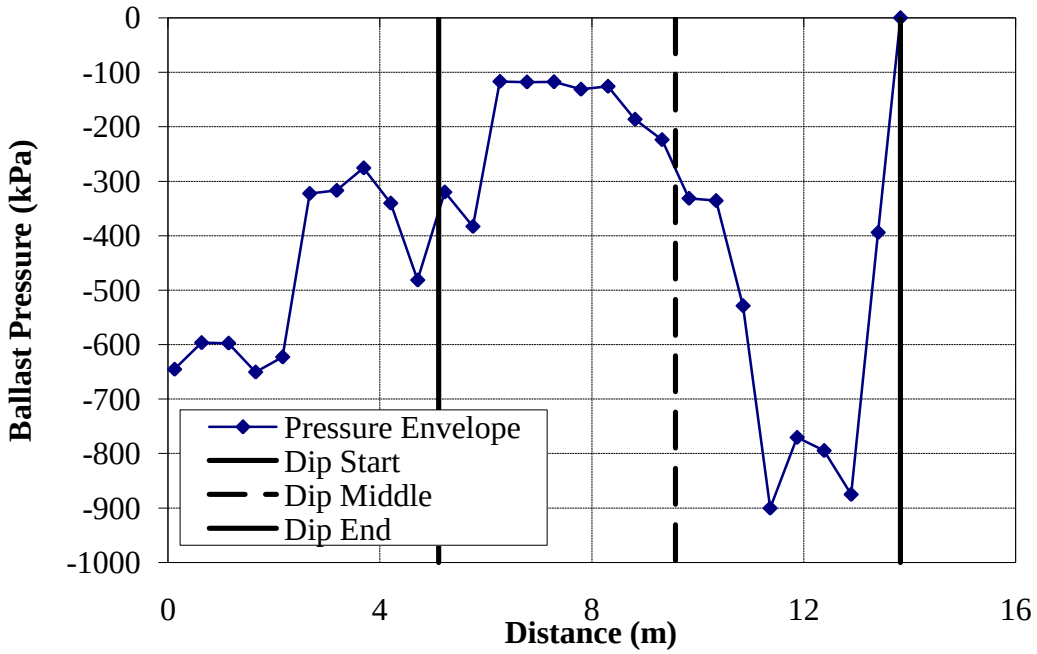

Figure F.77 – Ballast pressures due to a 1:250 Dip at a Bridge/Approach Location (Equal Height, v = 44.7 m/s)

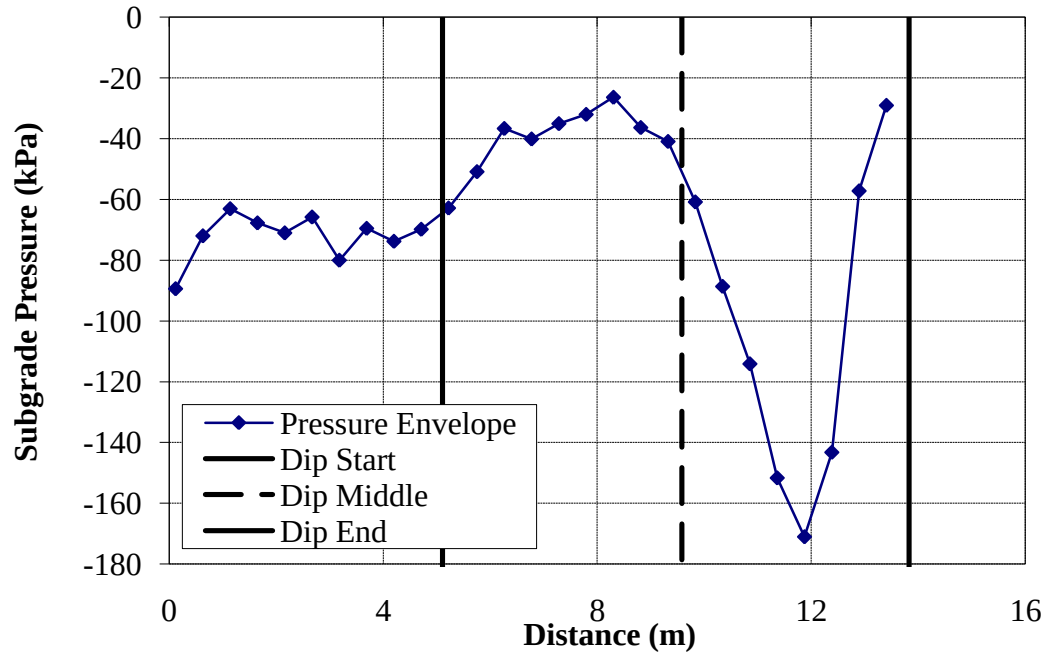

Figure F.78 - Subgrade pressures due to a 1:250 Dip at a Bridge/Approach Location (Equal Height, v = 44.7 m/s)

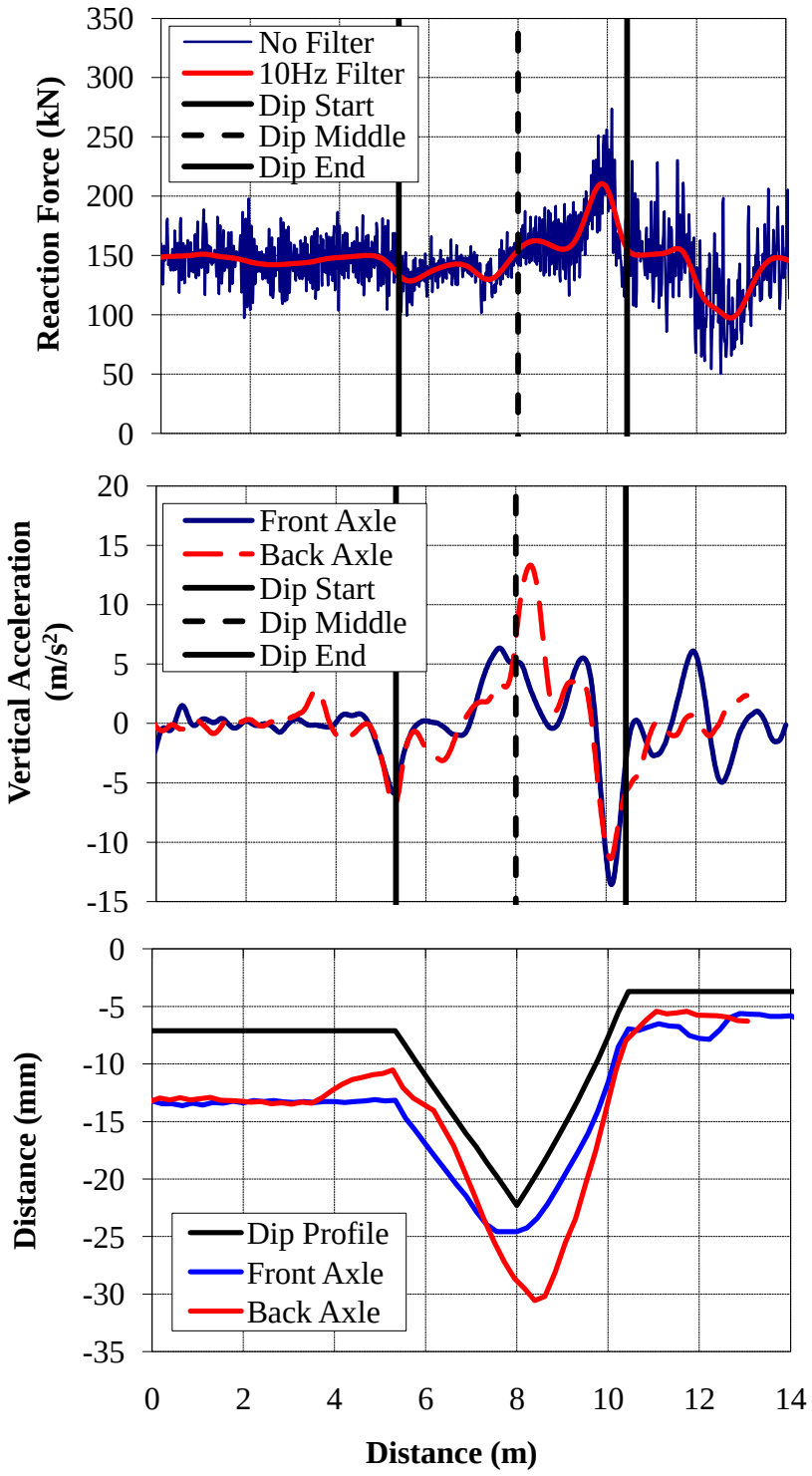

Figure F.79 - (a) Wheel/Rail Forces (b) Axle Accelerations and (c) Track Deflection due to a 1:150 Dip at a Bridge/Approach Location (20 MPa Soil and Fill Modulus, v = 22.2 m/s)

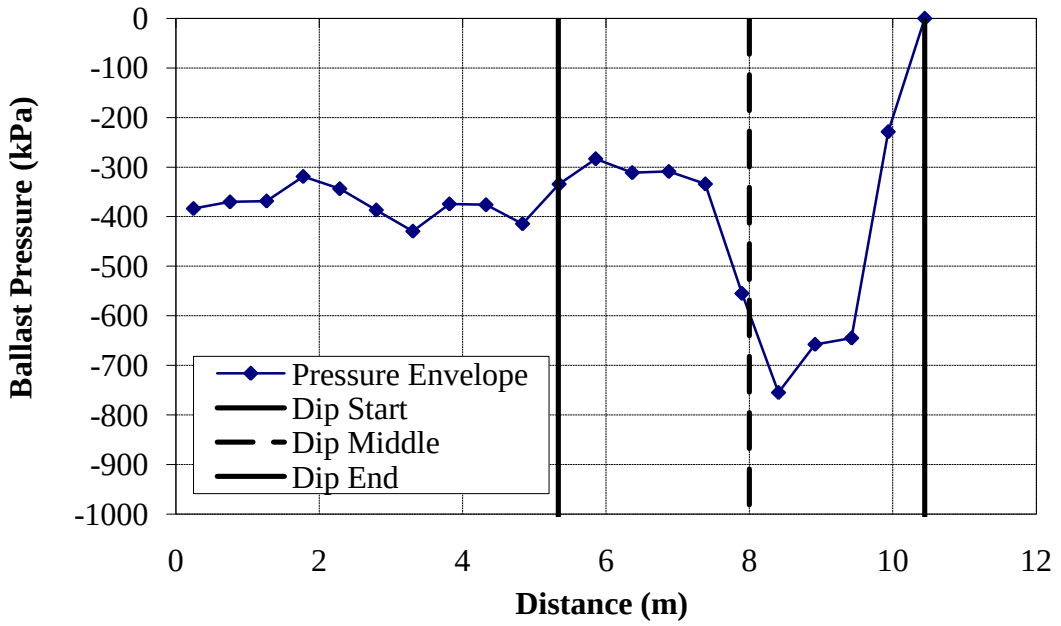

Figure F.80 – Ballast Pressures due to a 1:150 Dip at a Bridge/Approach Location (20 MPa Soil and Fill Modulus, v = 22.2 m/s)

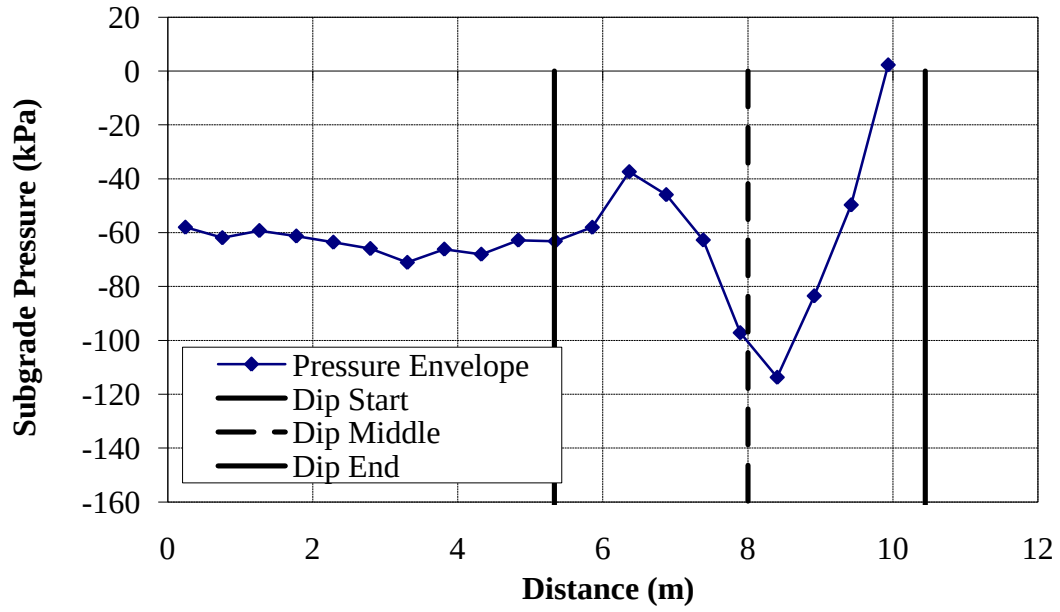

Figure F.81 - Subgrade Pressures due to a 1:150 Dip at a Bridge/Approach Location (20 MPa Soil and Fill Modulus, v = 22.2 m/s)

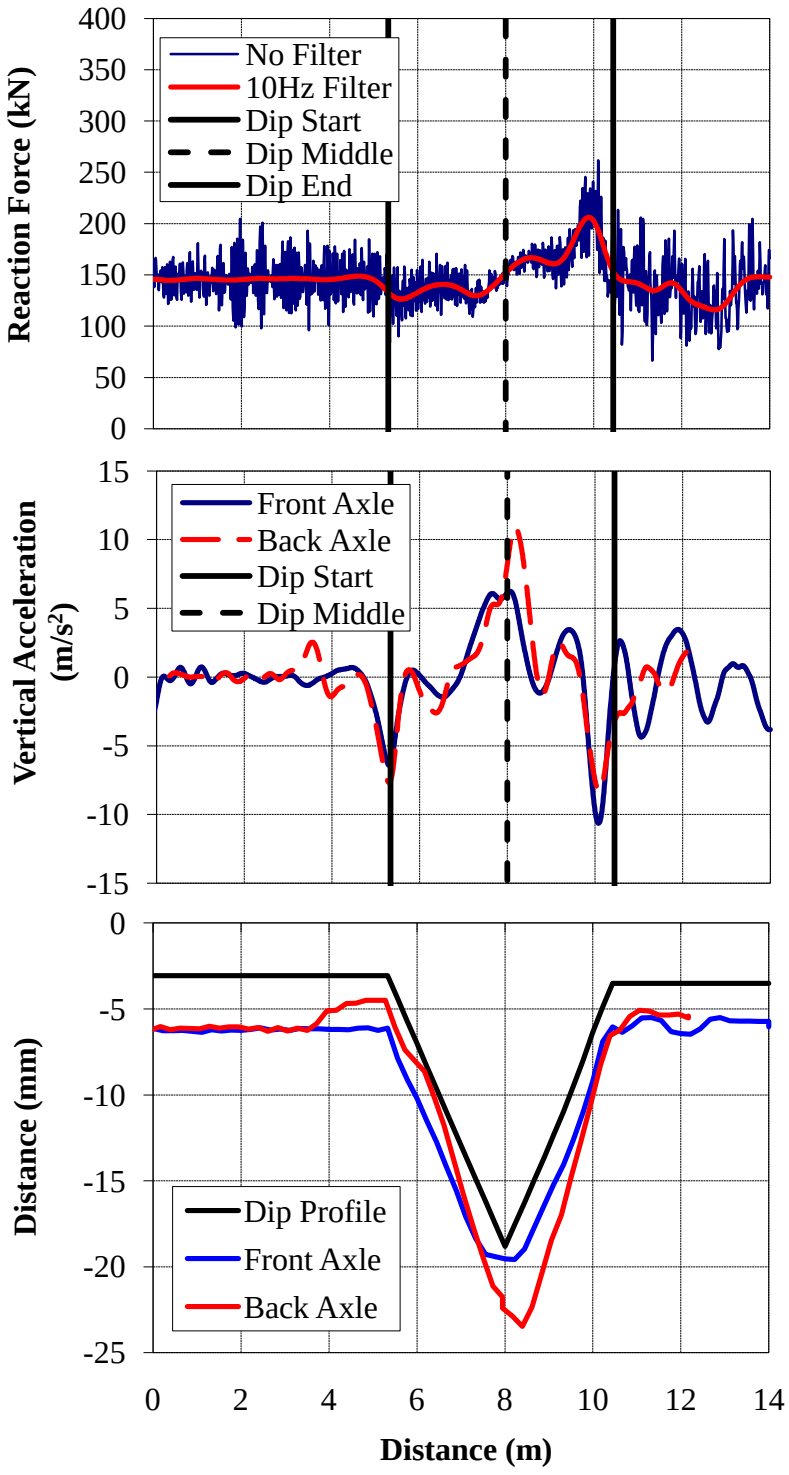

Figure F.82 - (a) Wheel/Rail Forces (b) Axle Accelerations and (c) Track Deflection due to a 1:150 Dip at a Bridge/Approach Location (50 MPa Soil and Fill Modulus, v = 22.2 m/s)

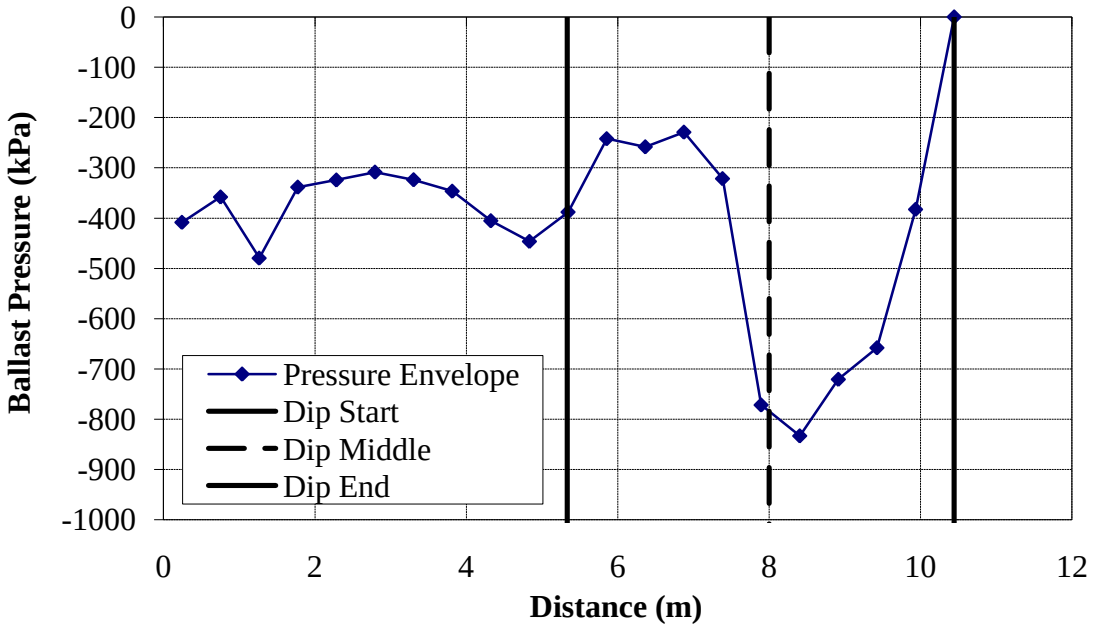

Figure F.83 – Ballast Pressures due to a 1:150 Dip at a Bridge/Approach Location (50 MPa Soil and Fill Modulus, v = 22.2 m/s)

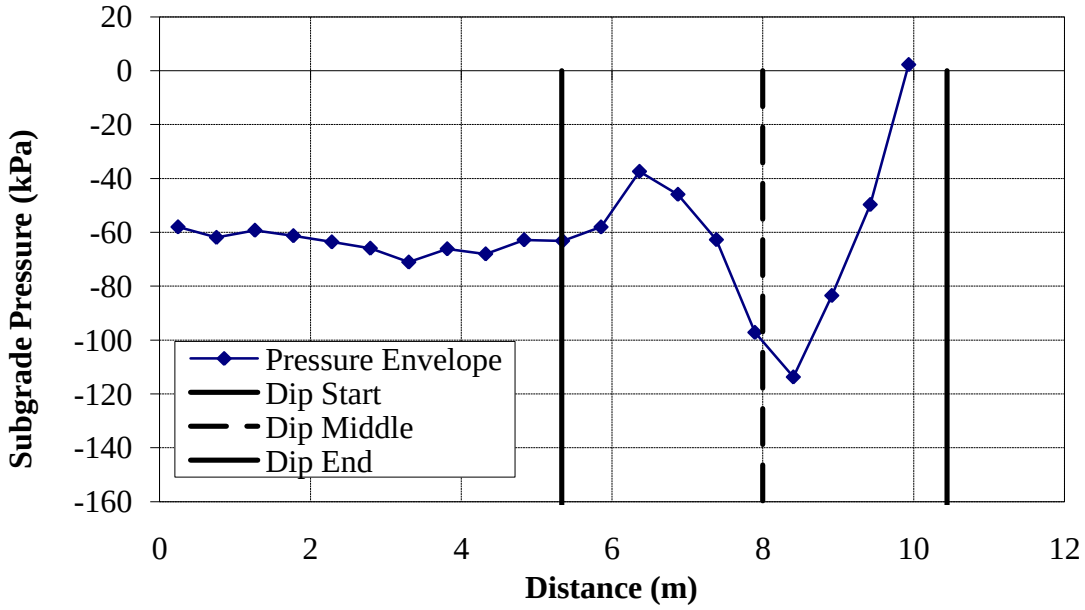

Figure F.84 - Subgrade Pressures due to a 1:150 Dip at a Bridge/Approach Location (50 MPa Soil and Fill Modulus, v = 22.2 m/s)

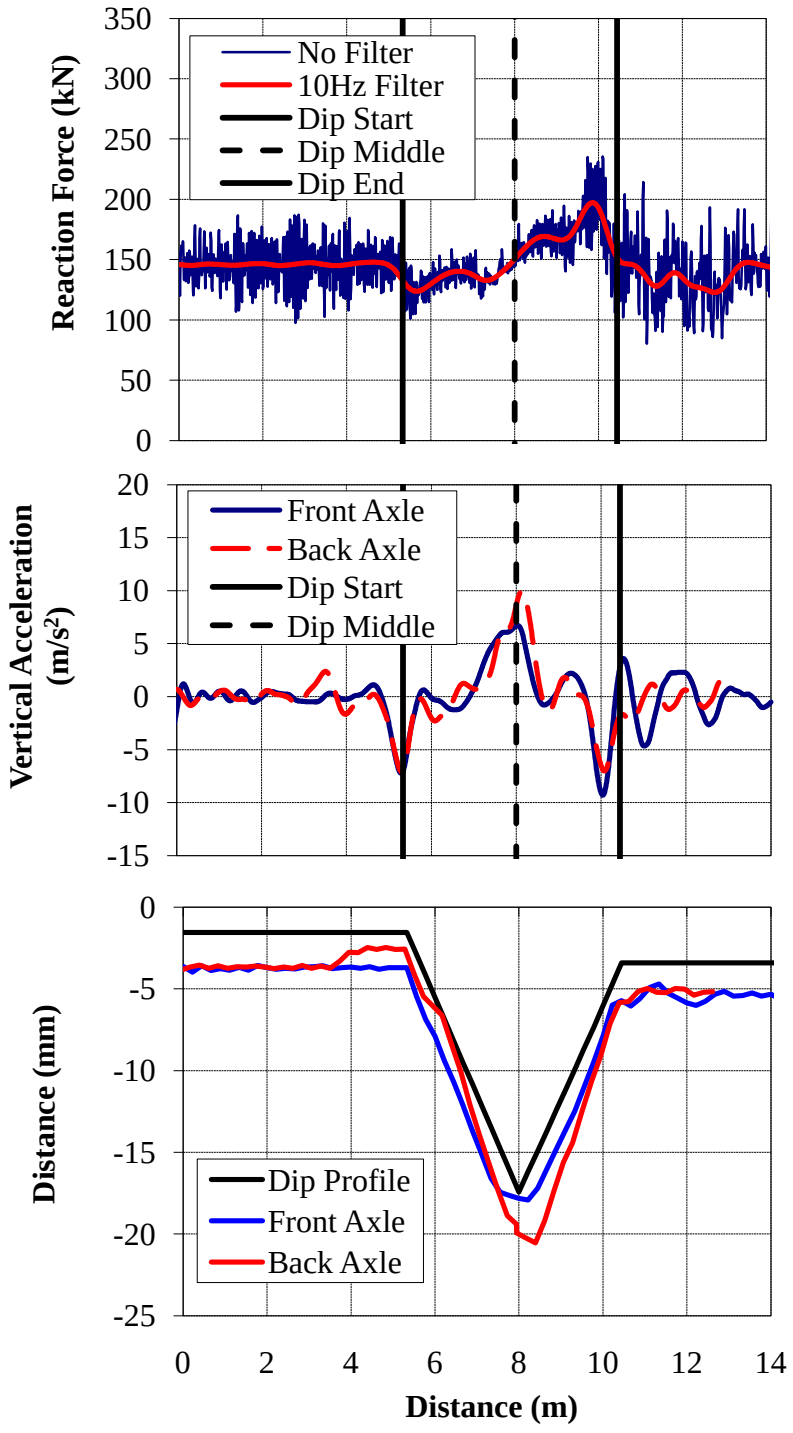

Figure F.85 - (a) Wheel/Rail Forces (b) Axle Accelerations and (c) Track Deflection due to a 1:150 Dip at a Bridge/Approach Location (100 MPa Soil and Fill Modulus, v = 22.2 m/s)

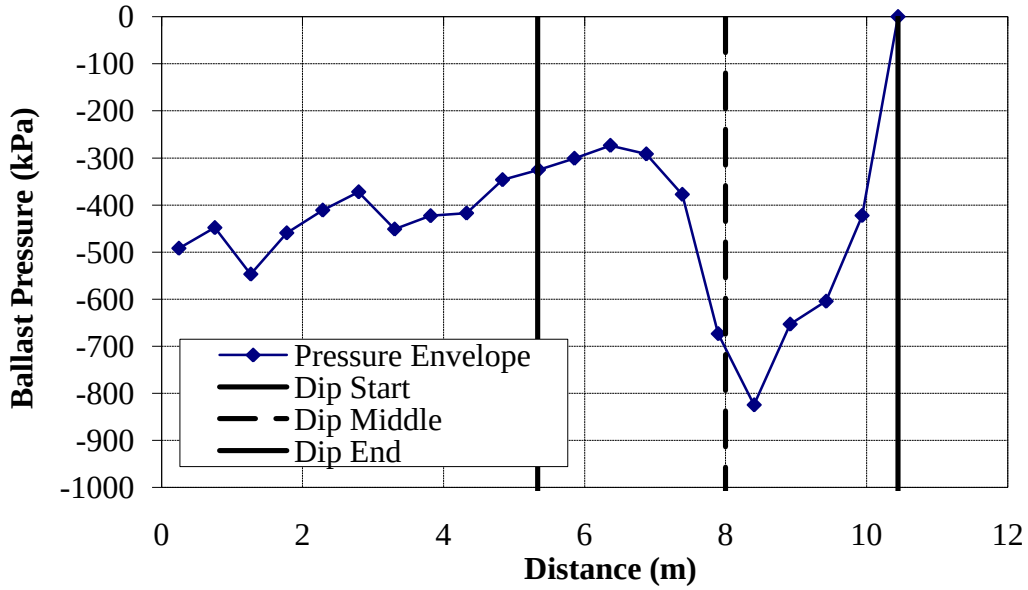

Figure F.86 – Ballast Pressures due to a 1:150 Dip at a Bridge/Approach Location (100 MPa Soil and Fill Modulus, v = 22.2 m/s)

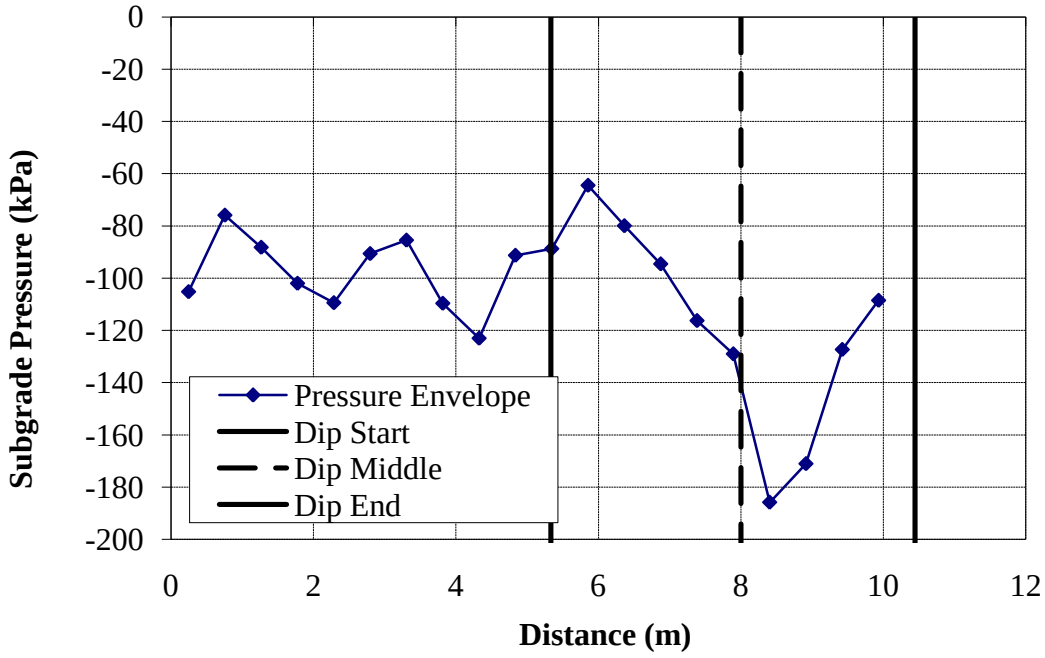

Figure F.87 - Subgrade Pressures due to a 1:150 Dip at a Bridge/Approach Location (100 MPa Soil and Fill Modulus, v = 22.2 m/s)

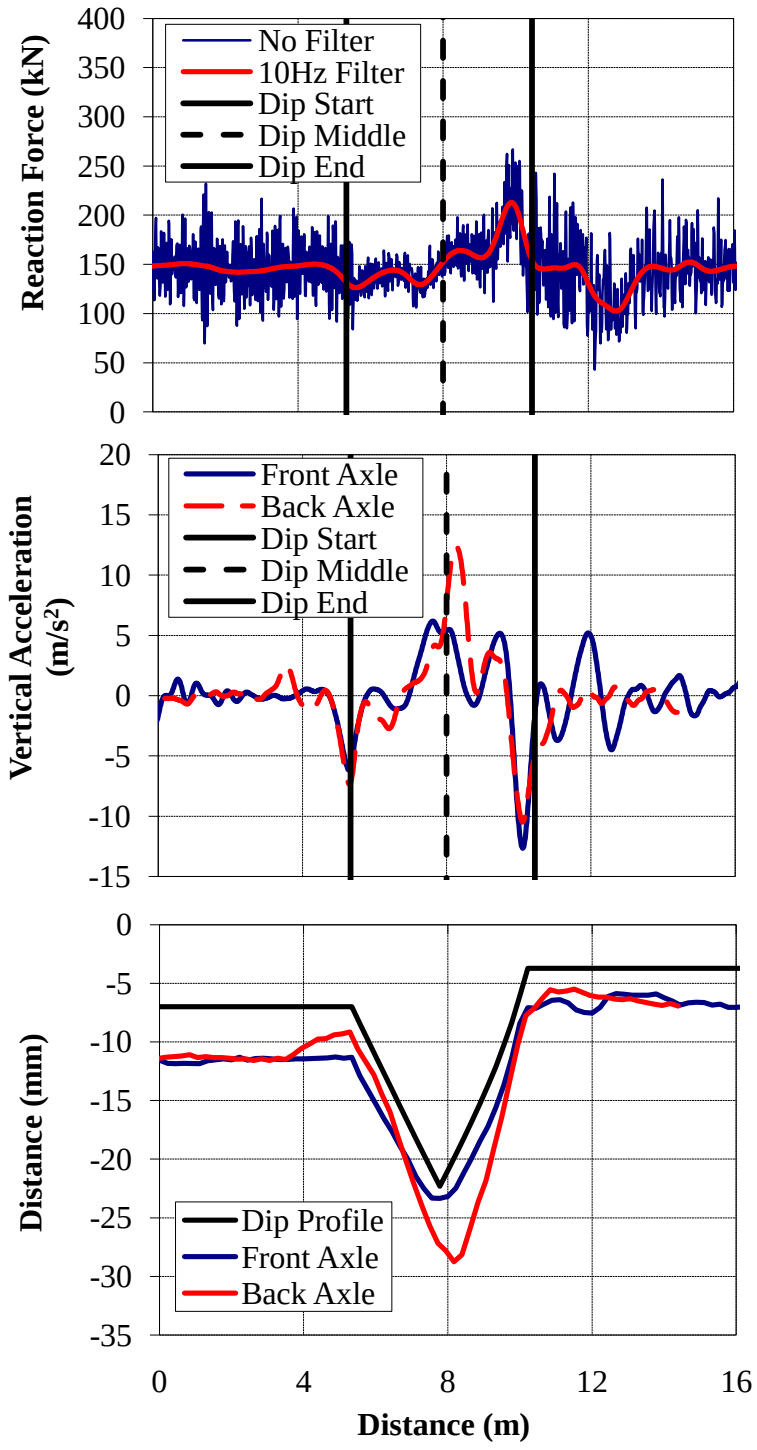

Figure F.88 - (a) Wheel/Rail Forces (b) Axle Accelerations and (c) Track Deflection due to a 1:150 Dip at a Bridge/Approach Location with Concrete Approach Ties (v = 22.2 m/s)

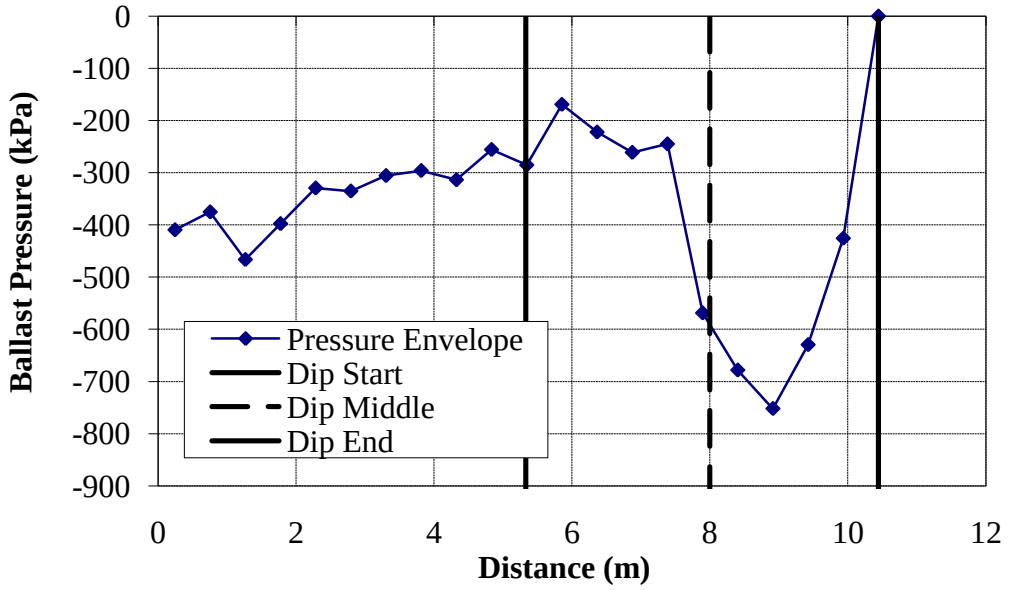

Figure F.89 – Ballast Pressures due to a 1:150 Dip at a Bridge/Approach Location with Concrete Approach Ties (v = 22.2 m/s)

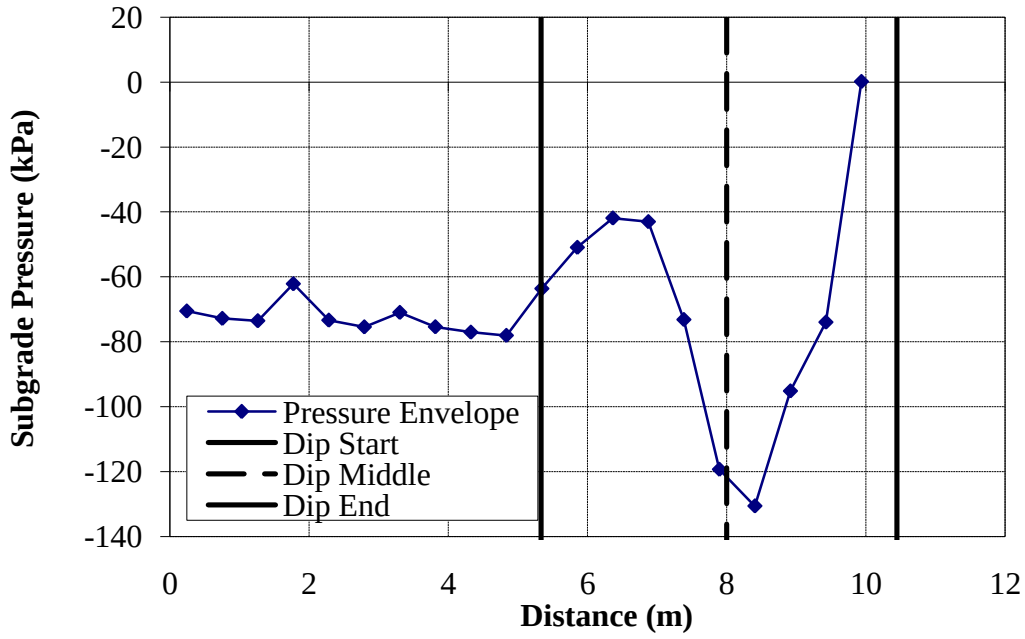

Figure F.90 - Subgrade Pressures due to a 1:150 Dip at a Bridge/Approach Location with Concrete Approach Ties (v = 22.2 m/s)

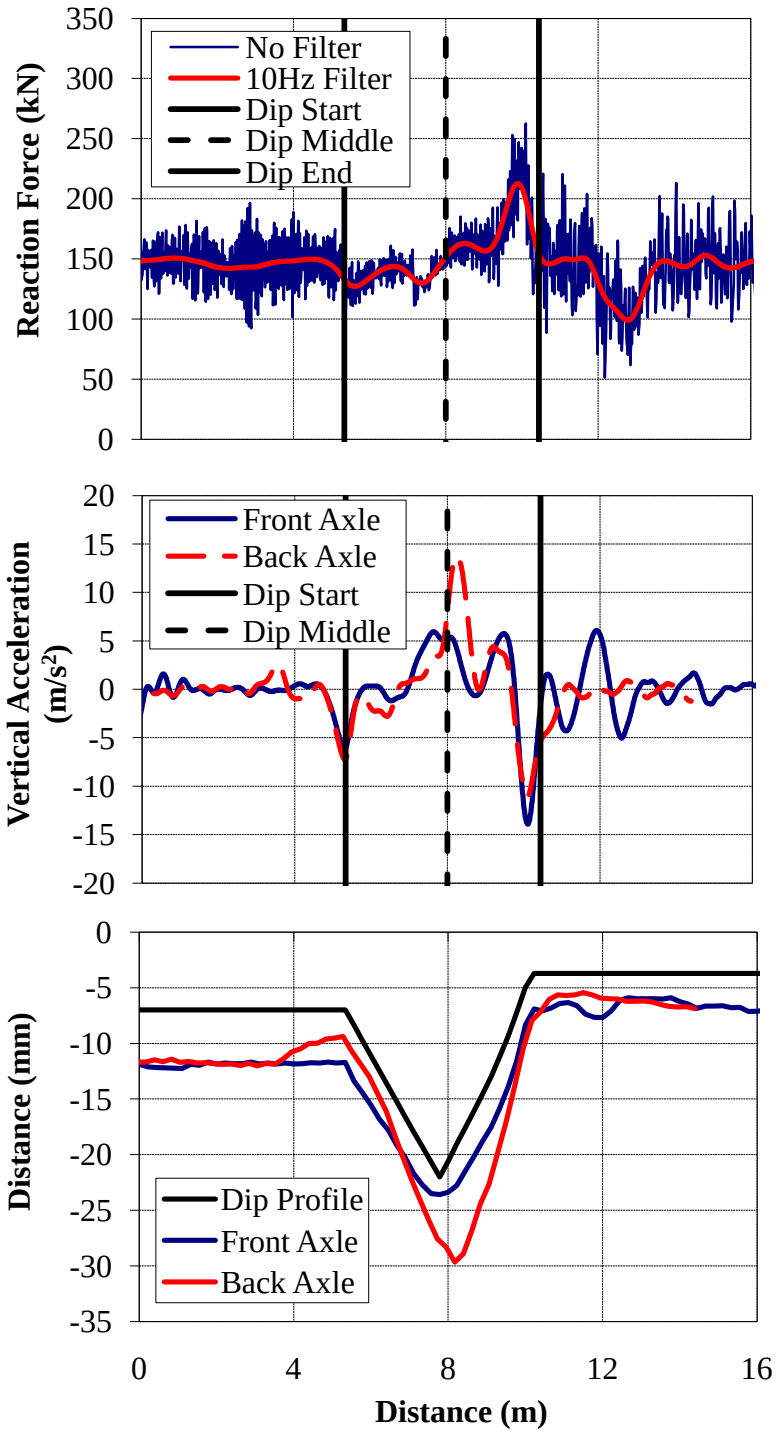

Figure F.91 - (a) Wheel/Rail Forces (b) Axle Accelerations and (c) Track Deflection due to a 1:150 Dip at a Bridge/Approach Location with Plastic Approach Ties (v = 22.2 m/s)

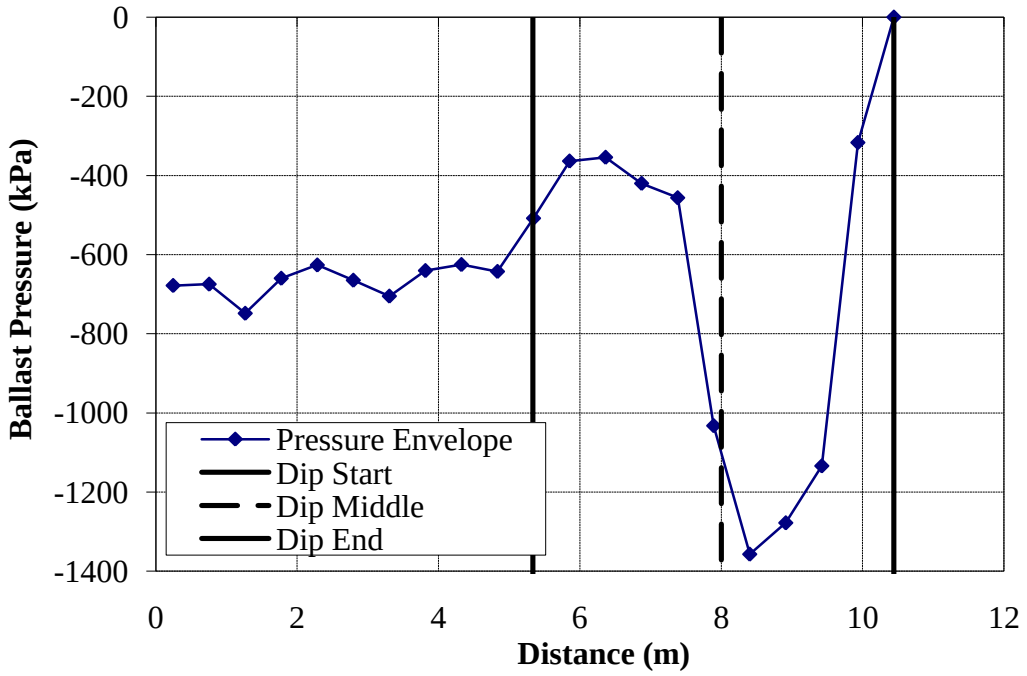

Figure F.92 – Ballast Pressures due to a 1:150 Dip at a Bridge/Approach Location with Plastic Approach Ties (v = 22.2 m/s)

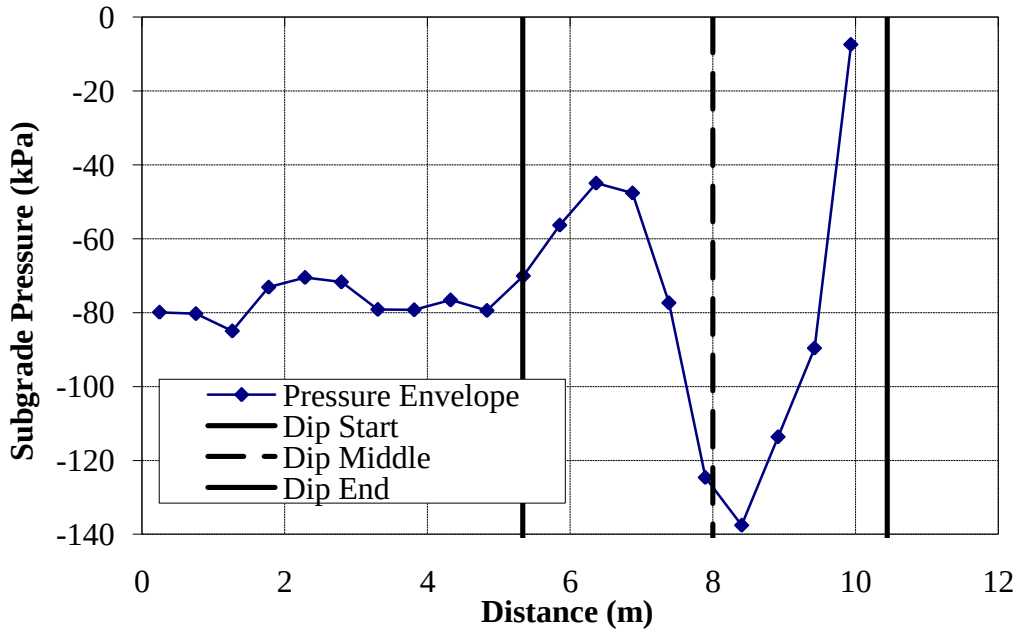

Figure F.93 - Subgrade Pressures due to a 1:150 Dip at a Bridge/Approach Location with Plastic Approach Ties (v = 22.2 m/s)

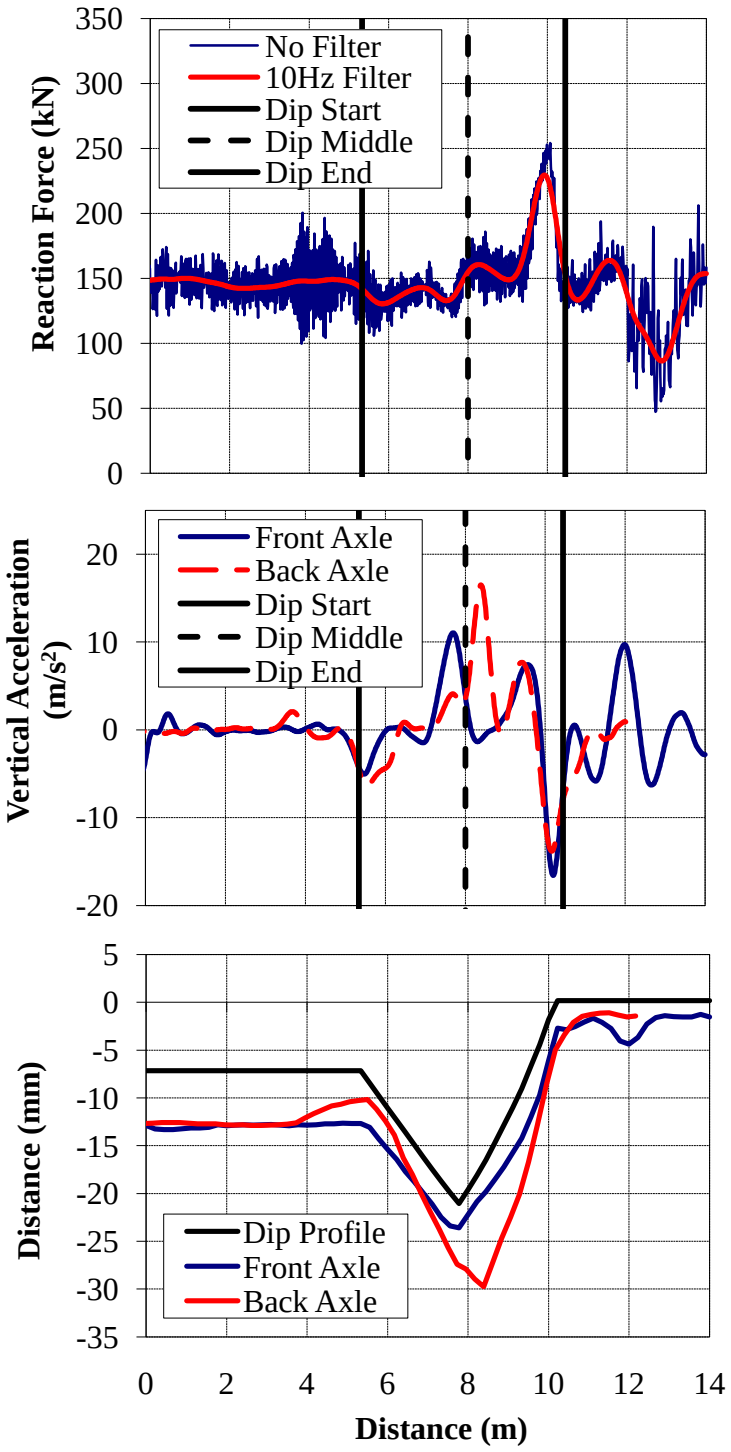

Figure F.94 - (a) Wheel/Rail Forces (b) Axle Accelerations and (c) Track Deflection due to a 1:150 Dip at a Bridge/Approach Location with Wood Approach Ties and Rubber Rail Seat Pads (v = 22.2 m/s)

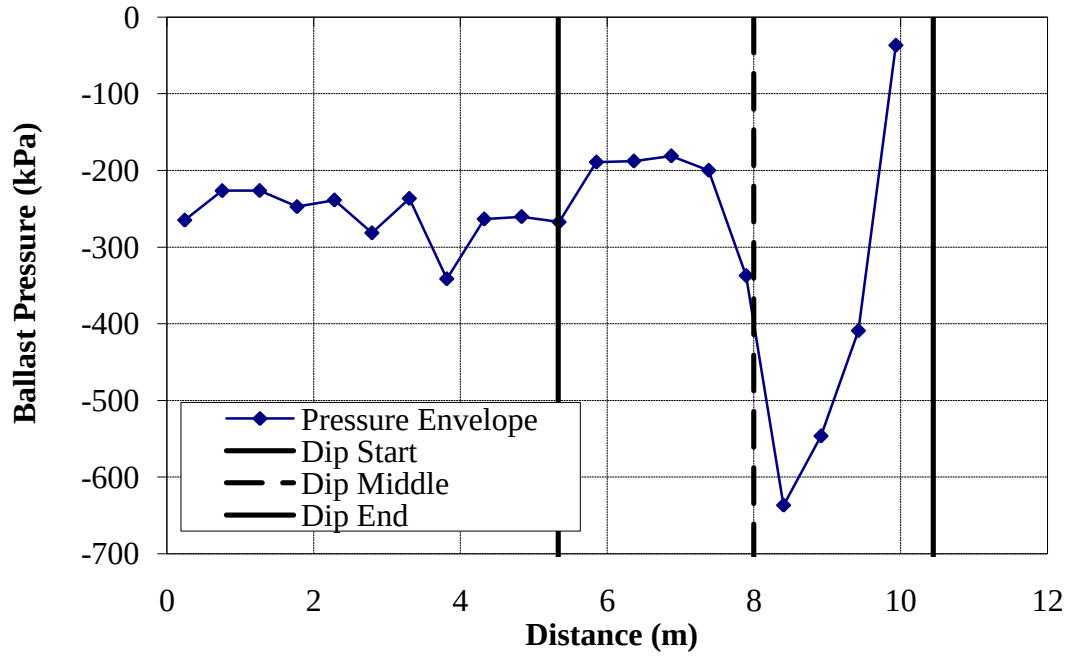

Figure F.95 – Ballast Pressures due to a 1:150 Dip at a Bridge/Approach Location with Wood Approach Ties and Rubber Rail Seat Pads (v = 22.2 m/s)

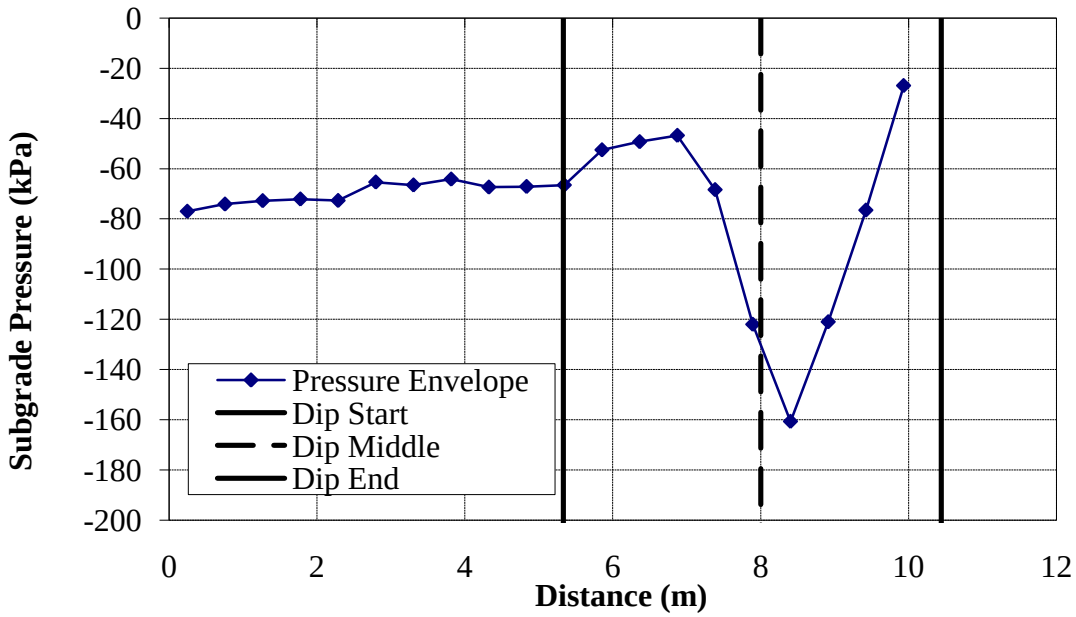

Figure F.96 - Subgrade Pressures due to a 1:150 Dip at a Bridge/Approach Location with Wood Approach Ties and Rubber Rail Seat Pads (v = 22.2 m/s)

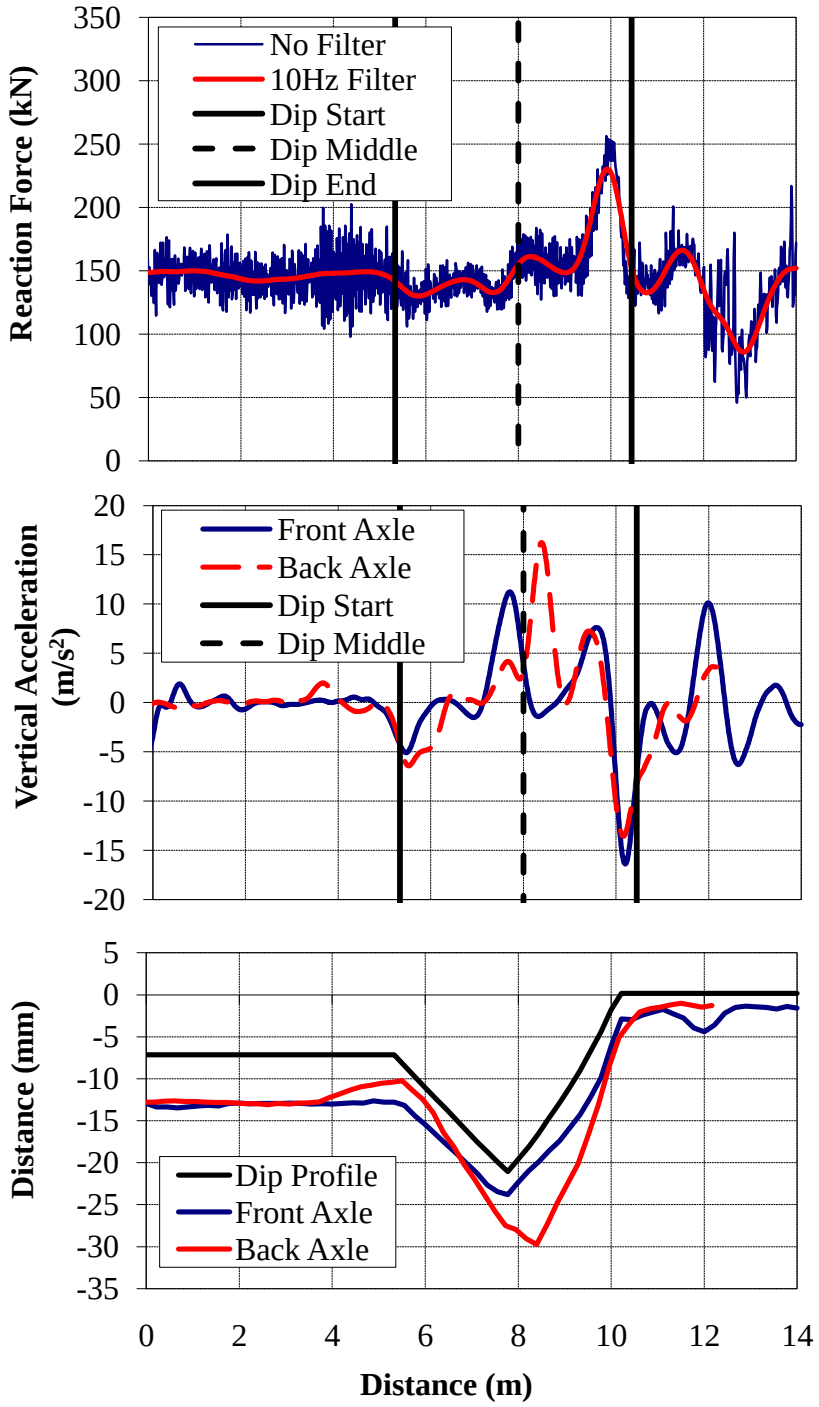

Figure F.97 - (a) Wheel/Rail Forces (b) Axle Accelerations and (c) Track Deflection due to a 1:150 Dip at a Bridge/Approach Location with Concrete Approach Ties and Rubber Rail Seat Pads (v = 22.2 m/s)

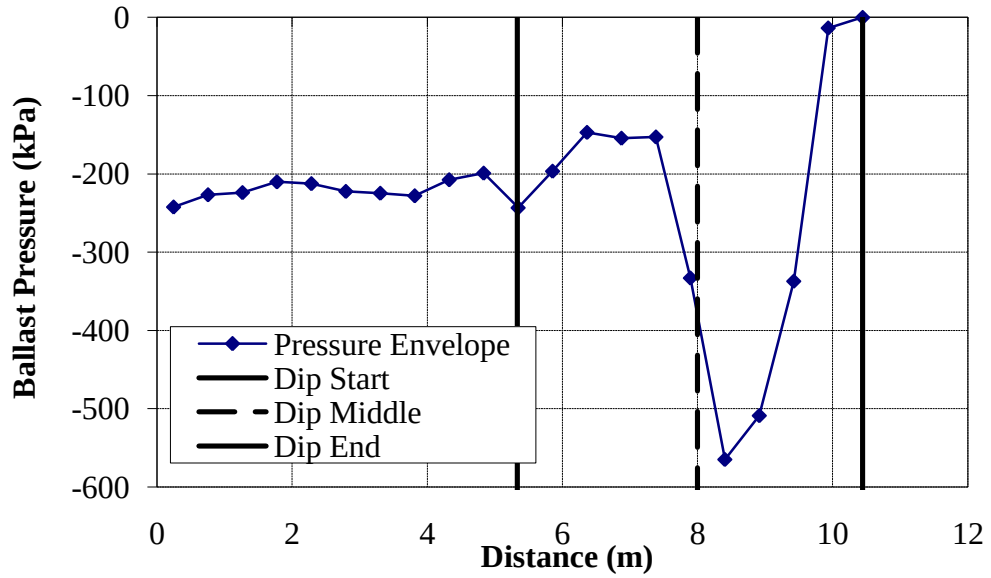

Figure F.98 – Ballast Pressures due to a 1:150 Dip at a Bridge/Approach Location with Concrete Approach Ties and Rubber Rail Seat Pads (v = 22.2 m/s)

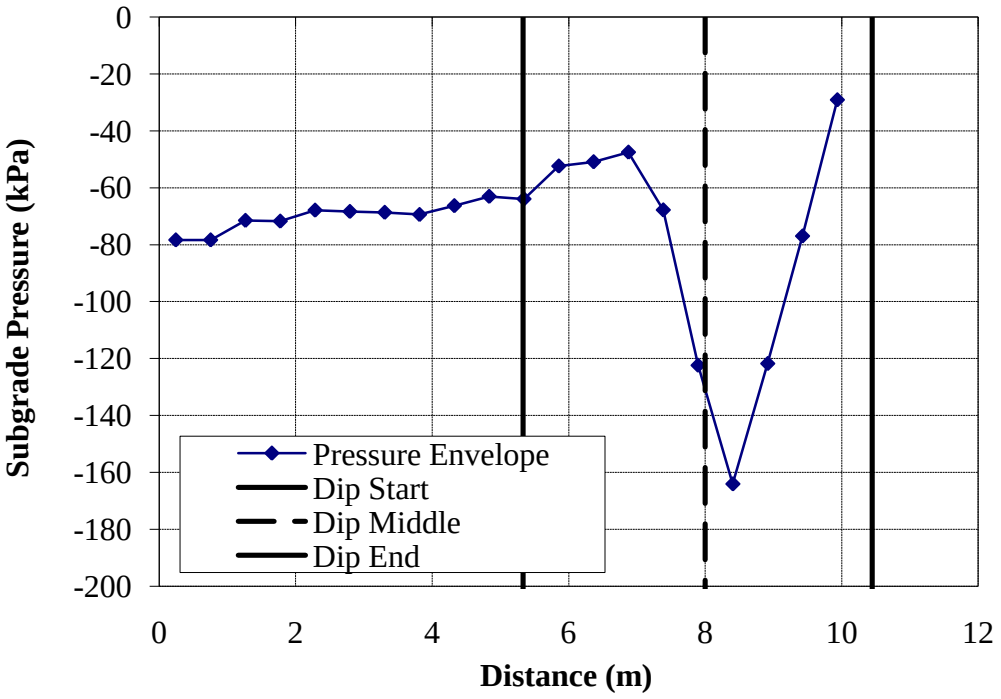

Figure F.99 - Subgrade Pressures due to a 1:150 Dip at a Bridge/Approach Location with Concrete Approach Ties and Rubber Rail Seat Pads (v = 22.2 m/s)

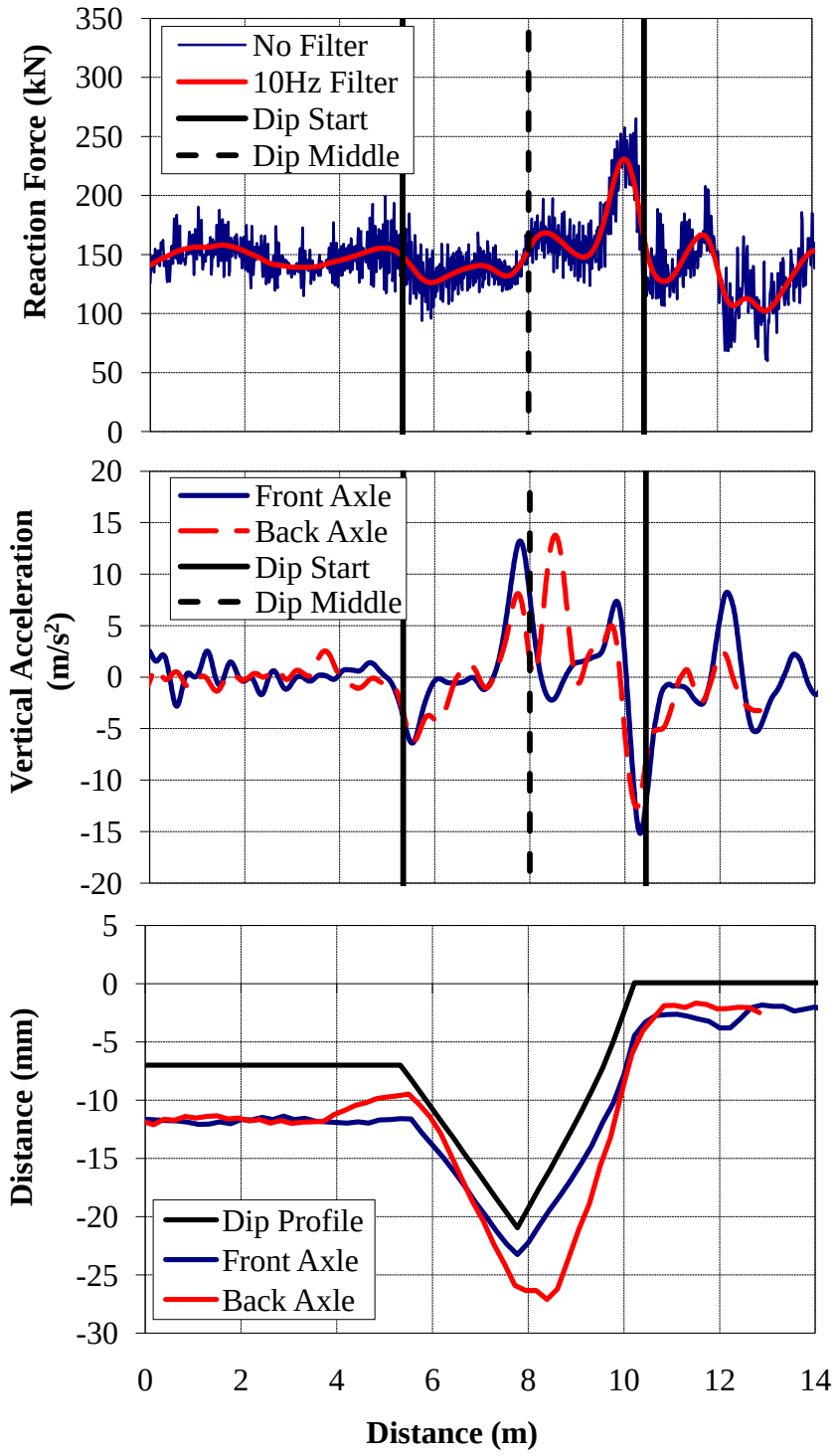

Figure F.100 - (a) Wheel/Rail Forces (b) Axle Accelerations and (c) Track Deflection due to a 1:150 Dip at a Bridge/Approach Location with Wood Approach Ties and Rubber Tie Pads (v = 22.2 m/s)

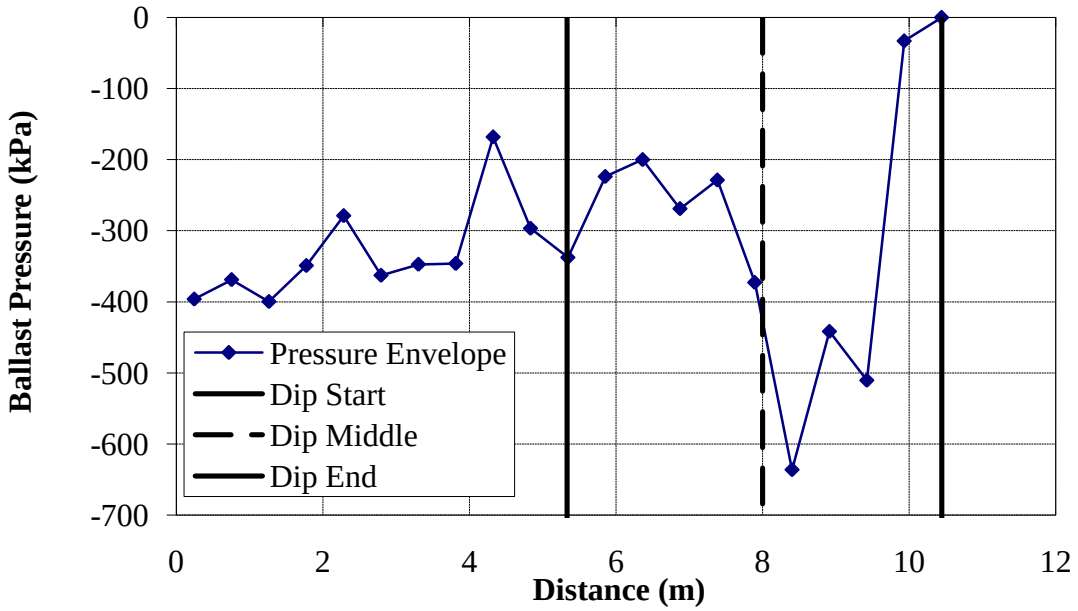

Figure F.101 – Ballast Pressures due to a 1:150 Dip at a Bridge/Approach Location with Wood Approach Ties and Rubber Tie Pads (v = 22.2 m/s)

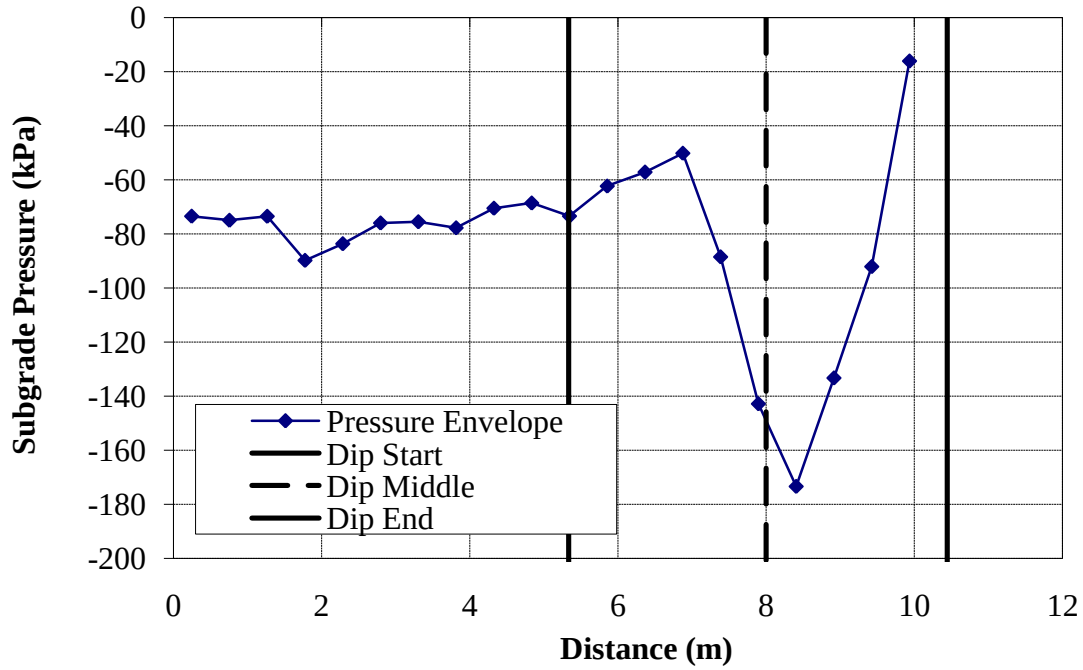

Figure F.102 - Subgrade Pressures due to a 1:150 Dip at a Bridge/Approach Location with Wood Approach Ties and Rubber Tie Pads (v = 22.2 m/s)

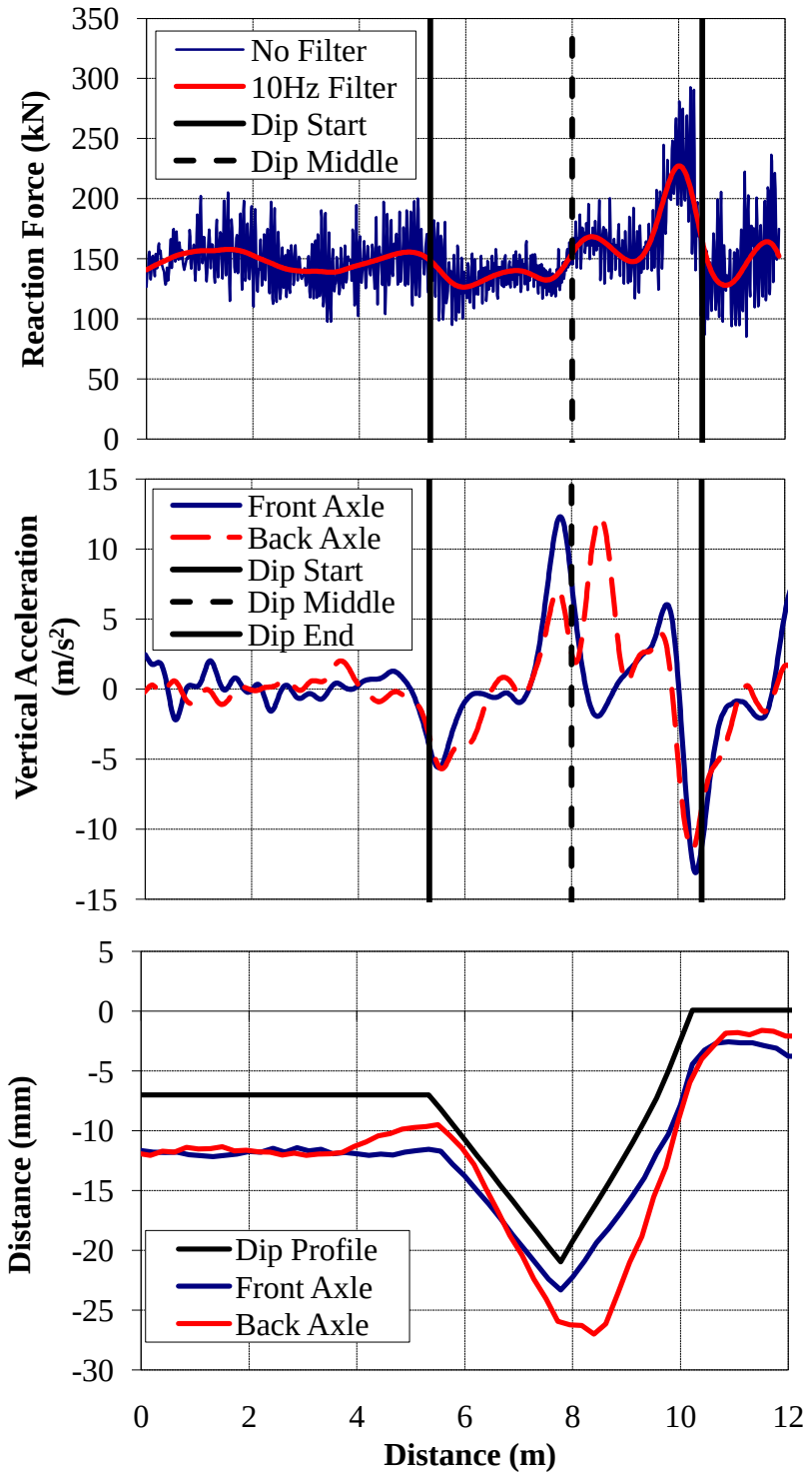

Figure F.103 - (a) Wheel/Rail Forces (b) Axle Accelerations and (c) Track Deflection due to a 1:150 Dip at a Bridge/Approach Location with Concrete Approach Ties and Rubber Tie Pads (v = 22.2 m/s)

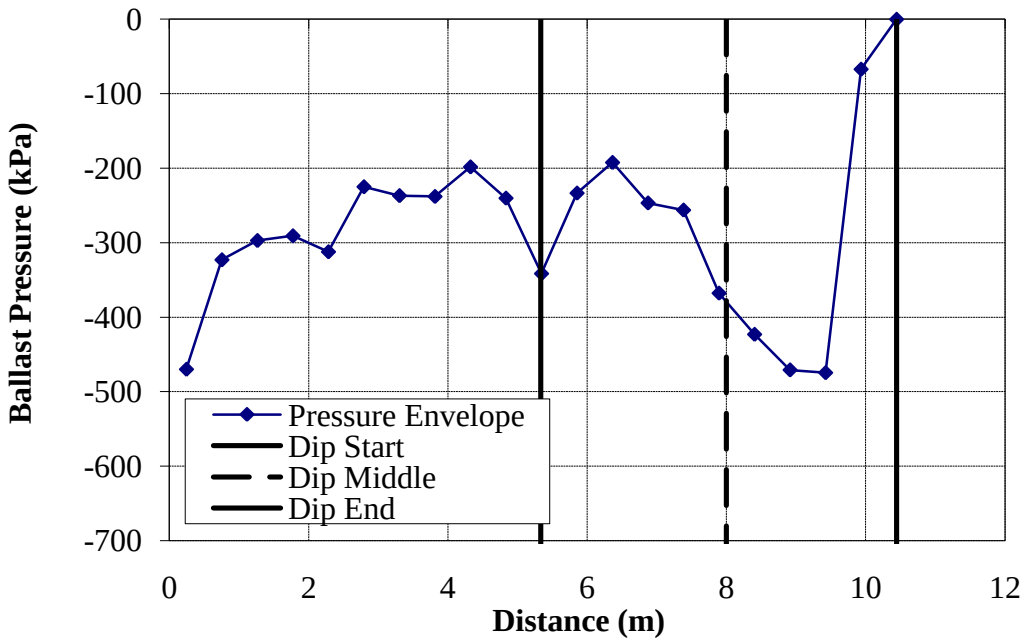

Figure F.104 – Ballast Pressures due to a 1:150 Dip at a Bridge/Approach Location with Concrete Approach Ties and Rubber Tie Pads (v = 22.2 m/s)

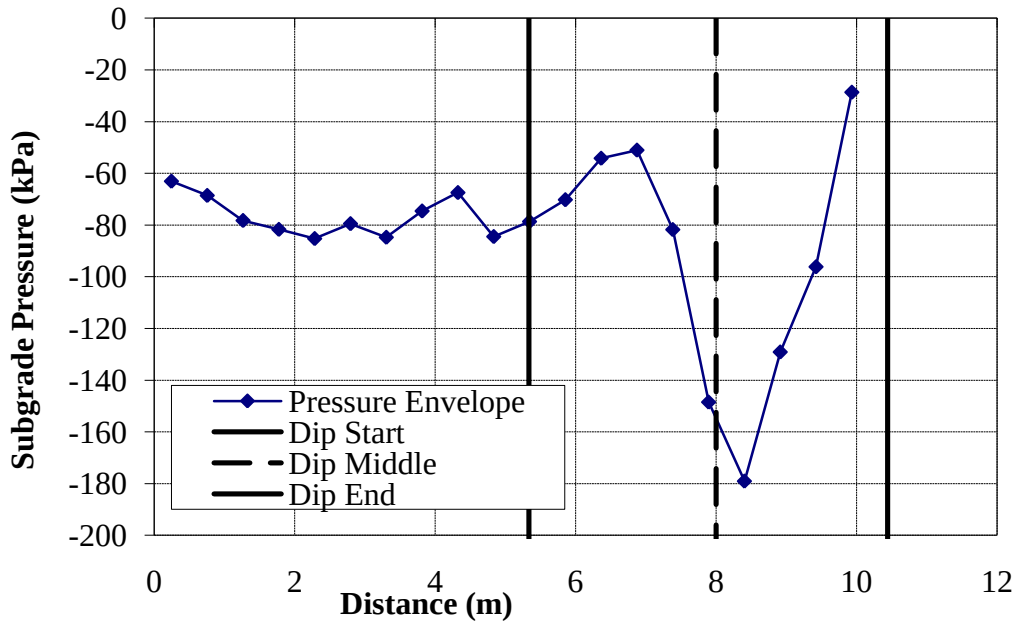

Figure F.105 - Subgrade Pressures due to a 1:150 Dip at a Bridge/Approach Location with Concrete Approach Ties and Rubber Tie Pads (v = 22.2 m/s)

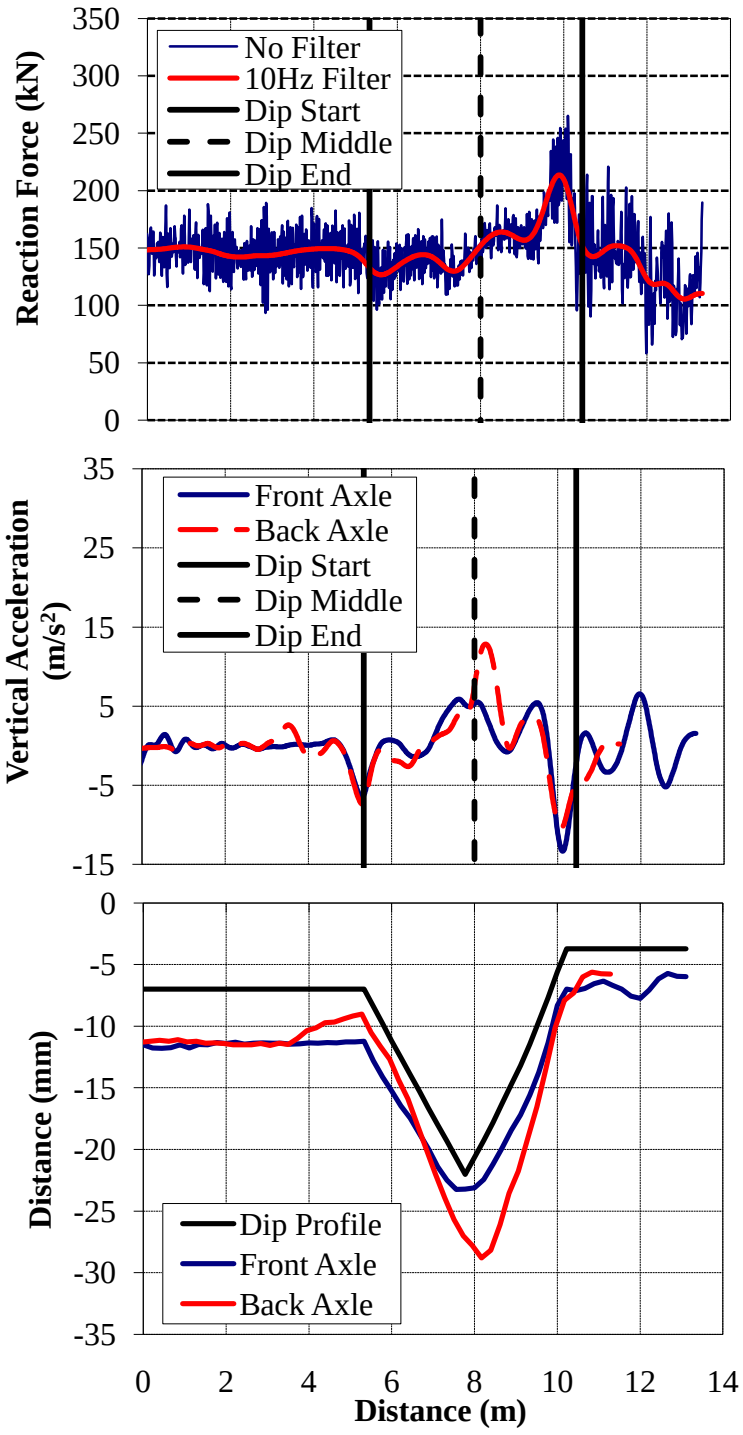

Figure F.106 - (a) Wheel/Rail Forces (b) Axle Accelerations and (c) Track Deflection due to a 1:150 Dip at a Bridge/Approach Location with Concrete Bridge Ties (v = 22.2 m/s)

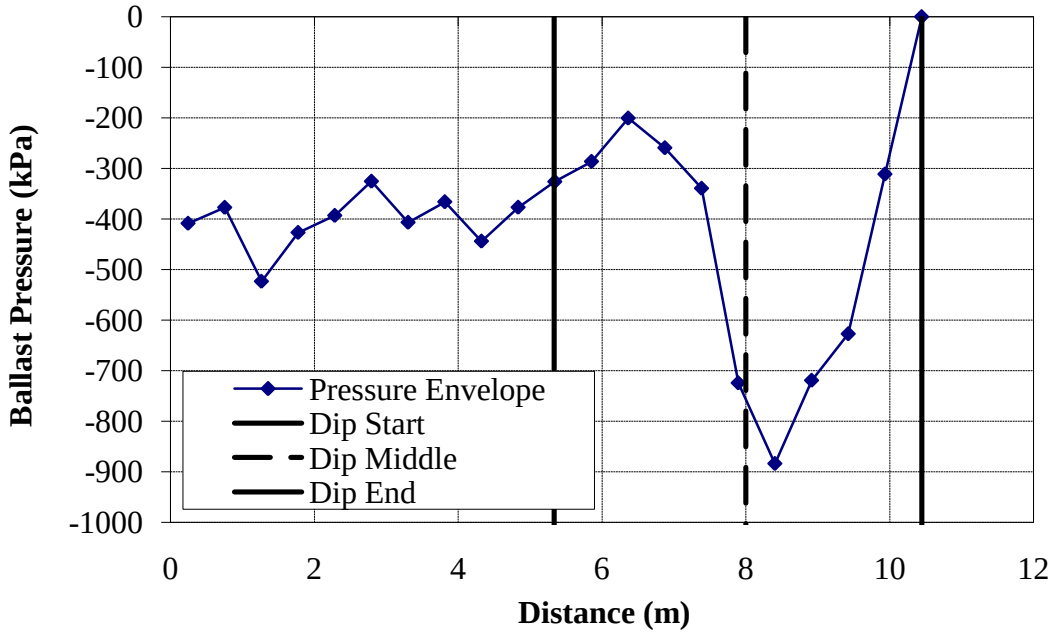

Figure F.107 – Ballast Pressures due to a 1:150 Dip at a Bridge/Approach Location with Concrete Bridge Ties (v = 22.2 m/s)

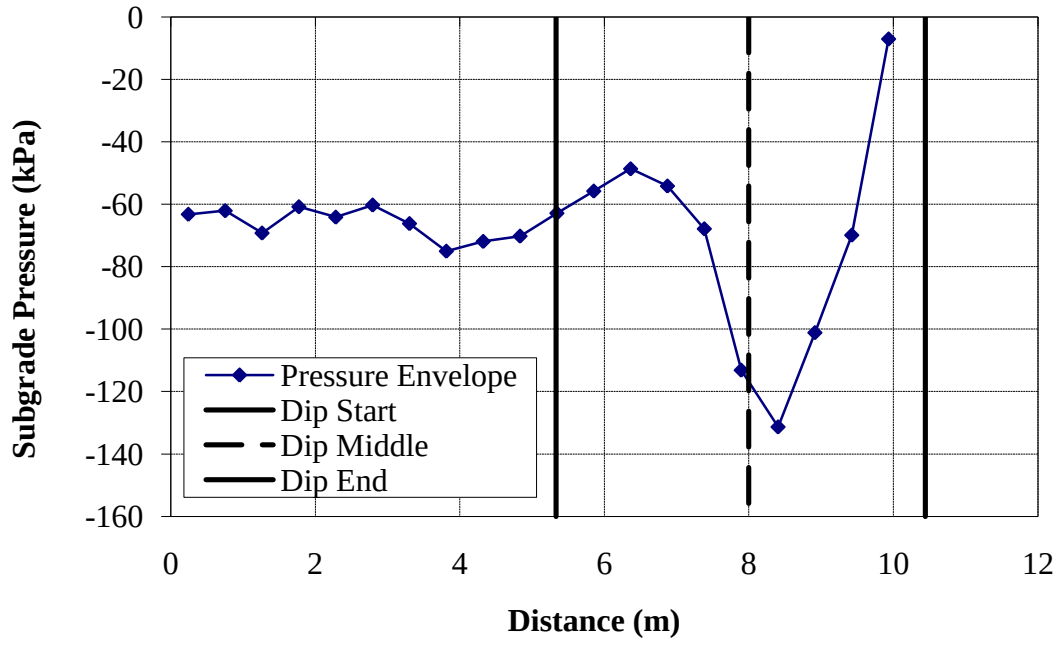

Figure F.108 - Subgrade Pressures due to a 1:150 Dip at a Bridge/Approach Location with Concrete Bridge Ties (v = 22.2 m/s)

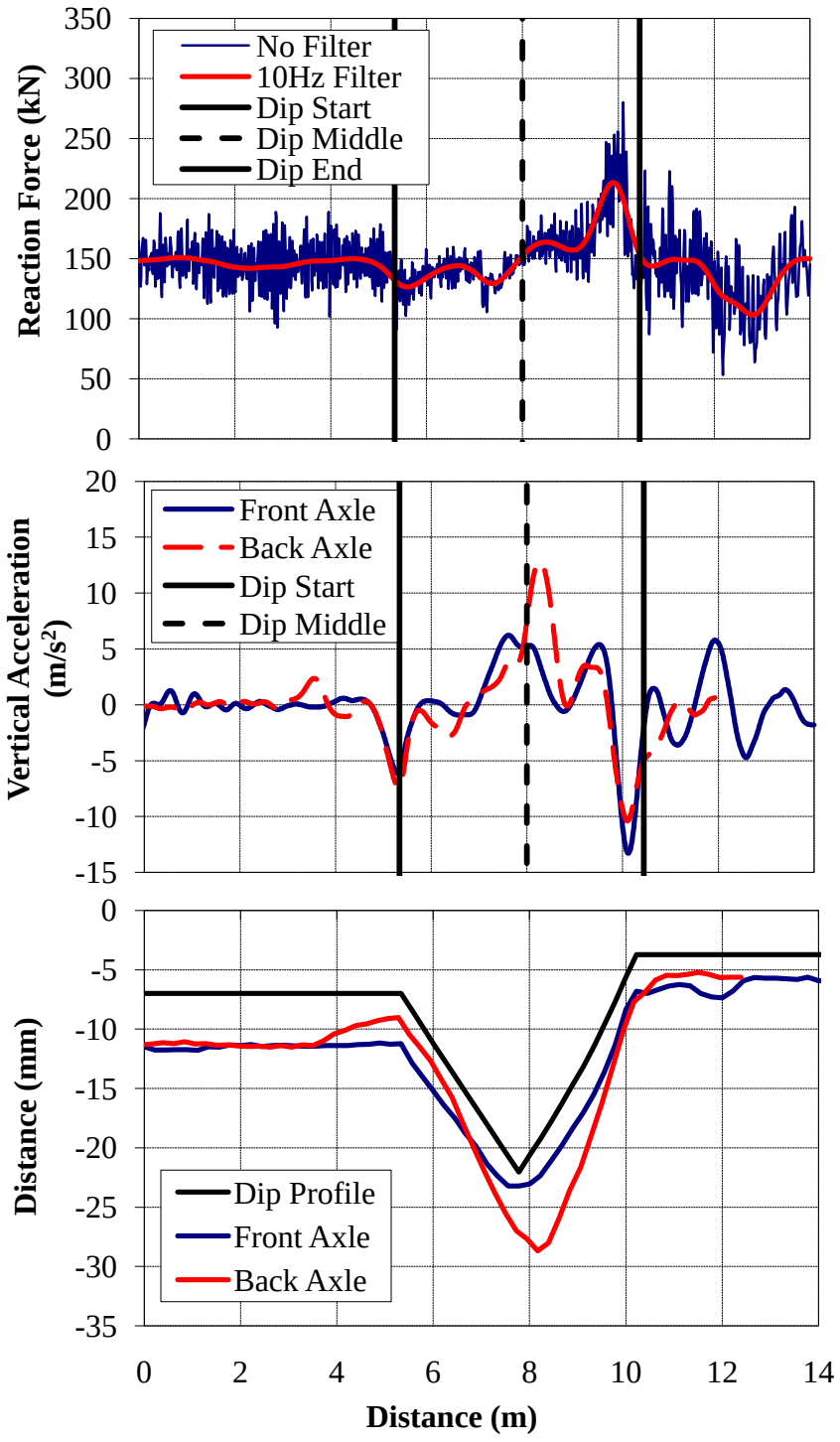

Figure F.109 - (a) Wheel/Rail Forces (b) Axle Accelerations and (c) Track Deflection due to a 1:150 Dip at a Bridge/Approach Location with Plastic Bridge Ties (v = 22.2 m/s)

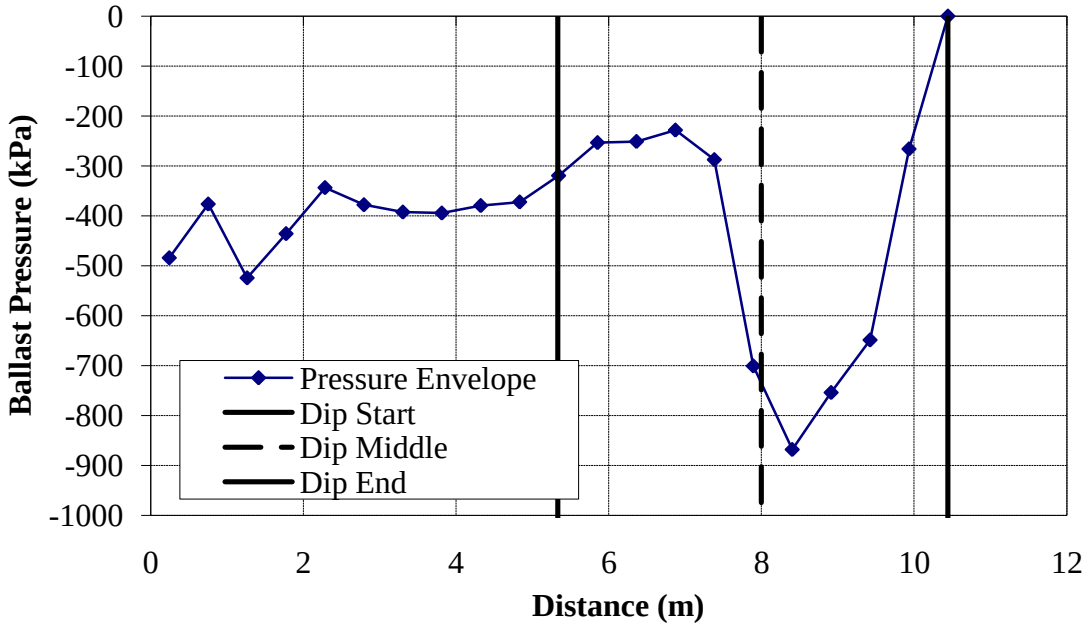

Figure F.110 – Ballast Pressures due to a 1:150 Dip at a Bridge/Approach Location with Plastic Bridge Ties (v = 22.2 m/s)

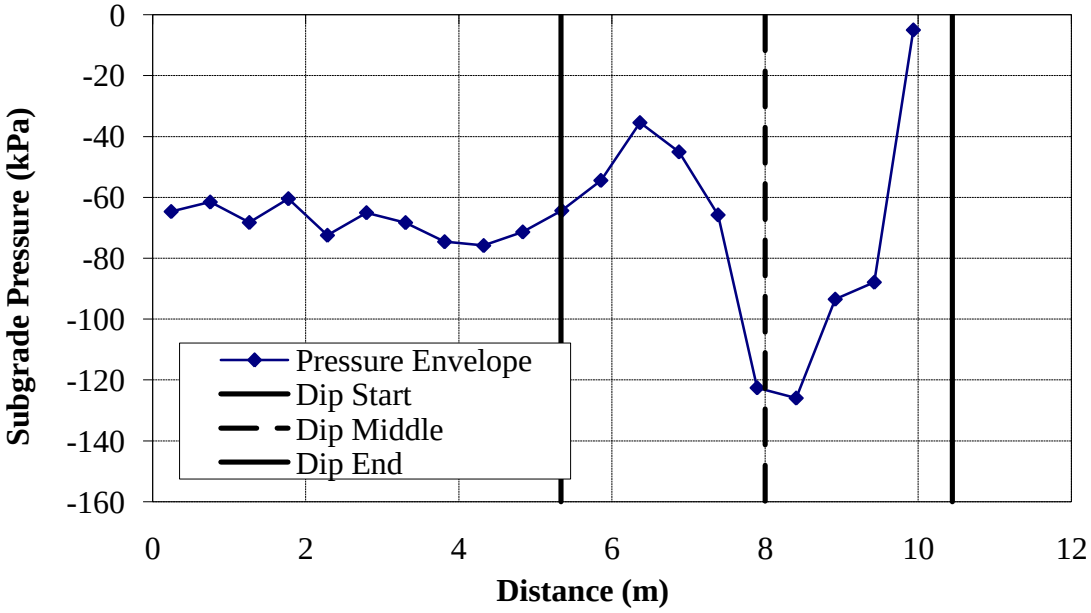

Figure F.111 - Subgrade Pressures due to a 1:150 Dip at a Bridge/Approach Location with Plastic Bridge Ties (v = 22.2 m/s)

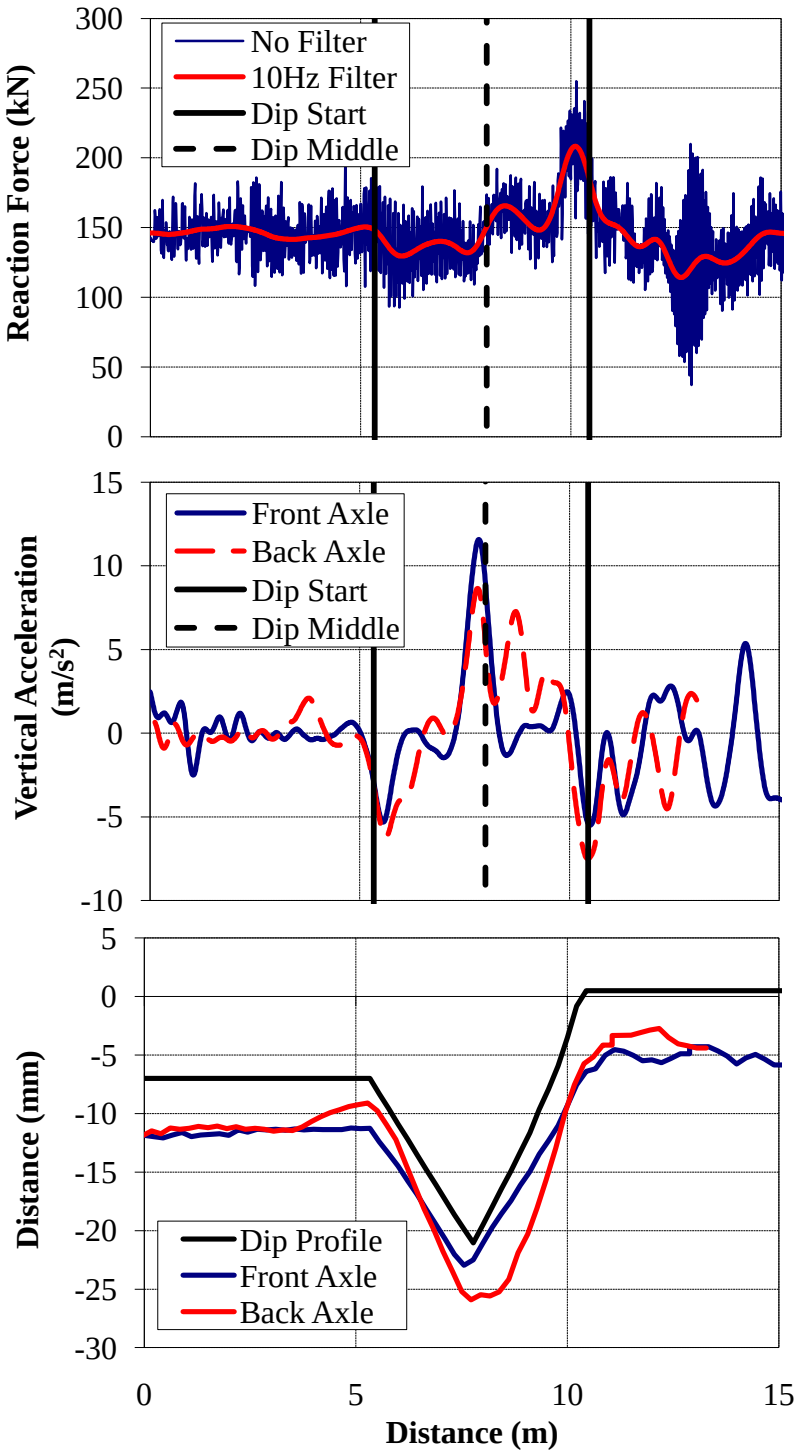

Figure F.11 - (a) Wheel/Rail Forces (b) Axle Accelerations and (c) Track Deflection due to a 1:150 Dip at a Bridge/Approach Location with Wood Bridge Ties and Rubber Rail Seat Pads (v = 22.2 m/s)

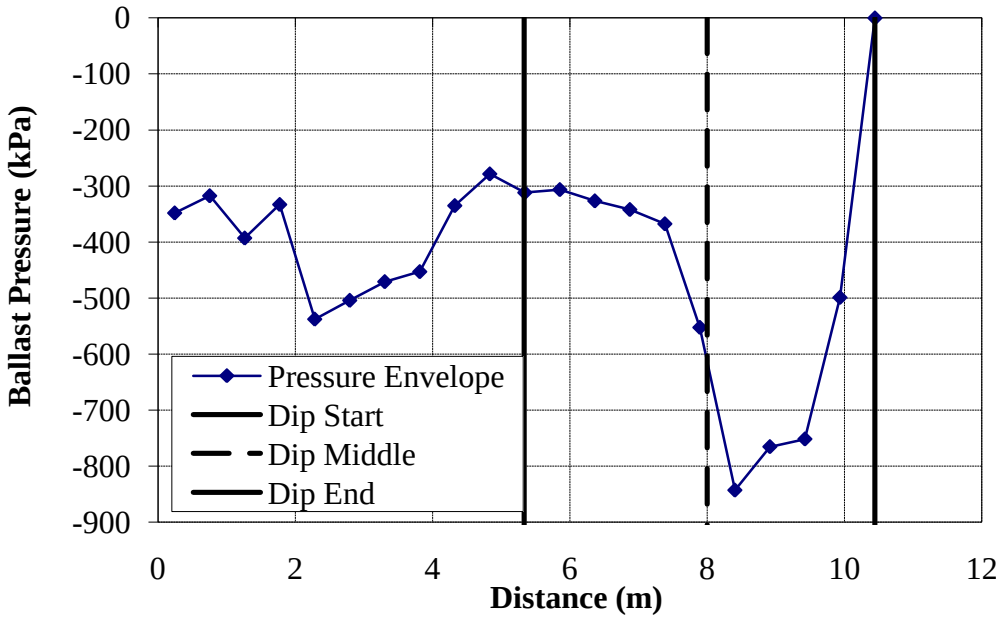

Figure F.113 – Ballast Pressures due to a 1:150 Dip at a Bridge/Approach Location with Wood Bridge Ties and Rubber Rail Seat Pads (v = 22.2 m/s)

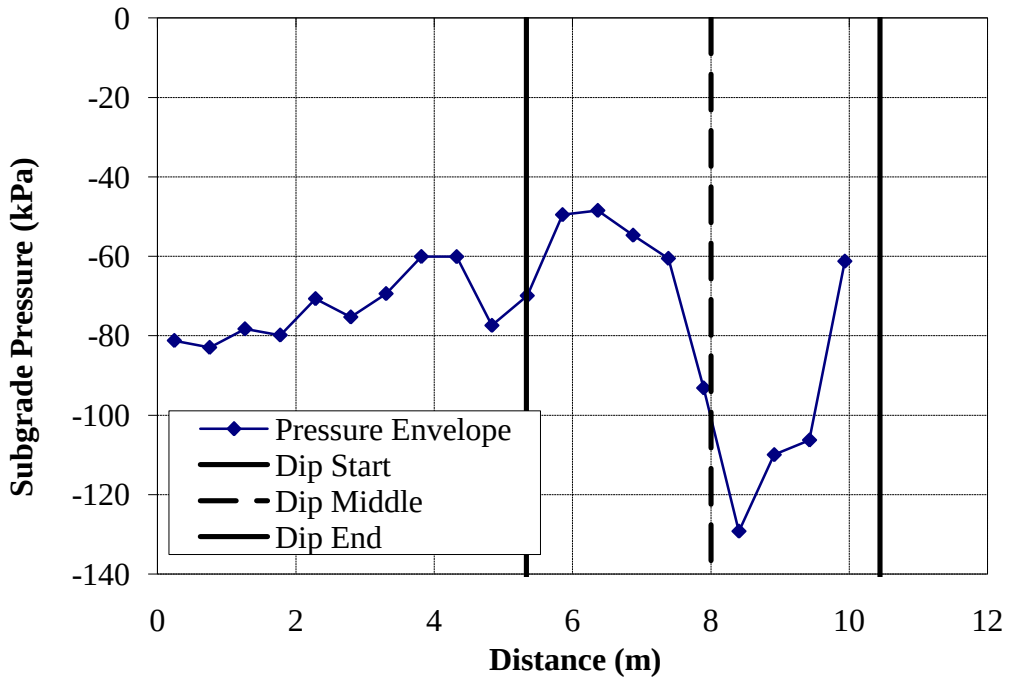

Figure F.114 - Subgrade Pressures due to a 1:150 Dip at a Bridge/Approach Location with Wood Bridge Ties and Rubber Rail Seat Pads (v = 22.2 m/s)

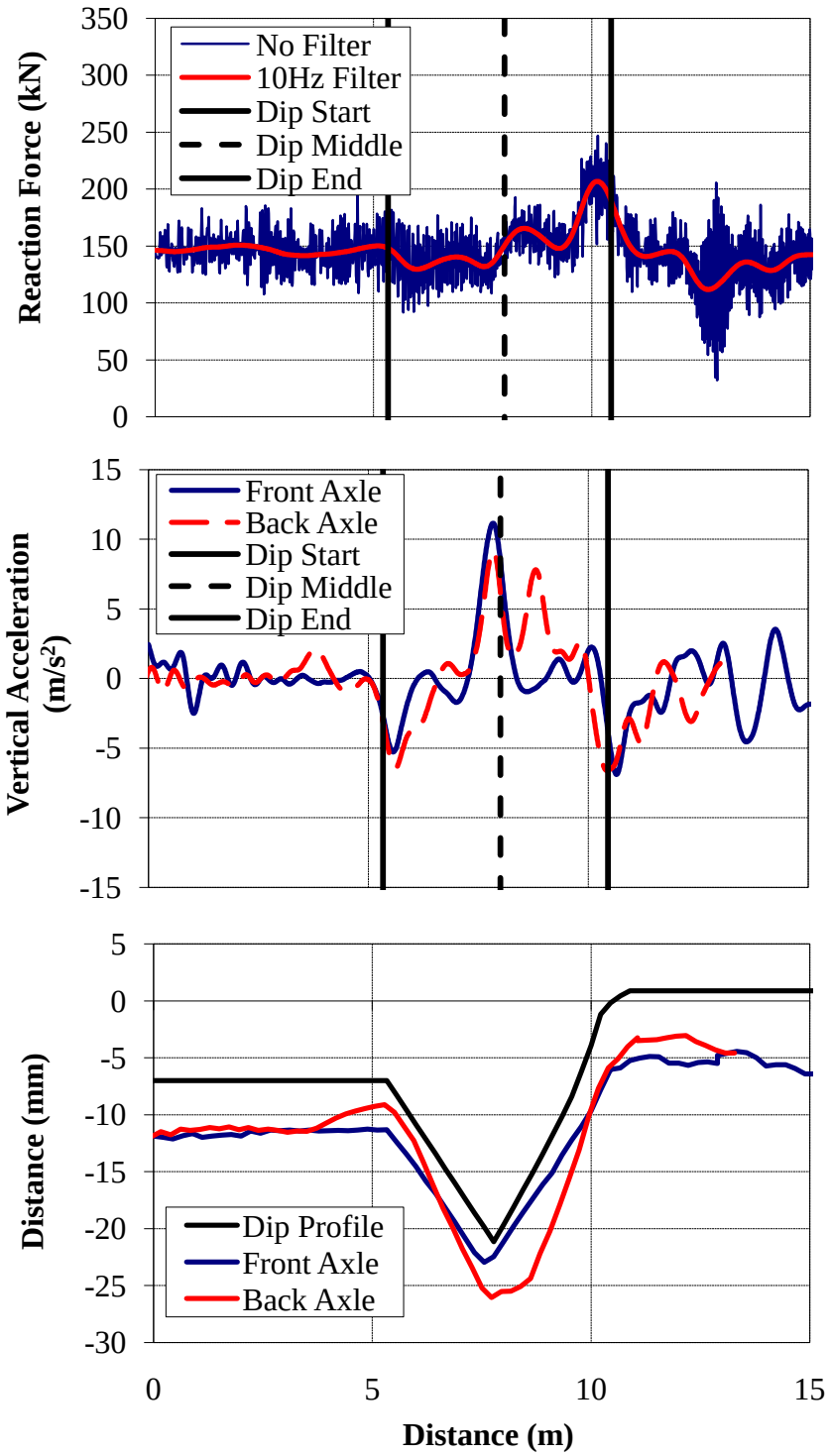

Figure F.115 - (a) Wheel/Rail Forces (b) Axle Accelerations and (c) Track Deflection due to a 1:150 Dip at a Bridge/Approach Location with Concrete Bridge Ties and Rubber Rail Seat Pads (v = 22.2 m/s)

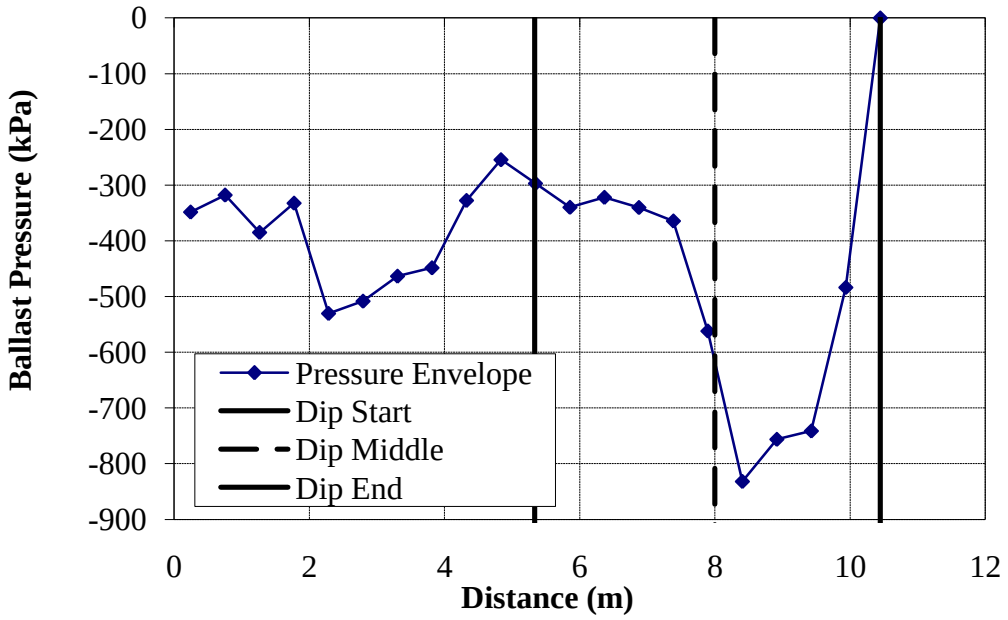

Figure F.116 – Ballast Pressures due to a 1:150 Dip at a Bridge/Approach Location with Concrete Bridge Ties and Rubber Rail Seat Pads (v = 22.2 m/s)

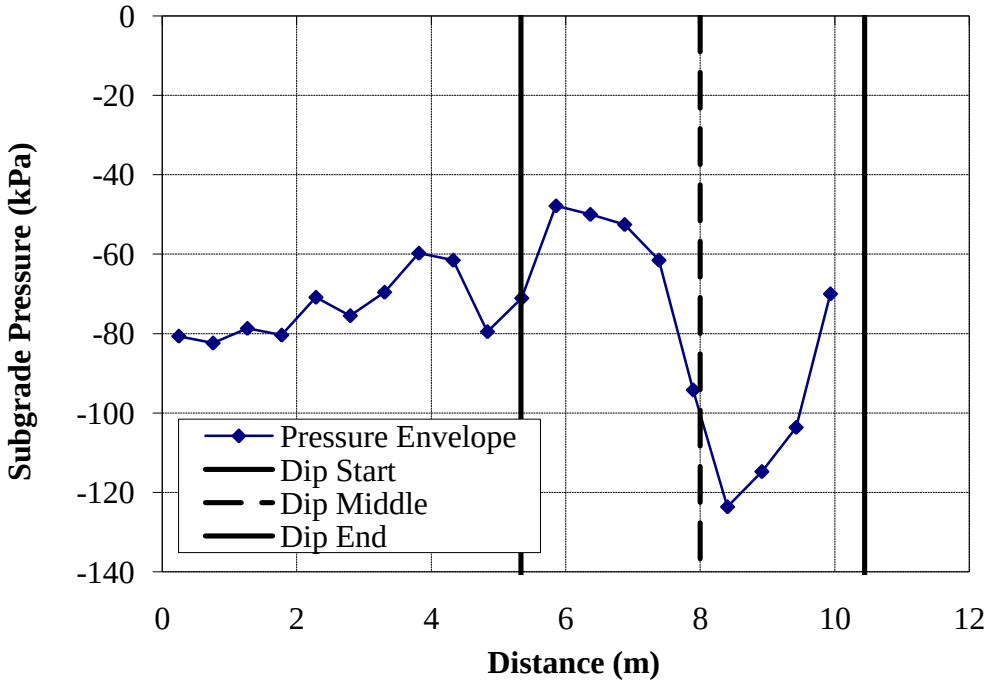

Figure F.117 - Subgrade Pressures due to a 1:150 Dip at a Bridge/Approach Location with Concrete Bridge Ties and Rubber Rail Seat Pads (v = 22.2 m/s)

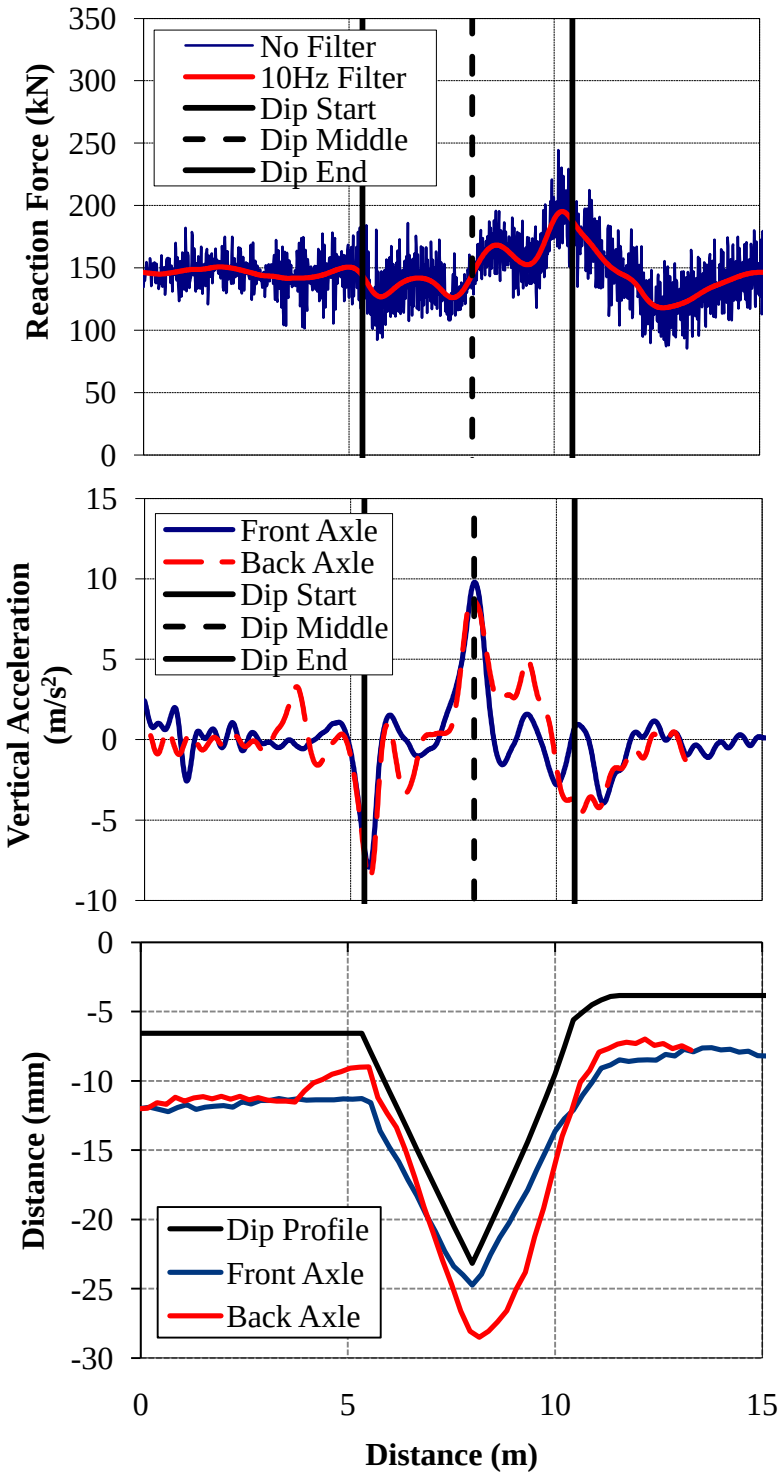

Figure F.118 - (a) Wheel/Rail Forces (b) Axle Accelerations and (c) Track Deflection due to a truck moving over a 1:150 Dip onto a Ballast Deck Bridge (v = 22.2 m/s)

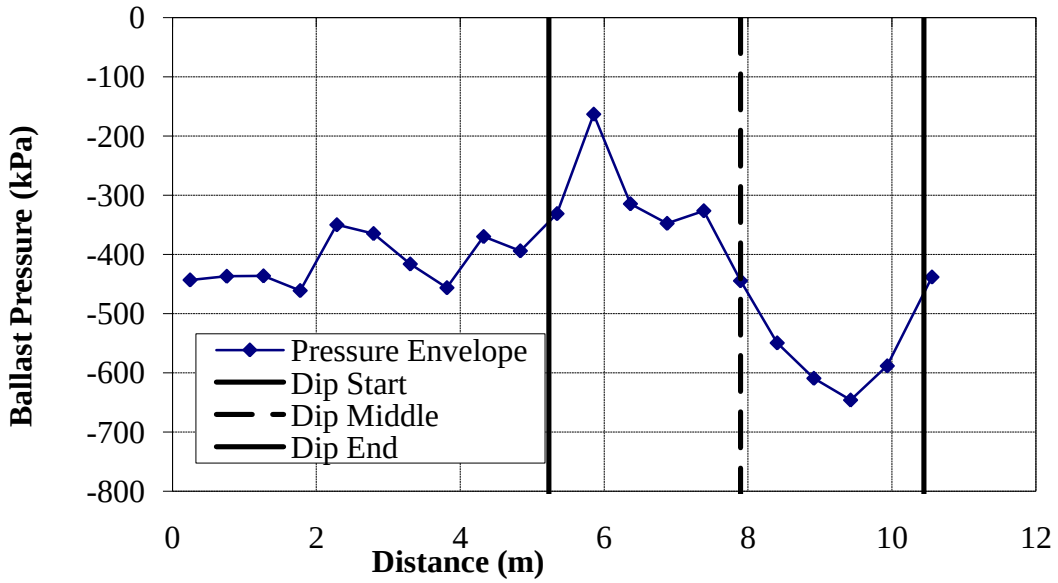

Figure F.119 – Ballast Pressures due to a truck moving over a 1:150 Dip onto a Ballast Deck Bridge (v = 22.2 m/s)

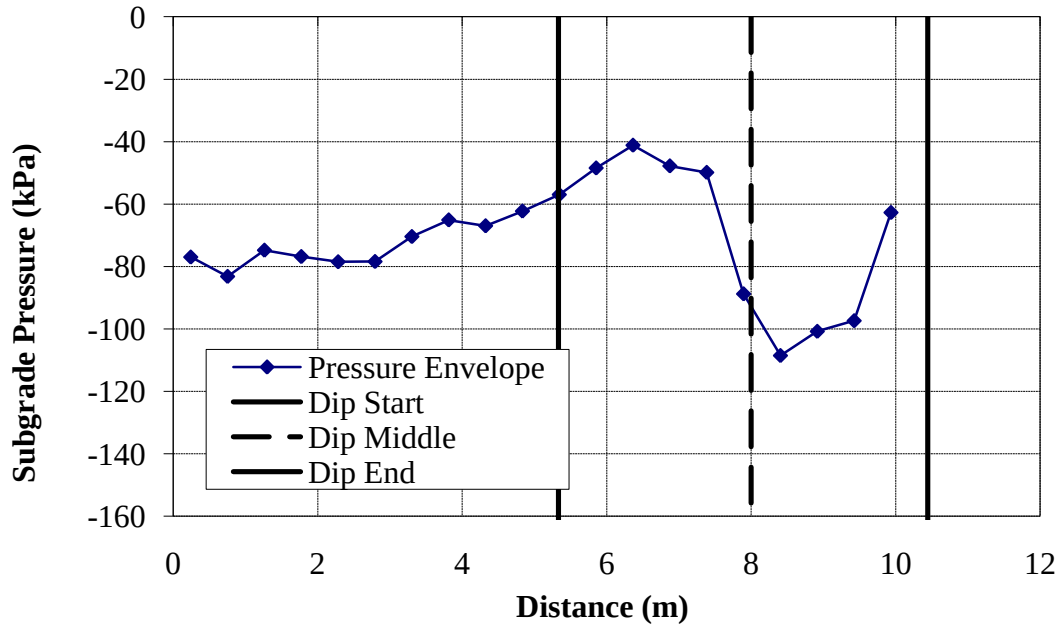

Figure F.120 – Subgrade Pressures due to a truck moving over a 1:150 Dip onto a Ballast Deck Bridge (v = 22.2 m/s)

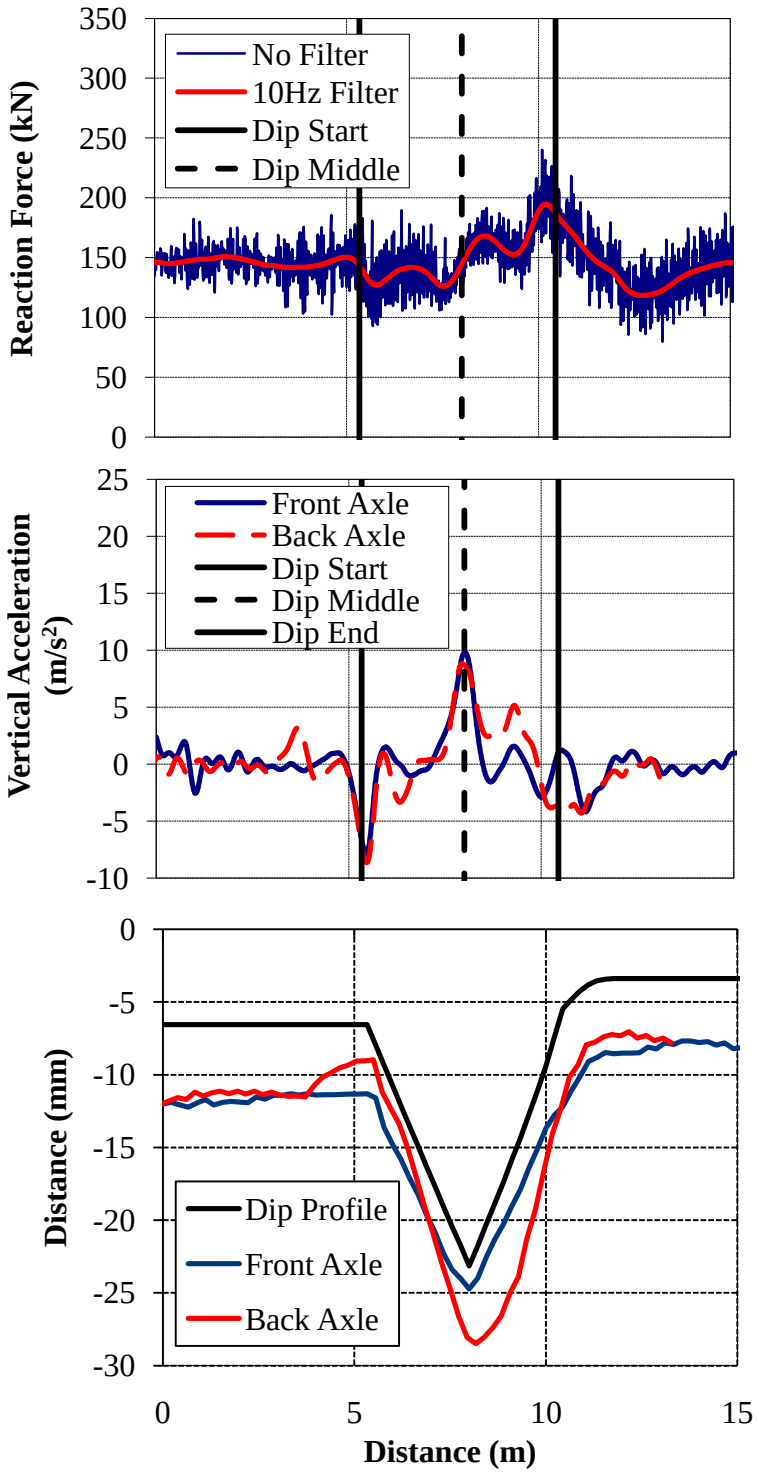

Figure F.121 - (a) Wheel/Rail Forces (b) Axle Accelerations and (c) Track Deflection due to a Truck Moving from an Approach Embankment with a 1:150 Dip onto a Ballast Deck Bridge with a Ballast Mat (v = 22.2 m/s)

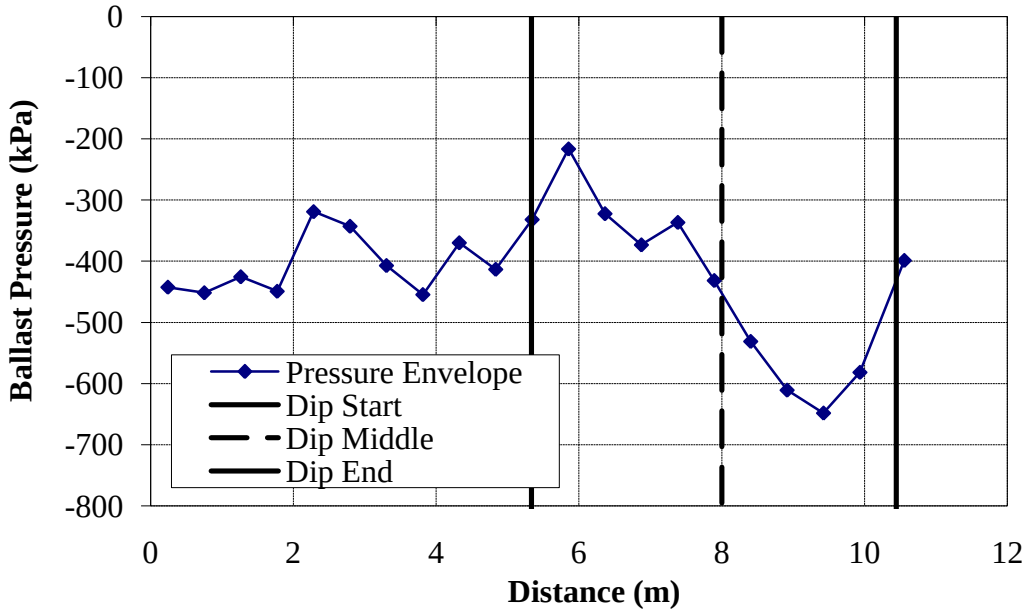

Figure F.122 – Ballast Pressures due to a Truck Moving from an Approach Embankment with a 1:150 Dip onto a Ballast Deck Bridge with a Ballast Mat (v = 22.2 m/s)

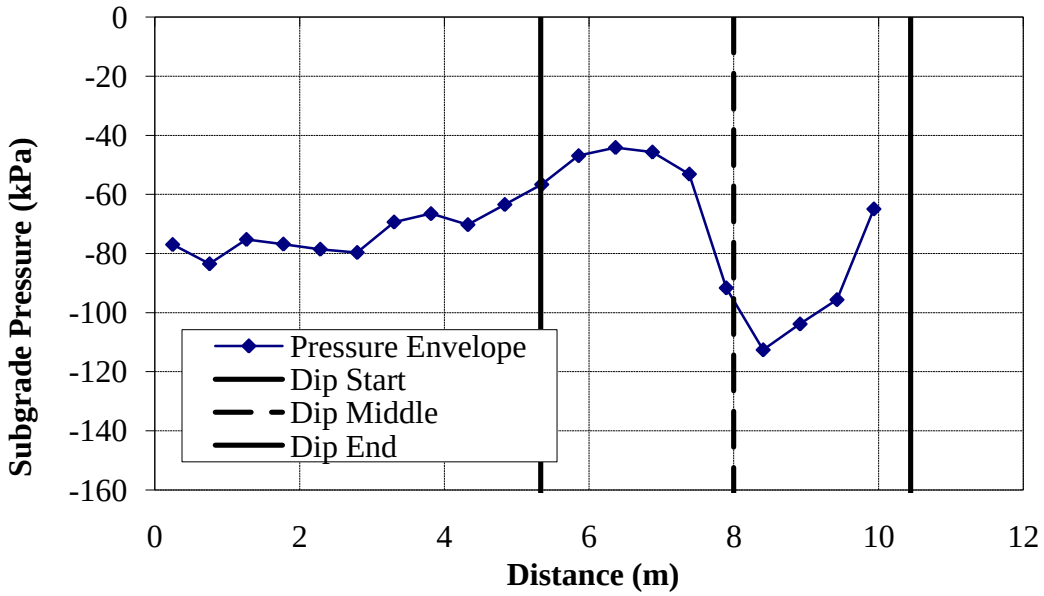

Figure F.123 - Subgrade Pressures due to a Truck Moving from an Approach Embankment with a 1:150 Dip onto a Ballast Deck Bridge with a Ballast Mat (v = 22.2 m/s)

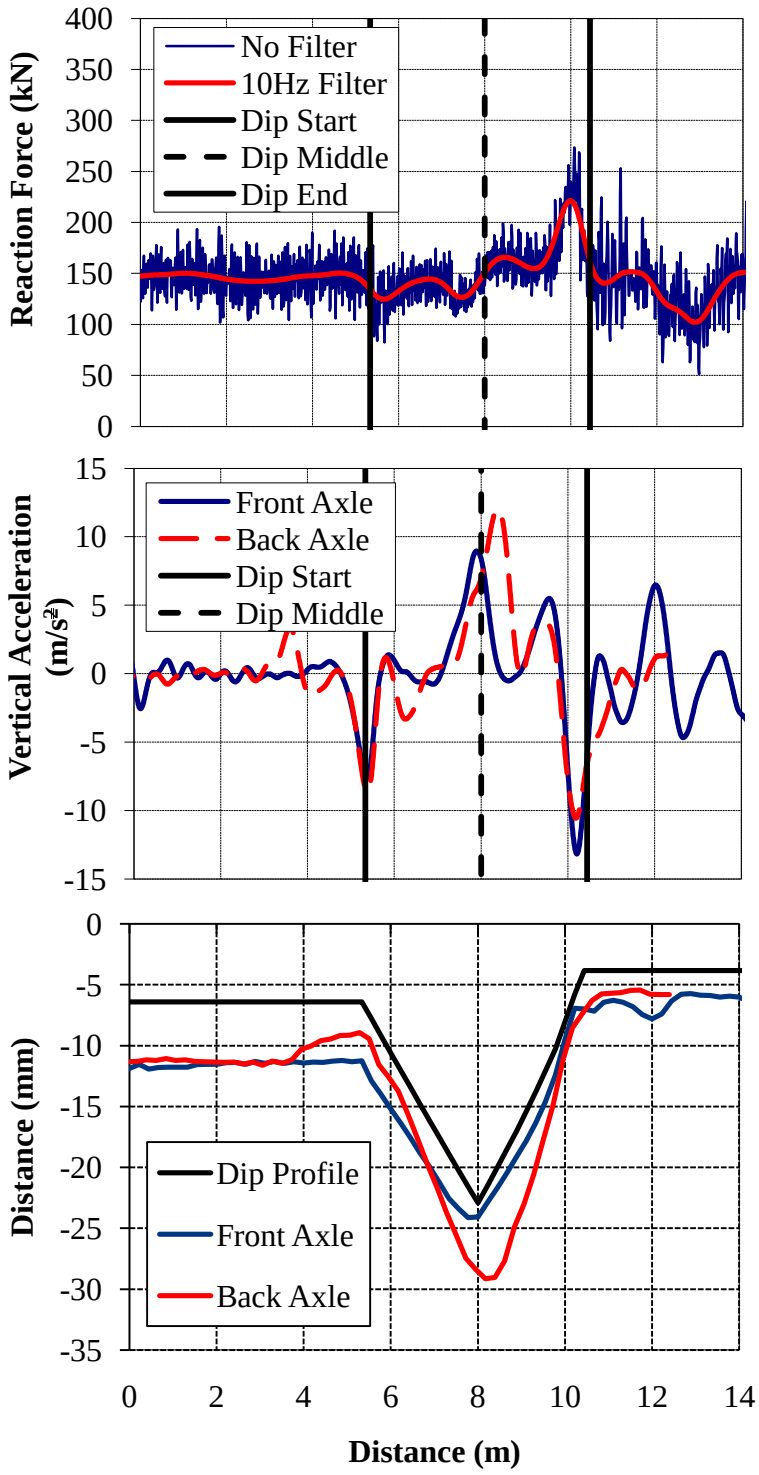

Figure F.124 - (a) Wheel/Rail Forces (b) Axle Accelerations and (c) Track Deflection due to a 1:150 Dip With an Approach Ballast Thickness of 152.4 mm (v = 22.2 m/s)

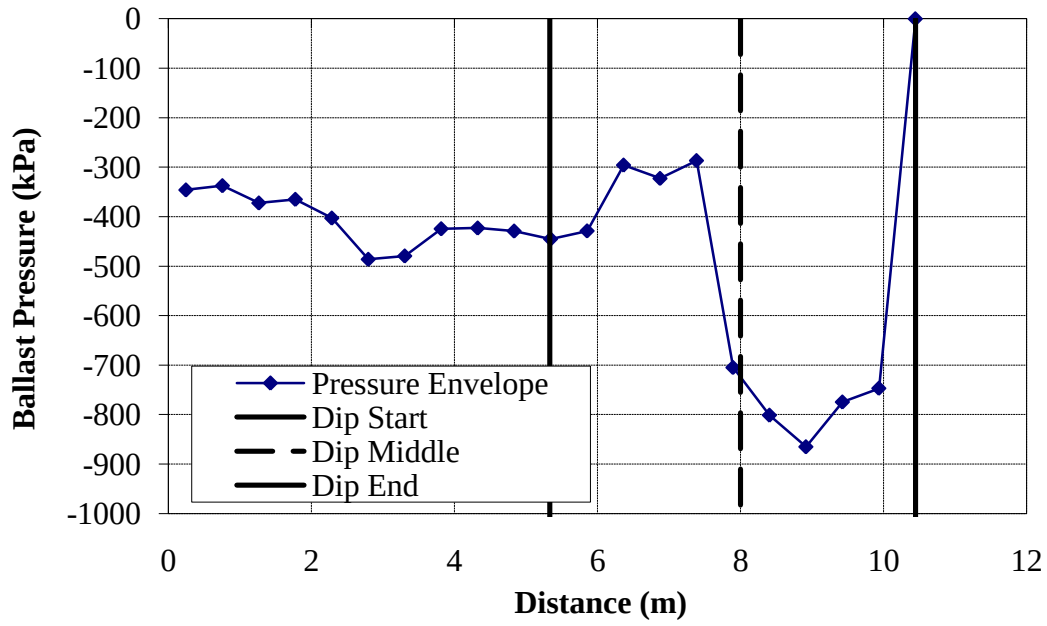

Figure F.125 – Ballast Pressures due to a 1:150 Dip With an Approach Ballast Thickness of 152.4 mm (v = 22.2 m/s)

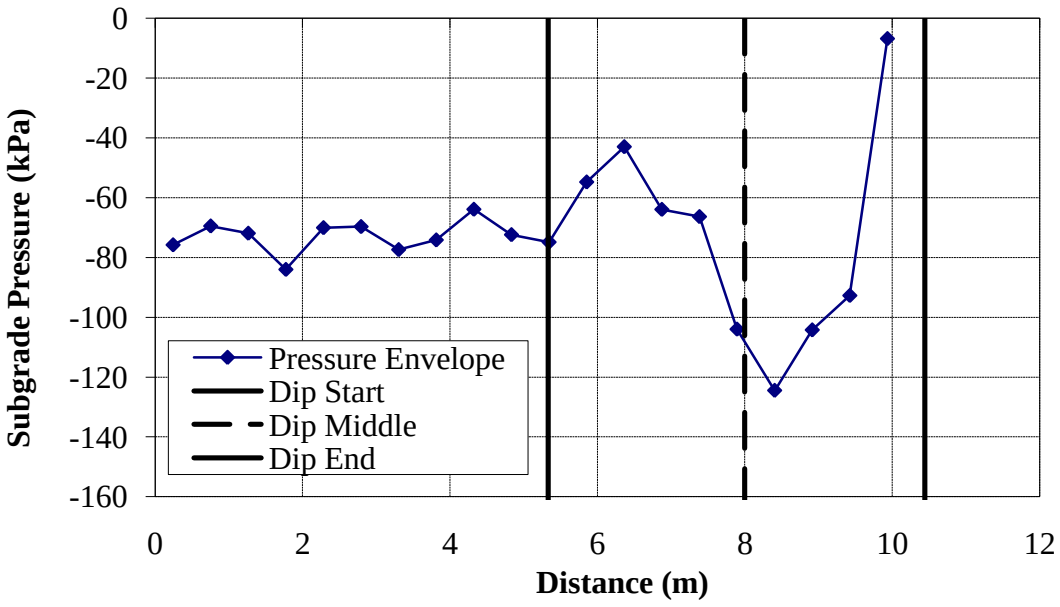

Figure F.126 - Subgrade Pressures due to a 1:150 Dip With an Approach Ballast Thickness of 152.4 mm (v = 22.2 m/s)

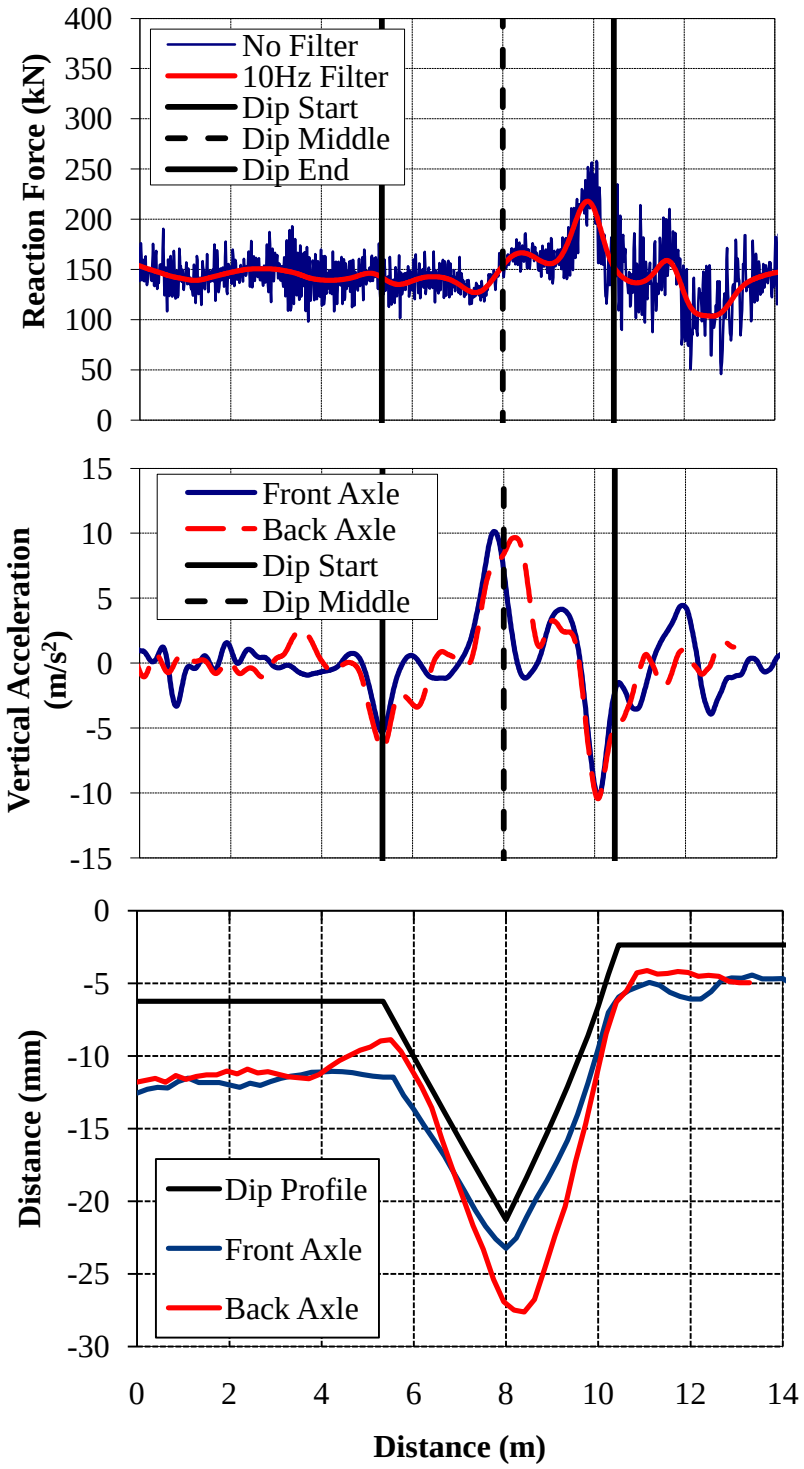

Figure F.127 - (a) Wheel/Rail Forces (b) Axle Accelerations and (c) Track Deflection due to a 1:150 Dip With an Approach Ballast Thickness of 203.2 mm (v = 22.2 m/s)

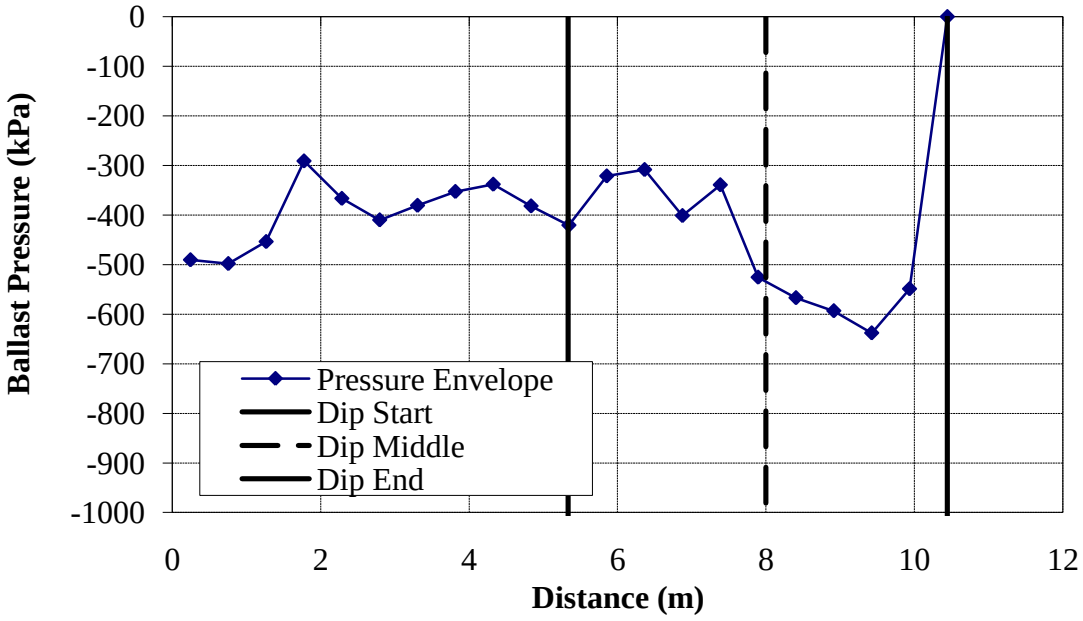

Figure F.128 – Ballast Pressures due to a 1:150 Dip With an Approach Ballast Thickness of 203.2 mm (v = 22.2 m/s)

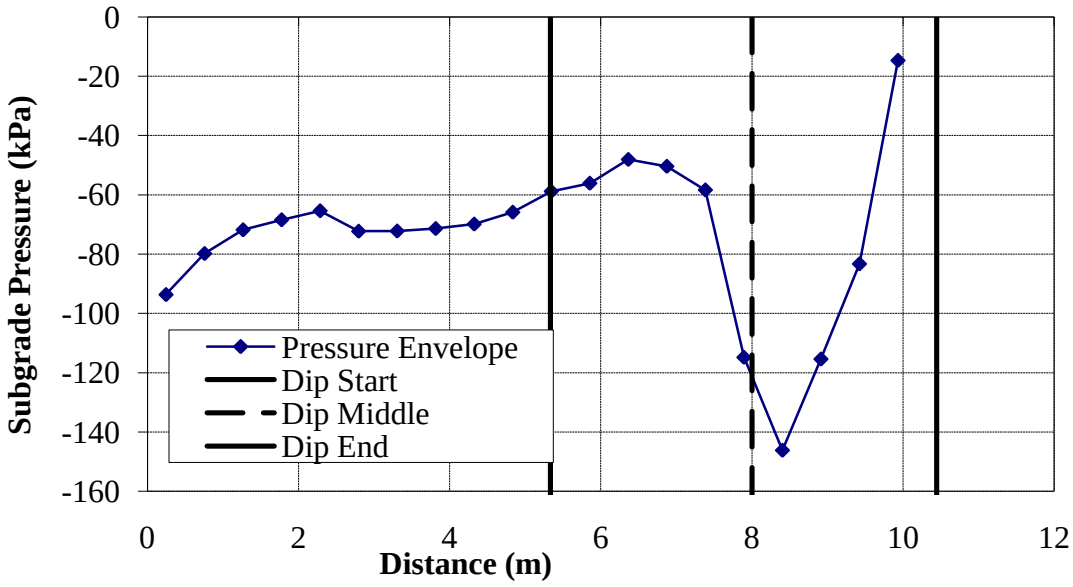

Figure F.129 - Subgrade Pressures due to a 1:150 Dip With an Approach Ballast Thickness of 203.2 mm (v = 22.2 m/s)

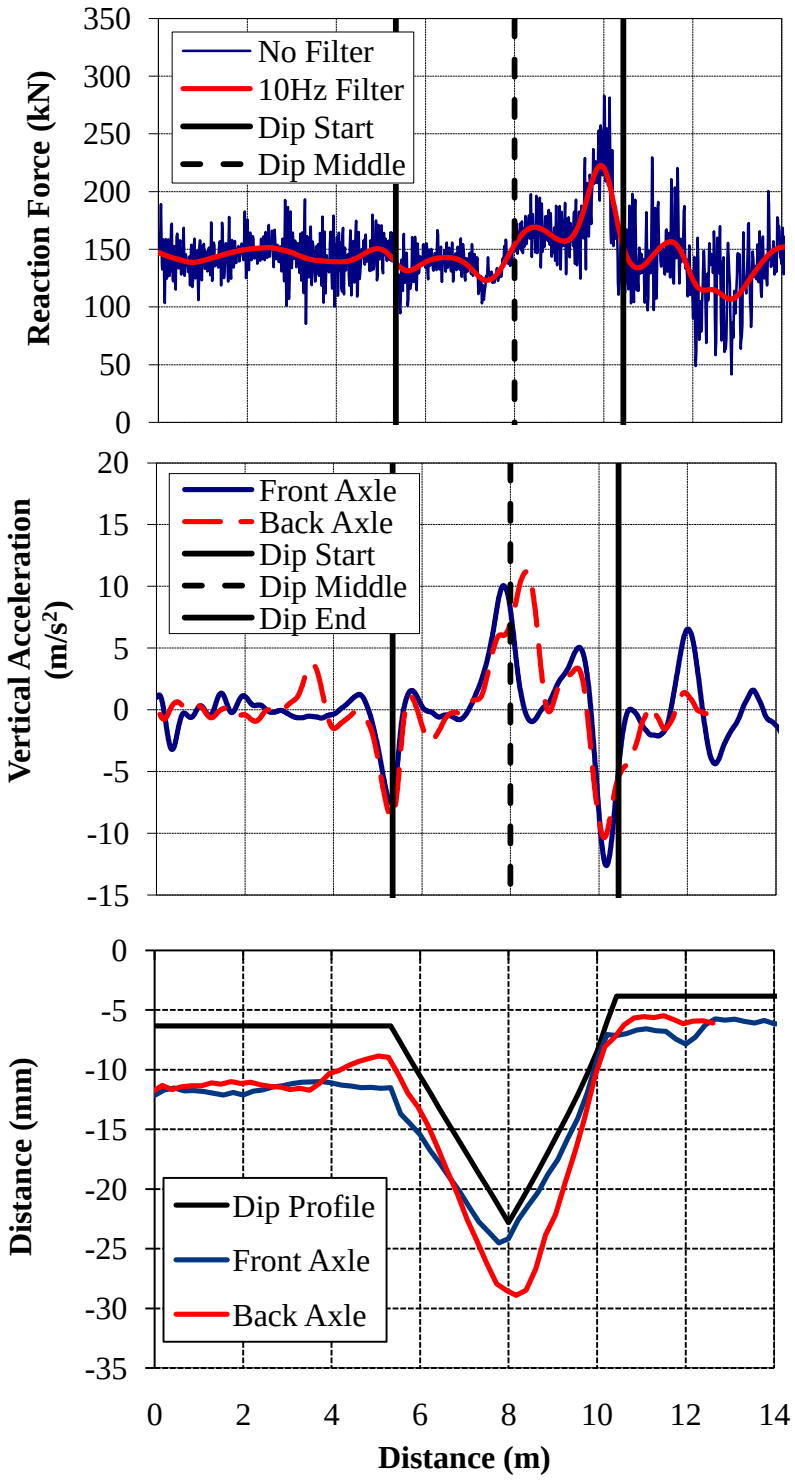

Figure F.130 - (a) Wheel/Rail Forces (b) Axle Accelerations and (c) Track Deflection due to a 1:150 Dip With an Approach Ballast Thickness of 304.8 mm (v = 22.2 m/s)

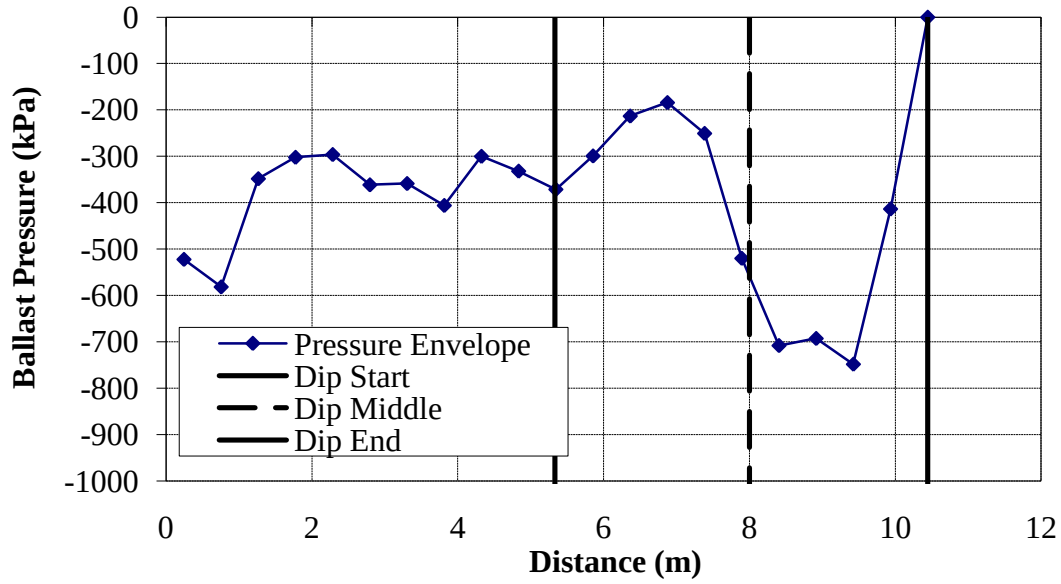

Figure F.131 – Ballast Pressures due to a 1:150 Dip With an Approach Ballast Thickness of 304.8 mm (v = 22.2 m/s)

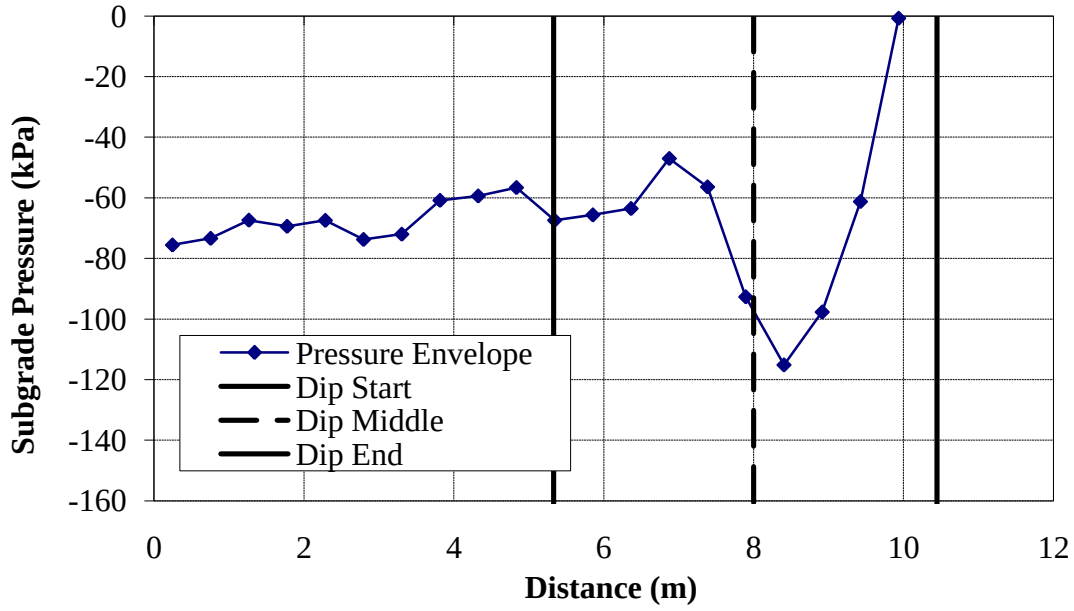

Figure F.132 - Subgrade Pressures due to a 1:150 Dip With an Approach Ballast Thickness of 304.8 mm (v = 22.2 m/s)

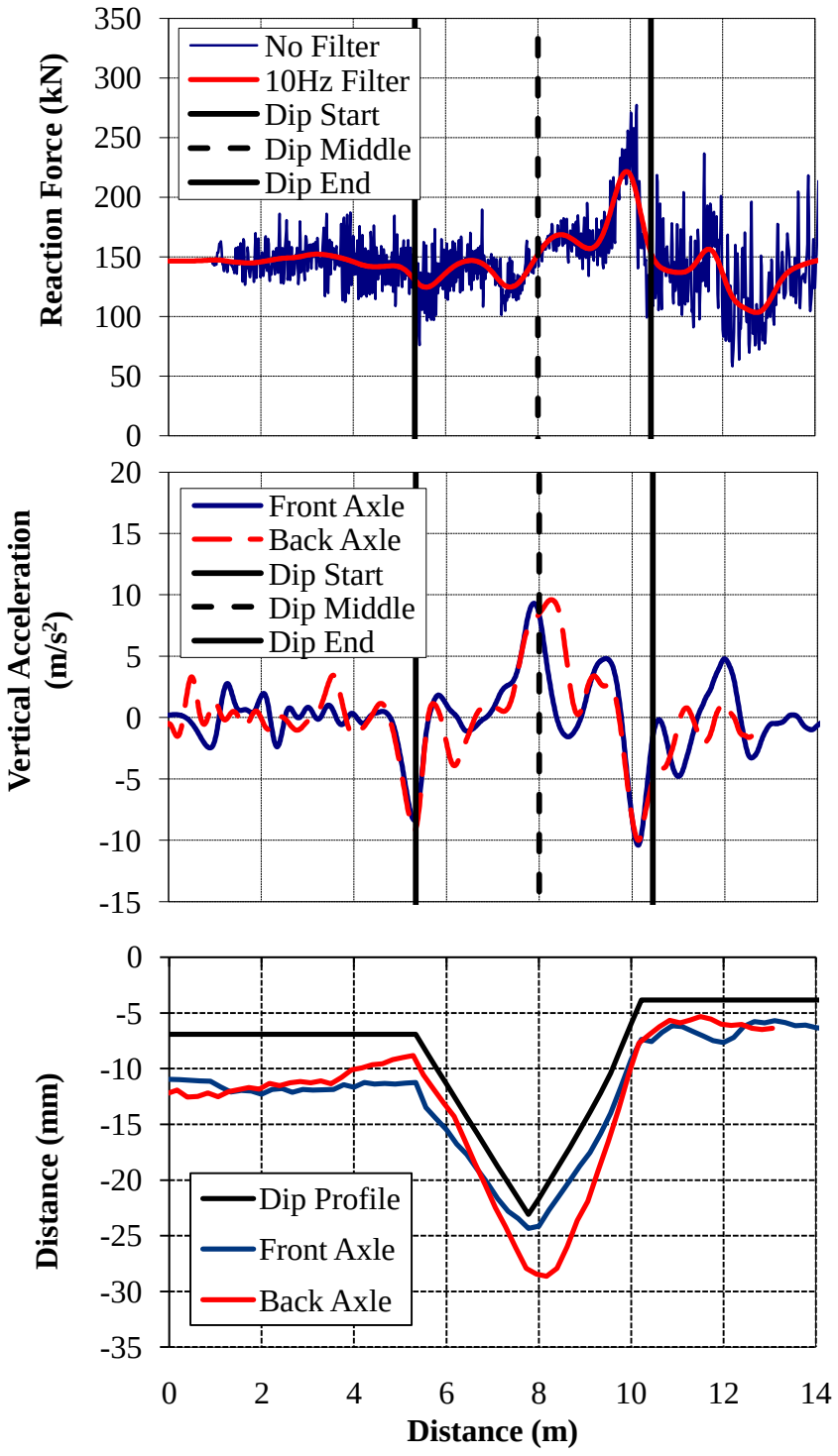

Figure F.133 - (a) Wheel/Rail Forces (b) Axle Accelerations and (c) Track Deflection due to a 1:150 Dip With an Approach Ballast Thickness of 406.4 mm (v = 22.2 m/s)

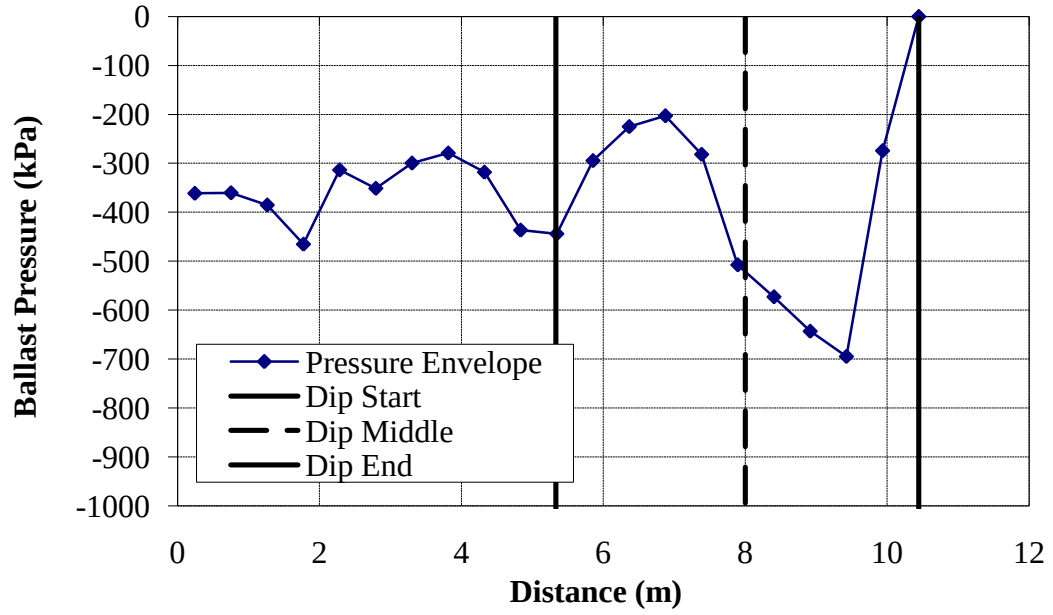

Figure F.134 – Ballast Pressures due to a 1:150 Dip With an Approach Ballast Thickness of 406.4 mm (v = 22.2 m/s)

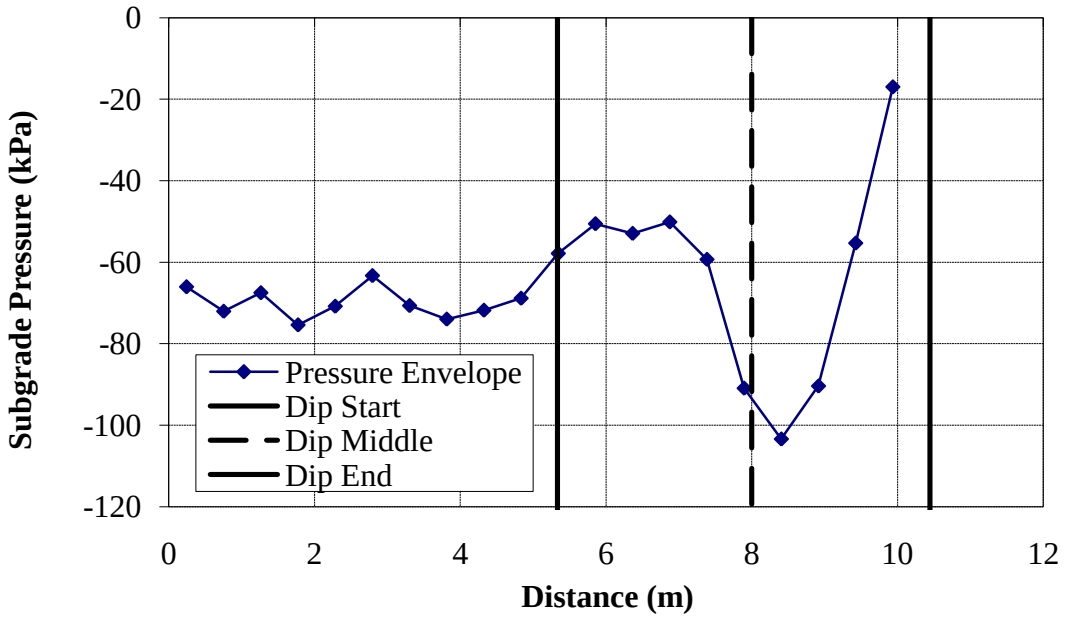

Figure F.135 - Subgrade Pressures due to a 1:150 Dip With an Approach Ballast Thickness of 406.4 mm (v = 22.2 m/s)

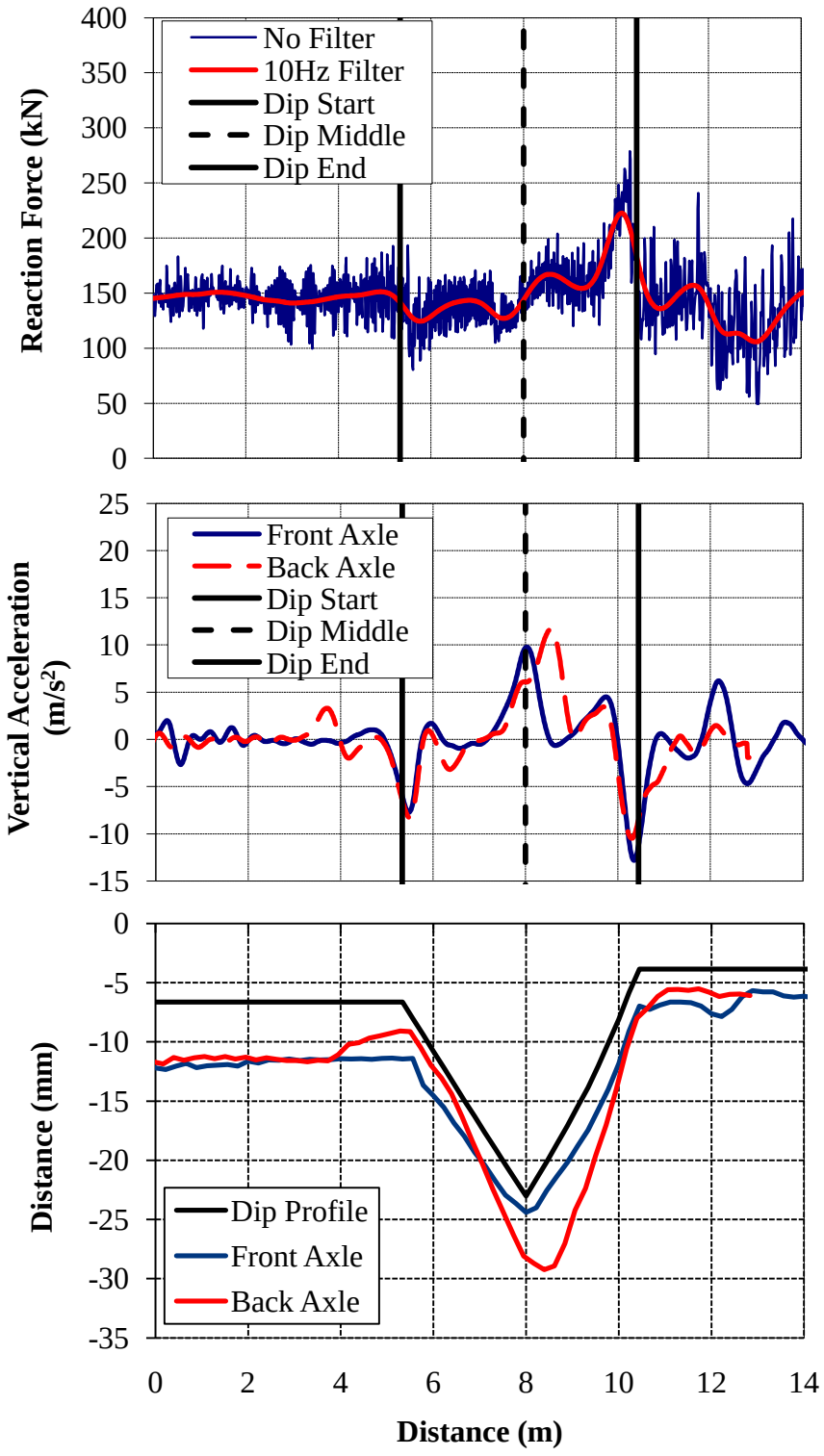

Figure F.136 - (a) Wheel/Rail Forces (b) Axle Accelerations and (c) Track Deflection due to a 1:150 Dip with 2.1-m Approach Tie Lengths (v = 22.2 m/s)

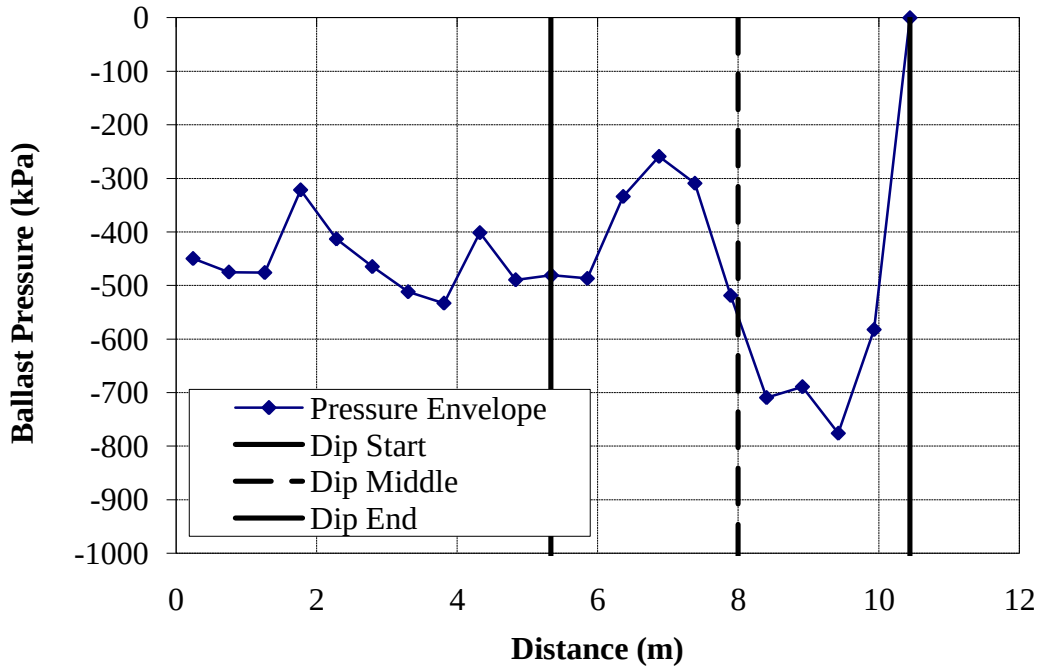

Figure F.137 – Ballast Pressures due to a 1:150 Dip with 2.1-m Approach Tie Lengths (v = 22.2 m/s)

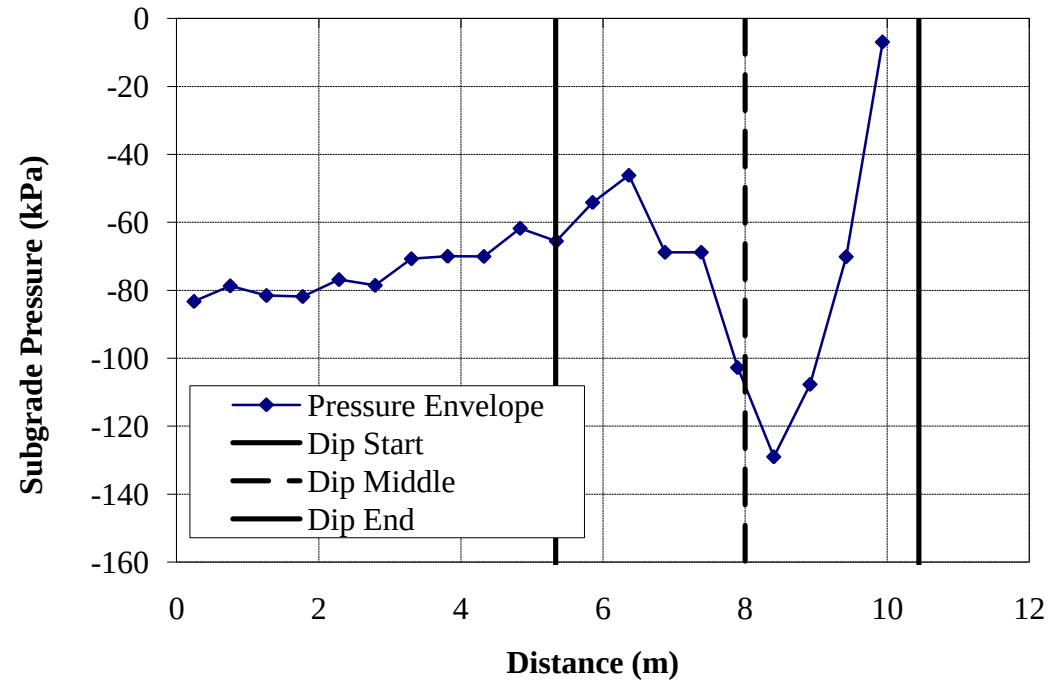

Figure F.138 - Subgrade Pressures due to a 1:150 Dip with 2.1-m Approach Tie Lengths (v = 22.2 m/s)

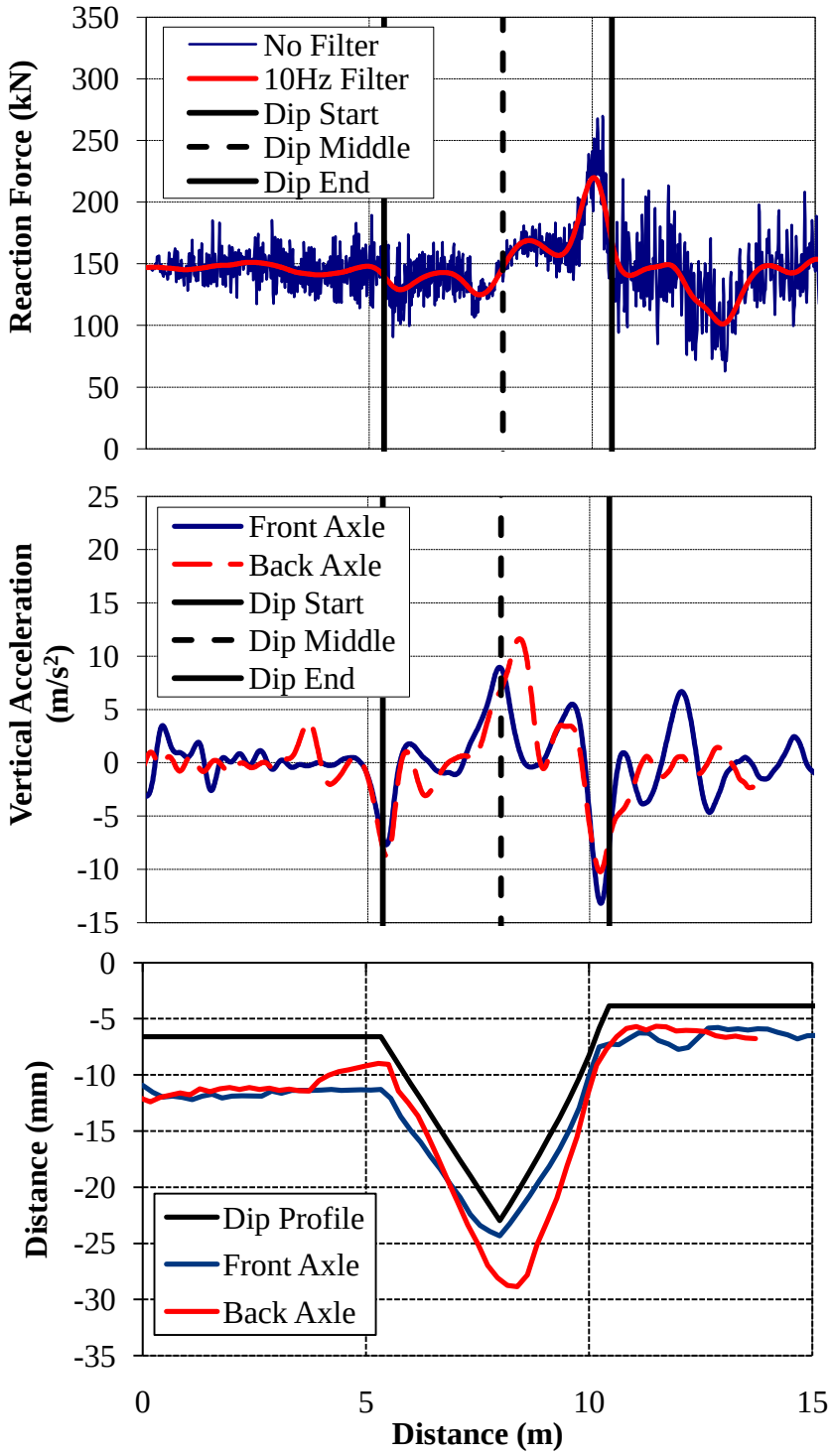

Figure F.139 - (a) Wheel/Rail Forces (b) Axle Accelerations and (c) Track Deflection due to a 1:150 Dip with 3-m Approach Tie Lengths (v = 22.2 m/s)

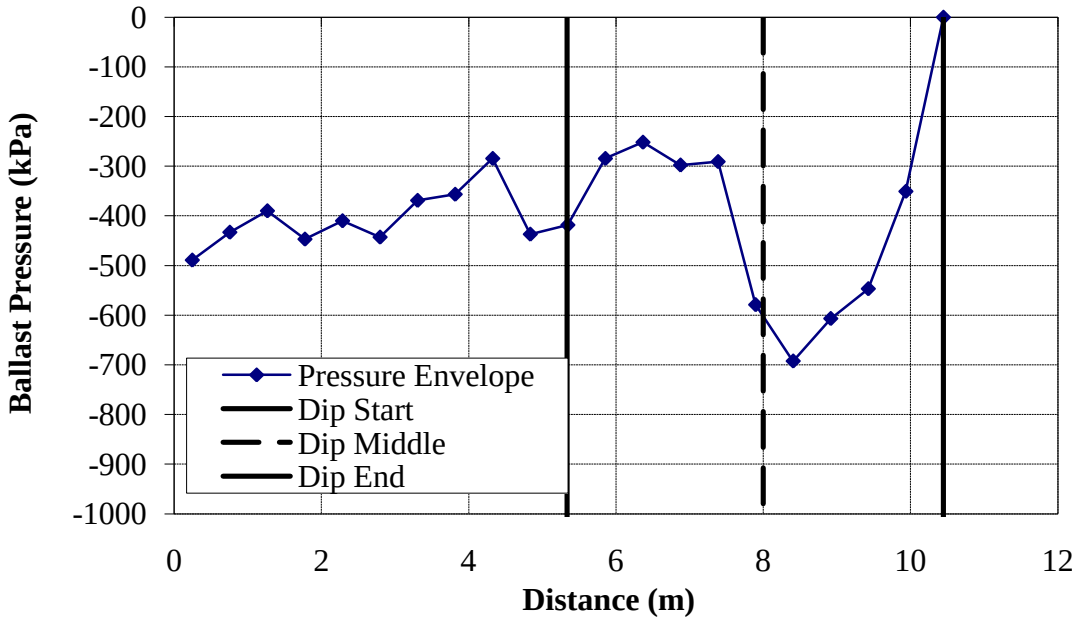

Figure F.140 – Ballast Pressures due to a 1:150 Dip with 3-m Approach Tie Lengths (v = 22.2 m/s)

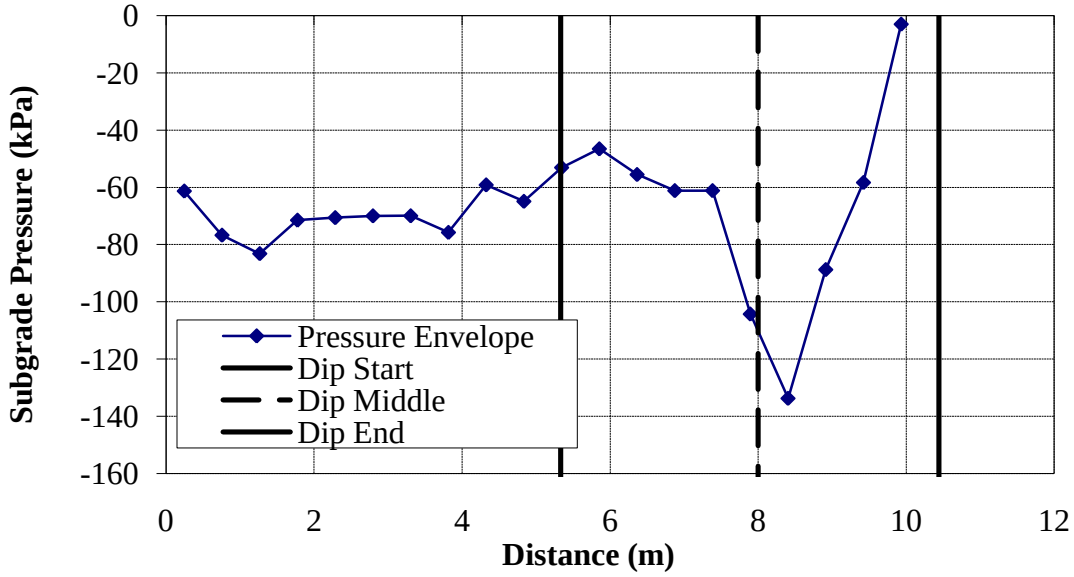

Figure F.141 - Subgrade Pressures due to a 1:150 Dip with 3-m Approach Tie Lengths (v = 22.2 m/s)

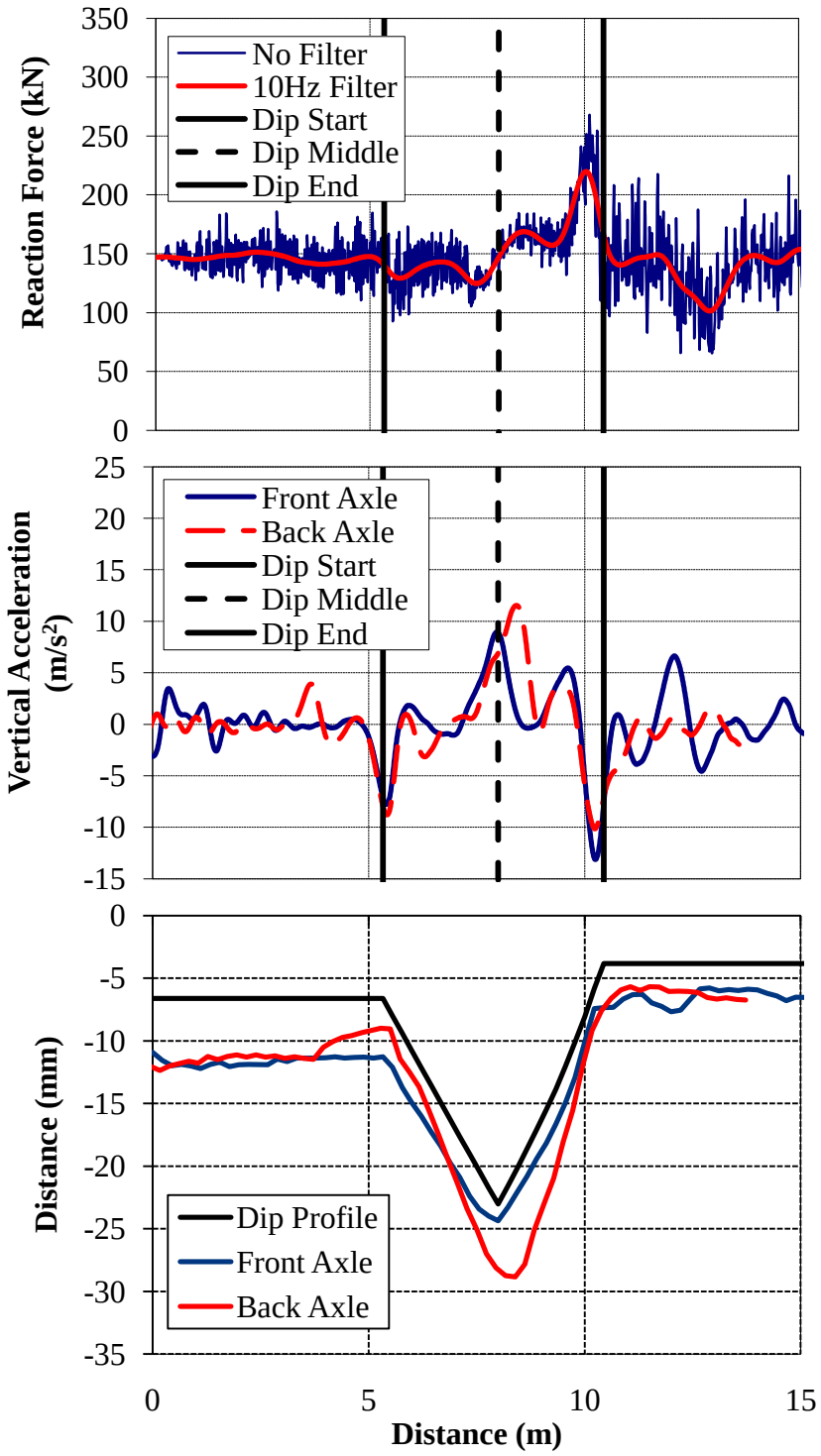

Figure F.142 - (a) Wheel/Rail Forces (b) Axle Accelerations and (c) Track Deflection due to a 1:150 Dip with 3.6-m Approach Tie Lengths (v = 22.2 m/s)

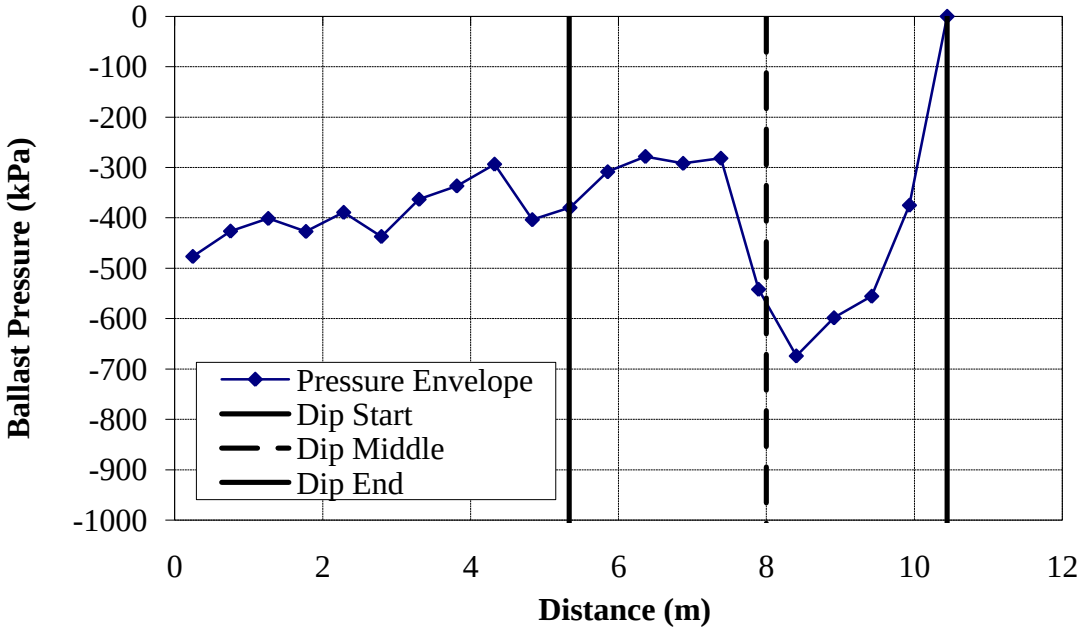

Figure F.143 – Ballast Pressures due to a 1:150 Dip with 3.6-m Approach Tie Lengths (v = 22.2 m/s)

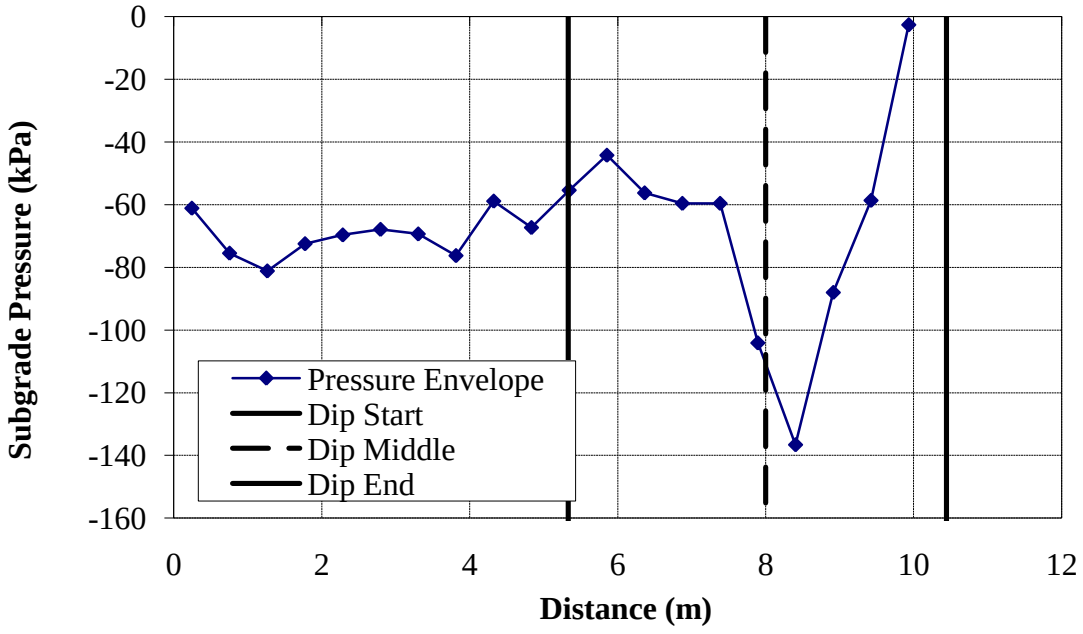

Figure F.144 - Subgrade Pressures due to a 1:150 Dip with 3.6-m Approach Tie Lengths (v = 22.2 m/s)

VITA

Jennifer Elizabeth Nicks received her Bachelor of Science degree in civil engineering from Texas A&M University in May 2004. She continued at Texas A&M University and received her Master of Engineering degree in civil engineering in December 2005. Her report was titled "The San Jacinto Monument Case History." During this time, she was a Teaching Assistant for the laboratory section of the "Introduction to Geotechnical Engineering" course. Jennifer continued at Texas A&M University by pursuing her Doctor of Philosophy degree in civil engineering (specifically geotechnical engineering) and graduated with her Ph.D. in December 2009. While working towards the Ph.D, Jennifer served as a Research Assistant for Dr. Jean-Louis Briaud investigating the topics of scour, erosion, shrink/swell soils, mat foundations, numerical modeling and consolidation. She was also actively involved in extracurricular activites including serving as Treasurer and President of the Texas A&M GSO of the Geo-Institute of ASCE (TAMU G-I), Co-Chair of the Geo-Institute's Student Presidential (G-I SPG) Group, Ambassador for the Zachry Department of Civil Engineering Aggie Ambassadors Program and geotechnical engineering representative for the Civil Engineering Student Advisory Committee (CESAC).

Ms. Nicks may be reached at 3136 TAMU, College Station, TX 77843-3136. Her email is jennifernicks@gmail.com.